UNCLASSIFIED

AD NUMBER
AD499885
CLASSIFICATION CHANGES
TO: unclassified
FROM: confidential
LIMITATION CHANGES
TO: Approved for public release, distribution unlimited
FROM: Distribution authorized to U.S. Gov't. agencies and their contractors; Administrative/Operational Use; 30 JUN 1950. Other requests shall be referred to Office of Naval Research, One Liberty Center, 875 North Randolph Street, Arlington, VA 22203-1995.
AUTHORITY
ONR ltr 30 Aug 2010; ONR ltr 30 Aug 2010

THIS PAGE IS UNCLASSIFIED

AD49885

JOSHUA HENDY CORPORATION
Contract No. N9onr-93201

FINAL REPORT

HYDROFOIL STUDIES
AND
PRELIMINARY DESIGN DATA

Copy No. 32

UNCLASSIFIED

DDC
RECEIVED
A

UNCLASSIFIED

DISTRIBUTION LIST

Copies	Addressee
15	Office of Naval Research Department of the Navy Washington 25, D. C. Attn: Fluid Mechanics Br. (Code 438)
1	Commanding Officer, Branch Office U.S. Navy Office of Naval Research 495 Summer Street Boston 10, Massachusetts
1	Commanding Officer, Branch Office U. S. Navy Office of Naval Research 346 Broadway New York 13, New York
1	Commanding Officer, Branch Office U. S. Navy Office of Naval Research 844 North Rush Street Chicago 11, Illinois
1	Commanding Officer, Branch Office U.S. Navy Office of Naval Research 801 Donahue Street San Francisco 24, California
2	Commanding Officer, Branch Office U.S. Navy Office of Naval Research 1030 East Green Street Pasadena 1, California
2	Assistant Naval Attache for Research U. S. Navy Office of Naval Research American Embassy, London, England Navy 100, F.P.O. New York, N.Y.
1	Navy Research Laboratory U.S. Navy Office of Naval Research Washington 20, D. C. Attn: Librarian (Code 2021)
1	Bureau of Aeronautics Department of the Navy Washington 25, D. C. Attn: Design Elements Division

Copies	Addressee
1	Bureau of Aeronautics Department of the Navy Washington 25, D. C. Attn: Research Division
1	Chief, Bureau of Ships Department of the Navy Washington 25, D.C.
1	Bureau of Ships Department of the Navy Washington 25, D. C. Attn: Ship Design Division
1	Bureau of Ships Department of the Navy Washington 25, D. C. Attn: Patrol District & Minecraft Branch
1	Bureau of Ships Department of the Navy Washington 25, D. C. Attn: Ass't Chief for Research & Development
2	David W. Taylor Model Basin Department of the Navy Washington 25, D. C. Attn: Hydromechanics Division
2	David W. Taylor Model Basin Department of the Navy Washington 25, D. C. Attn: Technical Library
1	Director of Aeronautical Research National Advisory Committee for Aeronautics 1724 F Street, N. W. Washington 25, D. C.
2	Director Langley Aeronautical Laboratory National Advisory Committee for Aeronautics Langley Air Force Base, Va.
1	Commanding General Wright-Patterson Air Force Base Dayton, Ohio Attn: Chief, Aircraft Laboratory (MCREXA)

Copies	Addressee
1	Central Air Documents Office Wright-Patterson Air Force Base Dayton, Ohio
1	Capt. G. C. Wright, Head New Developments & Operational Evaluation Branch (Op 312) National Defense Bldg. Rm. 4B548 Washington 25, D.C.
1	RAdm. C. B. Momsen, Head Underseas Warfare & Shipping Control Div. (Op 31) National Defense Building, Rm. 4E552 Washington 25, D. C.
1	Dr. S. D. Cornell, Director Planning Division Research and Development Board National Defense Building, Room 3E1036 Washington 25, D.C.
1	Dr. Ellis A. Johnson, Director Operations Research Office Department of the Army Fort Leslie J. McNair Washington 25, D. C.
1	Hon J. F. Floberg Assistant Secretary of the Navy for Air National Defense Building, Rm. 4E728 Washington 25, D.C.
1	Office of Naval Intelligence, Op 322F2 National Defense Building, Rm. 5E719 Washington 25, D. C.
1	Director, Weapons System Evaluation Group Office of Secretary of Defense National Defense Building, Rm. 2E995 Washington 25, D. C.
1	Dr. Vannevar Bush, President Carnegie Institution of Washington 1530 P Street, N.W. Washington 5, D.C.
1	Mr. Oscar Cox, President The Hydrofoil Corporation 1210 18th Street, N.W. Washington 6, D.C.
1	Mr. W. P. Carl, Jr. John H. Carl & Sons, Inc. 150 Merrick Road Rockville Centre, New York

Copies	Addressee
1	Mr. W. R. Ryan Edo Aircraft Corporation College Point Long Island, New York
1	Mr. E. G. Stout Hydrodynamics Research Laboratory Consolidated-Vultee Aircraft Corporation San Diego, California
1	Dr. K.S.M. Davidson, Director Experimental Towing Tank Stevens Institute of Technology Hoboken, New Jersey
1	Mr. John S. Coleman, Secretary Undersea Warfare Committee National Research Council 2101 Constitution Avenue, N.W. Washington 25, D.C.
1	Mr. F. L. Thompson Langley Aeronautical Laboratory National Advisory Committee for Aeronautics Langley Air Force Base, Va.
1	Capt. W. S. Diehl, USN Bureau of Aeronautics, Code AER-23 Department of the Navy Washington 25, D. C.
1	VAdm. E. L. Cochrane, USN (Ret.) Dept. of Naval Architecture & Marine Engineering, Rm. 5-228 Massachusetts Institute of Technology Cambridge 38, Mass.
1	RAdm. A. I. McKee, USN (Ret.) Design Director Electric Boat Co. Groton, Conn.
1	RAdm. P. F. Lee, USN (Ret.) Gibbs & Cox, Inc. 1 Broadway New York 4, N.Y.
1	Dr. G. F. Wislicenus Department of Mechanical Engineering John Hopkins University Baltimore, Maryland

JOSHUA HENDY CORPORATION

HYDROFOIL STUDY

Contract No. N9onr-93201

OBJECTIVE

It is the objective of this study to obtain and analyze available data on the subject of hydrofoils, to make necessary calculations, obtain necessary experimental data toward the end of determining the desirability and applicability of hydrofoils to surface vessels and, if and as the studies warrant, to assemble and present in practical usable form engineering and scientific data to be used as a basis for the preliminary design of surface vessels. The contract target requirement of obtaining maximum lift-drag ratio is a governing objective of all of the studies.

BASIC DATA

Because of the classified nature of the contract, all data reviewed has been obtained through the Office of Naval Research, which has supplied not only requested information, but such other data as was considered pertinent, covering a considerable amount of foreign information of a classified nature and some covering recent United States experience. Current work on hydrofoils by other groups has been reviewed only if the information was supplied through the Office of Naval Research.

METHOD OF ATTACK

The study approaches the problem of hydrofoil craft from the point of view of a possible designer, recognizing the interdependence of structural, hydrodynamic, stability and propulsive requirements. A considerable amount of detailed study has been given to each of these subjects and a great many preliminary design charts have been prepared to indicate the effect of the variation of each of the parameters on the final design. While many of these charts will have only occasional use, it is hoped that they will save a future designer a considerable amount of work and time in retracing the tedious and lengthy calculations necessary to find out what may be expected to happen when one of the parameters is varied. Where

possible, previous experimental results have been checked against these data. It is recognized, however, that additional experimental data is needed to complete the usefulness of the charts.

The studies were conducted as a coordinated effort of various specialists but for convenience of reference, this report has been divided into sections by subjects, with the primary responsibility for each section assigned to the subject specialist. The staff responsible for this work is as follows:

Project Director	W. C. Ryan
Hydrodynamics	W. C. Holmes, Jr.
Structures	Edmund G. Wodrich
Stability	Warren Amster
Propulsion	M. W. Beardsley

GENERAL

Brief Historical Background

Hydrofoils have been used sporadically on various types of craft for many years. As early as 1911 Guidoni used them successfully in Italy to assist landing and take-off of seaplanes and continued their successful use for a number of years on aircraft with a range of gross weights from 1400 to 55,000 pounds. Their successful use was in the era of relatively low speeds for aircraft, and as take-off and landing speeds increased, the use of hydrofoils for this purpose apparently declined. Although other nations were aware of the Italian results, no others saw fit to use hydrofoils extensively for this purpose.

About 1918 Dr. Alexander Graham Bell's laboratories developed a hydrofoil craft utilizing multiple fixed foils which apparently operated successfully at high speeds as high as 60 to 70 knots. Reports indicate that it attained a lift-drag ratio of about 8.

Recently in England Christopher Hook built and operated small hydrofoil craft utilizing foils whose angle of attack was automatically controlled by the use of a small surface sensing float. Apparently he achieved lift-drag ratios in the order of 8 with very small craft. His is the only known attempt to vary angle of attack.

Small fixed-foil craft have been recently constructed and operated by Swedish engineers, with interesting results reported in popular magazines, but no technical data concerning them has been reviewed by us.

The most extensive development of hydrofoil craft for which records are available was done by the Germans prior to and during World War II. They were of two types — those developed by Tietjens and those developed by the Sachsenberg Brothers. Tietjens utilized one large

main foil forward carrying the major portion of the load, with a small tail foil aft. The Sachsenberg Brothers' craft utilized two foils of approximately equal area, one forward and one aft. Both used fixed foils of relatively low aspect ratio and both attained stability by variation in the submerged area of the foils and by the use of V-shaped foils piercing the surface. Less data seems to be available on the Tietjens craft and there are indications that less development time was spent on this type of craft than on the other, due to war interruption, and there are also indications that it was less satisfactory in rough water performance from a stability point of view than was the Sachsenberg Brothers' craft.

The Sachsenberg Brothers apparently gave extended study to the subject and built numerous craft of various displacements, up to 80 tons, with power plants as high as 5000 H.P. These craft were operated with varying degrees of success up to speeds in excess of 50 knots. Progress was made gradually over a number of years of effort and the records indicate that there were many problems still requiring extensive research; there were also mixed opinions as to the effectiveness of hydrofoil craft at the time work was discontinued, due to bombings and enemy action. There is, however, ample evidence that these craft performed very well. Apparently the Russian Effort is along these lines.

None of the foreign craft of the past for which records were reviewed resulted in very high lift-drag ratios and the best results were of the order of 8. Apparently considerations of strength and stability and the desire to obtain workable craft in a short time dictated the course of design and required compromise which resulted in relatively low values of L/D. We have reviewed no evidence which indicates that a consistent concerted effort has been made in the past, aimed at the attainment of maximum L/D at moderate speeds as a prime objective.

Hydrofoil Craft - Summary and Conclusions

The particular appeal of hydrofoil craft as compared to conventional surface displacement craft lies in their lower power requirements at higher speeds and in their greater smoothness of operation and relative freedom from rolling and pitching due to surface disturbances. The curve of power required for a displacement or planing hull increases rapidly with increase of speed. The power curve of the hydrofoil craft, on the other hand, reaches a peak or hump value prior to the time the weight of the craft is supported dynamically on the foils and then drops appreciably lower than the curve for an equivalent surface craft and rises again. The difference between these curves represents an appreciable saving in power at higher speeds in the order of 50% or greater with high L/D craft.

The classic criterion of efficiency is the so-called Gliding Coefficient which is defined as the ratio R/D, where R is the resistance in pounds and D is the displacement of the vessel in pounds. This ratio for various vessels of various sizes and speeds is expressed as a function of the Froude number $F = \frac{V}{\sqrt{gL}}$ where V is the speed of the vessel in feet per second and L is the length of the vessel in feet.

Average values of R/D for planing craft against Froude numbers have been plotted by Tietjens and for various types of craft by J. H. Curry and are included in the Hydrodynamics section of this report. To get some idea of how the various types of craft fit into the picture, consider the following:

1. 10-Ton V Bottom Boat with Length - 33'

Speed in Knots	Froude Number	Gliding Coefficient	Corresponding L/D Req'd.
10	.519	.085	11.75
20	1.037	.165	6.06
30	1.557	.222	4.52

2. 100-Ton P.T. Boat with Length - 100'

Speed in Knots	Froude Number	Gliding Coefficient	Corresponding L/D Req'd.
20	.595	.095	21.0
30	.892	.130	7.7
50	1.49	.178	5.6

3. 1898-Ton Destroyer with Length - 334'

Speed in Knots	Froude Number	Gliding Coefficient	Corresponding L/D Req'd.
30	.483	.062	16.1
40	.644	.092	10.9

4. 13,790-Ton Cargo Ship with Length - 427'

Speed in Knots	Froude Number	Gliding Coefficient	Corresponding L/D Req'd.
14	.202	.00225	443.0

The familiar lift-drag ratio or L/D which is the reciprocal of the Gliding Number is the measure of the effectiveness of a hydrofoil craft once its weight is complete supported on its foils. A glance at the last column of the above table shows the values of L/D which must be obtained by hydrofoil craft to be economically competitive with displacement or planing vessels. Small hydrofoil vessels are superior at relatively low speeds, but large vessels are only competitive with surface craft at very high speeds.

Due to strength considerations and their effect on the geometry of hydrofoils, maximum attainable L/D ratios are extremely high at low speeds and gradually decrease with increasing speed so that, for instance, the maximum attainable L/D of a hydrofoil which has the necessary strength to withstand the forces generated at 50 knots is somewhat lower than the maximum attainable L/D at 20 knots. This is illustrated graphically in the Hydrodynamics Section of this report. This section also shows that L/D decreases with increases of unit foil loading.

Another limit on the performance of hydrofoils is introduced by cavitation, which reduces the lift and decreases the attainable L/D of hydrofoils. The speed at which incipient cavitation may be expected to occur for various types and thicknesses of hydrofoil sections is shown in the Hydrodynamics Section of this report. In general, cavitation-free operation requires progressively thinner sections as speed is increased. Thinner sections, in turn, require smaller spans between struts for structural reasons and also result in lower L/D ratios.

The results of European experience as exemplified by the Sachsenberg Brothers in Germany and others utilizing foils piercing the surface produced L/D ratios in the order of 8. The effort to attain "built-in" stability in a simple manner and performance at reasonably high speeds, coupled with strength requirements, were probably primarily responsible for these results.

Dr. Vannevar Bush has suggested the possibility that considerably higher values of L/D would probably be obtained if the hydrofoils were left completely submerged during all operation and stability obtained by automatic action of movable control surfaces actuated by depth sensing mechanisms.

In the Hydrodynamics section of this report it is theoretically demonstrated that for reasonable speeds and foil loadings, prior to the onset of cavitation, appreciably higher values of L/D may be obtained than those recorded in foreign results. It is recog-

nized that flaps and the means used for their control and actuation will reduce the attainable L/D somewhat over that predicted for a solid foil, but even with conservative allowance for this reduction it is anticipated that L/D ratios over 20 may be obtained at speeds in the neighborhood of 35 knots with careful design. This is based on conservative assumptions and turbulent flow. Under ideal conditions of laminar flow, considerably higher values might be attained.

The problem of longitudinal and lateral stability by the use of movable control surfaces and depth and motion sensing devices has been carefully studied and a system has been designed which is believed to be practicable and workable. Theoretically it should produce satisfactory stability and control under rough water conditions. The system utilizes readily obtainable components previously proved out in auto-pilot design. It is believed that a relatively straightforward simple program of testing can demonstrate the adequacy of the system and all of its components prior to installation in an actual vessel.

A small self-propelled test craft was constructed and tested to determine experimentally, under actual operating conditions, the validity of the data developed in the Hydrodynamics section of this report for predicting performance. The results of these tests are analyzed in detail in the Performance section of the report and indicate excellent agreement between experimental results and theoretical predictions. Briefly, the craft with a light weight of 351 pounds successfully lifted four people for a gross load of 1161 pounds. The maximum L/D developed by the craft as a whole was approximately 12 and it obtained a maximum speed of 24 miles per hour with a ten horsepower outboard engine. Analysis of the performance results indicates that an L/D of over 22 was obtained from the main foil-strut combination alone. The craft operated much more smoothly and stably in rough water than a displacement craft of the same size and weight.

The theoretical and experimental evidence developed in this report indicates that fully submerged foils will probably develop the highest possible L/D. The use of movable control surfaces seems to offer the possibility of sacrificing the least hydrodynamic performance to satisfy stability requirements but requires the utilization of mechanical means of some complexity to obtain automatic control of stability.

It was demonstrated that L/D ratios of a higher order than those recorded in European reports based on surface-piercing foils could be obtained by utilizing a fully submerged main foil of high aspect

ratio located aft of the center of gravity of the craft supporting most of the weight of the vessel, with auxiliary planing surfaces forward designed to provide necessary longitudinal and lateral stability without the use of mechanical methods of control. Some sacrifice of L/D of the craft was made in the attainment of stability and it is probable that less sacrifice of performance for stability would be made in a craft with movable flaps and all foils submerged than with auxiliary planing surfaces. However, it is believed that a careful development of auxiliary surfaces will ultimately result in very satisfactory values of L/D and the configuration with fixed main foil and surfaces is well worth further investigation.

The problem of propulsion for hydrofoil craft offers a field for a considerable amount of future investigation. The necessity of providing adequate thrust at relatively low forward speeds to get over the "hump" in the resistance curve, together with reasonable propeller efficiency at relatively high speeds, poses a difficult problem for a standard marine power plant and fixed pitch propeller. The use of controllable pitch propellers would undoubtedly help. Also, the necessity of mounting the propeller at some distance below the hull introduces complications in the intermediate drive, which is only partly answered by right angle gear transitions and inclined drive shafts. Other types of propulsion should be investigated. It is to be expected that some of the gains made in hydrodynamic efficiency will be offset by losses in propulsive efficiency of marine propellers as craft speeds become very high. In the propulsion section of this report, a theoretical investigation points out the possibility of increasing propulsive efficiency at high speeds by the reduction of cavitation effects through the use of shrouds. It is believed that the development of marine propulsion at high speeds should be carried on simultaneously with the development of hydrofoil craft.

The proper selection of materials for the construction of foils and struts proved to be a major problem in the German work. High strength steels were used extensively, but corrosion and erosion proved very serious. In an attempt to solve this problem, the Germans tried to protect the surface by numerous methods, including plating, painting and covering the surface with plastics and vulcanized rubber. At the time their work was discontinued, none of these methods had apparently proven completely satisfactory. It is believed that research along these lines is very necessary in hydrofoil craft. There seems to be some hope in the use of fibreglas plastic for this purpose because of its resistance to both corrosion and marine growths, and it is our opinion that a steel core wrapped with fibreglas may offer possibilities.

Although there are many new problems introduced in the design, construction and operation of practical hydrofoil craft, all seem capable of solution by research and experiment and the ultimate possibilities of high economy coupled with desirable military characteristics appear to justify continued and expanded efforts in this field.

C O N F I D E N T I A L

DESIGN CHARTS

June 1950

W. C. Holmes, Jr.

Contract No. N9onr-93201

DESIGN CHARTS

Based upon the general methods of configuration studies outlined in the Hydrodynamics section of this report, preliminary Design Charts are presented to indicate the order of magnitude of attainable (L/D) ratios which can reasonably be expected of hydrofoil craft which have high (L/D), rather than high speed, as their governing design consideration. The geometries, power requirements, performance and operating conditions necessary to the attainment of high (L/D) are indicated as well as the effects of variations of the principal design parameters.

Determination of maximum (L/D) and definition of the optimum configurations corresponding to such maximum involves a procedure in which both hydrodynamic and structural requirements are simultaneously satisfied. It is of course necessary, in the conduct of such studies, to make certain assumptions, predictions, and estimates of the relationships among the numerous parameters. Those made in the present studies are considered to represent a realistic estimate of attainment which can be realised with good, but not unreasonable, manufacturing technique. It is hoped that the results presented will prove useful in the evaluation of the potentialities of hydrofoil craft and will form a foundation upon which more refined studies can be based.

The general assumptions are discussed in some detail in the sections of this report dealing with Hydrodynamics and Structures. Some of the more essential ones are repeated here. It is, of course, possible that somewhat higher values of (L/D) could be estimated by the use of more optimistic basic assumptions. Where uncertainties exist, however, the present studies were based upon conservative estimates, and are therefore considered to be quite realistic.

The primary basic assumptions are:

1. Foil and strut sections are assumed to be solid, symmetrical sections. Some drag improvements can doubtless be realized, in certain cases, by the use of cambered foils, and fabricated sections can doubtless be used to advantage on large craft. Detailed consideration of these effects, however is considered beyond the scope of this preliminary report.

2. Strut slenderness ratio, limited by buckling considerations, is assumed no greater than 120. The use of tapered or stepped

struts are contemplated as means of decreasing strut thickness or increasing length. The present studies assume that average strut requirements are adequately considered by the general assumptions that foil and strut chords are equal, and that strut length is one-fifth the foil span.

3. Foil depth of submergence is assumed to be one-tenth its span. Particular design studies should of course include depth of submersion as a design variable. The value used in these studies, however, is considered to represent a fair estimate of the proper depth compatible with permissible roll angles, freedom from cavitation, and minimum strut drag.

4. The design load is assumed to be carried by a single, entirely submerged main foil, with control and stabilization provided by movable surfaces on the foil and, as necessary, completely submerged auxiliary foils. Such a configuration is considered to permit higher values of (L/D) than does that which utilizes oblique foils which pierce the water surface.

5. The main foil planform is assumed to be rectangular, of constant thickness. The effect of planform taper is indicated for the particular case of the single-strut configuration and is discussed in more detail in the Hydrodynamics section of this report. It is assumed that taper, particularly of the outer foil panels, in the case of multi-strut configurations is a design refinement which will be applied to particular designs as permissible.

6. It is understood that tests of a most promising type of endplate are in progress as this report is being prepared, and it is considered likely that some improvement of (L/D) will accrue from the use of endplates of this type. No attempt is made in the present studies, however, to include the effects of such devices upon maximum (L/D).

7. High-strength (150,000 psi) steel is assumed as the material of construction of foils and struts. Design safety factor is assumed to be 2.0, and dynamic load factor is assumed to be no greater than 2.0. The effects of using lower strength materials are indicated for the particular cases of mild steel (50,000 psi) and laminated fibreglas (40,000 psi). Design working stresses, based upon static loads, are therefore 37,500 for high-strength steel; 12,500 for mild steel; and 10,000 for fibreglas.

More detailed discussion of the variations of the major design parameters is presented in the following pages.

Chart A - VARIATION OF MAXIMUM (L/D) AND REQUIRED POWER WITH DESIGN SPEED

The effects of design speed upon maximum attainable (L/D) and corresponding required horsepower are indicated, for varying numbers of struts. Of particular significance to the general subject of hydrofoil craft is the decrease of attainable (L/D), and increase of required power, with increasing design speed. This is, primarily, affected by permissible foil loading. Low design speeds correspond to low foil loading, hence high aspect ratio and low foil and strut thicknesses, which in turn permit high values of (L/D). Conversely, high speeds correspond to high foil loading, low aspect ratio, greater thicknesses, and lower attainable values of (L/D). This is of course a familiar picture to aircraft designers.

Of almost equal importance is the indicated effect of the number of struts upon attainable values of (L/D). As the number of struts is increased, it can be expected that aspect ratio increases, or foil thickness decreases, permitting drag reductions which, in turn, result in higher values of (L/D). The trend does not, however, continue indefinitely, since the addition of struts is accompanied by increased strut parasite drag. A point is reached at which the addition of strut drag outweighs the advantages gained through reduction of foil drag, and the net (L/D) is reduced.

Chart B - OPTIMUM GEOMETRY FOR MAXIMUM (L/D)

Combinations of foil loading, design speed, foil thickness, and strut thickness required for attainment of maximum (L/D) are indicated. Optimization of the geometry is affected as outlined in the Hydrodynamic Section of this report. It is to be noted that the indicated variations of the geometrical parameters with foil loading are dictated primarily by structural considerations, with design speeds and (L/D) based upon hydrodynamic evaluations of the performance of structurally acceptable configurations.

Chart C - VARIATION OF (L/D) WITH OPERATING SPEED

Of particular significance to studies of hydrofoil craft is the variation of (L/D) with speed, as the operating speed differs from that corresponding to maximum (L/D) conditions. Serious consideration should be accorded this variation in the evaluation of particular craft. As indicated by the Chart, whereas high values of (L/D) are attainable with combinations of low speed and low foil loading, the (L/D) deteriorates rapidly with increasing speed and becomes considerably lower than the value attainable with a higher foil loading configuration which may have a relatively lower peak value of maximum possible (L/D).

It is immediately apparent that maximum (L/D), alone, is not of itself sufficient basis for the realistic evaluation of the merit of a hydrofoil craft. The speed range through which operation of the craft is to be expected becomes equally important. Thus, considering the three-strut configuration as an example, whereas a maximum (L/D) of about 35 is attainable with a foil loading of 0.1 tons per square foot (224 pounds) at ten knots, the (L/D) attainable with the same loading is only about 14 at 25 knots. More economical operation over this entire speed range could be obtained with a higher foil loading which, although its maximum (L/D) would be lower, would have a higher average value. A craft with a foil loading of 0.3 tons per square foot, for example, would show an (L/D) of 25 at 25 knots, with a peak value of 29 at 19 knots. The similarity to aircraft performance is readily apparent. The reasons for this variation of (L/D) with operating speed are discussed in the Hydrodynamic Section of this report.

Chart D - VARIATION OF REQUIRED POWER WITH OPERATING SPEED

Variations of power requirements as speed differs from that corresponding to maximum (L/D) are indicated, as based upon the (L/D) variations of Chart C. Here, again, it is readily apparent that (L/D) alone does not constitute sufficient basis upon which to evaluate the merit of a hydrofoil craft. It is also apparent that, as in the case of aircraft, high speed and maximum possible (L/D) are not compatible requirements.

Chart E - REDUCTION OF ATTAINABLE (L/D) DUE TO DEVIATIONS OF MAJOR PARAMETERS FROM OPTIMUM VALUES

The effects of variations from optimum values of speed and the major geometrical parameters are indicated. The effect of speed, reflected in Charts C and D, is seen to be of considerable magnitude. It is seen that, in the interest of economy, a craft designed for the attainment of maximum possible (L/D) should operate at speeds near that for such attainment.

The effects of the geometrical parameters appear, at first glance, to be relatively minor. Thus, a twenty percent error in aspect ratio is seen to result in only a ten percent loss in attainable (L/D). It should be noted, however, that when high (L/D) is the primary consideration, as is the case in the present studies, the apparently great margin of error permissible in each of the major parameters should not be construed as justification for laxity in maintenance of the proper values. If lower (L/D) values are to be considered acceptable, economy would dictate simplification of design, rather than the lowering of design standards. Thus, if a ten percent reduction of maximum (L/D) is acceptable with a four-strut craft, for example, Chart A indicates that it would be more judicious to concentrate efforts on a simpler two-strut craft.

A more detailed treatment of the effects of deviations of the major design parameters is given in the Hydrodynamic Section of this report.

Chart F - INFLUENCE OF MATERIALS OF CONSTRUCTION UPON MAXIMUM (L/D)

As indicated in the general introduction to this section, high-strength steel is assumed as the material of construction in the analyses upon which Charts A through E are based. It is of interest to determine the reduction of attainable (L/D) which results from the use of lower stress, or less critical, materials. Mild steel and laminated fibreglas are chosen as materials of interest. Mild steel is chosen for its obvious advantage with regard to availability, while glass is chosen for its light weight, resistance to corrosion, relative ease of fabrication, low cost, and reasonably good strength characteristics. The four-strut configuration is used as the basis for comparison, although the reductions, in percentage, can be expected to apply to the other cases.

CONFIDENTIAL

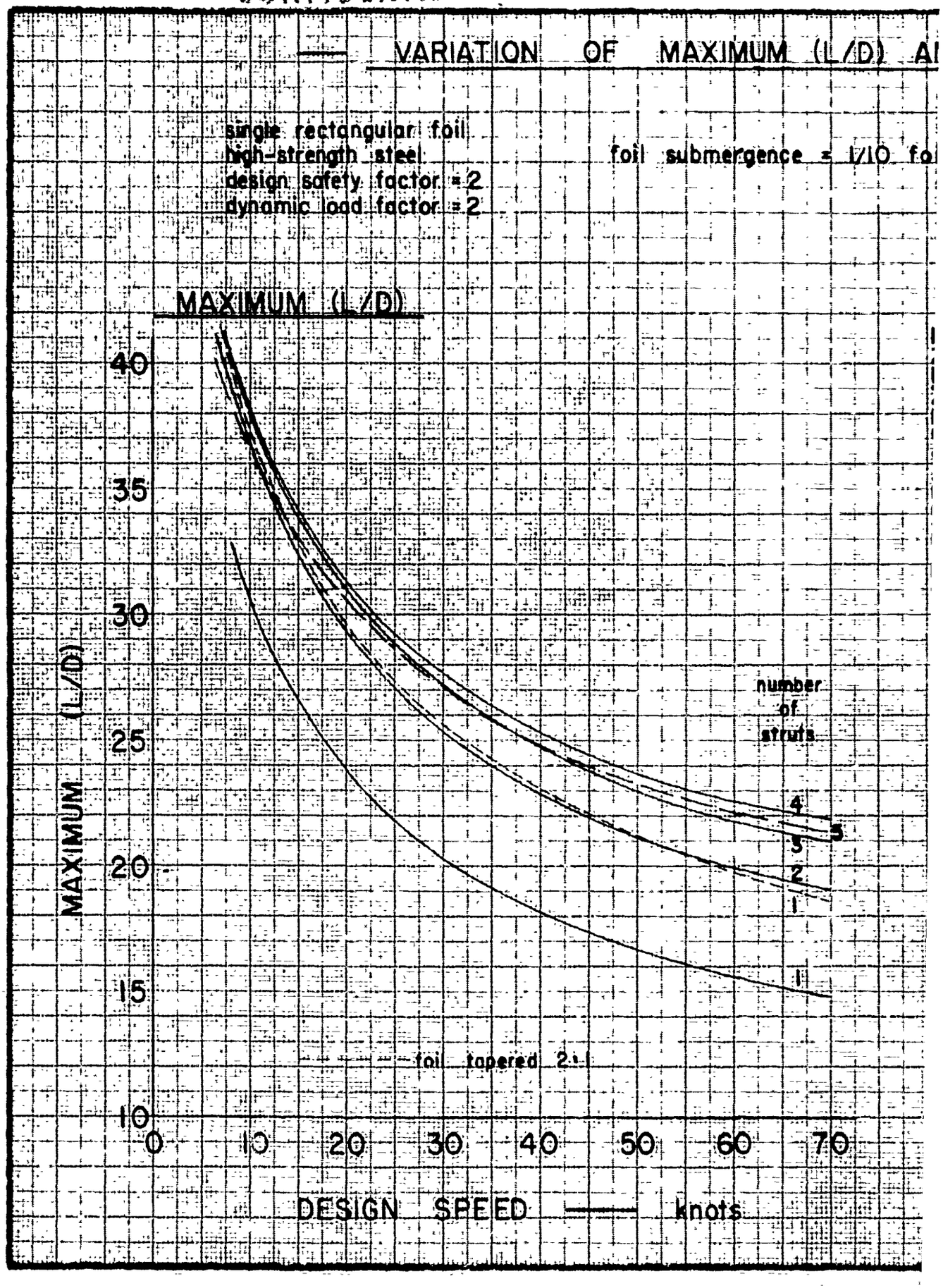

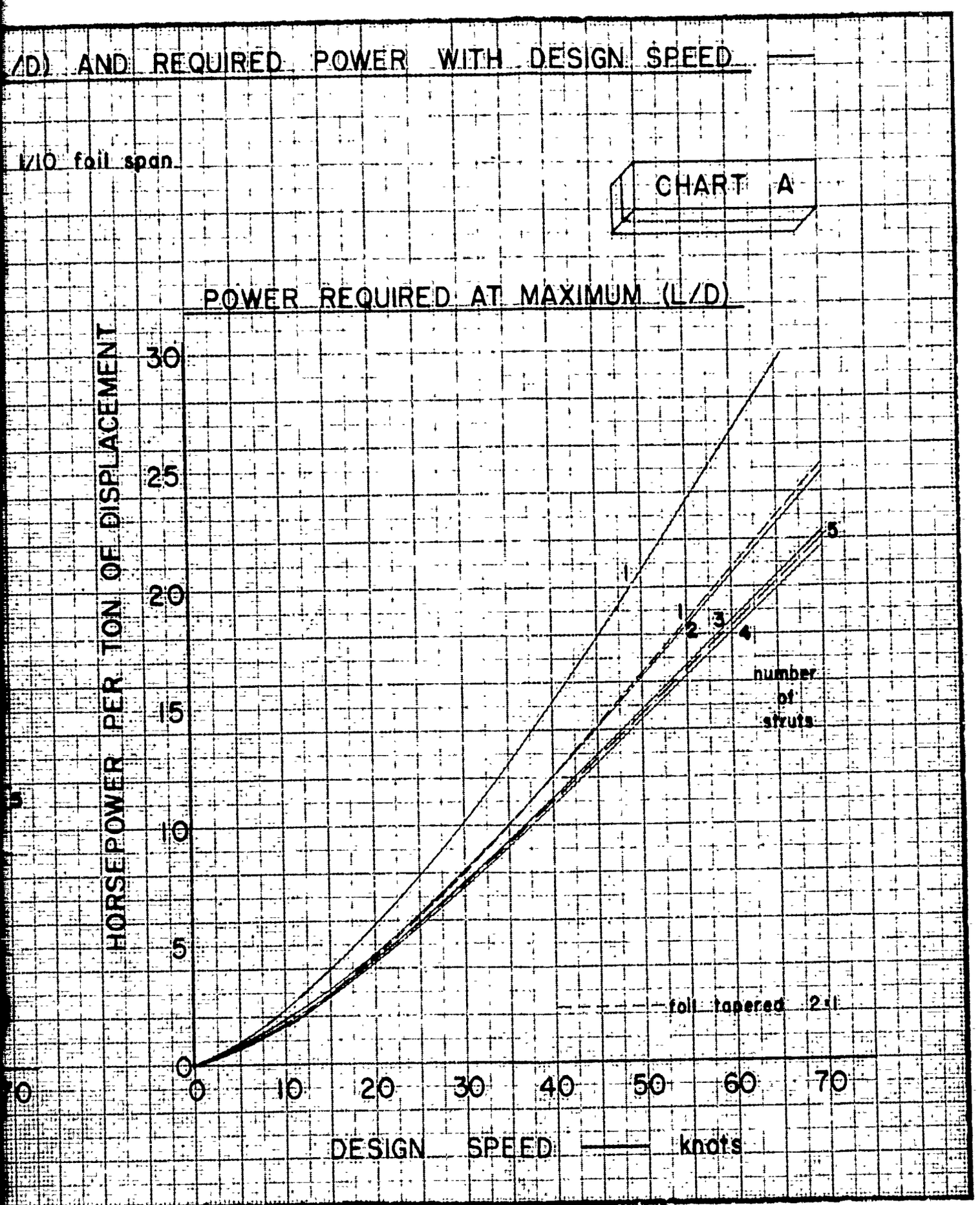
/D) AND REQUIRED POWER WITH DESIGN SPEED
l/10 foil span
CHART A
POWER REQUIRED AT MAXIMUM (L/D)
HORSEPOWER PER TON OF DISPLACEMENT
30
25
20
15
10
5
0
0
10
20
30
40
50
60
70
1
2
3
4
5
number of struts
foil tapered 2:1
DESIGN SPEED —— knots

CONFIDENTIAL

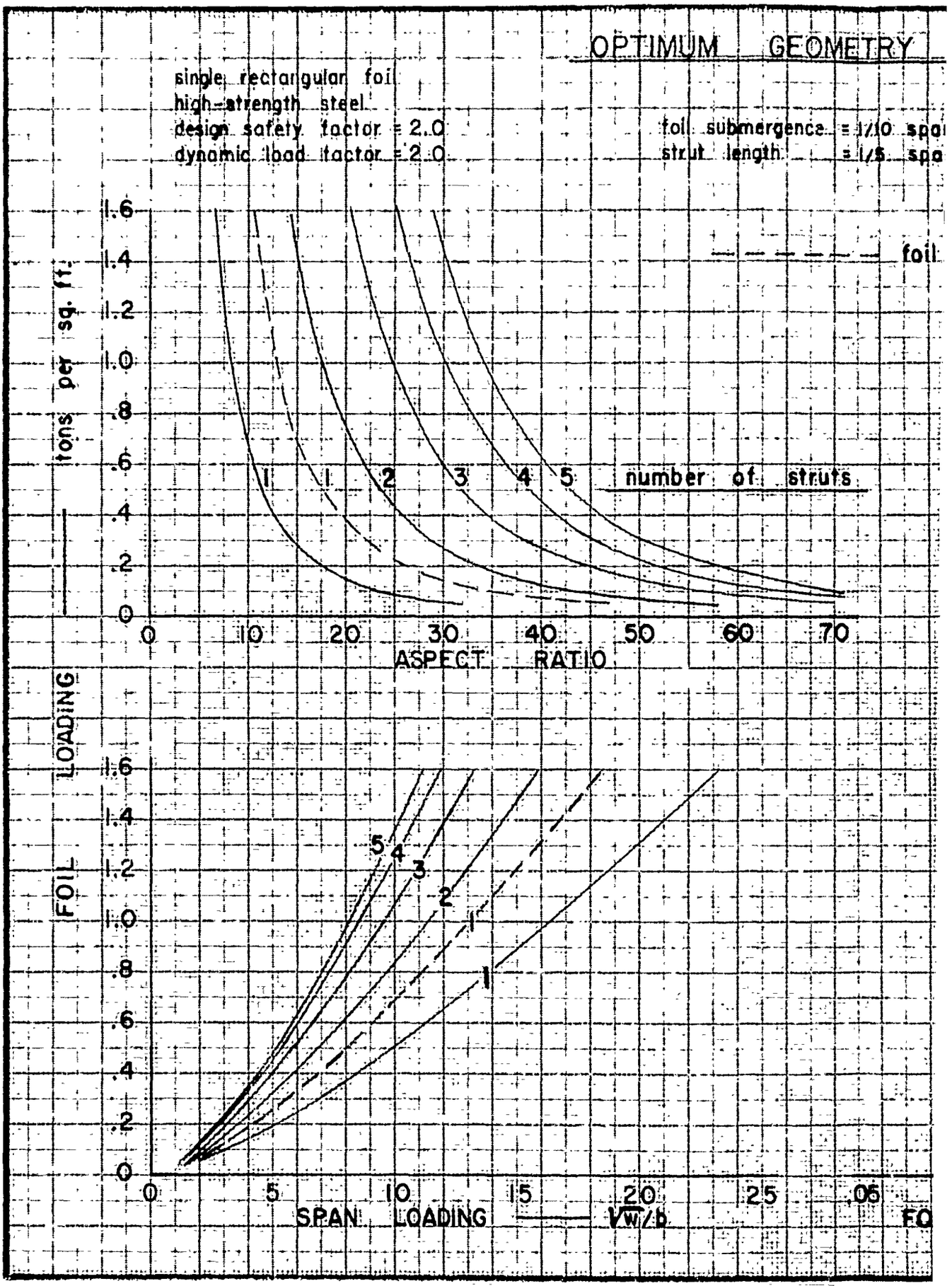

20

OMETRY FOR MAXIMUM (L/D)

ce. = 1/10 span
= 1/5 span

foil tapered 2:1

ruts.

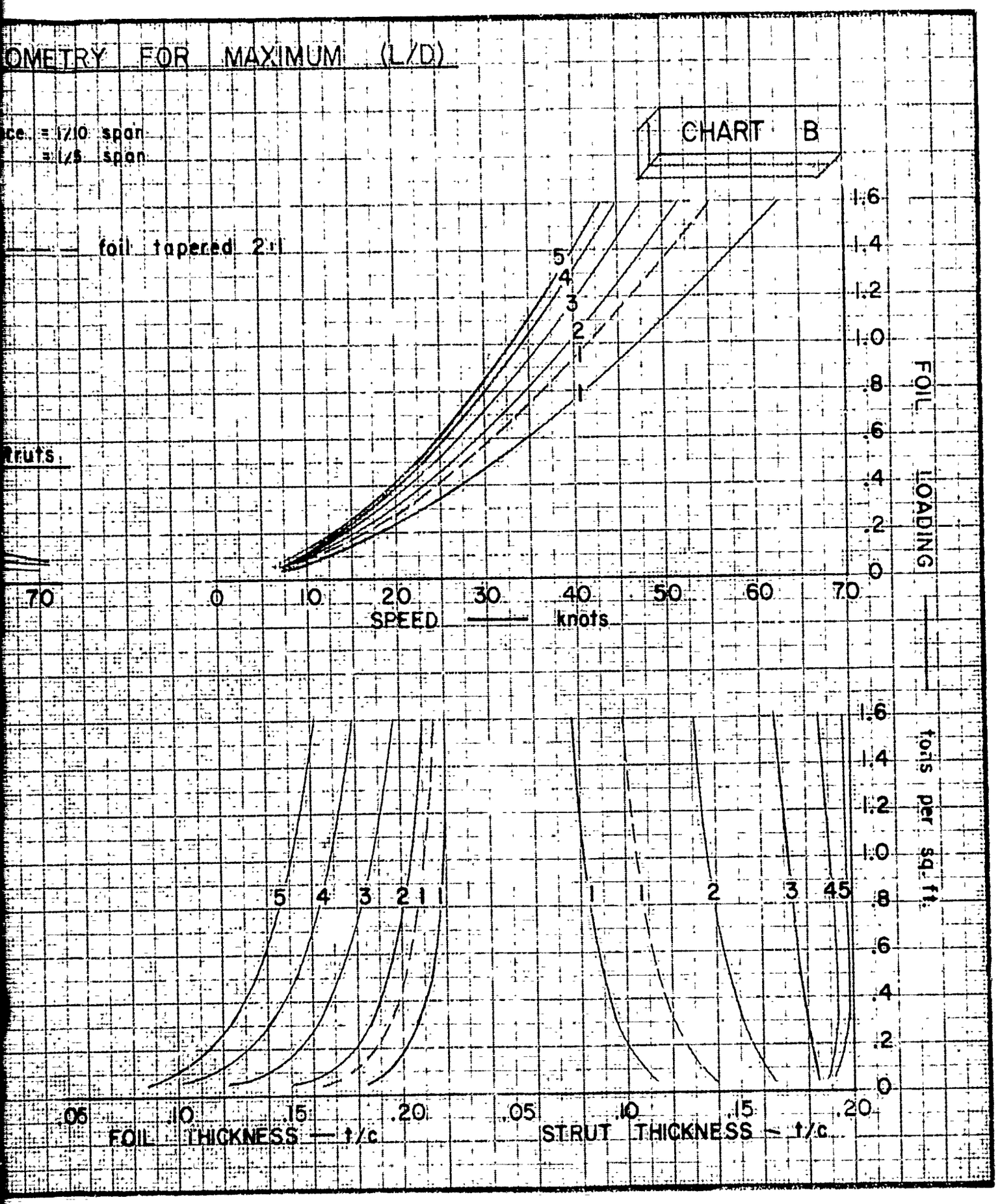

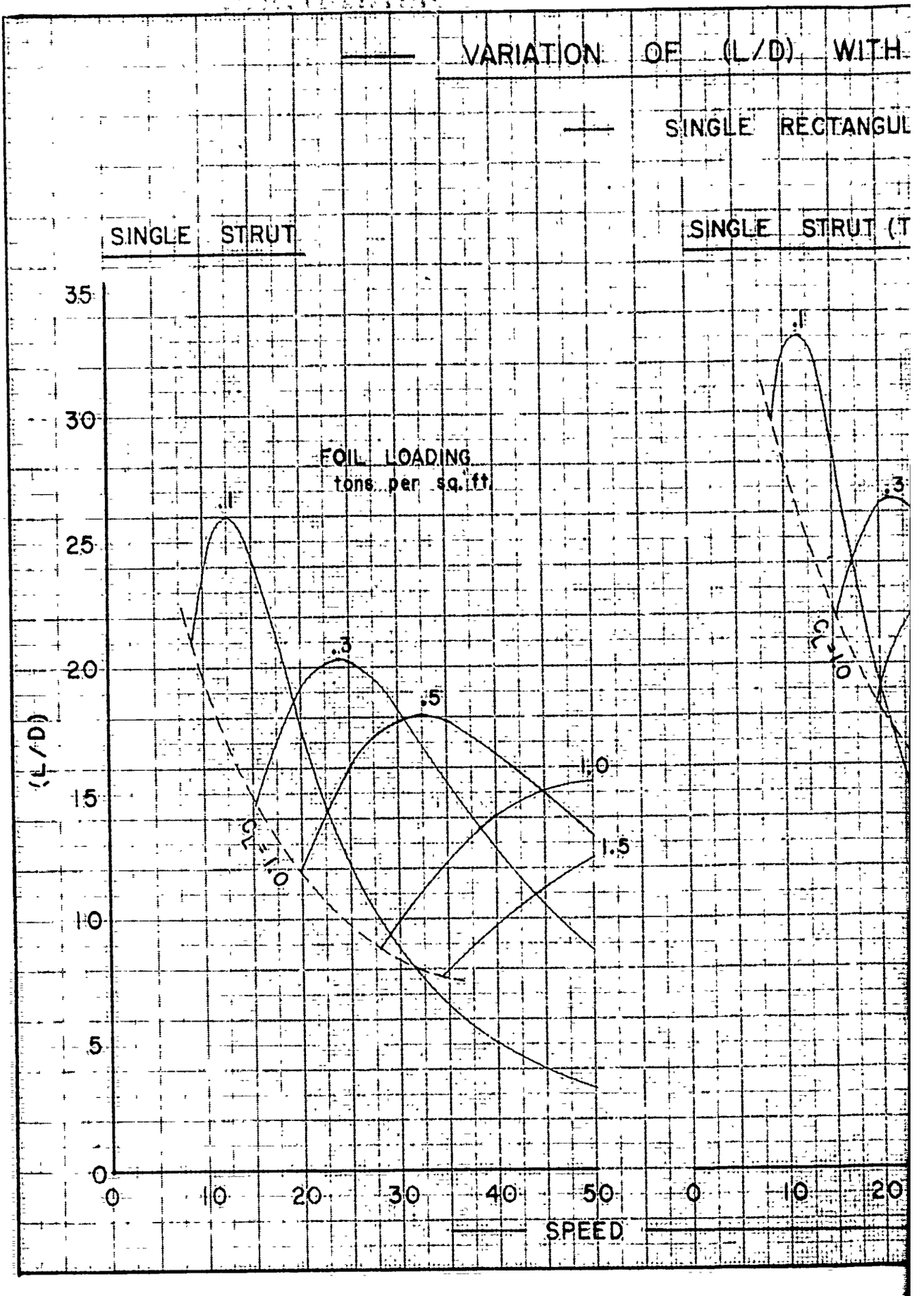
VARIATION OF (L/D) WITH
SINGLE RECTANGUL
SINGLE STRUT
SINGLE STRUT (T
FOIL LOADING
tons per sq.ft
(L/D)
SPEED
35
30
25
20
15
10
5
0
0
10
20
30
40
50
.1
.2
.3
.5
1.0
1.5
$C_L = 1.0$

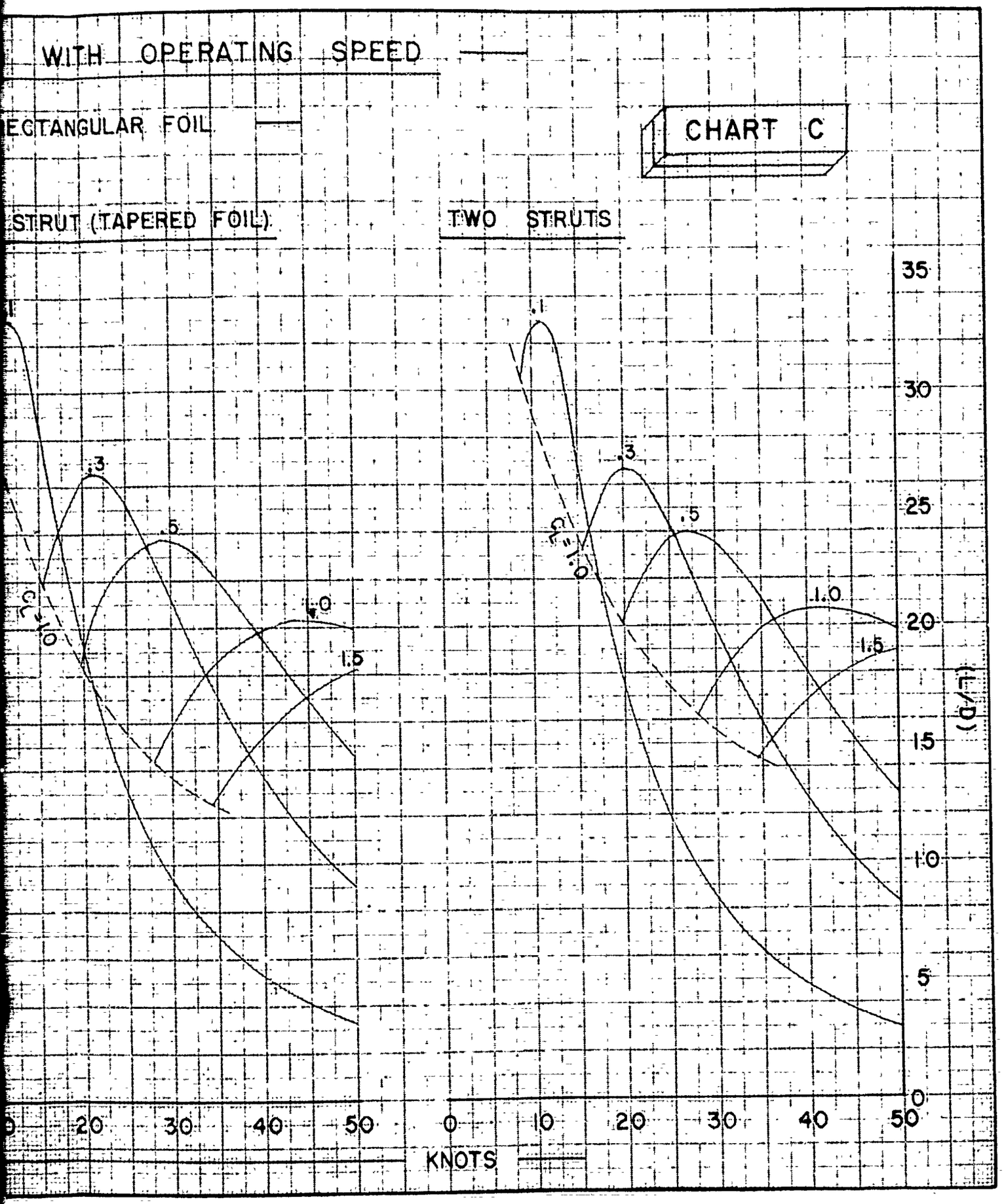
WITH OPERATING SPEED
ECTANGULAR FOIL
CHART C
STRUT (TAPERED FOIL)
TWO STRUTS
.1
.3
.5
1.0
1.5
C_L=1.0
35
30
25
20
15
10
5
0
(L/D)
0
10
20
30
40
50
KNOTS

CONFIDENTIAL

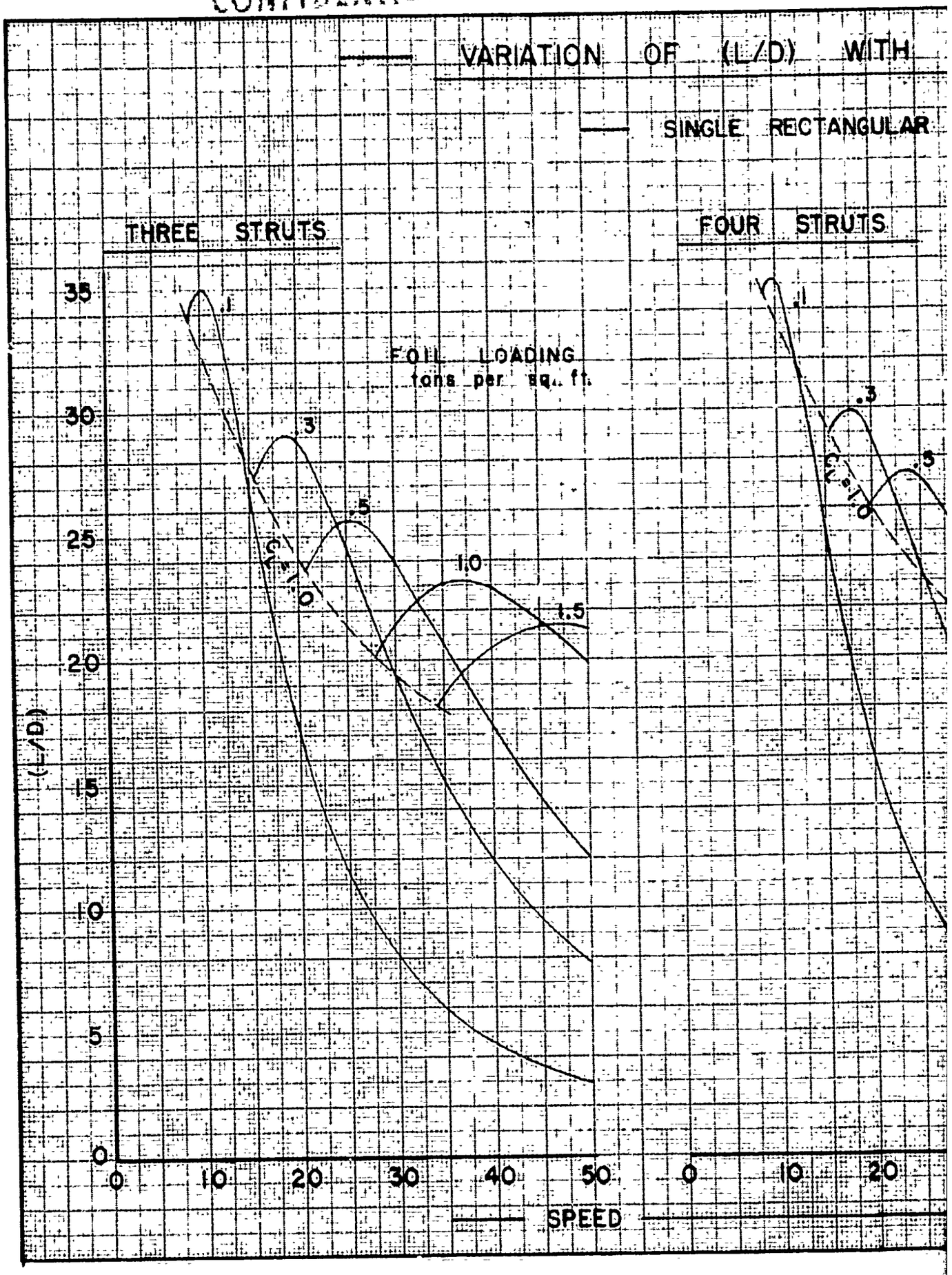

KEUFFEL & ESSER CO. N. Y. NO. 339 1/2F

WITH OPERATING SPEED

ECTANGULAR FOIL

CHART C

STRUTS

FIVE STRUTS

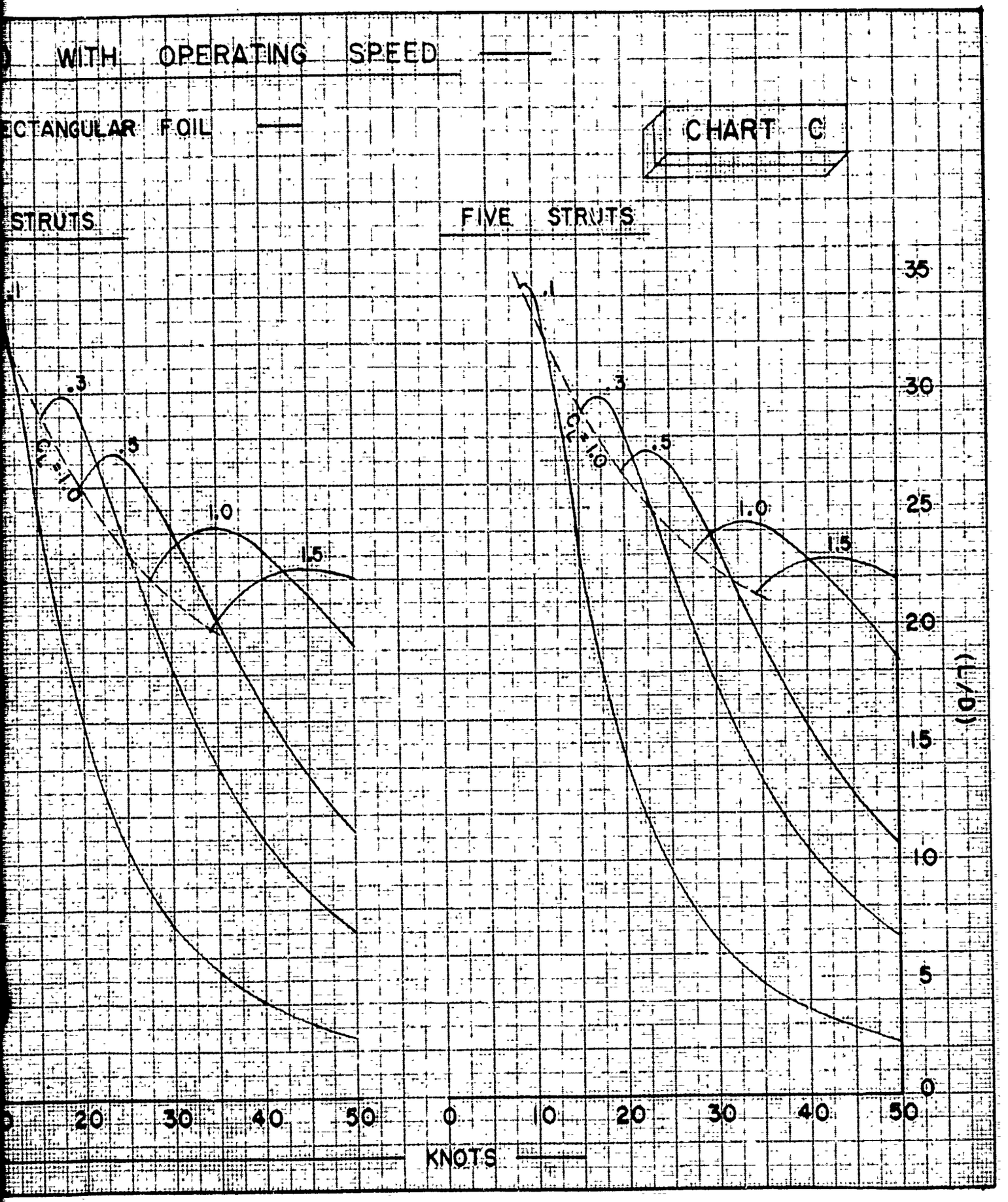

CONFIDENTIAL

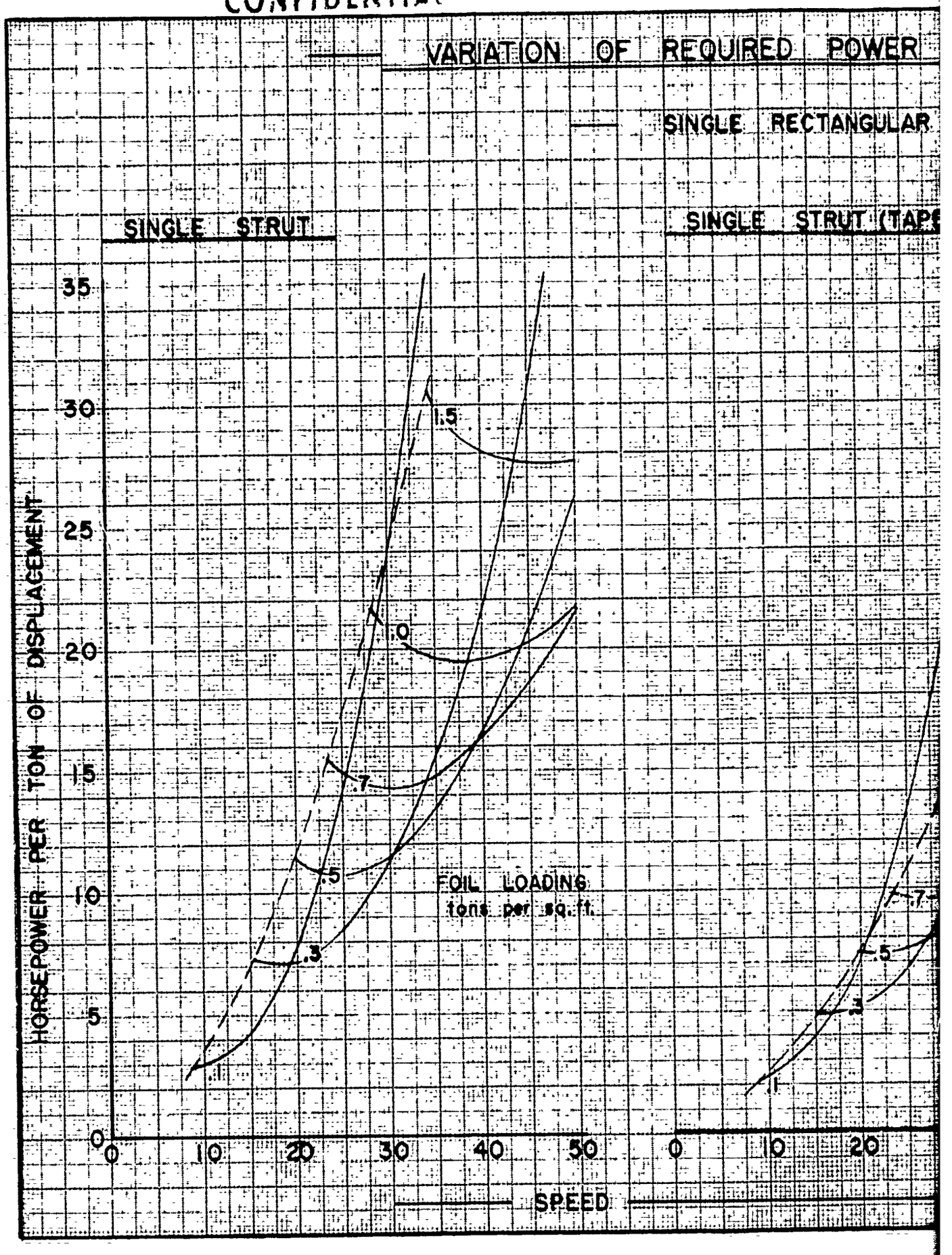

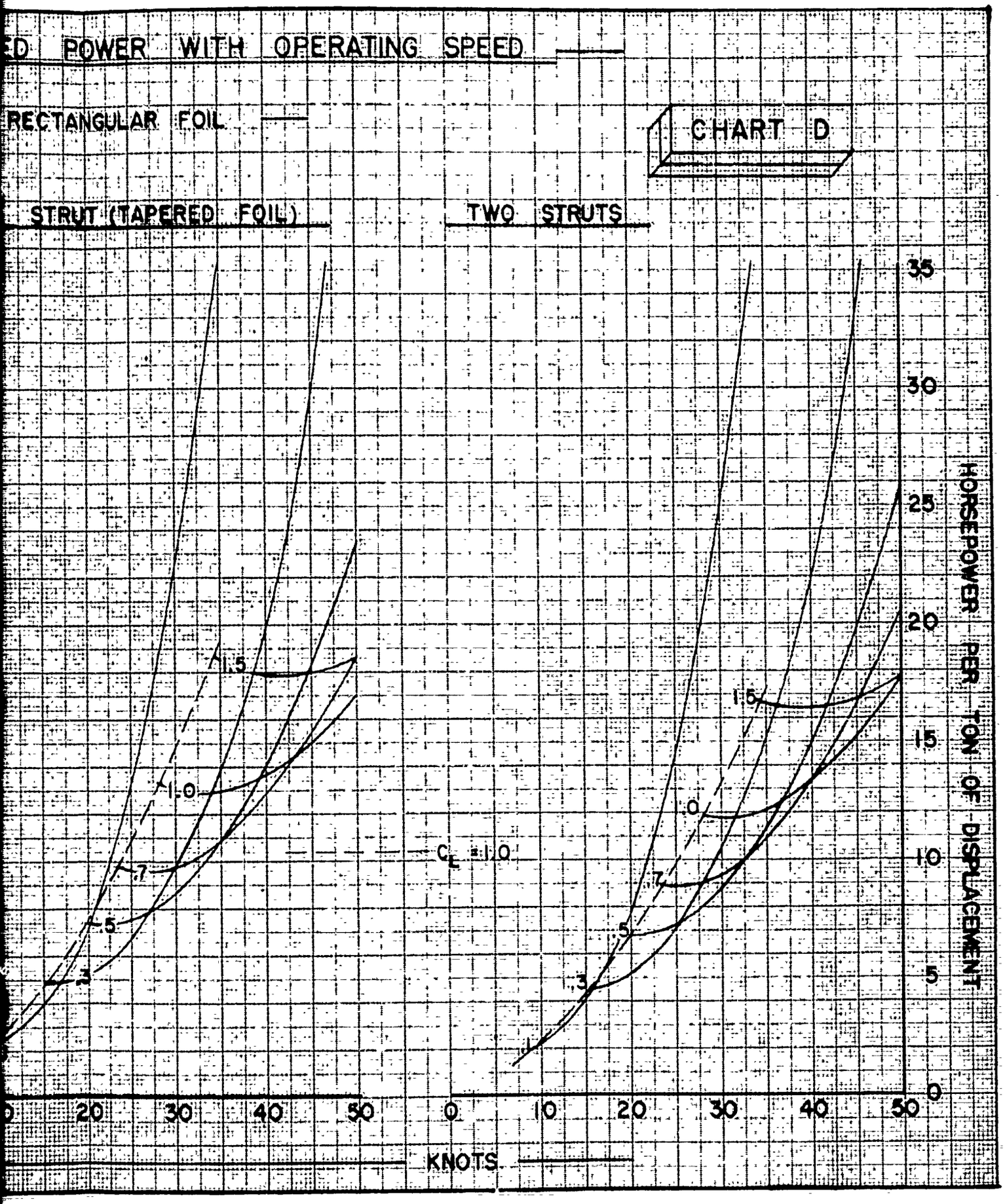
ED POWER WITH OPERATING SPEED
RECTANGULAR FOIL
CHART D
STRUT (TAPERED FOIL)
TWO STRUTS
1.5
1.0
.7
.5
.3
C_L = 1.0
1.5
1.0
.7
.5
.3
HORSEPOWER PER TON OF DISPLACEMENT
35
30
25
20
15
10
5
0
20
30
40
50
0
10
20
30
40
50
KNOTS

CONFIDENTIAL

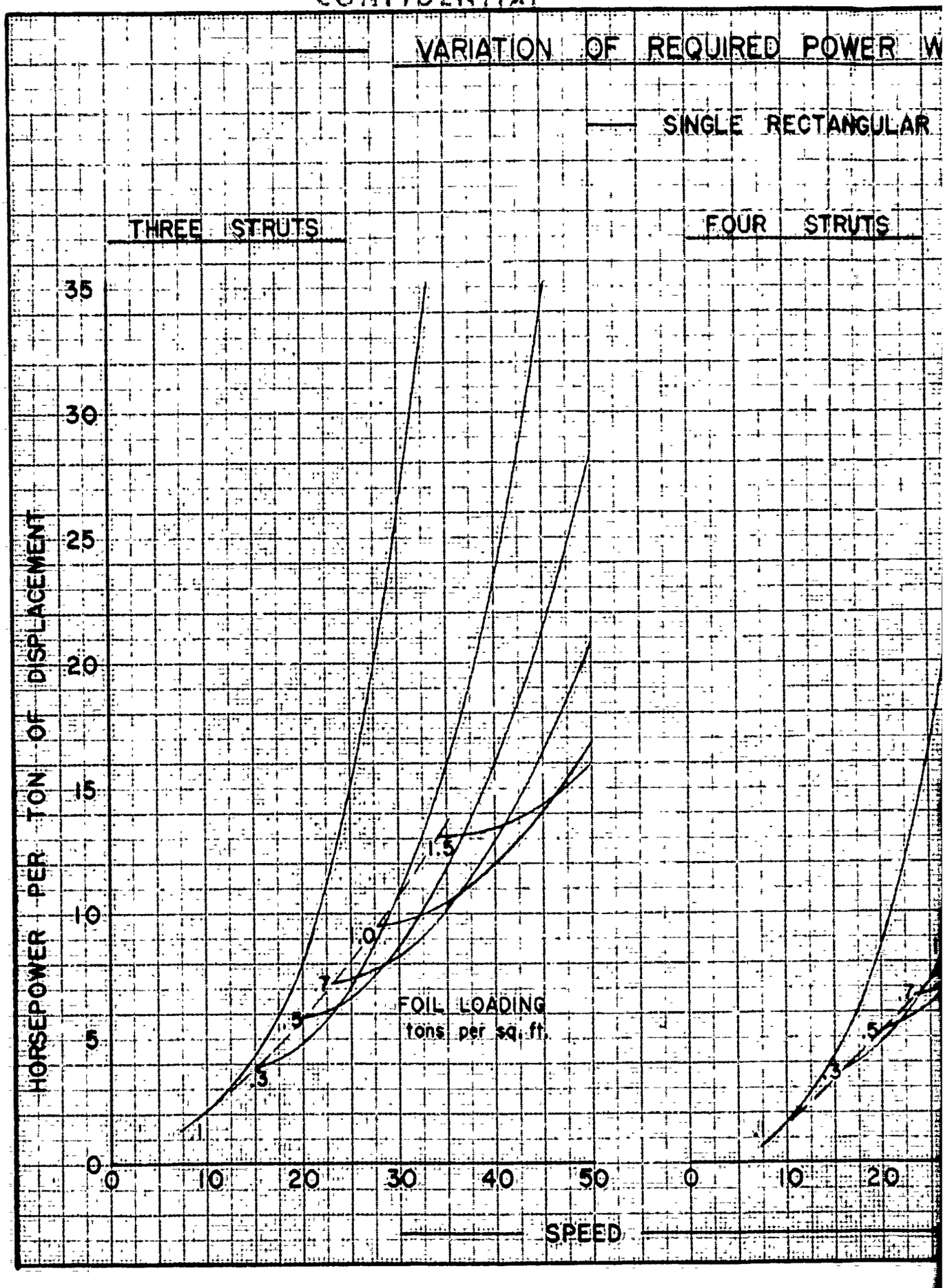

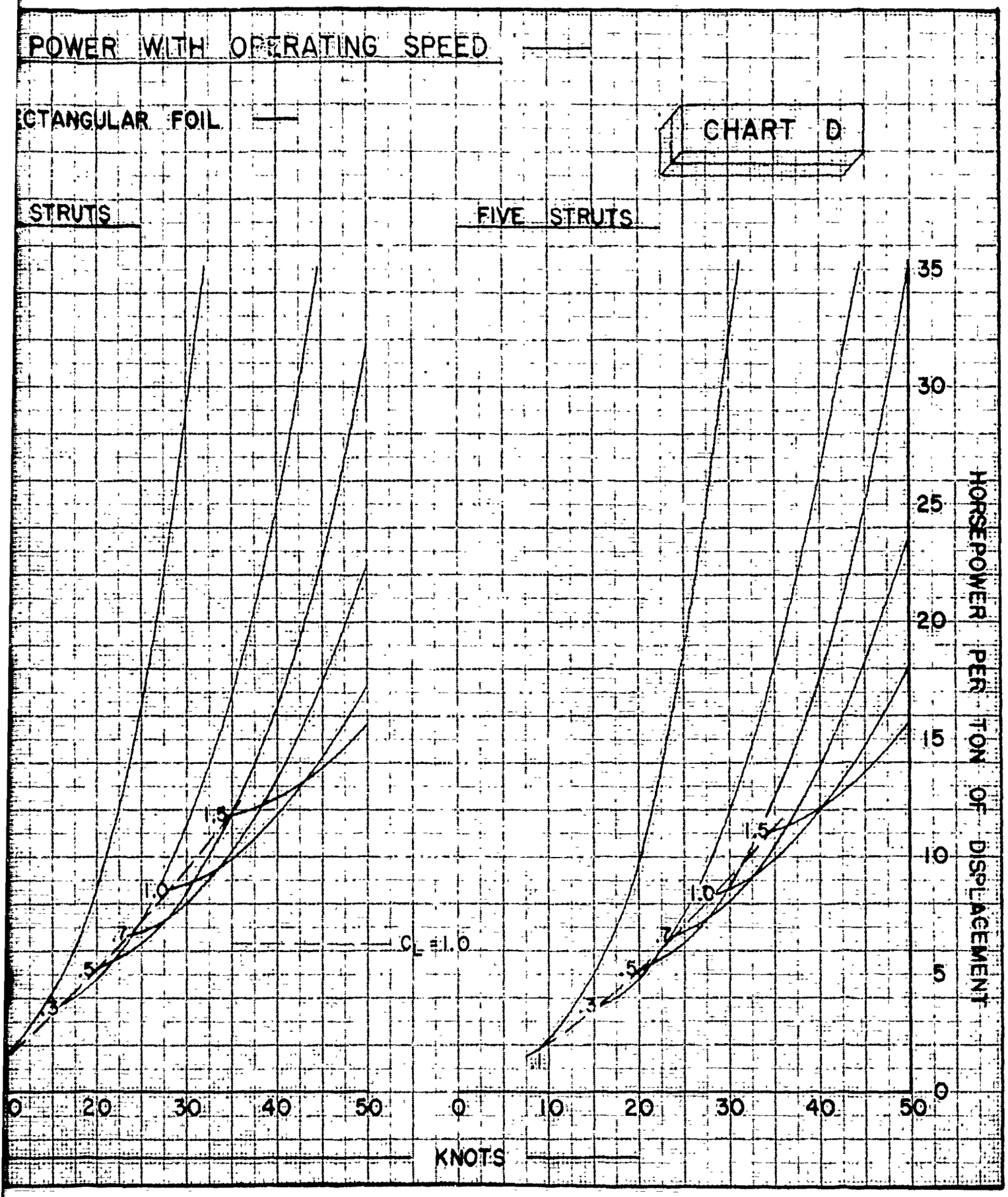
POWER WITH OPERATING SPEED
ECTANGULAR FOIL
CHART D
STRUTS
FIVE STRUTS
35
30
25
20
15
10
5
0
HORSEPOWER PER TON OF DISPLACEMENT
1.5
1.0
.7
.5
.3
$C_L = 1.0$
0
20
30
40
50
0
10
20
30
40
50
KNOTS

CONFIDENTIAL

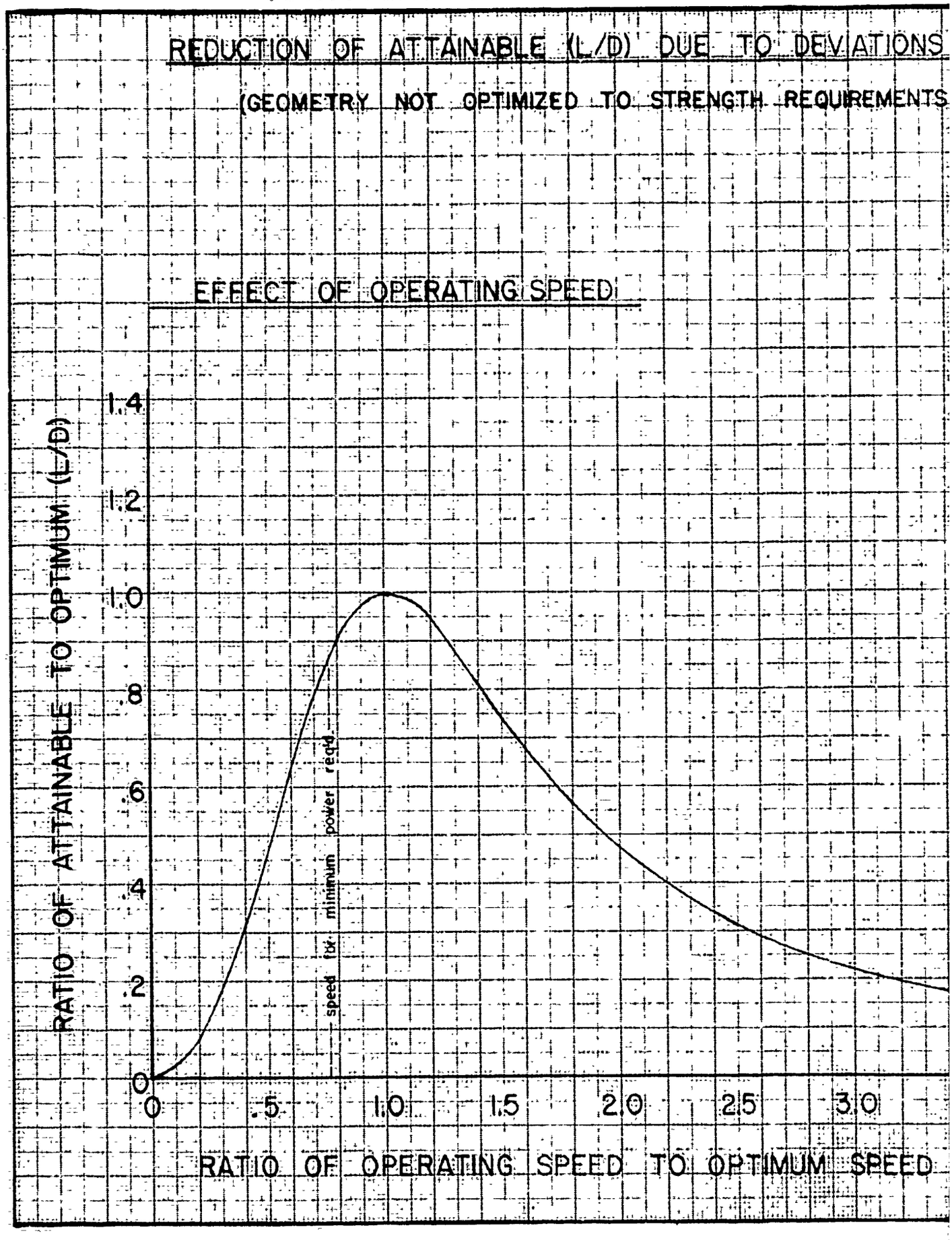

DEVIATIONS OF MAJOR PARAMETERS FROM OPTIMUM VALUES

EQUIREMENTS)

CHART E

EFFECT OF GEOMETRY

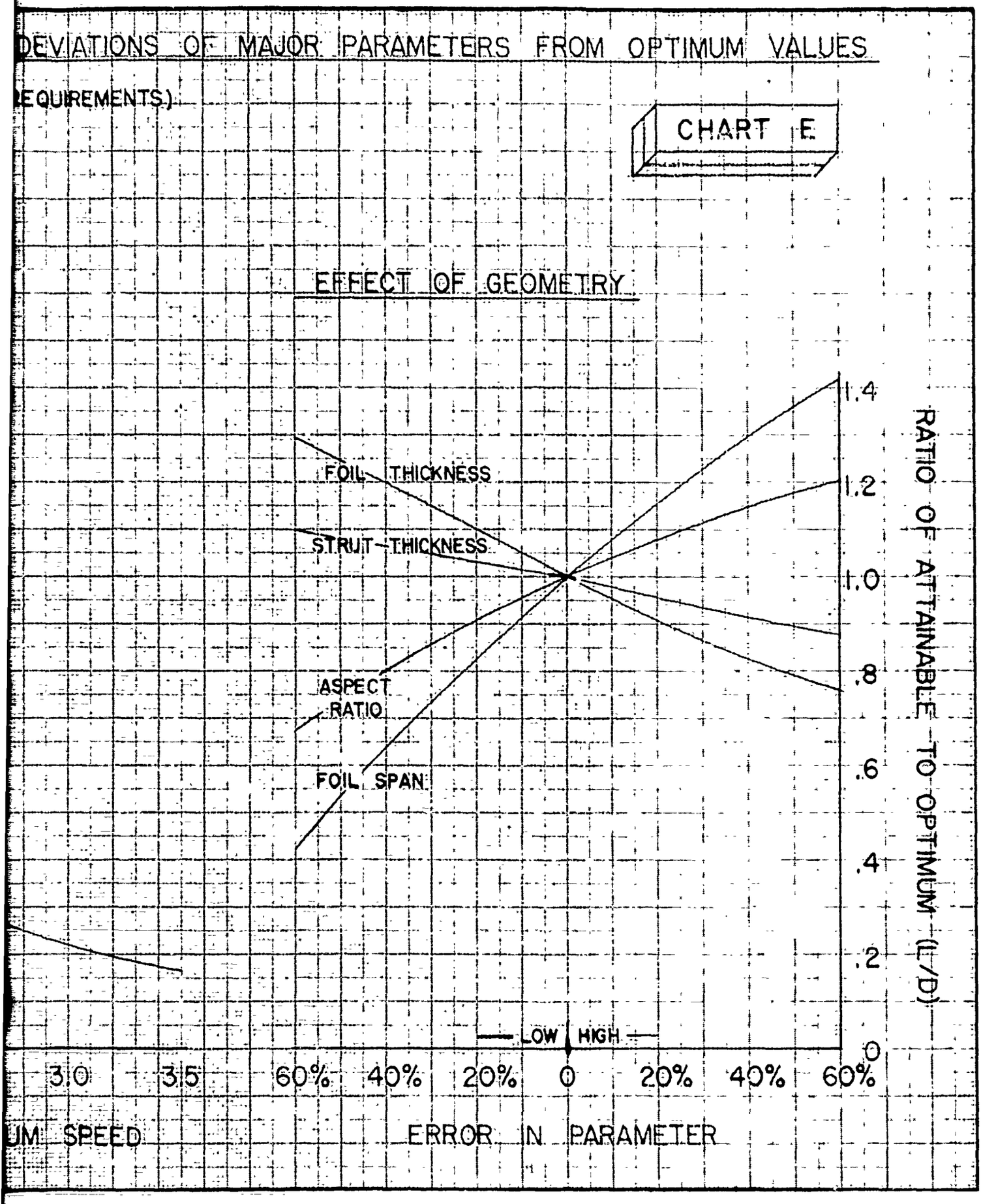

CONFIDENTIAL

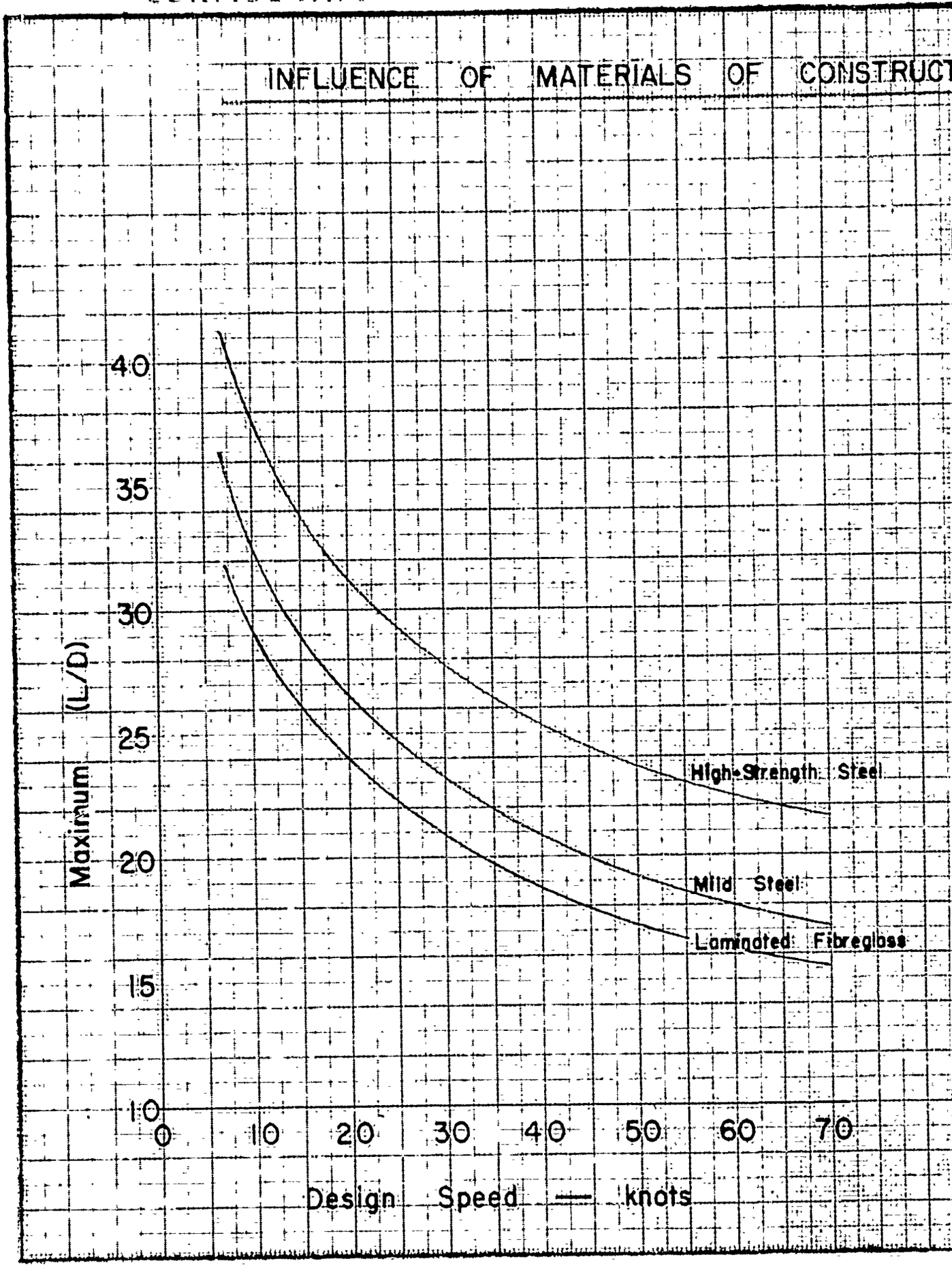

CONSTRUCTION UPON MAXIMUM (L/D)

CHART F

Design Safety Factor	2
Dynamic Load Factor	2
Foil Ultimate Stress	
high-strength steel	150,000
mild steel	50,000
glass	40,000
Strut Tangent Modulus	
high-strength steel	28,000,000
mild steel	28,000,000
glass	4,000,000

Single Rectangular Foil

Four Struts

th Steel

Fibreglass

2

C O N F I D E N T I A L

HYDRODYNAMICS, PERFORMANCE, AND DESIGN STUDIES OF HYDROFOIL CRAFT

June 1950

W. C. Holmes, Jr.

Contract No. N9onr-93201

CONTENTS

Introduction a

Notation 1

BASIC LIFT AND DRAG OF HYDROFOIL SYSTEMS 4
- Skin Friction Drag
- Basic Profile Drag
- Basic Induced Drag
- End Plates
- Interference Drag
- Strut Drag
- Air Drag
- Summary of Drag Equations
- Hull Drag
- Lift Curve Slope

PERFORMANCE OF HYDROFOIL CRAFT 14
- Conditions for Maximum (L/D)
- Variation of (L/D) with Speed
- Power Requirements
- Endurance and Range

CONFIGURATION STUDIES 20
- Optimum Geometry of Single-Foil Craft
- Effects of Deviations of Major Parameters
- Special Case of Single-Strut Configuration
- Special Case of Tandem Configuration
- Effects of Stabilizing Surfaces upon (L/D)
- Effects of Control Surfaces, Flaps, etc.

CAVITATION CONSIDERATIONS 42
- Incipient Cavitation
- Critical Cavitation Speed
- Significance of "Critical Cavitation Speed"
- Possible Advantages of Sweepback and Boundary Layer Control

References

Figures

HYDRODYNAMICS

A study of the hydrodynamics of hydrofoil craft involves a combination of the philosophies of both Naval Architecture and Aeronautical Engineering. Although it is not considered within the scope of the present studies to attempt to familiarize either group with all of the terminologies and methods of approach used by the other, some explanation is considered necessary to the purposes of this report. It is suggested that more detailed consideration can be obtained from any of the standard texts pertaining to either subject.

The naval architect usually regards lift, or supporting force, as being a function of bouyancy due to displacement of a volume of water, dynamic forces due to planing of a body upon the water surface, or a combination of both. Early efforts to derive theories of flight attempted to apply the same theories to lift in air. The lighter-than-air craft, such as the dirigible or balloon, is of course a direct application of the bouyancy familiar to the naval architect.

The most logical theory of lift of heavier-than-air craft, upon which modern aerodynamic theory is based, attributes the attainment of lift to the effect of superposition of a circulatory flow upon the free-stream flow around a body moving through a fluid. A resultant force is generated which may be resolved into forces parallel and normal to the general direction of movement. The normal force is designated "Lift" and the parallel force "Drag". It is interesting to note that the "planing force" of naval architecture is but a special case of circulatory lift, in which the medium is discontinuous at the water surface.

The lift forces upon a complete hydrofoil craft can thus be seen to comprise a combination of the lifts of both naval architecture and aerodynamics. At rest the craft is supported entirely by bouyancy. As forward motion is imparted to the craft, the hydrofoils develop hydrodynamic lift, reducing the portion of support which must be contributed by the hull, which portion may include planing lift as speed is increased. Then, when the speed is great enough to permit the foils to support the entire weight of the craft, the hull lift is reduced to zero and the craft is running, or more properly "flying", on its foils. It is thus seen that the lift of a hydrofoil craft embraces both the naval architect's and the aerodynamicist's concepts of supporting force, involving a smooth transition from one to the other.

The naval architect considers drag, usually denoted "resistance", to be composed of Frictional Resistance, Eddy Resistance, and Wave Resistance. Frictional Resistance arises from the frictional forces generated as a body is moved through the water, and is dependent upon the Reynolds Number of flow. Eddy Resistance arises from the creation of eddies, vortices, or turbulence, and depends upon the shape of the body. Wave Resistance arises from the creation and propagation of surface waves as the body is moved through the water. A great wealth of both theoretical and experimental information is available regarding these various types of ship resistance.

Drag in aerodynamic theory is, as in naval architecture, the resistance of a body to motion through a fluid. It consists of a combination of Parasite Drag and Drag Due to Lift. Parasite Drag includes that portion of the total drag which is independent of the creation of lift, whereas Drag Due to Lift consists of that portion which vanishes when the flow is such that there is no lift.

Parasite Drag is usually, for the sake of convenience, considered to consist of two principal components. That portion which is chargeable only to the lift-producing wing or foil is denoted Profile Drag, whereas that associated with non-lifting components of the craft is denoted Pure Parasite Drag. Both are composed of Friction Drag and Form Drag, which are directly analagous to the Friction Resistance and Eddy Resistance of the naval architect.

Drag Due to Lift also consists of two principal components. The force parallel to the general direction of flow which arises from circulation about the body is denoted Induced Drag. It is merely the drag component of the total force which results from circulation. The other component which is usually associated with lift, although it is actually a parasite drag analagous to Eddy Resistance, is that which arises as a body is operated at an "angle of attack" to the general direction of flow. It vanishes as the angle of attack approaches zero. Since lift also varies with angle of attack, it is usually convenient to charge to lift that portion of parasite drag which depends upon angle of attack.

It is thus apparent that, insofar as Friction Resistance, Eddy Resistance, Profile Drag, and Pure Parasite Drag are concerned, the naval architect and aerodynamicist are on common ground. The aerodynamicist usually combines his frictional and form drags into a single function, merely for convenience, whereas the naval architect regards them as separate items. Since in either case reliance upon experimental data is necessary, it would appear to make little difference which method is used.

The concepts of Wave Resistance and Induced Drag, however, would appear to be the primary subjects in which there is some difference of philosophy between the naval architect and aerodynamicist. The naval architect, in order to properly consider the performance of hydrofoil craft, must add Induced Drag to his usual concepts of resistance, and the aerodynamicist must add Wave Resistance. The subjects are not new, however, to either profession.

The present report approaches the hydrofoil problem from the aerodynamicist's viewpoint, with appropriate additions to his usual theories to account for the differences herein discussed. Wherever possible, notation is defined as it is introduced. For convenience, however, a separate table of notation for this, the "Hydrodynamics" section of the general report, is included, although it should be noted that the notation is intended to apply only to this section and may contain some duplication of terms used in the other sections.

The method of approach employed in the present studies attempts, first, to derive expressions for the various drags associated with hydrofoil craft; second, to outline methods of analysis of hydrofoil craft performance; and third, to indicate the processes by which it is possible to approximate the geometry required for the attainment of maximum lift to drag ratio (L/D), without requiring tedious trial-and-error studies of a great many specific configurations.

BASIC LIFT AND DRAG OF HYDROFOIL SYSTEMS

Of considerable importance to the study of hydrofoils is their marked similarity to airfoils as usually considered in incompressible flow aerodynamic theory. This similarity is first noted in studies of drag due to skin friction, then in both theoretical and experimental studies of the lift and drag characteristics of foils operating both in water and in air. From a theoretical standpoint, this similarity is of course not at all surprising. It is comforting to note, however, that the theory consistently receives substantial experimental verification. It is therefore possible to approach the problem of hydrofoil design with much the same philosophy usually applied to airfoil design.

Throughout the analyses presented here the usual aerodynamic assumptions of incompressible flow theory are made with regard to coefficients, lift and drag, lift curve slope, etc. It is

assumed, further, that these assumptions remain valid up to critical cavitation speeds. It is shown that here, again, the similarity to aerodynamic theory is manifested by the analogy between critical cavitation speed in water and critical Mach Number in air. No attempt is made to predict the changes which take place at speeds above those for commencement of cavitation, this portion of the general subject of hydrofoil design being considered of sufficient importance to warrant considerable further investigation as a separate study.

Expressions are developed for friction drag, profile drag, parasite drag, and induced drag of the foils and struts of a hydrofoil craft, and for hull drag. It should be noted, however, that since the aerodynamicist usually includes friction drag in his concepts of profile and parasite drags, the expression for skin friction is not used directly in the general studies. It is included primarily to illustrate the similarities b etween the philosophies of naval architects and aerodynamicists. It is, therefore, tacitly assumed in the studies that variations of Reynolds Numbers are such that the expressions developed for profile and parasite drags are of sufficient reliability for the purposes of these general studies. More exact studies should of course include detailed consideration of skin friction as a separate item.

Standard aerodynamic practices are used with regard to the use of coefficients, to a greater extent than is usually the case with naval architects. Lift and drag are expressed in terms of standard aerodynamic coefficients, as follows:

Lift $$L = C_L S \frac{\rho}{2} V^2 = C_L S q$$

Drag $$D = C_D S \frac{\rho}{2} V^2 = C_D S q$$

(L) is Lift

(D) is Drag

(C_L) is Lift Coefficient

(C_D) is Drag Coefficient

(S) is Area of the surface under consideration, projected upon the plane parallel to the direction of flow.

(ρ) is fluid density

(V) is forward speed

(q) is Dynamic Pressure

PERFORMANCE OF HYDROFOIL CRAFT

Methods of analysis of performance of hydrofoil craft are indicated, for the conditions after take-off from the water. The flow is assumed incompressible, and speeds are assumed to remain below critical cavitation speeds.

Conditions necessary to the attainment of maximum (L/D) are defined, and expressions are developed for variations of (L/D) with speed.

Power requirements for hydrofoil craft, in the "flying range", are defined. The speed for minimum power required to maintain the craft foilborne is defined, as are the speeds for maximum endurance and maximum range.

CONFIGURATION STUDIES

Recognizing the impracticability of attempting a study of all phases of the hydrofoil problem with the time available, and in an effort to derive some practically useful conclusions, the studies presented herein are confined for the most part to determination of the applicability of hydrofoils to the design of load-carrying craft which can demonstrate acceptable lift to drag ratios at speeds below critical cavitation speeds. The study is not, therefore, intended to serve as a guide to the design of high speed, rather than high (L/D), craft. An understanding of the philosophy of design for high load-carrying capacity should, however, indicate the nature of modifications which may be necessary to the attainment of high speed.

The study is based upon the basic assumption that the main lifting system of the hydrofoil craft consists of a single foil, with struts extending vertically upward through the water surface to the hull. The geometry of the single foil required for the attainment of maximum (L/D) is defined, for various conditions of loading, speed, number of struts, etc. Throughout the study, the foil is arbitrarily assumed to have a depth of submergence equal to one-tenth its span. This assumption, although admittedly arbitrary, is considered to be entirely reasonable, based upon what would appear to be about the minimum angle of roll through which a craft could be expected to roll without having its foil tips break water. The effects upon performance of deviations in foil or strut geometry from optimum values are indicated.

Although the general study is based upon the assumption of a single foil as the main lifting system of the hydrofoil craft, a brief analysis of tandem configurations is presented. It is shown that approximately equal performance should be attained with either type of configuration, and that considerations other than performance should probably dictate a decision between the use of a single foil or tandem arrangement.

A brief analysis of the performance losses which might be associated with control and stabilization of hydrofoil craft is presented. It is deduced that such losses, assuming that control mechanisms are designed to add minimum drag, should be of a second order.

CAVITATION CONSIDERATIONS

Although no attempt is made to present a rigorous treatment of the subject of cavitation, some remarks concerning this phenomenon are included. It is shown that predictions of the cavitation characteristics of a hydrofoil can be greatly facilitated by analogy to the critical Mach Number characteristics familiar to aerodynamic theory.

NOTATION

The following principal notations are used throughout the Hydrodynamics Section. Where others are used, they are defined as presented.

Symbol	Definition	See Page
(AR)	Aspect Ratio	7
(b)	Foil Span	7
(C_F, C_S)	Foil and Strut Chords	22
(C_f)	Skin Friction Coefficient	4
(C_{D_o})	Profile Drag Coefficient	6
(C_{d_o})	Section Zero-Lift Drag Coeff.	6
(C_{D_i})	Induced Drag Coefficient	7
(C_{D_S})	Strut Drag Coefficient	9
(C_D)	Total Drag Coefficient	14
(C_{Dp})	Total Parasite Drag Coefficient	14
(C_{D_L})	Total Drag Due To Lift Coeff.	14
(C_L)	Lift Coefficient	d
(C_p)	Pressure Coefficient	47
(D_f)	Friction Drag	5
(D_H)	Hull Drag	11
(D_p)	Parasite Drag	14
(D_L)	Drag Due To Lift	14
(D_i)	Induced Drag	34
(D)	Total Drag	14
(E_T)	Tangent Modulus of Elasticity	22

Symbol	Definition	See Page
(F_F, F_S)	Foil and Strut Design Safety Factors	22
(h)	Foil Depth of Submersion	8
(K_i)	Induced Drag Parameter	8
(k)	Total Drag Due to Lift Parameter ($K_i+.005$)	15
(L)	Lift	d
(l_s)	Strut Length	22
(M)	Mach Number in Air	47
(m_o)	Infinite Aspect Ratio Lift Curve Slope	12
(N)	Number of Struts	9
(n)	Design Load Factor	22
(P)	Power	17
(p)	Local Static Pressure	42
(p_v)	Vapor Pressure	42
(p_o)	Free-Stream Static Pressure	43
(q)	Dynamic Pressure	d
(R_N)	Reynolds Number	4
(R_s)	Strut Load Distribution Factor	22
(S, S_s)	Foil and Strut Projected Areas	d,9
(t)	Thickness Ratio (thickness/chord)	6
(V)	Forward Speed	d
(V_{TO})	Take-Off Speed	11
(V_o)	Speed for Maximum (L/D)	16
(V_{CR})	Critical Cavitation Speed	47
(W)	Gross Weight in Pounds	16

Symbol	Definition	See Page
(δ_i, τ_i)	Induction Planform Parameters	7, 13
(ϕ)	Interface Reflection Parameter	7
(δ_c)	Cavitation Number	42
(δ_L)	Location Cavitation Number	44
(δ_s)	Section Cavitation Number	44
(ω)	Downwash Velocity	35
(Δ)	Total Displacement in Tons	16
$(\frac{dC_L}{d\alpha})$	Lift Curve Slope	12
(σ_A)	Ultimate Stress	22
(ψ)	Ratio of (L/D) to Maximum (L/D)	27

Additional arbitrary constants are introduced and defined on the following pages:

Symbol	Page
(A)	23
(B)	23
(G)	23
(H)	23
(K)	22
(K_f)	23
(K_s)	23
(m)	22

BASIC LIFT AND DRAG OF HYDROFOIL SYSTEMS

Skin Friction Drag

It is interesting to note the similarity between the skin friction drag expressions postulated by Friedrich Gebers in 1916 (ref. 1) and von Karman in 1934 (ref. 2 and 3). Whereas Gebers' equation is based upon experimental work in a towing tank, Karman's expression was derived theoretically for turbulent flow. Both expressions appear to closely verify the results obtained experimentally by William Froude (1874), R. E. Froude (1888), and C. Tideman (1900).

The two expressions for turbulent skin friction drag coefficient are:

(1) Gebers $$C_f = 0.02058\, R_N^{-1/6}$$

(2) Karman $$\log_{10}(R_N C_f) = 0.242\, C_f^{-1/2}$$

In both equations the term (R_N) denotes the Reynolds Number, and is defined by: (for speed in knots and length in feet, in 50° sea-water)

(3) $$R_N = \frac{Vl}{8.66} \times 10^6$$

It is also interesting to note that no reference has been found, in the literature on skin friction drag in water, to the expression for drag in laminar flow as postulated by Blasius in 1911 (ref. 3).

(4) Blasius $$C_f = 1.328\, R_N^{-1/2}$$

The coefficients defined by these three fundamental equations (1, 2, and 4) are shown in Figure (1).

Typical Reynolds Number values encountered in hydrofoil studies can be expected to range from about 500,000 to about 10,000,000 for the speed ranges of interest to the high (L/D) studies outlined herein. High speed studies can be expected to involve Reynolds Numbers up to about 50,000,000.

In view of the apparent lack of experimental evidence in favor of the assumption of laminar flow conditions in actual operations of the type to be expected with hydrofoil craft, it is assumed that in all cases the flow will be turbulent, with friction drag as expressed by Gebers. Typical values of the skin friction drag coefficient to be expected are then shown by Figure (2). It should be noted that the skin friction drag, using this coefficient, is a function of the total wetted area, and is expressed by:

(5) $$D_f = C_f A q$$

in which

D_f is friction drag in pounds.

C_f is skin friction coefficient.

A is total wetted area.

q is dynamic pressure.

Assuming the density of 50° sea-water to be 64.4 p.c.f., the dynamic pressure, for speed in knots, is

(6) $$q = 2.85 V^2$$

This value is used throughout the present studies.

Basic Profile Drag

From a review of literature on hydrofoils (ref. 4-22), it appears that the most desirable section profiles for the attainment of high (L/D) over a reasonable range of speeds are of the type represented by the NACA High-Speed series airfoils (ref. 23). For the purposes of these general studies, therefore, it is assumed that lift and drag characteristics of typical hydrofoil sections are as expressed below, based upon the characteristics of such NACA airfoils. A more detailed analysis of particular configurations should, of course, include more exact information regarding section characteristics. The assumptions made, however, are considered to be entirely adequate for the purposes of preliminary investigations, and to represent reasonably good design practice.

Examination of the drag data of reference 23 indicates that typical profile drags can be expected to be of the order shown by Figure (3), for profiles of the "aerodynamic cleanness" to be expected of hydrofoils which can be free of the doors, ports, and other sundry protuberances usually found on airplane wings. For the purposes of preliminary studies, it appears entirely reasonable to express these profile drags empirically as

$$(5) \qquad C_{D_o} \approx C_{d_o} + 0.005\, C_L^2$$

in which (C_{D_o}) is net profile drag coefficient, (C_{d_o}) is section drag coefficient at zero lift, and (C_L) is section operating lift coefficient. Figure (4), summarizing typical coefficients to be expected, indicates that, approximately,

$$(6) \qquad C_{d_o} \approx 0.0048 + 0.10\, t^2$$

in which (t) is the section thickness ratio (thickness divided by chord). Combining equations (5) and (6), the general equation for profile drag coefficient becomes

$$(7) \qquad C_{D_o} \approx 0.0048 + 0.10 t^2 + 0.005\, C_L^2$$

It should be noted that this expression represents only an average value, since it implies no change of profile drag with Reynolds Number. Since friction drag is included in profile drag, however, such is of course not strictly true. The expression is considered to represent a good approximation over the range of Reynolds Numbers to be expected after take-off of the hydrofoil craft, and is included for simplification of the analysis. Specific design studies should of course consider friction drag in more detail.

Basic Induced Drag

The basic induced drag of a lifting hydrofoil, as usually expressed in aerodynamic theory, is (ref. 24)

$$(8) \qquad C_{D_i} = \frac{C_L^2}{\pi R}(1+\delta_i)$$

in which (C_{D_i}) is induced drag coefficient

(C_L) is foil lift coefficient

(R) is foil aspect ratio (b^2/S)
(b is span, S is area)

(δ_i) is the standard planform induction parameter

Typical values of the planform induction parameter (δ_i) are shown by Figure (5), as functions of foil thickness, aspect ratio, and two-dimensional (infinite aspect ratio) section characteristics.

Equation (8) expresses the induced drag encountered under "infinite flow" conditions, in which it is assumed that the surrounding extends effectively to infinity. The presence of the free water surface, or interface, above the foil can be expected to modify circulation about the foil in such a manner as to alter the usual concepts of induction effects.

The subject of flow around a foil which is located near a boundary of the surrounding medium is one which has received a great deal of attention in aerodynamic theory, since it is directly concerned with conditions which exist in a wind tunnel, or when an airplane is flown very close to the ground. The particular condition encountered in hydrofoil studies, in which the boundary is actually a free surface, is included in the rather extensive treatment of boundaries in reference 25. It is shown that a free surface above the foil can be expected to increase the induction effects, hence the induced drag of the foil.

The correction factor to be applied to the induced drag, to account for the effects of operation near the interface, then modifies equation (8) to read

$$(9) \qquad C_{D_i} = \frac{C_L^2}{\pi R}(1+\delta_i)(1+\phi)$$

in which the "interface reflection parameter" (ϕ) is, as published

by Prandtl (1923), and since established experimentally,

"Reflection Parameter" (ϕ), as function of depth of submersion (h) and foil span (b):

(h/b)	0	.1	.2	.3	.4	.5
(ϕ)	1.000	.780	.655	.561	.485	.420

Intermediate values of (ϕ) are shown by Figure (6).

A rigorous drag analysis should include detailed consideration of both the induction parameter (δi) and reflection parameter (ϕ). For use in preliminary studies, however, in which order of magnitude rather than precise values are useful to preliminary design selection, it appears quite reasonable to combine these parameters and represent the term ($(1+\delta i)(1+\phi)/\pi = Ki$) by a series of empirical curves as shown by Figure (7).

The induced drag coefficient then becomes

$$(10) \qquad C_{D_i} = \frac{K_i}{R} C_L^2$$

End Plates

Results of early experiments with end plates as a means of reducing the induced drag of rather low aspect ratio wings show that some reduction can be expected if the end plates are properly designed (ref. 26 and 27). The studies examined, however, were all concerned with rather low aspect ratios, and the economy of application of conventional end plates to high aspect ratio hydrofoils appears to be of sufficient uncertainty to preclude their consideration in studies of the type outlined here.

It is understood that tests of end plates based upon what appears to be a most promising design philosophy are in progress as the present studies are being conducted. It is considered quite likely that this new approach to the end plate problem may represent a most practical means of reducing the induced drag of high aspect ratio foils. Present plans with regard to tests of hydrofoil craft include provisions for rather extensive tests of the new type end plates.

Interference Drag

It is assumed that the hydrofoil-strut combinations under consideration consist of foils running under the surface of the water, with vertical, or nearly vertical, struts projecting upward from the upper surface of the foils, through the water surface, to the main load carrying hull or body. As a general rule, it can be expected that intersections of struts and foils will be reasonably well faired, to produce minimum interference. Under the assumption of turbulent flow, it appears entirely reasonable to assume that such interference is of a second order (ref. 28-30), and produces a net drag increase of about five percent for each strut-foil intersection. This increase is arbitrarily assumed to be equally divided between strut profile and foil induced drag (for reduction of lift-curve slope).

Strut Drag

The drag produced by the portions of the supporting struts running below the water surface can be considered equivalent to that defined by equation (6), in which the strut is assumed to operate at zero lift. An additional drag, however, can be expected as a result of the wave-making action of the strut extensions through the water surface, although it is assumed that the struts are of such profile that their wave-making characteristics are reduced to a practical minimum. It is considered reasonable to allow approximately a fifty-percent increase of the drag predicted by equation (6), to cover the wave making drag interference as predicted above, and the probability of the addition of rudders, flap actuating mechanisms, etc., to the basic strut configuration.

The strut drag is then, in terms of foil area, and for (N) struts,

(11) $$C_{D_S} = 1.5 N \left(\frac{S_s}{S}\right)\left(0.0048 + 0.10 t_s^2\right)$$

in which

N is the number of struts.

S_s is the strut submerged area.

S is the foil area.

t_s is the strut thickness ratio.

Air Drag

Air Drag is assumed, for the relatively low speed studies presented here, to be of a second order. It should be realized, however, that as design speeds are increased beyond, say, forty knots, estimates of air drag should be included in the general drag analysis, and every effort should be made to provide designs of aerodynamic cleanness.

Summary of Drag Equations

The drag equations which define performance of a hydrofoil craft after it is foilborne can be summarized for preliminary design purposes. It is considered significant that the methods of analysis outlined here were used in prediction of performance of a full-scale test craft, reported in a separate section of these general studies, with gratifying agreement between predicted and observed performance. They would appear, therefore, to represent reasonably reliable preliminary estimates.

Total Drag After Take-Off

(12) $$C_D = C_{D_o} + C_{D_i} + C_{D_s}$$

Foil Profile Drag

(13) $$C_{D_o} = 0.0048 + 0.10 t_F^2 + 0.005 C_L^2$$

Foil Induced Drag

(14) $$C_{D_i} = (1 + 0.025 N)\frac{C_L^2}{\pi AR}(1+\delta_i)(1+\phi) = (1+0.025N)\frac{K_i}{AR} C_L^2$$

Strut Drag

(15) $$C_{D_S} = 1.5 N \left(\frac{S_s}{S}\right)(0.0048 + 0.10 t_s^2)$$

TOTAL PARASITE DRAG

$$C_{D_p} = 0.0048 + 0.10 t_F^2 + 1.5 N \left(\frac{S_s}{S}\right)(0.0048 + 0.10 t_s^2)$$

TOTAL DRAG DUE TO LIFT

$$C_{D_L} = C_L^2 \left[(1 + 0.025 N)\frac{K_i}{R} + 0.005\right]$$

Hull Drag Prior to Take-Off

The drag of a hydrofoil craft, from the condition at rest until its weight is completely supported by the foils at take-off, includes the frictional and wave-making resistance of the hull, as well as the drag of the foils and struts. The hull resistance is equal to that of a conventional displacement or planing hull, appropriately modified as speed increases and lift is transferred from the hull to the foils, reducing the apparent displacement.

The resistances of typical planing hulls of various types have been summarized and plotted by J. H. Curry, as shown by Figure (8), and have also been examined and averaged into a single curve by Teitjens, as shown by Figure (9). In both cases the Planing Numbers, or Resistance divided by Displacement, are plotted against Froude Numbers. The resistance of a hull as a surface craft at any speed prior to take-off can be estimated from such curves as these, or from actual test data pertaining to the particular hull under consideration, if such is available.

It appears reasonable to assume, for preliminary design purposes, that the foils will be set at their maximum practicable angle of attack prior to take-off, hence the lift coefficient will be essentially constant. The transfer of lift will then be a function of the square of the speed, and the modification of hull resistance to account for the reduction of apparent displacement can be determined as a function of the ratio of actual speed to take-off speed.

For the preliminary design studies reported herein, it is assumed that hull resistance varies as the two-thirds power of displacement, and that the average curve presented by Teitjens, Figure (9), is applicable at Froude Numbers greater than unity. An empirical equation for hull resistance, including the correction for reduction of apparent displacement, is derived, as shown by equation (16). For more detailed studies, or for the special cases in which Froude Number is less than untiy, the curves of Figure (8), or actual test data for a particular hull, can be used, bearing in mind that the correction for transfer of lift must be applied to the Resistance Numbers indicated.

The general equation for hull resistance used in these studies is

$$(16) \qquad D_H = \left[1 - \left(\frac{V}{V_{TO}}\right)^2\right]^{2/3} \left[0.00582 \frac{V^2}{\ell_H} + 0.0987\right] [\Delta]$$

in which

D_H is hull drag in pounds.

V is speed in knots.

V_{TO} is take-off speed in knots.

ℓ_* is waterline length in feet.

Δ is total displacement in tons.

Typical values of hull drag predicted by equation (16) are shown by Figure (10).

It is significant to note that the total resistance prior to take-off, including both hull drag and strut-foil drags, is characterized by a "hump" which reaches its peak at a speed slightly below that for take-off. The power required to propel the craft through this region of increased resistance, and beyond to the take-off speed, is an extremely important consideration in the design of a hydrofoil craft, and should be carefully analyzed. It is possible to maintain some control over the magnitude of the peak power required in this region by varying the design take-off speed, or lift coefficient. As a general rule, the peak drag will be reduced if the take-off speed is made as low as possible, or if take-off lift coefficient is made as great as possible. Stalling or cavitating of the foil may impose practical limits to the maximum value of lift coefficient which can be utilized.

Typical curves of the total drag of a particular hydrofoil craft, showing the peak values reached in the region of the "hump," are shown by Figure (11), in which the design take-off speed, hence lift coefficient, are varied between the limits indicated.

Lift Curve Slope

The lift curve slope of a foil, as usually predicted in aerodynamic theory is (ref. 24)

(17) $$\frac{dC_L}{d\alpha} = \frac{m_o}{1 + \frac{m_o}{\pi AR}(1 + \tau_2)}$$

in which (τ_i) is the conventional induction parameter, as shown by Figure (12) and (m_o) is the lift curve slope for infinite aspect ratio.

(18) $$m_o = 2\pi - 4\tau_F$$

As in the case of induced drag, the presence of the water surface alters the lift curve slope. The reflection parameter (ϕ) is therefore applied to equation (17) to obtain the expression for lift curve slope used in the present studies:

(19) $$\frac{dC_L}{d\alpha} = \frac{m_o}{1 + \frac{m_o}{\pi R}(1+\tau_i)(1+\phi)}$$

PERFORMANCE OF HYDROFOIL CRAFT

Preliminary analyses of the performance of hydrofoil craft are based upon the general assumptions of steady rectilinear flight in which the effects of linear and rotational accelerations are neglected. Determination of probable accelerations at take-off, as lift is finally transferred from the hull to the foils, will require more specific definition of the variation of power with speed than is possible in the general studies presented herein. As in the case of conventional displacement craft, trial runs will be necessary before such definition of power characteristics can be considered reliable. Preliminary investigation of some of the more important performance parameters is possible, however, as indicated in the following discussion.

Conditions for Maximum (L/D)

In view of the contractual requirements that the studies presented herein have attainment of maximum (L/D) as their principal objective, it is well to define the conditions of operation necessary for such attainment. From the drag analyses indicated in the previous discussion, it is possible to define these conditions.

The total drag after take-off is equal to parasite drag plus drag due to lift

$$D = D_p + D_L \tag{20}$$

or, in coefficient form,

$$C_D = C_{D_p} + C_{D_L} \tag{21}$$

Combining equations (13), (14), and (15)

$$C_D = 0.0048 + 0.10 t_F^2 + 1.5N\left(\frac{S_s}{S}\right)(0.0048 + 0.10 t_s^2) + C_L^2\left[0.0050 + (1 + 0.025N)\left(\frac{1+\delta_i}{\pi R}\right)(1+\phi)\right] \tag{22}$$

From equation (22) it is seen that

$$(23) \quad C_{D_p} = 0.0048 + 0.10 t_F^2 + 1.5 N \frac{S_s}{S} \left[0.0048 + 0.10 t_s^2 \right]$$

$$(24) \quad C_{D_L} = C_L^2 \left[0.0050 + (1 + 0.025 N) \left(\frac{1+\delta_i}{AR\,\pi} \right) (1+\phi) \right]$$

$$= k C_L^2$$

whence

$$(25) \quad C_D = C_{D_p} + k C_L^2$$

The condition for maximum (L/D) is found by minimizing the term (C_D/C_L), in which

$$(26) \quad \frac{C_D}{C_L} = \frac{C_{D_p}}{C_L} + k C_L$$

Differentiating with respect to (C_L),

$$(27) \quad \frac{d\left(\frac{C_D}{C_L}\right)}{d C_L} = 0 = -\frac{C_{D_p}}{C_L^2} + k$$

whence it is seen that the condition for maximum (L/D) is satisfied if

$$(28) \quad C_{D_p} = k C_L^2 = \frac{1}{2} C_D$$

From equation (28) it is seen that the lift coefficient (C_{L_o}) for maximum (L/D) is defined by

$$(29) \quad C_{L_o} = \sqrt{\frac{C_{D_p}}{k}}$$

And Maximum (L/D) has the value

$$(30) \qquad \left(\frac{L}{D}\right)_o = \frac{1}{2}\left[k C_{D_p}\right]^{-1/2}$$

Equating lift to total weight (W in pounds), the speed at which maximum (L/D) is attained is found from equation (29)

$$(31) \qquad C_{L_o} = \frac{W}{2.85 S V^2} = \sqrt{\frac{C_{D_p}}{k}}$$

$$(32) \qquad V_o^2 = \frac{W}{2.85 S}\sqrt{\frac{k}{C_{D_p}}}$$

or, for total weight (Δ) in tons,

$$(33) \qquad V_o^2 = 786\left(\frac{\Delta}{S}\right)\sqrt{\frac{k}{C_{D_p}}}$$

L/D Attainable at Any Speed

Equation (30) defines the maximum (L/D) attainable with any particular configuration, at the optimum speed defined by equation (33). It is desirable to ascertain the (L/D) which is attainable at speeds other than optimum.

From equation (26)

$$(34) \qquad \frac{C_L}{C_D} = \frac{C_L}{C_{D_p} + k C_L^2}$$

Maximum (L/D) is, in this form,

$$(35) \qquad \left(\frac{C_L}{C_D}\right)_o = \frac{C_{L_o}}{C_{D_p} + k C_{L_o}^2}$$

Dividing (34) by (35) and substituting (31) as necessary

$$(36) \qquad \frac{L/D}{(L/D)_o} = \frac{2}{\frac{C_L}{C_{L_o}} + \frac{C_{L_o}}{C_L}}$$

which, in terms of speed, becomes

$$(37) \qquad \frac{L/D}{(L/D)_o} = \frac{2}{\left(\frac{V}{V_o}\right)^2 + \left(\frac{V_o}{V}\right)^2}$$

These variations of (L/D) with lift coefficient and speed are shown by Figure (13).

Power Requirements

Analyses of power requirements of hydrofoil craft are based on the assumptions that:

(1) Thrust is equal to total Drag.

(2) Required Power is equal to Thrust Power divided by Propulsive Efficiency.

(3) Propulsive Efficiency is constant over the speed ranges involved, below critical cavitation speeds and in the region near cruising speeds.

The Thrust Power after take-off is

$$(38) \qquad P_T = \frac{DV}{326} = \frac{WV}{326(L/D)} = 6.87 V \frac{\Delta}{(L/D)}$$

and the Required Power is

$$(39) \qquad P = P_T \left(\frac{1}{\eta}\right) = 6.87 \frac{V\Delta}{\eta (L/D)}$$

The speed for minimum power is determined by writing (P) in terms of (D) and differentiating with respect to speed.

$$(40) \qquad P = \frac{V}{326\eta}\left[2.85 C_{D_p} S V^2 + \frac{k W^2}{2.85 S V^2}\right]$$

$$(41) \qquad \frac{dP}{dV} = 0 = \frac{1}{326\eta}\left[(3)(2.85 S C_{D_p} V^2) - \frac{k W^2}{2.85 S V^2}\right]$$

whence the speed for minimum power is

$$(42) \qquad V_{P_{MIN}}^2 = \frac{W}{2.85 S}\sqrt{\frac{k}{3 C_{D_p}}} = 786\left(\frac{\Delta}{S}\right)\sqrt{\frac{k}{3 C_{D_p}}}$$

This is related to speed for maximum (L/D) by

$$(43) \qquad \left[\frac{V_{P_{MIN}}}{V_o}\right]^2 = \sqrt{\frac{1}{3}}$$

whence

$$(44) \qquad \frac{V_{P_{MIN}}}{V_o} = 0.760$$

Thus minimum power is required at the speed seventy-six percent of that at which maximum (L/D) is attained.

Endurance and Range

The attainable endurance and range of a hydrofoil craft are determined, under the assumption that fuel consumption (c) in pounds per horsepower hour remains constant, in the cruising speed region.

The fuel consumption per hour is

$$(45) \qquad \frac{dw}{dt} = cP = \frac{c D V}{326\eta}$$

Maximum endurance is attained if fuel consumption per hour is minimized. Thus, minimizing equation (45), it is seen that:

MAXIMUM ENDURANCE IS ATTAINED AT THE SPEED FOR MINIMUM POWER.

Maximum range is obtained when fuel consumption per mile travelled is minimized.

The range rate is

$$\frac{dR}{dt} = V \qquad (46)$$

Dividing (45) by (46), the fuel consumption per mile is

$$\frac{dw}{dR} = \frac{cP}{V} = \frac{cD}{326\eta} \qquad (47)$$

Thus, minimizing equation (47), it is seen that:

MAXIMUM RANGE IS ATTAINED AT THE SPEED FOR MAXIMUM (L/D).

From equations (45) and (47), it is also seen that:

Endurance and range both vary directly with drag, fuel consumption, and propulsive efficiency. Is is therefore mandatory that every effort be made to achieve:

Low Drag
Low Fuel Consumption
High Propulsive Efficiency

Optimum design for endurance and range is achieved by obtaining the best balance among these three parameters. Effort should not be concentrated solely on any one of them, at the expense of the others, without due consideration for the balance which must be maintained.

CONFIGURATION STUDIES

Optimum Geometry of Single Foil Craft

In accordance with the requirement that the present studies have attainment of maximum (L/D) as their primary objective, it is desirable to define, first, the conditions for attainment of maximum (L/D) and, second, the optimum configurations with which such maximum can be realized. The conditions for attainment are defined in the general performance analysis.

As a first step toward definition of the optimum configuration, it is appropriate to determine the maximum (L/D) which can be attained with a single foil, including its struts, but not including allowances for flaps, rudders, or auxiliary stabilizing foils or planing surfaces. The (L/D) thus defined represents the practical maximum which can conceivably be attained with the least compromised configuration, and can be used as the reference with which to evaluate configurations which include such items necessarily added for purposes of trim, stability, propulsion, etc.

Whereas the literature indicates that the great majority of hydrofoil configurations considered have had stability or high speed as their primary design parameters, no evidence has been found to indicate that serious consideration has been given to maximum attainable (L/D) as the governing criterion. The configurations given most serious consideration have utilized main foils incorporating either dihedral with the foil piercing the water surface, or low aspect ratio foils coupled to auxiliary skating foils. Both of these design philosophies appear to have been dictated by stability considerations, with high speed as their secondary objective.

It is considered quite likely, however, that greater attainable values of (L/D) can be realized with a hydrofoil craft if its main lifting foil is designed with maximum (L/D) as its governing parameter, with stability and trim requirements met by provision for auxiliary foils, flaps, or modifications designed to satisfy such requirements with the minimum compromise of the main foil (L/D).

The basic configuration upon which this design philosophy is

based is one using a single rectangular foil, without dihedral, with struts extending vertically upward from the foil through the water surface to the load-carrying hull or body. A study of the (L/D) values attainable with such a configuration will provide a convenient reference with which to compare particular configurations, and will indicate the order of magnitude of limits which may be imposed upon the design of hydrofoil craft.

The optimum geometry for attainment of maximum (L/D) can be established by combining the hydrodynamic conditions for such attainment with necessary structural limitations. Thus, whereas hydrodynamic theory alone implies that maximum (L/D) requires a combination of "infinite" aspect ratio with "zero" foil and strut thicknesses, structural considerations place definite physical limits upon these parameters. The definition of optimum geometry then becomes a problem of simultaneous optimization of both hydrodynamic and structural parameters.

From equation (30), maximum (L/D) is defined as

$$(48) \qquad (L/D)_{MAX.} = \frac{1}{2}\left[\mathcal{A} C_{D_P}\right]^{-1/2}$$

In which, from equations (23) and (24)

$$(49) \qquad C_{D_P} = 0.0048 + 0.10\, t_F^2 + 1.5\, N \left(\frac{s_s}{s}\right)(0.0048 + 0.10\, t_s^2)$$

$$(50) \qquad k = \left[1 + 0.025\, N\right]\left[\frac{(1+\delta_i)(1+\phi)}{\pi \mathcal{A}}\right] + 0.005 = (1 + 0.025\, N)\frac{K_i}{\mathcal{A}} + 0.005$$

Now, from structural considerations, the permissible foil thickness can be written, in terms of aspect ratio ($\mathcal{A}$), foil loading (Δ/S), design load factor (n), number of supporting struts (N), and material properties,

$$(51) \qquad t_F = \frac{4.125}{[N - 0.1835]}\, \mathcal{A} \left(\frac{\Delta}{S} n\right)^{1/2} \left(\frac{F_P}{\sigma_A}\right)^{1/2}$$

in which

t_F is the foil thickness in percent of chord.

N is the number of struts.

Δ is the total load in tons (2240 Pounds).

S is foil area in square feet.

n is design load factor.

F_F is foil design safety factor.

σ_A is foil ultimate stress.

Similarly, the required strut thickness is

$$t_s^3 = 1655 \frac{m^2}{K^4} K^3 \left(\frac{\Delta}{S} n\right)\left(\frac{F_s}{E_T}\right)(R_s) \tag{52}$$

in which

t_s is strut thickness in percent of chord.

m is ratio of strut length to chord.

K is ratio of strut chord to foil chord.

f_s is strut design safety factor.

E_T is strut tangent modulus of elasticity.

R_s is strut load distribution factor.

The general drag equation can then be written:

$$C_D = C_{D_p} + k C_L^2 \tag{53}$$

$$C_{D_p} = 0.0048 + \frac{K_F}{10} R^2 \left(\frac{\Delta}{S} N\right) + 1.5 N \frac{S_s}{S}\left[0.0048 + \frac{K_s}{10} R^2 \left(\frac{\Delta}{S} n\right)^{2/3}\right] \tag{54}$$

$$k = 0.0050 + \frac{1}{R}\left[(1 + 0.025 N)\left(\frac{1+\phi}{\pi}\right)(1+\phi)\right] \tag{55}$$

in which

(56) $$t_F^2 = K_F R^2 \left(\frac{\Delta}{S} n\right)$$

$$K_F = \frac{17.013}{(N-.1835)^2}\left(\frac{F_F}{\sigma_A}\right)$$

(57) $$t_S^2 = K_S R^2 \left(\frac{\Delta}{S} n\right)^{2/3}$$

$$K_S = \left(165.5\,\frac{R_S F_S}{E_T}\right)^{2/3}\left(\frac{l_S}{b}\right)^{4/3}\left(\frac{1}{K^4}\right)^{2/3}$$

Whence the drag equations can be written, in terms of foil aspect ratio,

(58) $$C_{D_P} = A + BR^2$$

(59) $$k = \frac{G}{R} + H$$

in which

$$A = 0.0048\left(1 + 1.5N\,\frac{S_S}{S}\right)$$

$$B = \frac{K_F}{10}\left(\frac{\Delta}{S} n\right) + 1.5N\,\frac{S_S}{S}\,\frac{K_S}{10}\left(\frac{\Delta}{S} n\right)^{2/3}$$

$$G = (1 + 0.025N)\left(\frac{1+\delta_S}{\pi}\right)(1+\phi)$$

$$H = 0.0050$$

and equation (48) becomes

$$(60) \qquad (L/D)_{max} = \frac{1}{2}\left[(A+BR^2)\left(\frac{G}{R}+H\right)\right]^{-1/2}$$

For any specified material of construction, it is then possible to determine the optimum Aspect Ratio, hence the complete geometry, for attainment of maximum (L/D) at any specified number of struts and foil loading.

Differentiating equation (60) with respect to Aspect Ratio,

$$(61) \qquad \frac{d(L/D)_{max}}{dR} = 0 = 2\left(\frac{L}{D}\right)^3_{max}\left[\frac{AG}{R^2} - BG - 2BHR\right]$$

whence the optimum Aspect Ratio is defined by

$$(62) \qquad R_o^3 + \frac{G}{2H}R_o^2 - \frac{AG}{2BH} = 0$$

Equation (62) has two solutions:

(I) If the term (A/B) is greater than 464.6,

$$(63\text{-I}) \qquad R_o = (X_1 + X_2) - 18.67$$

$$X_1^3 = 28\left[\frac{A}{B} - 232.3 + \sqrt{\frac{A}{B}\left(\frac{A}{B} - 464.6\right)}\right]$$

$$X_2^3 = 28\left[\frac{A}{B} - 232.3 - \sqrt{\frac{A}{B}\left(\frac{A}{B} - 464.6\right)}\right]$$

(II) If the term (A/B) is less than 464.6,

$$(63\text{-II}) \qquad R_o = 18.67\left[2\cos\theta - 1\right]$$

$$\theta = \frac{1}{3}\cos^{-1}\left(\frac{\frac{A}{B} - 232.3}{232.3}\right)$$

Thus the optimum Aspect Ratio can be determined for assumed combinations of strut number, foil loading, load factor, and material of construction. The corresponding foil and strut thicknesses can be determined from equations (56) and (57), and the maximum (L/D) from equation (60). The lift coefficient, speed, and required power can be determined from equations (29), (33), and (39).

Typical values of the parameters corresponding to maximum (L/D) are shown by Figure (14). Results of more comprehensive studies are presented in the general Design Charts which constitute a separate division of this report.

Effects of Deviations of the Major Parameters from Their Optimum Values

Two principal conditions for variation of the major parameters from their optimum values are of interest in a study of the effects of such variations upon maximum attainable (L/D).

First, it is assumed that as each parameter is varied the remaining items are adjusted to maintain the most efficient structure, as defined by equations (56) and (57). Thus, if aspect ratio is reduced, the foil and strut thicknesses are reduced as allowed by these equations.

Second, it is assumed that each parameter is varied, alone, without optimization of the remaining items. Thus, if aspect ratio is reduced, the foil and strut thicknesses are not reduced as allowed by equations (56) and (57), but are held constant. The configuration could then be considered "overstrength", since the equations define the most efficient structure possible under the assumptions made in their development. These second studies therefore also show the effects of changes in the basic structural assumptions which would result in modifications of the allowable relationships among the various parameters.

A rigorous study should include the analyses of variations of all parameters which affect maximum (L/D). Practical considerations, however, justify the elimination of certain of the parameters, for reasons which appear logical.

It is considered likely that interest in the effects of variations of the parameters centers about relatively small changes in the physical dimensions of a particular hydrofoil. Thus, a configuration near the optimum is selected from the Design Charts, and a craft defined with certain fixed values of displacement, number of struts, design load factor and material of construction. It is then of interest to determine the effects of deviations of aspect ratio, span, foil thickness, and strut thickness from their optimum values.

Such effects can be determined by consideration of the general equation for maximum (L/D),

$$(64) \quad \left(\frac{D}{L}\right)^2 = 4\left[A + 4\left(\frac{t_f}{t_{f_0}}\right)^2 + 3\left(\frac{t_s}{t_{s_0}}\right)^2\right]\left[\frac{C}{R_0}\left(\frac{R_0}{R}\right) + H\right]$$

in which

A, B, G, H are as defined in equation (59).

$(_o)$ the subscript denotes optimum values.

ψ is $0.10 t_{F_c}^2$

γ is $0.15 N \frac{S}{S_o} t_{s_o}^2$

$\psi + \gamma$ is (BR_o^2).

The ratio of attainable (L/D) at any geometry to that corresponding to optimum conditions is then

$$(65) \quad \left[\frac{L/D}{(L/D)_o}\right]^2 = \frac{[A+BR_o^2][S/R_o + H]}{\left[A+\psi\left(\frac{t_F}{t_{F_o}}\right)^2+\gamma\left(\frac{t_s}{t_{s_o}}\right)^2\right]\left[\frac{S}{R_o}\left(\frac{R_o}{R}\right)+H\right]} = \Psi^2$$

The effects of variations of each parameter from its optimum value can be determined by use of equation (65), using equations (56) and (57) to optimize the remaining items. The general equations which define such effects are as follows: (Note: constant total weight in all cases)

a. Effect of Aspect Ratio - See Figure (15)

1. Constant Area, other items optimized.

$$(65\text{-a-1}) \quad \Psi^2 = \frac{[A+BR_o^2][S/R_o + H]}{\left[A+BR_o^2\left(\frac{R}{R_o}\right)^2\right]\left[\frac{S}{R_o}\left(\frac{R_o}{R}\right)+H\right]}$$

2. Constant Span, other items optimized.

$$(65\text{-a-2}) \quad \Psi^2 = \frac{[A+BR_o^2][S/R_o + H]}{\left[A+\psi\left(\frac{R}{R_o}\right)^3+\gamma\left(\frac{R}{R_o}\right)^{3/2}\right]\left[\frac{S}{R_o}\left(\frac{R_o}{R}\right)+H\right]}$$

3. Constant Foil Thickness, other items optimized.

$$(65\text{-a-}3)\qquad \psi^2 = \frac{[A+BR_o^2][G/R_o + H]}{[A+\gamma+\zeta(\frac{R}{R_o})^{3/2}][\frac{G}{R_o}(\frac{R_o}{R}) + H]}$$

4. Geometry Not Optimized.

$$(65\text{-a-}4)\qquad \psi^2 = \frac{G/R_o + H}{\frac{G}{R_o}(\frac{R_o}{R}) + H}$$

b. Effect of Foil Span - see Figure (16)

1. Constant Area, other items optimized.

$$(65\text{-b-}1)\qquad \psi^2 = \frac{[A+BR_o^2][\frac{G}{R_o} + H]}{[A+BR_o^2(\frac{b}{b_o})^4][\frac{G}{R_o}(\frac{b_o}{b})^2 + H]}$$

2. Constant Aspect Ratio, other items optimized.

$$(65\text{-b-}2)\qquad \psi^2 = \frac{A+BR_o^2}{A+\gamma(\frac{b_o}{b})^2+\zeta(\frac{b_o}{b})^{4/3}}$$

3. Constant Foil Thickness, other items optimized.

$$(65\text{-b-}3)\qquad \psi^2 = \frac{[A+BR_o^2][\frac{G}{R_o} + H]}{[A+\gamma+\zeta(\frac{b}{b_o})^{4/3}][\frac{G}{R_o}(\frac{b_o}{b})^2 + H]}$$

4. Geometry Not Optimized.

$$(65\text{-b-}4)\qquad \psi^2 = \frac{G/R_o + H}{\frac{G}{R_o}(\frac{b_o}{b})^2 + H}$$

c. Effect of Foil Thickness - See Figure (17)

1. Constart Area, other items optimized.

$$(65\text{-}c\text{-}1) \qquad \psi^2 = \frac{\left[A + BR_o^2\right]\left[\frac{S}{R_o} + H\right]}{\left[A + BR_o^2\left(\frac{t_F}{t_{F_o}}\right)^2\right]\left[\frac{S}{R_o}\left(\frac{t_{F_o}}{t_F}\right)^2 + H\right]}$$

2. Constant Span, other items optimized.

$$(65\text{-}c\text{-}2) \qquad \psi^2 = \frac{\left[A + BR_o^2\right]\left[\frac{S}{R_o} + H\right]}{\left[A + \gamma\left(\frac{t_F}{t_{F_o}}\right)^2 + \zeta\left(\frac{t_F}{t_{F_o}}\right)^{4/3}\right]\left[\frac{S}{R_o}\left(\frac{t_{F_o}}{t_F}\right)^{2/3} + H\right]}$$

3. Constant Aspect Ratio, other items optimized.

$$(65\text{-}c\text{-}3) \qquad \psi^2 = \frac{A + BR_o^2}{A + \gamma\left(\frac{t_F}{t_{F_o}}\right)^2 + \zeta\left(\frac{t_F}{t_{F_o}}\right)^{4/3}}$$

4. Geometry Not Optimized.

$$(65\text{-}c\text{-}4) \qquad \psi^2 = \frac{A + BR_o^2}{A + \gamma\left(\frac{t_F}{t_{F_o}}\right)^2 + \zeta}$$

d. Effect of Strut Thickness

It is assumed that in all cases where possible the strut thickness will be no greater than absolutely necessary. The addition of flap actuating mechanisms, depth sensing devices, or other such equipment may make it necessary, however, to increase the strut thickness beyond the value required for adequate strength. It is therefore of interest to analyze the effects of changes in strut thickness, with all other parameters optimized. (See Figure 18)

$$(65\text{-d-1}) \qquad \psi^2 = \frac{A + BR_o^2}{A + \gamma + \beta\left(\frac{t_s}{t_{s_o}}\right)^2}$$

Figures (15), (16), (17), and (18) indicate, respectively, the effects of variations of aspect ratio, foil span, foil thickness, and strut thickness. It is appropriate to discuss briefly the effects shown. Constant weight, load factor, and material of construction are assumed in all cases.

It is necessary, in an analysis of the effects of variations of each parameter, to stipulate which of the remaining parameters are to be held constant. Thus, considering the equation for aspect ratio, ($R = b^2/S$), it is seen that variations of aspect ratio can be affected by variations of span, area, or both.

From equations (56) and (57), for constant values of (α), (n), (K_F), and (K_s), it is possible to derive the following general expressions for the terms (t_F/t_{F_o}) and (t_s/t_{s_o}) which appear in equation (65),

$$(65\text{-e}) \qquad \left(\frac{t_F}{t_{F_o}}\right)^2 = \frac{R^2}{R_o^2}\frac{S_o}{S} = \frac{b^4}{b_o^4}\frac{S_o^3}{S^3} = \frac{R^3}{R_o^3}\frac{b_o^2}{b^2}$$

$$(65\text{-f}) \qquad \left(\frac{t_s}{t_{s_o}}\right)^2 = \frac{R^2}{R_o^2}\left(\frac{S_o}{S}\right)^{2/3} = \frac{b^4}{b_o^4}\left(\frac{S_o}{S}\right)^{8/3} = \left(\frac{R}{R_o}\right)^{8/3}\left(\frac{b_o}{b}\right)^{4/3}$$

The relationships among the various parameters then become, holding certain of them constant,

at constant area ($S_o = S$)

$$\left(\frac{t_F}{t_{F_o}}\right)^2 = \left(\frac{R}{R_o}\right)^2 = \left(\frac{b}{b_o}\right)^4$$

$$\left(\frac{t_s}{t_{s_o}}\right)^2 = \left(\frac{R}{R_o}\right)^2 = \left(\frac{b}{b_o}\right)^4$$

at constant span ($b_o = b$)

$$\left(\frac{t_F}{t_{F_o}}\right)^2 = \left(\frac{R}{R_o}\right)^3 = \left(\frac{S_o}{S}\right)^3$$

$$\left(\frac{t_s}{t_{s_o}}\right)^2 = \left(\frac{R}{R_o}\right)^{8/3} = \left(\frac{S_o}{S}\right)^{8/3}$$

at constant aspect ratio ($AR_o = AR$)

$$\left(\frac{t_F}{t_{F_o}}\right)^2 = \left(\frac{b_o}{b}\right)^2 = \frac{S_o}{S}$$

$$\left(\frac{t_s}{t_{s_o}}\right)^2 = \left(\frac{b_o}{b}\right)^{4/3} = \left(\frac{S_o}{S}\right)^{2/3}$$

at constant foil thickness ($t_{F_o} = t_F$)

$$\left(\frac{t_F}{t_{F_o}}\right)^2 = 1.$$

$$\left(\frac{t_s}{t_{s_o}}\right)^2 = \left(\frac{AR}{AR_o}\right)^{2/3} = \left(\frac{b}{b_o}\right)^{4/3} = \left(\frac{S}{S_o}\right)^{1/3}$$

These relationships are used in development of the equations (65-a-1, etc.) which define the variations of (L/D), and can be used in an analysis of the effects shown by Figures (15-18).

a. Effect of Aspect Ratio

Variations of aspect ratio are accompanied by variations of the remaining parameters, as shown above. At constant area, a decrease of aspect ratio permits a decrease of both foil and strut thicknesses. The reduction of aspect ratio increases induced drag, whereas the decreased foil and strut thicknesses decrease the profile drag. It is seen in Figure (15) that induced drag has the more powerful effect.

The same reasoning can be applied to the effects shown for constant span, and constant foil thickness. At constant span, as aspect ratio is decreased, foil and strut thicknesses decrease, but the area increases, reducing the foil loading. At constant foil thickness, as aspect ratio is decreased, strut thickness decreases, and both span and area decrease. In each case, the increase or decrease of (L/D) is determined by the relative magnitudes of the changes in induced and profile drags. The same is true of the effects shown for the case in which the geometry is not optimized as the aspect ratio is varied.

b. Effect of Foil Span
c. Effect of Foil Thickness
d. Effect of Strut Thickness

The effects of span, foil thickness, and strut thickness, shown by Figures (16), (17), and (18), respectively, can be

analyzed in the same manner as indicated above for the effects of aspect ratio. In these cases, also, the change in attainable (L/D) is determined by the relative magnitudes of the changes in induced and profile drags.

It is of particular importance to note the significance of the effects of changes of the major design parameters, as shown by Figures (15-18). As indicated by these figures, appreciable errors can be made with respect to each of the parameters, without affecting enormous changes in the attainable (L/D).

It should be noted, however, that the apparently great margin of error permissible in each of the major parameters should not be construed as justification for laxity in maintenance of the proper values. It is, after all, the entire purpose of these studies to demonstrate high values of attainable (L/D), and to indicate the general design conditions under which such high (L/D) may be obtained. If lower values are to be considered acceptable, economy would dictate simplification of the design, rather than laxity in control over the major parameters (e.g., if a ten percent reduction in maximum L/D is considered acceptable with a four-strut craft, due to permissible errors in the major parameters, the Design Charts show that it would be better to build a two-strut craft).

Special Case of Single-Strut Configuration

Of notable significance to the design of hydrofoil craft, particularly with regard to application to small boats, is the special case of the single-strut configuration. Structural considerations permit the use of foils tapered in planform, which can be expected to result in appreciable improvements in attainable (L/D) over that permissible with the rectangular planform assumed in the general studies.

As indicated in the general discussion of structural considerations, an increase of Aspect Ratio can be realized, without increasing foil thickness, by tapering the foil planform. This is of course implied by equation (56), in which it is seen that aspect ratio must increase if the area is held constant and the planform tapered, at constant thickness.

The same increase of aspect ratio, hence (L/D), is of course possible, regardless of the number of struts. It appears logical to assume, however, that multi-strut configurations will utilize foils of constant chord between struts. The advantages of taper will then be applicable only to the cantilevered portions of the foils outboard of the outer struts, and cannot be expected to produce advantages as marked as is the case with a single strut in which the entire foil can be tapered. Tapering of the outer panels of multi-strut configurations are therefore treated as design improvements which can be applied to particular designs, and are not included in these general studies.

The increase of attainable (L/D) achieved by tapering of the single-strut planform is affected by two considerations. First, the aspect ratio is increased as indicated above; and, second, the induced drag parameter is decreased as indicated by Figure (7). A typical increase of attainable (L/D) is shown by Figure (19).

Special Case of Tandem Configuration

It is probable that size limitations may make it undesirable to use a single foil for the main lifting system of a hydrofoil craft, in which case it may be necessary to distribute the load between two or more foils arranged in tandem. It is of interest to analyse the effects of such tandem arrangement upon the attainable (L/D) ratios.

In the case of assumed infinite flow conditions it is possible to estimate the effects of forward foil downwash upon the rear foil. Such an assumption, however, appears to impose undue restrictions upon the analysis of tandem craft performance, since the creation of the well known standing wave behind a hydrofoil running near the water surface indicates that the downwash must, in fact, become an upwash at some distance behind the foil. An investigation of tandem configurations must therefore include predictions of the probable behavior of the downwash pattern behind the forward foil.

A completely rigorous analysis of the downwash pattern behind a hydrofoil becomes an extremely tedious, and questionably accurate process. Although some theoretical work has been derived regarding this phenomenon, little experimental verification of the predicted characteristics has been made available. Pending development of more reliable analyses, therefore, the present study will attempt only to estimate the order of magnitude of probable downwash behavior, rather than precise values. The results should be sufficiently accurate for the purposes of the general design studies with which this report is concerned.

It may be possible to deduce some useful conclusions regarding downwash characteristics, without the necessity of detailed theoretical analyses. Consider, for example, the basic equation for the drag induced by a lifting foil of finite span,

$$D_i = -L\left(\frac{\omega}{V}\right) \tag{66}$$

in which (L) is foil lift, (ω) is downwash velocity at the foil, and (V) is free-stream velocity parallel to the direction of motion.

Reducing equation (66) to coefficient form and comparing it with equation (9) it is seen that the downwash velocity (ω) is defined by

$$\omega = -\frac{K_i C_L V}{AR} \tag{67}$$

Since the factor (K_i) includes the effects of three-dimensional flow and depth of submersion, it is seen that equation (67) defines downwash, as expected, in terms of foil planform characteristics, submersion, lift, and forward speed.

It would appear reasonable to expect that, at least near the water surface, the resultant velocity of the water stream has the direction closely approximated by the slope of the surface wave created. If it then is assumed that this resultant velocity is composed of a horizontal component (V) and a vertical component (ω), it should then be possible to determine the strength of the vertical, or downwash, component at any distance behind the foil.

If the distance behind the foil is then denoted by (x) and the deflection of the water surface by (y), the shape of the water surface can be represented, to a first approximation, by the sine curve,

$$y = -X \sin\left(\frac{xg}{V^2}\right) \tag{68}$$

The strength of the vertical component (ω) is then

$$\omega = \frac{dy}{dt} = \frac{dy}{dx}\frac{dx}{dt} = -\frac{g}{V^2} X \cos\left(\frac{xg}{V^2}\right) \tag{69}$$

Solving for (X) by combining equations (67) and (69) at ($x = 0$), the downwash velocity becomes, at any point behind the foil,

$$\omega = -\frac{K_i C_L V}{R} \cos\left(\frac{xg}{V^2}\right) \tag{70}$$

Now the induced drag of a tandem configuration is composed of the self-induced drags of the individual foils which would exist if they were acting independently, plus the mutually-induced drag imposed upon the rear foil by the downwash from the forward foil. Denoting the forward foil by the subscript ($_1$) and the rear foil by ($_2$), the induced drag of the tandem system is then defined by

$$\begin{aligned} D_i &= D_{L_1} + D_{i_2} + D_{i_{12}} \\ &= -L_1 \frac{\omega_1}{V} - L_2 \frac{\omega_2}{V} - L_2 \frac{\omega_1}{V} \\ &= \frac{K_{i_1} L_1^2}{s_1 q R_1} + \frac{K_{i_2} L_2^2}{s_2 q R_2} + \frac{K_{i_1} L_1 L_2}{s_1 q R_1} \cos\left(\frac{xg}{V^2}\right) \end{aligned} \tag{71}$$

It is immediately apparent that the vertical induced velocity behind the forward foil varies from full downwash immediately behind it, through undisturbed flow at one-quarter wave length, to full upwash at one-half wave length. The most favorable location for the rear foil is, then, at the point of full upwash at which the mutually induced drag assumes a negative value, equivalent to an effective forward thrust. The location is a function only of speed and can be tabulated independently of the geometry of the craft. As can be noted, the foil separation required for full upwash at the rear foil becomes somewhat excessive with appreciable speeds.

Foil Separation for Full Upwash at Rear Foil

Speed (knots)	15	30	45	60
Separation (ft.)	63	250	563	1000

Values of the cosine function in the expression for downwash are presented in Figure (20), for use in analysis of specific tandem configurations. As indicated by the figure, the realization of full upwash at the rear foil can be expected only with very large craft, unless the operating speeds are rather low.

The complete analysis of tandem configuration becomes a problem of optimization of hydrodynamic and structural requirements, similar to that conducted for the single foil. It may be possible, however, to derive some significant conclusions from inspection of typical examples, without the elaborate studies necessary for a rigorous analysis.

Consider, for example, a case in which a single foil has been selected, at a specified design speed and craft gross weight, for the attainment of maximum (L/D). It is desired to determine whether an equivalent tandem configuration can be designed to produce the same performance as that of the single foil. It will be assumed that the two tandem foils are identical, and each carry one-half the total gross weight; and that each foil carries the same number of struts as the single foil. Each tandem foil can then be considered as a scaled-down counterpart of the single foil.

If the tandem configuration is to have the same performance characteristics as the single foil, its parasite and induced drags must be equal to those of the single foil. Inspection of equations (58) and (59) reveals that these requirements can be met if certain geometrical conditions are satisfied, neglecting for the moment the possible effects of downwash or upwash.

For equality of parasite drags, denoting the single foil by the subscript (o),

(72) $$C_{D_{P_o}} = C_{D_{P_1}}$$
$$A_o + B_o R_o^2 = A_1 + B_1 R_1^2$$

For equality of induced drags, neglecting the possibilities of upwash for the moment,

(73) $$k_o = k_1$$
$$\frac{G_o}{R_o} = \frac{G_1}{R_1}$$
$$R_1^2 = \left(R_o \frac{G_1}{G_o}\right)^2$$

Combining equations (72) and (73), the conditions of equality of both parasite and induced drags are satisfied if

(74) $$R_o^2 \left[B_o - B_1 \frac{G_1}{G_o}\right] + \left[A_o - A_1\right] = 0$$

The relationships defined by the various symbols in equation (74), defined in equation (59), can be studied to ascertain if equation (75) can be reasonably satisfied.

Considering first the quantity ($A_o - A_1$), it is seen that, if the strut chord is assumed to vary directly with foil chord, this quantity vanishes if the ratio of foil submergence to span is held constant. This would appear to be an entirely reasonable allowance, since the same roll angle would then be possible with either configuration.

If the same ratio of foil submergence to span is maintained, it is seen that the quantity (G_1/G_o) is unity. Equation (74) can then be satisfied if ($B_o = B_1$). From the definition of the term (B), it is seen that, since the single and tandem foils have the same unit loadings, the desired equality is satisfied if the struts have the same ratios of length to foil span. It is thus apparently possible, quite aside from considerations of upwash, to design a tandem configuration which has performance equal to that of the equivalent single foil.

Certain practical considerations should be noted, however, before too much credence is attached to this rather elementary analysis of the potentialities of tandem craft. First it should be noted that the example studied permitted equal performance of the tandem and single foil craft if the

ratios of strut length to foil span were held constant. Since the aspect ratios were constant and the area of the tandem foil was one-half that of the single foil, however, the span of the tandem foil was reduced, hence the length of strut above the water surface was reduced. Such would appear to be not permissible, since, if the hull can safely be run closer to the water, it would be only reasonable to shorten the struts of the single foil with which comparison is made, thus making its (L/D) higher.

It would therefore appear that a more reasonable requirement would specify that the strut length above the water surface should remain constant, in which case ($B_1 > B_0$). The desired condition that ($B_0 = B_1 \sigma_1/\sigma_0$) would be possible only if ($\sigma_1 < \sigma_0$). This would, however, require that the tandem foil ratio of submergence to span be greater than that of the single foil, which would in turn cause (A_1) to be greater than (A_{1_0}). The condition for equality of parasite and induced drags of the tandem and single foils would then not be satisfied.

Applying the same reasoning to other possible variations of geometry, it is apparent that the use of tandem foils is accompanied by some increases of either parasite drag, induced drag, or both. The magnitudes of such increases depend, of course, upon the particular geometries under consideration.

It is of course readily apparent that the effects of downwash upon the rear foil would aggravate the situation with regard to increase of tandem drag over that of the equivalent single foil. It is thus immediately apparent that, if the tandem arrangement is to have performance equal to that of the single foil, the rear foil must be operated in a region of upwash. It is entirely probable that the effects of such upwash would compensate for the inherent inferiority of the tandem arrangement. It has already been shown, however, that location of the rear foil in the upwash region may involve rather large craft.

It would appear, therefore, that consideration of tandem arrangements should be based upon other than maximum (L/D) requirements, unless full confidence is placed in the existing, rather inadequate theories with regard to upwash. It should be further noted, however, that the losses inherent in tandem arrangements are probably relatively small, and that entirely acceptable performance should be obtained with either tandem or single foil craft.

Effect of Stabilizing Surfaces upon Attainable (L/D)

Whereas the general configuration studies outlined in the previous discussion are based upon a single-foil configuration, without allowances for the effects of stabilizing foils or planing surfaces, it is of course necessary to include consideration of the requirements for such means of stabilization in the design of any particular hydrofoil craft. Although the design details of the stabilizing surface, hence its effect upon performance, will depend upon the characteristics of the craft for which it is required, certain general estimates can be made of the order of magnitude of the effects which can be expected with the type of craft under consideration in these studies.

On the basis of preliminary static and dynamic stability studies, outlined in a separate division of this report, it is possible to write an equation which defines the required tail area in terms of main foil area. This equation is useful in preliminary design studies, but it should be emphasized that more detailed studies should be made before considering the design completely defined.

The preliminary equation for tail size is

$$\frac{S_T}{S} = \left(\frac{m}{m_T}\right)\left(\frac{1.075 - \omega_F/W}{\frac{\omega_F}{W} - 0.075}\right)\left(\frac{1}{1 - \frac{d\epsilon}{d\alpha}}\right) \tag{75}$$

in which

S_T is the tail area.

S is the main foil area.

m is the main foil lift curve slope. $(dC_L/d\alpha)$

m_T is the tail lift curve slope. $(dC_L/d\alpha)_T$

$\frac{\omega_F}{W}$ is the proportion of the total load carried by the main foil in the most critical design condition (usually: most aft c.g.)

$\frac{d\epsilon}{d\alpha}$ is the main foil downwash parameter $\left(2K_i \frac{dC_L}{d\alpha}\right)$

Determination of required tail size for any particular configuration becomes a trial and error process in which assumed tail geometries are checked both against equation (75), and the allowable structural limits of equations (51) and (52). As is the usual case with design of aircraft stabilizing surfaces, such a trial and error process is repeated until the desired stability conditions are satisfied at the minimum cost in added tail drag.

Preliminary design studies conducted concurrently with the general studies which are the subject of this report indicate that reasonable approximations to tail size and tail drag can be made in a relatively short time. Again as in aircraft design, it is anticipated that actual tests of full scale hydrofoil craft will greatly clarify many of the problems with regard to stabilization, with the result that estimation of requirements, and prediction of the penalties involved, will be greatly facilitated.

Based upon the studies conducted with several preliminary designs under consideration, it appears likely that tail area requirements will be of the order of twenty-five percent of the main foil area, with an accompanying drag increase of approximately twenty-five percent. Under the assumption that at the cruise condition the tail will contribute no lift to the craft, its drag increase can be changed entirely to parasite drag.

It is therefore possible to generally state the order to magnitude of the effects of stabilizing tails upon the attainable (L/D) of the craft:

Tail size will probably be of the order of twenty-five percent of the main foil area.

Net parasite drag will probably be increased about twenty-five percent.

Maximum attainable (L/D) will probably be reduced about ten to twelve percent.

The speed at which maximum (L/D) is attained will probably be increased about five to six percent.

Effect of Control Surfaces, Flaps, etc. upon Attainable (L/D)

It appears that the great majority of design studies, as well as actual construction programs, with regard to hydrofoil craft, have utilized the water surface as a primary controlling element in the stabilization of the craft. This has been achieved by providing either oblique foils which pierce the water surface, or planing surfaces which rely upon direct contact with the water surface for their successful operation. It is considered obvious that the drag losses inherent in either system are appreciable.

On the other hand, it is considered highly probable that an effective means of stabilization can be provided, at an appreciably lower cost in drag, by utilizing movable control surfaces located directly on the main foil. The craft can then be virtually divorced from the water surface, except of course for its struts which can be designed to produce minimum drag. Elimination of the requirement that the foils pierce the surface also eliminates the necessity for dihedral, and the foil can be designed with a horizontal, maximum (L/D), geometry.

A review of some tests made in Germany upon flap effectiveness indicates remarkable similarity between flap performance on hydrofoils and flap performance as usually found in aircraft practice. It therefore appears quite reasonable to apply the same control surface design philosophy to hydrofoil craft as is ordinarily applied to aircraft design.

The most serious limitation with regard to the application of movable surfaces to hydrofoils is physical, rather than theoretical. Some drag increase is probably to be expected, due to the restricted dimensions of the basic hydrofoils involved and the probability that the addition of control surfaces will require that such dimensions be increased if the hinges and actuating mechanisms are to be carried internally, or that such items be carried outside the basic structure, where they can be expected to contribute some drag.

Under the conditions of relatively turbulent flow assumed in the studies outlined herein, however, it is considered quite likely that the drag contribution of control surfaces will be appreciably lower than that of the oblique foils or planing surfaces which they replace.

Based primarily upon experience with similar applications in aircraft design, it is assumed that a reasonable estimate of the order of magnitude of the drag increases chargeable to control surfaces will be approximately ten percent, with a consequent reduction of attainable (L/D) of about five percent.

CAVITATION CONSIDERATIONS

Incipient Cavitation

An extremely important, if not the most important, consideration in the design of hydrofoil craft is the phenomenon of cavitation. Although there appears to be some mystery as to just what happens when cavitation is present, it is possible to predict with some degree of accuracy both where and when it commences.

It is generally agreed that cavitation begins when the local pressure at any point on a submerged surface is at or below the local vapor pressure of the surrounding water. A vapor bubble forms, due to the vaporization of the water. This bubble may remain relatively stationary, or may be carried downstream if the pressure distribution along the surface is near enough to vapor pressure to permit it to do so.

Two phenomena are of interest in the study of cavitation. First, if cavitation takes place on a lifting surface such as a hydrofoil, formation of the cavitation bubble is usually accompanied by a simultaneous loss of lift and increase of drag. Second, and most dramatic, is the erossive, sometimes catastrophically so, effect of cavitation upon the surface of the body involved. One explanation of this errosion attributes it to the enormous water-hammer forces exerted upon the surface when the cavitation bubble collapses. It is with the lift and drag changes, however, that principal interest is centered in the present studies.

It is convenient to express the excess of pressure over that of vaporization in coefficient form, the "Cavitation Number" usually referred to in hydrodynamic work,

(76) $$\delta_c = \frac{p - p_v}{q}$$

in which

p is the local static pressure.

p_v is the local vapor pressure.

q is free-stream dynamic pressure.

The pressure coefficient at any chordwise location on a lifting hydrofoil is

$$(77) \qquad C_p = \frac{H_o - p}{q}$$

in which (H_o) is free-stream total pressure.

From Bernoulli's Equation,

$$(78) \qquad H_o = p_o + q$$

in which (p_o) is free-stream static pressure.

Combining equations (77) and (78),

$$(79) \qquad p = p_o - q\,(C_p - 1)$$

Then, combining equations (76) and (79), the cavitation number, referred to the hydrofoil section pressure coefficient, is

$$(80) \qquad \delta_c = \frac{p_o - p_v}{q} - (C_p - 1)$$

Typical values of (p_v) in sea-water are:

Water Temp. (°F)	40°	50°	60°	70°	80°
Vapor Press. (psf)	17.28	25.92	36.00	53.30	72.00

The cavitation number expressed by equation (80) is thus seen to consist of two independent terms. The first, $(p_o - p_v)/q$, is entirely a function of depth of submersion, water temperature, and free-stream conditions. The second, $(C_p - 1)$, is a function of the pressure distribution characteristics of the particular foil section under consideration, and is independent of its location. It is therefore possible to ascertain, easily, the

cavitation limits of a foil by comparing its minimum pressure coefficient with the first term of equation (80), which can be designated the "Location Cavitation Number."

(81) "Location Cavitation Number"

$$\delta_L = \frac{p_o - p_v}{q}$$

For depth of submersion (h) in feet, velocity (V) in knots, and assuming standard sea-water at 50°F., equation (81) becomes,

(82) $$\delta_L = \frac{22.6(h+32.5)}{V^2}$$

Typical values of this "Location Cavitation Number," against which the characteristics of particular hydrofoils can be compared, are shown by Figure (21).

The second term of equation (80), being entirely dependent upon the pressure characteristics of each hydrofoil under consideration, can be designated the "Section Cavitation Number," and has the value

(83) "Section Cavitation Number"

$$\delta_S = (C_p - 1)$$

It is now readily apparent that incipient cavitation conditions are defined by the condition that

(84) $$\delta_L = \delta_S$$

Selection of a hydrofoil profile must take into account several requirements. Unfortunately, it is seldom possible to find a foil section which satisfied all of the desires of the designer of the craft upon which it is to be used. Sections with inherently high (L/D) characteristics, for example, are usually limited to relatively low speeds by their cavitation characteristics. On the other hand, sections with high incipient cavitation speeds are usually poor sections with which to attempt to attain high (L/D) values.

As a general rule, cavitation speeds can be increased by slightly rounding the foil leading edge, providing some camber, and making the foil as thin as possible. The effects of camber upon Section Cavitation Number are shown by figure (22). The effects of thickness are shown by Figure (23).

It is immediately apparent that, whereas minimum thickness is desirable from the standpoint of cavitation, structural considerations place definite limits upon thickness. These limits become rather severe when, as in the present studies, high (L/D) is the primary objective of the designer. As indicated by equation (51), minimum thickness and maximum aspect ratio are not compatible requirements. It therefore appears quite logical to conclude that the attainment of high values of (L/D) must be at the expense of cavitation speeds, and, conversely, high cavitation speeds must preclude the attainment of the highest (L/D).

The similarity of this conclusion to that which is considered almost axiomatic in aircraft design is readily apparent. High (L/D), or high speed, hydrofoil craft are seen to present problems analogous to those of high (L/D) transport, or high speed fighter type, aircraft.

Critical Cavitation Speed

Selection of a hydrofoil section for operation at a desired speed is, as indicated in the previous discussion, a matter of determination of the Section Cavitation Number from the section pressure distribution, then comparison of that number with the Location Cavitation Number corresponding to the speed and depth of submersion desired. For profiles for which the data at hand include pressure distributions, this is a relatively simple task. The distribution shown by Figures (22) and (23), for example, can be directly compared with the Location Cavitation Numbers of Figure (21) to obtain the limits of cavitation-free operation of the particular sections shown.

Such a process, however, can become extremely tedious when it is necessary to analyse foil sections for which pressure distributions are not available. It is therefore desirable to find another method of estimation of the speed corresponding to incipient cavitation conditions, or the "Critical Cavitation Speed."

Much of the published data regarding characteristics of high speed airfoils include predictions of the critical Mach numbers of the profiles. This critical Mach number is defined as the speed, expressed as a percentage of the velocity of sound, at which the local flow velocity at some point on the section reaches sonic velocity. Thus, a section with a critical Mach number of 0.9 (speed is nine-tenths sonic velocity) has, somewhere on its surface, a local velocity equal to the speed of sound (Mach number of unity).

Critical Mach number derives its significance from the fact that, at the free-stream speed necessary to produce sonic velocity somewhere on the foil surface, the lift commences to drop off and the drag to rise. This is of course recognized as the same process which takes place after the speed for incipient cavitation is reached. If the equivalence of critical cavitation speed in water and critical Mach number in air can be established, a great deal of published data regarding high speed airfoils can be made available to the study of hydrofoils.

Since the critical Mach number represents a free-stream flight speed, it can be expressed as a pressure coefficient, for any foil section under consideration. It can then be compared directly with the Location Cavitation Number which is, as indicated

by equation (81), merely a pressure coefficient corresponding to critical cavitation conditions.

Typical values of the critical pressure coefficient corresponding to critical Mach number are: (Ref. 31)

(M_{icR})	.9	.8	.7	.6	.5	.4
$(C_{p_{icR}})$	.0779	.2380	.4960	[illegible]	1.620	2.900

Critical pressure coefficient is plotted as a function of critical Mach number in Figure (24).

Equating the critical pressure coefficient to the Location Cavitation Number of equation (82), and solving for speed, the critical cavitation speed is then defined by

$$V_{CR} = 4.75(h+32.5)^{1/2}(C_{p_{cR}})^{-1/2} \tag{85}$$

This can be plotted as in Figure (25), to obtain a convenient conversion from critical Mach number in air to critical cavitation speed in water.

Typical section data, giving critical Mach numbers as functions of operating lift coefficient, are as shown by Figure (26). These can be converted to cavitation speeds by use of Figure (25), to obtain the relationships between critical cavitation number and lift coefficient, as shown by Figure (27).

Examination of a representative number of airfoil sections, and conversion of their critical Mach numbers in air to critical cavitation speeds in water, indicates that practical hydrofoil sections can be expected to demonstrate critical cavitation speeds as shown by Figure (28). Some improvement can doubtless be realized by design refinement, but the curve shown is considered to represent a reasonable prediction of the limits attainable with average design techniques.

Significance of "Critical Cavitation Speed"

Although it appears quite possible to predict the critical cavitation speed of a hydrofoil, either by comparison of its pressure coefficient with the Location Cavitation Number or by conversion of its critical Mach number to critical cavitation speed, it is not at all clear just how serious this limitation is upon hydrofoil operation. As in the aerodynamic case, attainment of critical speed does not appear to bring immediately disastrous results.

Although the lift and drag changes which appear after the critical speed is passed deserve, at least according to airfoil theory, serious consideration, they do not appear to manifest themselves until the critical speed has been exceeded by about ten percent. Numerous tests of airfoils, and a few hydrofoil tests, seem to substantiate this conclusion. It therefore appears quite reasonable to assume that the critical cavitation speed can be exceeded by about ten percent without seriously affecting the performance of the hydrofoil craft.

There is very little data available, however, regarding the lift and drag characteristics of hydrofoils operating at speeds in excess of the critical speed, particularly in the speed range between incipient and complete cavitation. It is considered quite likely that the drag rise which starts soon after the critical speed is reached probably approaches a maximum value after the foil is completely cavitated. No reliable estimates of such characteristics have been found, however, to either confirm or deny this assumption, although some German work (Ref. 32) indicates that the problem was given consideration in the design of the high speed hydrofoil boats built in that country.

The determination of performance characteristics of hydrofoils at speeds in excess of the critical cavitation speed is therefore considered to be a subject warranting a high priority in any studies in which high speed is of primary interest.

Possible Advantages of Sweepback and Boundary Layer Control

The analogy between critical cavitation number in water and critical Mach Number in air suggests the possibility of delaying cavitation by application of the same philosophy to hydrofoils as that applied to airfoils for delay of critical Mach Number. The use of high speed section profiles has already been established as desirable. It appears likely that sweepback and boundary layer control can also prove advantageous

The application of sweepback to hydrofoil planform can be expected, as in the case of airplane wings, to reduce the section pressure coefficient by a factor proportional to the square of the cosine of the angle of sweep. This reduction is primarily a function of the velocity component normal to the foil leading edge, the component parallel to the leading edge having no influence upon the section pressure coefficient. Although the precise correction is affected by aspect ratio as well as sweepback angle, the order of magnitude is approximated by the cosine relationship stated.

It is of course necessary, in the use of sweepback to increase critical cavitation speeds, to properly assess the structural modifications necessary to achieve such sweepback. Torsion and bending can no longer be considered as independent phenomena, as is usually the case with straight foils, and some penalty can be expected in the form of increased thickness, reduced aspect ratio, etc. It is considered highly probable, however, that the net gains can be highly attractive, as evidenced by the almost universal use of sweepback on high speed aircraft.

The use of boundary layer control as a means of improving hydrofoil performance appears to offer some advantages, although no attempt is made here to assess the costs of such control in terms of power requirements. It would of course be theoretically desirable to completely remove the boundary layer and possibly reduce the flow to laminar conditions. Practical considerations, however, based upon studies of the subject with aircraft, indicate that the power requirements for such complete removal would probably negate the advantages to be gained, and a reasonable compromise involves control, rather than complete removal, of the boundary layer.

The use of boundary layer control is therefore suggested as a possible means of improving hydrofoil performance, although no attempt is made to predict the improvements which might be expected. It is considered highly probable that, quite aside from

performance considerations, control of the cavitation bubble may reduce erosion difficulties which constitute a serious aspect of the cavitation problem. Further investigation of the general subject of hydrofoils should probably include some consideration of the possibilities of boundary layer control.

HYDRODYNAMICS

REFERENCES

1. Taylor, D.W., "The Speed and Power of Ships"
2. von Karman, Th., "Turbulence and Skin Friction," J.Ae.Sc., Jan. 1934
3. Millikan, Clark B., "Aerodynamics of The Airplane"
4. Warren, C.H.E., "A Theoretical Approach to The Design of Hydrofoil Lifting Surfaces," R.A.E. Tech. Note No. Aero 1826, Sept. 1946
5. Benson, J.M. & Land, N.S., "An Investigation of Hydrofoils in The NACA Tank," NACA ACR, Sept. 1942
6. Land, N.S., "Characteristics of an NACA 66,S-209 Section Hydrofoil at Several Depths," NACA Conf. Bull., May 1943.
7. Ward, K.E. & Land, N.S., "Preliminary Tests in The NACA Tank to Investigate The Fundamental Characteristics of Hydrofoils" NACA ACR Sept. 1940
8. Knapp, R.T. & Dailey, J.W., "Force and Cavitation Characteristics of The NACA 4412 Hydrofoil" Div.6 sr 207-1273 OSRD 3953
9. Gott, J.P., "Note on Hydrofoils for Flying Boats," RAE T.N. Aero 1353 Jan. 1944 (trans.)
10. Tietjens, P.O., "Boat with Supporting Foils," April 1947 (Trans.)
11. "Hydrofoil Craft" F2-s-536-47 (trans.)
12. "German Hydrofoil Research and Development" F2-S-435-47 (trans.)
13. "Speed Boat after The Schertel-Sachsenberg System" (trans.)
14. "The Schertel-Sachsenberg Commercial High Speed Boats for Inland Waterways" (trans.)
15. NACA RB L4C28
16. NACA T.N. 1060
17. NACA ACR, Sept. 1942
18. NACA T.N. 1078
19. NACA T.N. 845
20. Grunberg, V., "Hydrodynamic Lift by Immersed Wings" (trans.)
21. Graff, Dr. Ing. W., "Reduction of Ship Resistance by The Lift of Wings" (trans.)
22. NACA T.N. 1211
23. Abbott, I.H., von Doenhoff, A.E., & Stivers, L.S., "Summary of Airfoil Data" NACA Rpt. 824, 1945
24. ANC-1(1) "Spanwise Airload Distribution" April 1938
25. Durand, W.F. "Aerodynamic Theory", Volume II, p. 219
26. Mangler, W., "The Lift Distribution of Wings with End Plates," NACA T.M. 856, April 1938

27. Bates, W.R., "Collection and Analysis of Wind Tunnel Data on the Characteristics of Isolated Tail Surfaces with and without End Plates," NACA T.N.1291, May 1947
28. Abbott, I.H., "Interference Effects of Longitudinal Flat Plates on Low-Drag Airfoils," NACA CB-16, Nov. 1942
29. "Interference Drag of Streamlined Struts," NACA TR 468
30. NACA Rpt. 669
31. Liepmann, H.W. & Puckett, A.E., "Introduction to Aerodynamics of A Compressible Fluid"
32. Graff, W., "Notes on the Problem of Cavitation" (trans.)

General References

1. Reid, E.G., "Applied Wing Theory"
2. Durand, W.F., "Aerodynamic Theory" Vol. I-VI
3. Weick, F.E., "Aircraft Propeller Design"
4. Diehl, W.S., "Engineering Aerodynamics"
5. Pope, Alan, "On Airfoil Theory and Experiment," J.Ae.Sc., July 1948
6. Carter, A.W., "Recent NACA Research on High Length-Beam Ratio Hulls," J.Ae.Sc., March 1949
7. Locke, F.W.S.,Jr., "An Empirical Study of Low Aspect Ratio Lifting Surfaces with Particular Regard to Planing Craft" J.Ae.Sc., March 1949
8. Wood, K.D., "Aspect Ratio Corrections," J.Ae.Sc., October 1943
9. Schairer, G.S., "Systematic Wing Section Development," J.Ae.Sc., Jan. 1947
10. Peebles, G.H., "A Method for Calculating Airfoil Sections from Specifications on the Pressure Distributions," J.Ae.Sc., Aug. 1947

INDEX OF FIGURES

1. Skin Friction Coefficient.
2. Friction Drag.
3. Section Drag Coefficient.
4. Profile Drag Coefficient.
5. Induced Drag Induction Parameter.
6. Interface Reflection Parameter.
7. Induced Drag.
8. Hull Resistance.
9. Hull Resistance.
10. Hull Drag Prior to Take-Off.
11. Effect of Take-Off Speed upon Required Take-Off Power.
12. Lift Curve Slope Induction Parameter.
13. Effect of Operating Speed upon (L/D).
14. Optimum Geometry for Maximum (L/D).
15. Effects of Deviation of Aspect Ratio from Optimum Value.
16. Effects of Deviations of Span from Optimum Value.
17. Effects of Deviations of Foil Thickness from Optimum Value.
18. Effects of Deviations of Strut Thickness from Optimum Value.
19. Maximum (L/D) of Single-Strut Configuration.
20. Values of Downwash Velocity Parameter
21. Location Cavitation Number.
22. Effect of Camber upon Typical Section Cavitation Number.
23. Effect of Thickness upon Typical Section Cavitation Number.
24. Critical Pressure Coefficient.
25. Conversion of Critical Mach Number in Air to Critical Cavitation Speed in Water.
26. Critical Mach Number in Air.
27. Critical Cavitation Speed in Water.
28. Estimated Critical Cavitation Speeds, Maximum Obtainable.

CONFIDENTIAL

Figure (1)

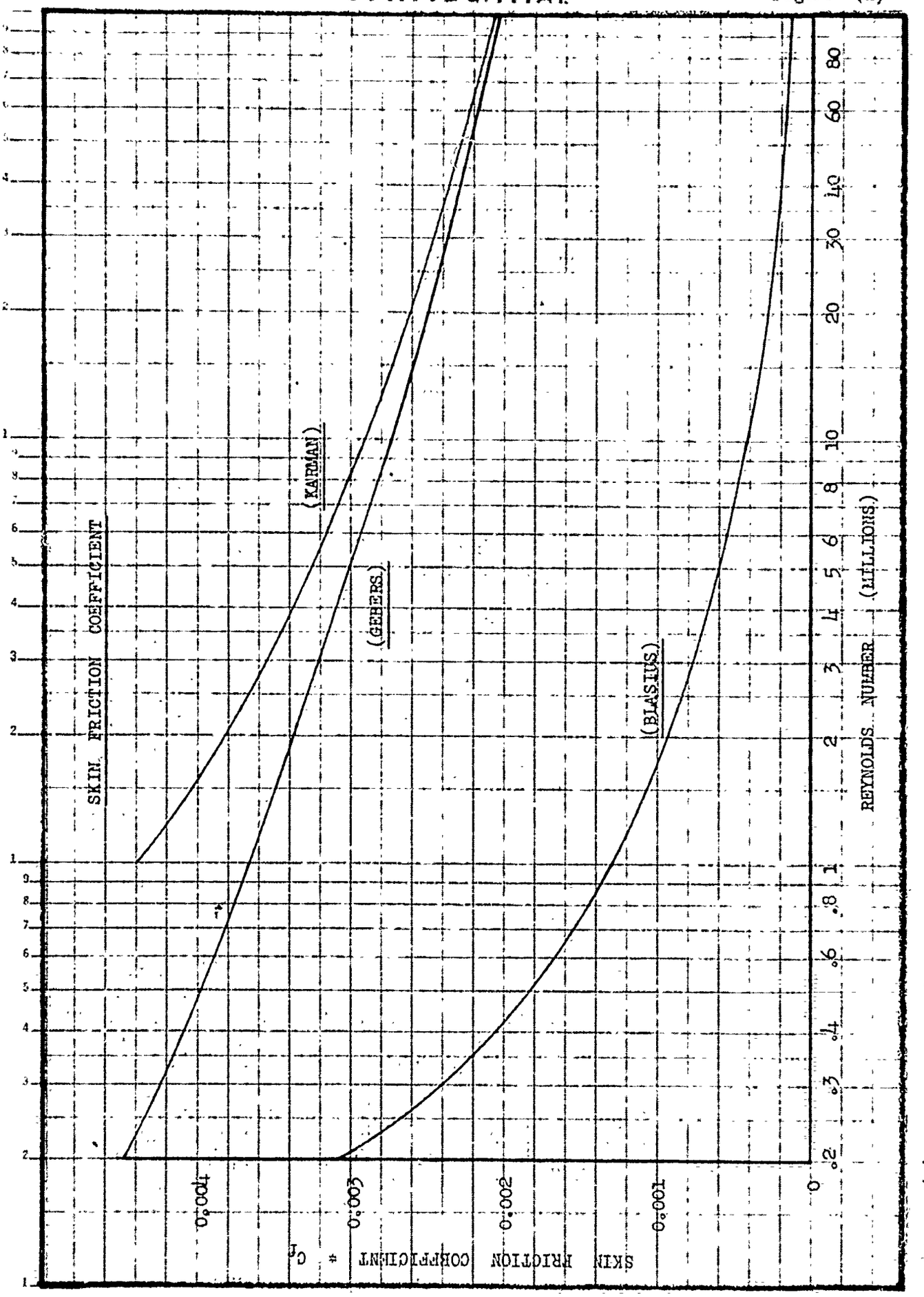

Figure (1)

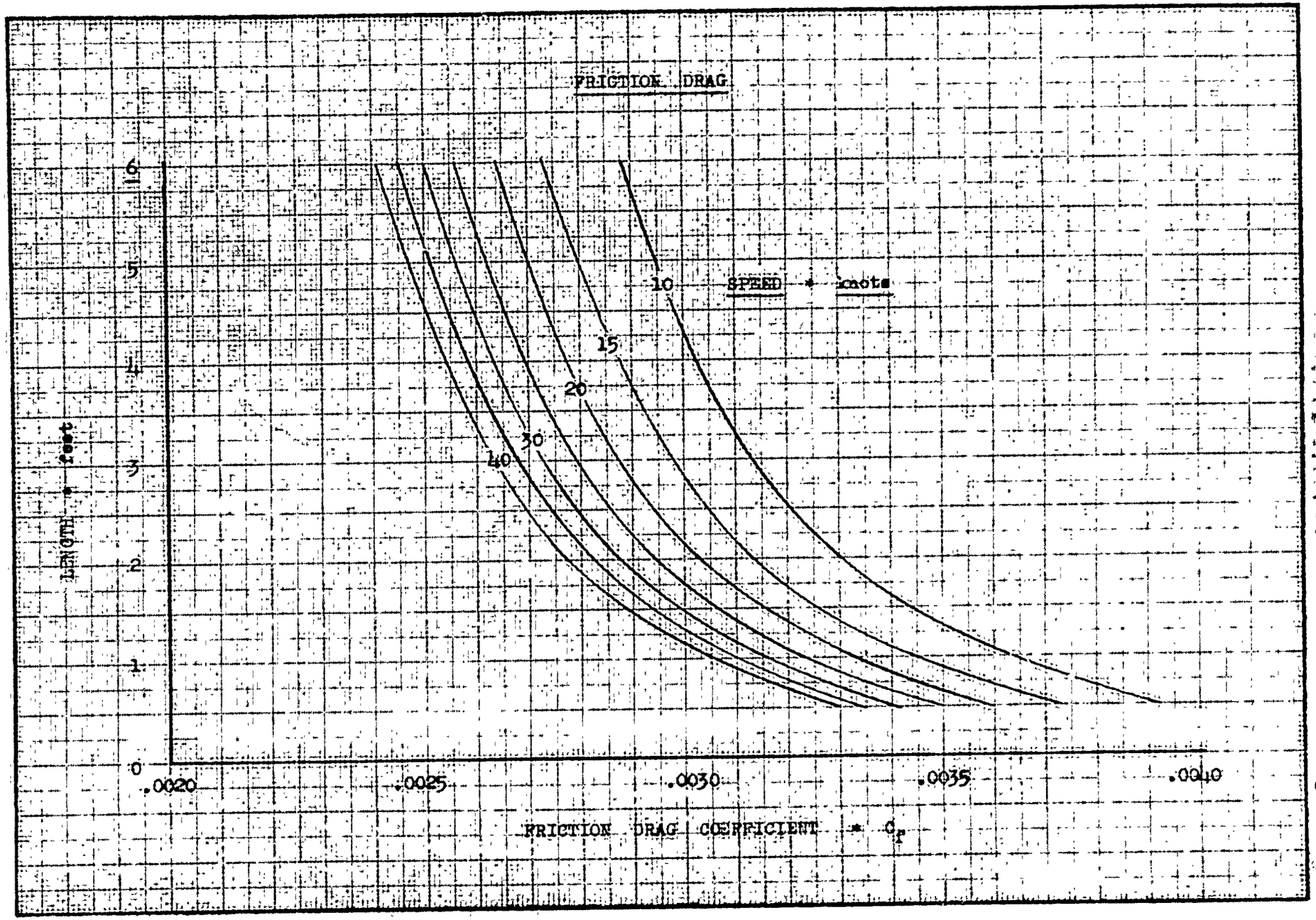

Figure (2)

Figure (2)

CONFIDENTIAL

Figure (3)

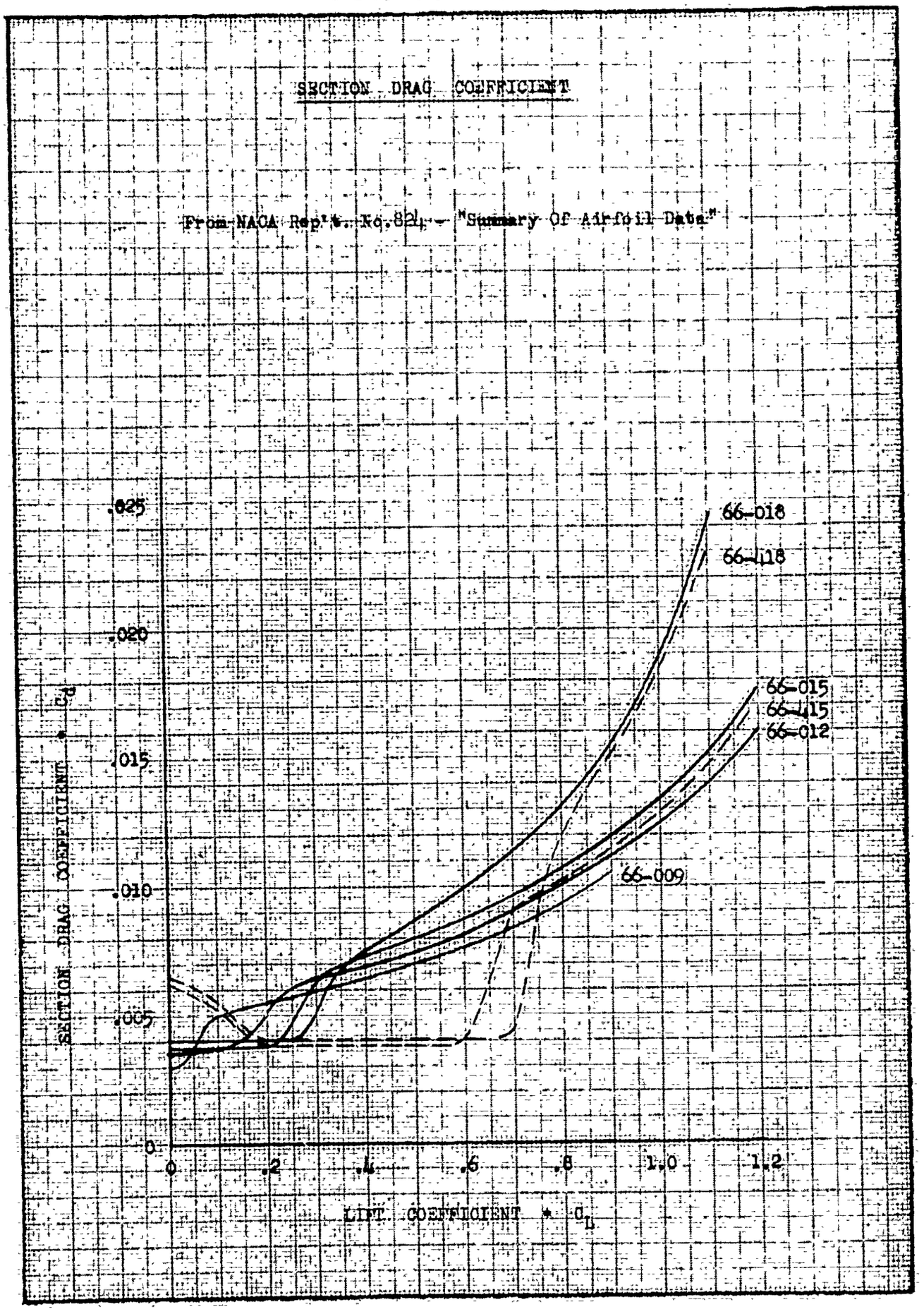

Figure (3)

3H

Figure (4)

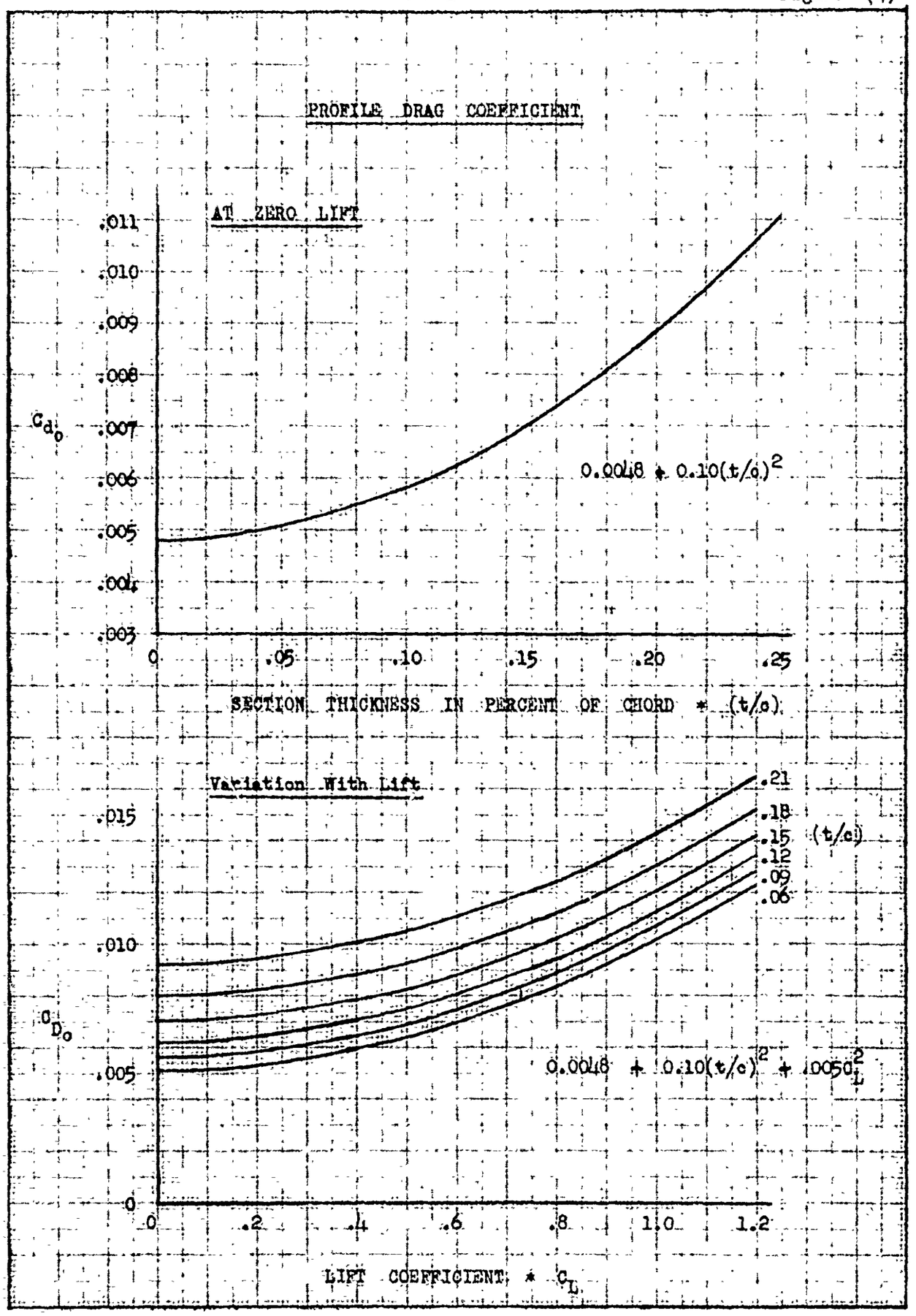

Figure (4)

Figure (5)

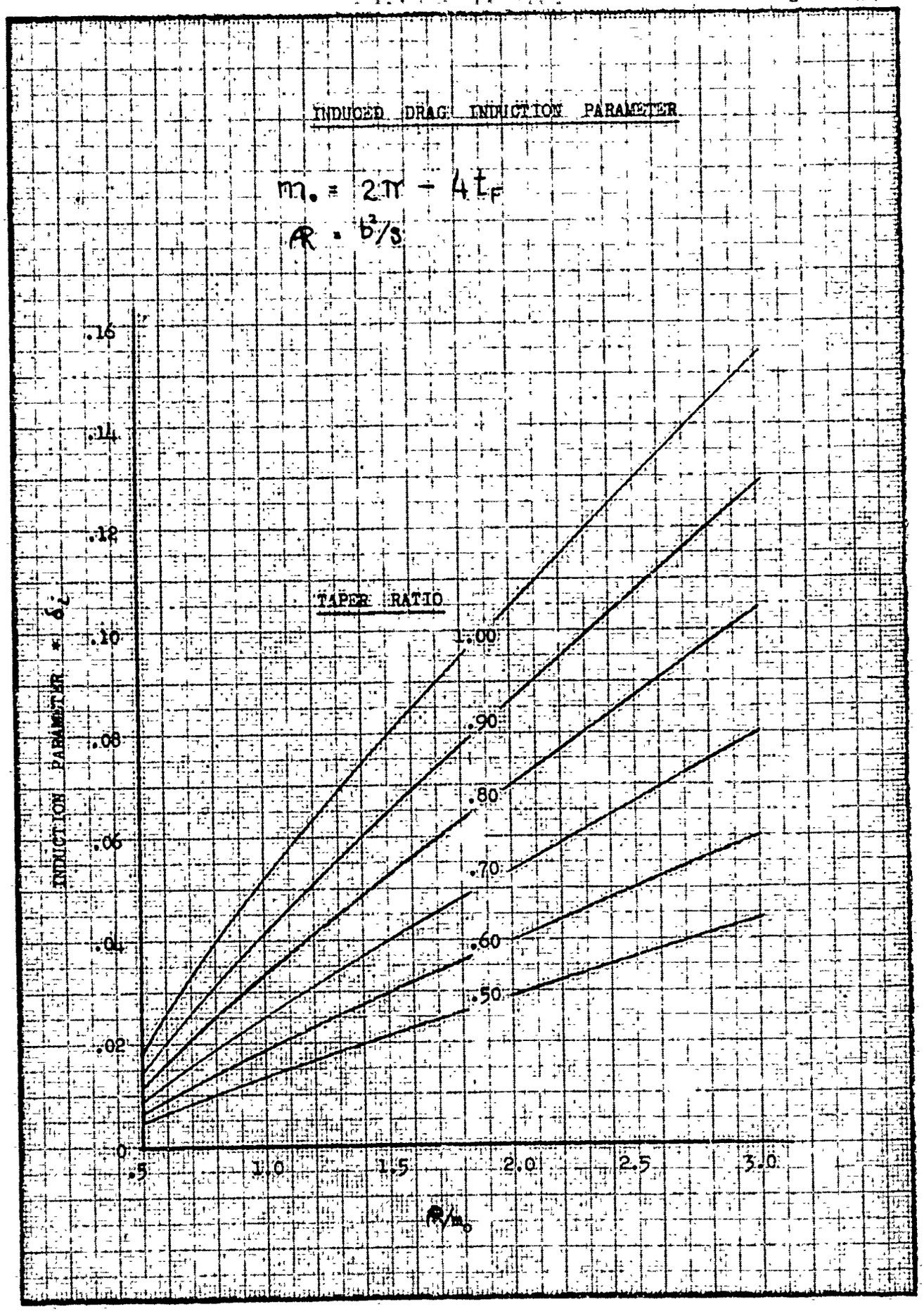

Figure (5)

5-H

CONFIDENTIAL

Figure (6)

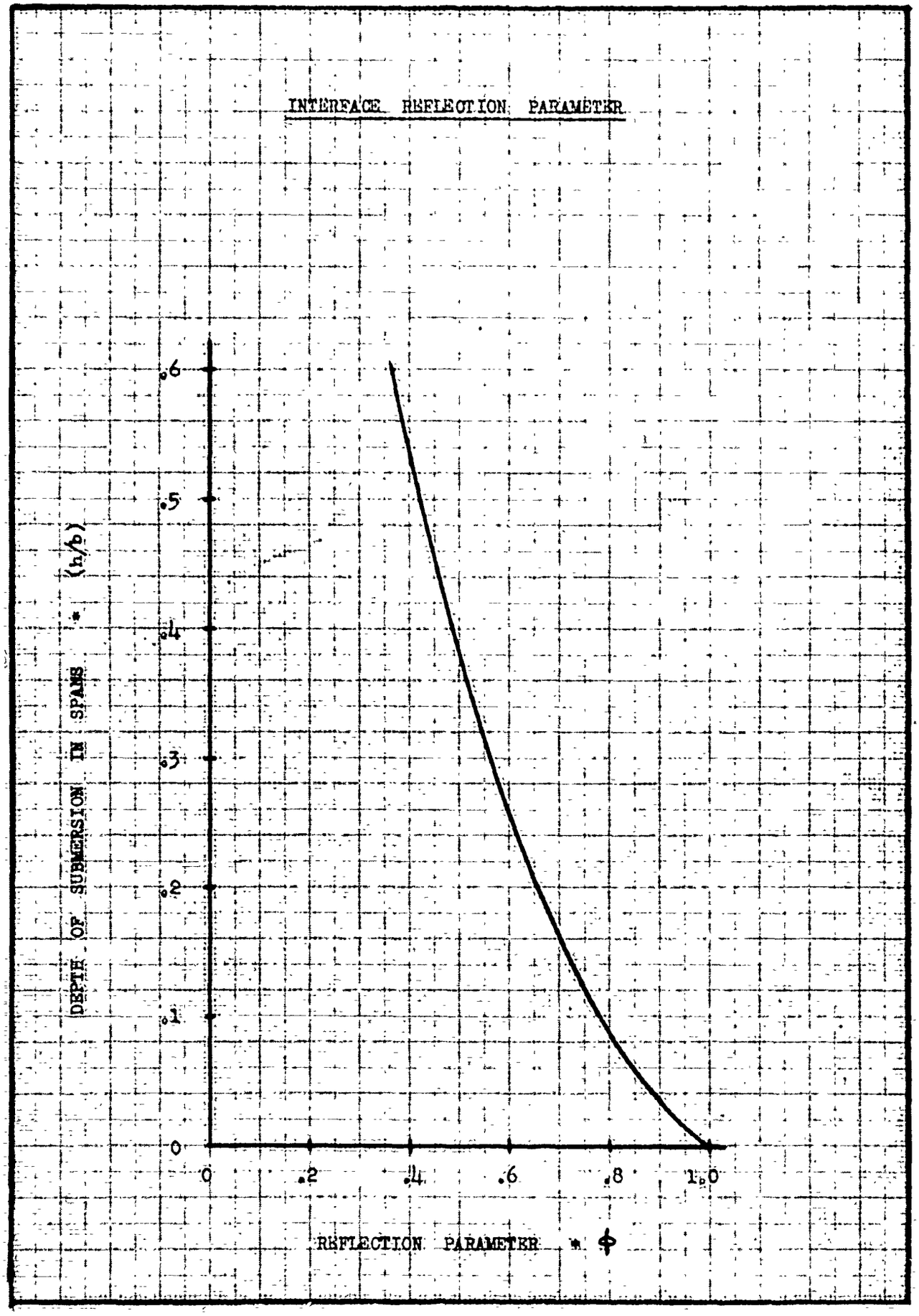

Figure (6)

Figure (7)

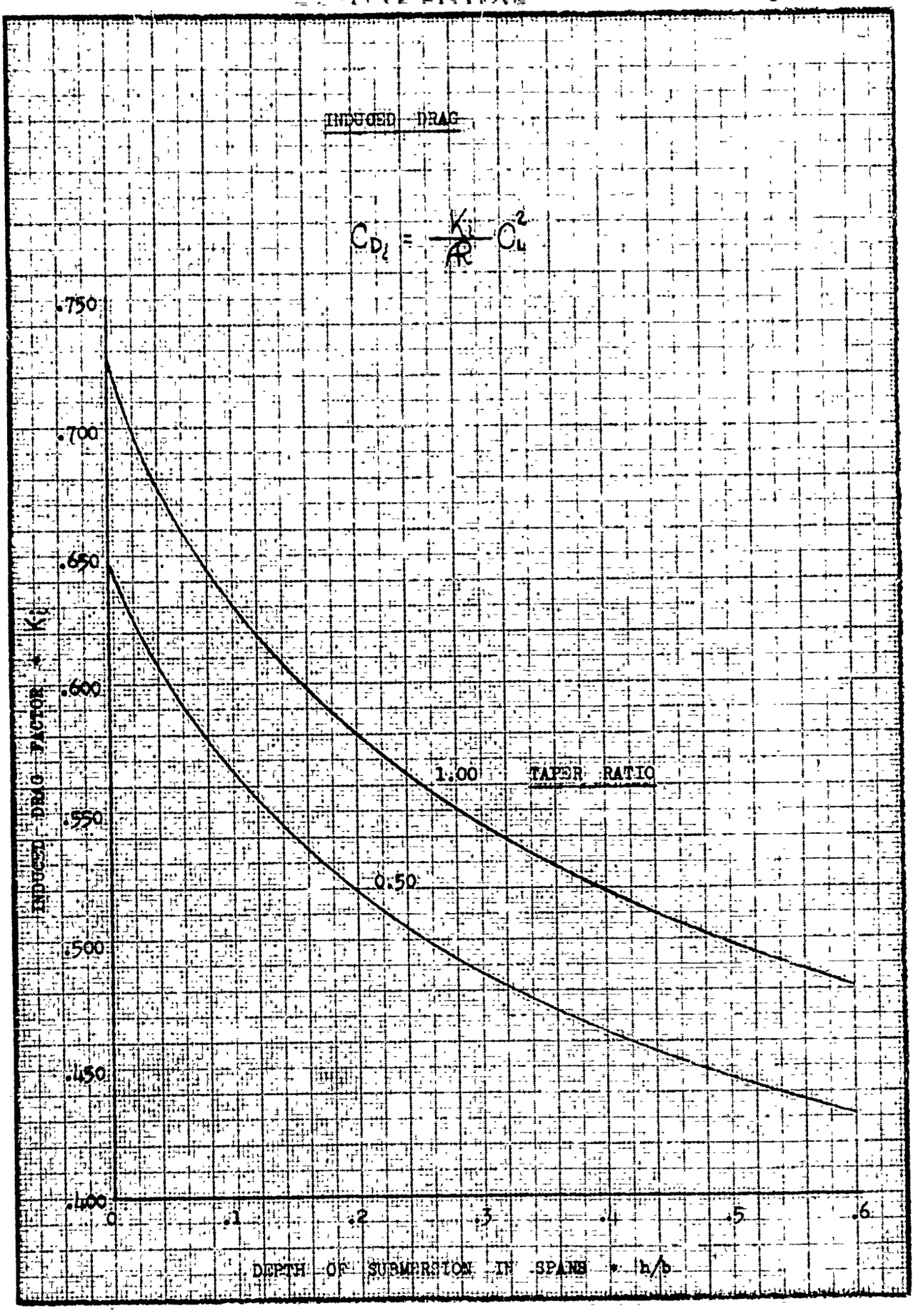

Figure (7)

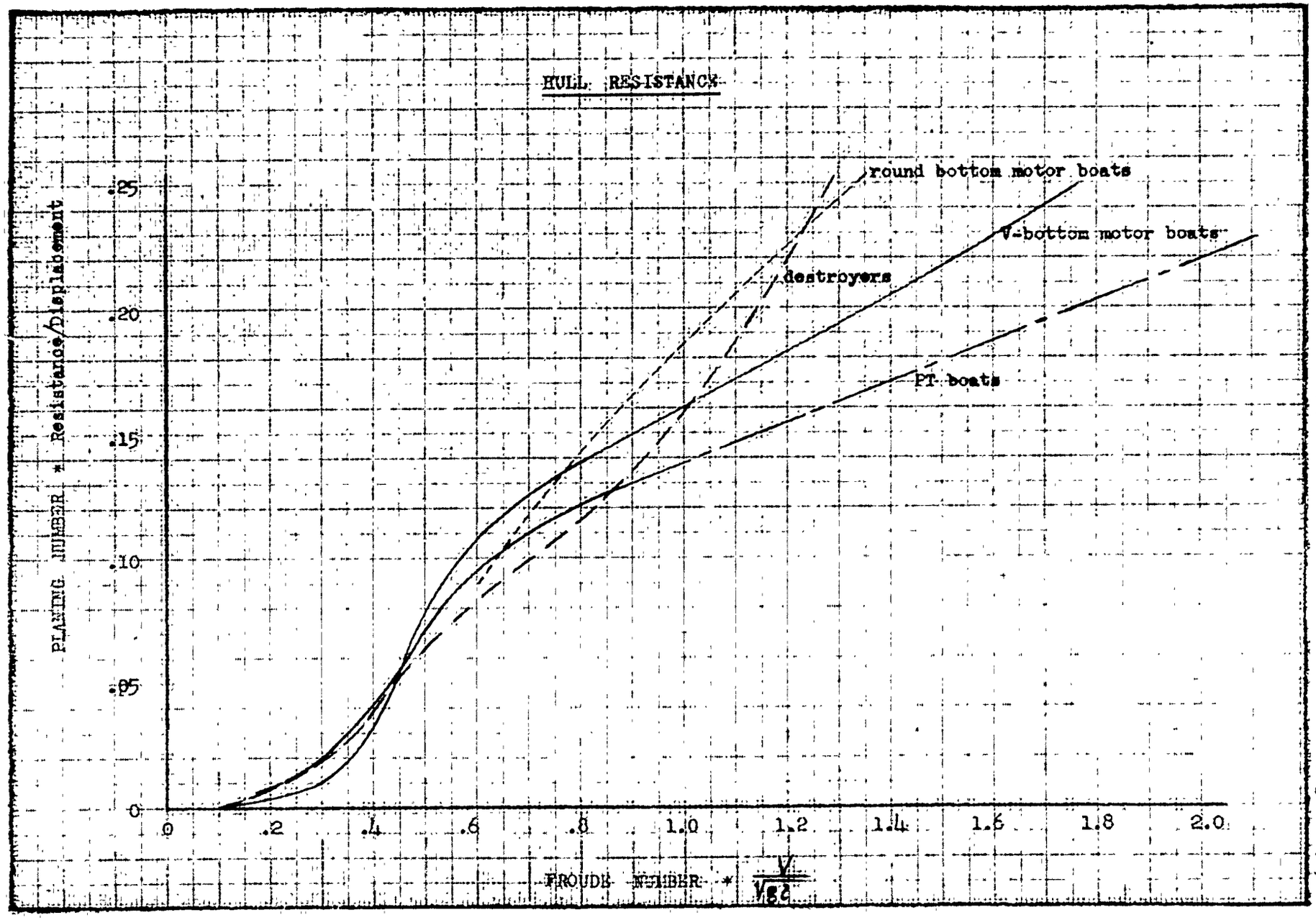
HULL RESISTANCE
round bottom motor boats
V-bottom motor boats
destroyers
PT boats
PLANING NUMBER * Resistance/displacement
.25
.20
.15
.10
.05
0
0
.2
.4
.6
.8
1.0
1.2
1.4
1.6
1.8
2.0
FROUDE NUMBER * V/√gL

Figure (8)

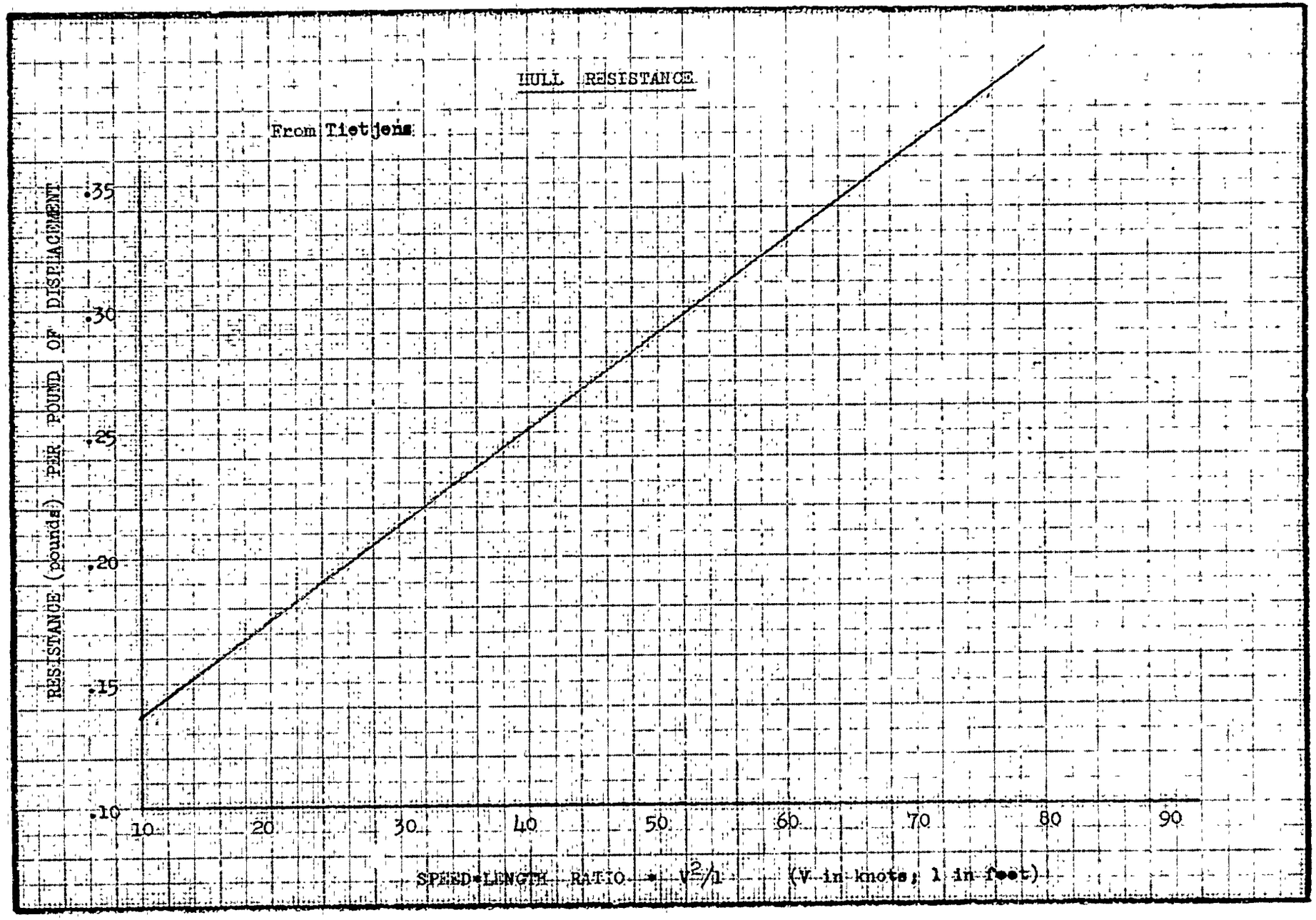

Figure (9)

Figure (9)

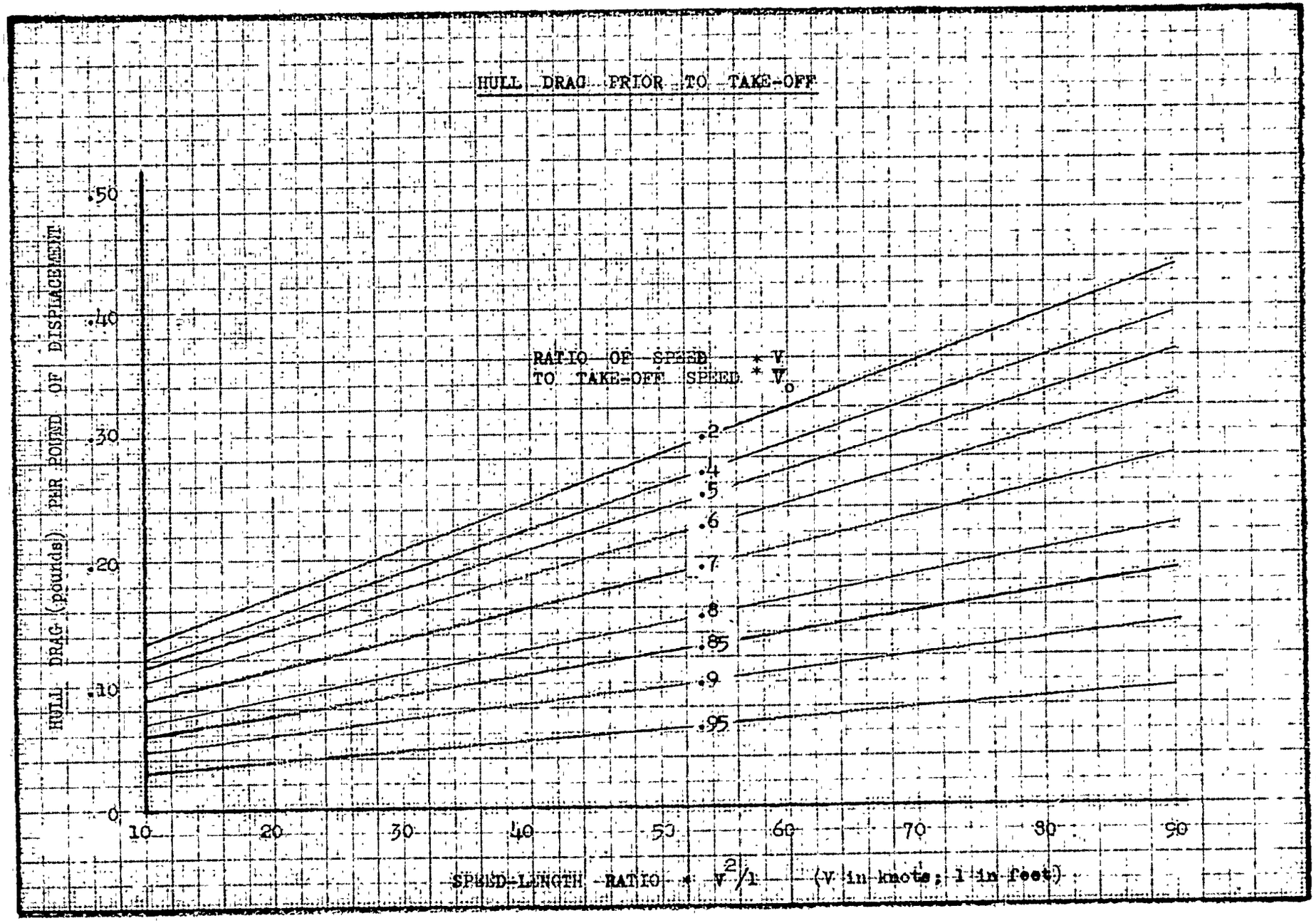

Figure (10)

Figure (10)

KEUFFEL & ESSER CO.
Made in U.S.A.

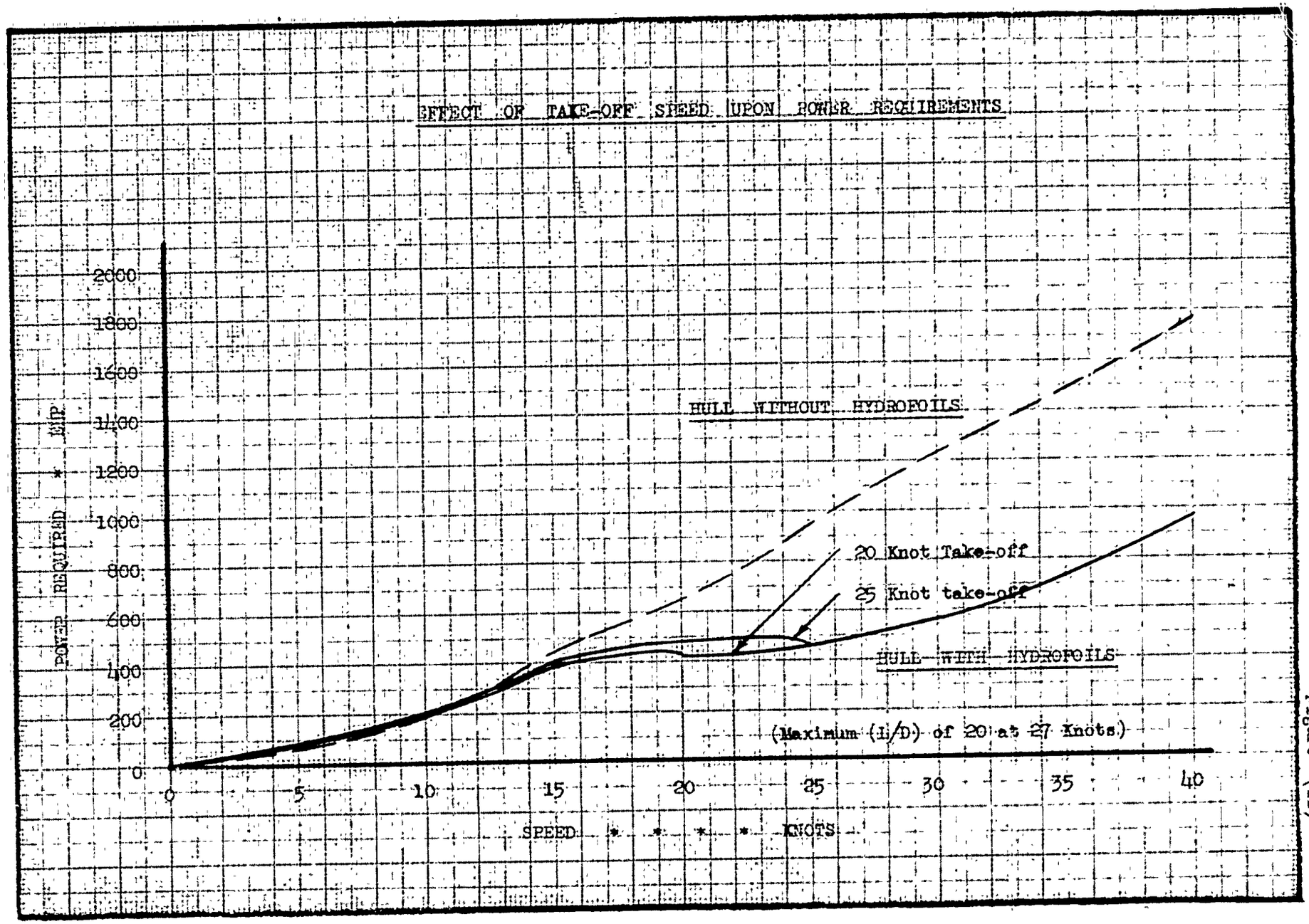

Figure (11)

Figure (11)

CONFIDENTIAL

Figure (12)

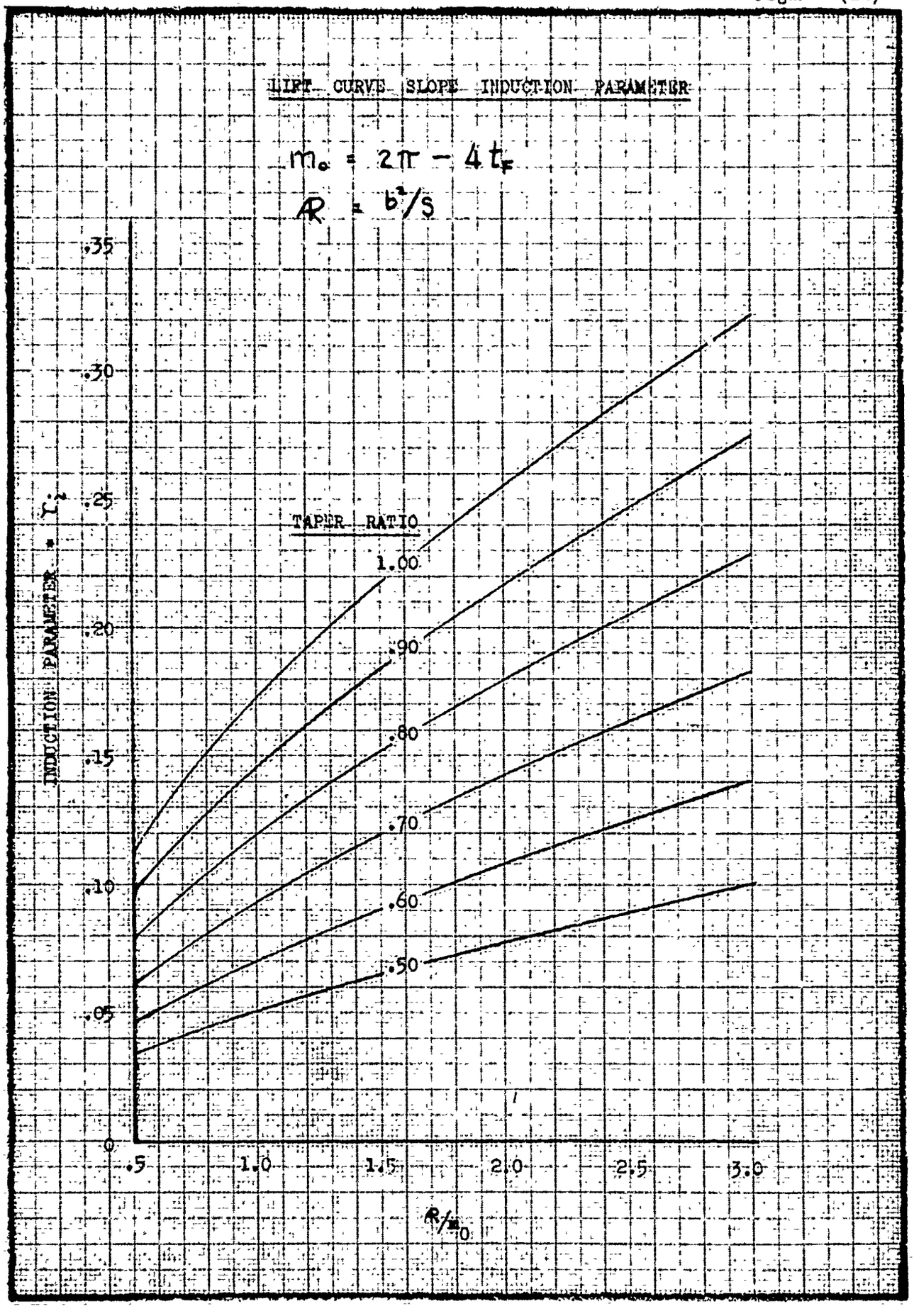

Figure (12)

12 H

CONFIDENTIAL

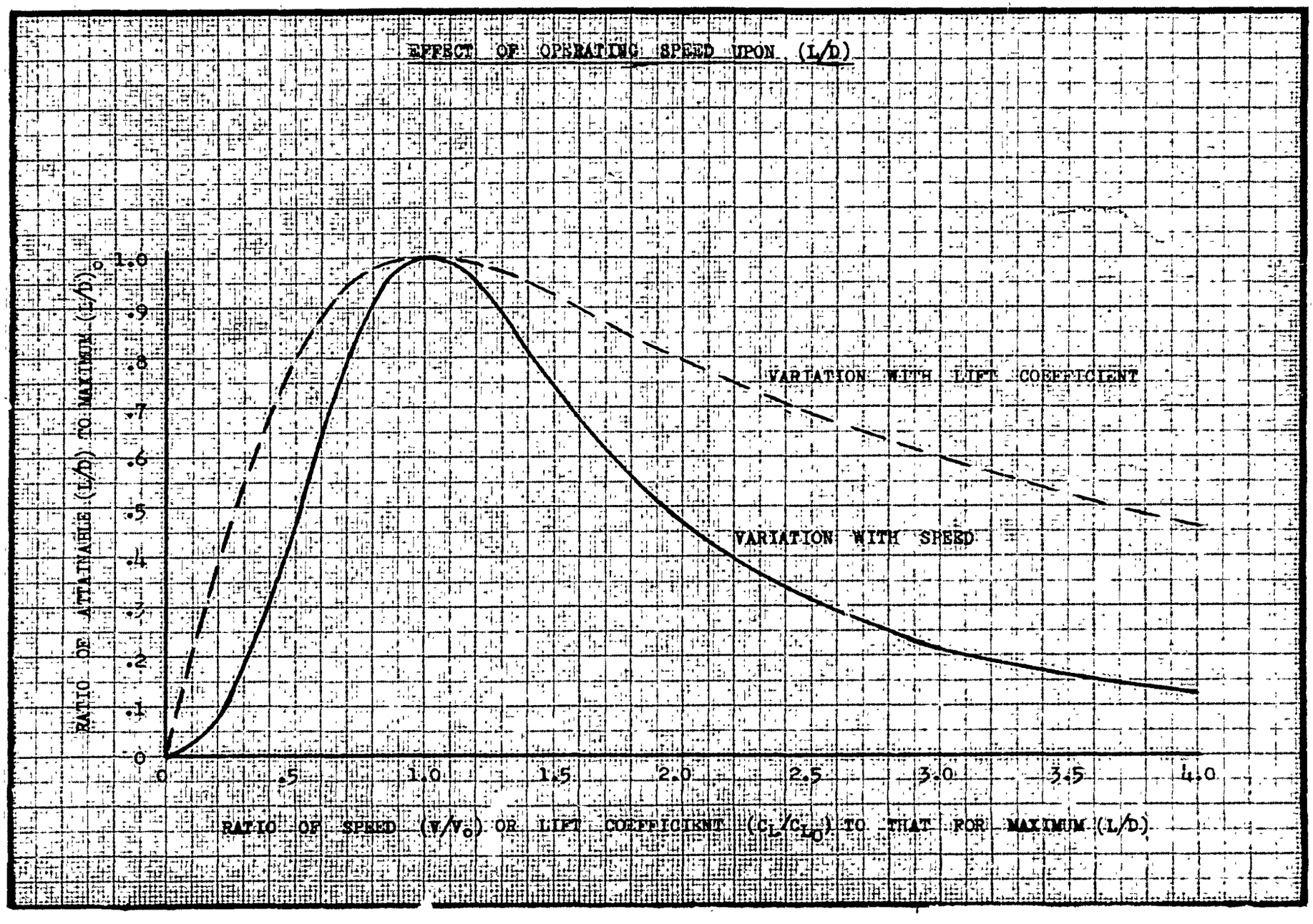

Figure (13)

Figure (13)

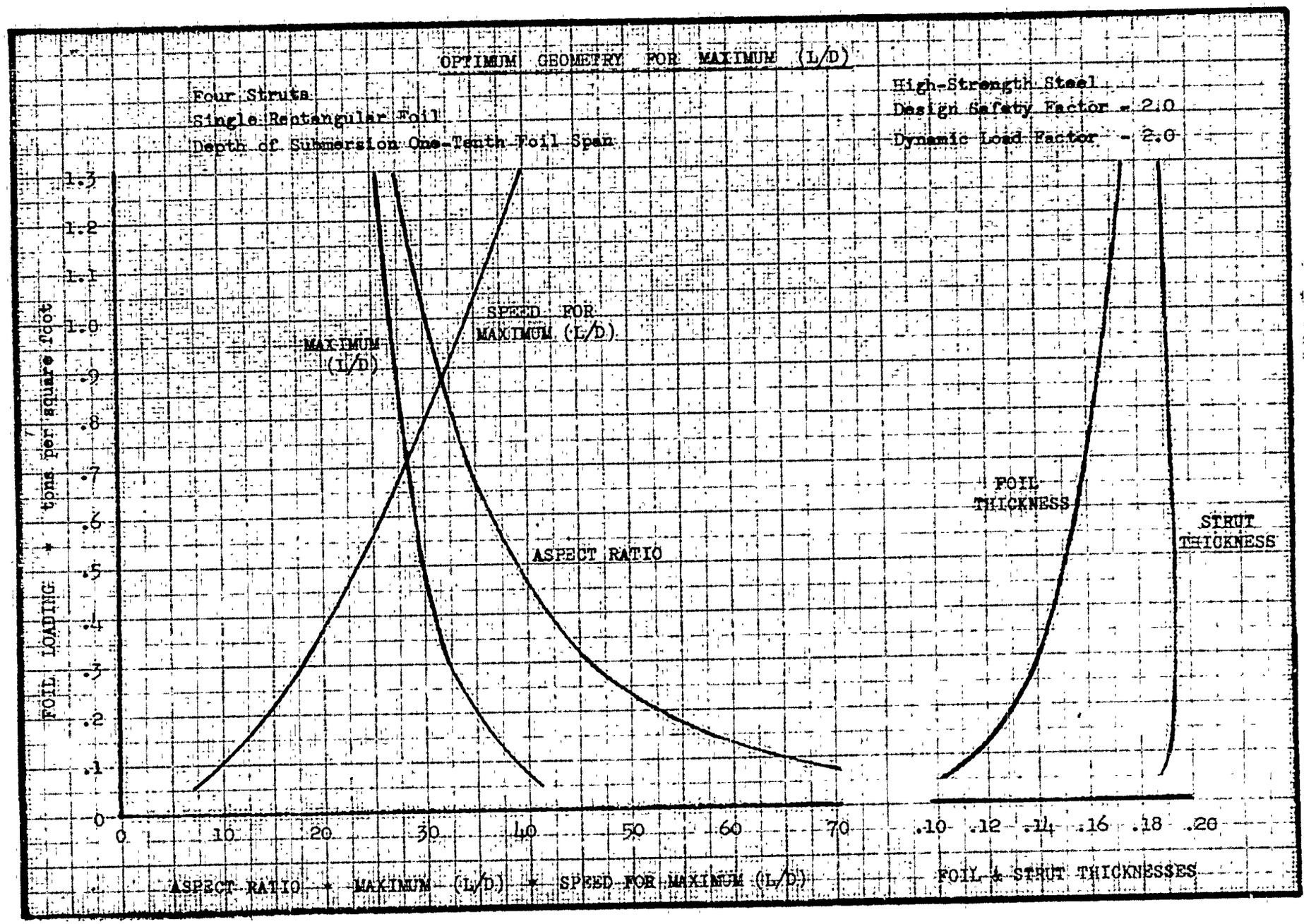

Figure (14)

Figure (14)

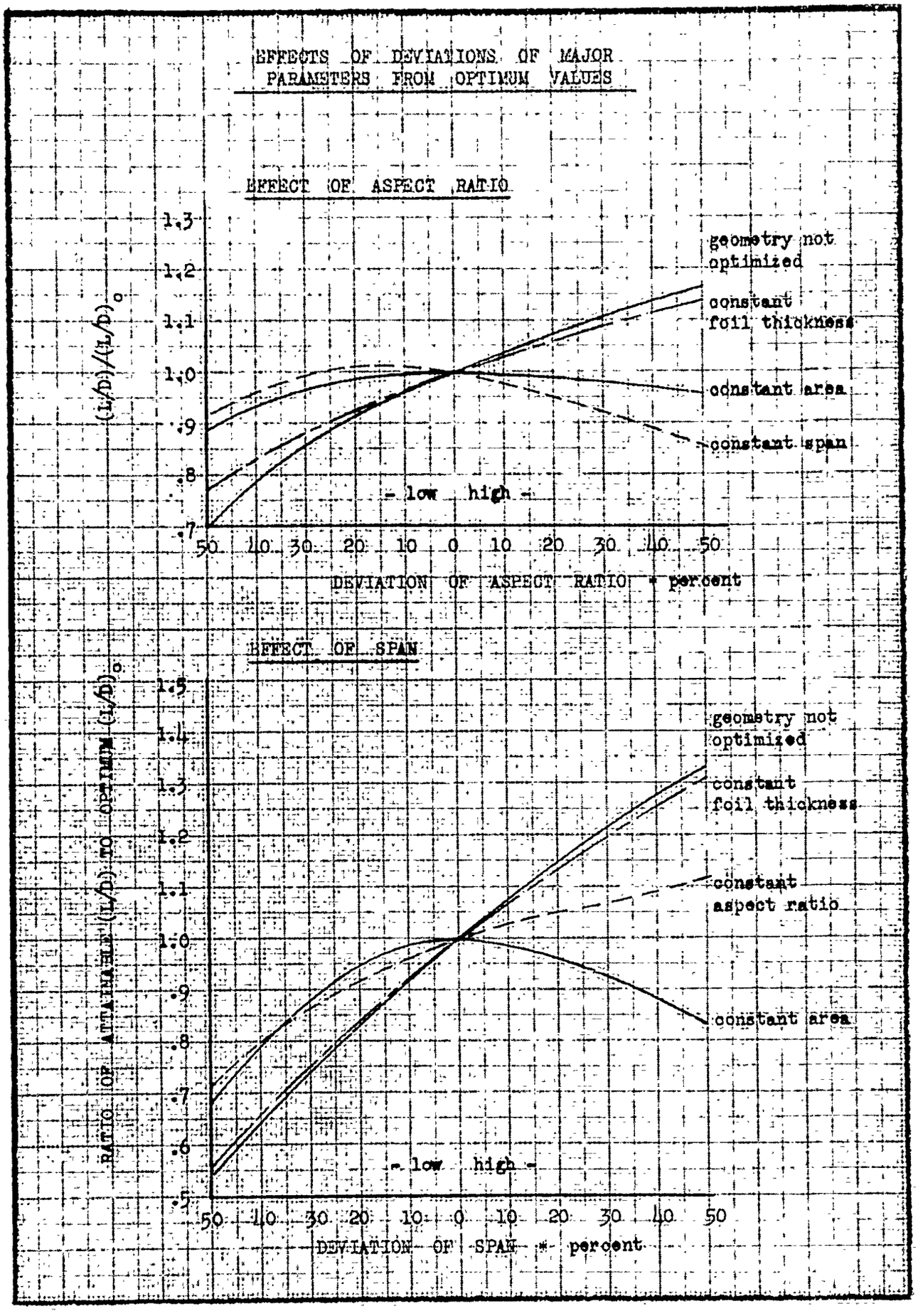
EFFECTS OF DEVIATIONS OF MAJOR PARAMETERS FROM OPTIMUM VALUES
EFFECT OF ASPECT RATIO
RATIO OF ATTAINED (L/D) TO OPTIMUM (L/D)
(L/D)/(L/D)o
1.3
1.2
1.1
1.0
.9
.8
.7
geometry not optimized
constant foil thickness
constant area
constant span
- low high -
50 40 30 20 10 0 10 20 30 40 50
DEVIATION OF ASPECT RATIO * percent
EFFECT OF SPAN
1.5
1.4
1.3
1.2
1.1
1.0
.9
.8
.7
.6
.5
geometry not optimized
constant foil thickness
constant aspect ratio
constant area
- low high -
50 40 30 20 10 0 10 20 30 40 50
DEVIATION OF SPAN * percent

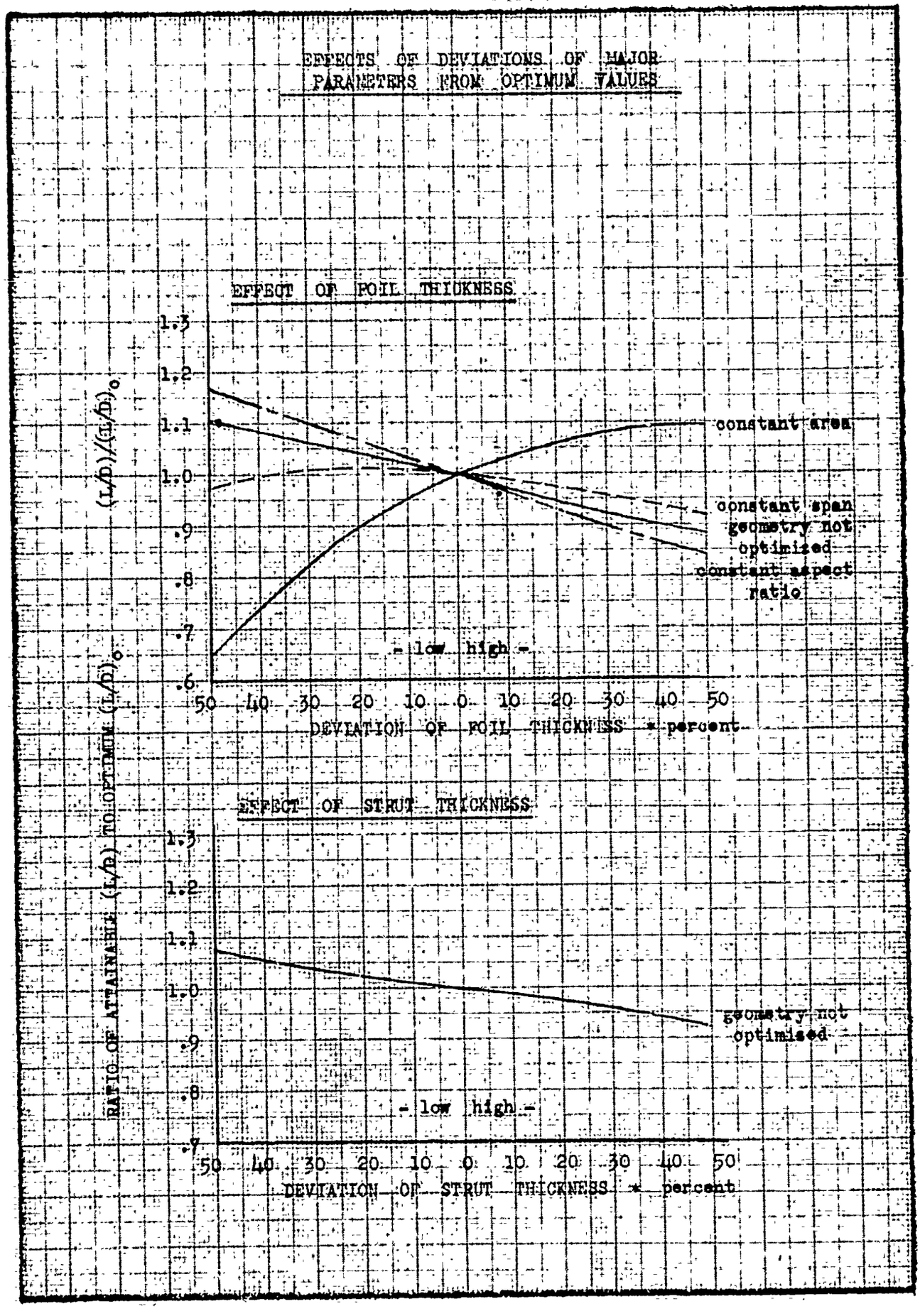
EFFECTS OF DEVIATIONS OF MAJOR PARAMETERS FROM OPTIMUM VALUES
EFFECT OF FOIL THICKNESS
RATIO OF ATTAINABLE (L/D) TO OPTIMUM (L/D)
(L/D)/(L/D)o
1.3
1.2
1.1
1.0
.9
.8
.7
.6
constant area
constant span geometry not optimized constant aspect ratio
- low high -
50 40 30 20 10 0 10 20 30 40 50
DEVIATION OF FOIL THICKNESS - percent
EFFECT OF STRUT THICKNESS
1.3
1.2
1.1
1.0
.9
.8
.7
geometry not optimized
- low high -
50 40 30 20 10 0 10 20 30 40 50
DEVIATION OF STRUT THICKNESS - percent

Figure (19)

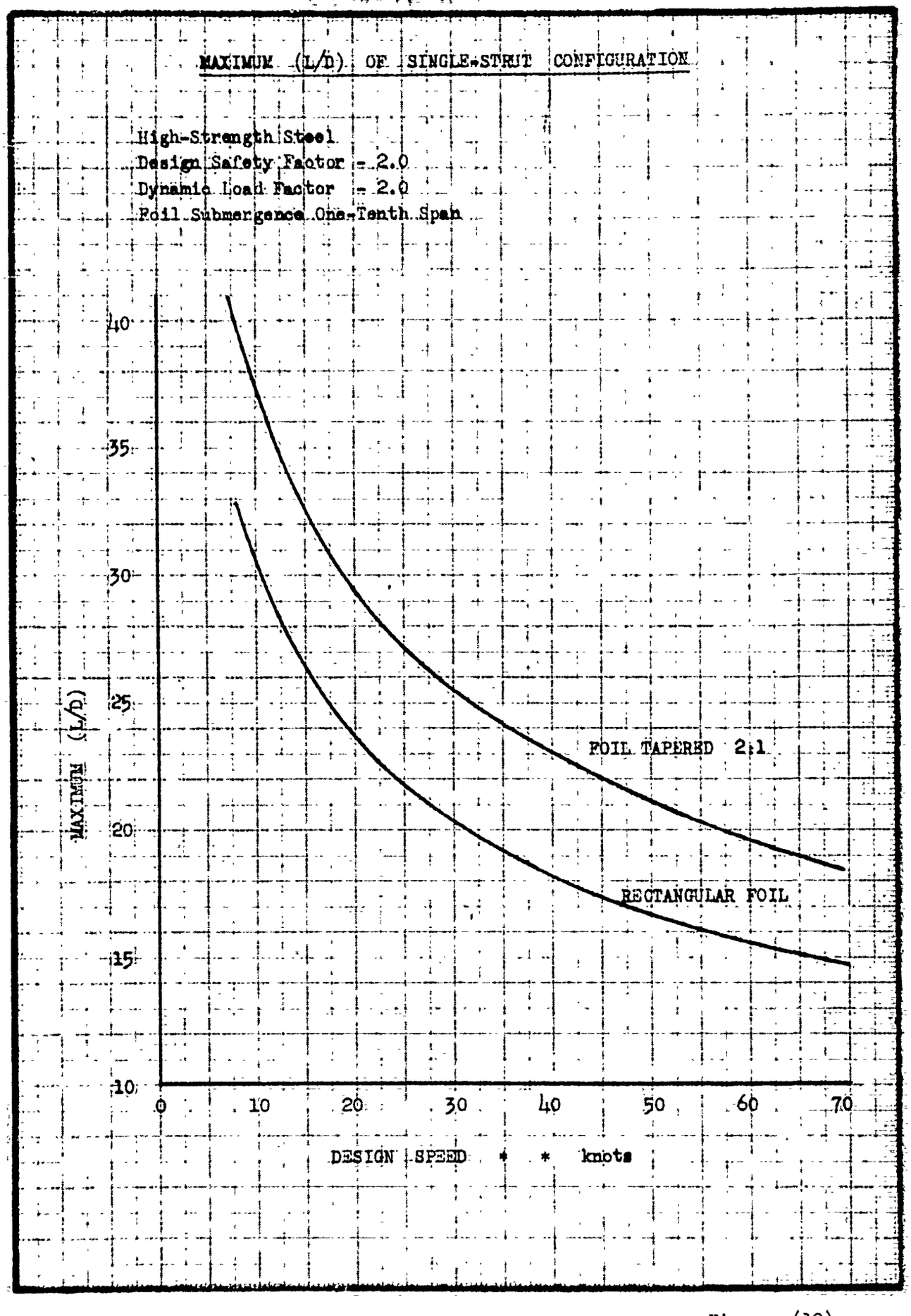

Figure (19)

Figure (20)

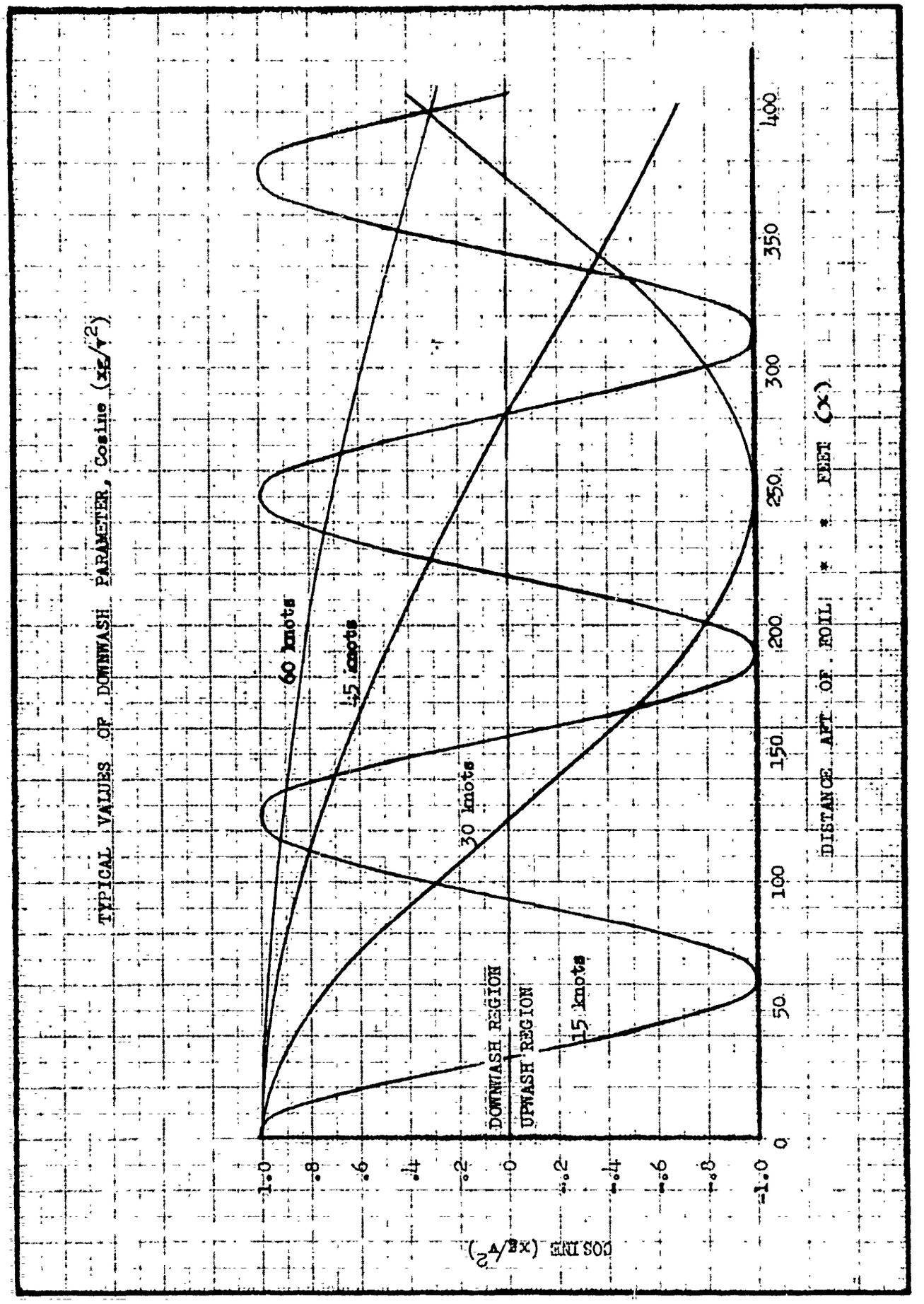

Figure (20)

Figure (21)

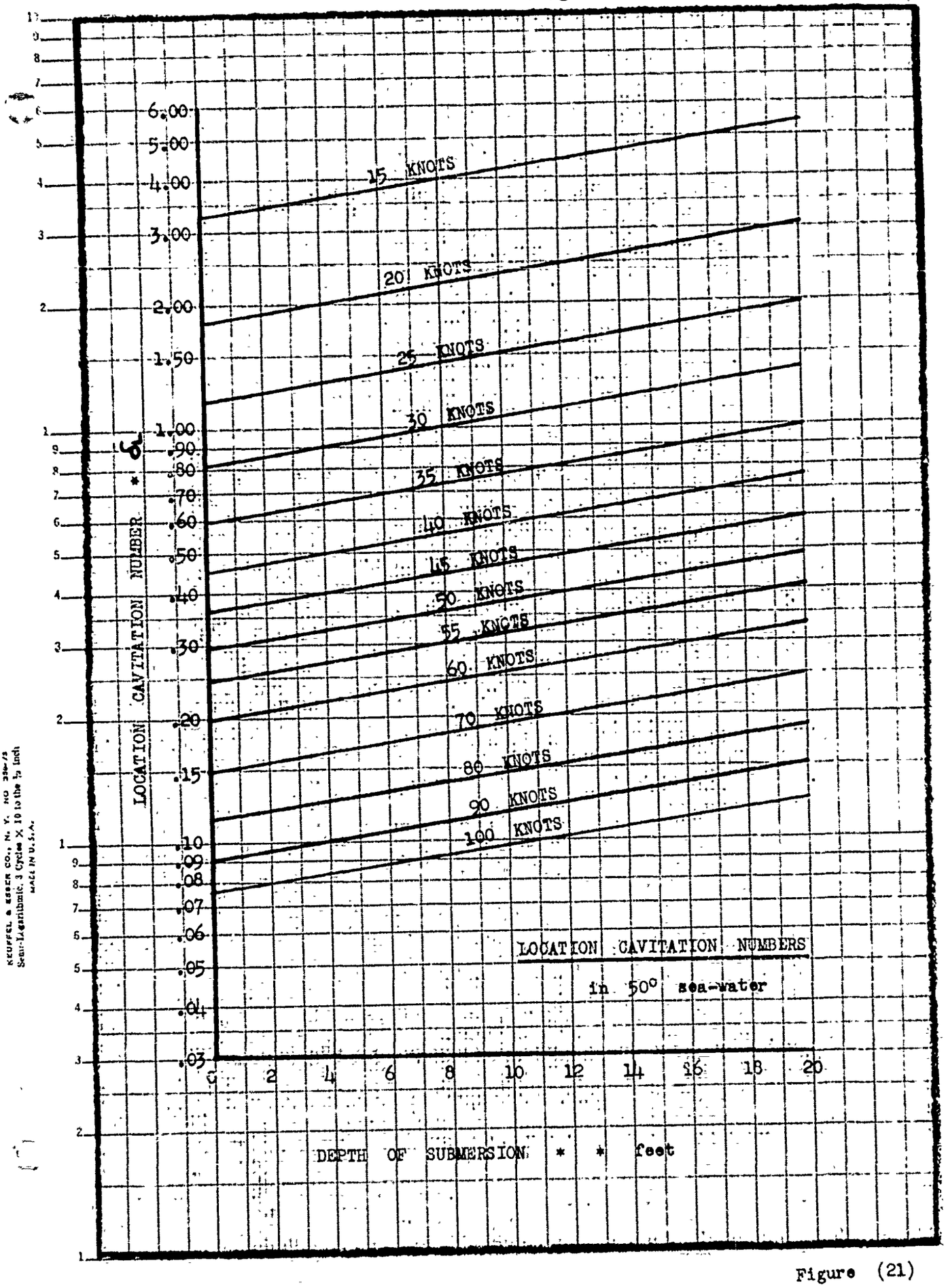

KEUFFEL & ESSER CO., N. Y. NO 358-23
Semi-Logarithmic, 3 Cycles X 10 to the ½ Inch
MADE IN U.S.A.

Figure (21)

194

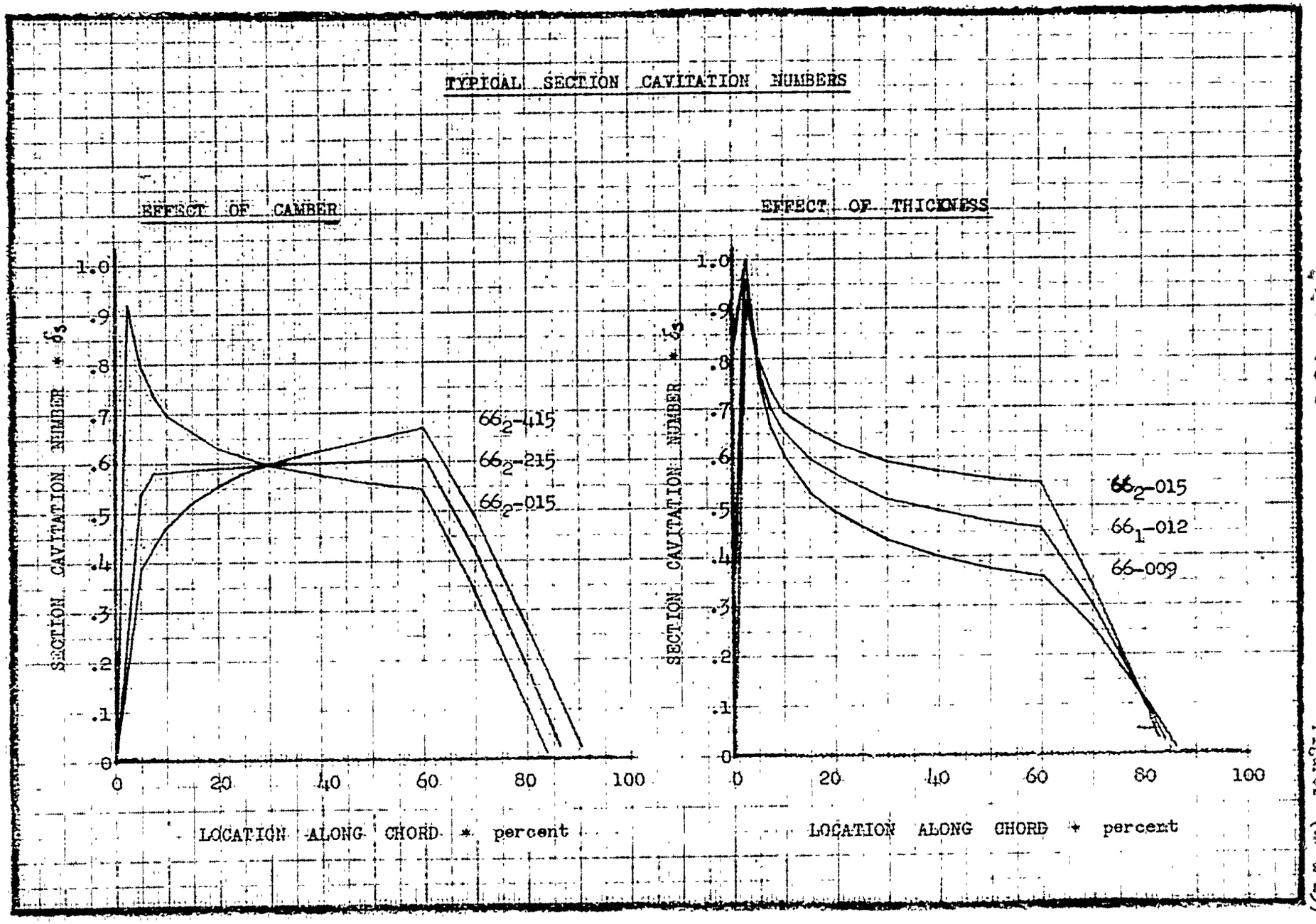

Figures (22 & 23)

Figure (22 & 23)

Figure (24)

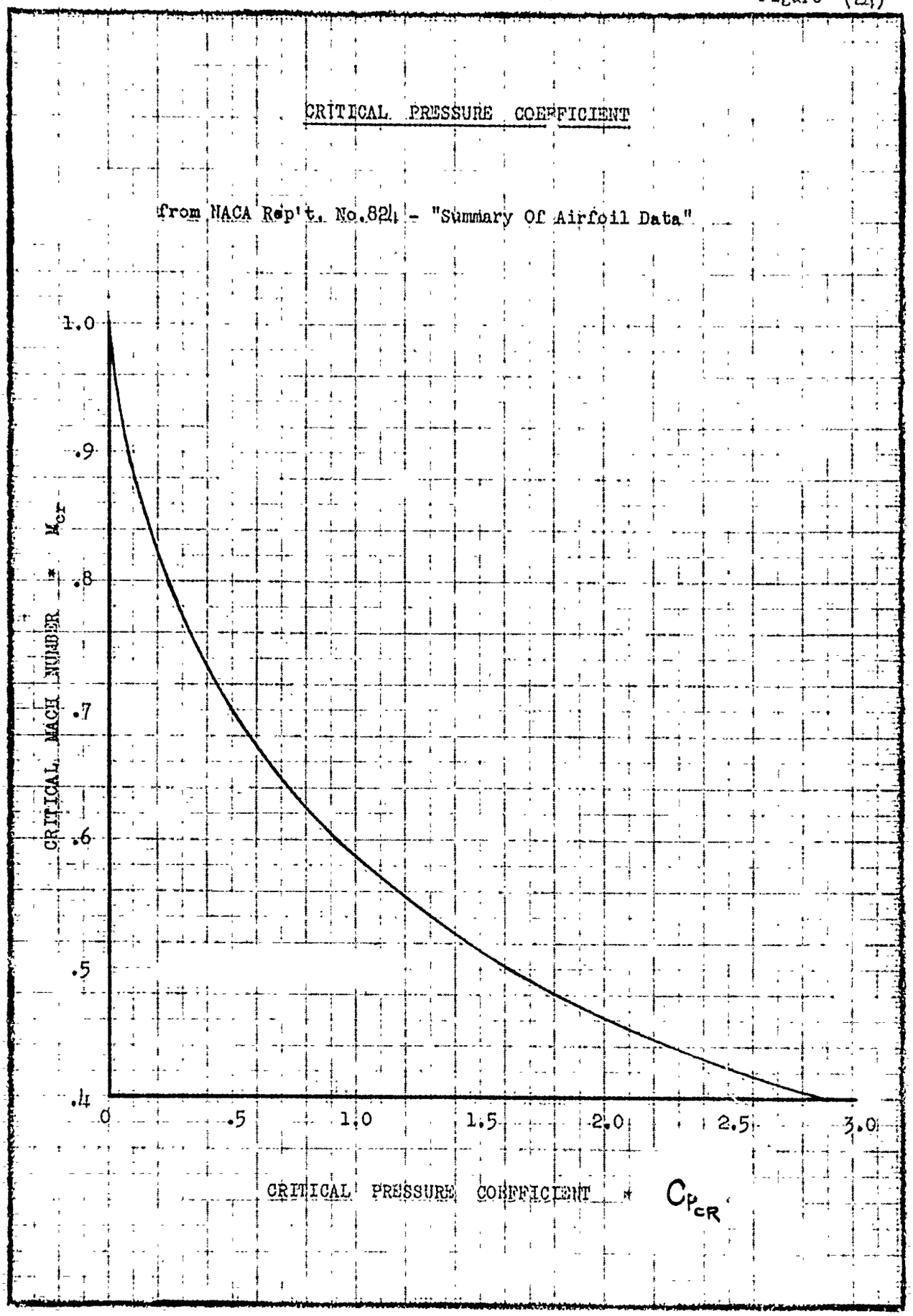

Figure (24)

24

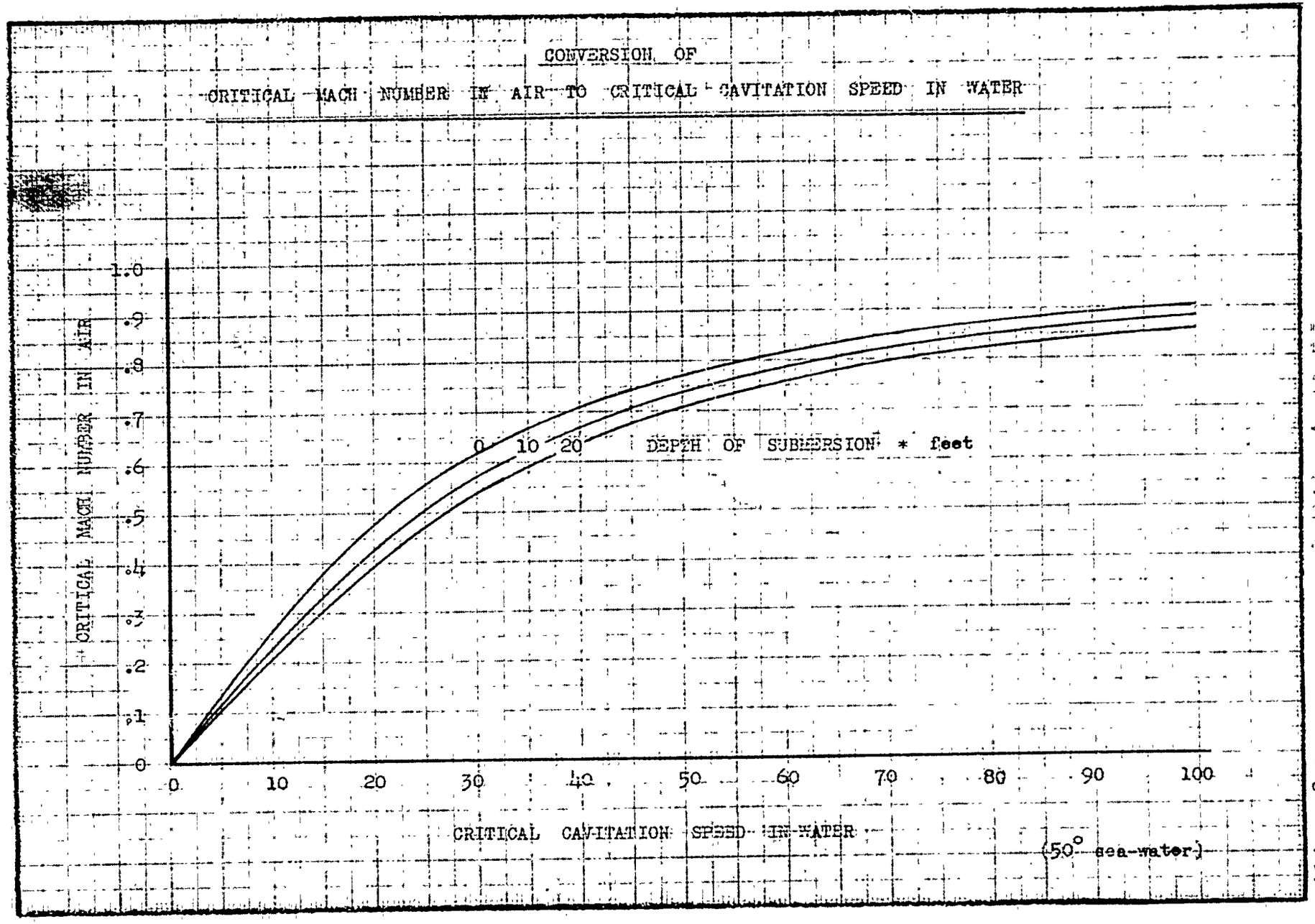

Figure (25)

Figure (25)

Figure (26)

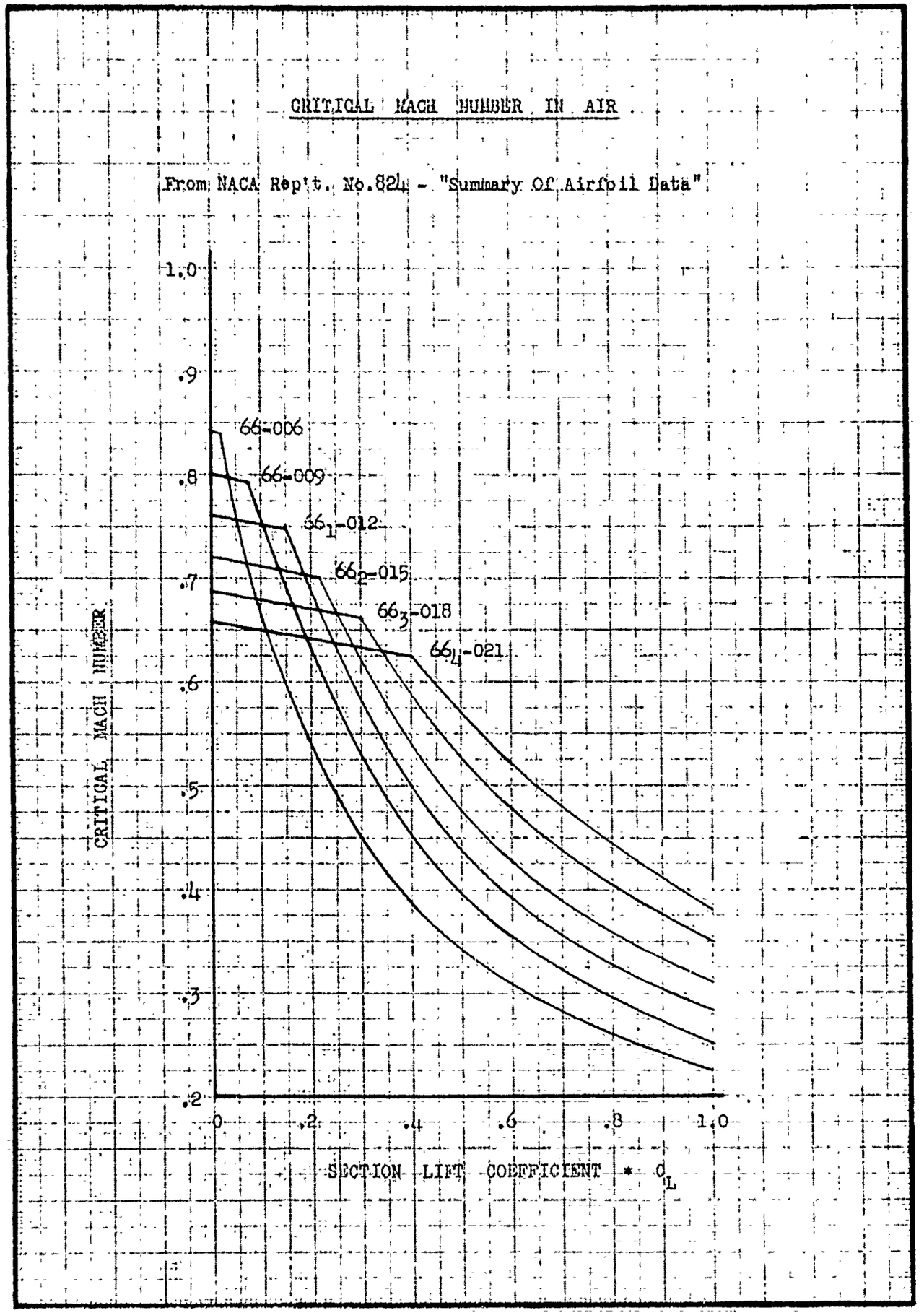

Figure (26)

2311

CONFIDENTIAL

Fig ure (27)

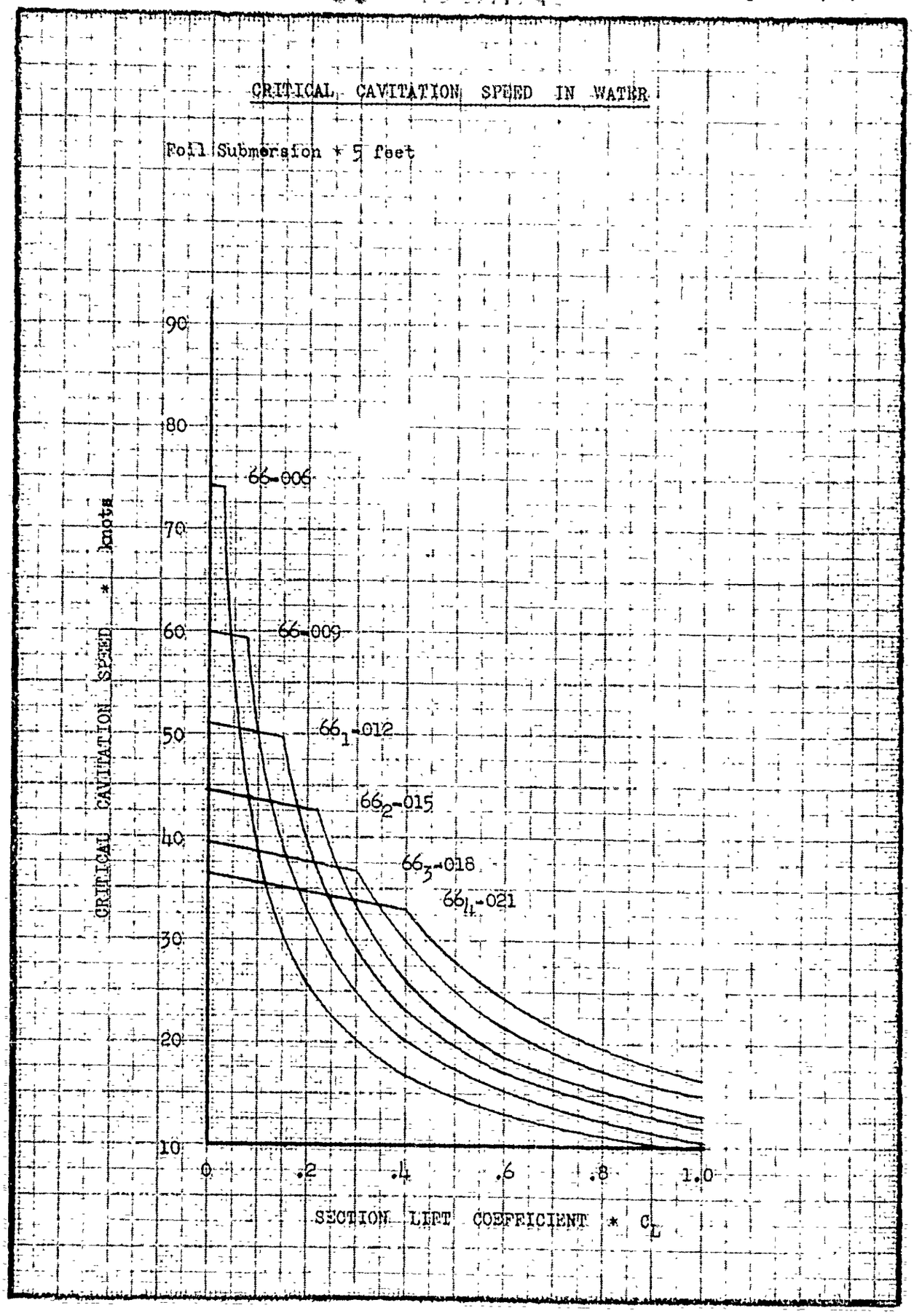

Figure (27)

Figure (28)

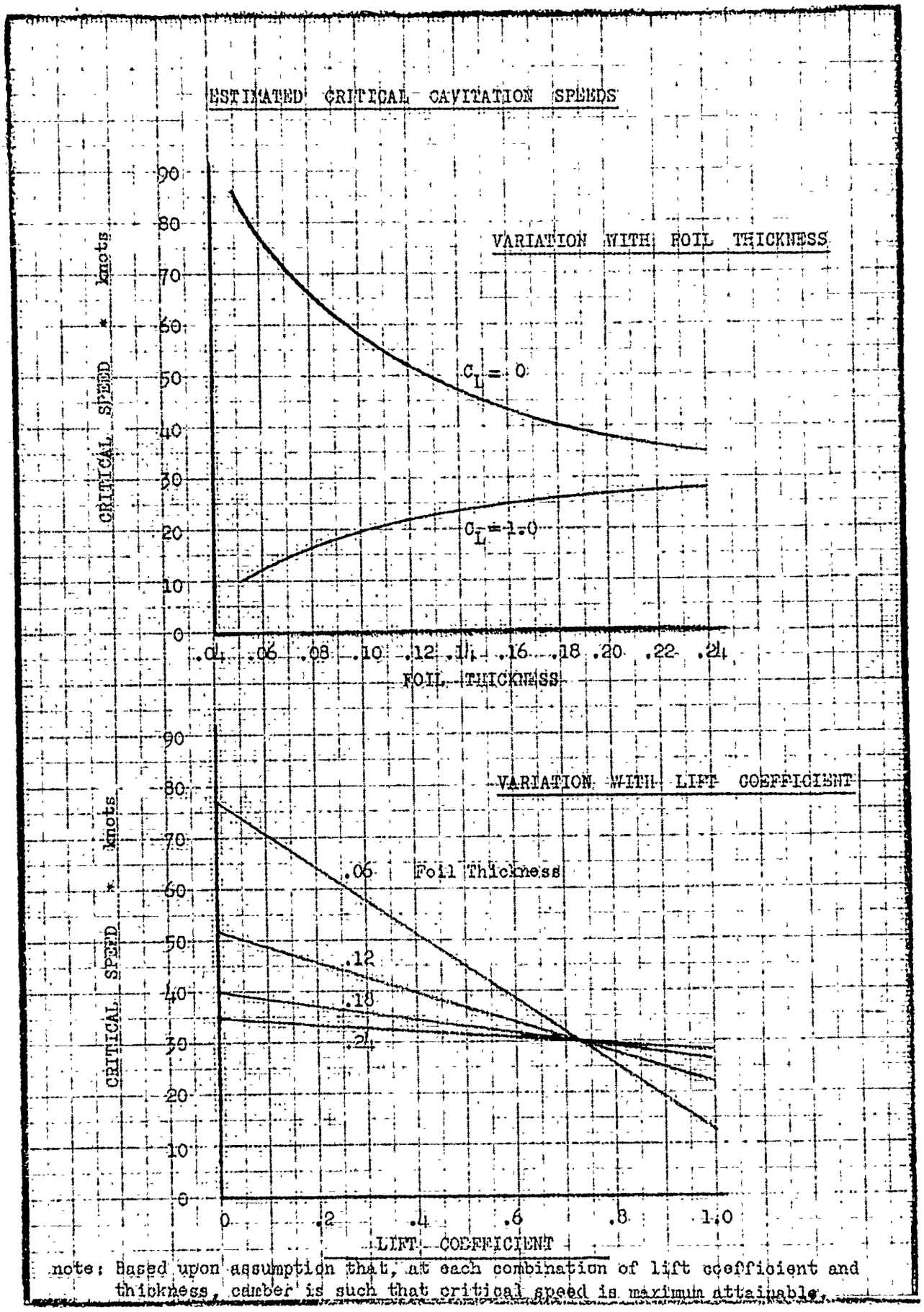

note: Based upon assumption that, at each combination of lift coefficient and thickness, camber is such that critical speed is maximum attainable.

Figure (28)

C O N F I D E N T I A L

A STRUCTURAL PRELIMINARY DESIGN INVESTIGATION CONCERNING STRUT & HYDROFOIL CONFIGURATIONS OF HYDROFOIL CRAFT

June 1950

Edmund G. Wodrich

Contract No. N9onr-93201

TABLE OF CONTENTS

STRUCTURES SECTION

Item	Page
List of Figures	iv
INTRODUCTION	1
Scope	2
Other Configurations	2
DEFINITIONS AND SYMBOLS	3
SECTION PROPERTIES	9
LOADING CRITERIA	13
Load Distribution (Hydrofoils & Struts)	13
Loading Conditions (Limit Load Factors)	14
Factor of Safety	14
CONFIGURATIONS (General)	15
Considerations	15
Hydrofoils	17
Governing Stresses	18
Shear	18
Torsion	18
Flaps	18
Bending Stress	19
Mono-Strut	20
Single-Bay Bent with Overhang	21
Multi-Bay Bent with Overhang	21
Bending Deflection	30
Tapered Beam and Varying Loading	30
Constant Beam and Constant Loading	33
Constant Beam and Varying Loading	34
Tapered Strut and Concentrated Load	36
Hydrofoil Deflection Formulae	37

Item	Page
Struts and Columns	48
Column Inaccuracies	48
Slenderness Ratios	49
End Fixity	50
Concentric Loading	50
Uniform Strut	51
Tapered Strut	57
Effect of Modulus of Elasticity	59
Eccentric Loading	64
Side Loading	70
Hydrofoil-Strut Combinations	77
Table I. Hydrofoil Strut Configurations.	78
Table II. Hydrofoil Strut Configurations.	79
Sample Calculations	80
Frames	83
Single-Bay Bent, Symmetrical Loading	83
Double-Bay Bent, Symmetrical Loading	85
Single-Bay Bent, Asymetrical Loading	86
STRUCTURAL CONSTRUCTION CONSIDERATIONS	88
REFERENCES	90
APPENDIX I. EFFECT OF CHANGE FROM SOLID TO HOLLOW SECTIONS	92
APPENDIX II. EFFECT OF TORSION ON HOLLOW HYDROFOILS	96

LIST OF FIGURES

Fig. No.	Title	Page
1	Biconvex Parabolic Arc Section	9
2	Moments of Inertia of Solid Biconvex Parabolic Arc Section	11
3	Moments of Inertia of Biconvex Parabolic Arc Sections with 0.5 Inch Thick Walls	12
4	Single Bent with Overhang	21
5	Variation of Minimum Permissible Hydrofoil thickness Ratio with Limit Loading, Aspect Ratio, Taper Ratio, Dihedral, and Factor of Safety	23
6	Variation of Permissible Hydrofoil Loading with Aspect Ratio and Allowable Bending Stress . .	24
7	Permissible Variation of Hydrofoil Percent Thickness with Aspect Ratio for Rectangular Planform	25
8	Permissible Variation of Hydrofoil Percent Thickness with Aspect Ratio for Planform Taper Ratio of 0.75	26
9	Permissible Variation of Hydrofoil Percent Thickness with Aspect Ratio for Planform Taper Ratio of 0.50	27
10	Variation of Hydrofoil Bending Stress with Aspect Ratio for Three Hydrofoil Thickness Ratios	28
11	Variation of Permissible Hydrofoil Loadings with Aspect Ratio for Three Different Hydrofoil Thickness Ratios	29
12	Geometry of Tapered Hydrofoil	31
13	Trapezoidal Load Distribution	34
14	Tapered Strut, Constant Load	36
15	Tip Deflection Ratio for Mono-Strut Configuration	40

Fig. No.	Title	Page
16	Tip Deflection Ratio for Mono-Strut Configuration	41
17	Hydrofoil Tip Deflection Ratio for Mono-Strut Configuration with Rectangular Planform and 1.0 ksf Hydrofoil Loading	42
18	Hydrofoil Deflection Ratio for Tip of Overhang on Two-Strut Configuration with Rectangular Planform and 1.0 ksf Hydrofoil Loading	43
19	Hydrofoil Deflection Ratio at Center of Span for Two-Strut Configuration with Rectangular Planform and 1.0 ksf Hydrofoil Loading	44
20	Hydrofoil Deflection Ratio at Tip of Overhang for Three-Strut Configuration with Rectangular Planform and 1.0 ksf Hydrofoil Loading	45
21	Hydrofoil Deflection Ratio at Midpoint between Struts for Three-Strut Configuration with Rectangular Planform and 1.0 ksf Hydrofoil Loading	46
22	Maximum Deflection at Center of Span of Three Strut Configuration	47
23	Variation of Minimum Permissible Strut Thickness Ratio with Hydrofoil Limit Loading & Geometry .	52
24	Variation in Strut Thickness Ratio with Hydrofoil Aspect Ratio for Six Different Hydrofoil Loadings of a Mono-Strut Configuration	53
25	Variation in Strut Thickness Ratio with Hydrofoil Aspect Ratio for Six Different Chord Ratios of a Mono-Strut Configuration	54
26	Variation in Strut Thickness Ratio with Hydrofoil Aspect Ratio for Six Different Strut Lengths of a Mono-Strut Configuration	55
27	Variation in Minimum Strut Thickness Ratio with Hydrofoil Loading for Various Aspect Ratios of a Mono-Strut Configuration	56
28	Tapered Strut	57

Fig. No.	Title	Page
29	Determination of Strut Geometry from Concentric Strut Load for Solid Biconvex Parabolic Arc Sections	60
30	Determination of Strut Geometry from Concentric Strut Load for Solid Biconvex Parabolic Arc Sections	61
31	Variation in Strut Thickness Ratio with Strut Chord for Center Strut of a Three-Strut Configuration	62
32	Variation of Strut Chord with Minimum Strut Thickness Ratio for Six Different Strut Lengths at a Slenderness Ratio of 140	65
33	Variation of Strut Chord with Minimum Strut Thickness Ratio for Various Strut Lengths at a Slenderness Ratio of 120	66
34	Variation of Strut Chord with Minimum Strut Thickness Ratio for Various Strut Lengths at an Effective Slenderness Ratio of 120	67
35	Critical Buckling Load for Solid Biconvex Strut of Mild Steel with 12-inch Chord	68
36	Critical Buckling Load for Solid Biconvex Strut of Fibreglas with 12-Inch Chord	69
37	Variation in Allowable Eccentricity of Axial Load with Strut Chord for Several Different Strut Thickness Ratios (20 Kip Axial Load) . .	71
38	Variation in Allowable Eccentricity of Axial Load with Strut Chord for Several Different Strut Thickness Ratios (25 Kip Axial Load) . .	72
39	Variation in Allowable Eccentricity of Axial Load with Strut Chord for a 15 Percent Thick Biconvex Solid Strut	73
40	Variation in Allowable Eccentricity of Axial Load with Strut Chord for an 18 Percent Thick Biconvex Solid Strut	74
41	Strut under Combined Loading	70

Fig. No.	Title	Page
42	Variation in Maximum Strut Bending Stress with Strut Chord for a Two-Strut Configuration under Combined Axial and Side Loads	75
43	Variation in Maximum Strut Bending Stress with Strut Chord for a Two-Strut Configuration under Combined Axial and Side Loads	76
44	Three-Strut Configuration with Uniform Loading	80
45	Single Bent, Symmetrical Loading	83
46	Single Bent, Forces and Moments	84
47	Double-Bay Bent, Symmetrical Loading	85
48	Single Bay Bent, Side Loading	86
49	Variation of Thickness Ratio for Hollow Sections with Thickness Ratio for Solid Sections with Several Chord Ratios to Give Equal Beam Bending Strength	94
50	Variation of Equivalent Hollow Strut Percent Thickness with Solid Strut Percent Thickness to Support Identical Loads	95

INTRODUCTION

The main objective of this contract, as stated in a preceding section, is to procure general preliminary design data for hydrofoil configurations that may be used in the design of hydrofoil craft, said designs to produce the greatest possible lift-drag ratio. For that reason and because experience is limited, the initial structural investigation on this hydrofoil project differs to some extent from the preliminary design investigation of a new type aircraft or surface vessel.

The structural investigation to obtain such preliminary design data is not primarily interested in the vessel's complete configuration, but the structural study is concerned with the particular configurations of the column-foil arrangements for any single unit. In other words, it isn't of any immediate structural interest whether the vessel's configuration obtains two, equal, tandem, column-foil arrangements; an auxiliary foil forward; or an auxiliary foil aft. The load distribution among the foils is also not of primary structural interest in the initial studies.

To obtain high lift-drag ratios, the aspect ratio and hydrofoil thickness ratio are of utmost importance. Likewise, these two items are of primary importance from the structural point of view. A high aspect ratio is of greater importance to hydrofoils which are to operate at large lift coefficients than for the hydrofoils which are to operate at low lift coefficients (see Hydrodynamics section). Thus, the aspect ratio and thickness ratio which are physically possible become functions of the type of loading which is assumed on the column-hydrofoil configuration. Also, they are a function of the mechanical properties of the materials from which they are to be fabricated. To a lesser extent, the aspect ratio and thickness ratio are functions of any auxiliary control device which is to be installed on the columns, struts or foils.

To obtain the highest possible lift-drag ratios, it also becomes requisite to submerge the foil to as great a depth below the water surface as is structurally permissible without increasing its thickness or chord (see Hydrodyanmics section for discussion of this). The distance from the water surface to the keel is a function of the wave conditions in which the ship is intended to operate. These two items have important bearings upon the struts and bents, as will be seen later.

At the outset, certain physical sizes are needed to permit the initial preliminary hydrodynamic estimates to be made. It was necessary, therefore, to determine quickly the likely ranges of sizes for struts and hydrofoils, using economically the various

structural materials. To this end the first series of charts and tables were prepared. As the project progressed, certain of the initial assumptions were found to need modification and some of the configurations were found unusable.

The approach to the problem is in a step-by-step fashion, commencing with the most elementary configuration. Many of the initial charts, figures, and tables remain useful in reaching the final design configuration. For that reason, the selections of the parameters which are used in the charts are based upon the order in which data are obtained in commencing any preliminary design.

The structural considerations are directed mainly to the hydrofoils and struts. Then considerations are given to available materials and methods of fabrication and to strength for control surfaces.

Scope:

Most hydrofoil-strut arrangements may be classed as single-foil and multi-foil, or as single-strut and multi-strut arrangements. The single-foil arrangements have been selected for the scope of this structural investigation. This consideration is based in part upon the short period of time available to investigate all possible configurations. It is also based upon the fact that the single-foil arrangement will eliminate great changes in load factor when passing through waves, will reduce interference effects, eliminate biplane effects and appears to possess less structural difficulties.

Other Configurations:

German experience (Ref.1) indicates that hydrofoils with dihedral were more satisfactory than hydrofoils with a circular spanwise shape . However, the circular spanwise shape was not tried with multi-struts, which would give a scalloped effect.

The use of this shape, with concomitant haunching, may permit a hydrofoil of less thickness than encountered with a flat hydrofoil. The total wetted area of strut and hydrofoil for any given depth of submersion would be less. It would work in reverse to that of the catenary configuration which has been proposed by Dr. V. Bush(1). But, like the catenary, the disadvantage of contouring a section with a curvature in span exists. A means of reducing deflection and racking moments in the bents would be to use gabled bents with inward sloping struts. These configurations are worthy of further consideration, but at the beginning, it is felt necessary to concentrate entirely on one configuration until that one has been thoroughly explored.

(1) Memo dated 15 Oct. 1949 from Paul Scheror to W. C. Ryan.

DEFINITIONS & SYMBOLS

The symbols and terms used in this Structures section are defined below. No rigid set of axes is adhered to in this report. The X and Y axes are used for the principal axes of both the struts and hydrofoils. However, where the complete set of axes are used, the right hand system is used: (see Fig. 12). The X-axis being positive aft, the Y-axis being positive up, and the Z-axis being positive from the centerline toward the left hand side.

A = $4E\Theta_A$ = constant in slope deflection equation.

A_{A_B} = aspect ratio of member "AB".

A_F = $\frac{b^2}{S}$ = hydrofoil aspect ratio (b & S are in same units).

A_{F_M} = aspect ratio of tapered planform mono-strut hydrofoil configuration with hydrofoil taper ratio of 0.5.

A_{F_r} = aspect ratio of rectangular planform mono-strut hydrofoil configuration.

A_m = mean inclosed area of a hollow section of regular shape, square inches.

A_o = cross section area of section under consideration.

A_s = $\frac{2}{3}\tau_o c^2$ = cross section area of biconvex parabolic arc section, square inches.

B = $4E\Theta_B$ = constant in slope deflection equation.

C = $4E\Theta_C$ = constant in slope deflection equation.

C_N = $\frac{\text{Normal Force}}{q\,S}$ = foil normal force coefficient.

E = modulus of elasticity, ksi.

E_r = reduced modulus, ksi.

E_t = tangent modulus, ksi.

F = factor of safety.

F_b = allowable bending stress of the material, ksi (modulus of rupture in bending).

F_{st} = modulus of rupture in torsion, ksi.

FM = fixed end moment, kip-inches.

G = modulus of rigidity in shear, ksi.

H = horizontal force at base of bent, kilopounds.

I = section moment of inertia, inches^4.

$I_x = \frac{4}{105} \tau_o^3 c^4$ = moment of inertia of a solid hydrofoil or strut of biconvex parabolic arc contour about its axis of symmetry, (least moment of inertia), inches^4.

I_1, I_2 = section moment of inertia of member no. 1, member no.2, et cetera.

$K = \frac{4 A_m^2 t_s}{U}$ = torsional constant, inches^4.

$K_1 = \frac{I_1}{l_1}$ = beam stiffness factor for member no. 1.

$K_2 = \frac{I_2}{l_2}$ = beam stiffness factor for member no. 2.

M = beam bending moment, kip-inches.

M_t = beam bending moment of tapered beam under trapezoidal load distribution, kip-inches.

N = number of struts.

P = axial load, kilopounds.

P_{CR} = critical buckling load, kilopounds.

$R = 6E\frac{\Delta}{l}$ = deflection constant in slope deflection equation.

R_A = strut reaction at panel point "A" in kips.

R_B = strut reaction at panel point "B" in kips.

R_S = strut constant, see Table I.

R_{S_A} = strut constant for strut "A", et cetera.

S = hydrofoil projected area, feet^2.

T = torque, kilopound-inches.

$U = \frac{l}{J}$, radians.

U_m = length of median boundary of hollow section of regular shape, inches.

V_K = velocity in knots

W = weight in kilopounds at 1.0 "g"

b = hydrofoil span normal to direction of motion

b_m = span of mono-strut hydrofoil configuration of taper ratio = 0.5.

b_r = span of mono-strut hydrofoil configuration of rectangular planform

c = chord, inches

c_F = hydrofoil chord, inches

c_{F_r} = hydrofoil root chord, inches

c_ℓ = section lift coefficient

c_n = section normal force coefficient

c_r = root chord, inches

c_s = strut chord, inches

c_t = tip chord, inches

c_y = distance from centroid of a section to extreme fiber, inches

e = eccentricity, inches

g = acceleration of gravity, ft./sec.^{2}

j = $\sqrt{\frac{EI}{p}}$ (length)

k = $\frac{c_s}{c_F}$ = chord ratio

k_1 = $\sqrt{\frac{p}{EI_1}}$

ℓ = length of strut, column, or bay; inches

ℓ_{FE} = length of fixed-ended beam, inches

ℓ_c = length of cantilever beam, inches

ℓ_s = length of strut, inches

ℓ_1 = length of member no. 1

ℓ_2 = length of member no. 2

m = $\frac{\ell_s}{c_r}$ = strut length ratio

n = limit load factor in terms of acceleration of gravity

q = $2.853\ V_K 2$ = dynamic pressure, psf

t = thickness of foil, skin, et cetera, inches

t_s = skin thickness, inches

w = load or weight per unit length, kips/inch

w_r = unit loading at root, kips/ inch

w_t = unit loading at tip, kips/inch

x = chordwise (longitudinal) direction, inches

x_r = $\frac{c_r}{2}$, inches

x_t = $\frac{c_t}{2}$, inches

y = vertical distance along y-axis, or deflection in "y" direction, inches

y_z = deflection at point "z" parallel to y-axis, inches

y_{tip} = deflection at beam tip in "y" direction, inches

y_{rect} = deflection of rectangular planform hydrofoil with constant moment of inertia and uniform load, inches

y_{taper} = deflection of uniformly tapered planform hydrofoil with uniformly varying moment of inertia and trapezoidal spanwise load distribution, inches

z = lateral direction, inches

z_o = $\frac{b}{2}$, inches

Subscripts:

A, B, C, D, E, et cetera = panel points
F = foil
FE = fixed ended span
b = bending
c = cantilever
f = fixed ends
h = hollow
n = normal force
o = initial or solid
r = root, rectangular
s = strut, skin
t = taper, tip, torsion

B = $\frac{4}{105}$ = section moment of inertia constants

Γ = dihedral of hydrofoil, degrees.

Δ = deflection of joint of bent, inches

θ = $\frac{dy}{dx}$ = slope, radians

θ_{AB}, θ_{AD} = slope of member AB at Panel Point "A", et cetera

δ = deflection, inches

η = ratio of inside chord to outside chord of hollow section

λ = $\frac{c_t}{c_r}$ = taper ratio of hydrofoil

π = 3.14159

ρ = $\sqrt{\frac{I}{A_o}}$ = radius of gyration, inches

σ = normal stress, ksi

σ_A = allowable stress, ksi

σ_b = bending stress, ksi

σ_c = compressive stress, ksi

σ_{bu} = ultimate bending stress, ksi

σ_{cr} = critical stress, ksi

σ_{tu} = tensile stress of material, ksi

$\tau_{.5}$ = thickness ratio of hydrofoil with taper ratio of 0.5.

τ_f = thickness ratio of hydrofoil

τ_h = thickness ratio of equivalent hollow section

τ_o = thickness ratio of initial solid section

τ_r = thickness ratio of hydrofoil of rectangular planform with mono-strut

τ_s = thickness ratio of strut

τ_t = torsional shear stress, ksi

τ_1 = thickness ratio of member no. 1

φ = total angle of twist, radians

$\frac{d^2y}{dz^2} = \frac{M}{EI}$

Definition of Terms:

A column is a long compression member which stands vertically.
A foil is that member supplying the vertical lifting force.
A strut is a long compression member which is diagonally placed.

Units: In general, lengths are in inches, areas are in square inches, loads are in kilopounds, and moments are in kilopound-inches, unless otherwise noted.

Factor of Safety is the ratio of the load that would cause failure of a structural member, to the load that is imposed upon it in service (normal operation).

Limit Load is the maximum load which is expected to be encountered in normal operation and is equal to the particular weight condition multiplied by the Limit Load Factor.

Limit Load Factor is the maximum load factor (related to a specific axis) which is expected to be encountered in normal operation.

Load Factor is the ratio of the total force upon the vessel to the weight of the vessel. In terms of the acceleration of gravity, it then becomes the ratio of the acceleration of the body divided by the acceleration of gravity.

Ultimate Load is the Limit Load increased by the Factor of Safety.

SECTION PROPERTIES: STRUTS & HYDROFOILS

A biconvex, parabolic arc, solid section is used in determining all of the preliminary structural design data for the struts and hydrofoils. These data are used in the preliminary hydrodynamic calculations. It was found that the properties of these sections reasonably represented those of the NACA 64, 65 or 66-series symmetrical airfoil sections which might later be employed. The cross-sectional area and the moment of inertia about the chord line, I_X, are used; and the moment of inertia, I_Y, normal thereto has not been used. (Those two properties which are used have been checked numerically on several chord sections).

For the solid, biconvex, parabolic arc section (see Fig. 1), represented by: $y = \frac{t}{2} - \frac{x^2 t}{2 x_o^2}$, where $\frac{t}{2} = c_y$ is the maximum thickness from chord line to extreme fiber, and $x_o = \frac{c}{2}$; the moment of inertia is determined to be:

$$I_x = \frac{4}{105} \tau_o^3 c^4 = B \tau_o^3 c^4 .$$

The cross-sectional area is determined to be: $A_s = \frac{2}{3} \tau_o c^2$.

Thus, the section modulus becomes: $\frac{I_x}{y} = \frac{8}{105} \tau_o^2 c^3 = 2 B \tau_o^2 c^3$.

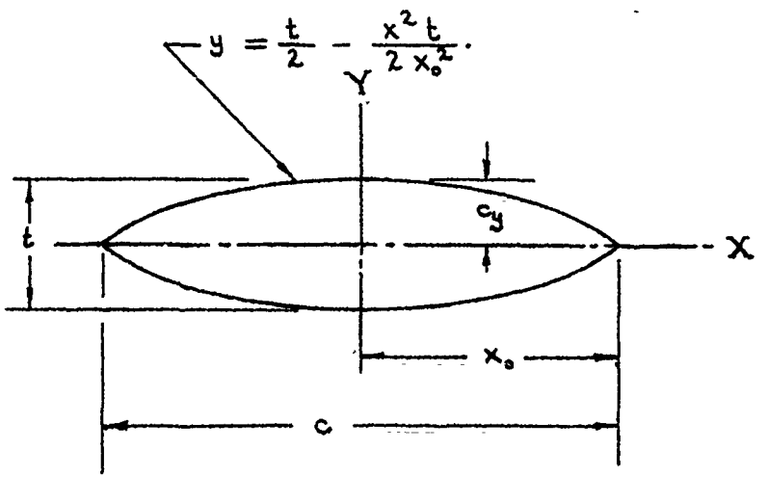

Biconvex Parabolic Arc Section
Fig. 1

Figures 2 and 3 are presented herein as examples to show the effects of varying certain physical parameters. The end result, the least moment of inertia of the section about its longitudinal axis is not non-dimensional. It appears best not to construct charts similar to these until after the size range for the ship under consideration is approximately known. Figure 2 presents moment of inertia as a variation in thickness ratios for constant chords. Figure 3 shows the variation of moment of inertia for hollow sections with the chord for various thickness ratios.

The effect on the struts and hydrofoils, when hollow sections are employed, are shown in Appendix I in non-dimensional form. The curves of Figures 49 and 50 (Appendix I) may be used in conjunction with the design charts (which are based on solid section) to obtain hollow struts and foils.

It must be remembered that as sizes become larger, the sections will become hollow and (percentage-wise) the skins will become thinner. Other considerations are delineated below which may influence the selection of strut and foil shapes and sizes in the ships of greater weights.

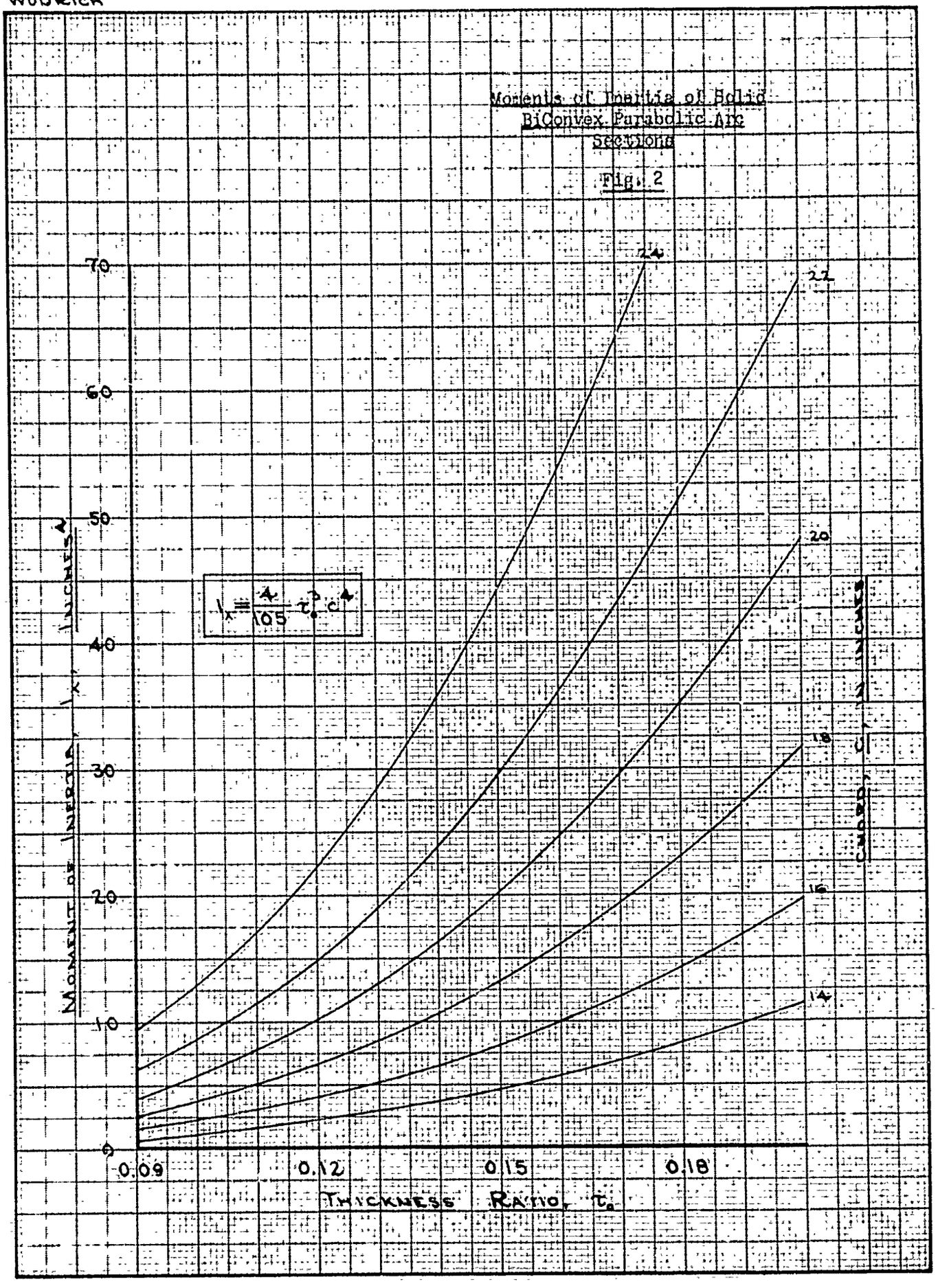
Moments of Inertia of Solid
BiConvex Parabolic Arc
Sections
Fig. 2
$I_x = \frac{A}{105} \tau_o^2 c^4$
MOMENT OF INERTIA, I_x, INCHES⁴
70
60
50
40
30
20
10
0
0.09
0.12
0.15
0.18
THICKNESS RATIO, τ_o
24
22
20
18
16
14
CHORD, c, INCHES

IF

Moments of Inertia of Solid Bi Convex Parabolic Arc Sections

Fig. 2

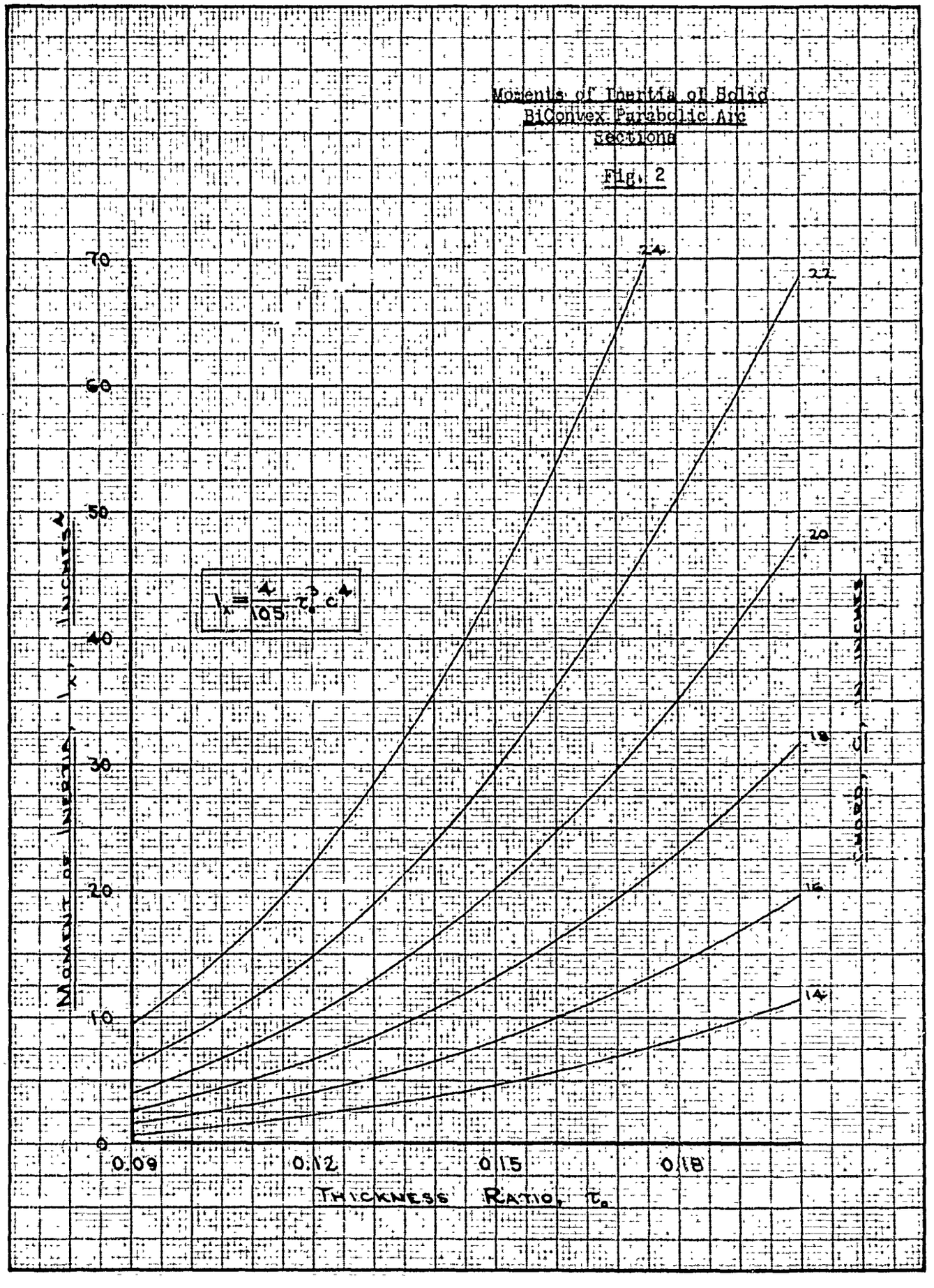

IF

Moments of Inertia of Bi-Convex Parabolic Arc Sections with 0.5 Inch Thick Walls

Fig. 3

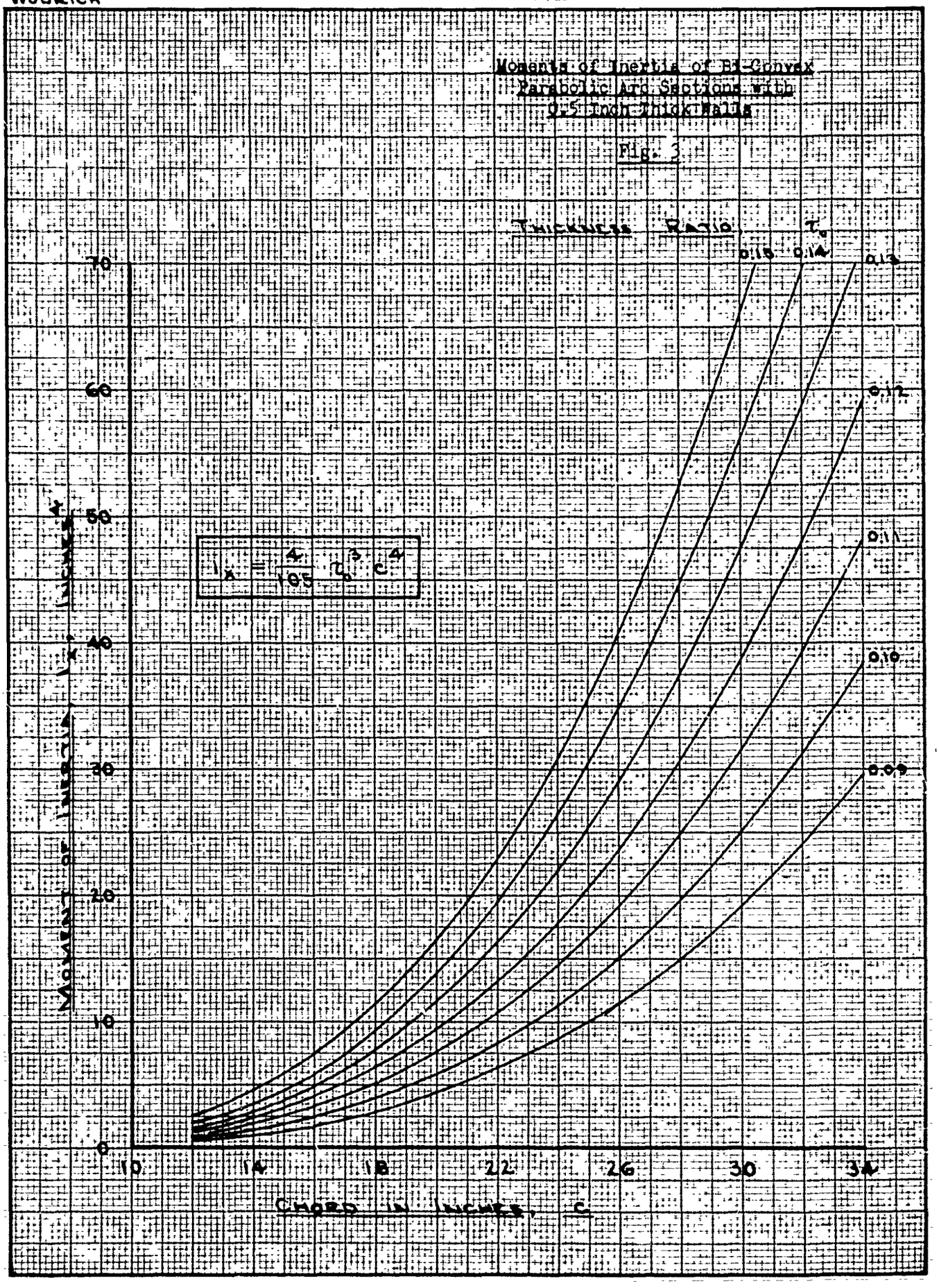

2F

LOADING CRITERIA

After perusing all of the data which have been available on hydrofoils and previous hydrofoil craft, it was ascertained that usable information concerning structural loads and applicable criteria is very limited. Before a large hydrofoil craft can be successfully designed, the vertical, longitudinal, and lateral load factors(1) and accelerations which are encountered at sea with the type of configuration under consideration must be previously determined. Also, the angular accelerations in pitch, roll and yaw must be determined. The accelerations of the ship while supported by the hydrofoils and struts may be dependent largely upon the type of the dynamic stability and control systems employed. These load factors and accelerations, as in aircraft design, must be determined in order to permit serviceable structural designs within the limits imposed by weight and sizes of members.

Load Distribution: (Hydrofoils & struts)

In this analysis no attempt is made to determine or use precise loadings on the struts or hydrofoils. The presence of struts which attach to the upper surface of the hydrofoil affects the chordwise and spanwise load distributions. The presence of stingers and/or nacelles at the strut-foil junctions likewise has an effect. NACA data will give the effect of nacelle shape and location upon the spanwise airload distribution for any particular planform. Since the struts are likely to cause a greater modification, and the magnitude is not precisely known, the use of precise basic distributions, for the hydrofoil alone, are not justified. However, an attempt has been made to select loading conditions and load distributions which would not be unduly conservative.

For instance, the spanwise water load distribution is considered to vary uniformly from root to tip in proportion to the chord, i.e.,

$$C_N = \int_{-\frac{b}{2}}^{\frac{b}{2}} c_f \cdot c_N \cdot d\bar{z} \cdot$$

For a taper ratio of 0.50 the resulting spanwise water load distribution closely approaches the theoretical load distribution. It gives a bending moment distribution which is not far different from the bending moment distribution for an elliptical load distribution. In the case of rectangular planforms with multi-struts, the presence of the struts induces a shift of the load away from the struts. But the distribution between the struts approaches that of a rectangular distribution. Then

(1) The term, "Load Factor," is defined under Definitions and Symbols.

the only deviation is that involved for cantilever overhang. If the overhang is tapered, the resulting moments will approach those for an elliptical load distribution.

For the preliminary design data on the hydrofoils, the chordwise center of pressure of the load is assumed to occur at the quarter-chord point of the unflapped hydrofoil. Where flaps are used, it is intended that the additional load due to flap deflection will be added in separately at its proper chordwise center of pressure, since the principal axes of the section also shift with flaps. Because the use of flaps on the main lifting surfaces for the vessel configurations which were under consideration hydrodynamically and dynamically was not contemplated until late in this contract phase, no general structural preliminary design charts are presented for them.

Loading Conditions:

In this analysis the external forces applied to the ship's structure are specified in terms of Limit Load Factor(1). The limit vertical load factors have been taken as plus 2g and zero g, and are assumed to amply account for the gust effects. This means that when flaps are employed, the flap deflections are limited to such a value that the resulting load will not exceed limit load factors of zero and 2. (Data from Reference 2 show that limit incremental vertical accelerations from 0.7 to 0.9 were not uncommon; i.e., total limit vertical load factors of 1.7 to 1.9. Those data indicate that the size of waves compared to vessel displacement, hull clearance, and forward velocity had considerable effect.)

Side loads on the struts are a result of the yaw angle of the craft. With a given forward velocity of the vessel, and with waves of a specific height in a beam sea, the orbital motion of the waves creates a certain yaw angle on the struts. Where a rudder becomes an integral part of a strut, side loads and torsion are imposed by deflection of the rudder. The limiting side load factor is assumed to be not more than 1.0 g and to act in combination with the vertical limit load factors of 2.0 g and zero.

Factor of Safety:

Factors of safety(2) are largely to account for ignorance in loads or allowables. In structural engineering, a factor of safety of 3.0 is often used to keep the maximum working stress safely below the proportional limit of the material. But in aircraft design, columns and struts are worked close to the yield stress. It seems likely that as loadings and allowables of the various configurations become better known the factor of safety may be lowered. This will be desirable not only from structural weight saving (which may become important), but also from hydrodynamic limit on physical sizes to obtain satisfactory performance.

(1) The term, "Limit Load Factor," is defined under Definitions and Symbols.
(2) The term, "Factor of Safety," is defined under Definitions and Symbols.

CONFIGURATIONS

The two main structural items comprising any configuration are struts and hydrofoils. Innumerable ways exist for assembling these essential parts; some appear better than others. Even in the single-foil arrangement, to which this report is confined (see Scope, Pg.2), many types of configurations exist.

Considerations:

For a hydrofoil craft to possess the hydrodynamic characteristics which are deemed essential (so that it may compete practically with the long established forms of water transportation), the physical dimensions of the struts and foils and their methods of attachments are of prime importance. The thinnest possible struts and the thinnest possible foils are needed to accomplish this mission. The resulting structure still must be practical from the standpoint of fabrication cost, reliability, and serviceability. The overall structural weight and the resulting center of gravity of the ship become very important: to possess a reasonable ratio of useful load to design gross weight, weight control is essential!

Therefore, the structural designs and the structural analyses of these components must be accomplished with precision. This is true not only in the determination of the stresses and strains within the structure under given loading assumptions, but also in the determination of the nature and magnitude of the external loads which are acting upon the structural components.

The approach to the problem of selecting a hydrofoil-strut configuration for a hydrofoil ship started with the most elementary configuration: one strut and one foil without dihedral, resembling a "T". It is one of the single foil class and is referred to as a mono-strut arrangement in this report. Having selected certain structural materials, their factors of safety, and modes of fabrication; having determined reasonable spanwise and chordwise water load distributions; and having a given planform, a specified loading in pounds per square foot, and a single symmetrical center strut; only one aspect ratio is permissible for a given thickness.

It was found from this initial investigation that the single-strut gives only a moderate lift-drag ratio. Means were in-

vestigated to raise the value of this lift-drag ratio. This resulted in the investigation of symmetrical bents with one, two and three bays. These, by their very geometry, imposed bending as well as compression loads on the struts. To eliminate primary bending in the struts and columns in the symmetrical loading conditions, the series of configurations with the hydrofoils extending outboard from the struts are considered. In the single hydrofoil system, the various hydrofoil-strut combinations or configurations may be divided into combinations of certain basic structural forms. These combinations are: mono-strut; two struts, pin-ended; three-struts, the two end struts pin-ended; four struts, all pin-ended; single rigid bent; and multi-bay bents, fix-ended with overhang.

Initially it was thought that these configurations would be with and without dihedral, but hydrofoils with appreciable dihedral which intersect the water surface have been covered by German data and work conducted by Carl & Sons. Joshua Hendy data (see the Hydrodynamics section) reveal that in order to obtain the best lift-drag ratio, the hydrofoil should not intersect the water obliquely. Hence, these strucutral studies are confined entirely to hydrofoils which are submerged completely below the water surface. The hydrofoil thickness varies inversely with the cosine of the dihedral angle (see Equation 6, Pg. 20). Thus, the smaller the dihedral, the greater the aspect ratio will become for a given thickness ratio. Since roll stabilization is being obtained by movable surfaces, all of the structural analyses which have been completed on the multi-struts are with zero dihedral.

The majority of the studies which have been made are devoted to the analyses of single, two or three strut systems with hydrofoil overhang. For the symmetrical loading assumptions which are made, the slopes of the hydrofoil at the hydrofoil-strut junctions are zero. These geometries are selected to obtain zero initial moments in the struts so that the maximum hydrofoil bending moments will occur at the hydrofoil-strut junctions.

The first family of multi-struts considered are of rectangular planform. Tapering the cantilever portion of the planform gives another family of configurations. The advantage for so doing may be seen in a test vehicle. An aspect ratio of approximately 16 results from two struts with a rectangular planform. By tapering the two outer panels, the aspect

ratio is increased to approximately 21 without any change in percent thickness.

The use of any of the hydrofoil strut configurations with concomitant haunching of the hydrofoil thickness will provide a gain in aspect ratio for a given maximum thickness ratio if methods of fabrication permit. The hydrofoils are haunched by increasing the percent thickness of the hydrofoils toward the strut intersections. Some of the German hydrofoil vessels had haunched foils which were obtained by varying the chord length (see References No. 3 & 4). The final selection of a given multi-strut configuration is based on hydrodynamic rather than structural considerations. From the economy of weight and fabrication, the fewer the struts, the lighter the struts and foils will become and the easier the construction. In order to meet the demand for high aspect ratio and minimum thickness, the multi-strut configurations are dictated.

For a specific load to be carried axially be columns, there exists a maximum number of members for maximum efficiency. Any increase beyond that number of struts lowers the efficiency of the structure. This is readily evident when the strut lengths for the configuration remain the same regardless of the number of struts. The column buckling allowable is a function of $\left(\frac{\rho}{l}\right)^2$. Thus, the buckling allowable varies directly as the square of the strut thickness ratio and the square of the strut chord. Then for a configuration to carry a given load, the point is reached at which the number of submerged struts in the configuration add more drag than the increase in hydrofoil aspect ratio and decrease in hydrofoil thickness reduce the drag (see Hydrodynamics section). This point may occur at three struts for many loading conditions. The multiple struts have two other disadvantages as compared with a mono-strut or two-strut configuration: (1) for a given yaw angle the magnitude of the side force in question increases since the strut side area increases; and (2) the slender struts of the multi-strut configuration impose greater bending stresses on the hydrofoil under asymmetrical loading conditions.

Hydrofoils:

For preliminary design purposes it is desirable to be able to ascertain the hydrofoil geometry with a minimum expenditure of time and effort. The important items of geometry which must be considered prior to performance calculations are the maximum span between struts, maximum overhang, total span, aspect

ratio, chord, and percent thickness. It is also desirable to have comparisons of spans, aspect ratios, and thickness ratios for the various strut-foil configurations.

Governing Stresses

The required hydrofoil section may be determined from the bending stress, the shearing stress, the torsional stress, or from a combination of all or any two of these. If flutter is serious or if a predetermined maximum deflection has been stipulated, the hydrofoil section may be determined from that size required to obtain the maximum specified deflection.

In solid hydrofoils of medium thickness, shear will not be serious, either alone or in combination with bending or torsion, due to the cross-sectional area.

Torsion is a function of the location of the principal axes of the section, the chordwise center of pressure of the load, the spanwise distribution of load, and the section pitching moment. If a symmetrical hydrofoil section is used, the pitching moment of the section will remain approximately constant and equal to zero through moderate angle of attack changes. (This is the range to be considered for hydrofoil vessels.) Thus, the only torsion acting upon the section is due to the distance between the chord load center of pressure of the section and the principal axes of the section. The principal Y-axis of the biconvex parabolic arc section passes through the 50 percent ordinate of the chord while the Y-axis location for the NACA 65- and 66-series airfoil sections, which are currently being considered, varies from approximately 40 to 47 percent. In the sizes likely to be encountered, the torque due to the chordwise center of pressure of the load not being along the neutral axis of the section is quite small, and the repression of the bending stress due to shear stress effect is neglible. For solid sections, if no other factors are present, the effect of torsion may be neglected. Therefore, the preliminary design sizes may be picked from bending and deflection considerations. (For hollow sections, see Appendices I & II.)

Should flaps be present on the foils, bending alone cannot be used for determining the hydrofoil geometry, but bending will be the primary consideration. The presence of a flap greatly reduces the moment of inertia of the section about the Y-axis, the cross-sectional area, and the torsional rigidity. Flaps shift the principal Y-axis forward on the hydrofoil, introduce appreciable pitching moments in the hydrofoils with flap deflections, and alter the chordwise load distribution. These moments cannot be properly evaluated until the chord of the flap in percent of hydrofoil chord, type of flap balance, the maximum flap

deflection, the rate of change in pitching moment with flap deflection and angle of attack, and the flap hinge moments are known.

Therefore, the best approach seems to be to determine the required sections, based upon bending, and to provide for a reduction in allowable bending stress due to the combined effect of bending and torsion. This may be done approximately by:

$$\left(\frac{\sigma_b}{F_b}\right)^2 + \left(\frac{\tau_t}{F_{tc}}\right)^2 = 1.0 \cdot \text{ (See Ref. 5)}$$

The amount of this reduction in allowable, converted into terms of greater hydrofoil thickness ratio or reduced aspect ratio, would need to be determined for the specific flap geometry being considered.

Bending Stress

The bending moment for a trapezoidal spanwise load distribution is given as:

$$M = \frac{w_r}{2}\left[\frac{(\ell-z)^2(1-\lambda)}{3\ell} + (\ell-z)^2\lambda\right] \quad \text{Equ. 1 (see Pg. 32)}$$

which, at the root of a mono-strut configuration, becomes:

$$M_{MAX.} = \frac{w_r \ell}{6}\left(1 + 2\lambda\right) \cdot \quad \text{Equ. 2}$$

Where dihedral is present in a hydrofoil,

$$W_N = \frac{W}{\cos\Gamma} \; \& \quad S_N = \frac{S}{\cos\Gamma} \cdot$$

$$\therefore \frac{W_N}{S_N} = \frac{W}{S} \; \& \quad b_N = \frac{b}{\cos\Gamma}$$

if b is the span along the hydrofoil in inches

Thus, Equ. 2 becomes:

$$M = \left[\frac{W}{S}n\right]\frac{c_{F_r}}{144}\,\frac{\ell^2(1+2\lambda)}{6} = \frac{1}{3456}\left[\frac{W}{S}n\right] c_{F_r} b^2(1+2\lambda) \text{ kip-inches}$$

$$\text{OR } M = \frac{1}{3456\cos^2\Gamma}\left[\frac{W}{S}n\right] c_{F_r} b_N^2\left(1 + 2\lambda\right) \cdot \quad \text{Equ. 3}$$

Then, dropping subscript N and using b as projected span, as defined under Definitions & Symbols,

and $\sigma_b = \frac{Mc_y}{I}$,

$$\sigma_b = \frac{108}{8 \cdot 24 \cdot 144} \left[\frac{W}{S} n\right] \frac{c_{r_r} b^2}{\cos^2 \Gamma} (1 + 2\lambda) \frac{1}{\tau_r^2 \cdot c_{r_r}^3}. \quad \text{Equ. 4}$$

Where $b^2 = \frac{A_r^2 c_{r_r}^2 (1+\lambda)^2}{4}$,

$$\text{then: } \sigma_b = \frac{35}{4 \cdot 64 \cdot 144} \left[\frac{W}{S} n\right] \frac{(1+2\lambda)(1+\lambda)^2}{\cos^2 \Gamma} \left(\frac{A_r}{\tau_r}\right)^2. \quad \text{Equ. 5}$$

Since $\sigma_{b_{MAX.}} = \frac{\sigma_{bu}}{F}$, by transposing,

$$\tau_r^2 = 0.0009495 \frac{F}{\sigma_{bu}} \left[\frac{W}{S} n\right] \left(\frac{A_r}{\cos \Gamma}\right)^2 (1 + 2\lambda)(1+\lambda)^2;$$

$$\therefore \tau_r = 0.0308 \frac{A_r}{\cos \Gamma} (1+\lambda) \left[\frac{W}{S} n\right]^{0.5} \left(\frac{F}{\sigma_{bu}}\right)^{0.5} (1 + 2\lambda)^{0.5}. \quad \text{Equ. 6}$$

which is the general equation for a mono-strut (root thickness).

For a taper, $\lambda = 0.5$, it becomes:

$$\tau_r = 0.0653 \frac{A_r}{\cos \Gamma} \left[\frac{W}{S} n\right]^{0.5} \left(\frac{F}{\sigma_{bu}}\right)^{0.5}. \quad \text{Equ. 7}$$

For a taper, $\lambda = 1.0$, it becomes:

$$\tau_r = 0.1068 \frac{A_r}{\cos \Gamma} \left[\frac{W}{S} n\right]^{0.5} \left(\frac{F}{\sigma_{bu}}\right)^{0.5}.$$

In the multi-strut rectangular configuration, to prevent bending in the bents other than the hydrofoil proper (i.e., in struts), the slope of the head of each strut must be zero. (See also discussion of configurations.)

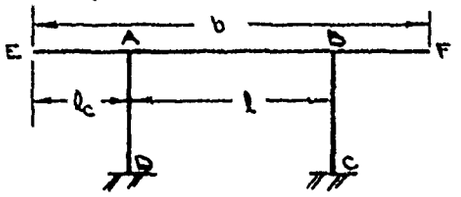

SINGLE BENT WITH OVERHANG
FIG. 4

To obtain $\Theta_{AE} = \Theta_{AB} = \Theta_{BA} = 0$,

$$M_{AE} = M_{AB}$$

and, $\frac{w l_c^2}{2} = \frac{w l}{12}$; (Table III, Ref. 6)

thus, $l_c = \frac{l}{\sqrt{6}} = \frac{l}{2.4499}$ (length in inches)

and $b = l\left(1 + \frac{2}{2.4499}\right) = l(1.8164)$. (inches)

If the number of struts becomes N, and the number of intermediate bays becomes (N-1),

then $b = l\left[(N-1) + 0.8164\right]$

and $l = b \Big/ \left[(N-1) + 0.8164\right]$

or $M_{MAX.} = \left[\frac{W}{S}\eta\right] \frac{b}{A_F} \frac{1}{1728} \frac{b^2}{\left[(N-1)+0.8164\right]^2}$ Equ. 8

in kip inches

from which

$$\tau_F = 0.0871\% \frac{1}{\left[(N-1)+0.8164\right]} A_F \left[\frac{W}{S}\eta\right]^{0.5} \left(\frac{F}{\sigma_{by}}\right)^{0.5}. \quad \text{Equ. 9}$$

Figure 5 presents hydrofoil thickness ratio (percent thickness) as a function of hydrofoil loading, aspect ratio, dihedral, taper ratio, and factor of safety assuming a maximum bending stress of 150 ksi. This chart applies to the basic mono-strut configuration; but, in conjunction with Tables I and II, it may be applied to most configurations which have been considered.

Once the approximate configuration has been selected, however, the data should be presented in a form which would permit reading to greater accuracy. Fig. 6 presents the variation of hydrofoil loading with aspect ratio for various allowable bending stresses for zero dihedral, a thickness of 12 percent, and a taper ratio of one-half. Knowing the aspect ratio of the equivalent mono-strut, and the bending allowable of the material,

$$\sigma_{b_{MAX.}} = \frac{\sigma_{bu}}{F} = \sigma_{ALLOW.},$$

it is readily possible to determine the permissible loading.

If the material is selected, by varying the thickness and holding $\sigma_{b_{MAX.}}$ constant, another useful family of curves for preliminary design purposes may be constructed. Examples of such a method of presenting data are shown on Figures 7, 8 and 9, where percent thickness variation with aspect ratio for different loadings is presented for taper ratios of 1.0, 0.75, and 0.50. These three figures show the effect of taper ratio where a single strut is involved and show the effect of increasing the hydrofoil loading. They were constructed for an allowable yield stress of 50 ksi.

Fig. 10 shows the variation of bending stress in the hydrofoil with aspect ratio for three different foil thicknesses in a single bent configuration with certain assumed geometry and with a strut thickness of 15 percent. Fig. 11 presents variation in hydrofoil loading with aspect ratio for these foil thicknesses and the geometry of Fig. 10.

CONFIDENTIAL

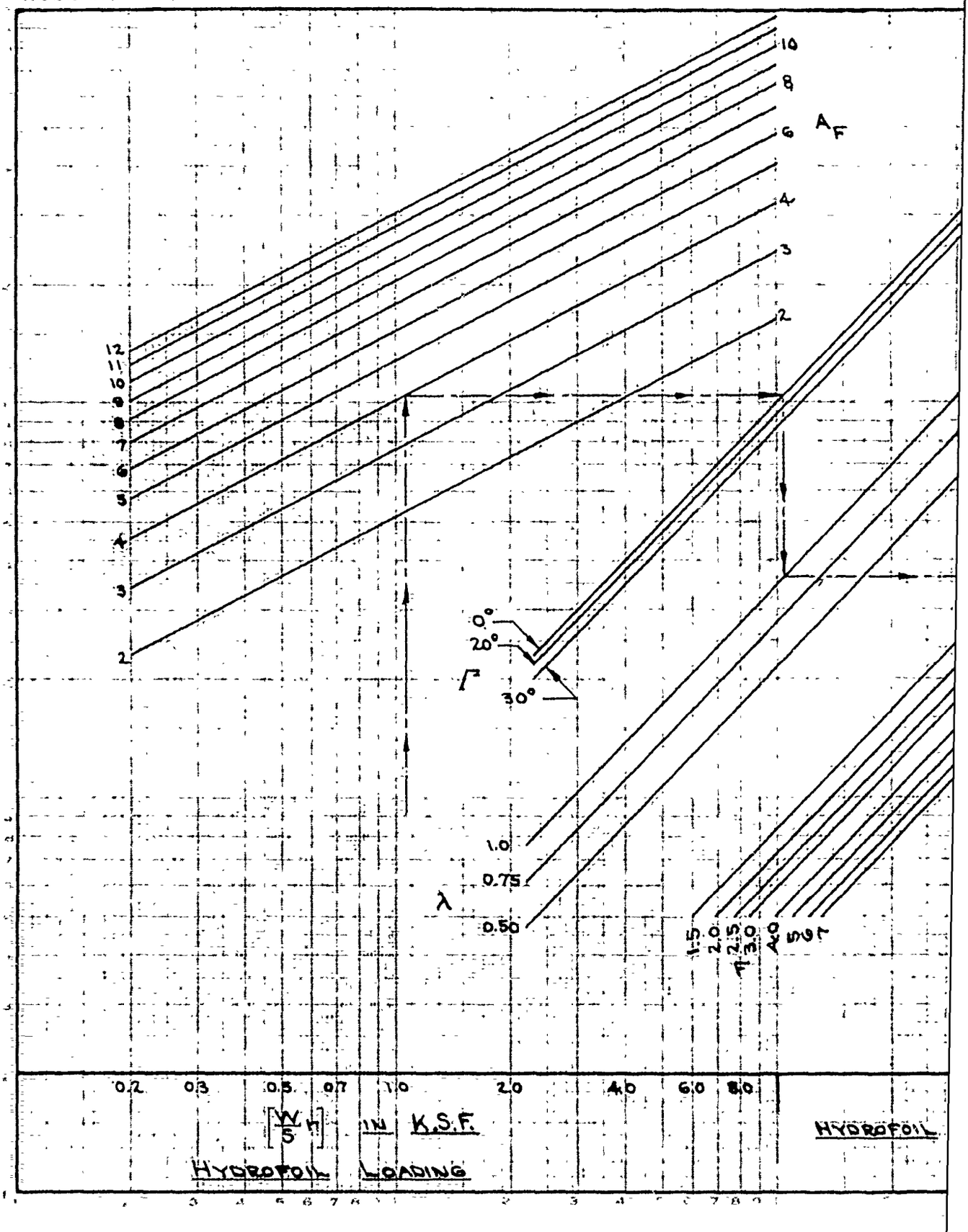

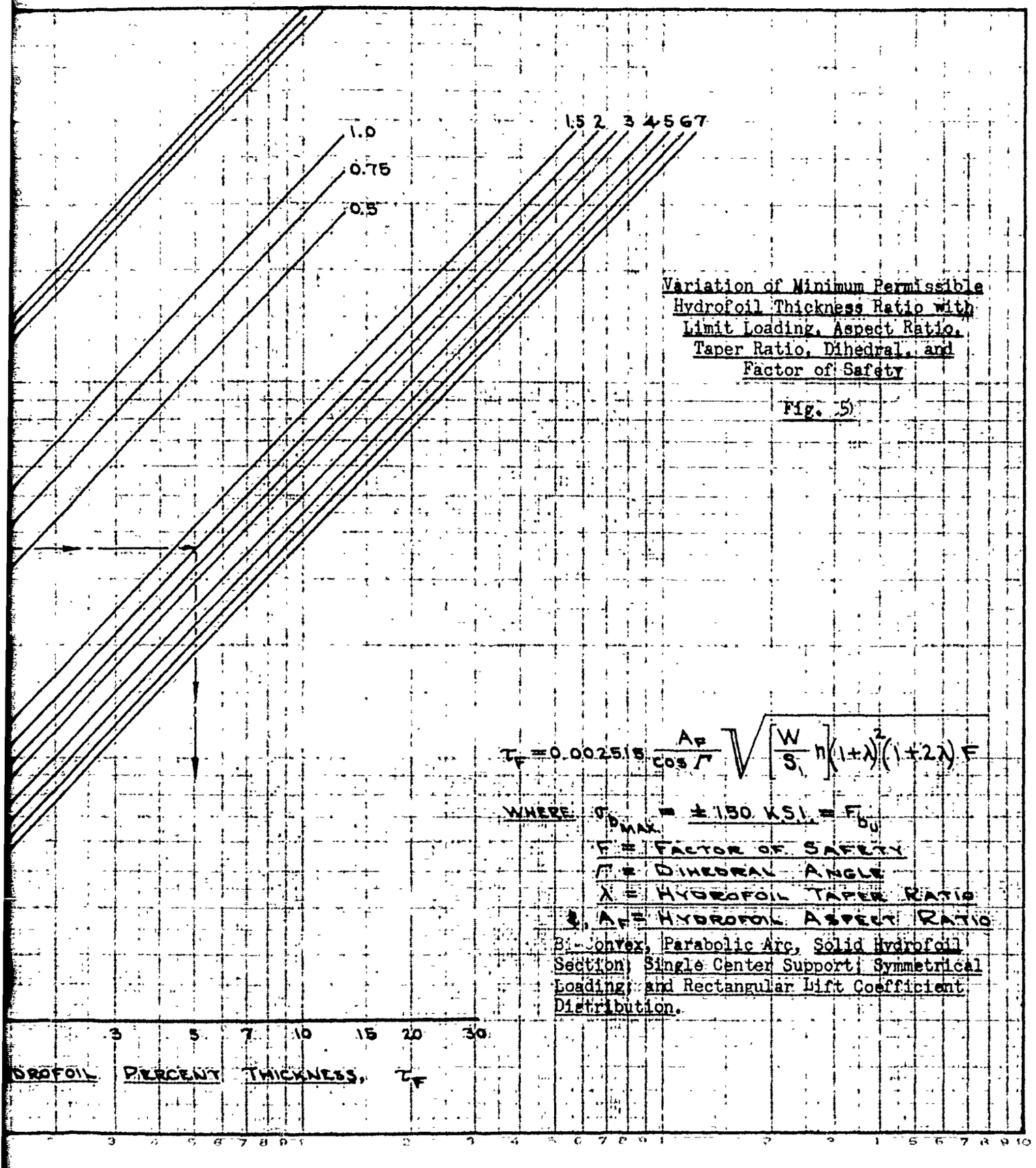

Variation of Minimum Permissible Hydrofoil Thickness Ratio with Limit Loading, Aspect Ratio, Taper Ratio, Dihedral, and Factor of Safety

Fig. 5)

$$\tau_F = 0.00251\,\frac{A_F}{\cos\Gamma}\sqrt{\left[\frac{W}{S_1}\,n\right]\left(1+\lambda\right)^2\left(1+2\lambda\right)F}$$

WHERE $\sigma_{b_{MAX.}} = \pm 150\ KSI = F_{bu}$

F = FACTOR OF SAFETY

Γ = DIHEDRAL ANGLE

λ = HYDROFOIL TAPER RATIO

& A_F = HYDROFOIL ASPECT RATIO

Bi-Convex, Parabolic Arc, Solid Hydrofoil Section, Single Center Support, Symmetrical Loading, and Rectangular Lift Coefficient Distribution.

WODRICH

Variation of Permissible Hydrofoil Loading with Aspect Ratio and Allowable Bending Stress

Fig. 6

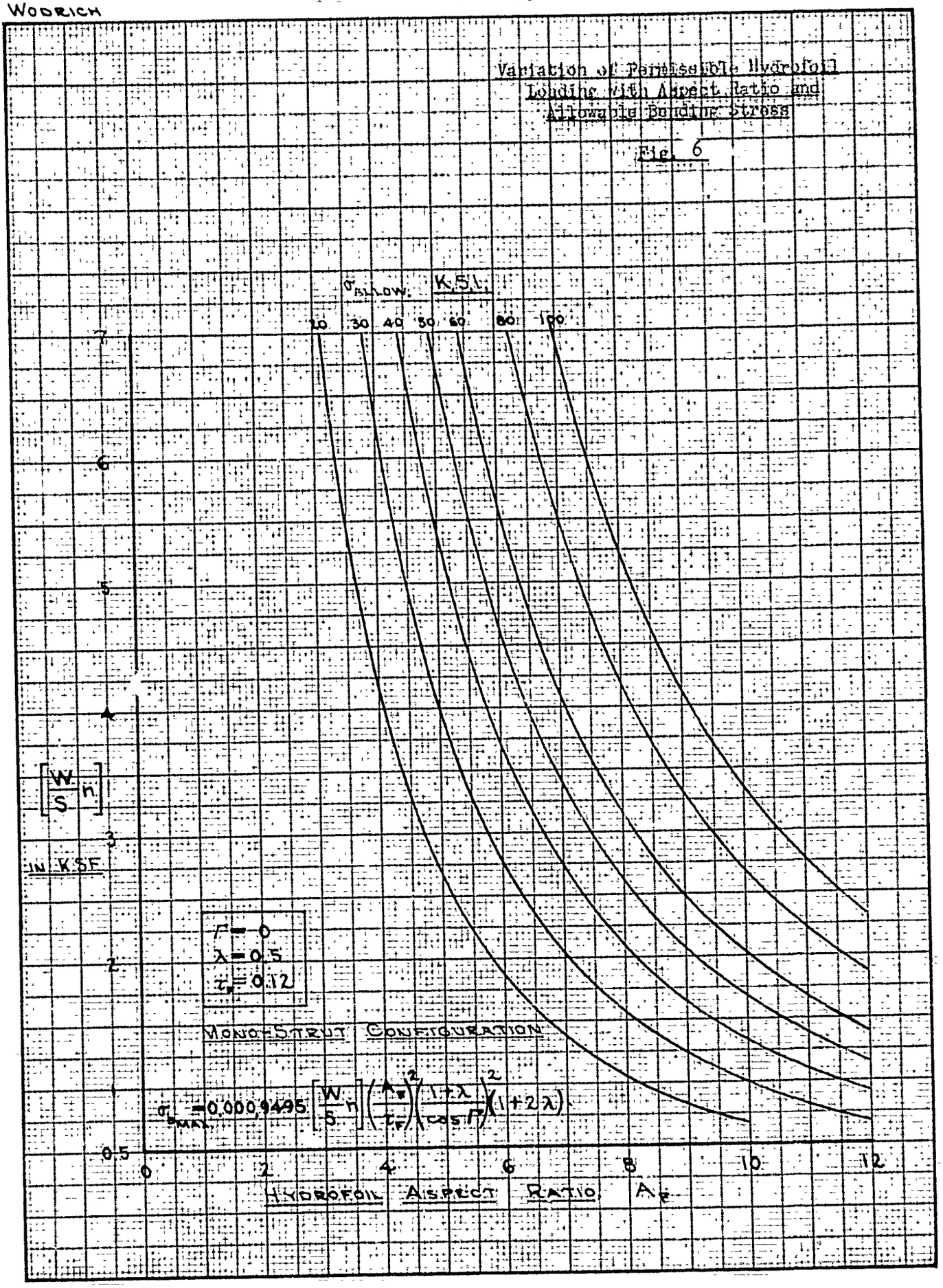

3F

CONFIDENTIAL

Permissible Variation of Hydrofoil Percent Thickness with Aspect Ratio for Rectangular Planform

Fig. 7

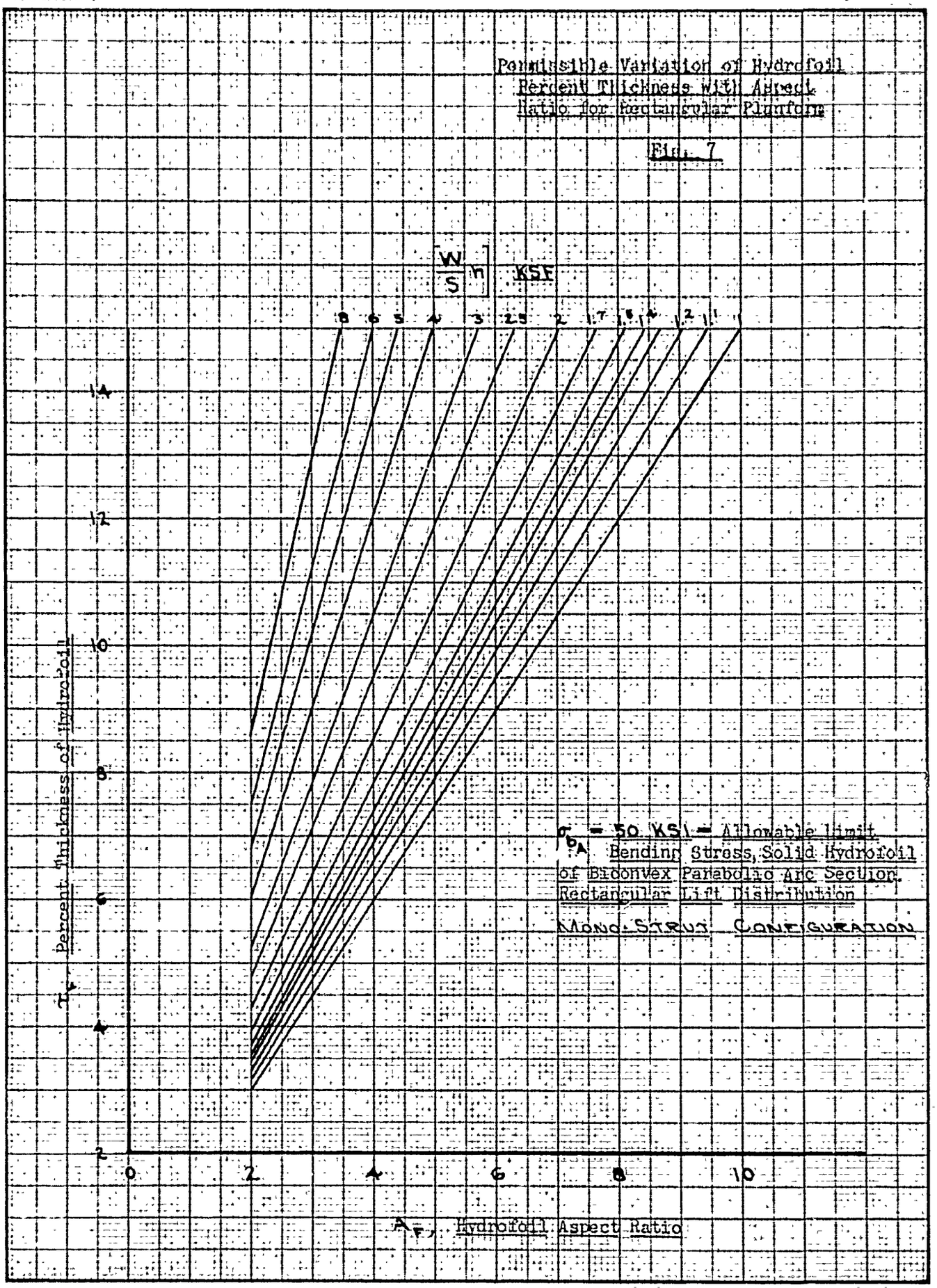

Permissible Variation of Hydrofoil Percent Thickness with Aspect ratio for Planform Taper Ratio of 0.75

Fig. 8

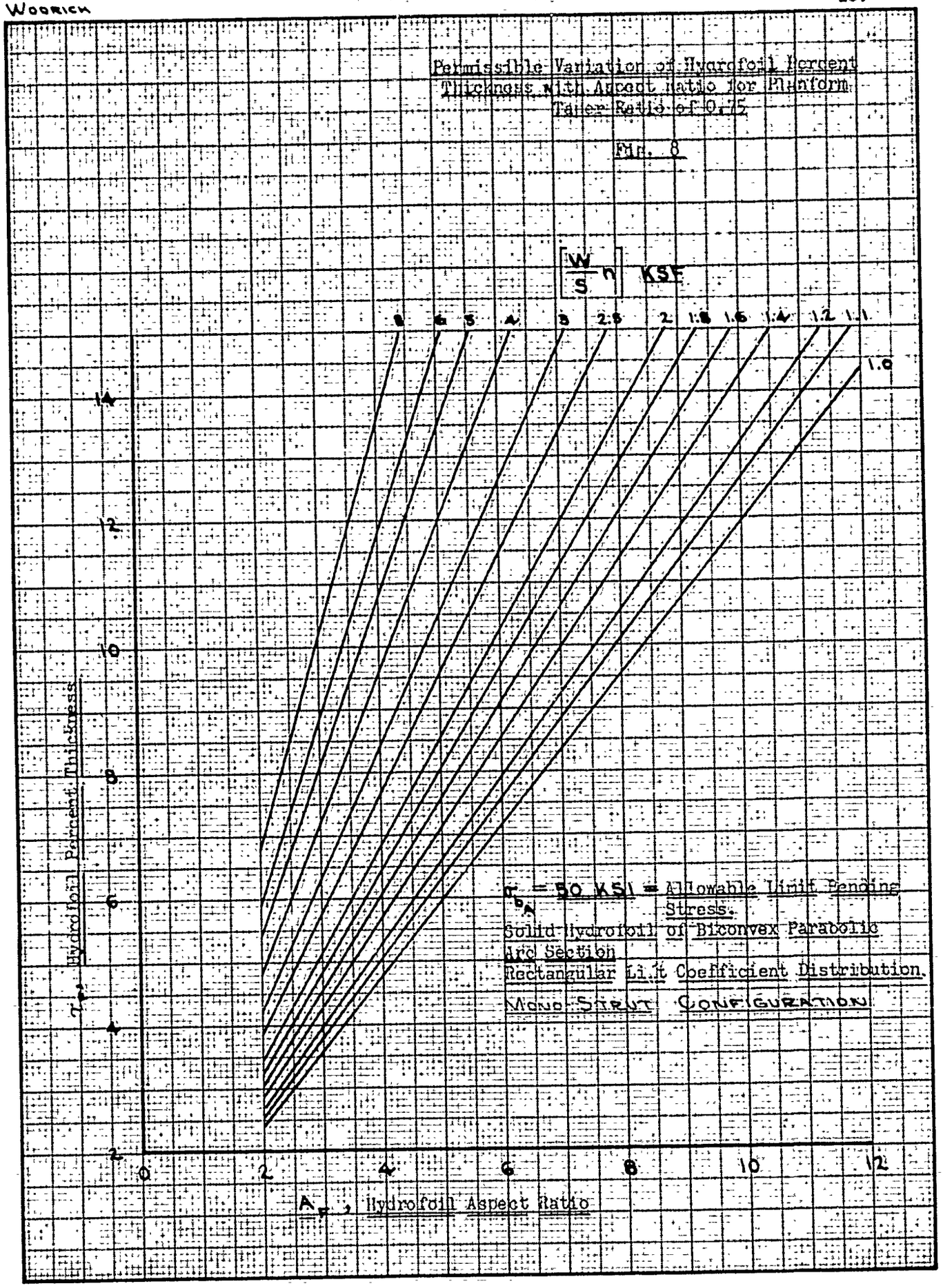

5F

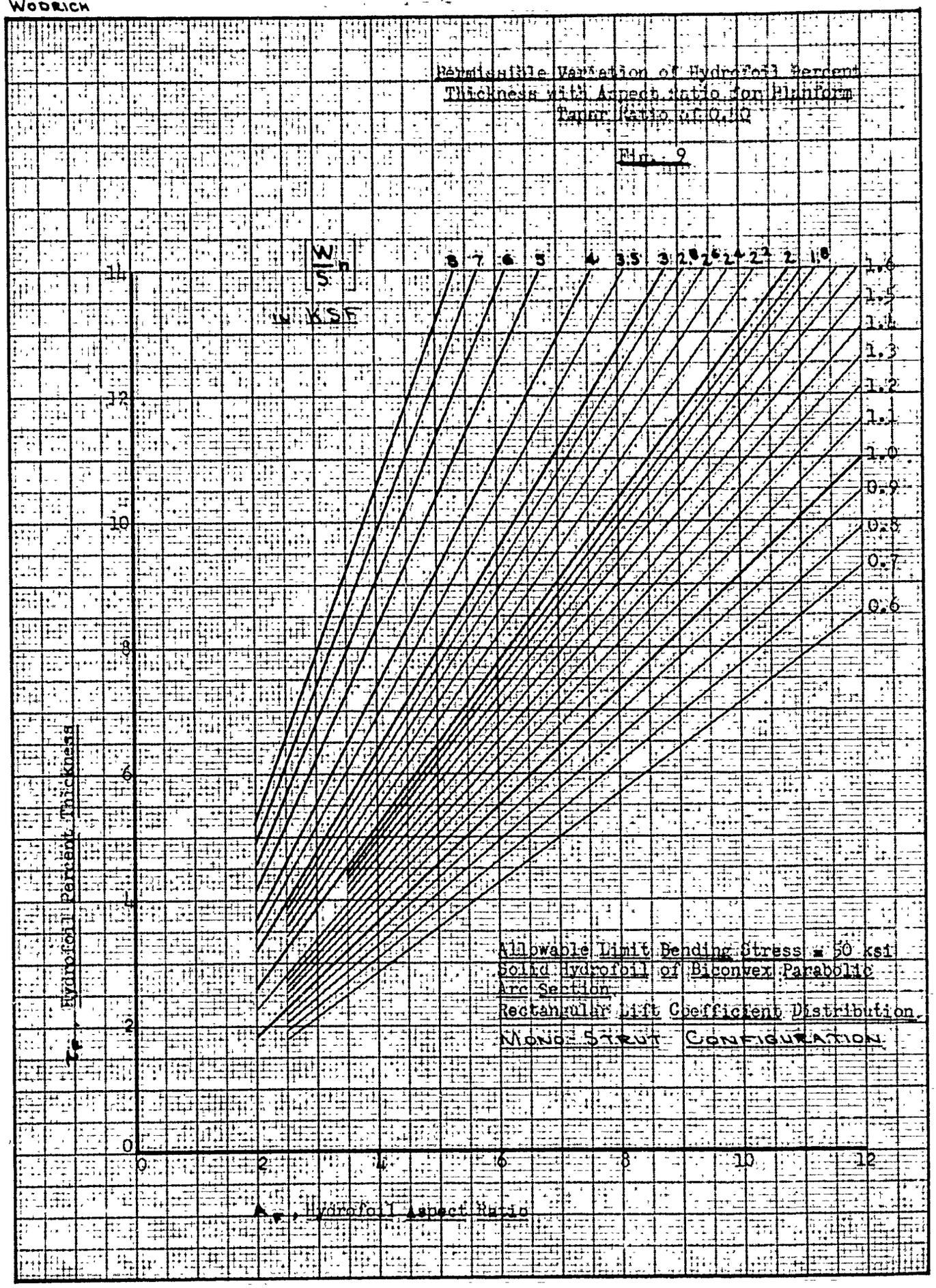
Permissible Variation of Hydrofoil Percent Thickness with Aspect Ratio for Planform Taper Ratio of 0.40
Fig. 9
$\left[\frac{W}{S}\right]_n$
4 KSF
8 7 6 5 4 3.5 3 2.8 2.6 2.4 2.2 2 1.8
1.6 1.5 1.4 1.3 1.2 1.1 1.0 0.9 0.8 0.7 0.6
Hydrofoil Percent Thickness $\frac{t}{c}$
14 12 10 8 6 4 2 0
0 2 4 6 8 10 12
Hydrofoil Aspect Ratio
Allowable Limit Bending Stress = 50 ksi
Solid Hydrofoil of Biconvex Parabolic Arc Section
Rectangular Lift Coefficient Distribution
MONO STRUT CONFIGURATION

CONFIDENTIAL

Variation of Hydrofoil Bending Stress with Aspect Ratio for Three Hydrofoil Thickness Ratios

Fig. 10

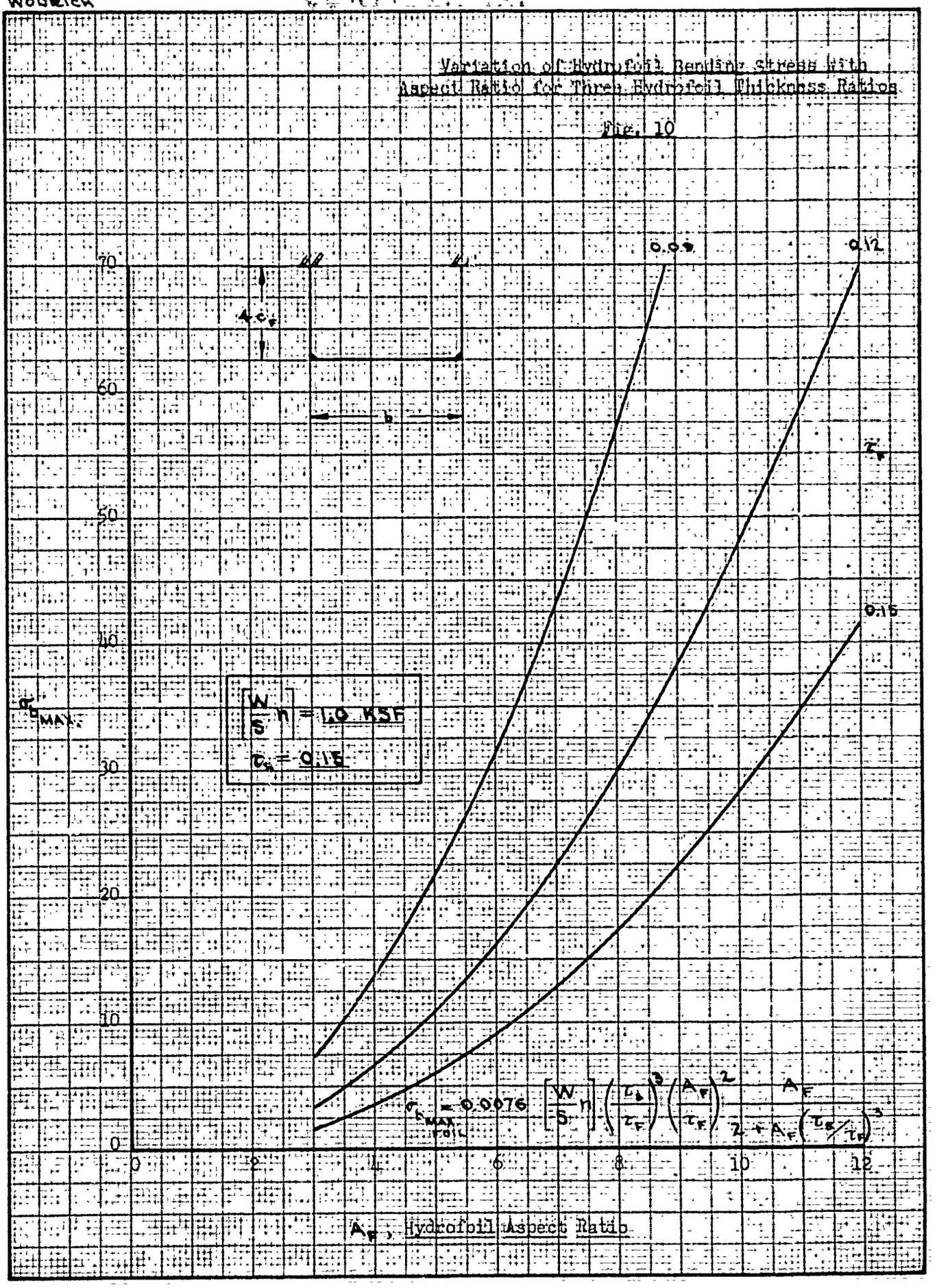

Variation of Permissible Hydrofoil Loadings with Aspect Ratio for Three Different Hydrofoil Thickness Ratios

Fig. 11

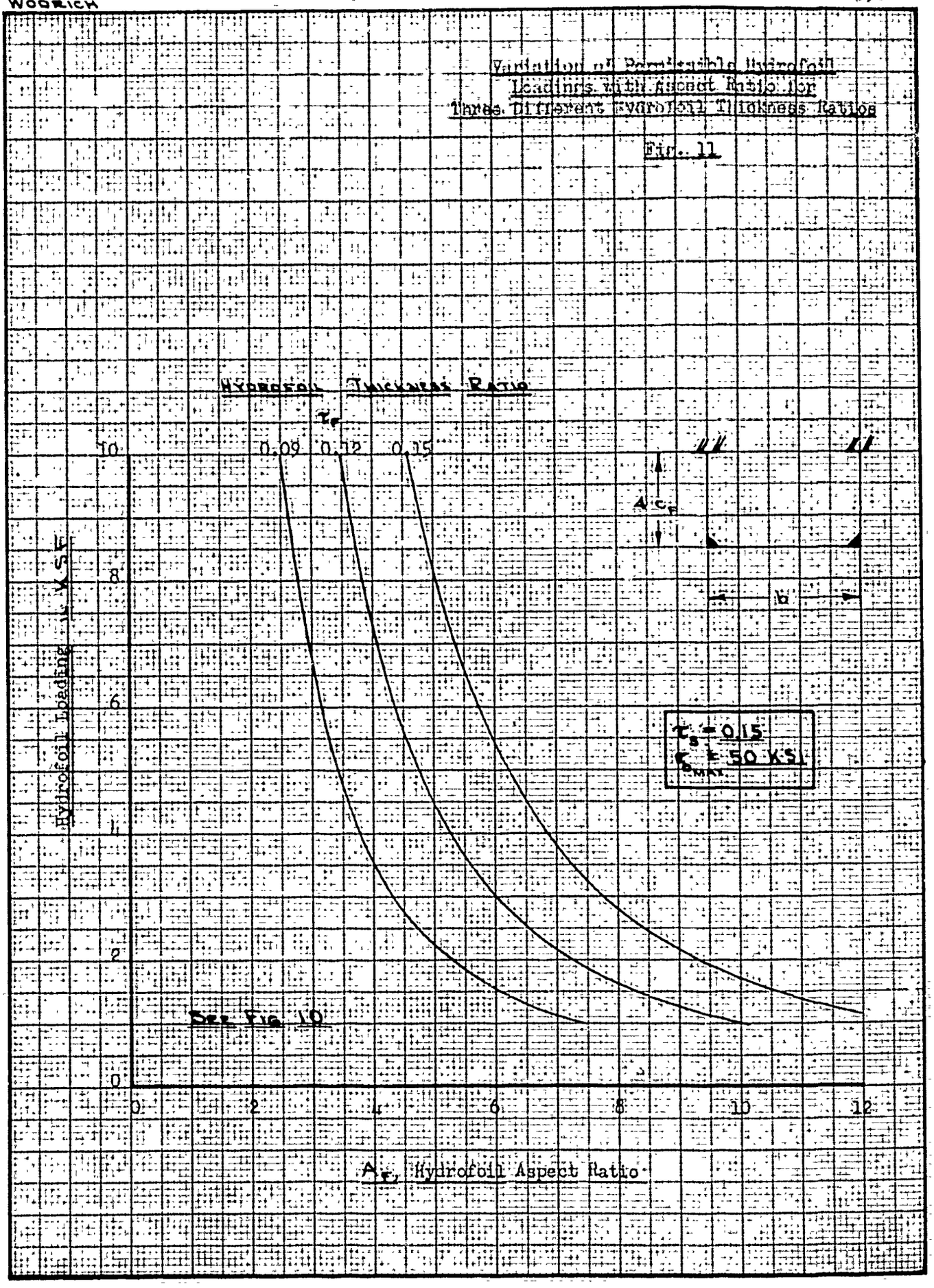

8.5

Recent hydrodynamic calculations indicate configurations of this geometry would not be usable because the strut length required is greater than the strut length which is used. However, they do show the general effect of such configurations: For instance, Fig. 7 indicates at $\left[\frac{W}{S}n\right] = 1.0$ ksf that if $\tau_r = 0.09$, $A_r = 6.0$; while Fig. 10 shows that for $\left[\frac{W}{S}n\right] = 1.0$, and $\tau_r = 0.09$ that $A_r = 7.5$ AT $\sigma = 50$ ksi, or a gain in aspect ratio of 25 percent, provided the struts will carry the moments.

Bending Deflection

The deflection of the tip of a uniformly tapered, cantilever hydrofoil under a uniformly tapered load is first developed in terms of the length of the beam, the unit loading of its root, and the section moment of inertia at the root. Then the tip deflection and deflection at any point of a constant section cantilever hydrofoil under a uniformly tapered load are presented.

The deflection at any point of a uniformly tapered hydrofoil under a trapezoidal load may be obtained by modifying Equation 12, p. 31, to read:

$$y_z = \delta = -\frac{w_r}{2BE}\int_{z_1=0}^{z_1=z} \frac{(z-z_1)\left[\frac{(\ell-z_1)^3}{3\ell}(1-\lambda)+(\ell-z_1)^2\lambda\right]dz_1}{\left[1+\frac{z_1}{\ell}(\lambda-1)\right]^4} \qquad \text{Equ. 10}$$

where z, as shown in Fig. 12, is the section at which the deflection is desired.

However, since the resulting equation becomes somewhat cumbersome (see Equation 21, p. 34, for constant moment of inertia), and since the present interest is in the magnitude of the tip deflection, solution of this equation has been omitted. Likewise, Equation 12 was simplified to Equation 13 by putting

since current interest is in that particular taper ratio. Solution of "y" without evaluation of "λ" is not of sufficient advantage to warrant the additional labor at this time.

Deflection of the end of a cantilever beam of uniformly varying moment of inertia (representatively of a tapered strut under a constant side force) has also been developed for various amounts of taper.

These equations are then rewritten in terms of the hydrofoil loading, the hydrofoil aspect ratio, and the hydrofoil taper ratio and are plotted as the non-dimensional ratio, $\left(\frac{\delta_{max}}{\ell}\right)$, for use in preliminary design.

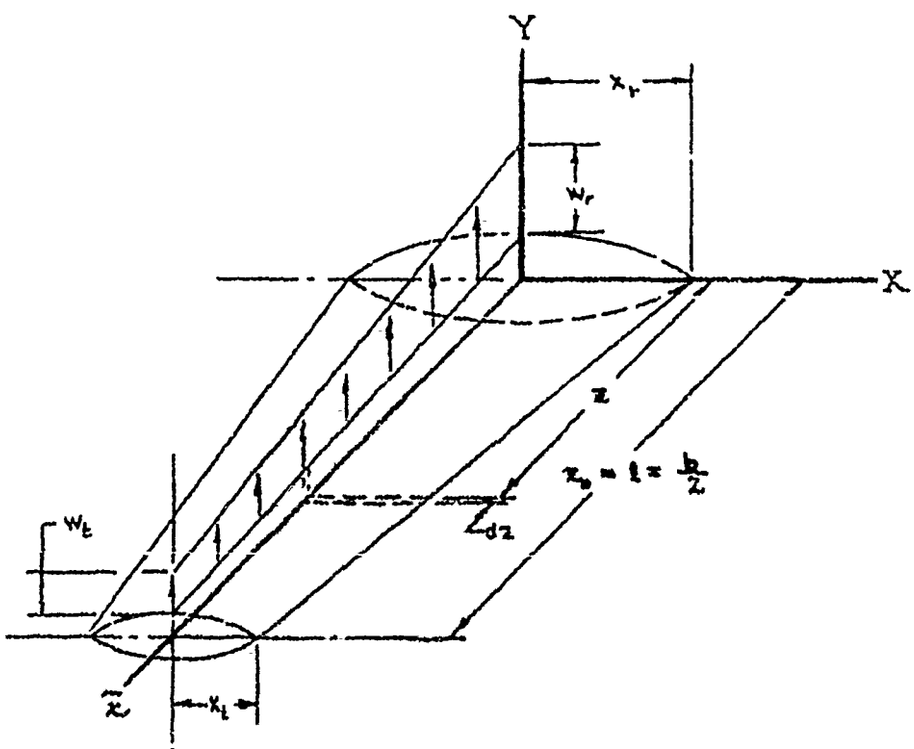

GEOMETRY OF TAPERED HYDROFOIL

FIG. 12

The deflection of a uniformly tapered cantilever hydrofoil under a trapezoidal load distribution, using the geometry of Fig. 12, is derived as follows:

Since $x = mz + k$, $\quad x = x_r\left[1 + \frac{z}{z_o}(\lambda - 1)\right]$.

$x_r = \frac{c_r}{2}$; $\quad z_o = l$.

Then $\quad x = \frac{c_r}{2}\left[1 + \frac{z}{l}(\lambda - 1)\right]$, & $I_x = \frac{4}{105}\tau^3 c_r^4\left[1 + \frac{z}{l}(\lambda - 1)\right]^4$

or $\quad I_x = B\tau^3 c_r^4\left[1 + \frac{z}{l}(\lambda - 1)\right]$. $\qquad$ Equ. 11

$$\Delta M_\Delta = \left(\frac{l-z}{2}\right) w_x \left(\frac{l-z}{3}\right) = \frac{(l-z)^3 w_x}{6}.$$

With $\quad w_x = \frac{(w_r - w_t)(l-z)}{l}$,

$$\Delta M_\Delta = \frac{(l-z)(w_r - w_t)}{6l}.$$

$$\Delta M_\square = \frac{(l-z)^2 w_t}{2}.$$

Where $\quad \frac{w_t}{w_r} = \lambda$,

$$M = \frac{w_r}{2}\left[\frac{(l-z)^3(1-\lambda)}{3l} + (l-z)^2\lambda\right], \qquad \text{Equ. (1)}$$

$$\& \quad y_{max} = \delta = -\frac{1}{E}\int_0^l \frac{(l-z)\frac{w_r}{2}\left[\frac{(l-z)^3(1-\lambda)}{3l} + (l-z)^2\lambda\right]dz}{B\left[1 + \frac{z}{l}(\lambda-1)\right]^4} \qquad \text{Equ. 12}$$

FOR $\lambda = 0.5$

$$y_{max} = -\frac{w_r}{4BE}\int_0^l \frac{(l-z)\left[\frac{(l-z)^3}{2l} + (l-z)^2\right]dz}{\left[1 - \frac{z}{2l}\right]^4} \qquad \text{Equ. 13}$$

$$\text{or } y = \delta = \frac{W_r}{4BE}\int_0^z \frac{(z-z_1)\left[\frac{(l-z_1)^3}{3l}+(l-z_1)^2\right]dz_1}{\left[1-\frac{z_1}{2l}\right]} \qquad \text{Equ. 13A}$$

for deflection at any point. WHEN $l = z$,

$$y_{tip} = -\frac{W_r l^4}{4BE}(0.522). \qquad \text{Equ. 14}$$

Where $B = I_o$, and I_o = moment of inertia of root section.

$$y_{tip} = -0.1305\,\frac{W_r l^4}{E I_o}. \qquad \text{Equ. 15}$$

By substituting the aspect ratio, thickness ratio, span, and hydrofoil loading into Equation 15 gives:

$$y = 0.001254\left(\frac{b}{2}\right)\left[\frac{W}{S}\eta\right]\left(\frac{A_F}{\tau_F}\right)^3\frac{1}{E}. \qquad \text{Equ. 16}$$

For a rectangular planform hydrofoil with a constant section moment of inertia and a uniform spanwise waterload distribution, $y = \frac{wl^4}{8EI}$. By substituting the aspect ratio, thickness ratio, span, and loading into that equation, the deflection becomes:

$$y = 0.002845\left(\frac{b}{2}\right)\left[\frac{W}{S}\eta\right]\left(\frac{A_F}{\tau_F}\right)^3\frac{1}{E}. \qquad \text{Equ. 17}$$

(b is in inches)

Where both planforms develop the same bending stresses and both have the same thickness ratios,

from Equ. 5, $A_{F_{TAPER}} = 1.632\,A_{F_{RECT.}}$. Equ. 18

Thus, from Equ. 16, 17 and 18,

$$\frac{y_{TAPER}}{\left(\frac{b}{2}\right)_{\lambda=0.5}} = \frac{y_{RECT}}{\left(\frac{b}{2}\right)_{\lambda=1.0}}(1.92). \qquad \text{Equ. 19}$$

Where τ_r, A_r, S, & b are equal

$y_{TAPER} = 0.441\ y_{RECT.}$ Equ. 20

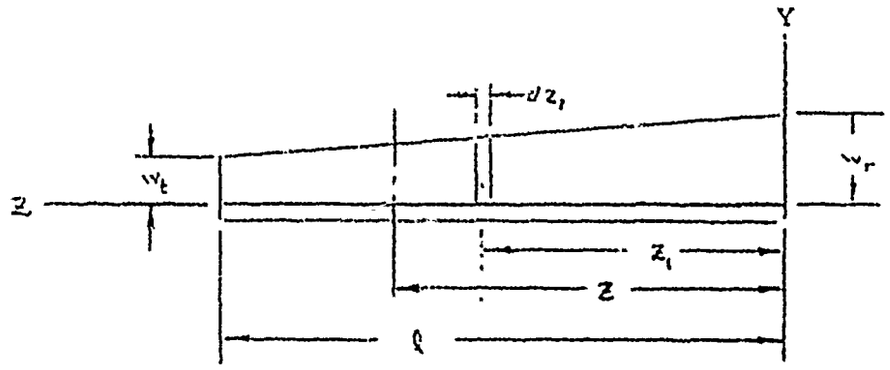

TRAPEZOIDAL LOAD DIST.
FIG. 13.

For a rectangular planform hydrofoil with a constant section moment of inertia and a trapezoidal spanwise waterload distribution, as shown in Fig. 13, the deflection, y, of any section, z, may be expressed as: (by the area-moment method)

$$y = -\frac{1}{E I_x}\int_{z_1=0}^{z_1=z}(z-z_1)\frac{w_r}{A}\left[\frac{(\ell-z_1)^3}{3\ell}+(\ell-z_1)^2\right]dz_1 \quad \text{Equ. 21}$$

Where $M = \frac{w_r}{A}\left[\frac{(\ell-z)^3}{3\ell}+(\ell-z)^2\right]$ is from Equ. 1, for $\lambda = 0.5$. Integrating and collecting terms, Equation 21 becomes:

$$y = -\frac{w_r}{4E I_x}\left[\frac{2l^2z^2}{3} - \frac{lz^3}{2} + \frac{z^4}{6} - \frac{z^5}{60l}\right]. \qquad \text{Equ. 22}$$

When $z = l$,

$$y_{max} = -\frac{w_r l^4}{4E I_x}\left(\frac{19}{60}\right). \qquad \text{Equ. 23}$$

Substituting for w_r, l, & I_x, gives:

$$\frac{y_{max}}{\left(\frac{b}{2}\right)} = 0.002405\left[\frac{W}{S}n\right]\left(\frac{A_r}{\tau}\right)^3\frac{1}{E}. \qquad \text{Equ. 24}$$

This may be derived also by double integration from the equation $M = E I_x \frac{d^2y}{dz^2}$ when M has the same value as in Equation 1:

$$E I_x \frac{d^2y}{dz^2} = \frac{w_t}{2}\left[\frac{4l^2}{3} - 3lz_1 + 2z_1^2 - \frac{z_1^3}{3l}\right].$$

PREVIOUS PG. BLURRED

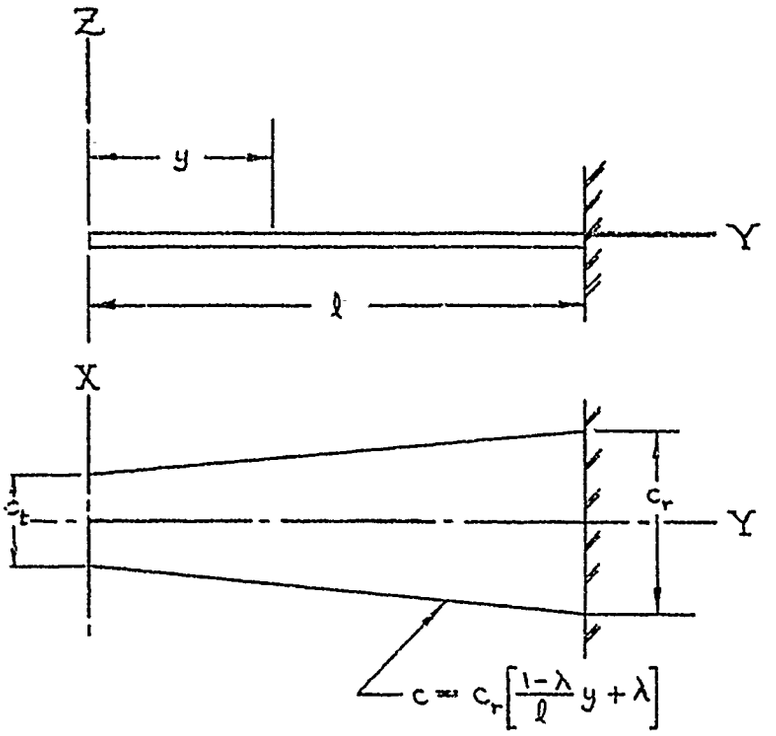

TAPERED STRUT, CONSTANT LOAD
FIG. 14

For a constant force, P, at the end of a cantilever strut of variable moment of inertia (see Fig. 14)

$$\delta = \int_0^{\ell} \frac{P x^2 dx}{E I}.$$

This, upon integrating, becomes:

$$\delta = \frac{P}{BE} \frac{\ell^3}{(1-\lambda)^3} \left[\frac{1 - 3\lambda + 3\lambda^2 - \lambda^3}{3\lambda}\right] \qquad \text{Equ. 25}$$

or

$$\delta = \frac{2 P \ell^3}{BE} \qquad \text{Equ. 26}$$

where $\lambda = 0.5$.

The hydrofoil deflection formulae which are presented in Figs. 16 through 22 are:

Mono-Strut:

$$\left(\frac{\delta_{max}}{\ell}\right) = 0.002645 \left[\frac{W}{S}\eta\right]\left(\frac{A_F}{\tau_F}\right)^3 \frac{1}{E} \cdot \qquad \text{Equ. 17}$$

$$\ell = \frac{b}{2}$$

Twin-Strut:

Overhang:
$$\left(\frac{\delta_{max}}{\ell}\right) = 0.000{,}2595 \left[\frac{W}{S}\eta\right]\left(\frac{A_F}{\tau_F}\right)^3 \frac{1}{E} \cdot \qquad \text{Equ. 27}$$

$$\ell = 0.225\, b$$

Center
$$\left(\frac{\delta_{max}}{\ell}\right) = 0.000{,}079 \left[\frac{W}{S}\eta\right]\left(\frac{A_F}{\tau_F}\right)^3 \frac{1}{E} \cdot \qquad \text{Equ. 28}$$

$$\ell = 0.55\, b$$

Three-Strut:

Overhang:
$$\left(\frac{\delta_{max}}{\ell}\right) = 0.000{,}0694 \left[\frac{W}{S}\eta\right]\left(\frac{A_F}{\tau_F}\right)^3 \frac{1}{E} \cdot \qquad \text{Equ. 29}$$

$$\ell = 0.145\, b$$

Center:
$$\left(\frac{\delta_{max}}{\ell}\right) \quad 0.000{,}02125 \left[\frac{W}{S}\eta\right]\left(\frac{A_F}{\tau_F}\right)^3 \frac{1}{E} \cdot \qquad \text{Equ. 30}$$

$$\ell = 0.355\, b$$

Other deflection formulae for the mono-strut, which were developed on the preceding pages, are summarized below. For varying moment of inertia, trapezoidal spanwise waterload distribution, and taper of one-half:

$$\left(\frac{\delta_{max}}{\ell}\right)_{\lambda=0.5} = 0.001254 \left[\frac{W}{S}\eta\right]\left(\frac{A_F}{\tau_F}\right)^3 \frac{1}{E} \cdot \qquad \text{Equ. 16}$$

$$\ell = \frac{b}{2}$$

$$\delta_{MAX.,\lambda=0.5} = 0.441\ \delta_{MAX.,\lambda=1.0}$$

(for equal span) Equ. 20

$$\left(\frac{\delta_{MAX.}}{l_t}\right)_{\lambda=0.5} = 1.92\left(\frac{\delta_{MAX.}}{l}\right)_{\lambda=1.0} \cdot$$ Equ. 19

For constant moment of inertia and a 2-to-1 trapezoidal spanwise waterload distribution:

$$\left(\frac{\delta_{MAX}}{l}\right) = 0.0024\left[\frac{W}{S}\eta\right]\left(\frac{A_F}{\tau_F}\right)^3\frac{1}{E} \cdot$$ Equ. 24

$$l = \frac{b}{2}$$

$$\delta_z = -\frac{W_r}{4EI}\left[\frac{2l^2z^2}{3} - \frac{lz^3}{2} + \frac{z^4}{6} - \frac{z^5}{60l}\right] \cdot$$ Equ. 22

$$\delta_z = -0.243\left[\frac{W}{S}\eta\right]\frac{1}{\tau^3 c^3 E}\left[\frac{2l^2z^2}{3} - \frac{lz^3}{2} + \frac{z^4}{6} - \frac{z^5}{60l}\right]$$ Equ. 31

Fig. 15 gives the variation of $\left(\frac{\delta_{max.}}{\ell}\right)$ with aspect ratio for various hydrofoil thickness ratios on a mono-strut configuration having a taper ratio of one-half. The spanwise load distribution varies with the chord and is for a 1.0 ksf hydrofoil loading. Figures 16 and 17 are for the same configuration with a rectangular planform. Figure 17 is included to show the effect of very thin hydrofoil sections.

For a rectangular two-strut configuration, Fig. 18 presents similar data for the overhanging portion of the hydrofoil while Fig. 19 is for the center portion of the hydrofoil. Similar three-strut data are presented in Figures 20 and 21, respectively. These are all for a hydrofoil loading of 1.0 ksf. Fig. 22 is for the center section of a three-strut configuration (like Fig.21), but includes the effect of variation of the hydrofoil loading.

The slight variation in the values for E which are used occurs because the original charts are constructed for chromium-nickel steels while the other charts are constructed for mild steel. (Data for configurations involving more than three struts do not seem of sufficient importance to justify their inclusion at the present time.)

Woodrich

Tip Deflection Ratio for
Homogeneous Construction

Fig. 15

$$\frac{\delta_{x=0.5}}{\left(\frac{b}{2}\right)} = 0.001254 \left[\frac{W}{S}_h\right] \left(\frac{A_T}{\tau_T}\right)^3 \frac{1}{E}$$

$\Delta = 0.5$
$E = 28{,}000$ KSI
Rect. Cg Dists.
$\left[\frac{W}{S}\right]_h = 10$ KSF

$\frac{\delta_{MAX.}}{\left(\frac{b}{2}\right)}$

0.13
0.12
0.11
0.10
0.09
0.08
0.07
0.06
0.05
0.04
0.03
0.02
0.01
0

0.09
0.10
0.11
0.12
0.13
0.14
0.15
0.16
0.17

HYDROFOIL THICKNESS RATIO $\frac{t}{c}$ τ_T

1 2 3 4 5 6 7 8 9 10 11 12 13 14

A_T Hydrofoil Aspect Ratio

YF

Tip Deflection Ratio for Mono-Strut Configuration

Fig. 16

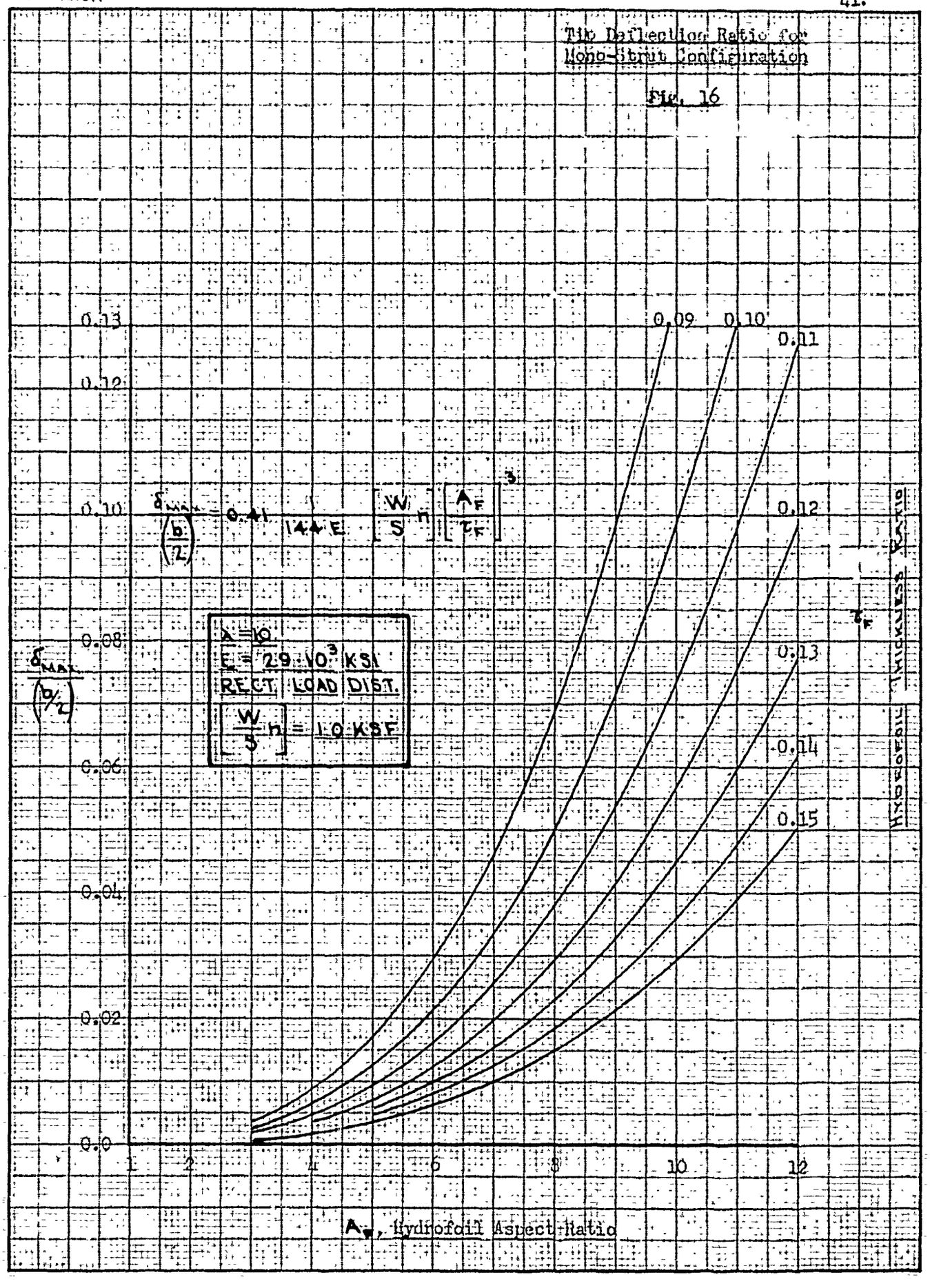

Hydrofoil with Deflection Ratio for Cross-Strut Configuration with Rectangular Planform and A.D.K.S.F. Hydrofoil Loading

Fig. 17

$$\frac{\delta_{MAX}}{\frac{b}{2}} = \frac{0.41}{AA\,E}\left[\frac{W}{S}H\right]\left[\frac{A_F}{\tau_F}\right]^3$$

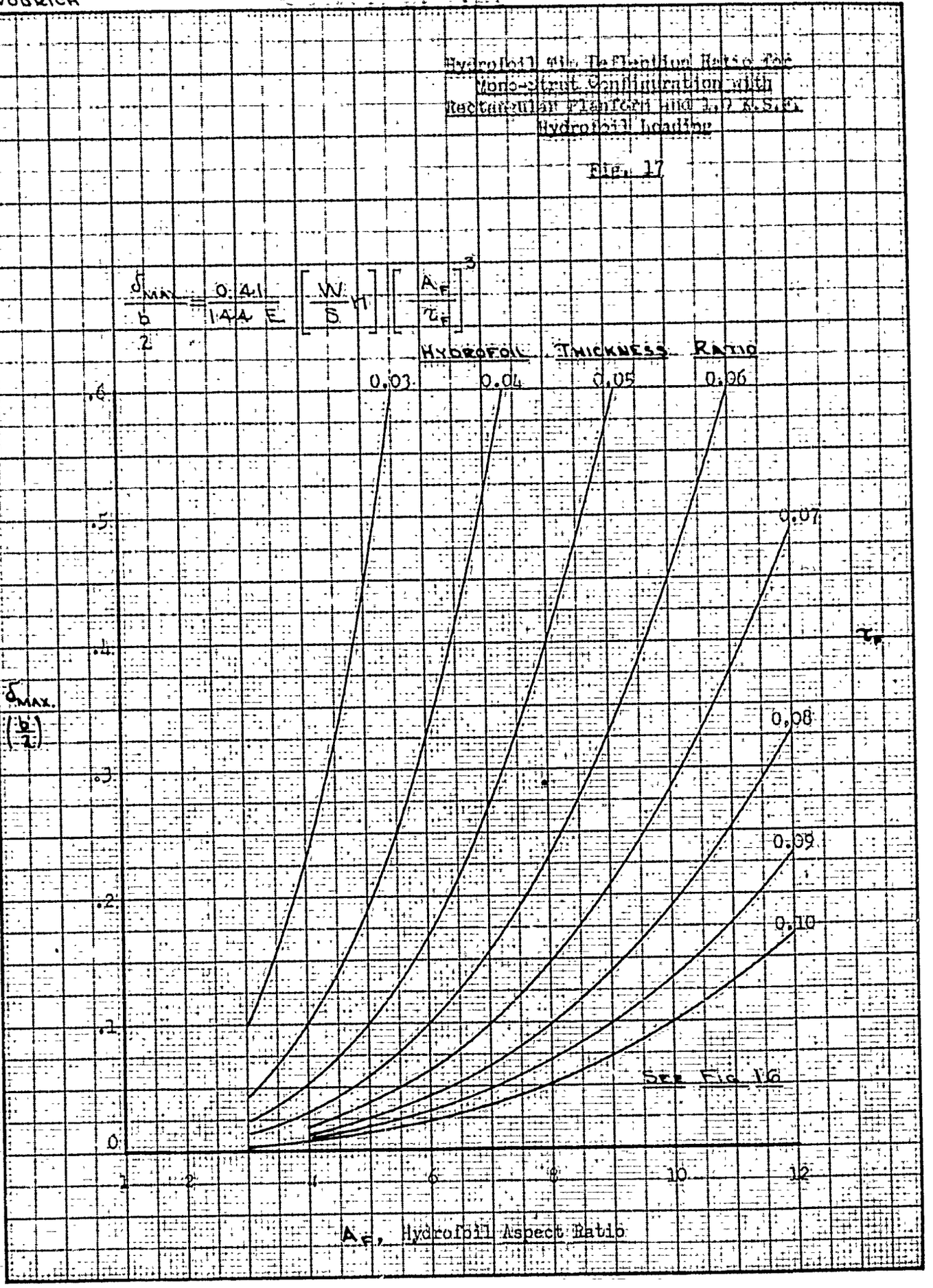

HF

Hydrofoil Deflection Ratio for Tip of Overlapped on Tee-Shaft Configuration with Rectangular Planform and 3.0 KSF Hydrofoil Loading

Fig. 18

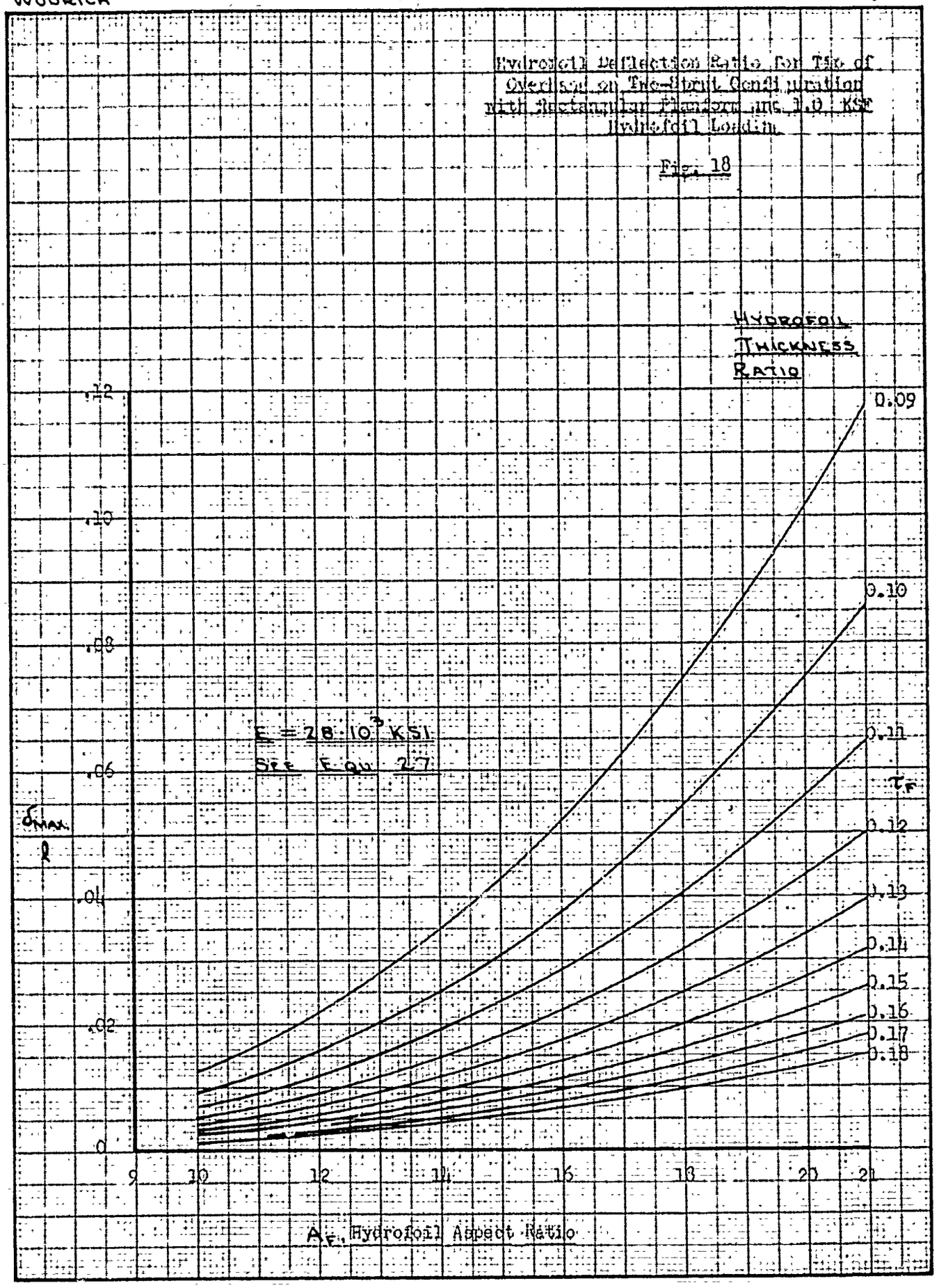

12F

Hydrofoil Deflection ratio at Center of Span for Two-Strut Configuration with Rectangular Planform and 5.0 KSF Hydrofoil Loading

Fig. 19

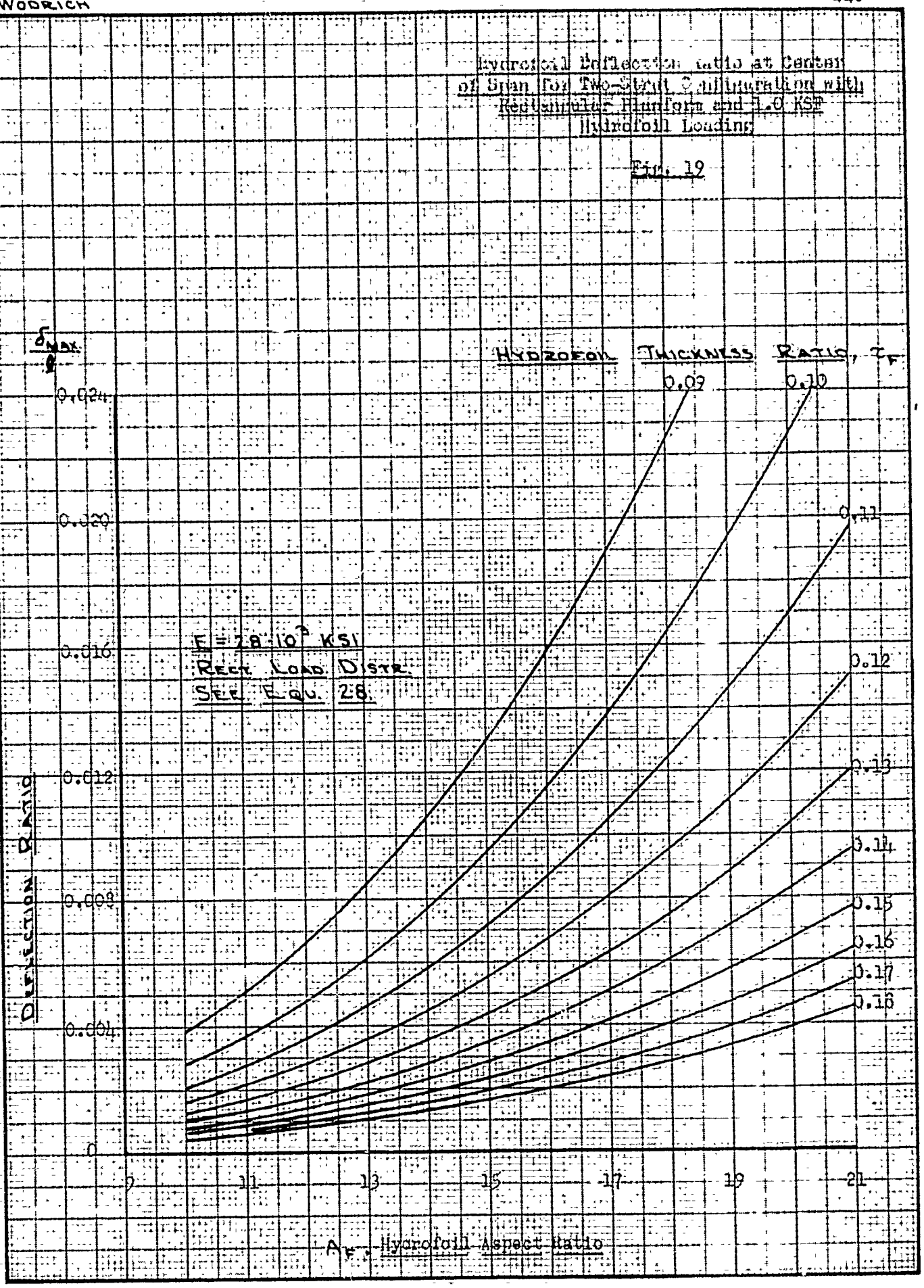

Variation of Deflection Ratio of Outboard Tip Hydrofoil with Tapered Planform and L.O KSF Hydrofoil Loading

Fig. 20

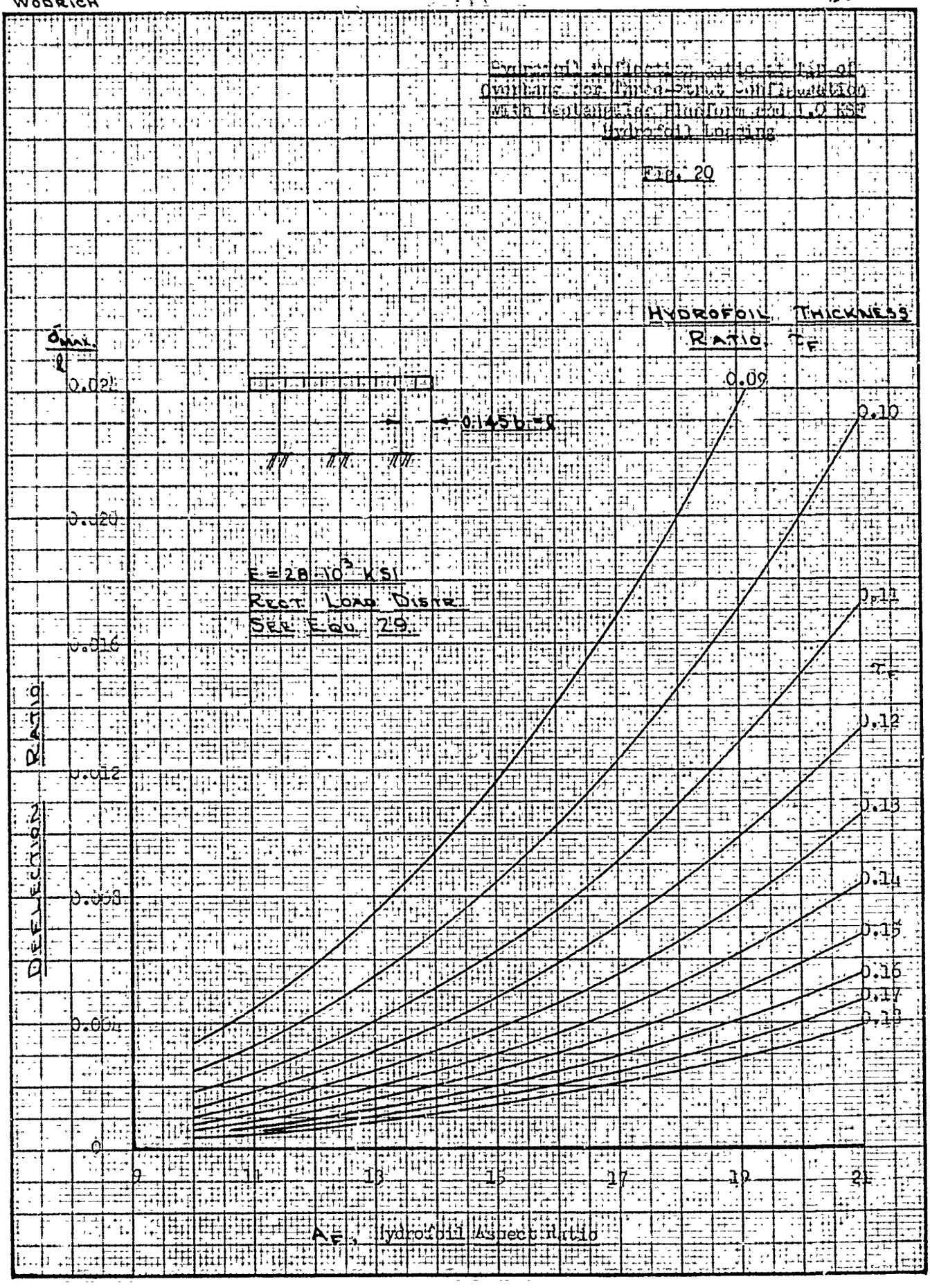

14F

Hydrofoil Deflection Ratio at Midpoint between Struts for Three-Strut Configuration with Rectangular Planform and 1.0 KSI Hydrofoil Loading

Fig. 21

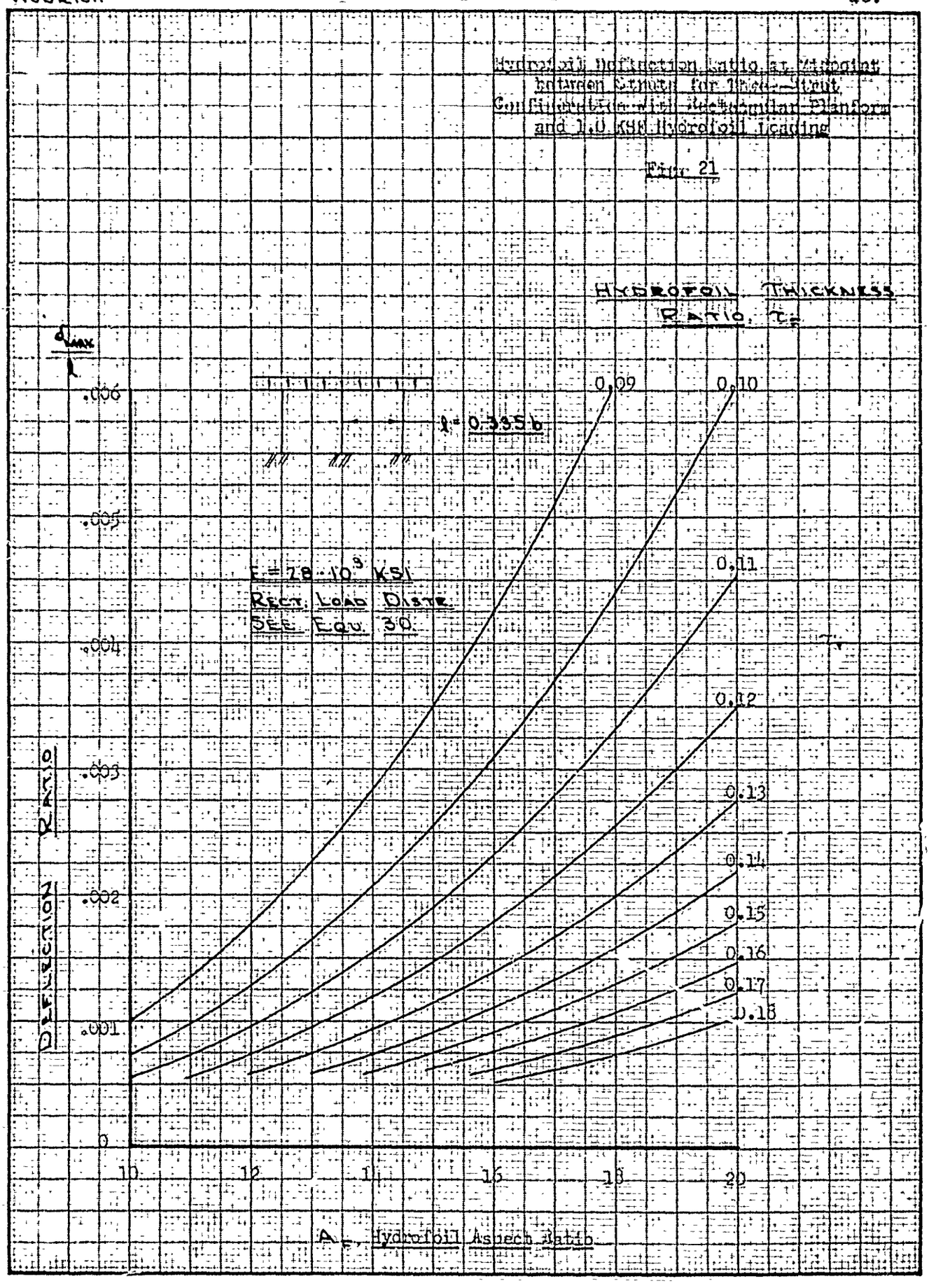

Woolrich
9 Nov 1949

CONFIDENTIAL

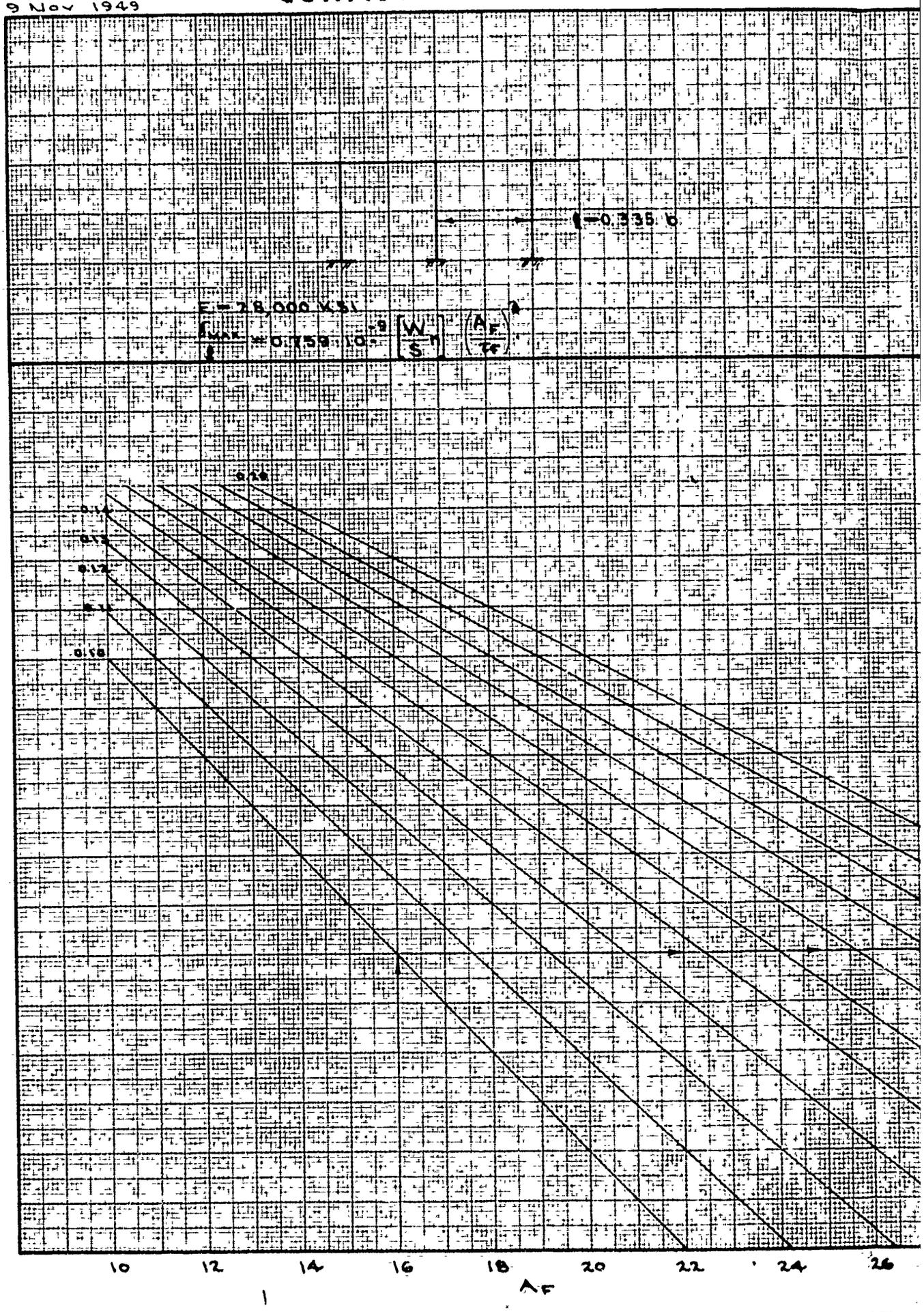

2E

Maximum Deflection at Center of Span of Three Strut Configuration

Fig. 22

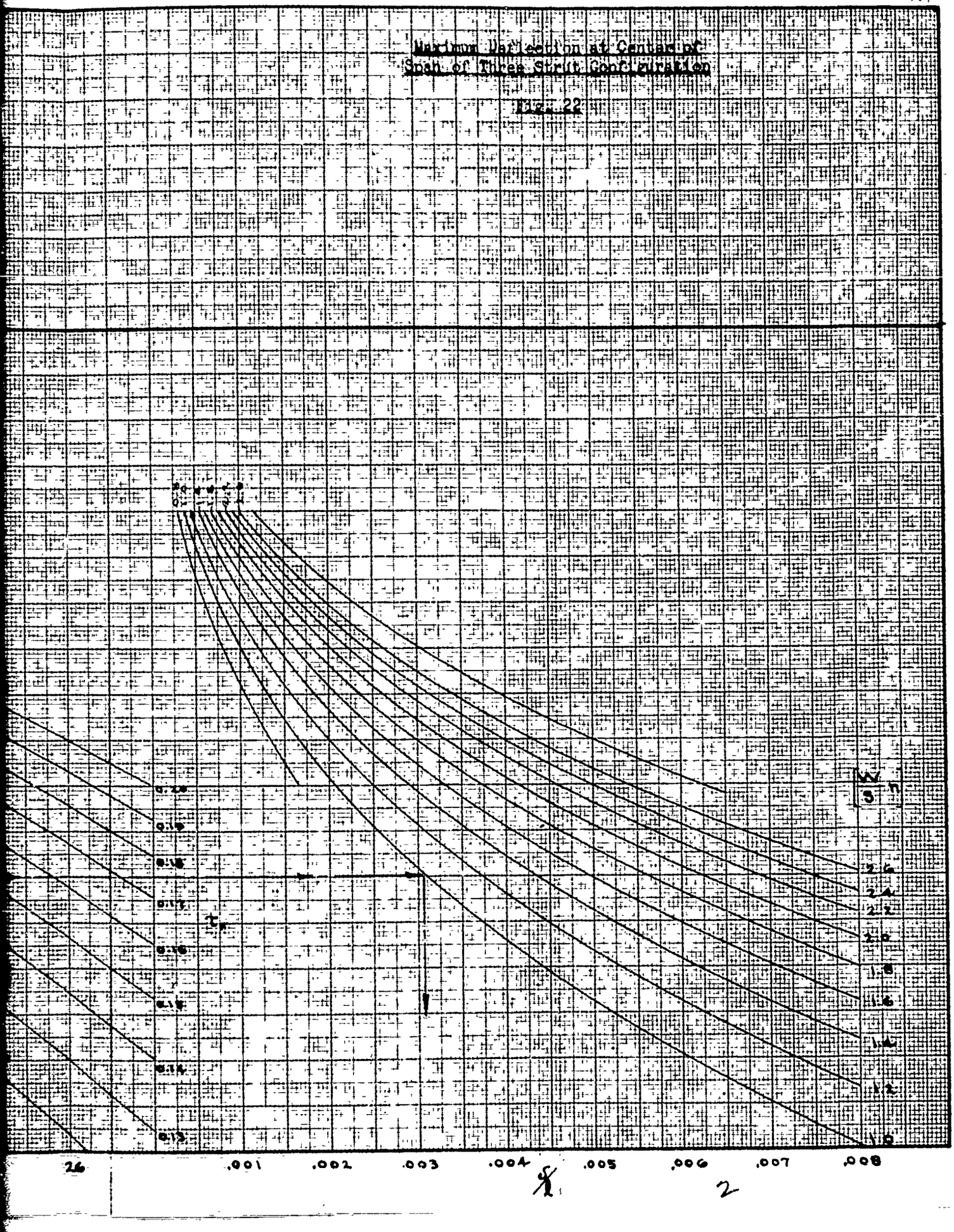

Struts and Columns:

The critical value for the compressive stress in slender, straight columns with concentrically applied compressive forces can be calculated with sufficient accuracy provided the compression-test diagram for the column material is known. Within the elastic range, Euler's formula must be used for such calculations: For use beyond the proportional limit, as in short columns, Euler's formula must be modified with the reduced modulus, E_r, or the tangent modulus, E_t, being used instead of E[1]. From such calculations, diagrams representing σ_{cr} as a function of the slenderness ratio can be obtained.

In the application of this formula to column and strut design, the selection of a proper factor of safety is the principal difficulty encountered: this factor of safety should compensate for the various column imperfections. It seems logical to assume certain inaccuracies in a column from the very beginning and to devise formulae which contain not only the column dimensions and the material, but also the values of the assumed inaccuracies. By incorporating these inaccuracies in the design formulae, the selection of a proper factor of safety can be put on a more reliable basis. (This assumes that the material and mode of fabrication have been selected). The simplest method of choosing the factor of safety is to assume that the effect of various imperfections on the deformation of columns and on the maximum fiber stress which is produced is independent of slenderness ratio, i.e., constant. But imperfections such as an initial curvature of the column are apt to increase with slenderness ratio.

The principal imperfections[2] which make the behavior of actual columns so different from those which are assumed in Euler's theory are: an unavoidable eccentricity in the application of the compressive load, initial curvature of the column, and non-homogeneity of the material, including

(1) See Ref. 7.

(2) Column inaccuracies are discussed in detail in Ref. 8.

variation in the cross-sectional area. All of these imperfections may be replaced by an equivalent initial column deflection.

The struts are initially considered to have uniform sections throughout their length. Struts which can carry the concentric loads, and no moments, have slenderness ratios between 160 and 180. To keep the slenderness ratio less than 120, as in structural engineering practice, tapered or stepped struts are necessary. By tapering or stepping the struts between the operating waterline and the hull, the change in thickness of the section will not affect the normal operating efficiency of the boat.

It is found that struts with slenderness ratios of less than 120 obtained with a step of one-third the strut length, and the thicker section having a section moment of inertia of four times the section moment of inertia of the thinner section, will automatically allow for the effects of normal loads on the struts caused by yaw at the instant of take-off. The thicker section, if but one-third of the strut length, will normally be above the water surface. (On a six-foot long strut with a depth of submergence of three feet, one-third of the strut length, or two feet, will permit a clearance of one foot between the cruise water line and the change in section.) This will also provide for a given amount of eccentricity in the application of the hydrofoil load.

Reference 9 indicates the considerable concern of the British about end fixity for the struts and foils. The amount of fixity which is actually realized in any condition will greatly affect distribution of the loads among struts and foils. If, in a "pi" configuration, the struts under load obtain a slope due to joint flexibility or flexibility in the hull of the vessel, the bending moment in the hydrofoil will be materially changed. In this study, perfect fixity is assumed at the hull or hulls, and in some cases pin-ended conditions are assumed at the column-foil and strut-foil junctions. Where necessary, overlapping assumptions are used. But it should be remembered that for any particular configuration, material,

and mode of fabrication, actual structural tests will be required in order to obtain the best structural-hydrodynamic compromise for the design.

The effect of side loadson the struts in combination with the axial compressive loads must be considered in determining the strut size. The most critical condition occurs either at take-off, when the maximum yaw angle exists and the strut is fully submerged, or at the maximum velocity of the vessel, when the minimum strut length is submerged and the greatest "q" occurs. Which of these will be the most critical depends upon the specific geometry and the maximum side load which can be developed within the 1g limitation.

Likewise, consideration must be given to the effect of eccentricity, the load on the strut either not being concentric or else having an induced moment due to the lack of balance over the supports. Pin-ending the strut-foil connections would eliminate this moment.

As stated on p. 9, biconvex, parabolic arc, solid sections are used in the calculations of the struts and columns. It appears likely that such sections will be found to be near the optimum from hydrodynamic considerations, as well as possessing definite structural advantages. A British document, Ref.10, discusses strut sections.

Concentric Loading

For a fixed-ended cantilever strut of uniform cross-section, the critical buckling stress may be expressed as:

$$\sigma_{cr} = \frac{\pi^2 E_t}{4\left(\frac{l}{\rho}\right)^2} \qquad \text{(Ref. 7)} \qquad \text{Equ. 32}$$

Where $\rho = \sqrt{\frac{I_s}{A_s}} = c_{F_r} k \tau_s \sqrt{\frac{2}{35}}$,

$$l = m\, c_{F_r} , \qquad \sigma_\lambda = \frac{\sigma_{cr}}{F} ,$$

(I_s = least moment of inertia of strut,
& A_s = cross section area of strut.)

and $\sigma_A = \frac{P}{A_s} = \frac{1}{384}\left[\frac{W}{S}\eta\right]\frac{A_F}{\tau_s k^2}(1+\lambda)^2$;

$$\sigma_A = \frac{P}{A_s} = \frac{\tau_s^2 k^2 \pi^2 E_t}{70 m^2 F} = \frac{1}{384}\left[\frac{W}{S}\eta\right]\frac{A_F(1+\lambda)^2}{\tau_s k^2} \quad \text{Equ. 33}$$

By transposing, $$\tau_s^3 = 0.01845\left[\frac{W}{S}\eta\right]\frac{A_F(1+\lambda)m^2F}{k^4 E_t} \quad \text{Equ. 34}$$

Using $E_t = 28{,}300$ ksi for $\frac{3}{4}$H, transverse, stress relieved, high tensile steel;

$$\tau_s = 0.00866\sqrt[3]{F\left[\frac{W}{S}\eta\right]\frac{A_F(1+\lambda)}{k^4}m^2} \quad . \qquad \text{Equ. 35}$$

See Ref. 11 for typical curves of the tangent modulus of elasticity.

Equation 35 is plotted in Fig. 23 without regard to strut slenderness ratio. This nomograph is for use in the initial phase of a configuration selection, but the sizes obtained must be modified to allow for eccentricity, side load, and reasonable slenderness ratios. However, the form of Figure 23 is not such that the effect of certain variables may be readily assessed. The effect of these are shown in Figures 24, 25, 26, and 27 for a monostrut configuration.

Figures 24, 25, and 26 present the variation of thickness ratio with aspect ratio for a rectangular hydrofoil planform. Figure 24 shows the effect of varying the hydrofoil loading; Figure 25 shows the effect of varying the chord ratio; Figure 26 shows the effect of varying the strut length; Figure 27 shows the variation of thickness ratio with hydrofoil loading on a tapered hydrofoil for the effect of aspect ratio.

Woodrich
27 Sept 1949

CONFIDENTIAL

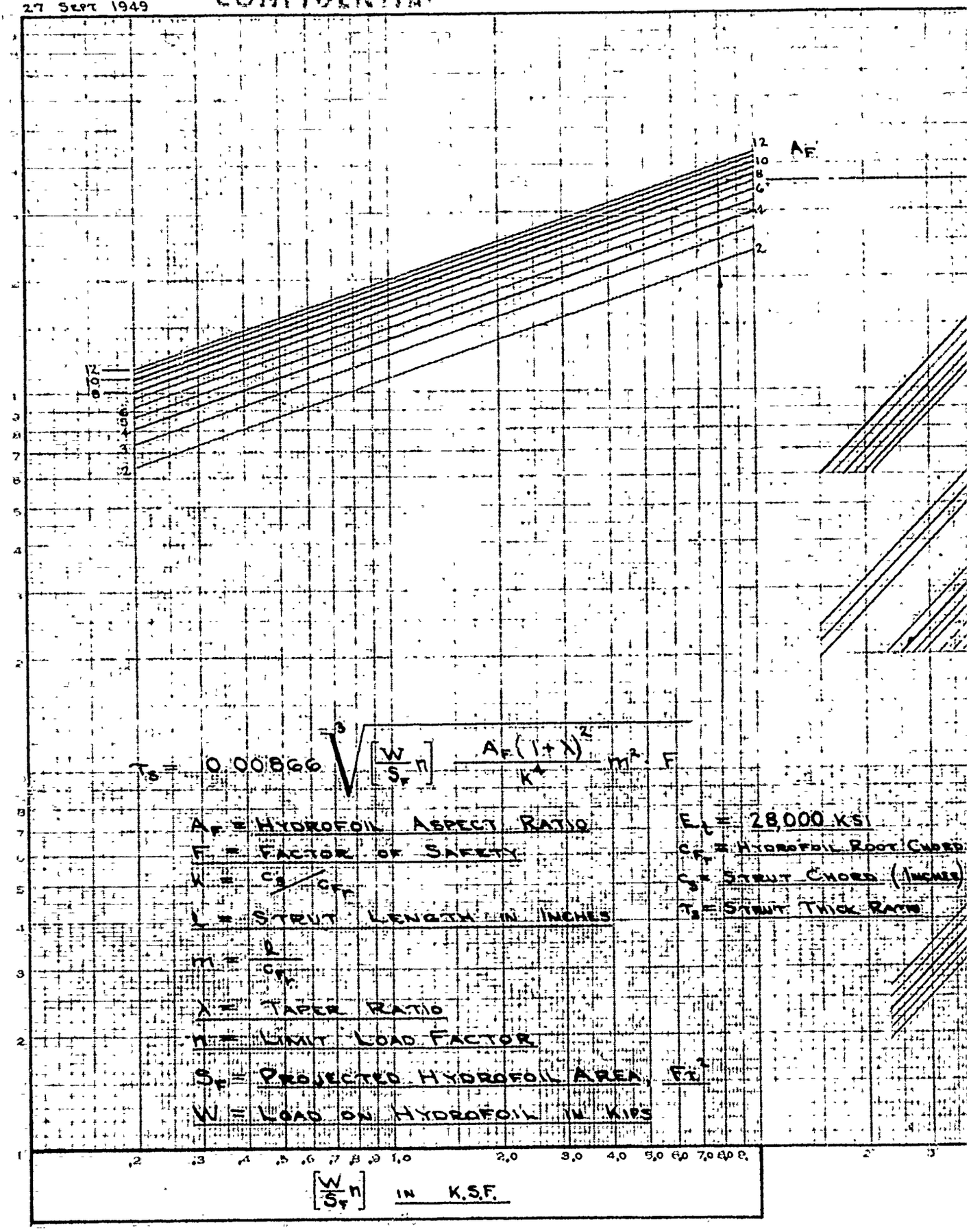

$$T_s = 0.00866 \sqrt[3]{\left[\frac{W}{S_F}\,n\right]\frac{A_F(1+\lambda)^2}{k^4}}\ m^2.F$$

A_F = HYDROFOIL ASPECT RATIO

F = FACTOR OF SAFETY

$W = \frac{C_s}{C_{FR}}$

L = STRUT LENGTH IN INCHES

$m = \frac{L}{C_{FR}}$

λ = TAPER RATIO

n = LIMIT LOAD FACTOR

S_F = PROJECTED HYDROFOIL AREA, FT^2

W = LOAD ON HYDROFOIL IN KIPS

E_L = 28,000 KSI

C_{FR} = HYDROFOIL ROOT CHORD

C_s = STRUT CHORD (INCHES)

T_s = STRUT THICK RATIO

3E

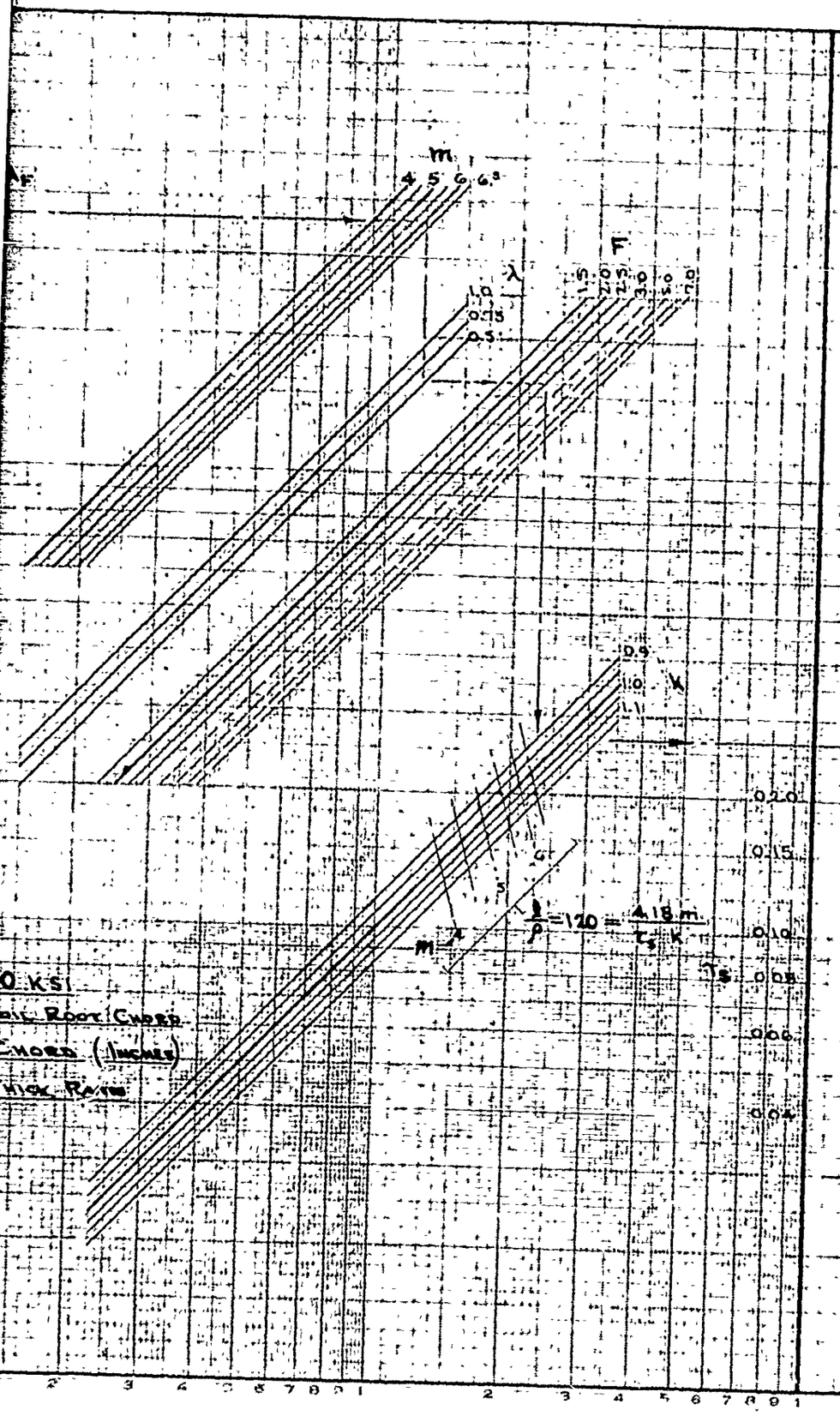

VARIATION OF MINIMUM PERMISSIBLE STRUT THICKNESS RATIO WITH HYDROFOIL LIMIT LOADING & GEOMETRY

FIG 23

BICONVEX, PARABOLIC ARC, SOLID HYDROFOIL
SINGLE CENTER SUPPORT
SYMMETRICAL LOAD
RECTANGULAR C_ℓ DISTR.

$$\tau_s^3 = \frac{35\,F\,m^2}{192\,\pi^4 E_F}\left[\frac{W_n}{S_F}\right]\frac{A_F(1+\lambda)^2}{K^4}$$

CONFIDENTIAL

Variation in Strut Thickness Ratio with Hydrofoil Aspect Ratio for Six Different Hydrofoil Loadings of a Mono-Strut Configuration

Fig. 24

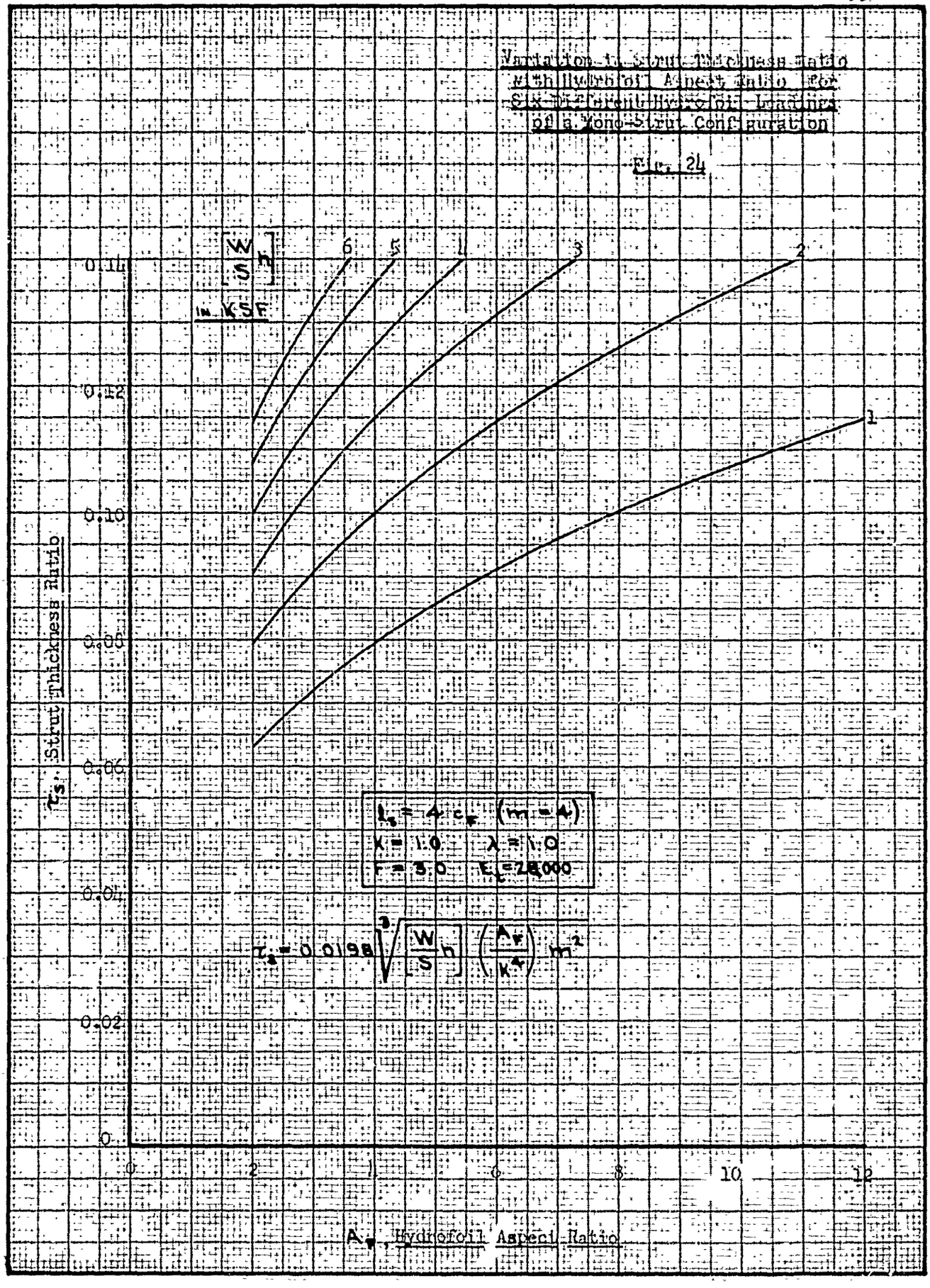

16F

Variation in Strut Thickness Ratio with Hydrofoil Aspect Ratio for Six Different Chord Ratios of a Mono-Strut Configuration

Fig. 25

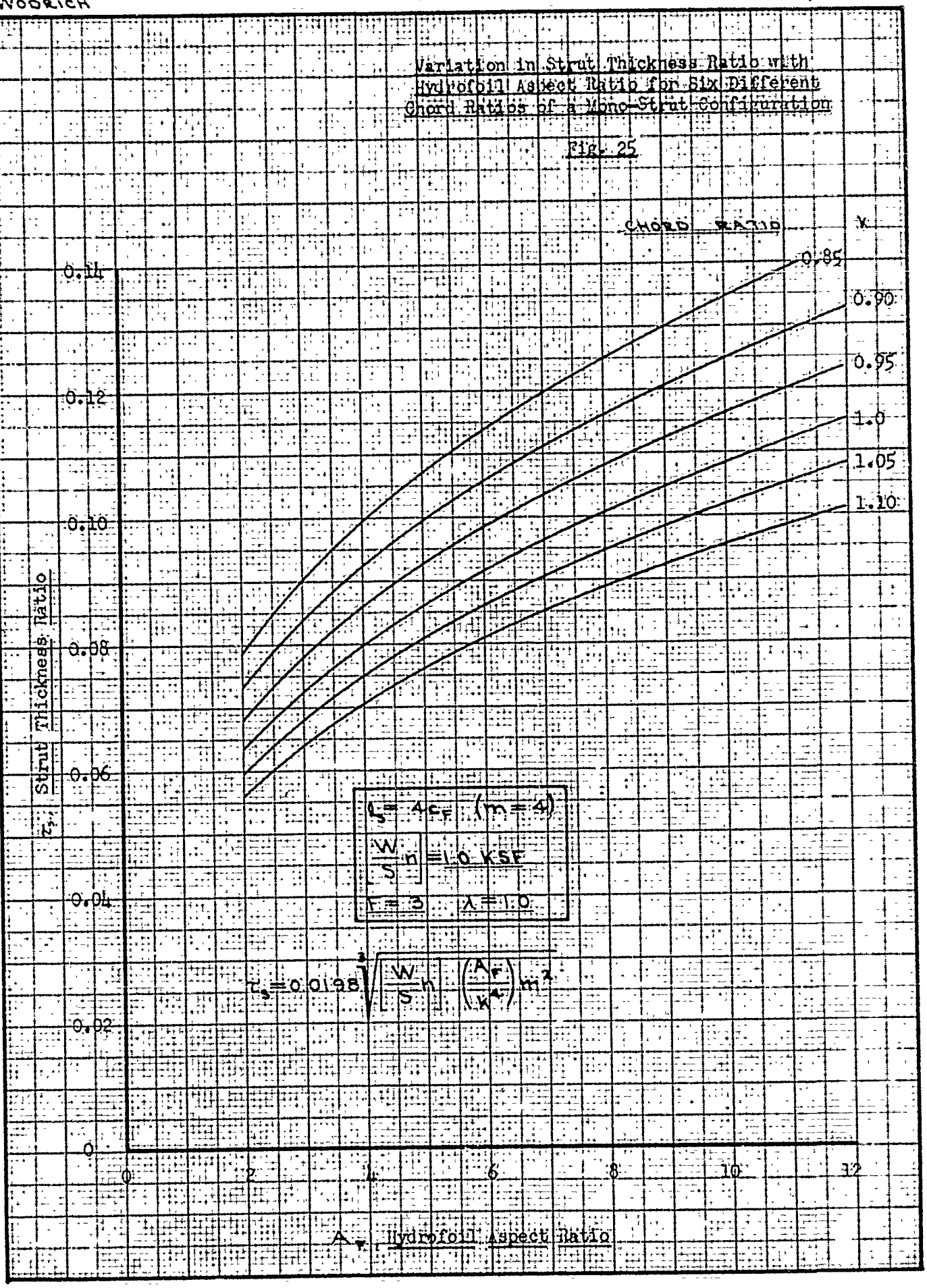

Variation in Strut Thickness Ratio with Hydrofoil Aspect Ratio for Six Different Strut Lengths of a Mono-Strut Configuration

Fig. 26

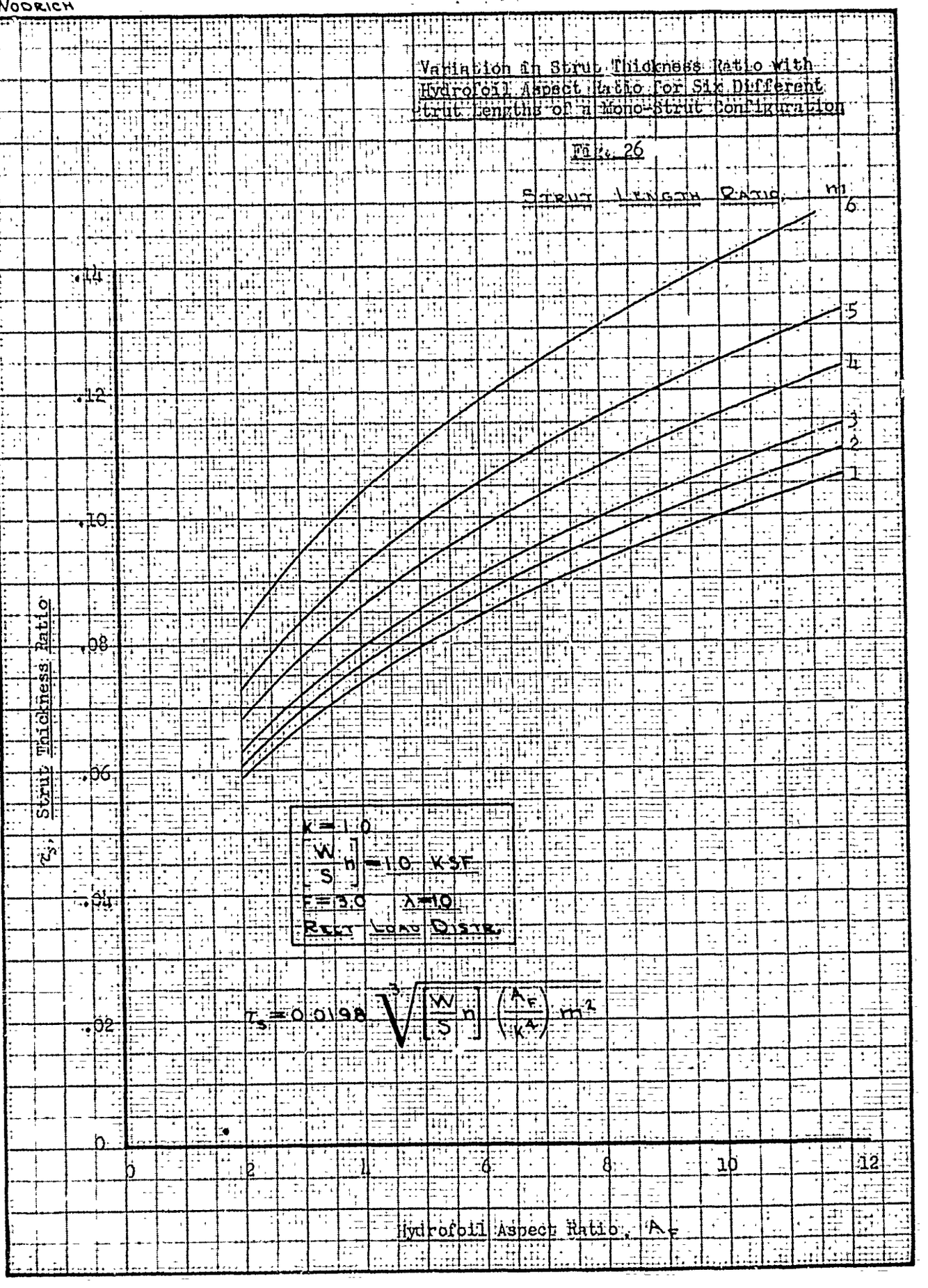

Variation in Minimum Strut Thickness Ratio with Hydrofoil Loading for Various Aspect Ratios of a Mono-Strut Configuration

FIG. 27

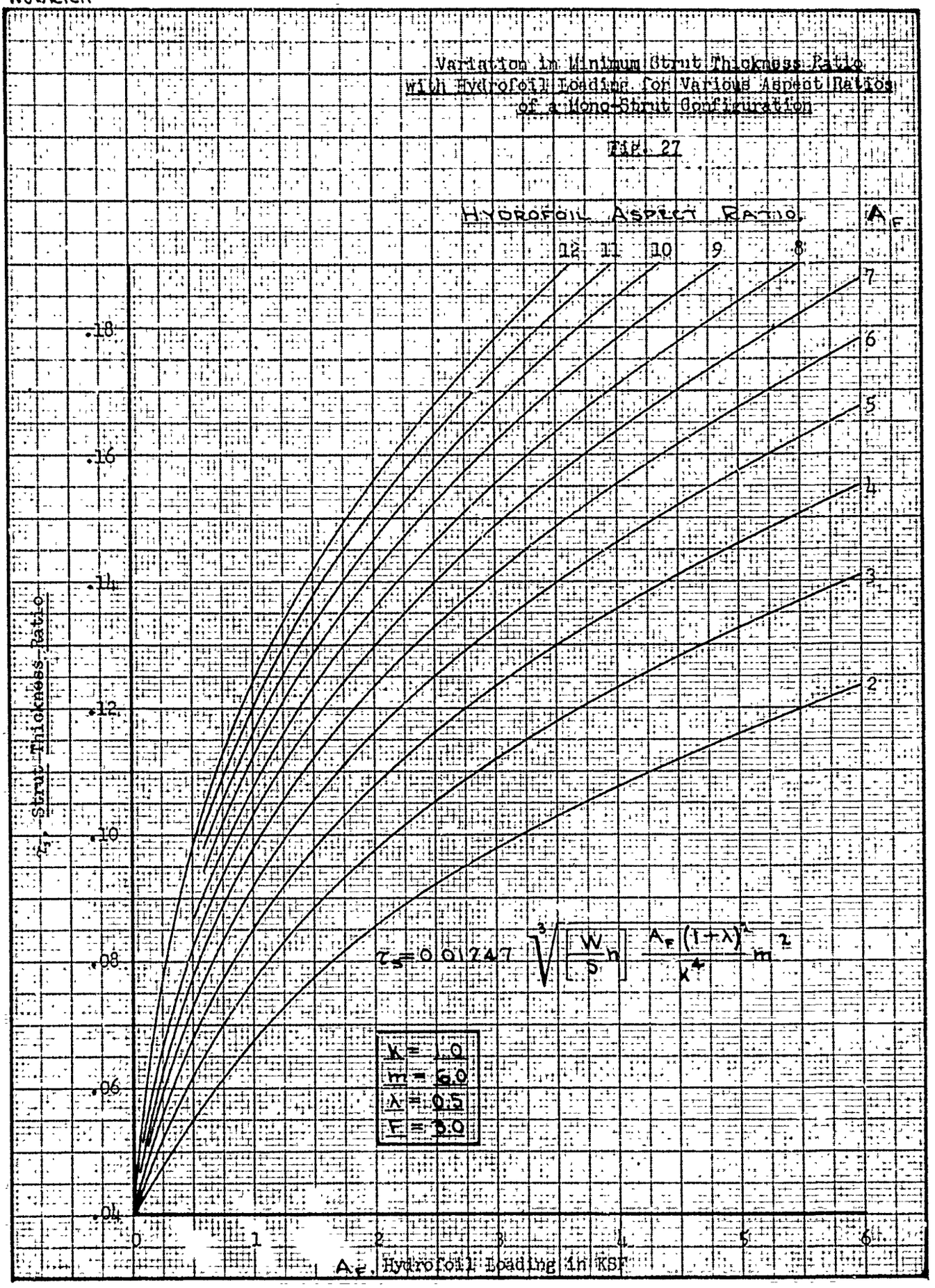

For a tapered strut subjected to a concentric load, the deflection is obtained as a function of the critical loading and strut geometry. Figure 28 depicts the type of column which could be utilized and impare the overall performance of the hydrofoil craft but little. The expression for the relation between critical load and geometry for this type of column has been developed by Timoshenko in Ref. 12. (For reference purposes, it will be repeated herein.) To obtain the critical load, P_{cr}, for the column of Fig. 28 with one end fixed and one end free, and consisting of two portions having moments of inertia of I_1 and I_2, it is necessary to write the differential equations of the two portions of the deflection curve. Where δ is the deflection of the top of the column during buckling, these equations are:

$$E I_1 = \frac{d^2 y_1}{dx^2} = P(\delta - y_1)$$

$$E I_2 = \frac{d^2 y_2}{dx^2} = P(\delta - y_2).$$

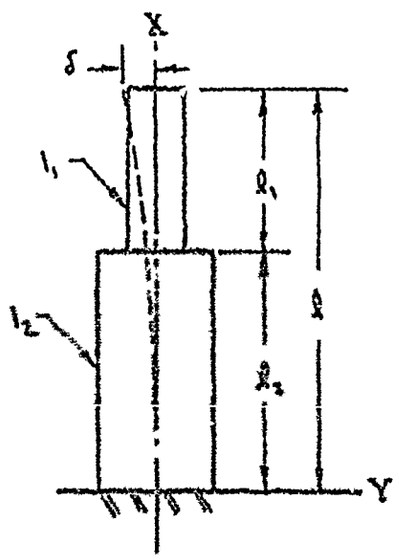

TAPERED STRUT

FIG. 28

Using, $\frac{P}{EI_1} = k_1^2$, & $\frac{P}{EI_2} = k_2^2$; the equations yield:

$$y_1 = \delta + C \cos k_1 x + D \sin k_1 x$$

& $$y_2 = \delta(1 - \cos k_2 x).$$

At $x = l_2$ the deflections of the two portions are equal, and at $x = l$ the deflection is δ. Thus,

$$\delta + C \cos k_1 l - D \sin k_1 l = \delta;$$

$$\delta + C \cos k_1 l_2 + D \sin k_1 l_2 = \delta (1 - \cos k_2 l_2);$$

from which

$$C = -D \tan k_1 l; \quad \& \quad D = \frac{\delta \cos k_2 l_2 \cos k_1 l}{\sin k_1 l_1}.$$

Since both portions of the deflection curve possess the same tangent of $x = l_2$, the equation obtains

$$\delta k_2 \sin k_2 l_2 = -C k_1 \sin k_1 l_2 + D k_1 \cos k_1 l_2.$$

Upon substituting the above values of C and D, the following transcendental equation is obtained for calculating the critical compressive load.

$$\tan k_1 l_1 \cdot \tan k_2 l_2 = \frac{k_1}{k_2}. \qquad \text{Equ. 36}$$

Since

$$I_1 = B \tau_1^3 c_{s_1}^4, \quad \& \quad I_2 = B \tau_2^3 c_{s_2}^4;$$

if $\tau_1 = \tau_2$,

then $$\frac{I_1}{I_2} = \left(\frac{c_{s_1}}{c_{s_2}}\right)^4 = \left(\frac{c_{s_1}}{a\, c_{s_1}}\right)^4 = \left(\frac{1}{a}\right)^4. \qquad \text{Equ. 37}$$

Where $\frac{l_1}{l_2} = \frac{1}{4}$; $q = 4^{0.25} = 1.414$ = ratio of chords, and

$$\frac{k_1}{k_2} = \sqrt{\frac{P}{E I_1}} \sqrt{\frac{E I_2}{P}} = \sqrt{\frac{I_2}{I_1}} = 2.0;$$

if $\ell_1 = 2 \ell_2$, then Equation 36 becomes:

$$\tan\left[\ell_1\sqrt{\frac{P}{E I_1}}\right]\tan\left[0.25\,\ell_1\sqrt{\frac{P}{E I_1}}\right] = 2.0. \quad \text{Equ. 38}$$

By trial and error it is found that for

$$\tan\left[\ell_1\sqrt{\frac{P}{E I_1}}\right] = \tan 1.393^r = 5.51176$$

and for $\tan\left[0.25\,\ell_1\sqrt{\frac{P}{E I_1}}\right] = \tan 0.3482^r = 0.36265$

the conditions of Equation 38 are met.

Then, $$\ell_1\sqrt{\frac{P}{E I_1}} = 1.393$$

or $$P = \left(\frac{1.393}{\ell_1}\right)^2 E I_1 . \quad \text{Equ. 39}$$

Equation 39 is plotted on Fig. 29 for a modulus of elasticity of 4,000 ksi (corresponding to laminated glass fiber based plastics) and in Fig. 30 for a modulus of elasticity of 28,000 ksi (corresponding to mild steel).

Since some use of fibreglas is contemplated in a test craft, and since the modulus of elasticity for such material depends upon technique in lay-up as well as material, the effect of moderate variations in modulus of elasticity upon the strut chord and thickness ratio is needed. By modifying Equation 33, p. 51, the data of Fig. 31 are obtained. For properties of laminated glass fabric based plastic materials, see Refs. 13 and 14.

Woolrich
21 Nov 1949

CONFIDENTIAL

$E = 4{,}000$ KSI
$C_1 = C_2$
$l_1 = 2\,l_2$
$I_{x_2} = 4\,I_{x_1}$
$C_2 = .414\,C_1$
$P_{ALLOW} = \frac{P_{CR}}{F}$

STRUT LENGTH, l_2 IN INCHES

76
74
72
70
68
66
64
62
60

$$\tan\left[l_1\sqrt{\frac{P_{CR}}{E\,I_{x_1}}}\right] \tan\left[l_2\sqrt{\frac{P_{CR}}{E\,I_{x_2}}}\right] = \sqrt{\frac{I_{x_2}}{I_{x_1}}}$$

$$P_{CR} = 7760\,\frac{I_{x_1}}{l_2^2}$$

2 4 6 8 10 12 14 16 18 20 22 24 26 28 30 32 34

CRITICAL BUCKLING LOAD OF STRUT, P_{CR}, IN KIPS

KEUFFEL & ESSER CO., N. Y., NO. 339 14L

4E

Determination of Strut Geometry from Concentric Strut Load for Solid Biconvex Parabolic Arc Sections

Fig. 29

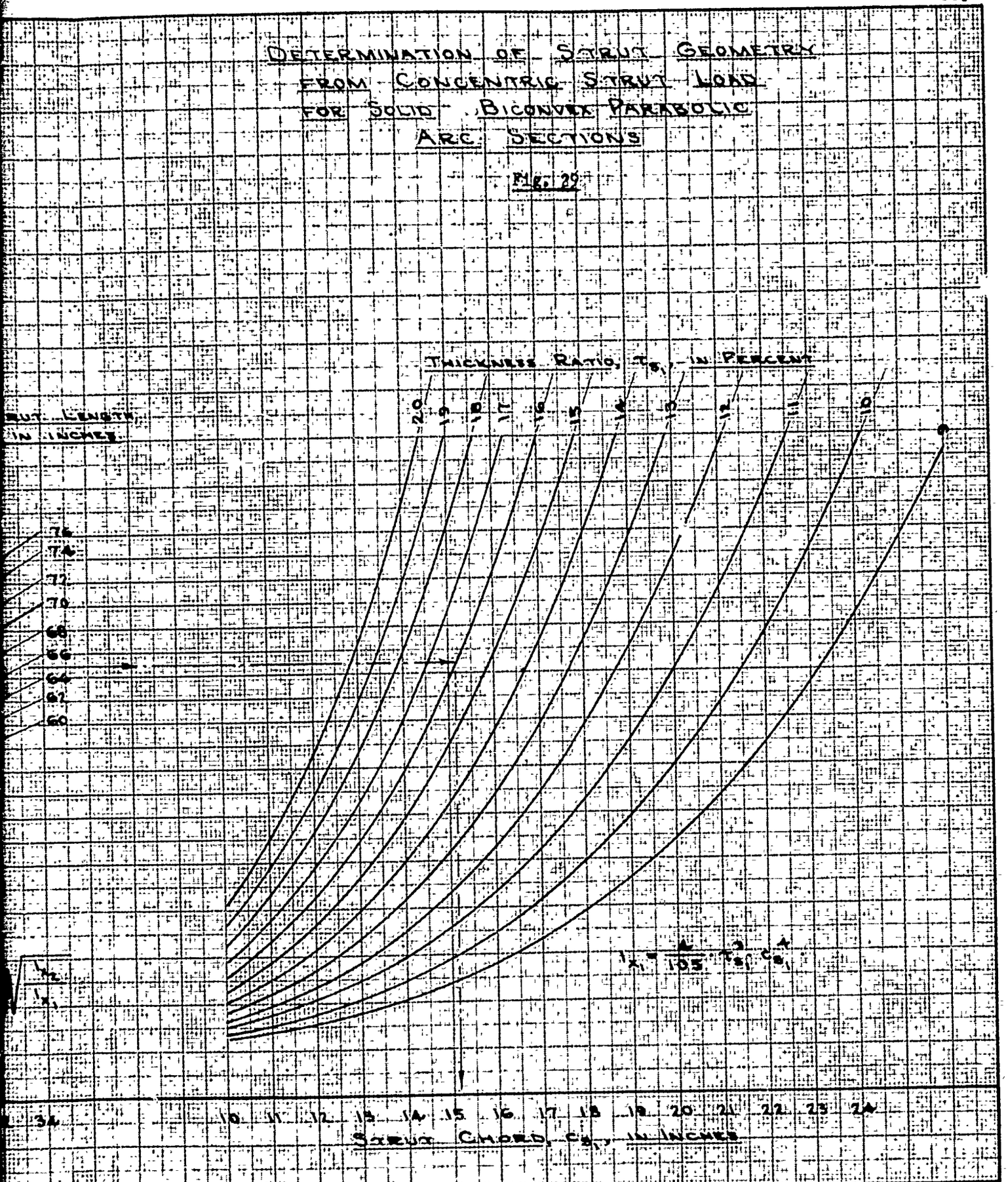

Woodrich
22 Nov. 1949

CONFIDENTIAL

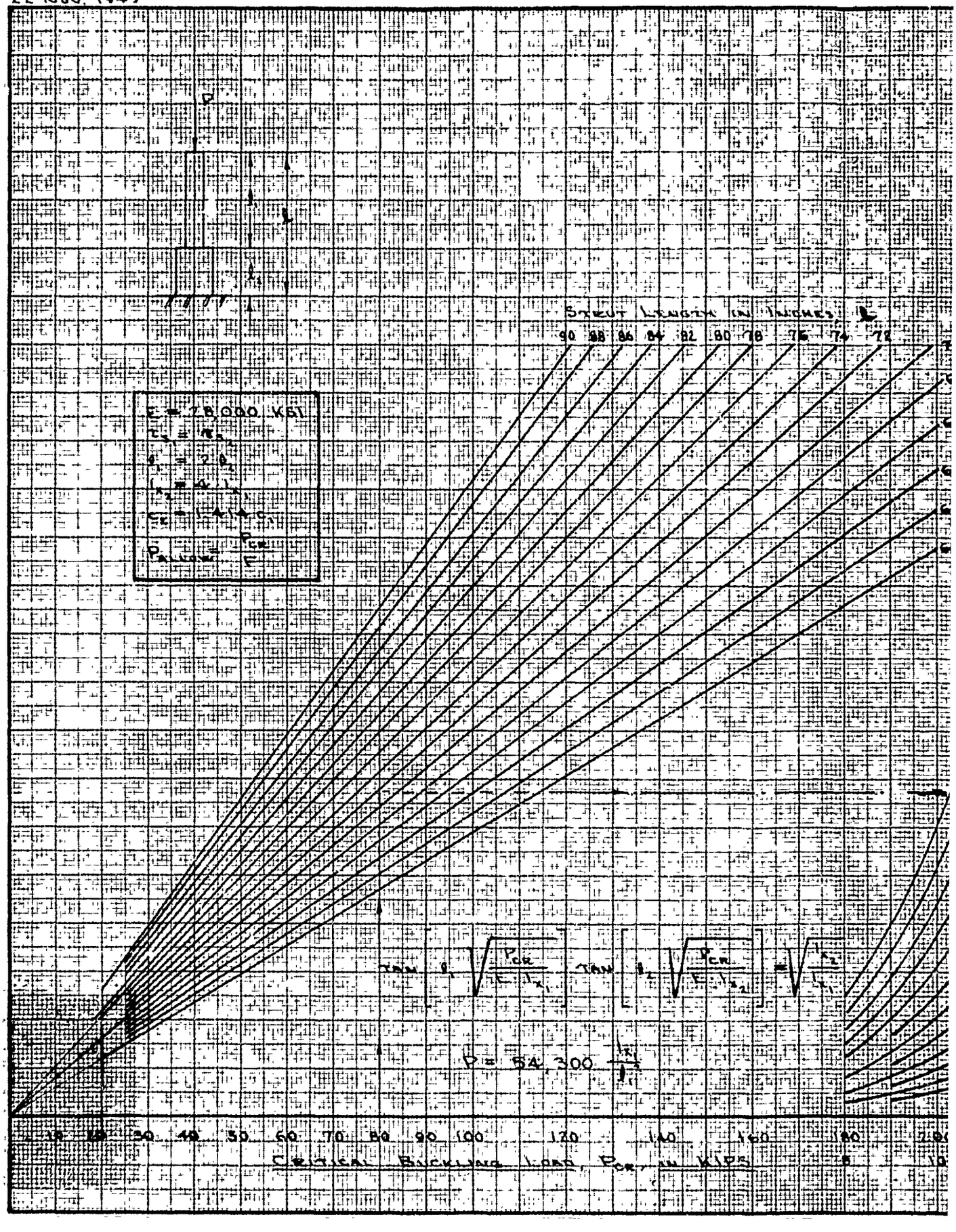

SE

Determination of Strut Geometry from Concentric Strut Loads for Solid Biconvex Parabolic Arc Sections

Fig. 30

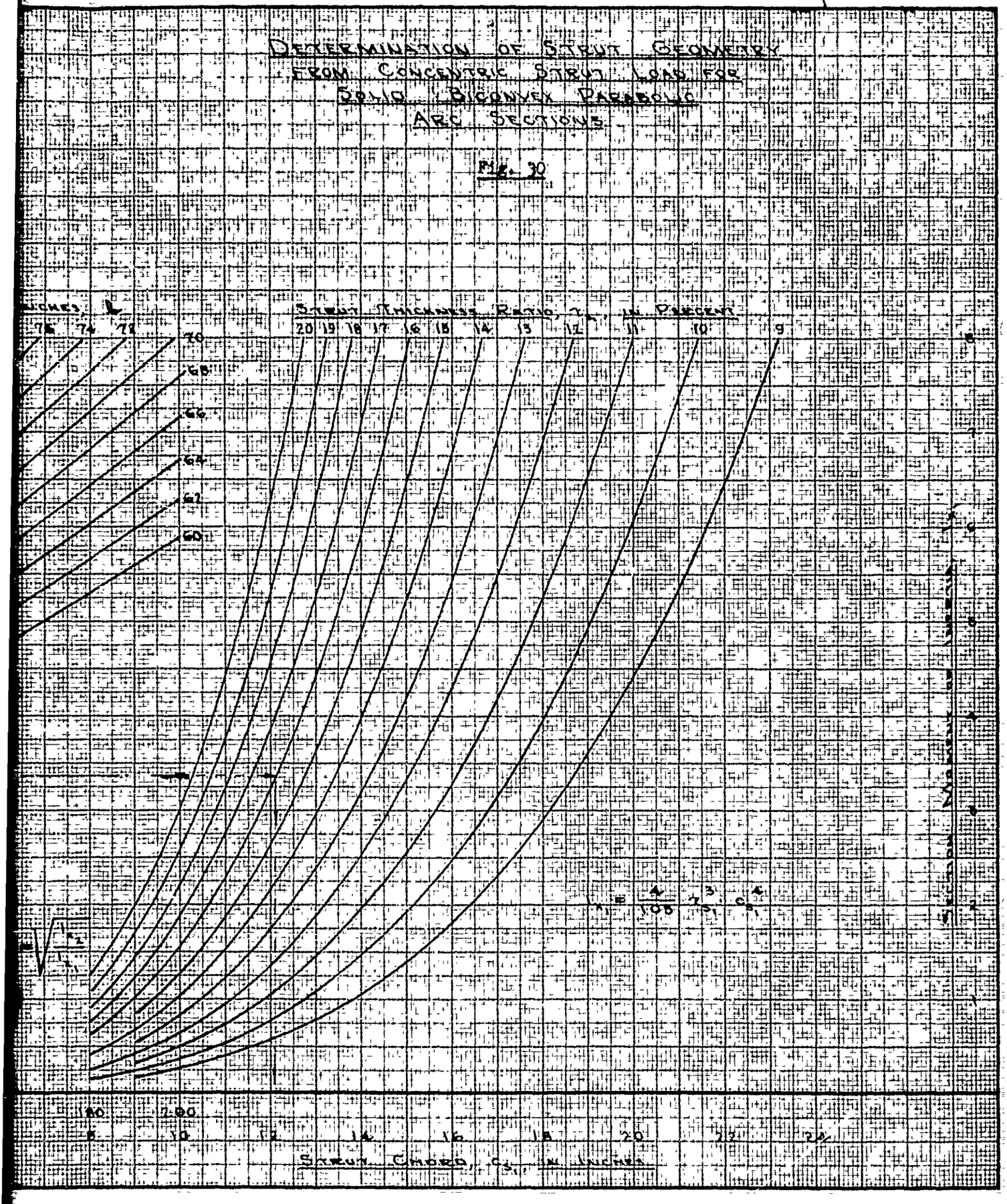

WOORICH

Variation in Strut Thickness Ratio with Strut Chord for Center Strut of a Three-Strut Combination

Fig. 31

$$\frac{\tau_s^3 c_s^4}{E} = \frac{16.88 L^2 F W}{E} = \frac{131000 W}{E}$$

Where L is in inches
& W is in Tons,
F = 1.50

W	$W^{0.33}$ / $10^{0.33}$
10	1.0
15	1.143
20	1.256
25	1.354
30	1.442

E
3,000
3,500
4,000
4,500
10,000

τ_s, Strut Thickness Ratio

.24 .22 .20 .18 .16 .14 .12 .10

10 12 14 16 18 20

c_s, Strut Chord in Inches

In hydrofoil craft of greater design gross weights, the required strut loads, of course, are greater. Therefore, it may be desirable to vary the ratios of the lengths and moments of inertia of the strut components. In such designs it may be advantageous to construct curves similar to Figure 30, which will include the variables peculiar to the specific design.

Figures 32, 33, and 34 show the variation of the strut chord with the strut thickness ratio for slenderness ratios of 140 and 120 on a uniform strut, and a slenderness ratio of 120 on a tapered strut, respectively. The slenderness ratio, $\left(\frac{l}{\rho}\right)$, in each case, was determined from the following:

$$\frac{l}{\rho} = \frac{l\sqrt{17.5}}{\tau c} \qquad \text{Equ. 40}$$

A comparison of the critical buckling loads for struts of mild steel and of fibreglas may be made from Figures 35 and 36. Figure 35 gives the column curves for mild steel in the Euler range for a chord of 12 inches and various thicknesses. The corresponding slenderness ratios and stresses are also shown. Figure 36 is for the same chord and thickness range for a column of fibreglas. This is a method of presenting data for ready comparison after one or more parameters have become known.

Eccentric Loading

The effect of an end moment, in addition to the axial compression, on a column may be accounted for by a given eccentricity of the axial load. From P. 38 of Ref. 12 or P. 245 of Ref. 6, the following relation for a free-ended column is obtained:

$$\sigma_A = \frac{nP}{A}\left(1 + \frac{2y}{\rho^2}\sec\frac{l}{\rho}\sqrt{\frac{nP}{EA}}\right). \qquad \text{Equ. 41}$$

This may be converted to the following:

$$\sigma_A = \frac{3FnWR_s}{2\tau_s c_s^2}\left[1 + \frac{8.75e}{\tau_s c_s}\sec\left(\frac{\sqrt{52.5}\,l}{\tau_s c_s^2}\sqrt{\frac{FP}{2\tau_s E}}\right)\right] \qquad \text{Equ. 42}$$

where $P = nWR_s$ and n, in Equation 41 equals F.

Variation of Strut Chord with Minimum Strut Thickness Ratio for Six Different Strut Lengths at A Slenderness Ratio of 110

Fig. 32

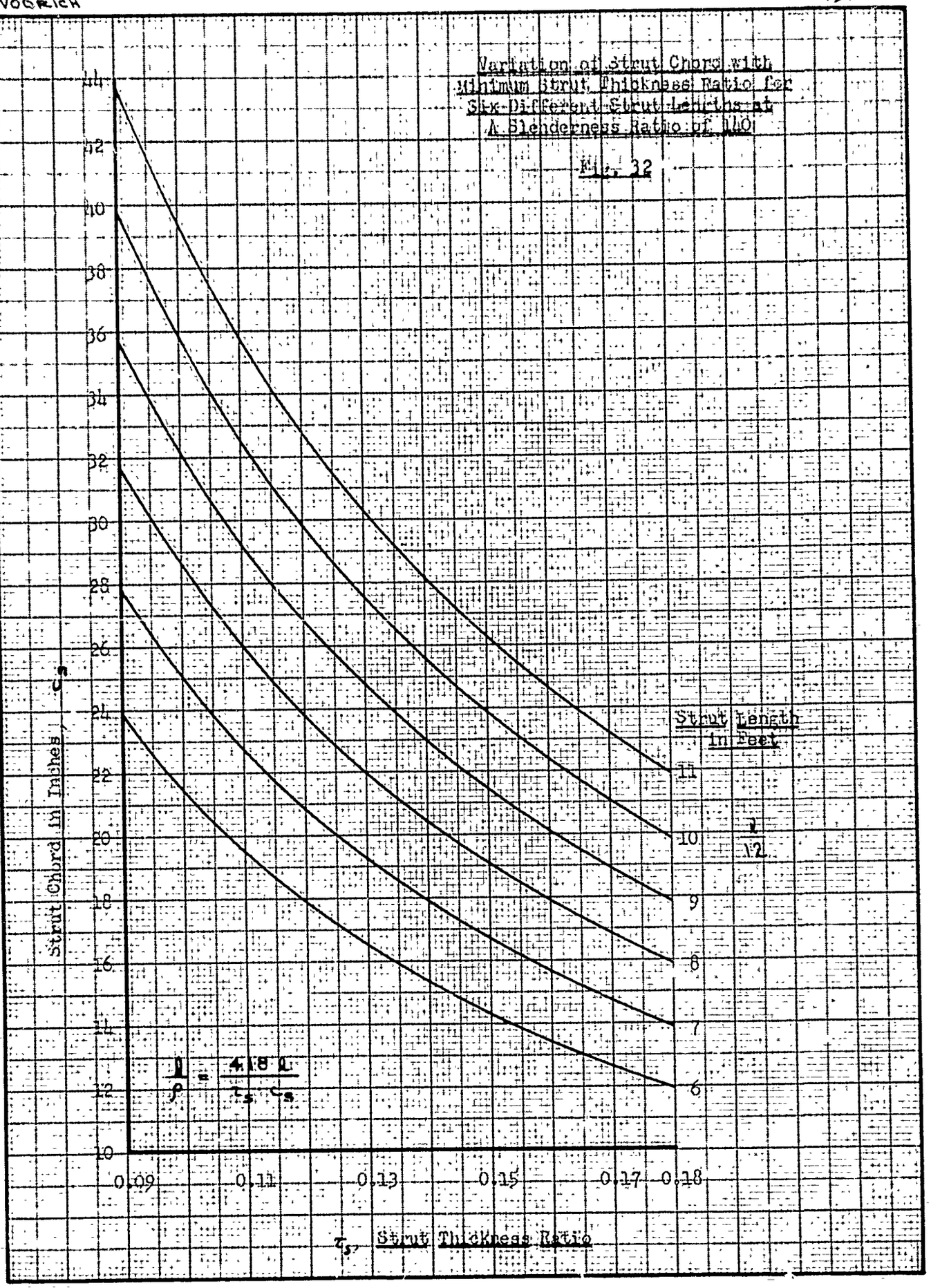

Variation of Strut Chord with Minimum Strut Thickness Ratio for Various Strut Lengths at a Slenderness Ratio of 120

Fig. 33

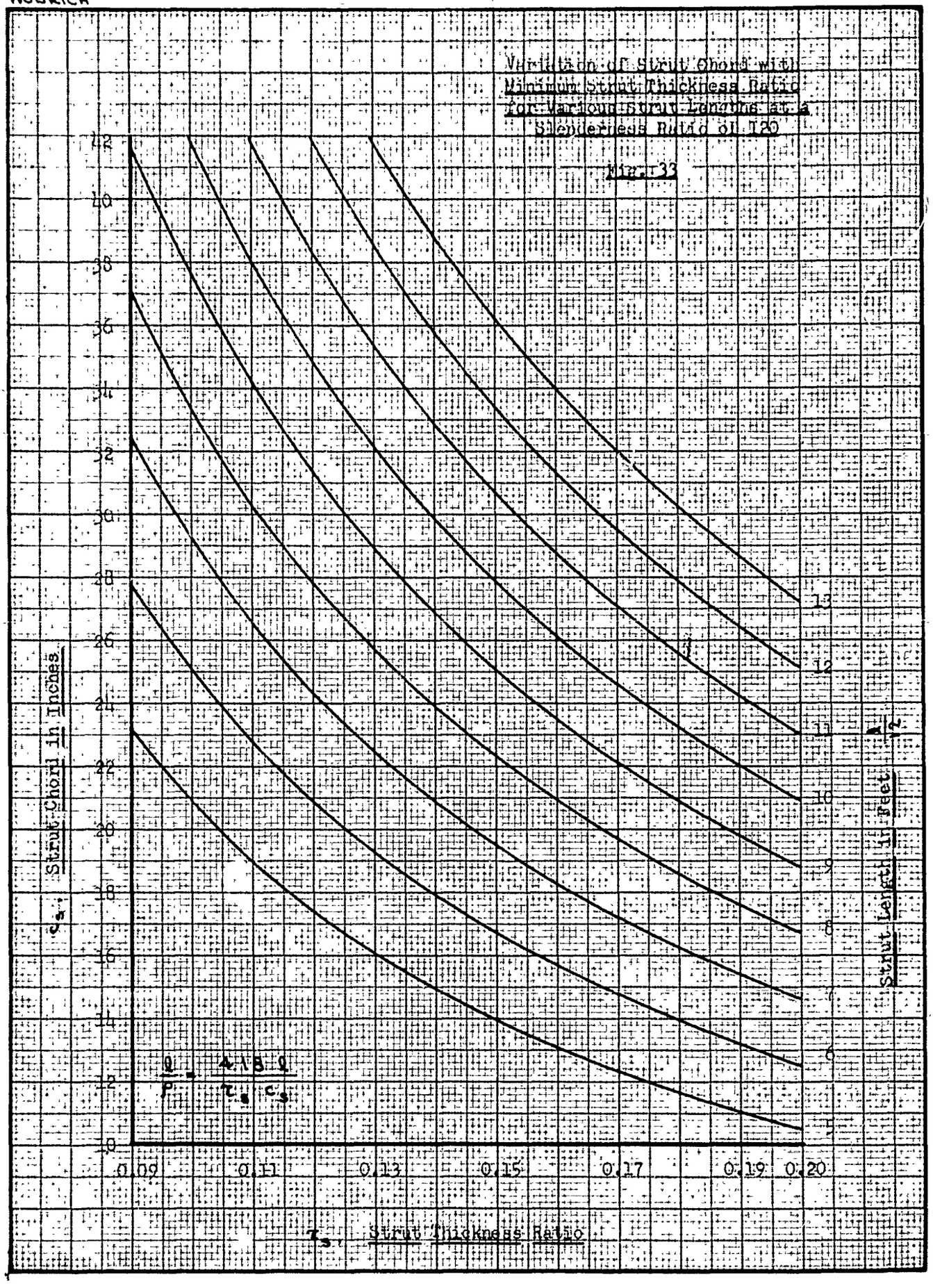

22F

Variation of Strut Chord with Minimum Strut Thickness Ratio for Various Strut Lengths at an Effective Slenderness Ratio of 120

Fig. 34

c_s, Strut Chord in Inches

$\tau_s = 0.03145 \frac{l}{c_s}$

τ_s, Strut Thickness Ratio

l, Strut Length in Inches

42 38 34 30 26 22 18 14 10

.09 .10 .11 .12 .13 .14 .15 .16 .17 .18 .19 .20

10 9 8 7 6 5

WOODRICH

Critical Buckling Load for Solid Biconvex Strut of Wire Gage with 22-Inch Chord

Fig. 35.

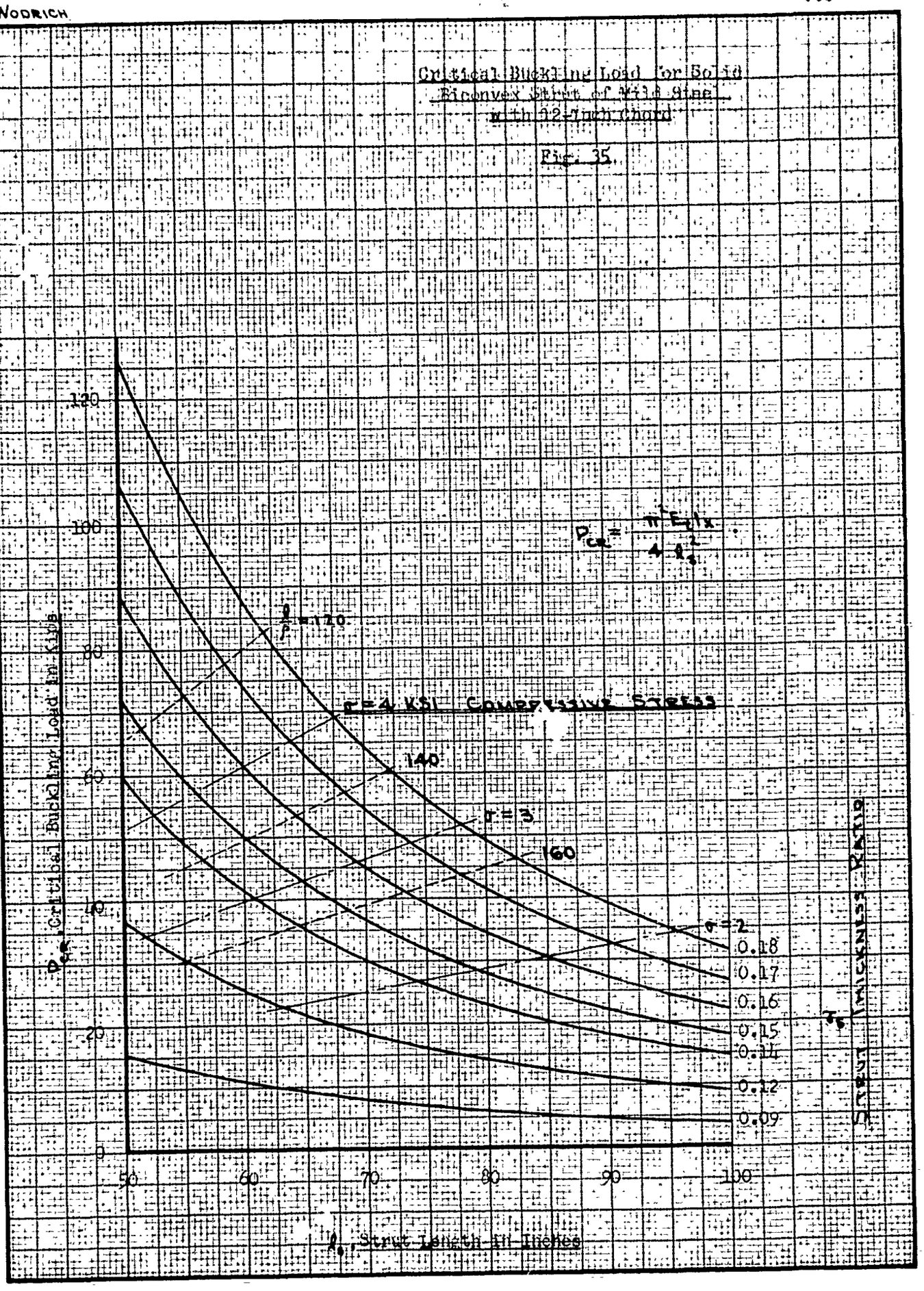

Critical Buckling Load for Solid Biconvex Strut of Fiberglas with 18-Inch Chord

Fig. 36

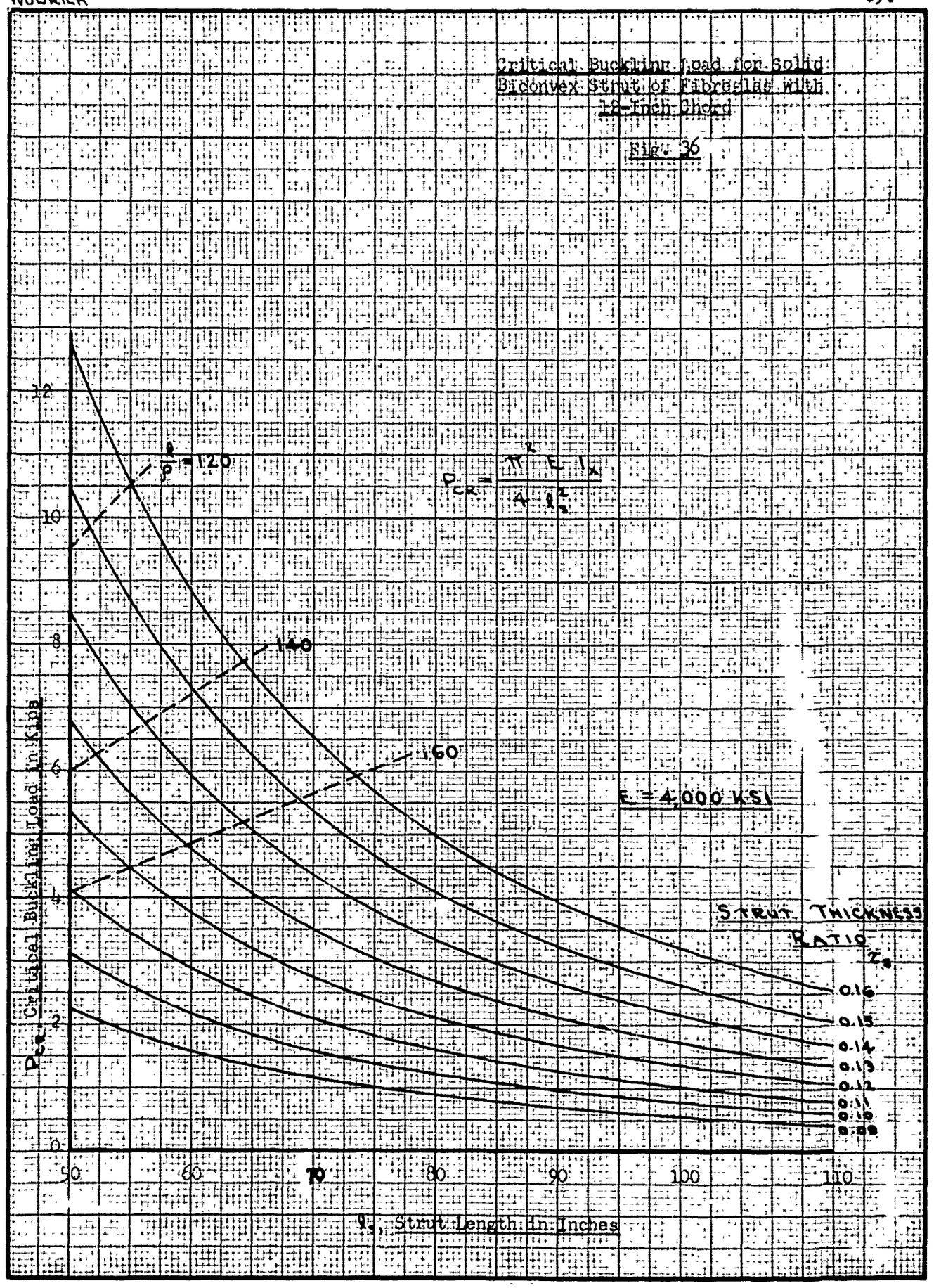

25F

This equation is used to plot Figures 37 through 40, which present the variation of allowable eccentricity with column chord for different axial loads and thicknesses. These charts may be used in determining safe limits of eccentricity due to fabrication and joint unbalance. For a specific configuration, Equ. 41 and Fig. 37 and 38 also indicate that certain dimensions of a strut configuration must be known unless large families of curves are to be constructed.

Side Loading

A cantilever strut under the effects of combined axial load and side load may be analyzed by application of the following equation:

$$M_{MAX_{(x=l)}} = -wj\left[j\left(1-\sec U\right)+l\tan U\right] . \qquad \text{Equ. 43}$$

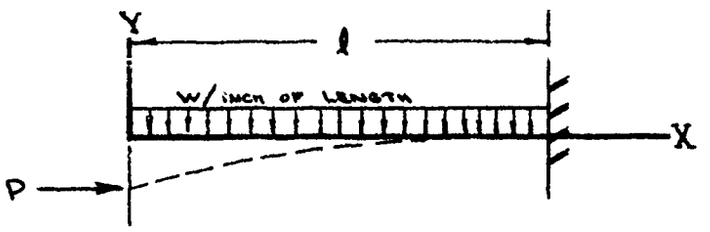

Strut under Combined Loading

Fig. 41

(See Table VI, P. 130, Ref. 6)

This equation is used to determine the allowable strut stress as a function of strut chord and strut thickness ratio. Such data are plotted on Figures 42 and 43, for comparison purposes.

Variation in Allowable Eccentricity of Axial Load with Strut Chord for Several Different Strut Thickness Ratios (20 Kip Axial Load)

Fig. 37

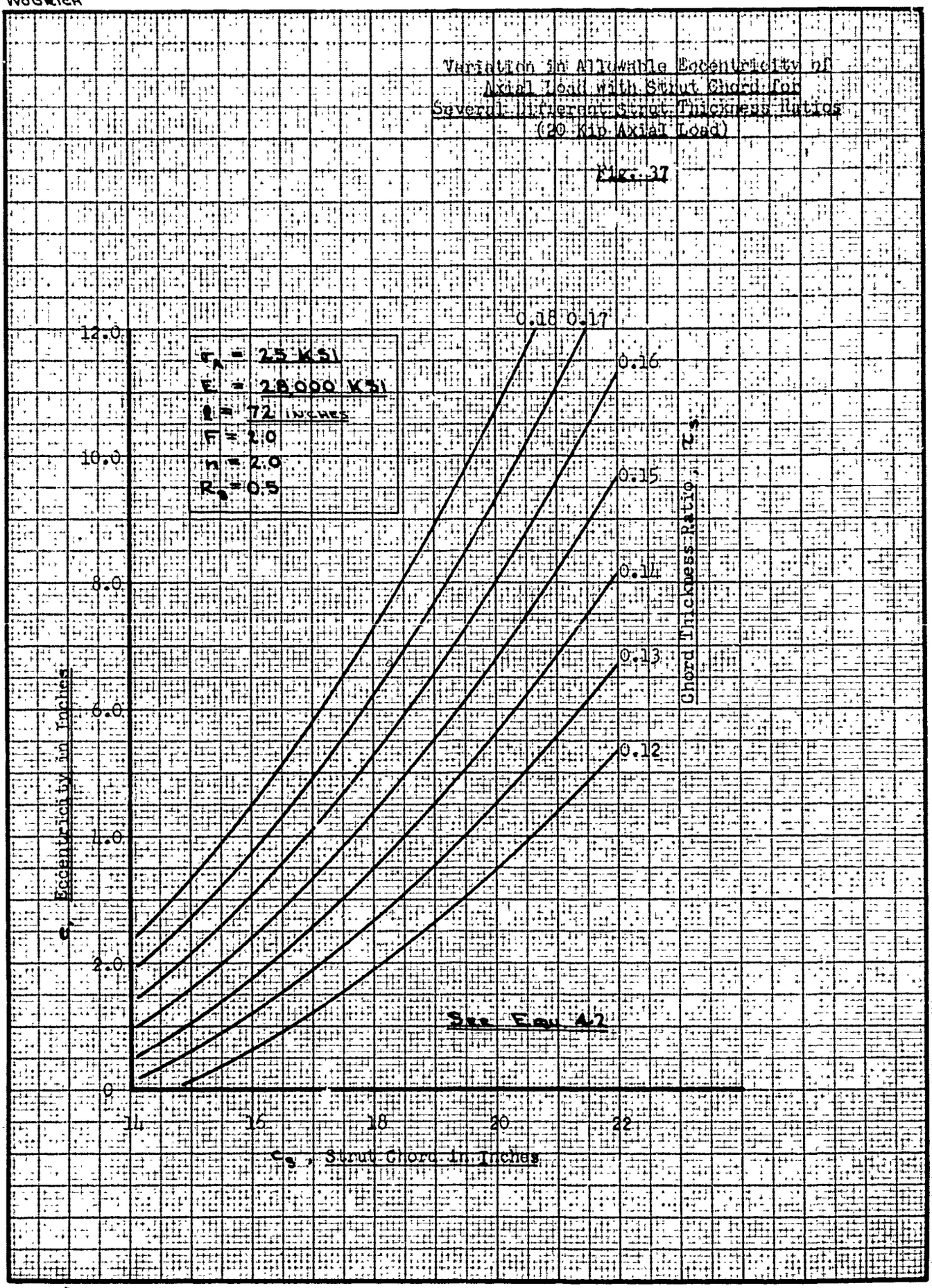

26F

Variation in Allowable Eccentricity of Axial Load With Strut Chord for Several Different Strut Thickness Ratios (25 KSI Axial Load)

Fig. 35

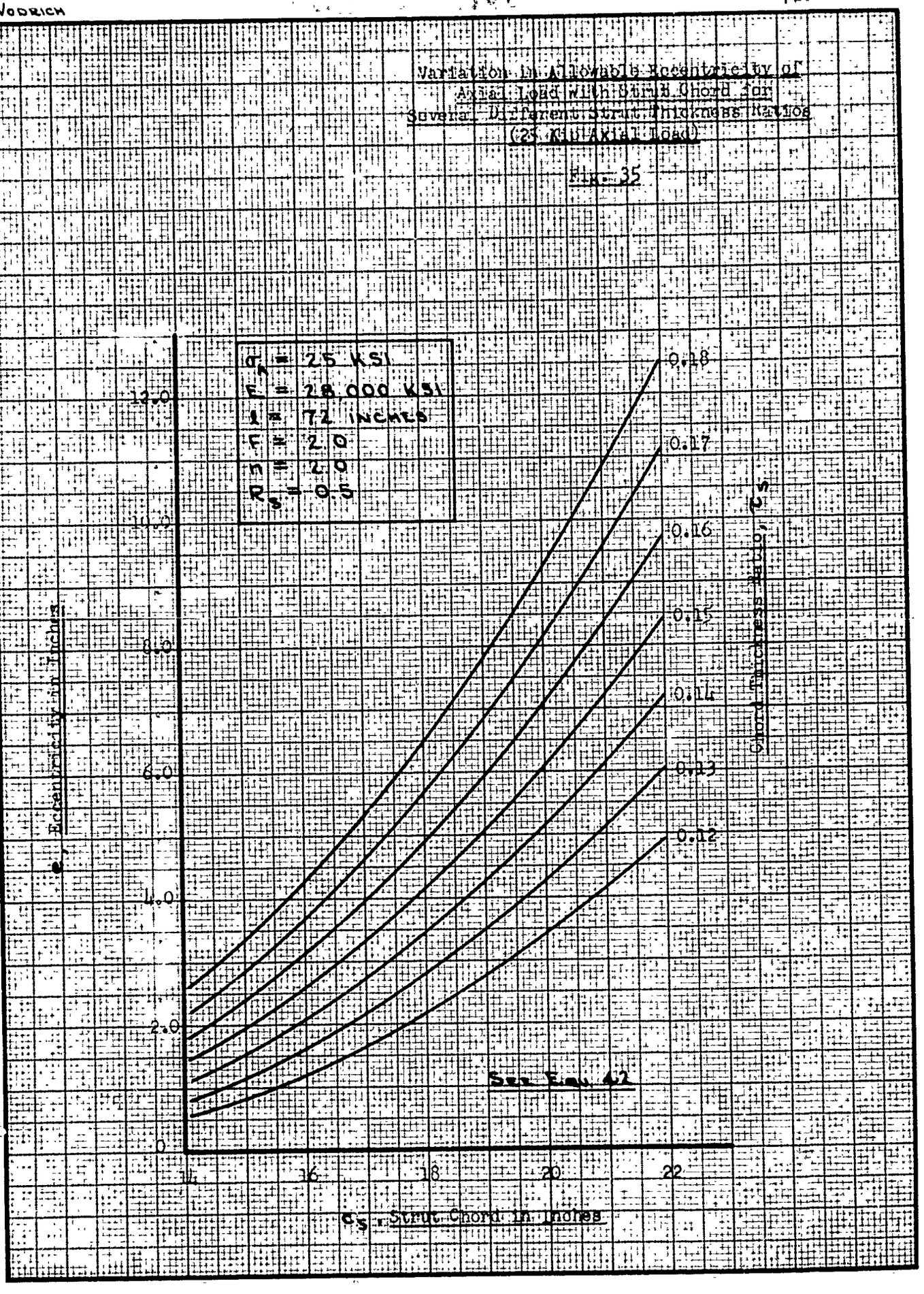

Variation in Allowable Eccentricity of Axial Load with Strut Chord for a 15 Percent Thick Biconvex Solid Strut

Fig. 39

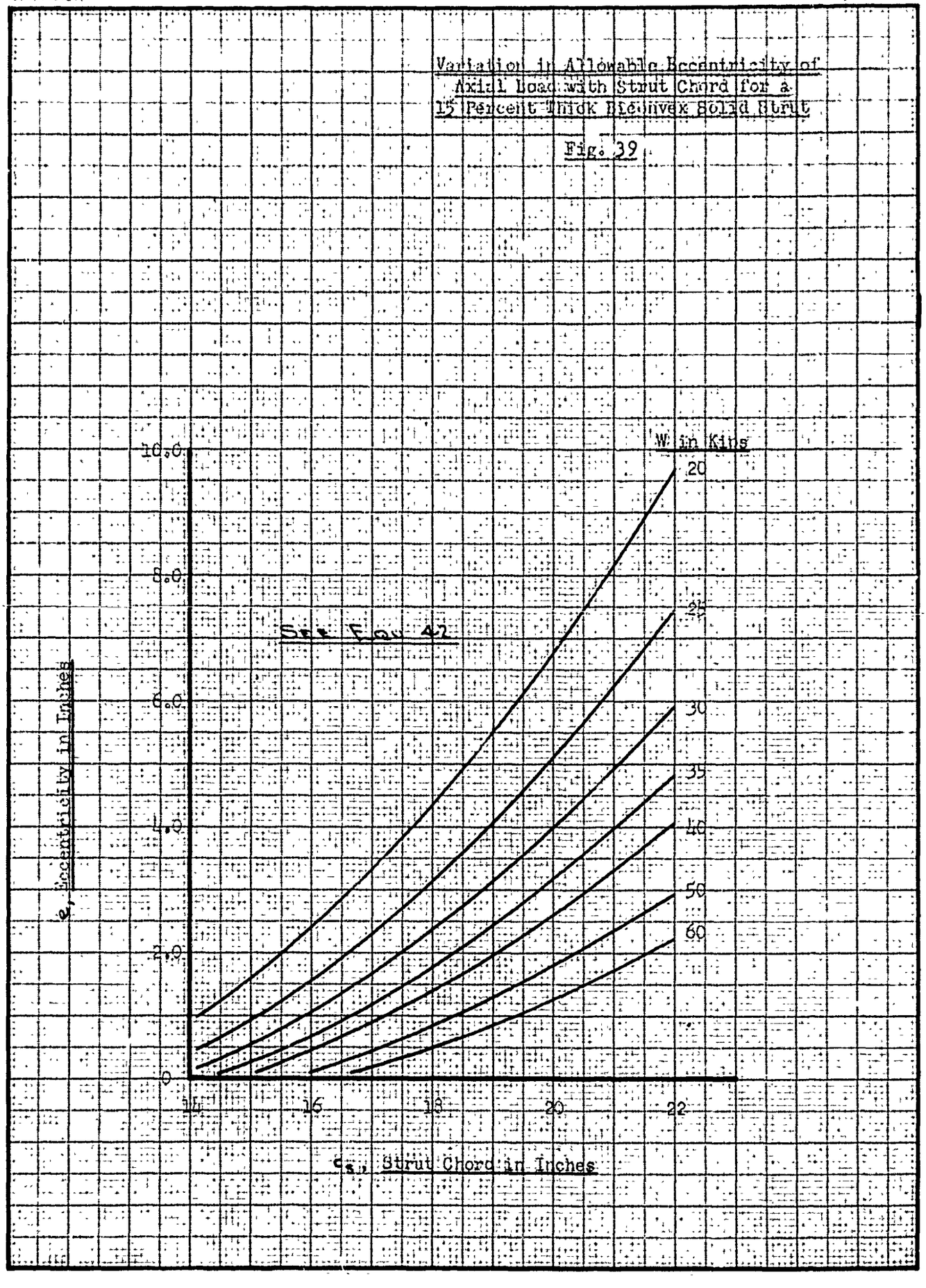

Variation in Allowable Eccentricity of Axial Load with Strut Chord for an 18 Percent Thick Bidonvex Solid Strut

Fig. 40

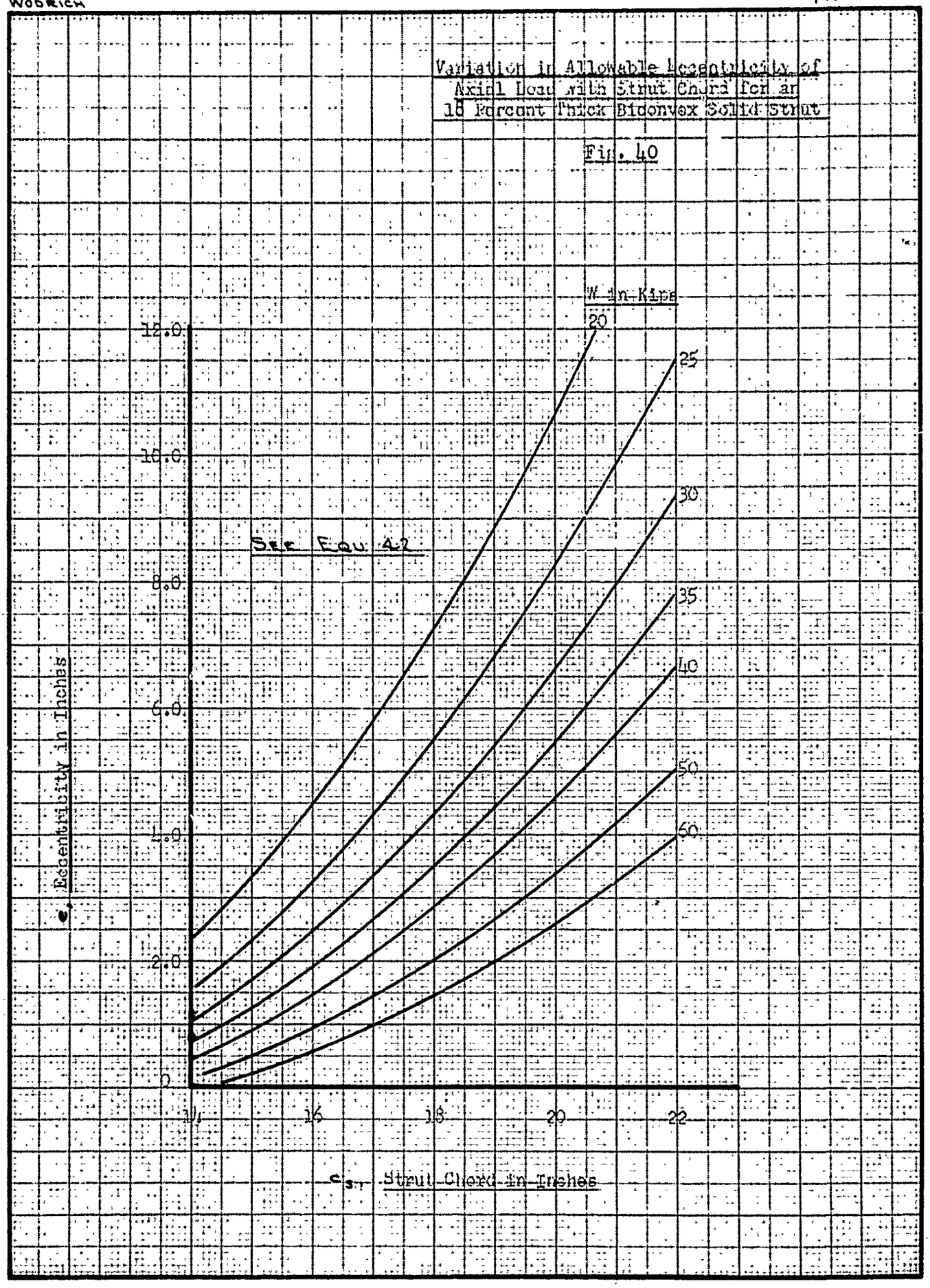

Woodrich

Variation in Maximum Strut Bending Stress with Strut Chord for a Two-Strut Configuration under Combined Axial and Side Loads

Fig. 42

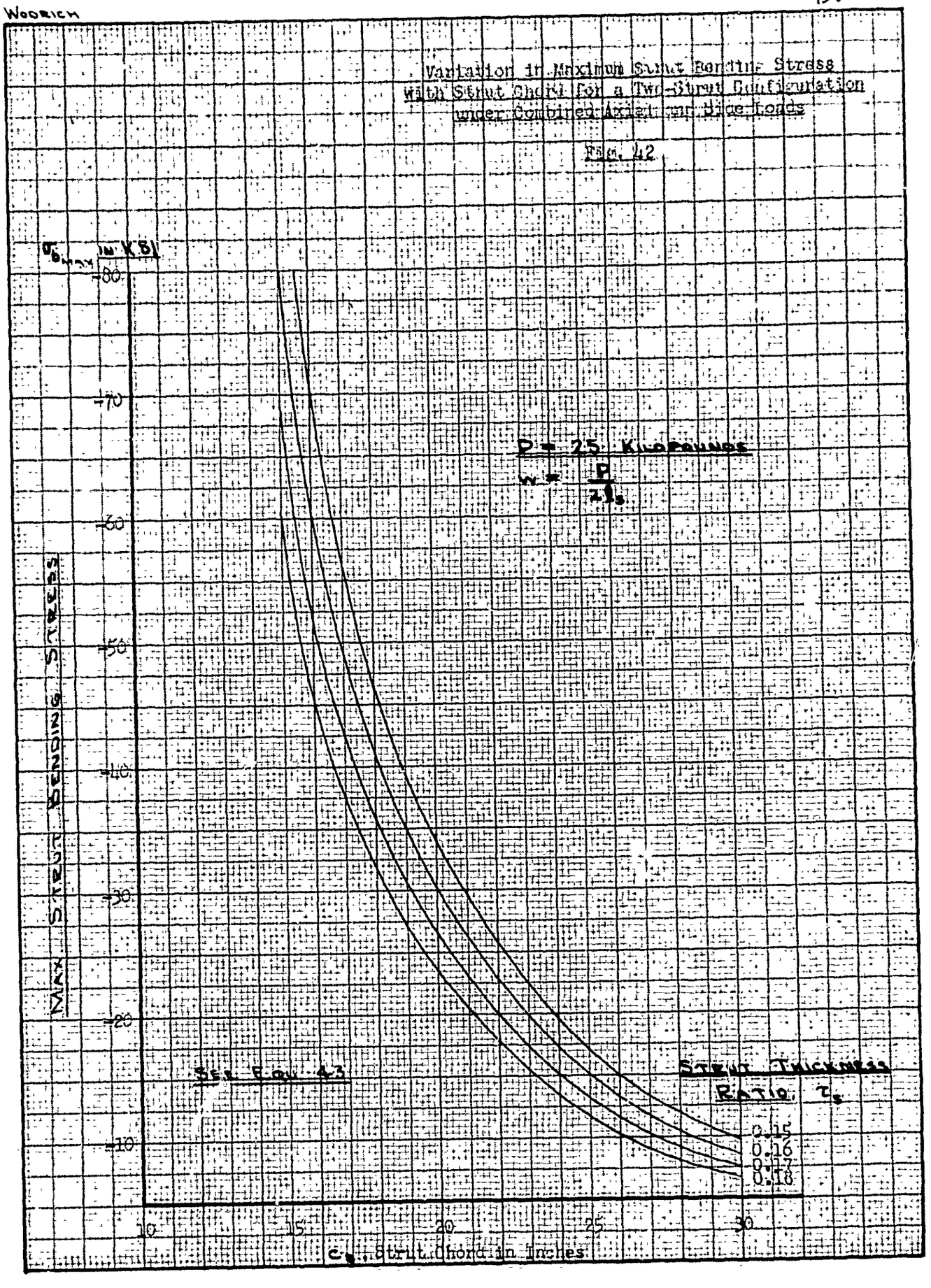

Variation in Maximum Strut Bending Stress with Strut Chord for a Tri-Strut Configuration under Combined Axial and Side Loads

Ref. 43

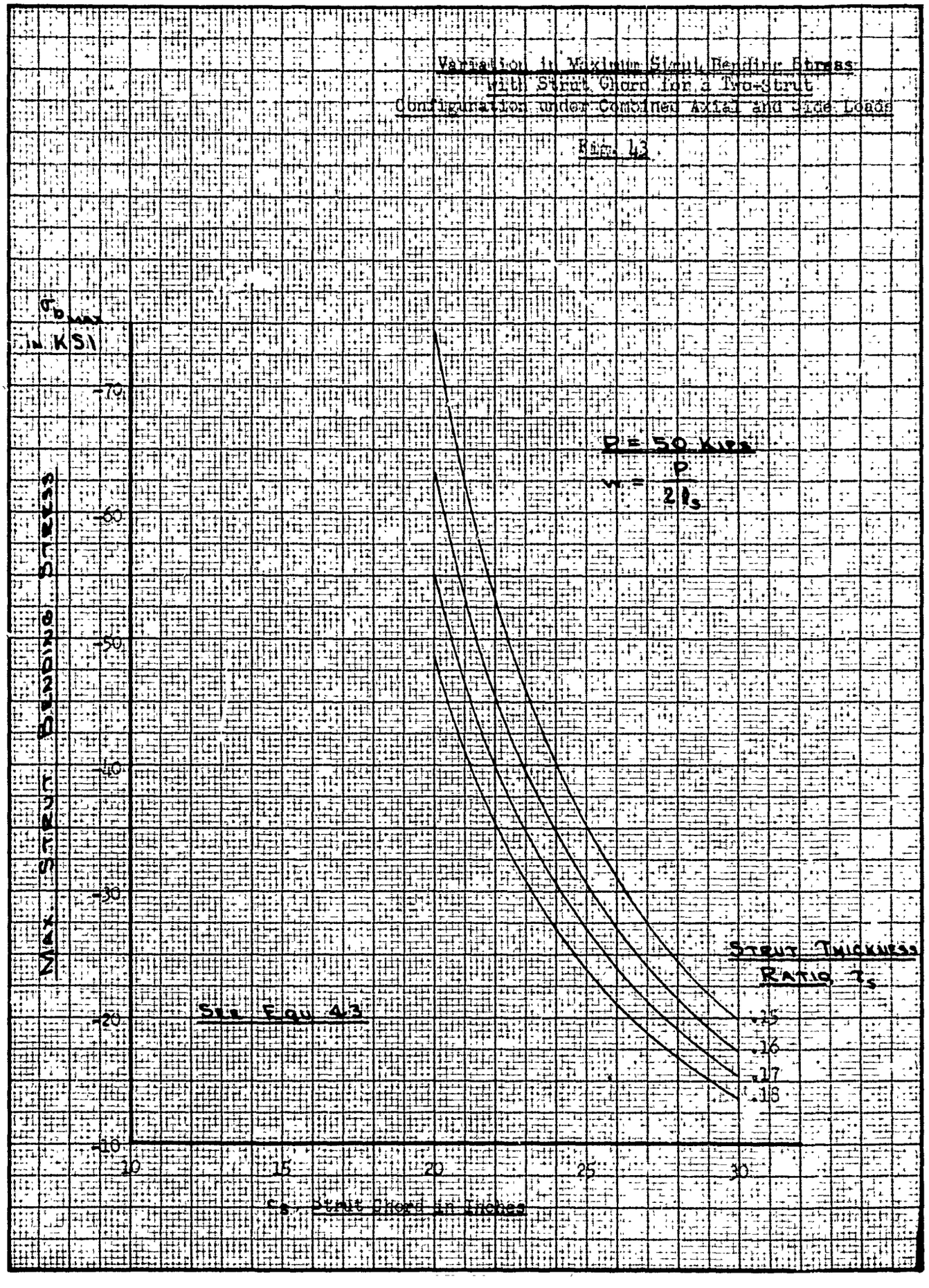

Hydrofoil-Strut Combinations:

From the general equations concerning hydrofoils and struts which were developed in the preceding portion of this report, it is now possible to set up relationships between the spans, aspect ratios, and strut thickness ratios of the various multi-strut configurations. The relationships which are presented herein are based solely upon bending stress considerations. Thus, the Hydrodynamics section, which uses these structural data, is based upon bending stress considerations. Similar relationships can be developed, based upon bending deflection considerations. However, a review of bending deflection data in a preceding section of this report seems to indicate that until either large craft are considered or craft with high hydrofoil loadings and hollow sections are considered, the deflection relationship is of little interest from a preliminary design viewpoint. Likewise, relationships based upon torsional shear stress and torsional deflection are of questionable value initially in the preliminary design phase. (One reason for this is that the torsion is greatly effected by minor variations in the assumed loadings and changes in cross-section; until more is known about those loadings, the bending basis will be more reliable.)

These strength determined configuration relationships are presented in Tables I and II. In order to use the factors contained in the tables, it is necessary to obtain the geometry of either the tapered mono-strut or the rectangular mono-strut configuration, depending upon which factors are used; that is, obtain the hydrofoil thickness ratio, aspect ratio, and span for the tapered mono-strut with a given hydrofoil loading. For any other desired configuration with the same hydrofoil loading and thickness ratio, the aspect ratio is obtained by multiplying the aspect ratio constant by the mono-strut aspect ratio. In similar manner the hydrofoil span and the strut thickness ratio are obtained.

WODRICH 21 OCT. 49

CONFIDENTIAL

CONFIGURATION	ASPECT RATIO	HYDROFOIL SPAN	STRUT THICKNESS RAT END	INTE
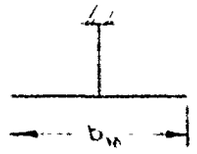 TAPER RATIO, $\lambda = 0.5$	A_{F_M}	b_M		
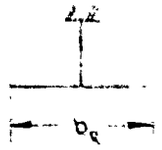 $\lambda = 1.0$	$0.6124\ A_{F_M}$ A_{F_r}	$0.7825\ b_M$ b_r		1.025
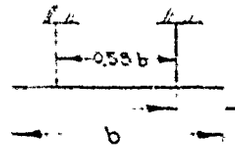 $\lambda = 1.0$	$1.362\ A_{F_M}$ $2.225\ A_{F_r}$	$1.167\ b_M$ [illegible] b_r	$1.066\ \tau_{s_M}$ $1.036\ \tau_r$	
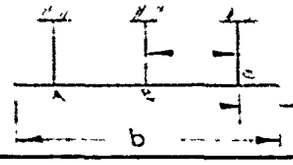	$2.113\ A_{F_M}$ $3.445\ A_{F_r}$	$1.452\ b_M$ [illegible] b_r	$1.067\ \tau_M$ $1.036\ \tau_r$	1.107 1.07
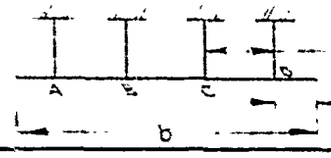	$2.86\ A_{F_M}$ $4.67\ A_{F_r}$	$1.69\ b_M$ [illegible] b_r		
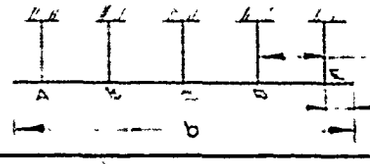	$3.615\ A_{F_M}$ $5.90\ A_{F_r}$	$1.90\ b_M$ [illegible] b_r	$\tau_{s_A} = 1.066\ \tau_M$	$\tau_{s_B} = 1$ $\tau_{s_C} = 1$
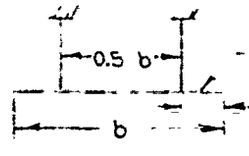 $\lambda = 0.5$ TAPERED OUTER PANELS $A_F = \frac{8}{7}\frac{b}{c_r}$ $S = \frac{7}{8} b c_r$	$1.715\ A_{F_M}$ $2.80\ A_{F_r}$	$1.31\ b_M$ $1.672\ b_r$		

HYDROFOIL - STRUT CONFIGURATIONS

TABLE I

STRUT SS RATIO	INTERMED.	R_s
	τ_M	1.0
	1.029 τ_M τ_r	1.0
τ_{sM} τ_r		$R_s = 0.5$
τ_M τ_r	1.102 τ_M 1.071 τ_r	$R_A = 0.323$ Wn $\left(R_{s_A}=0.323\right)$ $R_B = 0.354$ Wn
		$R_{s_A} = 0.238$ $R_{s_B} = 0.262$
τ_M	$\tau_{s_B} = 1.0986\ \tau_M$ $\tau_{s_C} = 1.124\ \tau_M$	$R_A = 0.1884$ Wn $R_B = 0.207$ Wn $R_C = 0.2092$ Wn

RECT. PLANFORM:

$$\tau_{FT} = 0.08715 \frac{1}{(N-1)+0.8164} A_F \left[\frac{W}{S} n\right]^{0.5} \left(\frac{F}{\sigma_A}\right)^{0.5}$$

$\sigma_A = \sigma_{Cu} = \sigma_{Tu}$ OR F_b

WHERE σ_{Cu} = ULT. COMP STRESS OF MATL., σ_{Tu} = TENSILE STRESS, & F_b = BENDING OR RUPTURE ALLOWABLE OF MATL.

$$\tau_s^3 = 0.0739 \left[\frac{W}{S} n\right] \frac{m^2}{k^4} A_F R_s \frac{F}{E_t}$$

WODRICH 19 Sept 49
19 Oct

HYDR
FOR
OR

CONFIDENTIAL

CONFIGURATION	ASPECT RATIO	TAPER RATIO	SPAN	SUPPORT THICKNESS LBS (EACH)
	A_M	0.5	b_M	
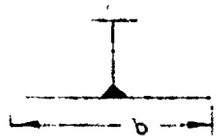	$0.6124 A_{FM}$	1.0	$0.7825\ b_M$	
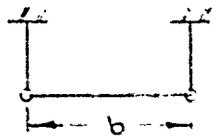	$< 0.624 A_{FM}$	1.0	$< .7825\ b_M$	19 Oct $0.816\ T_M$
	$1.225\ A_{FM}$	1.0	$1.108\ b_M$	19 Oct $0.742\ T_M$
19 Oct 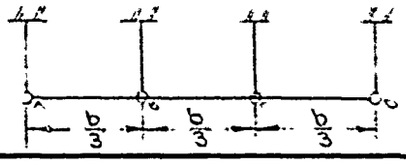	1.100 $2.055\ A_{FM}$	1.0	17-10 $1.432\ b_M$	19 Oct $0.786\ T_M$
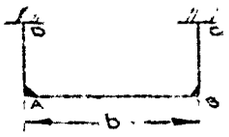	$0.919\ A_{FM}$	1.0	$0.958\ b_M$	
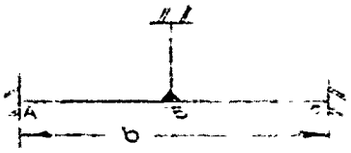	$1.499\ A_{FM}$	1.0	$1.222\ b_M$	
19 Oct Rect. 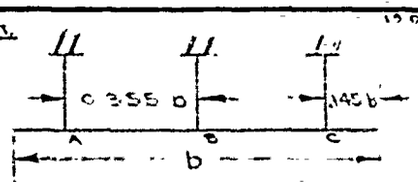	19 Oct $2.113\ A_{FM}$	1.0	$1.452\ b_M$	$1.067\ T_M$
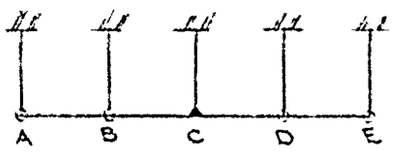	$2.65\ A_{FM}$	1.0	$1.628\ b_M$	

7E

HYDROFOIL STRUT CONFIGURATIONS

FOR BICONVEX, SOLID, PARABOLIC ARC OR NACA 66-SERIES AIRFOILS

TABLE II

STRUT THICKNESS RATIO		BENDING MOMENT	
END (EACH)	INTERM. (EACH)		
	T_M	$M = \frac{A_F^2 c_{F_r}^3}{96 \cos^2\Gamma} (1+\lambda)^2(1+2\lambda) \frac{Wn}{144S}$	$T_F = 0.002515 \frac{A}{\cos\Gamma} \sqrt{\left[\frac{W}{S}n\right](1+\lambda)^2(1+2\lambda) F}$ WHEN $\sigma_{D_A} = 150$ KSI
	$1.029\, T_M$	$M = \frac{Wn}{144S} \frac{b^2 c_F}{8}$ b IS IN INCHES	
$0.816\, T_M$		$M_{MID} = \frac{W}{S} \frac{n}{144} \frac{b^2 c_F}{8}$	
$0.742\, T_M$	$1.108\, T_M$	$M_B = \frac{Wn}{144S} \cdot \frac{b^2 c_F}{32}$	$R_A = 0.1875\ Wn$ $R_B = 0.625\ Wn$
$0.798\, T_M$	$1.102\, T_M$	$M_B = \frac{Wn}{144S} \cdot \frac{b^2 c_F}{90}$	$R_A = 0.133\ Wn$ $R_B = 0.3665\ Wn$
		$M_{AB} = \frac{Wn}{144S} \cdot \frac{b^2 c_F}{18}$	STIFFNESS FACTOR = K $K_S = \frac{I_S}{l}$ $K_F = \frac{I_F}{b}$ ASSUMED: $K_S = K_F$
		$M_{AB} = \frac{Wn}{144S} \cdot \frac{b^2 c_F}{12}$ $M_{BA} = \frac{Wn}{144S} \cdot \frac{b^2 c_F}{48}$	
$1.067\, T_M$	$1.102\, T_M$		$R_A = 0.323\ Wn$ $R_B = 0.354\ Wn$

Sample Calculations:

In the case of the mono-strut configuration, the maximum bending moment and, correspondingly, the maximum percent thickness are obtained at the root of the cantilever: i.e., at the strut junction. If the thickness ratio is to be kept constant, the root thickness ratio is then the required hydrofoil thickness ratio. (See Equ. 6, Pg. 20) However, if it is economical from fabrication aspects, the percent thickness may be tapered from root to tip. Should that be considered, though, careful study must be given to bending and torsional deflections.

In the multi-strut configurations with cantilever overhang, the geometry relationships are obtained by equating bending stresses at the critical points in the span to those for the critical mono-strut bending stresses. As an example, calculations for the three-strut, rectangular overhang configuration of Table I are shown below. The geometry is shown in Fig. 44

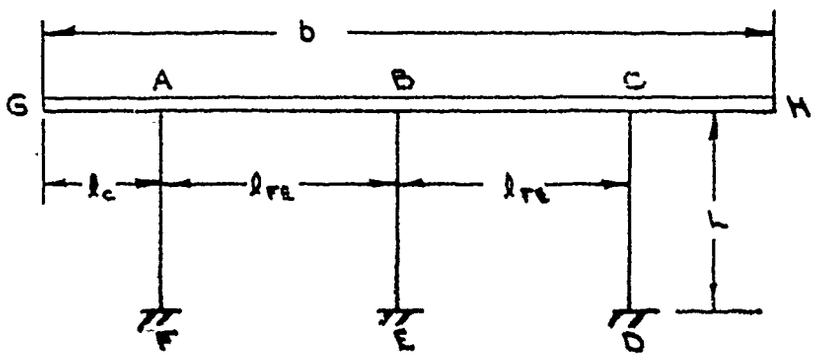

Three-Strut Configuration
with Uniform Loading

Fig. 44

For a cantilever beam, $M_{AG} = \frac{w l_{AG}^2}{2}$; For a fixed-ended beam, $M_{AB} = \frac{w l_{AB}^2}{12}$. To obtain $\theta_{AG} - \vartheta_{AB} = 0$, M_{AG} must equal M_{AB}. Since the unit loadings, , are equal, $b = 2.816\, l_{FE}$ (see p. 21).
where b is span in inches.

The maximum moment occurs at the top of the columns for a fixed-ended beam. Thus,

$$M_{MAX.} = \left[\frac{W}{S}\eta\right] \frac{b^3}{1728(2.816)^2 A_F}, \qquad \text{(see Equ. 8)}$$

$$\& \quad \sigma = \left[\frac{W}{S}\eta\right] \frac{b^3}{1728\,(2.816)^2 A_F} \; \frac{1}{B\,\tau_F^2 c_F^3}$$

$$\text{or} \quad \sigma = \left[\frac{W}{S}\eta\right] \frac{b^3}{1728\,(2.816)^2 A_F} \; \frac{1}{B\,\tau_F^2 \left(\frac{b}{A_F}\right)^3}.$$

This reduces to: $\sigma = \left[\frac{W}{S}\eta\right]\left(\frac{A_F}{\tau_F}\right)^2 \frac{1}{1728\,(2.816)^2 B}$.

For a mono-strut configuration with rectangular planform:

$$\sigma_R = \left[\frac{W}{S}\eta\right]\left(\frac{A_{F_R}}{\tau_{F_R}}\right)^2 \frac{1}{8 \cdot 144 \cdot B}.$$

By equating the bending stresses for the two configurations, and putting $\tau_F = \tau_{F_R}$, gives:

$$A_F = \sqrt{1.5 \cdot (2.816)^2}\; A_{F_R} = 3.445\, A_{F_R}.$$

Applying the factor of Table I for the ratio between the rectangular and tapered mono-strut configurations makes:

$$A_F = 2.113\, A_{F_M}.$$

To determine the strut sizes, it is necessary to obtain first the strut loads (using beam notation and the three-moment equation).

$$M_A + 4M_B + M_C = -\frac{w l_{FE}^2}{2} = -\frac{w(0.355b)^2}{2}.$$

With $M_A = M_C = -\frac{0.145b}{2}(0.145b)w$ for the cantilevers, yields,

$$M_B = \frac{wb^2}{4}\left[-\frac{(0.355)^2}{2} - (0.145)^2\right].$$

Also, by summing the moments at B,

$$M_B = R_A(0.355b) - \frac{wb^2}{8}.$$

By equating identities and solving for the strut reaction, gives: $R_A = 0.323\,wb$. (or $R_{S_A} = 0.323$)

Since $R_A = R_C$, $R_B = 0.354\,wb$. (or $R_{S_B} = 0.354$)

Now since $wb = Wn$,

$$R_A = 0.323\left[\frac{Wn}{5.144}\right]\frac{b_F^2}{A_F}$$

and $$\frac{R_A}{A} = 0.323\frac{W}{5}n \cdot \frac{b_F^2}{A_F}\cdot\frac{3}{2.88}\cdot\frac{1}{\tau_3 k^2}\cdot\left(\frac{A_F}{b_F}\right)^2 = \frac{\tau_3^2 k^2 \pi^2 E_t}{70\, m^2 F}.$$

(see Equ. 33, P. 51)

This yields $$\tau_{3_A}^3 = 0.323\frac{35}{48}\frac{W}{S}n\frac{A_F}{k^4}\frac{m^2 F}{\pi^2 E_t}.$$

(Equ. 34, P. 51, modified)

With $A_F = 2.113 \cdot A_M$, $\tau_{3_A}^3 = 0.323 \cdot 2.113 \cdot A_M \cdot C$.

Since $\tau_{3_M}^3 = A_M C \frac{9}{16}$

$$\tau_{3_A}^3 = \tau_{3_M}^3 \frac{16}{9} \cdot 2.113 \cdot 0.323$$

or $\tau_{3_A} = 1.067\,\tau_{3_M}$.

Frames:

A two-strut configuration with good joint efficiencies becomes a single bay bent. For symmetrical configurations, where the slope of the hydrofoil at the strut point is not zero; and for configurations both with and without overhang, which are subjected to assymetrical loadings; the strut and hydrofoil bending moments must be determined by rigid frame analysis. References 15, 16 and 17 are used in the study of the bent configurations.

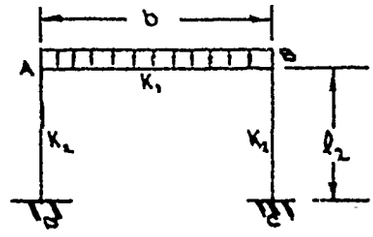

Single Bent, Symmetrical Loading

Fig. 45

Fig. 45 shows a single bent subjected to a uniform spanwise loading over the hydrofoils. Since the loading is symmetrical, $M_{AB} = M_{BA}$, and R = 0. Thus,

$$\text{Thus, } M_{AB} = \frac{2K_2}{K_1+2K_2} FM_{AB} \qquad \text{Equ. 44}$$

$$M_{AD} = \frac{-2K_2}{K_1+2K_2} FM_{AB} \qquad \text{Equ. 45}$$

$$M_{BA} = \frac{-K_2}{K_1+2K_2} FM_{AB} \qquad \text{Equ. 46}$$

For a uniform load on a rectangular hydrofoil

$$FM_{AB} = \frac{1}{1728}\left[\frac{W}{S}n\right]\frac{b^3}{A_{AB}}$$ where $C_F = C_S$, & b is in inches

Then, $M_{AB} = \frac{b^3}{864}\left[\frac{W}{S}n\right]\left(\frac{\tau_s}{\tau_F}\right)^3 \frac{1}{m+2A_F\left(\frac{\tau_s}{\tau_F}\right)^3}$ kip inches; Equ. 47

$M_{AD} = -M_{AB}$;

and $M_{DA} = -\frac{M_{AD}}{2}$.

From these equations, the maximum bending stress in the hydrofoil, $\sigma_{b_{MAX.}}$, becomes:

$$\sigma_{b_{MAX.F}} = 0.01519\left[\frac{W}{S}n\right]\left(\frac{\tau_s}{\tau_F}\right)^3\left(\frac{A_F}{\tau_F}\right)^2 \frac{A_F}{m+2A_F\left(\frac{\tau_s}{\tau_F}\right)^3}; \qquad \text{Equ. 48}$$

and the maximum bending stress in the strut becomes:

$$\sigma_{b_{MAX.S}} = \left(\frac{\tau_F}{\tau_s}\right)^2 \sigma_{b_{MAX.F}} \qquad \text{Equ. 49}$$

For $K_1 = K_2$ it would be necessary for $\frac{l_F}{b} = \frac{l_s}{m c_F}$, or $\frac{l_F}{l_s} = \frac{b}{m c_F} = \frac{A_F}{m}$. But the required l_s increases with m, and is initially greater than l_F, while A_F is greater than m. Therefore K_1 can never be equal to K_2.

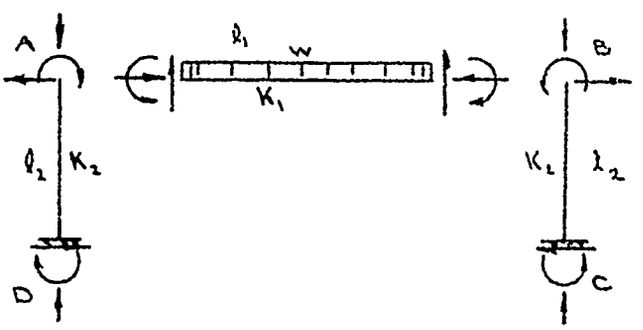

Single Bent, Forces and Moments

Fig. 46

The effect of axial load in the hydrofoil of the single bent was neglected in the foregoing. From Equations 45 and 46 the axial load at A becomes:

From the stress due to bending, and the stress due to axial load, the effect of the axial load may be found.

$$\sigma_b = \left[\frac{W}{S}\eta\right] \frac{b^3}{864} \left[\frac{\left(\frac{\tau_s}{\tau_F}\right)^3 k^4}{m + 2A_F\left(\frac{\tau_s}{\tau_F}\right)^3 k^4}\right] \frac{105}{8} \frac{1}{\tau_F^2} \left(\frac{A_F}{b}\right)^3 . \qquad \text{Equ. 48 (modified)}$$

$$\sigma_c = \frac{P}{A_o} = \frac{b^3}{864} \left[\frac{W}{S}\eta\right] \left[\frac{\left(\frac{\tau_s}{\tau_F}\right)^3 k^4}{m + 2A_F\left(\frac{\tau_s}{\tau_F}\right)^3 k^4}\right] \frac{1.5}{m\, c_{F_r}} \frac{1}{\frac{2}{3}\tau_F\, c_{F_r}^2} .$$

$$\sigma_{TOT} = \sigma_b + \sigma_c .$$

$$\sigma_{TOT} = \frac{b^3}{864} \left[\frac{W}{S}\eta\right] \left[\frac{\left(\frac{\tau_s}{\tau_F}\right)^3 k^4}{m + 2A_F\left(\frac{\tau_s}{\tau_F}\right)^3 k^4}\right] \frac{105}{8\,\tau_F^2\, c_{F_r}^3} \left(1 + \frac{18\,\tau_F}{105\, m}\right) .$$

Thus the axial component in the hydrofoil is negligible.

A double-bay bent under symmetrical loading is depicted in Fig. 47.

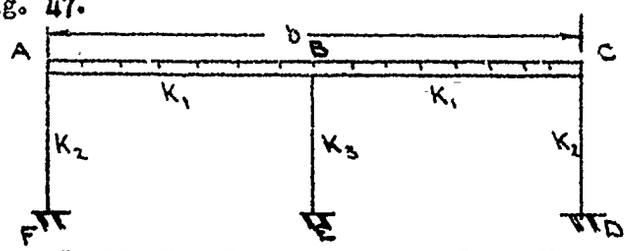

Double-Bay Bent, Symmetrical Loading

Fig. 47

The joint moments become: $M_{AF} = -\frac{K_2}{K_1 + K_2} FM_{AB}$;

$M_{BA} = -\frac{K_1}{2(K_1 + K_2)} FM_{AB} - FM_{AB}$;

and $M_{FA} = -\frac{K_2}{2(K_1 - K_2)}$; where $FM_{BE} = 0$. } Equ. 50

Then by geometric relations, $FM_{AB} = \left[\frac{W}{5}\eta\right]\frac{b^3}{4.1728\ A_F}$,

$K_1 = \frac{2I_F}{b}$, & $K_2 = \frac{I_F \left(\frac{r_g}{r_F}\right)^3}{m \cdot c_F}$; from which the joint moments may be obtained. (b = span in inches)

In a single bay bent subjected to side load, as shown in Fig. 48, the equations for the joint moments may be expressed as follows:

$$M_{AB} = 2E\frac{I_1}{l_1}\left(2\Theta_A + \Theta_B - 3\frac{\Delta_1}{l_1}\right) + FM_{AB}$$

$$M_{AD} = 2E\frac{I_2}{l_2}\left(2\Theta_A + \Theta_D - 3\frac{\Delta_2}{l_2}\right) + FM_{AD} \quad \text{Equ. 51}$$

$$M_{DA} = 2E\frac{I_2}{l_2}\left(2\Theta_D + \Theta_A - 3\frac{\Delta_2}{l_2}\right) + FM_{DA}$$

Or, using the notation of Ref. 15, $M_{AB} = K_1\left(A + \frac{B}{2}\right)$.

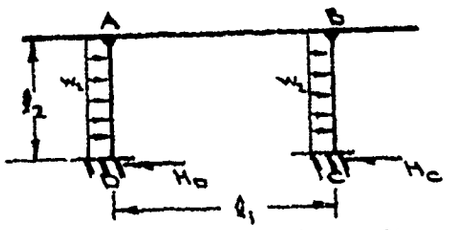

Single Bay Bent, Side Loading

Fig. 48

From Equation 51, $M_{AB} = \frac{w_2 l_2^2 K_1}{3(r_3 K_1 + K_2)} = -M_{AD}$ Equ. 52

(The equations for the joint moments may also be obtained from Ref. 16, Table 47, by combining loadings.)

From the foregoing, it may be seen that the magnitude of the bending moment, M_{AB}, in the hydrofoil, due to side load, is an appreciable proportion of the bending moment in the hydrofoil due to a symmetrical loading between points A and B. It should be noted that if the hydrofoil has a symmetrical lift load imposed upon it, and it is so distributed that the slopes at joints A and B are zero, then the resulting joint moment, M_{AB}, is appreciably greater than that resulting from Equation 44. Since the zero slope method of determining hydrofoil size is used in preliminary design charts, the effect of side load, if combined with a reduced normal load factor, is of little importance.

Example: If $K_2 = 7K_1$ (typical for a 10-ton craft which is under investigation), then $M_{AB} = \frac{w_1 l_1^2}{90}$ from Equ. 44 while $M_{AB} = \frac{w_1 l_1^2}{12}$ for zero slope, as used in the design charts (see P. 21). At the same time, due to side load, $M_{AB_S} = \frac{w_1 l_2}{13}$ from Equation 52. Upon substituting the corresponding loadings and lengths,

$M_{AB_V} = 46$ kip-inches.

$M_{AB_{FLV}} = 345$ kip-inches.

and $M_{AB_S} = 20$ kip-inches.

STRUCTURAL CONSTRUCTION CONSIDERATIONS

The immediate concern with regard to structural materials and fabrication centers on cost for construction of a small test vehicle with a design gross weight somewhere between 10 and 25 tons. Solid hydrofoils and struts, to be fashioned from steel, become very costly due to the necessary machining operations to obtain the required cross-sections. Mild steel must be treated to prevent corrosion. German literature indicates that they had not obtained any satisfactory solutions. Erosion, as the Germans found, apparently is a serious factor with mild steel. Ackert's work on cavitation (Ref. 18) in 1930 and data on brasses by Dr. Uhlig (Ref. 19, p. 76) indicates that erosion on various brasses at high velocities will be serious. However, Ref. 19 states that the copper-tin alloys (high-tin bronzes) show good resistances to such attack. The use of high tensile corrosion resistant steels increases the cost of the basic material and multiplies the manufacturing costs. (In time of conflict, such material would be in short supply and some substitute would need to be found).

The use of a laminated glass fiber base plastic material for the construction of the exterior surface of hydrofoils and struts may have several advantages over the use of steel. The material is light in weight and will give a smooth, easily fabricated surface which may be free from corrosion and fouling worries.

To obtain struts, which by their very shape are critical items, fabricated entirely from fibreglas would require struts of greater thickness than the comparable steel struts except where propeller shafts and controls dictate the strut sizes. The modulus of elasticity for fibreglas is approximately one-seventh that of steel and the allowable working stress is somewhat lower than that for mild steel. The problems of making joints between the struts and foils and between the struts and hull are much more difficult in the laminated glass fiber reinforced plastic than in the steel structure. The problem of proper quality control is also of extreme importance in fibreglas, especially in thick sections. The work of the Structures Branch, Aircraft Laboratory, Hq., Air Materiel Command, during World War II in applications of laminated glass fiber based plastics to aircraft fuselages bears this out.

From Ref. 3 it appears that the Germans came to the conclusion that only high strength alloy steels are suitable for large craft. Although it is noted from some of the literature that aluminum alloys had been used for construction of foils on one of the vessels, the advisability of its use in large ships may be seriously questioned. The Germans also concluded that steel castings and forgings could not be used. Without the substantiating evidence, the logic behind such conculsions cannot be ascertained.

Consideration has been given to the use of aluminum alloy extrusions for the fabrication of foils (and possibly struts) in a 10-ton hydrofoil test craft where the corrosion prevention would be supplied by a layer of fibreglas laminate, Plywell, metal spray coat, or Resoweld. This appears promising from the standpoint of quality control of strength, from cost, from strength and from weight.

REFERENCES

1. "17-Ton Special Speed-Boat with Immersed Hydrofoils Used as Minelayer-Test Boat; Testing Various Lift-Producing Sections at Sea; and as Sub-Chaser." Ref. 062 084. Translated from German. Confidential.

2. "Measurements of the Dynamic Behavior of a Free to Trim and Heave Hydrofoil System in Waves Encountered Head-on." John H. Carl & Sons, Inc., Rept. No. 3; October 1949. Confidential.

3. "Technology of Lift-Producing Immersed Water Wings." Ref. 062 084. Translated from German. Confidential.

4. Admiralty Hydrofoil Development Committee: "Interim Report on Hydrofoil Craft." Report No. C.F.M. 2109/45. Secret.

5. "Strength of Metal Aircraft Elements." Document ANC-5a. Munitions Board Aircraft Committee. U.S. Govt. Printing Office. May 1949.

6. Roark, Raymond L.: "Formulas for Stress and Strain." McGraw-Hill Book Co., Inc.; 1943.

7. Wolford, Don S.: "Significance of the Secant and Tangent Moduli of Elasticity in Structural Design." Journal of the Aeronautical Sciences. June 1943.

8. Salmon, E.H.: "Columns." Oxford Technical Publications, London, 1921.

9. "Strength of Hydrofoils-Preliminary Tests." Naval Construction Research Establishment (British). Report No. NCRE/R.11.

"Test of Hydrofoil from Ex-German High-Speed Motor Boat." Naval Construction Research Establishment Report No. NCRE/R.71. August 1948.

10. Warren, C.H.E.: "A Theoretical Approach to the Design of Hydrofoil Strut Sections." R.A.E. Technical Note No. Aero. 1739. January 1946.

11. "Design Data on High Tensile Stainless Steel Sheets for Structural Purposes." American Rolling Mill Company, 1944.

12. Timoshenko, S.: "Theory of Elastic Stability." McGraw-Hill Book Co., Inc. 1936.

13. "Plastic Materials; Laminated Glass Fabric Base, Low Pressure Molded"; U.S. Air Force Specification No. 12051, 3 August 1949.

14. Werren, Fred and Norris, C.B.: "Directional Properties of Glass-Fabric-Base Plastic Laminate Panels of Sizes That Do Not Buckle"; U. S. Forest Products Laboratory Report No. 1803, April 1949.

15. Amirikian, A.: "Analysis of Rigid Frames." U. S. Govt. Printing Office. 1942.

16. Hool, G.A. and Kinne, W.S.: "Stresses in Framed Structures." McGraw-Hill Book Co., Inc. 1942.

17. Parcel and Maney: "Statically Indeterminate Stresses." John Wiley and Sons, Inc. 1936.

18. Ackert, J.: "Experimental and Theoretical Investigations of Cavitation in Water"; National Advisory Committee for Aeronautics, Technical Memorandum No. 1078; May 1945.

19. Uhlig, H.H.: "Corrosion Handbook"; John Wiley & Sons, Inc. 1948.

APPENDIX I

EFFECT OF CHANGE FROM SOLID TO HOLLOW SECTIONS

The structural data which are used in the Hydrodynamics section to determine preliminary performance charts are for solid struts and foils. As the gross weight of the hydrofoil craft increases, the struts and foils will change from solid to hollow sections to provide feasible methods of fabrication and to provide for reasonable structural weight. It is desirable, therefore, to know what effect this structural modification has upon: 1. the estimated hydrodynamic performance, and 2. the structural factor of safety if the exterior dimensions are held.

The skin thickness and chord affect the percent thickness required in order to have a section with the same sectional moment of inertia as the solid section. Basing consideration only upon beam bending, to determine the increase in thickness of the hollow section over the solid section, the section modulus of the hollow section must equal that of the solid section. This gives:

$$\tau_h = \frac{\tau_o}{\sqrt{1-\eta^4}} \qquad \text{Equ. 53}$$

where τ_h = thickness ratio of the equivalent hollow section,
τ_o = thickness ratio of the initial solid section,
and η = ratio of inside chord to outside chord.

Equation 53 is plotted in Figure (49) with the thickness ratio of the hollow section as ordinate and the thickness ratio of the solid section as abscissa and various chord ratios.

The skin thickness, too, then becomes:

$$t_s = \frac{\tau_h \cdot c\,(1-\eta)}{2} \quad \text{(APPROXIMATELY)} \qquad \text{Equ. 54.}$$

The ratio of the hollow section moment of inertia to that of the solid section moment of inertia, where the outside chord and thickness ratio for the two are identical, gives the decrease in bending moment. In other words, it gives the decrease in the margin of safety or the factor of safety to maintain zero margin of safety. This ratio is equal to $(1-\eta^4)$.

Example: An indication of the effects of this structural modification is shown with a 500-ton vessel. A four-strut configuration with a limit hydrofoil loading of 2.2 ksf is selected. The structural material selected is mild steel with

$$\frac{F}{\sigma_A} = \frac{2}{50} = \frac{1}{26}$$

From Equation 9, p. 26, the thickness ratio of the hydrofoil becomes 13.55 percent for an aspect ratio of 20. Thus, the hydrofoil area is 1020 square feet, the chord length becomes 7.15 feet, the span becomes 143 feet, and the maximum thickness becomes 11.62 inches.

If the skin thickness of the hydrofoil is selected as 2.0 inches, then from Equation 54, $\eta = 0.701$ (approx.) if $\tau_h = 15.6$ percent. For that value of η, Equation 53 yields $\tau_h = 15.58$ percent. Hence, the thickness increases approximately 14.8 percent. However, had the thickness been held constant, from Equation 54 (replacing τ_h by τ_o) $\eta = 0.655$, and $(1-\eta^4) = 1-0.184 = 0.816$. The factor of safety would then be reduced from 2.0 to 1.632.

For a hollow strut to support the same axial column load, the hollow strut must possess the same least moment moment of inertia as the solid strut because:

$$P = \frac{\pi^2 E_t I_x}{4 l^2}.$$

thus,

$$\tau_h = \frac{\tau_o}{\sqrt[3]{1-\eta^4}}. \qquad \text{Equ. 55}$$

Such variation is presented in Figure 50.

Variation of Thickness Ratio for Hollow Sections with Thickness Ratio for Solid Sections with Several Chord Ratios to give Equal Beam Bending Strength

Fig. 49

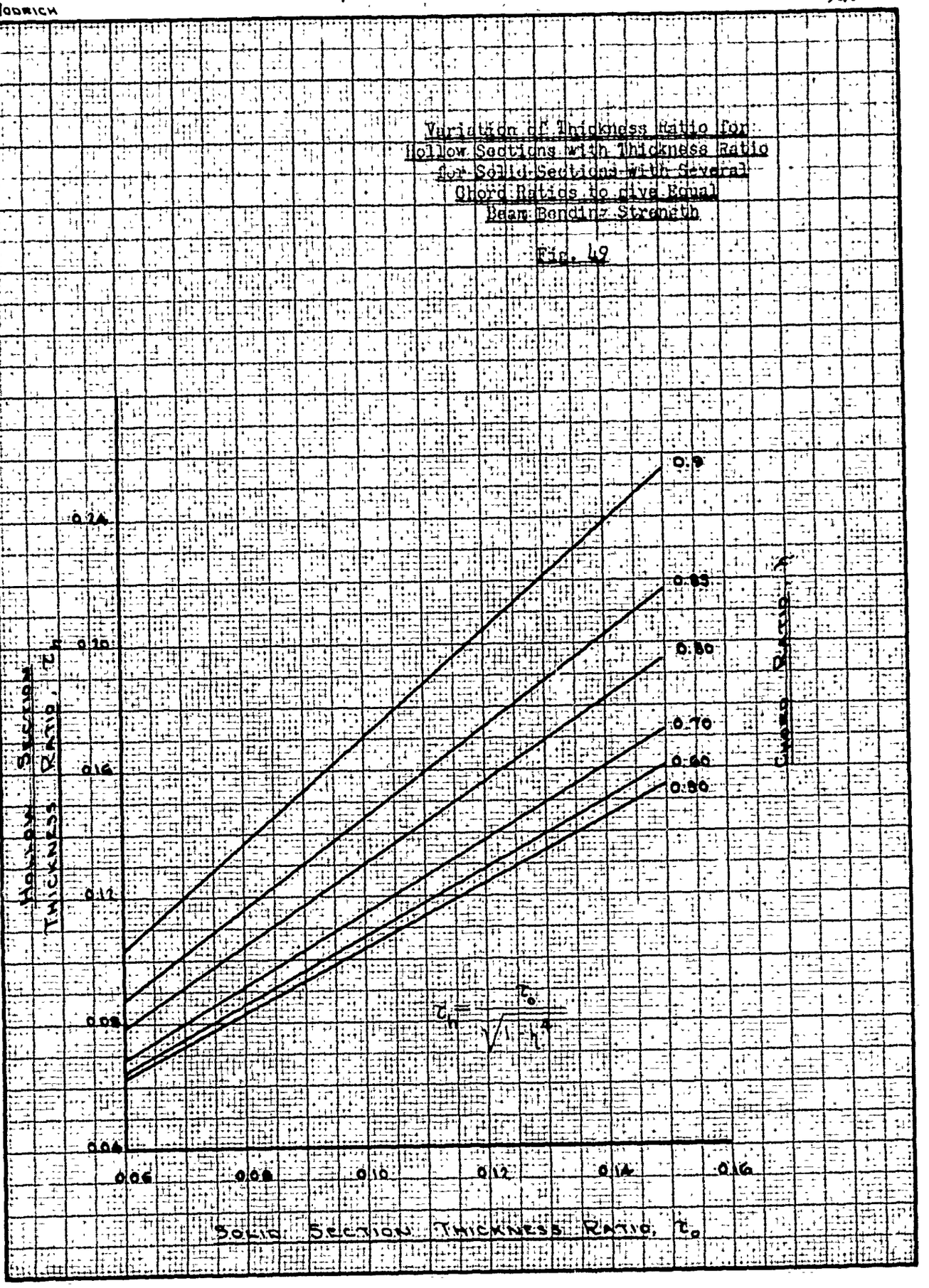

Variation of Equivalent Hollow Strut Percent Thickness with Solid Strut Percent Thickness to Support Tangential Loads

Fig. 50

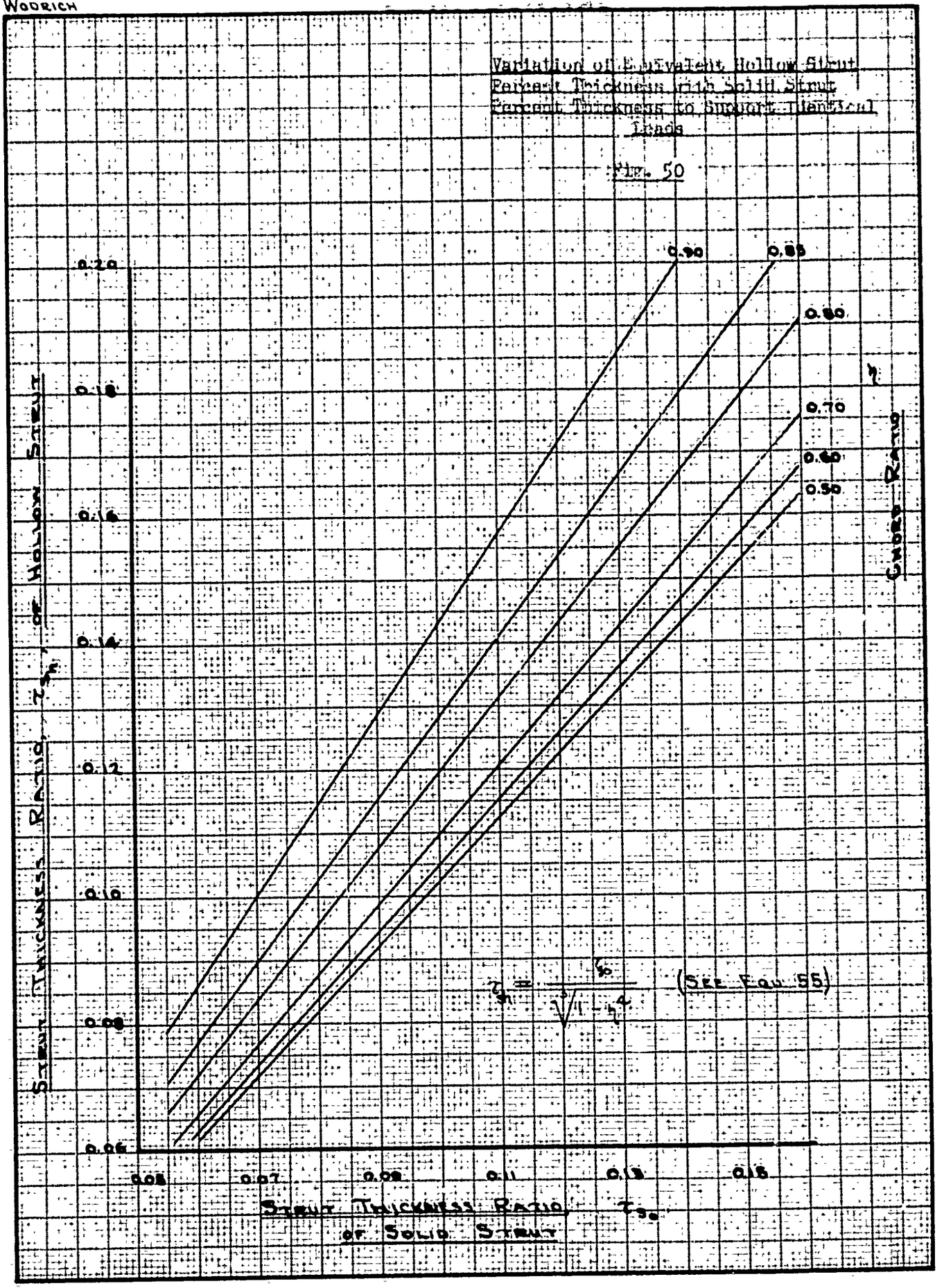

APPENDIX II

EFFECT OF TORSION ON HOLLOW HYDROFOILS

The effect of the shear stress due to torsion in hollow hydrofoils must be combined with the normal bending stresses and the normal shear stresses in determining margins of safety and skin thicknesses for hollow hydrofoils. The torsional shear stress for a hollow section is normally expresses as:

$$\tau_t = \frac{T}{2 A_m t_s} \quad \text{IN KSI} \qquad \text{Equ. 56}$$

Since $A_s = \frac{2}{3} \tau_h c$, the mean enclosed area becomes:

$$A_m = \frac{\frac{2}{3}\tau_h c^2 + \frac{2}{3}\tau_h (\eta c)^2}{2} \text{ , OR}$$

$$A_m = \frac{\tau_h c^2}{3}\left(1 + \eta^2\right). \qquad \text{Equ. 57}$$

Substituting the value of A_m from Equation 57 and the value of t_s from Equation 54 into Equation 56 gives:

$$\tau_t = \frac{3T}{\tau_h^2 c^3 (1+\eta^2)(1-\eta)} . \qquad \text{Equ. 58}$$

The torsional deflection for a hollow hydrofoil of constant section may be expressed as:

$$\phi = \frac{T l}{K G} \qquad \text{(RADIANS)} . \qquad \text{Equ. 59}$$

Here, ϕ is the angle of twist in radians, l is the length under consideration in inches, T is the torque at length l in kip-inches and K is the torsional constant of the section in inches^4.

Where $K = \frac{4 A_m^2 t_s}{U_m}$ (Ref. 6) Equ. 60

and U_m is length of the median boundary.
For thin skins, U_m approximately equals $\frac{\pi c}{4}\left(3 + \tau_h^2\right)$.

Thus, by substituting the above value for U, and the value of A_m from Equation 57 into Equation 60,

$$K = \frac{8}{9} \frac{\tau_h^3 c^4 (1+\eta^2)^2 (1-\eta)}{\pi (3+\tau_h^2)} . \qquad \text{Equ. 61}$$

And Equation 59 becomes:

$$\phi = \frac{Tl}{G} \left[\frac{8 \tau_h^3 c^4 (1+\eta^2)^2 (1-\eta)}{9 \pi (3+\tau_h^2)} \right] . \qquad \text{Equ. 62}$$

C O N F I D E N T I A L

AN INVESTIGATION OF THE STABILITY OF HYDROFOIL CRAFT

June 1950

Warren Amster

Contract No. N9onr-93201

TABLE OF CONTENTS

Section	Page
Table of Contents	i
Index of Figures	iv
Index of Tables	vi
Symbols	vii
I. Introduction	1
II. Analysis of Stability and Control	3
A. Stability Requirements	4
1. Performance Considerations	4
a. High Speed	4
b. Lift to Drag Ratio	5
2. Wave Response	5
3. Necessary Stability Conditions	7
a. Longitudinal and Lateral Trim	8
b. Static Longitudinal Stability, Directional and Roll Stability	8
c. Stability to Height above Surface	9
d. Dynamic Stability	9
B. Configurations with All Foils Fixed	10
1. Slanting Foils	11
2. Planing Foils	11
3. Ladder Foils	12
4. Underwater Wings	12
5. Combinations of Fixed Foil Types	13
C. Configurations with All Foils Submerged and Movable Controls	15
1. Single Foil Craft	15
2. Stabilizer Forward	15
3. Stabilizer Aft	16
4. Types of Control Surfaces	16
a. All Movable Surfaces	17
b. Hinged Control Surfaces	18

TABLE OF CONTENTS (cont.)

	Page
D. Control Systems for Craft with Movable Surfaces	20
1. Orientation Sensing Elements	20
a. Water Surface Sensing	20
(1) Hydrodynamic Pressure	21
(2) Hydrostatic Pressure	21
(3) Float or Skating Foil	21
(4) Electrical System	22
b. Motion Sensing	22
(1) Accelerometer	22
(2) Gyroscope	23
(3) Flow Direction Vane	23
c. Command Signals	23
2. Control Surface Actuators	24
a. Mechanical	24
b. Hydrodynamic Pressure	25
c. Hydraulic	25
d. Electrical	25
e. Pneumatic	26
E. Static Stability and Trim	27
1. Longitudinal Static Conditions	27
a. Longitudinal Trim Equations	27
(1) All Foils Fixed	28
(2) Foils with Movable Controls	29
b. Longitudinal Static Stability	31
(1) All Foils Fixed	32
(2) Foils with Movable Controls	34
2. Lateral Static Conditions	35
a. Lateral Trim	35
b. Lateral Static Stability, Metacentric Height	36
F. Dynamic Stability of Hydrofoil Craft	37
1. Theory of Small Disturbances	37
2. Longitudinal Motions	38
a. Axes, Coordinates and Notations	38
b. Equations of Motion	42
c. Stability Derivatives	47
3. Lateral Motions	49
a. Axes, Coordinates and Notations	49
b. Equations of Motion	52
c. Stability Derivatives	53
d. Steady Turns	53

TABLE OF CONTENTS (cont.)

		Page
G.	Dynamic Stability of Fixed Foil Craft . . .	56
H.	Dynamic Stability of Movable Foil Craft . .	58
	1. Servomechanism Approach	58
	2. Equivalent Stability Derivative Approach.	59
	3. Longitudinal System	60
	a. Calculation of Stability Derivatives	60
	b. Transient Approximation	66
	c. Feedback Loops.	68
	4. Lateral System.	70
	a. Calculation of Stability Derivatives	71
	b. Feedback Loops.	72
I.	Summary and Conclusions	73
III.	Design of 10 Ton Test Vehicle	75
A.	Configuration and Operating Conditions. . .	75
B.	Longitudinal Analysis	76
	1. Trim Curves	76
	2. Static Stability Curves	76
	3. Stability Derivatives and Coefficients.	76
	4. Solutions to Equations of Motion. . . .	76
	5. Perfect Servomechanism Curves	77
C.	Lateral Analysis.	78
	1. Stability Derivatives and Coefficients.	78
	2. Perfect Servomechanism Analysis	80
	3. Steady Turns.	81
D.	Description of Control System	82
E.	Alternative Control Systems	85
References.		87
Figures		89
Tables.		110

INDEX OF FIGURES

No.	Title	Page
1.	Frequencies of Encountering Waves.	89
2.	Orbital Velocities and Wave Heights.	90
3.	Inertia Coefficient for Elliptic Flat Plate with Initial Acceleration Normal to Plate Face.	91
4.	Foil Configuration and Center of Gravity Location - 10 Ton Test Craft.	92
5.	$C_{m_{trim}}$ and Θ versus C_L, Forward C.G.	93
6.	$C_{m_{trim}}$ and Θ versus C_L, Design C.G.	94
7.	$C_{m_{trim}}$ and Θ versus C_L, Aft C.G.	95
8.	$C_{m_{stability}}$ and Θ versus C_L, Forward C.G.	96
9.	$C_{m_{stability}}$ and Θ versus C_L, Design C.G.	97
10.	$C_{m_{stability}}$ and Θ versus C_L, Aft C.G.	98
11.	Attenuation and Phase vs. Frequency, Cruise Condition, Stabilizing Foils Used as Control Surfaces.	99
12.	Attenuation and Phase vs. Frequency, Forward C.G., Take-Off.	100
13.	Attenuation and Phase vs. Frequency, Aft C.G., Take-Off.	101
14.	Attenuation and Phase vs. Frequency, Design C.G., Cruise.	102
15.	Attenuation and Phase vs. Frequency, Forward C.G., High Speed.	103
16.	Attenuation and Phase vs. Frequency, Aft C.G., High Speed.	104

INDEX OF FIGURES (cont.)

No.	Title	Page
17.	Longitudinal Frequency Response, Design C.G., Cruise.	105
18.	Lateral Attenuation and Phase vs. Frequency, Design C.G., Cruise.	106
19.	Lateral Frequency Response Design C.G., Cruise.	107
20.	Hydrofoil Test Vehicle - Schematic Diagram - Stabilization and Trim System.	108
21.	Circuit Diagram of a Typical 10 Contact Electrical Height Sensing Stabilization System.	109

INDEX OF TABLES

No.	Title	Page
1.	Roots of Longitudinal Characteristic Equations.	110
2.	Configuration Properties of Ten Ton Test Craft.	111
3.	Longitudinal Stability Derivatives.	112
4.	Longitudinal Stability Coefficients.	113
5.	Lateral Stability Derivatives.	114
6.	Lateral Stability Coefficients.	115

SYMBOLS

Symbol	Description	Unit
AR_m	Forward foil aspect ratio.	---
AR_t	Aft foil aspect ratio.	---
b	Foil span used as lateral reference length.	ft.
b_m	Forward foil span.	ft.
b_t	Aft foil span.	ft.
C_D	Total drag coefficient, based on S.	---
C_{D_m}	Forward foil drag coefficient based on S_m.	---
$C_{D_{o_m}}$	Forward foil parasite drag coefficient based on S_m.	---
$dC_{D_m}/dC_{L_m}^2$	Forward foil induced drag coefficient index based on S_m.	---
C_{D_t}	Aft foil drag coefficient based on S_t.	---
$C_{D_{o_t}}$	Aft foil parasite drag coefficient based on S_t.	---
$dC_{D_t}/dC_{L_t}^2$	Aft foil induced drag coefficient index based on S_t.	---
C_h	Hinge moment coefficient.	---
C_L	Lift coefficient based on S.	---
C_{L_m}	Forward foil lift coefficient based on S_m.	---
$C_{L_{\alpha_m}}$	Forward foil lift curve slope based on S_m.	1/rad.
C_{L_t}	Aft foil lift coefficient based on S_t.	---
$C_{L_{\alpha_t}}$	Aft foil lift curve slope based on S_t.	---

SYMBOLS (cont.)

Symbol	Description	Unit
C_l	Rolling moment coefficient.	---
$C_{l\dot{\psi}}$, etc.	Typical lateral stability derivative.	---
C_m	Pitching moment coefficient.	---
C_{m_θ}, etc.	Typical longitudinal stability derivative.	---
C_n	Yawing moment coefficient.	---
C_x	Longitudinal force coefficient.	---
C_y	Side force coefficient.	---
C_z	Vertical force coefficient.	---
$\bar{c}_m$	Forward foil center of area chord, $\bar{c}_m = \frac{1}{S_m}\int_0^{b_m} c^2 dy$.	ft.
$\bar{c}_t$	Aft foil center of area chord, $\bar{c}_t = \frac{1}{S_t}\int_0^{b_t} c^2 dy$	ft.
D	Differential operator, d/dt	1/sec.
d	Height of wave surface above mean water level at height measuring device.	ft.
d_m	Distance of center of drag of forward foil below center of gravity.	ft.
d_p	Normal distance between thrust line and center of gravity.	ft.
d_s	Distance of center of side force on aft strut below center of gravity.	ft.
d_t	Distance of center of drag of aft foil below center of gravity.	ft.
e	Roll angle measured by lateral sensing system.	rad.
$G_i(s)$, etc.	Typical servo component transfer function.	

SYMBOLS (cont.)

Symbol	Description	Unit
g	Acceleration of gravity.	ft./sec.^{2}
h	Vertical disturbance of craft center of gravity from equilibrium.	ft.
H	Laplace transform of h.	ft.sec.
I_{xz}	Lateral product of inertia.	slugs ft.^{2}
K	Weight coefficient.	—
K_1, etc.	Typical servo component gain ratio.	—
k_m	Forward foil inertia coefficient.	—
k_t	Aft foil inertia coefficient.	—
k_x	Roll radius of gyration.	ft.
k_y	Pitch radius of gyration.	ft.
k_z	Yaw radius of gyration.	ft.
$\mathcal{L}$	Rolling moment.	lb.ft.
l	Longitudinal reference length.	ft.
l_m	Forward foil arm.	ft.
l_t	Aft foil arm.	ft.
l_φ, etc.	Typical lateral stability coefficient.	—
M	Pitching moment.	lb.ft.
m	Craft mass.	slugs
m_θ, etc.	Typical longitudinal stability coefficient.	—
N	Yawing moment.	lb.ft.
q	Dynamic pressure.	lb./ft.^{2}
R_t	Terminal turning radius.	ft.

SYMBOLS (cont.)

Symbol	Description	Unit
r	Rate of turn.	rad./sec.
r_t	Terminal rate of turn in steady turn.	rad./sec.
S	Reference area, usually chosen as area of largest foil.	$ft.^2$
S_m	Area of forward foil.	$ft.^2$
S_{sm}	Wetted side area of forward struts.	$ft.^2$
S_{st}	Wetted side area of aft foil struts.	$ft.^2$
S_t	Aft foil area.	$ft.^2$
s	Laplace transform variable.	1/sec.
U	Equilibrium forward speed.	ft./sec.
u	Forward speed pertibation from equilibrium.	ft./sec.
X	Longitudinal force.	lb.
Y	Side force.	lb.
Z	Vertical Force.	lb.
α	Angle of attack.	rad.
β	Sideslip angle, positive for slipping to right.	rad.
γ	Angle between thrust line and x axis, positive for thrust line inclined upward at bow.	rad.
δ_f	Flap deflection, either symmetric or asymmetric, positive for left flap trailing edge down.	rad.
δ_r	Rudder deflection, positive for trailing edge to right.	rad.
δ_t	Aft foil deflection, positive for trailing edge down.	rad.

SYMBOLS (cont.)

Symbol	Description	Unit
Δ	Laplace transform of δ_f	rad.sec.
$d\epsilon/d\alpha$	Downwash angle gradient at rear foil due to lift of forward foil.	--
θ	Pitch angle, positive for bow up.	rad.
Θ	Laplace transform of θ	rad.sec.
μ	Longitudinal density ratio, $\mu = \frac{m}{\rho S \ell}$	--
μ_1	Lateral density ratio, $\mu_1 = \frac{m}{\rho S b}$	--
ρ	Water density.	slugs/ft.^{3}
τ	Time factor, $\tau = \frac{m}{\rho S V}$	
φ	Roll angle, positive for right side down.	rad.
φ_t	Roll angle in steady turn.	rad.
Ω	Denominator of longitudinal approximate transfer function.	sec.$^{-4}$

I. INTRODUCTION

In this report the stability analysis is divided into two distinct parts. Sec. II considers the general problem of stability of a variety of types of hydrofoil configurations. Sec. III presents the results of a basic stability analysis for a test vehicle preliminary design which incorporates the results of performance and structural studies.

A hydrofoil craft design based on rational consideration of performance, strength and stability requirements must represent a series of design decisions and compromises. Performance and strength characteristics can be studied rather generally by the use of design charts representing envelops of limiting configurations which conform to certain reasonable fixed criteria. Unfortunately, the stability of families of configurations cannot be studied usefully in this manner because of the complexity of the requirements and the lack of definite numerical criteria. In general, it is only possible to present the results of detailed studies of specific configurations and an outline of the relative advantages or disadvantages of each configuration studied.

Sec. II includes a group of necessary conditions which must be satisfied in order to demonstrate minimum satisfactory stability characteristics. Equations for the investigation of these conditions are derived and presented in terms of dimensionless coefficients.

Various types of hydrofoil configurations are discussed from a purely functional point of view. No attempt is made to evaluate the merits of complete craft employing the foil types mentioned.

The investigation of stabilization of completely submerged foil configurations by movable controls was first suggested to the personnel of this project by Dr. Vannevar Bush. This method of stabilization has since proved to offer the most promise for the type of craft with which this report is most intimately concerned. During the course of the investigation, Dr. Bush has made many valuable suggestions concerning the methods and the control systems used in achieving stability by this means.

Sec. III presents the results of an investigation of necessary stability conditions for the proposed test vehicle. This

vehicle is designed to demonstrate the performance of a type of hydrofoil arrangement which can achieve lift to drag ratios in a useful range for transportation vehicles. The stability system used in this craft makes use of movable controls on completely submerged foils and the analysis of the system follows servomechanism methods.

The heavy reliance on theory in the stability considerations of this report is in marked contrast to the experimental methods used almost exclusively by previous investigators in the field of hydrofoil craft. This report is intended as a theoretical background for the study of load carrying hydrofoil craft and the methods, assumptions and equipment presented here must be proven experimentally before the theory can be accepted as properly representative of the behavior of this type of vehicle.

Symbol notation is similar to the notation used in aircraft stability analyses. Whenever possible, the notation is arranged to avoid confusion with the symbols used in the structures and performance divisions of this report. However, all the symbols do not conform with the notation of the other divisions and the list of symbols is intended to apply to this division only.

II. ANALYSIS OF STABILITY AND CONTROL

In this section, methods for the investigation of stability and control of hydrofoil craft are developed. The analysis presented is intended to be applicable to a hydrofoil craft when operating completely supported on its foils. The very important trim considerations during take-off can be treated by methods similar to those used in hull design and a useful treatment of this subject is beyond the scope of this report.

Part of the purpose of this section is to present a summary of literature available on the subject of hydrofoil craft stability. Many of the references given in this report contain information on stability of specific configurations. However, the total of the information available is fragmentary and often simply qualitative so that a comprehensive study and comparison of the configurations which have been tested is not possible. The summary of configurations includes the broad aspects of the stability characteristics of most of the important hydrofoil craft which are discussed in the available literature.

The methods and nomenclature associated directly with the theoretical stability calculations of this report are most closely related to those employed in the study of aircraft stability. Some of the investigation employs the methods and nomenclature of electrical engineering and servomechanism analysis. The references which are cited as detailed background for the equations presented here are recommended for clarification of nomenclature for those not familiar with these fields.

Although the theoretical treatments of various types of hydrofoil craft follow parallel lines, the practical achievement of different types of designs may require very different approaches. Hydrofoil craft with foils which pierce the surface or plane on the surface usually have characteristics which are best investigated experimentally. This has been the approach of most design efforts to date. The theoretical analysis which is presented in this report is of limited usefulness in the development of such a craft. On the other hand, a configuration employing foils which are completely submerged at all times can be investigated quite thoroughly by the methods of theoretical hydrodynamics and free body dynamics. These differences in design procedure are discussed in greater detail in the portion of this section which deals with hydrofoil configurations.

A. STABILITY REQUIREMENTS

A hydrofoil craft has stability requirements which are a combination of those found in aircraft and ships. The proximity of the foils to the water surface imposes requirements similar to those found associated with displacement or planing surface vessels. The craft must stay at a proper attitude with respect to the surface and it must be capable of operation in waves or swells. On the other hand, its lift and control members operate by pressure induced by their shapes, attitudes and speed through the water. A satisfactory specification for stability requirements must recognize the similarities and differences of the principles of operation of hydrofoil vessels and other types of fluid-borne vehicles.

Various types of hydrofoils are potentially capable of operating usefully over a wide range of conditions. In the actual design of a vessel, emphasis should be placed on best performance for one particular type of operation and this will almost always penalize the performance for other purposes. In the same way, the emphasis in designing for stability will be determined by stability requirements which depend to a certain extent on the region of operation. Thus, a specific requirement which may be loosely specified and easily achieved for one type of craft may be very critical and difficult to accomplish for another. However, in spite of where the emphasis is placed, all the basic requirements of stability must be present in some form for every craft and for all operating conditions.

1. PERFORMANCE CONSIDERATIONS.

In another section of this report, the performance potentialities of hydrofoils as load carrying devices are analyzed. There are several types of water-borne vehicles with design emphasis on different features for which hydrofoil designs potentially offer distinct advantages over displacement vessels.

a. High Speed.

The design emphasis for most existing hydrofoil craft has been on speed. However, there are no available reports which show comprehensive studies of the problem of obtaining high speed. There are some reports, such as in Ref. (1), on the development of foil sections to inhibit incipient cavitation without a

clear demonstration of the effect of cavitation on high speed.

The stability problems peculiar to craft designed specifically for high speed appear to be divided roughly into two types. First, the trim and stabilization must be achieved with the smallest possible drag penalty. This does not necessarily mean that the lifting surfaces should also be used for stabilization. It may turn out to be of considerable advantage to develop the best high speed configuration and then stabilize it with surfaces which are for that purpose alone. The second consideration is that the craft must be able to respond to waves sufficiently to keep the hull out of the water without riding excessively hard. The problem of providing proper wave response at very high speeds may be the most important single factor in the selection of a final configuration.

b. Lift-to-Drag Ratio.

A performance parameter which is of greater importance than high speed for hydrofoil craft intended as transportation vehicles is the ratio of lift to drag. In another section of this report the means of obtaining good lift-to-drag ratios with foil systems designed to reasonable structural strength criteria are explored. A basic lifting foil with relatively high aspect ratio that operates completely below the surface appears to be capable of achieving lift-to-drag ratios of a high enough order to be acceptable for many transportation purposes at reasonably high speeds.

Two arrangements employing high aspect ratio foils offer the most promise. One configuration consists of a single, large foil supporting most of the weight of the craft and small auxiliary submerged foils for balance purposes. Another configuration is a tandem arrangement of two foils, each of which carries a part of the craft weight. Neither of these foil systems has height-seeking stability so that some type of stabilization must be provided.

The stability analysis of this report is particularly applicable to exploring means of stabilizing completely submerged foils. It must be kept in mind that in order to achieve the best overall vehicle design, the drag due to stabilization should be as small as possible.

2. WAVE RESPONSE

The requirements for wave response characteristics of hydrofoil craft can only be specified in general terms without actual operating experience. The riding qualities of any craft must lie

somewhere between two conflicting ideal requirements. From the point of view of crew comfort, the craft should position to the mean location of the water surface and not respond at all to surface irregularities. From the point of view of keeping the hull out of the water, the craft should follow the surface very closely. In general, neither of these characteristics would be satisfactory and sometning in between is desirable, depending on wave height and speed. The actual characteristics of a craft will be a further compromise between the response characteristics which are finally chosen and the extent to which they can be achieved within the selection of configurations available for the design.

Without attempting to write rigid specifications, it is possible to outline some qualitative response requirements. The craft should ride perfectly smooth on water with a chop light enough so that there is no danger of water hitting the hull. As the wave size increases, the craft should tend to follow the waves more closely. For large waves, it should follow almost exactly. The actual size of waves for which these regions of response characteristics apply is determined by the clearance which the hull is intended to maintain above the water surface. Tight following action should begin at wave height about the same as the clearance dimension.

In order to find the expected frequencies of encountering waves for various speeds, wave heights and directions of travel, it was necessary to consult a study of wave characteristics. From the information presented in Ref. (2), the following general properties of deep water waves appear to be reasonable assumptions for frequency response purposes:

Length to height ratio averages 17 for waves less than 100 feet long. Height is measured from crest to trough and length from crest to crest.

Wave velocity can be computed from deep water wave theory:

$$C = \sqrt{\frac{g}{2\pi} L}$$

C - velocity of advance (ft./sec.)
g - acceleration of gravity (ft./sec.^{2})
L - length of wave (ft.)

Deep water wave theory indicates that water particles have a circular motion and the diameter of the circle at the surface is the wave height.

The diameter of the circle of wave motion decreases with depth according to the formula:

$$\frac{d}{d_o} = e^{-2\pi\frac{y}{L}}$$

d = diameter of circle at depth y. (ft.)
d_o = diameter at surface. (ft.)
y = depth of center of circle. (ft.)
L = wave height. (ft.)

The period of the motion does not change with depth so that velocities decay with depth in the same manner as the particle circle.

Fig. (1) shows the frequencies of encountering waves as functions of wave height and craft speed for a following sea and a head sea based on the assumptions above. These curves serve as a guide to the disturbance frequencies and amplitudes that can be expected for hydrofoil craft. Fig. (2) shows the orbital motion velocities that can be expected at and below the surface, based on these assumptions. These orbital motions may be important because of the load factors they can cause on foils operating completely below the surface.

The conclusion which can be drawn from this brief consideration of wave frequencies is that every craft has a maximum rough water speed, depending on three factors. These factors are hull clearance above water, wave height and direction of travel relative to the wave propagation direction. There is also some wave size below which it is possible to operate the craft at any speed without discomfort and regardless of direction of wave propagation

3. NECESSARY STABILITY CONDITIONS.

In order to demonstrate that a hydrofoil vessel will maintain a desired attitude in calm water for an extended period of time, a series of necessary conditions must be satisfied. No single one of these conditions is sufficient to guarantee satisfactory operation and the lack of any one of them will cause the

craft to be unsatisfactory. They represent the minimum stability requirements. Each of the quantitative measures of stability can be modified by configuration or mechanism changes to achieve characteristics which are more desirable for various ranges of operation.

a. Longitudinal and Lateral Trim.

The first requirement for stability is that there be some attitude of equilibrium in steady undisturbed operation at each speed.

For longitudinal trim where all forces and moments remain in the plane of symmetry, the following relationships must be satisfied. Lift equals weight. Thrust equals drag. The pitching moment about the center of gravity must be zero.

Lateral trim places requirements on forces and moments notin the plane of symmetry. The rolling moment about an axis through the center of gravity and pointing in the direction of motion must be zero. The yawing moment about a vertical axis through the center of gravity must be zero. The side force in a direction normal to the plane of symmetry must be zero in straight operation and must be in balance with centrifugal acceleration and forces due to the roll angle in a steady turn.

It should be remembered that these requirements are simply equilibrium conditions and no mention has yet been made of the behavior of the craft if it is disturbed from equilibrium.

b. Static Longitudinal Stability, Directional and Roll Stability.

The next requirement is that a craft which has an angular disturbance from equilibrium must tend to return toward the equilibrium position.

The longitudinal requirement is called "longitudinal static stability" and specified that a disturbance pitch angle which raises the bow must cause a bow down pitching moment on the craft.

There are two lateral static stability requirements. Directional stability requires that a disturbance yaw angle with the bow to the right from equilibrium must result in a yawing moment which tends to turn the bow to the left. Roll stability requires that a roll angle from equilibrium must result in a righting rolling moment.

Note that the satisfaction of these requirements does not necessarily imply that the craft will actually return and remain in the equilibrium position following a disturbance.

c. Stability to Height above Surface.

In order for a hydrofoil craft to remain at the desired height above the water surface, it must lose lift if it rises above that height and gain lift if it sinks deeper. This requirement may be satisfied by having a bow down pitching moment result from rising too high and the decreased angle of attack, caused by the pitching moment, can then cause the decreased lift. Regardless of how it is accomplished, a hydrofoil vessel must demonstrate a tendency to return to an equilibrium height above the water when it rises or sinks from that position.

d. Dynamic Stability.

In order for a dynamically supported vehicle to continue to operate for an extended time, it must return to equilibrium following a disturbance. This may be accomplished by a damped oscillation or by an exponental decay of the disturbance, or both. The failure to return to equilibrium may be evidenced by a divergent oscillation or by an exponental divergence. The occurence of a neutrally damped mode is usually considered unsatisfactory dynamic behavior.

It might appear at first that dynamic stability is a sufficient condition for satisfactory hydrofoil craft operation. However, a configuration with fixed foils submerged completely below the water can have angle and velocity disturbances damp to zero and still lack height stability and have insufficient roll stability.

B. CONFIGURATIONS WITH ALL FOILS FIXED

There is a considerable body of technical literature reporting on design, construction and testing of various hydrofoil craft. These efforts vary from simple attempts to improve the high speed water-borne characteristics of seaplanes to extensive testing of good sized vessels and proposals for very large craft. Unfortunately most of the literature is lacking in consistent test data and theoretical analyses so that it is not of great use as a guide for new design attempts. With a few exceptions, the craft about which reports are available have employed foils fixed rigidly to a hull and operating at the surface of the water.

A fixed foil system at the surface of the water is intended to accomplish four purposes. First, it must support the weight of the craft. Second, it must tend to maintain the craft at some specific average height above the water surface. Third, it must provide roll stability by tending to right the craft if it should start to roll over. Fourth, the system must be dynamically stable both laterally and longitudinally so that disturbance amplitudes subside instead of increasing.

In most fixed hydrofoil craft to date, the underwater configuration has consisted of two foil systems in tandem, with the craft center of gravity located somewhere between them. In almost all cases both systems have been designed to contribute directly to the first three objectives mentioned above. Thus, the lifting surfaces are required to provide height and roll stability so that the foil designs become compromises in order to satisfy several requirements. Little thought has evidently been given to the design of foils to best accomplish each separate objective. The possibility of designing a foil to give the best lift and drag characteristics for a specific application and then stabilizing it with foils specially designed for that purpose appears not to have been explored in the literature. Such a design philosophy should yield better craft for both performance and stability than designs where foils are required to perform several functions.

Hydrofoils which contribute to height or roll stability by operating at the water surface can be divided roughly into three classes, according to principle of operation.

1. SLANTING FOILS

One type of hydrofoil which has been used extensively has its lifting members at a slant with respect to the water surface. They are usually shaped like a "V" or "U" in front elevation and planforms are sometimes constant chord and sometimes tapered to a smaller chord at the center. When a craft using this type of foil settles into the water below the equilibrium position, added foil area is submerged and the lift increases, causing the vessel to rise. A righting rolling moment is also developed when the craft rolls if the center of gravity is not too high.

There is a large amount of descriptive literature about craft incorporating this type of hydrofoil, but very little consistent data on the foils themselves. Ref. (3) describes several craft using "V" and "U" foils of various types. Ref. (4) contains some data on their characteristics.

There are several types of slanting foils which have not appeared in the literature but which might prove to have desirable characteristics. The "inverted V", the "W", and "inverted W" foils might give better roll stability than the "V" or "U" foils. Another type of foil system which has structural advantages looks, in front elevation, somewhat as follows, "><".

The initial design of hydrofoil craft using slanting foils for lift or stabilization, or both, is severely hampered by lack of data on their operating characteristics. Scale effects have not been properly evaluated and unsteady lift characteristics have not been investigated in any quantitative manner. Until such investigations have yielded basic data on the characteristics of slanting foils, the design of hydrofoil craft employing them must remain largely a matter of testing models of progressively larger sizes in order to develop a satisfactory configuration.

2. PLANING FOILS

Several successful hydrofoil craft designs have employed planing surfaces to position the craft with respect to the water surface. Such surfaces have no better performance characteristics than conventional planing hulls so they are not used for the main lifting system. However, as stabilizing surfaces, they are quite satisfactory because they provide a very positive tendency to locate the craft correctly with respect to the water surface. Their principal disadvantage is their tendency to skip and their generally light damping of disturbance motions.

From a design standpoint the planing foil has the advantage that the characteristics of planing surfaces have been studied extensively by hull designers. This information can be used directly for the design of planing foils for hydrofoil craft. Ref. (5) contains descriptive material on the use of planing foils for hydrofoil craft.

3. LADDER FOILS.

A vertical cascade of horizontal foils mounted like the rungs of a ladder will provide height stability. Such a system is particularly attractive for performance because area which is not needed for lifting is raised out of the water and its drag is eliminated. By placing "ladders" on each side of a craft, excellent roll stability is attainable. Several designs have been tested with some portion of their foil system employing this principle. Ref. (6) describes craft using "ladder" foils.

Unfortunately the rough water characteristics of this type of system are undesirable. If the craft is running at high speed on the lower rungs of the ladder, with the others raised out of the water, and it encounters a wave which submerges the other foils, the lift and drag of the "ladder" can be increased three or four times. Such load factors are very hard on the structure and the craft's occupants. At least one instance of the destruction of a craft from this cause is noted in the literature.

The steady characteristics of a lifting foil cascade operating near the surface can be treated theoretically by incompressible cascade theory so as to yield answers sufficiently accurate for preliminary design purposes. However, the problem of the unsteady characteristics of such a system, especially as foils enter or leave the water, can be treated best experimentally. No consistent test data on foil cascades appear to be available.

4. UNDERWATER WINGS.

The well-developed theory of lifting surfaces operating in an incompressible fluid can be used to predict the lift and drag-due-to-lift of a completely submerged hydrofoil. The effect of the surface can be predicted by assuming that it is a flat, free surface and using the principle of reflection. The effect of specified surface irregularities can be treated, although the mathematics would be involved. There are even some closed solutions, in Ref. (7), for two dimensional wings which include the disturbance of the surface due to the presence of a lifting hydrofoil and the

resulting effect on the hydrofoil. This extensive theoretical background and the vast amount of test data on wings operating in air are available for the design of hydrofoils which operate completely under water at all times. Such methods make it possible to design underwater wings which best perform some specified type of operation. The limits imposed by cavitation and by "air cavitation" can be estimated theoretically, but only determined accurately by experiment. To date, no hydrofoil craft described in the available literature has been designed to take advantage of this theoretical and experimental background.

The great disadvantage of the fixed underwater hydrofoil is that it is not stable to height or roll, and neither are combinations of foils of this type alone. Dihedral in a foil with the tips submerged does not give satisfactory roll stability because of the high center of gravity inherent in hydrofoil craft. The high center of gravity also means that dihedral does not produce the same effects as it does with aircraft which employ it to improve lateral dynamic stability. Special means of stabilization for both height and roll are required in order to take advantage of the desirable and predictable performance characteristics of the fixed underwater hydrofoil.

5. COMBINATIONS OF FIXED FOIL TYPES

Many of the successful hydrofoil craft reported in the literature have employed two or more types of hydrofoils for the overall configuration. These combinations are intended to take advantage of certain characteristics of some of the foils mentioned above in order to achieve designs with some desirable stability, performance or rough water behavior. Ref. (8) describes several craft of this type.

There are some general principles which are usually followed in these designs. Planing foils are almost always located forward because they have strong depth stability and poor lift curve slopes. Slanting foils are used most widely and usually serve for main lifting surfaces as well as stabilizing members. "Ladder" foils are usually located symmetrically on opposite sides of a craft to help give roll stability.

A configuration which can combine the low drag-due-to-lift of the completely submerged foil and the positive stabilization of the planing foil offers excellent possibilities for a satisfactory overall craft. A self-propelled test craft using planing foils forward and a high aspect ratio underwater wing just aft of the center of gravity has been tested extensively as part of the present investigation. This craft is very stable and well damped

laterally and longitudinally. It has excellent take-off, landing and rough water handling characteristics. The turning properties are, in general, excellent although it is possible to raise the forward planing foil on the inside of a turn out of the water by suddenly applying rudder to tighten the turn. No special skill is necessary to operate the craft.

The purpose of the test vehicle was to obtain experimental data on the performance of the type of foil-strut configuration which is recommended in the division of this report dealing with performance. The forward planing foils were used because it was felt that they would give satisfactory stability with a minimum of detailed development. Measurement of the drag of the entire craft shows that the forward foils impare the craft performance quite severely and that the best performance is obtained when the forward foils are most lightly loaded, which corresponds to the most aft permissible center of gravity location.

No detailed stability analysis for this test vehicle is presented here because of the lack of data on the properties of planing foils and the uncertainty in methods for computing stability derivatives for such configurations. Even such simple calculations as static trim yield very uncertain results because of lack of data. However, the dynamic stability equations presented in a later section of this report apply to this as well as the other fixed foil configurations. Presumably it is possible by experience to develop techniques of hydrofoil craft design to the point where dynamic stability analyses have real meaning for fixed foil craft. Lacking such experience, the best stability analysis appears to involve building a craft and trying it out.

C. CONFIGURATIONS WITH ALL FOILS SUBMERGED AND MOVABLE CONTROLS

In the logical development of a dynamically supported water-borne vehicle, a configuration with all lifting and stabilizing surfaces submerged offers considerable promise for several reasons. Foremost among these reasons are freedom from surface irregularities, theoretical and experimental information available for design, and better performance because of lack of surface wave drag. There is also the advantage of simple control of "air cavitation" and theoretical prediction and, under some conditions, elimination of cavitation.

Balanced against these advantages are the difficulties resulting from the necessity for movable controls required for trim and stabilization.

1. SINGLE FOIL CRAFT

From a performance standpoint, the most desirable configuration is a single underwater wing. A straight wing alone supporting a load several chord lengths above it would be very difficult to trim for a stable center of gravity location. This configuration might be made to give satisfactory stability if the foil had a high aspect ratio and was swept back. Such a foil has not been considered in this investigation because of the difficult structural and hydroelastic problems.

2. STABILIZER FORWARD

A configuration which can be trimmed for a stable center of gravity location and has good longitudinal damping consists of a large foil just aft of the center of gravity and a small stabilizing foil forward. One advantage of this configuration is that the downwash from the main lifting foil does not affect the lift of the stabilizing foil. For most configurations, the separation of the foils will be large enough compared to the stabilizing foil span so that its downwash will not have a large effect on the main foil.

Several promising-looking configurations with this arrangement were investigated for longitudinal trim and stability. It was found that this configuration has unsatisfactory allowable center of gravity travel, due largely to the high center of gravity location inherent in hydrofoil craft. The aft center of gravity limit is determined by static stability. The high center of

gravity location causes the neutral point to be farther forward than it would be if the center of gravity were located at the same height as the main foil. The forward center of gravity location is limited by stalling of the stabilizing surface at take off due to the required trim load. Since liberal limits on center of gravity travel is one of the characteristics which is desired in any useful vessel, this limitation imposes a severe handicap on the configuration.

3. STABILIZER AFT

The conventional aircraft configuration consisting of a main lifting surface just forward of the center of gravity and a small stabilizing surface aft offers satisfactory trim, stability and damping. However, all three of these quantities are influenced by the effect of main foil downwash on the stabilizing foil. Also, the trim loads on the stabilizing foil act downward so that the maximum lift coefficient of the craft suffers. An advantage of the configuration is that the main foil operates in undisturbed water.

Several variations of this configuration were investigated for trim and stability. It was assumed that the downwash at the stabilizing foil due to the lift on the main foil was the full theoretical value, including effect of the water surface. This is a conservative assumption for stability and a non-conservative assumption for longitudinal damping. The permissible travel of the center of gravity for the configurations investigated proved satisfactory, although at the most forward center of gravity location the lift-drag ratio suffered due to a down load on the stabilizing foil. In general this configuration appears to be quite satisfactory for hydrofoil craft.

4. TYPES OF CONTROL SURFACES.

The purpose of control surfaces is to impose forces or moments on the craft in order to trim it and to correct orientation errors. Some special control elements such as spoilers, slots, rotors, variable camber or suction could possibly be used on a hydrofoil craft. However, the consideration of control devices in this investigation will be confined to movable surfaces.

For the type of hydrofoil craft considered in this section, the control surfaces must perform two types of functions. First, they must trim the craft longitudinally to the proper lift coefficient and trim in roll to counteract asymmetric loading. This function

can be accomplished by relatively slow deflection of the controls. The second function of control surfaces is to maintain proper height above the water and correct tendencies to roll. The speed at which the surfaces must move for this purpose depends on the geometry of the craft and on its velocity. Control deflection rates of the order of 60°/sec. and frequencies of the order of two cycles per second are typical of requirements of craft for which detailed calculations were made.

a. All-Movable Surfaces

One or more of the foils on a hydrofoil craft can be mounted on bearings and rotated in pitch to provide pitch and roll trim and stabilization. Such foils should be mounted near their aerodynamic centers to minimize the control loads. It is not necessary to move both forward and aft foils since their relative angular attitude determines the lift coefficient for longitudinal trim. However, if it is required that the hydrofoil craft hull remain level at all speeds, both foils must be able to move. It is ordinarily desirable to have roll controls deflect differentially in order not to change lift coefficient when applying a rolling moment.

The structural and mechanical problems associated with mounting the main lifting foil on bearings have been considered as a general design problem. Such an arrangement would be difficult for design, construction and maintenance. There appear to be simpler means of accomplishing longitudinal trim and stability so this type of control has not been used in any detail design. Its hydrodynamic advantages are spanwise lift distribution, which does not change with deflection, and profile drag, which is not harmed by hinges or gaps. Roll control with an all movable main foil might be accomplished by twisting the foil or by splitting it in the center and having the two halves deflect separately.

Stabilizing foils can be mounted on bearings and rotated rather simply because the static loads on them are usually a small fraction of the weight of the craft. Such foils can be designed with a small enough aspect ratio to be mounted on a single strut. This makes the bearing problem somewhat simpler by removing the tendency for bearings to bind which can occur with multiple strut configurations. The control effectiveness of all movable stabilizing foils is excellent. The all movable stabilizing foil has the advantage of removing the hinge, control surface gap, and actuation problems from the design of a surface which should be

kept as thin as possible to reduce the drag.

b. Hinged Control Surfaces

The type of control surfaces which are used almost exclusively on aircraft can be adapted theoretically to hydrofoil craft design quite easily. The practical problems of hinges, control actuation, high hinge moments and gap seal appear to be somewhat exacting design considerations. Hinged control flaps offer the advantage of permitting the main structure of the foil to be rigidly attached to the hull and still be effective in applying control forces and moments. For small deflections, these surfaces do not have a marked adverse effect on the drag if they are properly designed. Such design is complicated for hydrofoil craft by the very high surface loadings, the desirability of thin foils, the submersion in water with the attendant lubrication problems, and the difficulties in sealing the gaps between the main surface and the movable portion.

Control surfaces on the main lifting foil serve the purpose of altering lift without changing the craft pitch angle and of applying a rolling moment. These surfaces can extend along the entire span or can be located over some portion of the outbound part of the foil. Partial span flaps alter the spanwise lift distribution which is detrimental to the induced drag of a properly designed foil. Also a redistribution of load can be difficult from a structural design standpoint. Despite the difficulties involved in their design, hinged flaps can be placed on foils whose physical dimensions are large enough to permit location of the necessary actuation mechanism. They appear to offer the simplest solution to control of the forces and moments on a main lifting foil.

Stabilizing foils can be made similar to the elevators on aircraft. Hydrodynamically they are very satisfactory, although they usually have a somewhat smaller trim range than the all movable stabilizer. The difficulty encountered in their design is that the physical dimensions of a stabilizing foil designed for stability, trim and damping of the craft will generally be small except on very large craft. The design of internal hinge and actuation mechanisms is very difficult under these circumstances. External equipment is detrimental to both drag and control effectiveness. This problem could possibly be solved very satisfactorily by the use of a non-binding piano hinge arrangement and torque tube actuation. No attempt has been made to design such equipment under the present investigation. Use of trim tabs is a next logical step for control surfaces on large craft.

No investigation has been made to determine the size craft for which hinged stabilizing foil control surfaces begin to offer design advantages.

The hydrodynamic characteristics of hinged control surfaces have been studies extensively in connection with aircraft design. Refs. (9 and 10) contain excellent summaries of design information covering a wide variety of control surfaces.

D. CONTROL SYSTEMS FOR CRAFT WITH MOVABLE SURFACES

It has been demonstrated that hydrofoil craft with all foils submerged must have control surfaces which trim and correct orientation errors. In the following section the possibilities for actuating the surfaces and for control of the actuators are explored.

1. ORIENTATION SENSING ELEMENTS

In order for a hydrofoil craft to remain at a fixed height above the water and in an upright position, there must be some means of correcting its attitude when it differs from the desired orientation. For a fixed foil craft this is done by having forces or moments act on the foils due to the error in attitude. For the type of craft under consideration here, some device must be made to sense the error and transmit it to the control surfaces. This function can be accomplished in a variety of ways, depending on the nature of the desired signal.

a. Water Surface Sensing

The most obvious means of stabilizing a hydrofoil craft is to have the control surfaces move in response to errors in its attitude with respect to the water surface. This is the function which is performed by surface foils and by a ship's hull. The most useful information about attitude with respect to the surface is height above the water and roll angle with respect to it. Another attitude which might be important for some craft is pitch angle with respect to the surface. The first two items of information can be obtained by determining the location of the water surface at two points located symmetrically on opposite sides of the craft. The average of these readings gives the height; and their difference, the roll angle. A third point located in the plane of symmetry, but not in line with the other two, would give pitch angle and determine the plane of the water. This is the maximum amount of practical information about orientation obtainable by this method. The information can then be used to dictate how far to deflect the surfaces in order to correct orientation errors. There are a variety of ways by which attitude with respect to the water surface can be obtained.

(1) Hydrodynamic Pressure.

The ratio of dynamic pressure in air and in water at the same velocity is the ratio of their densities. It is possible to detect the surface of the water with a moving object by detecting the total head pressure and determining whether it corresponds to air or water.

A vertical row of pressure orifices can be made to control the static pressure in a chamber so that there is a unique relationship between height of the orifice array and the pressure in the chamber at a given speed. The pressure in the chamber can then be used to control the flap deflection or actually used to operate the actuator. There are several difficulties with this system. No design is immediately apparent which will have fast enough response to meet hydrofoil craft requirements and yet be compact enough for installation in the supporting struts. The hydrostatic pressure varies with speed so a pressure sensing device will not operate in the desired manner. The pressures available are too low to operate controls for any but the smallest craft.

A more promising system makes use of a vertical row of pressure sensing buttons which tell simply whether they are in water or air. Such a step system will act almost like a linear system if the buttons are close enough together. The signal from such buttons would be electrical or mechanical.

(2) Hydrostatic Pressure.

Theoretically, a very good way to detect depth is to measure hydrostatic pressure. Practically, this is very difficult because it is hard to find a place on a moving body where the pressure is hydrostatic and will remain that way for all angles of attack and yaw. The hydrodynamic pressure is usually so much higher than the expected hydrostatic errors that very small pressure coefficients can give large false hydrostatic pressure signals.

(3) Float or Skating Foil.

One successful hydrofoil craft based on the movable surface principle uses a small skating foil to detect the location of the water surface. Ref. (11) presents the principles of the design of this craft, called the Hook Hydrofin, in some detail.

The use of a positive mechanical follower to detect the location of the water surface is very attractive because of simplicity and reliability. Such a follower can be used to operate the control surfaces if hinge moments are not too large. Other possible applications include operation of a potentiometer or selsyn transmitter or a hydraulic valve by the action of a surface follower.

Whether or not mechanical ruggedness is a real design problem for floats or skating foils can only be determined by their actual use in rough water.

(4) Electrical Systems.

There are several types of electrical fluid sensing devices which can be used to detect the location of a water surface. Commercial capacity-type fuel gauges might be applicable, although the conductivity of water would probably make their use difficult. However, a high frequency capacity device could probably be made to operate satisfactorily. Making use of the electrical conductivity of water results in a much simpler type of device. The difference in electrical conductivity between sea water and fresh water is not sufficient to require different equipment in this type of arrangement. The water can be made to close a series of direct or alternating current circuits, each of which corresponds to a particular water level.

b. Motion Sensing

Certain types of response or damping qualities can be artificially imparted to a hydrofoil craft by having the control surfaces respond to motions of the craft without reference to the water surface. This means might be required under certain circumstances to inhibit porpoising or other undesirable dynamic behavior of a craft which has proper height sensitivity.

(1) Accelerometer.

Vertical, fore and aft or side accelerations can be detected by accelerometers and the signals translated into control surface deflections. The signal can also be integrated electronically to give velocity or displacement signals if they are desired. Angular accelerometers can also be used to detect pitching, rolling or yawing accelerations, and their signals can likewise be integrated. The riding qualities of a hydrofoil

craft might be improved by use of a vertical accelerometer if the amount of improvement warranted the added complication.

(2) Gyroscope.

Angular orientation and rate of angular deflection can be used as a signal for control surface deflection. Gyroscopes, to accomplish this end, have been developed for aircraft autopilots.

(3) Flow Direction Vane.

Angle of attack and angle of sideslip can be detected, measured and translated into control surface deflection by the use of flow direction vanes. Such vanes can be of the weather-vane type with a selsyn follower or a nulling follow-up type which has controlled damping properties.

(4) Strain Gauge.

The output from strategically located strain gauges can be used as a signal for control surface deflection. Such a use would probably be principally as a structural safety feature to relieve loads before they cause failure.

c. Command Signals

One of the simplest ways to govern the movement of control surfaces is in response to command signals from the craft operator. A craft incorporating only command control would have to be flown continuously whenever it was up on the foils. In theory, such an arrangement might work in calm water. The section on wave response indicates that the frequency of encountering waves is too high for a human pilot to follow, even at relatively low speeds. No further consideration has been given to designs based on this means of obtaining height or roll stabilization.

Command signals are necessary for steering the craft. For this application it is essential that the means of steering be so arranged that it is not possible to turn so tightly that some essential portion of the lifting system leaves the water.

The roll and height control systems can be provided with manual overrides for take-off purposes or for emergency landings in

the event of a stabilization system failure. Further investigation and experience in operation may reveal other circumstances under which a manual override or even a full command signal control system might be desirable.

2. CONTROL SURFACE ACTUATORS

On a craft with movable surfaces, some means must be provided to supply the moments to move the surfaces. Surface actuators can be divided roughly into two classes. The first class provides a given amount of moment and the surface moves until the hinge moment from the water just balances the applied moment. In order to use such a system it is necessary to know both how effective the surface is and how much hinge moment it needs. The second class deflects the surface a given amount and holds it there unless the resisting hinge moment is greater than the maximum available control moment. This system does not require detailed information about hinge moment characteristics of the surfaces.

In general, the second class of control actuator is superior because of its freedom from the very uncertain hinge moment characteristics of hinged control surfaces.

A consideration which is easily overlooked in the selection of control actuators is the control power required. The speed with which a surface must be actuated should be considered together with the moment required. Sometimes a low force actuator and a high mechanical advantage look promising until the actuator travel and power are found to be prohibitive.

a. Mechanical

Control surfaces can be operated by purely mechanical means for some applications. Manual systems are usually arranged to transmit control loads from a wheel or stick directly to the surface by means of cables, push rods or torque tubes. Controls for steering are an excellent application of such a system if the loads are not too high.

Buoyancy or hydrodynamics force on a float or small planing foil is also a possibility for the operation of a mechanical system. The size of the float or foil tends to become large

in order to provide sufficient control power for any but small hydrofoil craft. This type of control system must be so arranged that the moments from the surface are not large enough to force the foil or float away from the water surface. A system such as is described here might be quite satisfactory for small pleasure craft.

b. Hydrodynamic Pressure

Ram pressure available from water which is trapped in a total head tube on a hydrofoil craft can be used to operate controls. This pressure, of course, varies with speed so the control system would probably be of the force type instead of the displacement type. Ram pressure is about 17.4 lb./in.^{2} at 50 ft./sec. (34.1 m.p.h. or 29.6 knots). The force available from a system operating at this pressure limits the type of control system very severely. Requirements of control power might make the flow required at such pressures prohibitive.

c. Hydraulic

The familiar hydraulic actuation system can be used to move control surfaces. Hydraulic motors are not ordinarily recommended for this purpose. Hydraulic cylinders are usually most satisfactory for this type of application. There is no question about being able to obtain sufficient control force or power from a hydraulic cylinder system. However, careful design is required in order to achieve satisfactory frequency response characteristics. For a properly designed hydraulic system, the frequency response is far better than is required for any contemplated hydrofoil craft application.

The hydraulic pump can be driven by an engine or, even better, by an electric motor for that purpose. Hydraulic system components are simple, inexpensive, light, small and reliable.

d. Electrical

Several types of irreversible electric actuators are available for operation of control surfaces. An electric motor with a gear train or worm drive is quite satisfactory if control speeds are not high. As control loads increase, it is increasingly difficult to find electrical actuators which have enough power and can still meet frequency response requirements. The best high-power, high-frequency-response electrical actuator

is the amplidyne. However, at about 2 horsepower, the frequency response of amplidynes is just marginal for hydrofoil craft. It is quite probable that stable amplidyne actuators could be designed in larger sizes and with the required frequency response.

e. Pneumatic

Very little information is available on the use of pneumatic actuators for high load and high frequency response applications. It is known, however, that the principal reason for failure of hydraulic systems to meet frequency response requirements is due to the cushioning effect of air dissolved in the hydraulic fluid. This difficulty is overcome by operating a hydraulic system at high pressure, which compresses the air and increases the fluid rigidity. A high pressure pneumatic system might be a possibility for a hydrofoil craft control actuator.

E. STATIC STABILITY AND TRIM

There are several necessary conditions which must be satisfied in order that a dynamically supported vehicle operate satisfactorily. These conditions specify that in undisturbed operations, the summations of forces in any direction, or moments about any axis, be zero. Furthermore, there must be an initial tendency for the craft to return to equilibrium if it is disturbed. These are necessary conditions for stability but they are not sufficient conditions to guarantee stable operation. Stability and trim both apply to two separate types of equilibrium. The longitudinal case involves lift, drag, thrust and pitching moment. The lateral case involves rolling and yawing moments. Trim conditions are investigated to determine the balance of the craft. Static stability is investigated because a craft cannot be dynamically stable without it. However, a properly trimmed and statically stable craft can still be dynamically unstable under certain circumstances. Such conditions can be investigated by the dynamic stability equations.

1. LONGITUDINAL STATIC CONDITIONS

Three equations govern the longitudinal trim conditions. First, lift equals weight. Second, thrust equals drag. Third, the pitching moment about the center of gravity is zero. Static stability means that a bow up angle of pitch disturbance causes a bow down pitching moment.

In order to remove craft weight and its speed as independent parameters, forces and moments are expressed as dimensionless coefficients. It should be remembered that coefficients representing forces on individual foils are given identifying subscripts and they are based on the area of the surface to which they apply.

a. Longitudinal Trim Equations

For most applications the three trim equations are too cumbersome to solve analytically, and it is much simpler to solve them graphically. These equations represent lift coefficient, drag coefficient and pitching moment coefficient as functions of two independent variables. It is desired to find the values of the variables for various lift coefficients and zero pitching moment coefficient. In this way, it is possible to find the balanced attitude of the craft for a given gross weight and speed.

(1) All Foils Fixed

The variables governing trim for a fixed foil craft are height of the center of gravity above the water, h , and pitch angle, Θ . In order to calculate trim conditions, it is necessary to know for each foil its lift and drag characteristics as functions of angle of attack and depth of submersion. The following sketch shows the forces on a fixed foil craft.

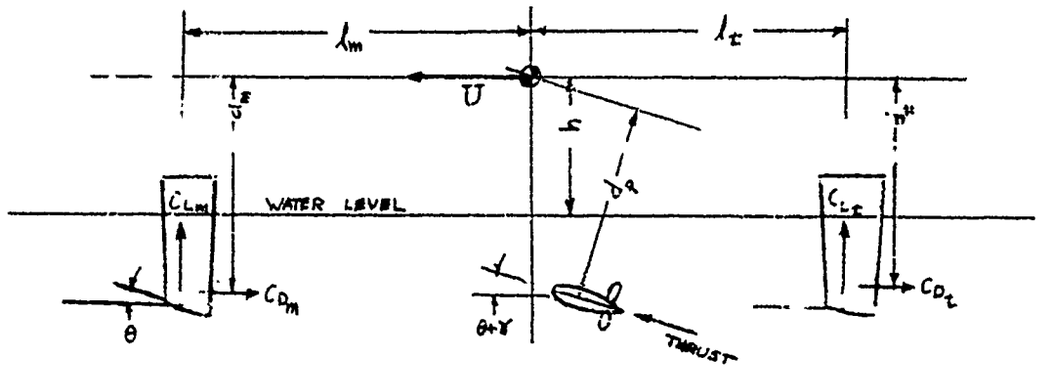

For this type of craft, the overall lift and drag coefficients are functions of Θ and h . Equally spaced increments of Θ and h are chosen as independent variables and values of the dependent variables computed. The lift and pitching moment coefficient for the entire craft are computed as follows:

C_{Lm} , C_{Lt} , C_{Dm} , C_{Dt} , l_m , l_t , d_m , d_t are determined for a series of values of Θ and h .

$$C_L = C_{Lm} + \frac{S_t}{S_m} C_{Lt} + \left(C_{Dm} + \frac{S_t}{S_m} C_{Dt}\right) \tan(\theta + \gamma)$$

$$C_{m_{(TRIM)}} = C_{Lm} \frac{l_m}{l} - C_{Dm} \frac{d_m}{l} - \frac{S_t}{S_m}\left(C_{Lt} \frac{l_t}{l} + C_{Dt} \frac{d_t}{l}\right) + \frac{\left(C_{Dm} + C_{Dt} \frac{S_t}{S_m}\right)}{\cos(\theta + \gamma)} \frac{d_p}{l}$$

Note that it is best to choose reference areas which do not change with submersion because of the complication imposed by keeping track of the amount of area submerged for each angle of attack and height. Also, the total lift coefficient has meaning for performance if it is based on some geometric area instead of a wetted area. Curves of C_m versus C_L are shaped somewhat as shown below for this type of configuration:

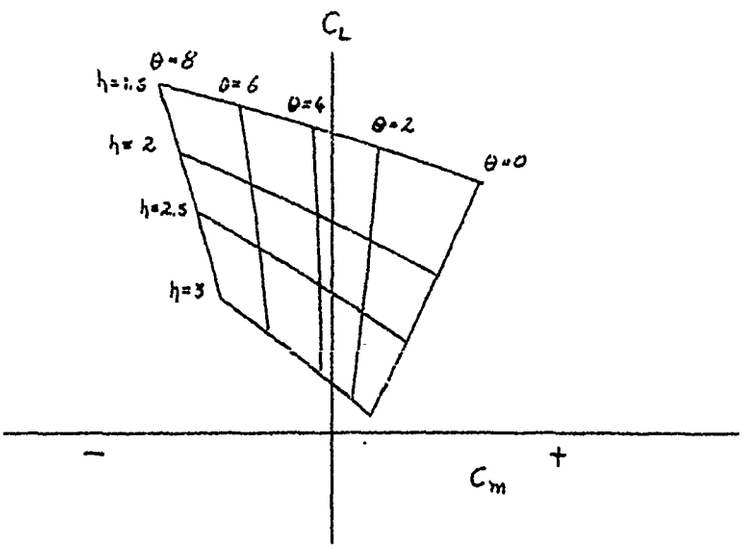

The values of h and θ along the line $C_m = 0$ correspond to the trim condition for each C_L value.

(2) Foils with Movable Controls.

The trim equations for hydrofoil craft with all foils submerged and movable controls use angle of pitch, θ, and surface deflection, σ, as independent variables. In the following analysis it is assumed that the aft foil is deflected an angle σ_t and the angle of pitch, θ, is referred to the front foil. Notice that the height of the center of gravity above the water does not enter into the calculations. The following sketch illustrates the notation:

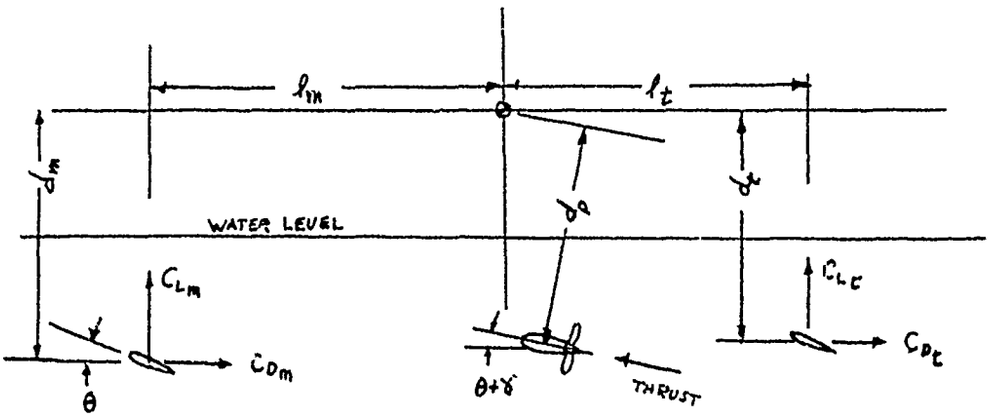

Lift and drag of the foils are assumed to act at their quarter chords so the dimensions ℓ_m , ℓ_t , d_m , d_t depend on angle of pitch only. If we identify the values of these dimensions for $\theta = 0$ by ℓ_{mo} , ℓ_{to} , d_{mo} , d_{to} , then for any other angle of attack:

$$\ell_m = \ell_{mo} \cos\theta + d_{mo} \sin\theta$$

$$\ell_t = \ell_{to} \cos\theta - d_{to} \sin\theta$$

$$d_m = d_{mo} \cos\theta - \ell_{mo} \sin\theta$$

$$d_t = d_{to} \cos\theta + \ell_{to} \sin\theta$$

Using lift curve slopes, drag characteristics and downwash flow angles from the performance analysis permits calculation of the trim equations:

$$C_{Lm} = C_{L\alpha_m}\,\theta$$

$$C_{Dm} = C_{Do_m} + \frac{dC_{Dm}}{dC_{L_m}^2}\,C_{L_m}^2$$

$$C_{Lt} = C_{L\alpha_t}\frac{S_t}{S_m}\left[\theta\left(1 - \frac{d\varepsilon}{d\alpha}\right) + \delta_t\right]$$

$$C_{Dt} = C_{Do_t} + \frac{dC_{Dt}}{dC_{Lt}^2}\,C_{Lt}^2 + \theta\frac{d\varepsilon}{d\alpha}\,C_{Lt}$$

$$C_L = C_{Lm} + C_{Lt}\left(\frac{S_t}{S_m}\right) + \left(C_{Dm} + \left(\frac{S_t}{S_m}\right)C_{Dt}\right)\tan(\theta+\gamma)$$

$$C_{m_{(cm)}} = C_{Lm}\frac{\ell_m}{\ell} - C_{Dm}\frac{d_m}{\ell} - \left(\frac{S_t}{S_m}\right)\left[C_{Lt}\frac{\ell_t}{\ell} + C_{Dt}\frac{d_t}{\ell}\right] + \left[\frac{C_{Dm} + C_{Dt}\left(\frac{S_t}{S_m}\right)}{\cos\theta + \gamma}\right]\frac{d_p}{\ell}$$

Curves of C_m and θ v.s. C_L for different values of δ_t permit determination of trim conditions. These curves look somewhat as follows:

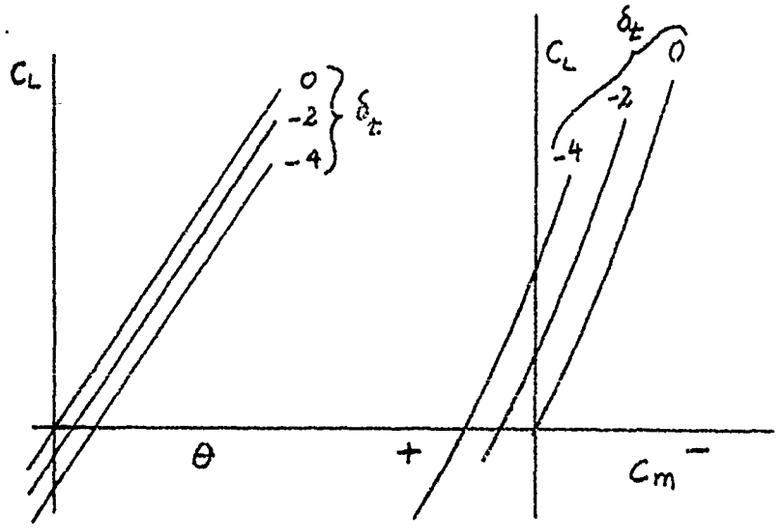

Trim conditions correspond to points along the vertical line $C_m \approx 0$. The values of θ and δ_t corresponding to a desired C_L give the craft attitude for trim.

b. Longitudinal Static Stability

The static stability requirements of a hydrofoil craft are somewhat the same as for a displacement hull. When the craft is disturbed by a small pitch angle it must develop a restoring

pitching moment. For a displacement hull this moment is measured by the longitudinal metacentric height. It is found by dividing the restoring moment by the hull displacement and the pitch angle. For hydrofoil craft, the measure of static stability is the stability derivative, C_{m_θ}. It represents the restoring pitching moment coefficient divided by the pitch angle. These quantities are related by:

$$\text{Longitudinal Metacentric Height} = \frac{-C_{m_\theta} l}{C_L}$$

It should be noted that the equivalent longitudinal metacentric height for a hydrofoil craft is a function of the speed at a given gross weight. This is not the case for a displacement hull.

Static stability is calculated in much the same way as trim. If the drag and thrust act through the center of gravity, the equations are identical. This is clearly not the case for a hydrofoil craft. There is a fine distinction between the two equations due to differences in the phenomena they represent.

The envelope of trim moments assumes that at each point the craft is operating at a constant velocity with the lift just equal to the weight and the thrust equal to the drag. The assumption of static stability calculations is that the craft is operating in trimmed equilibrium and it is given a disturbance angle of pitch. The speed of the craft is assumed to remain constant, so a pitch angle increase causes a change in lift and drag. However, the propulsive thrust does not change so there are no longer balances between lift and weight or thrust and drag.

A static stability value corresponds to a specific center of gravity location and a specific operating condition. It is necessary to establish the trim condition before determining static stability.

(1) All Foils Fixed.

To calculate a curve from which static stability can be determined for a fixed hydrofoil craft, it is necessary to find the lift, drag, height and angle of pitch of the trim condition for which static stability is desired. It is then assumed that the height and thrust remain fixed and the lift, drag and pitching moment coefficients are computed as functions

of angle of pitch. Let the subscript $(\ )_s$ identify quantities corresponding to the trim condition. Notice that θ is the only variable in the following expressions:

$$C_{Lm}\ ,\ C_{Lt}\ ,\ C_{Dm}\ ,\ C_{Dt}\ ,\ l_m\ ,\ l_t\ ,\ d_m\ ,\ d_t$$

are determined for $h = h_s$ and a series of values of θ .

$$C_{m_{(STABILITY)}} = C_{Lm}\frac{l_m}{l} - C_{Dm}\frac{d_m}{l} - \frac{S_t}{S_m}\left(C_{Lt}\frac{l_t}{l} + C_{Dt}\frac{d_t}{l}\right) + \frac{\left(C_{Dm_s} + \frac{S_t}{S_m}C_{Dt_s}\right)}{\cos(\theta+\gamma)}\frac{d_t}{l}$$

This equation is best plotted as C_m VS. θ ; it looks somewhat as follows:

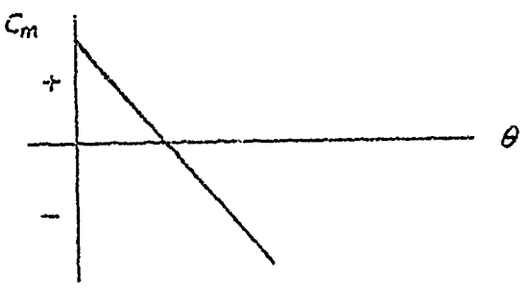

The amount of static stability is determined by the value and sign of the slope of this curve.

$$\left.\frac{dC_m}{d\theta}\right|_{C_m=0} < 0 \quad \text{Statically Stable}$$

$$\left.\frac{dC_m}{d\theta}\right|_{C_m=0} = 0 \quad \text{Statically Neutral}$$

$$\left.\frac{dC_m}{d\theta}\right|_{C_m=0} > 0 \quad \text{Statically Unstable}$$

(2) Foils with Movable Controls.

The static stability of a craft with all foils submerged is best expressed as dC_m/dC_L instead of $dC_m/d\theta$ because the numerical value of the former has the significance of a stability margin expressed as a decimal of the foil separation distance. The trim attitude must be established corresponding to the condition for which the static stability is desired. The trim angle of pitch is θ_s and the trim aft foil deflection is σ_{ts}. It is now necessary to compute C_L and C_m for $\sigma_t = \sigma_{ts}$ and a series of values for θ.

$$C_{Lm} = C_{L\alpha m}\,\theta$$

$$C_{Dm} = C_{Do_m} - \frac{dC_{Dm}}{dC_{L^2_m}}\,C_{L^2_m}$$

$$C_{Lt} = C_{L\alpha_t}\,\frac{S_t}{S_m}\left[\theta\left(1 - \frac{d\varepsilon}{d\alpha}\right) + \sigma_{ts}\right]$$

$$C_{Dt} = C_{Do_t} + \frac{dC_{Dt}}{dC_{L^2_t}}\,C_{L^2_t} + \theta\,\frac{d\varepsilon}{d\alpha}\,C_{Lt}$$

$$C_L = C_{Lm} + C_{Lt}\left(\frac{S_t}{S_m}\right) + \left(C_{Dm_s} + \frac{S_t}{S_m}\,C_{Dt_s}\right)\tan(\theta+\gamma)$$

$$C_{m_{(STABILITY)}} = C_{Lm}\,\frac{l_m}{l} - C_{Dm}\,\frac{l_t}{l} - \left(\frac{S_t}{S_m}\right)\left[C_{Lt}\,\frac{l_t}{l} + C_{Dt}\,\frac{d_t}{l}\right] + \left[\frac{C_{Dm_s} + C_{Dt_s}\left(\frac{S_t}{S_m}\right)}{\cos(\theta+\gamma)}\right]\frac{d_p}{l}$$

A plot of C_m vs. C_L now looks somewhat as follows:

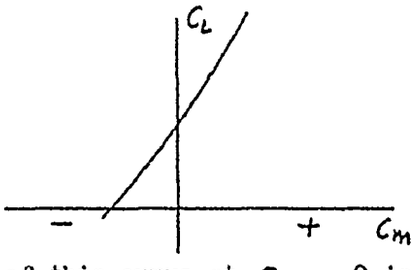

The slope of this curve at $C_m = 0$ is the static stability margin.

$\frac{dC_m}{dC_L} < 0$ Statically Stable

$\frac{dC_m}{dC_L} = 0$ Statically Neutral

$\frac{dC_m}{dC_L} > 0$ Statically Unstable

2. LATERAL STATIC CONDITIONS

a. Lateral Trim

If the center of gravity of a craft moves out of the geometric plane of symmetry, an unbalanced rolling moment is caused by the lift which continues to act in the plane of symmetry. Some means must be devised to counteract the unbalance or the craft will continue to roll over.

A fixed foil craft which is asymmetrically loaded and which has static roll stability assumes an angle of roll which has the proper rolling restoring moment to counteract the asymmetry. If this angle of roll produces a yawing moment, it in turn must be balanced by the rudder. Thus it is possible to hold a straight course by rudder action under an asymmetric load.

For a craft stabilized by moving surfaces, an asymmetric deflection of the surfaces is required to counteract an asymmetric load. The craft may trim upright or it may assume a roll angle in developing the balancing rolling moment, depending on the type of stabilization system.

b. Lateral Static Stability, Metacentric Height

A displacement hull develops a righting rolling moment when it rolls. If this rolling moment is divided by the hull displacement and the angle producing the roll, a length is obtained which is called the metacentric height. It is a measure of the craft's rolling static stability. In much the same way a hydrofoil craft with fixed foils must have roll static stability. The magnitude of the rolling static stability can be expressed as metacentric height or as a stability derivative. The relationship between them is:

$$\text{Metacentric Height} = -\frac{C_{l_\varphi} b}{C_L}$$

The derivative C_{l_φ} is the rolling moment coefficient due to a roll angle, φ, divided by φ. Some data on the rolling characteristics of fixed foil arrangements are available. Ref. (12) gives some information on one type of modified "V" slanting foil.

A craft with all foils under water and movable controls for roll stability must be designed so that the controls deflect asymmetrically when the craft rolls. The amount of the control deflection per unit angle of roll and the rolling effectiveness can be combined to give an effective metacentric height. However, it is more useful for dynamic stability purposes to express this roll stability in terms of a stability derivative.

Another lateral static stability requirement is directional stability. If a craft assumes a yaw angle without changing direction so that it sideslips, it must develop a yawing moment which tends to straighten it out. Once again this may be accomplished by proper location and size of vertical struts or other surfaces, or it may be achieved by moving a rudder in response to a sideslip vane signal. In this particular respect, there is a considerable difference between the properties of slanting, planing and "ladder" foils. One type may show distinct advantages for directional stability in certain applications where otherwise all the surface foils appear to have equal merit.

F. DYNAMIC STABILITY OF HYDROFOIL CRAFT

1. THEORY OF SMALL DISTURBANCES.

Dynamically supported vehicles are completely free from fixed restraints so they have six degrees of freedom for disturbance motions. There is a well-developed theory and a large amount of experience concerning the motions which such vehicles may develop. In brief, the theory is based on equations which relate the three linear accelerations and three angular accelerations to the forces and moments which produce them. A complete expression involving all possible means by which these forces and moments can arise would be extremely complicated besides being non-linear. In order to produce equations which may be solved by reasonable methods and in a reasonable time, some simplifying assumptions are made concerning the nature of the forces and moments. It is assumed that all disturbances are small so that, to a first approximation, forces and moments vary linearly with the disturbances from trimmed equilibrium which cause them. Furthermore a plane of symmetry is assumed for the vehicle and this suggests the assumption that motions which leave the plane of symmetry in its original plane do not produce moments or forces which tend to alter the plane of symmetry. Another assumption which is not as clearly justifiable is that motions which are purely asymmetrical do not produce moments or forces which leave the plane of symmetry unchanged.

When all these assumptions are incorporated into the six equations of motion, they separate into groups of three which are independent of each other. One group is the so called longitudinal equations which relate vertical motions, forward motions, and pitching angular motions in a system of three simultaneous linear total differential equations. The other group is the lateral equations relating sideward motions, rolling angular motions and yawing angular motions. These groups of equations can be solved rather easily because they are linear and the use of the Laplace Transform facilitates obtaining complete characteristics and transient solutions with relatively little labor.

A question naturally arises concerning the validity of these equations because of the rather limiting assumptions which have

been made. In general it has been the experience in the aircraft and guided missile field, where these equations are used extensively, that the major shortcoming of the system of equations is not in the assumptions made but in a lack of knowledge about the characteristics of the vehicles whose motions they describe. Actual testing of a properly instrumented hydrofoil craft will be required to determine the regions of validity of the equations which are used in this report for the dynamic stability analysis

2. LONGITUDINAL MOTIONS.

a. Axes, Coordinates and Notations.

In order to derive the longitudinal equations of motion, the craft is assumed to be operating initially in steady trimmed equilibrium on perfectly smooth water. A Cartesian coordinate system is established with origin at the center of gravity. The X axis is positive forward along the line of motion, the Z axis is positive downward in the plane of symmetry normal to the X axis. This coordinate system is fixed rigid to the craft and moves with it when it is disturbed. The forward velocity of the undisturbed craft is U . The fundamental disturbances of the craft from equilibrium are: a change in forward speed, u , positive for increased speed; a change in pitch angle, θ , positive nose up; and a vertical displacement of the center of gravity, h , positive downward. The time derivatives of these quantities are measured in the same sense.

It should be noted here that the fundamental disturbances are not the same as those used for aircraft and missile dynamics. The vertical displacement is used here instead of angle of attack. It can be demonstrated rigorously that within the assumption of small disturbances, the equations used here and those customarily used for aircraft yield the same final solutions although they differ in details. Since one of the requirements of a hydrofoil craft is to be stable to height above the water, the choice of disturbances of this report is very convenient to describe their motions.

Forces and moments resulting from disturbances are always resolved into components in the direction of the defined axes fixed in the

craft. X denotes a force along the x axis, Z a force along the z axis, and M a moment which tends to give a positive pitching angular acceleration.

Time derivatives of motions are denoted as follows:

$$\frac{dh}{dt} \equiv h^{\circ} \qquad \frac{d^2\theta}{dt^2} \equiv \ddot{\theta}$$

The assumptions of small disturbances and linear dependence of forces and moments on motions means that the quantities X, Z, and M can be expressed as a series of characteristic constants of the craft multiplied by each of the disturbance motions as follows:

$$Z = Z_o + \frac{\partial Z}{\partial h}h + \frac{\partial Z}{\partial \dot{h}}\dot{h} + \frac{\partial Z}{\partial \ddot{h}}\ddot{h} + \frac{\partial Z}{\partial \theta}\theta + \frac{\partial Z}{\partial \dot{\theta}}\dot{\theta} + \frac{\partial Z}{\partial \ddot{\theta}}\ddot{\theta} + \frac{\partial Z}{\partial u}u$$

Similar equations can be written for X and M. Since the condition where h, θ, u and their derivatives are zero corresponds to equilibrium, $Z_o = M_o = X_o = 0$. The assumptions of this theory require that each of these partial derivatives be a constant for a given craft and operating conditions. Thus $\frac{\partial Z}{\partial \theta}$ means change in lift force per unit change in pitch angle.

In using the equations of motion about to be developed, it is most convenient to express forces and moments in terms of coefficients defined by dynamic pressure and dimensions of the craft. The notation used is as follows for defining <u>force and moment coefficients</u>:

$$C_z = \frac{Z}{\frac{\rho}{2}U^2 S} \qquad C_m = \frac{M}{\frac{\rho}{2}U^2 S l}$$

$$C_x = \frac{X}{\frac{\rho}{2}U^2 S}$$

The partial derivatives used in the series expansion of forces or moments due to disturbance can be made dimensionless by converting the forces to coefficients and the motions to dimensionless ratios. The following illustrations include typical examples of all the motions involved in the longitudinal analysis. These quantities are called stability derivatives:

$$\frac{\partial C_X}{\partial(h/l)} = C_{X_h} \qquad \frac{\partial C_X}{\partial(\theta)} = C_{X_\theta}$$

$$\frac{\partial C_Z}{\partial(\dot{h}/U)} = C_{Z_{\dot{h}}} \qquad \frac{\partial C_m}{\partial\left(\frac{\dot{\theta} l}{U}\right)} = C_{m_{\dot{\theta}}}$$

$$\frac{\partial C_m}{\partial(\ddot{h} l/U^2)} = C_{m_{\ddot{h}}} \qquad \frac{\partial C_Z}{\partial\left(\frac{\ddot{\theta} l^2}{U^2}\right)} = C_{Z_{\ddot{\theta}}}$$

$$\frac{\partial C_Z}{\partial(u/U)} = C_{Z_u}$$

It should be emphasized here that these are partial derivatives and other motions must be absent during differentiation. A complete typical definition would include the following restrictions:

$$C_{Z_{\dot{\theta}}} = \left.\frac{\partial C_Z}{\partial\left(\frac{\dot{\theta} l}{U}\right)}\right|_{h = \dot{h} = \ddot{h} = \theta = \ddot{\theta} = u = 0}$$

In order to include the dynamic characteristics of the craft in the dimensionless notation of the equations of motion, it is necessary to include the radius of gyration in pitch of the craft. When the equations of motion are derived in the next section, the

significance of the following coefficients will be explained. The following terms appear directly in the longitudinal equations of motion; they are called stability coefficients:

$$X_h = \tfrac{1}{2} C X_h \qquad Z_h = \tfrac{1}{2} C Z_h$$

$$X_{\dot{h}} = \tfrac{1}{2} C X_{\dot{h}} \qquad Z_{\dot{h}} = \tfrac{1}{2} C Z_{\dot{h}}$$

$$X_{\ddot{h}} = \tfrac{1}{2} C X_{\ddot{h}} \qquad Z_{\ddot{h}} = \tfrac{1}{2} C Z_{\ddot{h}}$$

$$m_h = \tfrac{1}{2}\left(\frac{l}{K_y}\right)^2 C m_h$$

$$m_{\dot{h}} = \tfrac{1}{2}\left(\frac{l}{K_y}\right)^2 C m_{\dot{h}}$$

$$m_{\ddot{h}} = \tfrac{1}{2}\left(\frac{l}{K_y}\right)^2 C m_{\ddot{h}}$$

$$X_\theta = \tfrac{1}{2} C X_\theta \qquad Z_\theta = \tfrac{1}{2} C Z_\theta$$

$$X_{\dot{\theta}} = \tfrac{1}{2} C X_{\dot{\theta}} \qquad Z_{\dot{\theta}} = \tfrac{1}{2} C Z_{\dot{\theta}}$$

$$X_{\ddot{\theta}} = \tfrac{1}{2} C X_{\ddot{\theta}} \qquad Z_{\ddot{\theta}} = \tfrac{1}{2} C Z_{\ddot{\theta}}$$

$$m_\theta = \tfrac{1}{2}\left(\frac{l}{K_y}\right)^2 C m_\theta$$

$$m_{\dot{\theta}} = \tfrac{1}{2}\left(\frac{l}{K_y}\right)^2 C m_{\dot{\theta}}$$

$$m_{\ddot{\theta}} = \tfrac{1}{2}\left(\frac{l}{K_y}\right)^2 C m_{\ddot{\theta}}$$

$$X_u = \tfrac{1}{2} C X_u$$

$$Z_u = \tfrac{1}{2} C Z_u$$

$$m_u = \tfrac{1}{2}\left(\frac{l}{K_y}\right)^2 C m_u$$

In addition to the stability derivatives, the effect of deflecting control surfaces symmetrically is reduced to coefficient form in order to incorporate these effects into the equations of motion. Once again it is assumed that the forces and moments caused by deflecting controls are proportional to the angle of deflection which causes them. This assumption permits definition of control effectiveness derivatives:

$$\frac{\partial C_m}{\partial \sigma} \equiv C_{m_\sigma} \quad ; \quad \frac{\partial C_z}{\partial \sigma} \equiv C_{z_\sigma}$$

$$\frac{\partial C_x}{\partial \sigma} = C_{x_\sigma}$$

The symbol σ stands for any symmetrical control deflection angle in radians and is usually identified by a subscript.

In a manner similar to the stability coefficients, it is possible to define control effectiveness coefficients:

$$z_\sigma = \tfrac{1}{2} C_{z_\sigma} \; ; \; X_\sigma = \tfrac{1}{2} C_{x_\sigma} \; ; \; m_\sigma = \tfrac{1}{2}\left(\frac{l}{K_Y}\right)^2 C_{m_\sigma}$$

b. Equations of Motions

Three perfectly general expressions to describe the longitudinal motions of a hydrofoil craft can be written in terms of forces, moments and accelerations:

$$m\ddot{x} = \Sigma X \qquad (1a)$$
$$m\ddot{z} = \Sigma Z \qquad (1b)$$
$$I_Y\ddot{\theta} = \Sigma M \qquad (1c)$$

The assumptions of the stability analysis are imposed when the forms of ΣX , ΣZ , and ΣM are expressed as linear terms of a series in motions and control deflections:

$$\Sigma X = X_0 + \frac{\partial X}{\partial \theta}\theta + \frac{\partial X}{\partial \dot{\theta}}\dot{\theta} + \frac{\partial X}{\partial \ddot{\theta}}\ddot{\theta} + \frac{\partial X}{\partial h}h + \frac{\partial X}{\partial \dot{h}}\dot{h} + \frac{\partial X}{\partial \ddot{h}}\ddot{h} + \frac{\partial X}{\partial u}u - mg\theta + \frac{\partial X}{\partial \delta}\delta \qquad (2a)$$

$$\Sigma Z = Z_0 + \frac{\partial Z}{\partial \theta}\theta + \frac{\partial Z}{\partial \dot{\theta}}\dot{\theta} + \frac{\partial Z}{\partial \ddot{\theta}}\ddot{\theta} + \frac{\partial Z}{\partial h}h + \frac{\partial Z}{\partial \dot{h}}\dot{h} + \frac{\partial Z}{\partial \ddot{h}}\ddot{h} + \frac{\partial Z}{\partial u}u + \frac{\partial Z}{\partial \delta}\delta \qquad (2b)$$

$$\Sigma M = M_0 + \frac{\partial M}{\partial \theta}\theta + \frac{\partial M}{\partial \dot{\theta}}\dot{\theta} + \frac{\partial M}{\partial \ddot{\theta}}\ddot{\theta} + \frac{\partial M}{\partial h}h + \frac{\partial M}{\partial \dot{h}}\dot{h} + \frac{\partial M}{\partial \ddot{h}}\ddot{h} + \frac{\partial M}{\partial u}u + \frac{\partial M}{\partial \delta}\delta \qquad (2c)$$

The term $-Mg\theta$ in Equ. 2a is the component of gravity due to the pitch angle θ because the x axis is fixed in the craft and the gravity vector remains vertical. Since the motions

are disturbances from equilibrium, $X_0 = Z_0 = M_0 = 0$ Eq. (2a, 2b, 2c) are substituted into Eq. (1a, 1b, 1c), regrouped and manipulated to put the equations in dimensionless form. Acceleration in the X direction can be related to a change in forward speed and that in the Z direction to a vertical acceleration.

$$u = \dot{x} \ , \ \dot{u} = \ddot{x} \ , \ \dot{z} = h \ , \ \ddot{z} = \ddot{h}$$

Eq. (1a, 1b, 1c) now become:

$$\left(\frac{\dot{u}}{U}\right) - X_u\left(\frac{\rho S U}{m}\right)\left(\frac{u}{U}\right) - X_h\left(\frac{\rho U S}{m}\right)\left(\frac{h}{l}\right) - X_{\dot{h}}\left(\frac{\rho S l}{m}\right)\left(\frac{\dot{h}}{l}\right)$$

$$- X_{\ddot{h}}\left(\frac{\rho S l}{m}\right)^2\left(\frac{m}{\rho S U}\right)\left(\frac{\ddot{h}}{l}\right) + \left[\frac{mg}{\rho U^2 S} - X_\theta\right]\left(\frac{\rho S U}{m}\right)\theta$$

$$- X_{\dot{\theta}}\left(\frac{\rho S l}{m}\right)\dot{\theta} - X_{\ddot{\theta}}\left(\frac{\rho S l}{m}\right)^2\left(\frac{m}{\rho S U}\right)\ddot{\theta} = X_\delta\left(\frac{\rho S U}{m}\right)\delta \quad (3a)$$

$$- Z_u\left(\frac{\rho U S}{m}\right)^2\left(\frac{m}{\rho S l}\right)\frac{u}{U} - Z_h\left(\frac{\rho U S}{m}\right)^2\left(\frac{m}{\rho S l}\right)\frac{h}{l} - Z_{\dot{h}}\left(\frac{\rho U S}{m}\right)\left(\frac{\dot{h}}{l}\right)$$

$$+ \left[1 - Z_{\ddot{h}}\left(\frac{\rho S l}{m}\right)\left(\frac{\ddot{h}}{l}\right)\right] - Z_\theta\left(\frac{\rho S U}{m}\right)^2\left(\frac{m}{\rho S l}\right)\theta - Z_{\dot{\theta}}\left(\frac{\rho S U}{m}\right)\dot{\theta}$$

$$- Z_{\ddot{\theta}}\left(\frac{\rho S l}{m}\right)\ddot{\theta} = Z_\delta\left(\frac{\rho S U}{m}\right)^2\left(\frac{m}{\rho S l}\right)\delta \quad (3b)$$

$$- m_u\left(\frac{\rho U S}{m}\right)^2\left(\frac{m}{\rho S l}\right)\frac{u}{U} - m_h\left(\frac{\rho U S}{m}\right)^2\left(\frac{m}{\rho S l}\right)\left(\frac{h}{l}\right) - m_{\dot{h}}\left(\frac{\rho S U}{m}\right)\left(\frac{\dot{h}}{l}\right)$$

$$- m_{\ddot{h}}\left(\frac{\rho S l}{m}\right)\left(\frac{\ddot{h}}{l}\right) - m_\theta\left(\frac{\rho U S}{m}\right)^2\left(\frac{m}{\rho S l}\right)\theta - m_{\dot{\theta}}\left(\frac{\rho S U}{m}\right)\dot{\theta}$$

$$+ \left[1 - m_{\ddot{\theta}}\left(\frac{\rho S l}{m}\right)\right]\ddot{\theta} = m_\delta\left(\frac{\rho U S}{m}\right)^2\left(\frac{m}{\rho S l}\right)\delta \quad (3c)$$

Certain groups of physical quantities appear repeatedly in the above expressions so they are given symbols:

$$\mu = \frac{m}{\rho S l}$$ Density Ratio

$$K = \frac{mg}{\rho v^2 S}$$ Weight Coefficient

$$\tau = \frac{m}{\rho S v}$$ Time Factor

Experience with the solutions of these equations for typical hydrofoil craft has shown that certain of these terms have a completely insignificant effect on the final solution. These terms will be neglected at this point:

$$X\dot{h} = X\dot{\theta} = X\ddot{\theta} = 0$$

In order to simplify writing these equations the time derivatives will be expressed in the form of differential operators which simply indicate that differentiation with respect to time is to be performed on the variable upon which it operated:

$$D \equiv \frac{d}{dt} \quad ; \quad D^2 \equiv \frac{d^2}{dt^2}$$

Substitution of μ , τ and D into Eq. (3a, 3b, 3c) yields the final form of the longitudinal equations of motion:

$$\left[D - \frac{X_u}{\tau}\right]\frac{u}{U} + \left[-\frac{DX_{\dot{\alpha}}}{\mu} - \frac{X_\alpha}{\tau}\right]\alpha + \left[(K - X_\theta)\right]\theta = \frac{X_\delta}{\tau}\delta \quad (4a)$$

$$\left[-\frac{\mu z_u}{\tau^2}\right]\frac{u}{U} + \left[D^2\left(1 - \frac{z_{\dot{\alpha}}}{\mu}\right) - D\frac{z_\alpha}{\tau} - \frac{\mu z_\alpha}{\tau^2}\right]\alpha$$

$$+ \left[-D^2\frac{z_{\dot{\theta}}}{\mu} - D\frac{z_\theta}{\tau} - \mu\frac{z_\theta}{\tau^2}\right]\theta = \frac{\mu z_\delta}{\tau^2}\delta \quad (4b)$$

$$\left[-\frac{\mu m_u}{\tau^2}\right]\frac{u}{U} + \left[-D^2\frac{m_{\dot{\alpha}}}{\mu} - D\frac{m_\alpha}{\tau} - \frac{\mu m_\alpha}{\tau^2}\right]\alpha$$

$$+\left[D^2\left(1 - \frac{m_{\dot{\theta}}}{\mu}\right) - D\frac{m_\theta}{\tau} - \frac{\mu m_\theta}{\tau^2}\right]\theta = \frac{\mu m_\delta}{\tau^2}\delta \quad (4c)$$

From a mathematical point of view the equations of motion are three simultaneous linear total differential equations with constant coefficients. They may be solved by assuming an harmonic solution and applying initial and terminal conditions. A particularly straightforward method of solution is to take the Laplace Transform of the equations, solve for some desired variable and then perform the inverse Laplace Transform by means of a partial fraction expansion as shown in Ref. (13).

From a purely physical point of view, these equations represent relations between small changes in pitch angle, forward speed and height. If all the motions are damped quickly, then the craft will operate satisfactorily. However, if the motions are not damped well, the craft will porpoise or, under the worst conditions, leave the water or settle until the hull hits the water. The terms on the right hand sides of the equations represent the effect of deflecting controls.

For a hydrofoil craft with all foils fixed, these equations represent a complete description of the longitudinal motions of the craft with the right hand sides all zero. With the values of stability derivatives and $M_{\dot{w}}$ and $Z_{\dot{w}}$ substituted, the response to an assumed disturbance such as encountering a wave can be computed. For a craft with all foils submerged and moveable controls to provide height stability, these equations are simply a means of determining the size, speed of operation and deflections required of the control surfaces.

c. Stability Derivatives

One of the most uncertain phases of aerodynamics or hydrodynamics is the computation of stability derivatives for use in the equations of motion. This uncertainty is due in part to the complexity of configurations and flow patterns and the associated difficulties in making theoretical calculations which have real meaning. The rest of the uncertainty results from the lack of a satisfactory means of determining stability derivatives from flight testing of the finished vehicle. For a hydrofoil craft there is the added difficulty of the proximity of the water surface to the lifting foils.

The exact definition of a stability derivative is the change in a force or moment coefficient caused by some small disturbance motion from equilibrium divided by some dimensionless measure of the motion which caused it in the limit as the motion becomes vanishingly small and with the condition imposed that all other motions be absent. Thus, the derivative to be computed might be the change in lift due to an increase in pitch angle. The pitching motion is assumed to occur with the condition imposed that the height of the center of gravity remains fixed. For a craft with all foils submerged, this

particular derivative is just the lift curve slope. For a craft with skating foils, a pitch angle causes the front foil to rise out of the water and the aft one to sink deeper so that the calculation of the pitching stability derivative is quite complicated. The rate derivatives such as those involving vertical velocity or rate of change of pitch angle are usually computed assuming that the motions cause local changes in apparent angle of attack for each lifting member. Derivatives which result from changes in angle of attack or from acceleration must include the effect of additional apparent mass of the foil surfaces. This effect can be computed theoretically and it is quite important for hydrofoil craft because of the high density of water.

Although certain of the stability derivatives used in this report look like similar ones used in aircraft or missile dynamics, there are basic differences in their definition. As an example, $C_{m_{\dot{\theta}}}$ has the meaning in this report:

$$C_{m_{\dot{\theta}}} = \left.\frac{\partial C_m}{\partial\left(\frac{\dot{\theta} l}{V}\right)}\right|_{\dot{h}=0}$$

This means that in the computation of the derivative, the craft is assumed to have a pitching velocity but no vertical velocity of the center of gravity. In the aircraft and missile system, the derivative which looks the same superficially is defined as follows:

$$C_{m_{\dot{\theta}}} = \left.\frac{\partial C_m}{\partial\left(\frac{\dot{\theta} l}{V}\right)}\right|_{\dot{\alpha}=0}$$

Note that in this case the angle of attack is assumed to be constant so the center of gravity must have a vertical velocity. Note also that for most aircraft and missile applications, the wing mean aerodynamic chord is used as the reference length instead of the longitudinal foil separation which is used in this report.

3. LATERAL MOTIONS

a. Axes, Coordinates and Notations.

Derivation of the lateral equations of motion involves the same sort of reasoning used in the longitudinal case. A Cartesian coordinate system is set up in the craft with origin at the center of gravity. The x axis points forward in the direction of motion, the z axis downward in the plane of symmetry and the y axis to the right, normal to the plane of symmetry. The fundamental disturbances of the craft from the level steady condition are: a sideslip angle, β, positive for nose to the left; a rate of yaw about the z axis, r, positive for clockwise rotation when viewed from above; a roll angle about the x axis, φ, positive for right side down. The time derivatives of these quantities are measured in the same sense.

These definitions and directions are chosen to form a complete right hand Cartesian coordinate system in force, moment, disturbance velocity and disturbance angle sign conventions. The complete definitions of angles and orientations of such a system are extremely complicated and they are explained in some detail in Ref. (14). This same reference points out that the equations presented below are valid only for small angles of disturbance from the level trimmed condition. These equations are the same as those used for aircraft and missile lateral dynamics.

Force in the direction of the y axis is denoted by Y, a moment about the x axis is denoted by $\mathcal{L}$ and it is positive if it tends to depress the right side of the craft, a moment about the z axis is denoted by N and it is positive if it tends to turn the craft to the right. Dividing forces and moments by the dynamic pressure and the proper craft dimensions yields lateral force and moment coefficients:

$$C_y = \frac{Y}{\frac{\rho}{2} U^2 S} \qquad C_l = \frac{\mathcal{L}}{\frac{\rho}{2} U^2 S b}$$

$$C_n = \frac{N}{\frac{\rho}{2} U^2 S b}$$

The discussion in Sec. II, F, 2, a, concerning time derivatives of motion and stability derivatives applies also to the notation used for lateral stability derivatives:

$$\frac{\partial C_y}{\partial \beta} = C_{y_\beta} \qquad \frac{\partial C_y}{\partial \left(\frac{\dot{\varphi} b}{V}\right)} = C_{y_{\dot{\varphi}}}$$

$$\frac{\partial C_n}{\partial \varphi} = C_{n_\varphi}$$

$$\frac{\partial C_l}{\partial \left(\frac{r b}{V}\right)} = C_{l_r}$$

The lateral stability derivatives have the same general nature as the longitudinal stability derivatives in that they are constants which depend on craft configuration and operating conditions. The same care must be taken in their definitions as was shown to be necessary in the longitudinal use. A typical complete definition of a lateral stability derivative is as follows:

$$C_{n_r} = \left.\frac{\partial C_n}{\partial \left(\frac{r b}{V}\right)}\right| \varphi = \dot{\varphi} = \beta = 0$$

The mass and moment of inertia properties of the craft are incorporated into the equations through the stability coefficients. The radius of gyration about the X axis is denoted by K_X and that about the Z axis by K_Z. The following are the lateral stability coefficients:

$$y_v = \tfrac{1}{2} C y_\beta \qquad y_{\dot\varphi} = \tfrac{1}{2} C y_{\dot\varphi}$$

$$y_r = \tfrac{1}{2} C y_r \qquad y_\varphi = \tfrac{1}{2} C y_\varphi$$

$$n_v = \tfrac{1}{2}\left(\tfrac{b}{K_z}\right)^2 C n_\beta \qquad n_{\dot\varphi} = \tfrac{1}{2}\left(\tfrac{b}{K_z}\right)^2 C n_{\dot\varphi}$$

$$n_r = \tfrac{1}{2}\left(\tfrac{b}{K_z}\right)^2 C n_r \qquad n_\varphi = \tfrac{1}{2}\left(\tfrac{b}{K_z}\right)^2 C n_\varphi$$

$$l_v = \tfrac{1}{2}\left(\tfrac{b}{K_x}\right)^2 C l_\beta \qquad l_{\dot\varphi} = \tfrac{1}{2}\left(\tfrac{b}{K_x}\right)^2 C l_{\dot\varphi}$$

$$l_r = \tfrac{1}{2}\left(\tfrac{b}{K_x}\right)^2 C l_r \qquad l_\varphi = \tfrac{1}{2}\left(\tfrac{b}{K_x}\right)^2 C l_\varphi$$

For hydrofoil craft configurations with a rudder or with control surfaces, there are control effectiveness derivatives and coefficients. Again the control deflection angle is δ, expressed in radians and identified by a suitable subscript. The following definitions give the lateral control effectiveness derivatives:

$$C n_\delta = \frac{\partial C n}{\partial \delta} \; ; \; C l_\delta = \frac{\partial C l}{\partial \delta}$$

Corresponding lateral control effectiveness coefficients are:

$$n_\delta = \tfrac{1}{2}\left(\tfrac{b}{K_z}\right)^2 C n_\delta \; ; \; l_\delta = \tfrac{1}{2}\left(\tfrac{b}{K_x}\right)^2 C l_\delta$$

The sign convention for rudder deflection is δ_r positive for the trailing edge of the rudder moved to the right. For differentially operated flaps or surfaces, the deflection is

positive for the trailing edge of the right hand surface moved up.

b. Equations of Motion.

The derivation of the lateral equations of motion follows the same steps as in the longitudinal case if the principal lateral inertia axes coincide with the X and Z axes of the craft. This situation can only be a coincidence and even then valid for only one attitude of the craft because the X and Z axes are determined by the direction of motion and the principal inertia axes are determined by mass distribution. It is beyond the scope of this report to present a complete derivation of the lateral equations of motion including the effects of product of inertia. The lateral equations of motion in the coordinate system chosen for this report are the same as those used for aircraft except that hydrofoil craft have several stability derivatives which are absent in aircraft. The equation of Ref. (14) will be used here with appropriate changes in notation and the addition of the required stability derivatives. In order to simplify the expressions, operator notation is used to designate differentiation with respect to time in the lateral equations of motion:

$$\left[D - \frac{Y_v}{\tau}\right]\beta - \left[D\,\frac{Y_{\dot\varphi}}{2\mu_1} + \frac{K}{\tau}\right]\varphi + \left[\frac{2\mu_1 - Y_r}{\tau}\right]\left(\frac{rb}{V}\right) = \frac{Y_\delta}{\tau}\,\delta$$

$$\left[-\frac{\mu_1 \ell_v}{\tau^2}\right]\beta + \left[D^2 - D\,\frac{\ell_{\dot\varphi}}{\tau} - \frac{\mu_1 \ell_\varphi}{\tau^2}\right]\varphi - \left[D\,\frac{\mu_1 I_{xz}}{\tau I_x} + \frac{\mu_1 \ell_r}{\tau^2}\left(\frac{rb}{V}\right)\right] = \frac{\mu_1 \ell_\delta}{\tau^2}\,\delta$$

$$\left[-\frac{n_v}{\tau}\right]\beta - \left[D^2\,\frac{\tau I_{xz}}{2\mu_1 I_z} + D\,\frac{n_{\dot\varphi}}{2\mu_1} + \frac{n_\varphi}{\tau^2}\right]\varphi + \left[D - \frac{n_r}{\tau}\right]\left(\frac{rb}{V}\right) = \frac{n_\delta}{\tau^2}\,\delta$$

In these equations the grouped parameters are defined as follows:

$$\mu_1 = \frac{m}{\rho S b}$$

$$\tau = \frac{m}{\rho S V}$$

$$K = \frac{m g}{\rho V^2 S}$$

c. Stability Derivatives.

The major difference between the lateral dynamics of hydrofoil craft and aircraft is in the roll stability derivatives. The terms f_φ and n_φ are not found in aircraft. These roll angle derivatives indicate that an angle of roll from equilibrium will tend to be corrected, but they do not necessarily guarantee lateral dynamic stability. No extensive study of the lateral equations of motion has been possible as part of the present investigation in order to determine regions of operation where satisfactory lateral dynamic stability can be expected.

The uncertainty in values of stability derivatives which was pointed out for the longitudinal case is probably even more prevalent in the lateral case. It is possible to compute lateral derivatives by the same effective angle of attack methods which were pointed out in the longitudinal analysis. However, such calculations can be considerably in error. Certain derivatives can be estimated by static model tests but others require various types of dynamic tests. These difficulties probably account for the small amount of serious work that has been done toward investigating the lateral characteristics of hydrofoil craft. Further clarification of the subject will require carefully planned tests both of models and full scale craft.

d. Steady Turns.

The lateral equations of motion provide a convenient means of computing the turning radius of a hydrofoil craft. These equations are not strictly applicable to maneuvers with disturbances from steady level operation as large as those which might be expected in a turn. However, the use of these equations offers the simplest means of predicting turning radius. For design calculations before a craft is built, the expected characteristics will probably not be known with accuracy which

warrants any more detailed calculations.

To obtain the conditions in a steady turn, assume that the rudder is deflected an amount δ_r and that all derivatives of V, φ and r have vanished. This means that the craft has reached a new equilibrium with a sideslip angle, a roll angle and a rate of turn.

$$-\frac{Y_v}{\tau}\beta_t - \frac{Y_\varphi}{\tau}\varphi + \left(\frac{\mu_1 - Y_r}{\tau}\right)\left(\frac{r_t b}{V}\right) = \frac{Y_{\delta_r}}{\tau}\delta_r$$

$$-\frac{\mu_1 \ell_v}{\tau^2}\beta_t - \frac{\mu_1 \ell_\varphi}{\tau^2}\varphi_t + \frac{\mu_1 \ell_r}{\tau^2}\left(\frac{r_t b}{V}\right) = \frac{\mu_1 \ell_{\delta_r}}{\tau^2}\delta_r$$

$$-\frac{n_v}{\tau}\beta_t - \frac{n_\varphi}{\tau}\varphi_t - \frac{n_r}{\tau}\left(\frac{r_t b}{V}\right) = \frac{n_{\delta_r}}{\tau}\delta_r$$

The subscript $(\quad)_t$ denotes a specific constant value of the variables corresponding to the control deflection δ_r. The above equations are three simultaneous algebraic equations in three unknowns and the values of β_t, φ_t, $\left(\frac{r_t b}{V}\right)$ can be found easily by the methods of elimination by variables or by determinants. The turn radius can be found from the rate of turn and the forward speed.

$$R_t = \text{TURNING RADIUS} = \frac{V}{r_t} = \frac{b}{\left(\frac{r_t b}{V}\right)}$$

$$R_t = \frac{b}{\delta_r}\left[\frac{(\mu_1 - Y_r)(\ell_v n_\varphi - n_v \ell_\varphi) + \ell_r(Y_v n_\varphi - K n_v) + n_r(K\ell_v - Y_v \ell_\varphi)}{Y_{\delta_r}(n_\varphi \ell_v - n_v \ell_\varphi) + \ell_{\delta_r}(K n_v - Y_v n_\varphi) + n_{\delta_r}(Y_v \ell_\varphi - K\ell_v)}\right]$$

The roll angle in a steady turn can be computed in the same way:

$$\varphi_t = \frac{\delta_r\left[Y_{\delta_r}(\ell_r n_v - \ell_v n_r) + \ell_{\delta_r}(Y_v n_r - \{\mu_1 - Y_r\} n_v) + n_{\delta_r}(Y_v \ell_r - \{\mu_1 - Y_r\}\ell_v)\right]}{\left[(\mu_1 - Y_r)(\ell_v n_\varphi - n_v \ell_\varphi) + \ell_r(Y_v n_r - K n_v) + n_r(K\ell_v - Y_v n_\varphi)\right]}$$

Note that the moments of inertia of the craft do not affect these answers because each term in both the numerator and denominator contains the squares of the radii of gyration in both roll and yaw.

Solutions for such information as how long it takes to achieve a steady turn and the form of the path covered can be obtained by assuming a step control surface deflection and solving the complete equations of motion for the associated transient response by the methods given in Ref. (13).

G. DYNAMIC STABILITY OF FIXED FOIL CRAFT.

The theory of the dynamic stability of fixed foil hydrofoil vessels is developed in Sec. F of this report. A solution of the equations which have been derived can be obtained for each particular configuration of interest and for each operating condition which appears to be significant. General properties of these equations can be investigated for certain ranges of stability derivatives by approximate factorizations or other special methods. However, there are no simple criteria for indicating satisfactory dynamic stability and no simple design rules which will guarantee it for all configurations.

The largest region of uncertainty concerning the properties of surface foils is their contributions to stability derivatives. The information which has been found experimentally about slanting foils is most useful for trim calculations. It can be used to compute certain stability derivatives such as the height, pitch angle and roll angle static derivatives. There is no experimental information available with which to estimate the damping derivatives or the apparent additional mass terms for surface foils. Theoretical treatment of these problems would be very difficult and any results would require experimental verification.

The most promising prospect for obtaining typical values of stability derivatives is to conduct special tests which yield the values of isolated derivatives. These tests can be conducted by mounting models of the foils free to move in certain restricted directions and recording their motions in response to disturbances. Such tests are best conducted in facilities where the water moves past the model rather than the towing tank type of arrangement.

Lacking such tests, there is some hope of developing a method for decomposing the motions of models into stability derivatives by assuming that the equations which have been derived represent the form which these motions take. Such a method could then be applied to the data which have been taken by several investigators with towed models of various configurations. To date no satisfactory means have been devised to analyze dynamic test data of self-propelled or towed vehicles and obtain stability derivatives.

The data on the motions of models with various degrees of freedom have been taken, mostly on relatively small models. The

information consists of traces of the time histories of motion of the models at various speeds, loadings and center of gravity locations. Refs. (15) show typical data of this nature. Almost all these data are concerned with longitudinal motions.

Due to the present lack of information about fixed foil configurations, it appears that a theoretical dynamic stability analysis has very little meaning. This does not mean that a rational design from a stability point of view is not possible. A configuration can be designed that will trim properly, that will have static longitudinal stability as well as roll, directional and height stability. With these requirements satisfied, dynamic stability is almost certain. Testing of the configuration is then the only certain means of determining if the design is satisfactory.

H. DYNAMIC STABILITY OF MOVABLE FOIL CRAFT

Hydrofoil systems with all foils submerged fail to meet several of the criteria of Sec. II, A, 3. of this report. It is necessary to provide the types of static stability which are lacking by deflecting movable surfaces to correct orientation errors. This type of stabilization is accomplished for many other applications by servomechanisms. A complete system involving the use of a servomechanism is called a servo system.

Without attempting any formal definition, a simple explanation of a servo system can best be given by an example. Most modern dwelling heating systems use an automatic temperature control. The desired temperature is set on a thermostat which also measures the actual temperature. The difference between the desired temperature is then used to control the heat output of the furnace. In much the same way, height stability can be obtained for a hydrofoil craft by selecting the desired height, measuring the actual height and moving height-changing control surfaces an amount proportional to the height error and in the appropriate direction. Thus, the theory and the equipment which have been developed in the field of servo systems can be utilized for the control and stabilization of hydrofoil craft. There are two types of approach to the design of hydrofoil configurations for servo stabilization. These two methods serve very different purposes and great care should be exercised in the choice of a method for any particular application.

1. SERVOMECHANISM APPROACH.

For any detailed analysis the standard methods of servo system design should be used. It is possible by such analysis to incorporate the characteristics of each component of the control system into the overall operating characteristics of the craft. These methods also facilitate proper choice of control system components.

An explanation of the details of a servo system analysis is beyond the scope of this report. Physical as well as mathematical treatments of the subject are available in texts such as Ref. (16). For the analysis of this report, the notation and nomenclature of Ref. (16) will be followed wherever possible. Detailed system analysis will be carried out by the "phase-attenuation" diagram method outlined in Sec. 4.8 of the reference. The purpose of any such analysis is to determine the best control surface size and the amount it should be deflected in response to an orientation error signal.

2. EQUIVALENT STABILITY DERIVATIVE APPROACH

For certain types of servo system applications, it is possible to obtain information about the system characteristics by simpler means than a full servomechanism analysis. The method is not nearly as general nor as reliable as the "phase-attenuation" analysis but it is adequate if the range of stable operation is not very critical. Also this method does not lend itself to incorporating the characteristics of the control system elements into the analysis.

In brief, the equivalent stability derivative method replaces the feedback loop by a term in the equations of motion. The case of servo roll stability is a good example. In this case, it is desired to keep the craft upright under circumstances where it has no inherent righting tendencies. The angle of roll is measured in some manner. The roll control surfaces are arranged to move an amount proportional to the roll angle error. K is the constant of proportionality:

$$\delta = K\varphi$$

The roll control effectiveness is expressed as a rolling moment proportional to the angle of control deflection. In coefficient form this is expressed as:

$$C_l = C_{l_\delta} \cdot \delta$$

The rolling moment coefficient due to a roll angle is then:

$$C_l = KC_{l_\delta}\varphi$$

Thus, the rolling moment coefficient per unit roll angle is a constant with the form of a stability derivative:

$$C_{l_\varphi}(\text{equivalent}) = KC_{l_\delta}$$

Equivalent stability derivatives can be used in the equations of motion in the same manner as actual stability derivatives to find characteristic motions.

This type of analysis is particularly useful as a means of exploring the general effects of various types of feedback on the motions of a system. It should be used with great care because

it does not indicate what is the best value of K or C_{l_δ} to use or how much it is possible to vary them before the system becomes dynamically unstable.

3. LONGITUDINAL SYSTEM.

The main purpose of the longitudinal stabilization system is to provide height stability. Ordinarily a configuration consisting of a main foil and stabilizing foil will be well damped in pitch so that the proper amount of height stability will usually result in a dynamically stable system. However, other types of feedback such as pitch angle or rate of pitch may be desirable to improve response characteristics.

a. Calculation of Stability Derivatives.

The lifting properties of foil systems with all foils submerged completely can be computed by theoretical methods which show good agreement with experiment. Although no experimental checks are available on the computation of stability derivatives, procedures similar to those used for aircraft should be applicable since the same type of lifting surface theory applies to both wings and foils. It should be pointed out that the methods which are used in this portion of the stability analysis usually yield satisfactory values when applied to aircraft. However, it is possible for the computed values to be considerably in error compared to experimental or flight test results. In general, the orders of magnitude of the stability derivatives computed by these methods should be correct and the solutions of the equations of motion based on them should be representative of the type of hydrofoil craft under investigation.

For craft with all foils submerged, the height derivatives are zero for all practical purposes.

$$m_h = Z_h = X_h = 0$$

These values simply imply that the craft can change its height a small amount with respect to the surface while maintaining the same pitch angle and no change in lift, drag or pitching moment will result. Actually the proximity of the surface will make these conditions not exactly true, but the effect of height will be negligibly small.

As an example of the general method for computing stability derivatives, one of the most intricate damping derivatives will be computed in detail. For such a computation, a definite configuration is required. The following sketch is applicable to both stabilizer forward and stabilizer aft configurations. It represents the attitude of a craft operating in steady trimmed equilibrium:

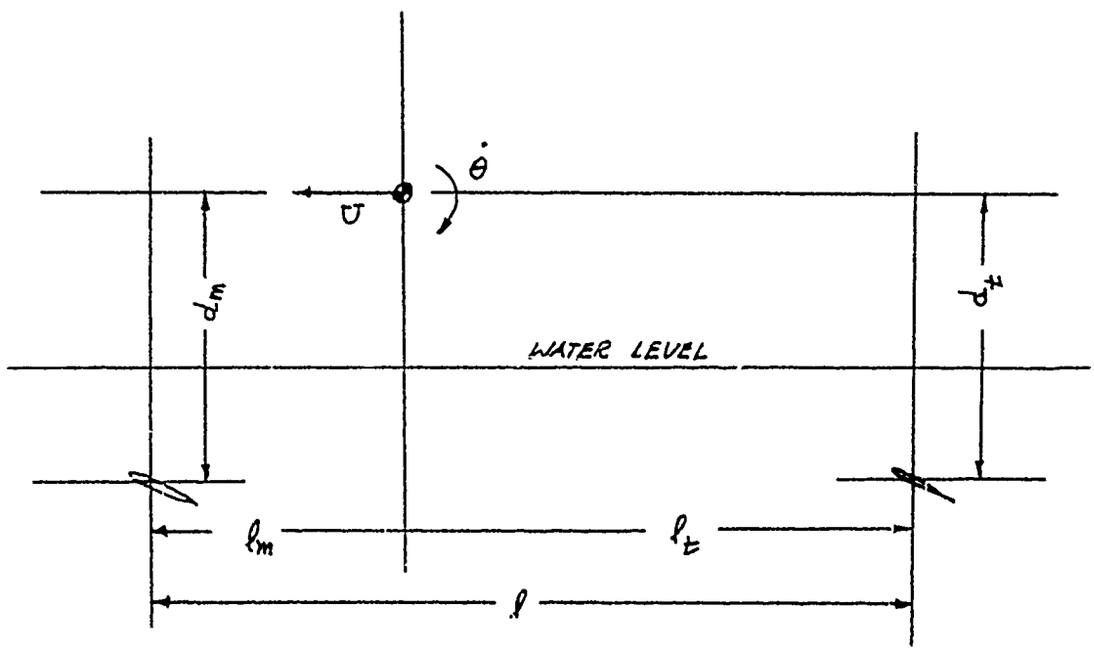

Consider the pitching moment, positive bow up, arising from the pitching velocity, $\dot{\theta}$, shown in the sketch with the condition imposed that the vertical location of the center of gravity remain fixed. The front foil has an upward velocity, $\dot{\theta} l_m$; so it has an apparent decrease in angle of attack of $\dot{\theta} l_m / V$. This gives a change of lift coefficient, $-\dot{\theta} l_m C_{L\alpha m} / V$, and a moment about the center of gravity:

$$M_1 = -\dot{\theta} l_m C_{L\alpha m} \frac{\rho}{2} V^2 S_m \times l_m / V$$

Similarly, the rear foil has an increased apparent angle of attack and a moment:

$$M_2 = -\dot{\theta} l_t C_{L\alpha_t} \frac{\rho}{2} V^2 S_t \times l_t / V$$

There is a lag in the effect of the downwash from the front foil due to the time it takes for the downwash to get from the front foil to the rear foil. The time required is l/V and the apparent angle of attack lag is $l\dot{\theta}/V$. The downwash angle lag is therefore $l\dot{\theta}\frac{d\varepsilon}{d\alpha}/V$. The moment on the rear foil due to the downwash lag is:

$$M_3 = -l\dot{\theta}\frac{d\varepsilon}{d\alpha} C_{L\alpha_t} \frac{\rho}{2} V^2 S_t \times l_t / V$$

The changes in lift on the two foils result in changes in drag and since the foils are below the center of gravity, a pitching moment results. On the forward foil the lift decreases so there is a positive pitching moment from the drag:

$$M_4 = 2\dot{\theta} l_m C_{Lm} C_{L\alpha_m} \frac{\rho}{2} V^2 S_m d_m \frac{dC_{Dm}}{dC_L^2} / V$$

On the rear foil the lift increases so the drag is greater and the pitching moment from the drag is negative:

$$M_5 = -2\dot{\theta} l_t C_{L_t} C_{L\alpha_t} \left(1 + \frac{l}{x_t}\frac{d\varepsilon}{d\alpha}\right) \frac{\rho}{2} V^2 S_t d_t \frac{dC_{D_t}}{dC_L^2} / V$$

It is physically apparent that a foil in a flow of velocity, V, with a vertical velocity, $\dot{h}$, experiences an apparent angle of attack $\dot{h}/V$. The flow pattern resulting from this vertical velocity is the same as that for a foil with an added angle of attack, $\alpha = \dot{h}/V$. In much the same way, a foil which is rotating with a pitch velocity, $\dot{\theta}$, has the same flow pattern as it would if it were not rotating but had a vertical acceleration $\dot{h}'/V$. Any solid body at rest in a fluid and subject to an unbalanced force receives an acceleration which depends on its mass and on an apparent additional mass due to the density of the fluid around it as shown in Ref. (17). This additional apparent mass depends on the shape of the body, the direction of acceleration and on the density of the fluid. There is a complete theoretical solution for a flat, elliptical plate of any aspect ratio, accelerating normal to its face. This planform is close enough to the types of foils which would be used for all underwater hydrofoil configurations, for calculation purposes. Ref. (18) gives tabulated values of this solution. Fig. (3) shows a dimensionless coefficient, k,

which is a measure of the apparent additional volume of a flat elliptical plate. The force due to the apparent additional mass acts at the center of area of the surface. Since the longitudinal reference dimensions are measured from the quarter chord of the mean aerodynamic chord, a term must be added to the moment arm to give the proper moment on the front foil:

$$M_6 = +\frac{K_m}{4}\pi S_m \bar{C}_m \rho\left(l_m - \frac{\bar{C}_m}{4}\right)\dot{\theta} V$$

The analagous term for the rear foil is:

$$M_7 = \frac{K_t}{4}\pi S_t \bar{C}_t \rho\left(l_t + \frac{\bar{C}_t}{4}\right)\dot{\theta} V$$

Dividing the sum of the moments by $\frac{\rho V^2 S_m \bar{c}}{2}$ yields the moment coefficient. This is then divided by $\dot{\theta}\bar{c}/V$ to give the stability derivative:

$$C_{m\dot{\theta}} = \frac{\partial C_m}{\partial\left(\frac{\dot{\theta}\bar{c}}{V}\right)} = -\left(\frac{l_m}{\bar{c}}\right)^2 C_{L\alpha_m} - \left(\frac{l_t^2 S_t}{\bar{c}^2 S_m}\right) C_{L\alpha_t}\left[1 + \frac{\bar{c}}{l_t}\frac{d\varepsilon}{d\alpha}\right]$$
$$+ 2\left(\frac{l_m d_m}{\bar{c}^2}\right) C_{L_m} C_{L\alpha_m} \frac{dC_{D_m}}{dC_{L^2_m}}$$
$$- 2\left(\frac{l_t d_t}{\bar{c}^2}\frac{S_t}{S_m}\right) C_{L_t} C_{L\alpha_t}\left(1 + \frac{\bar{c}}{l_t}\frac{d\varepsilon}{d\alpha}\right)\frac{dC_{D_t}}{dC_{L^2_t}}$$
$$+ \frac{K_m \pi \bar{C}_m}{2\bar{c}}\left(\frac{l_m - \frac{\bar{C}_m}{4}}{\bar{c}}\right) - \frac{K_t \pi \bar{C}_t S_t}{2\bar{c} S_m}\left(\frac{l_t + \frac{\bar{C}_t}{4}}{\bar{c}}\right)$$

The other derivatives are computed by similar types of analyses:

$$C_{z_\theta} = C_{z_{\dot{\alpha}}} = -\left[C_{L\alpha_m} + \frac{S_t}{S_m}\left(1 - \frac{d\varepsilon}{d\alpha}\right) C_{L\alpha_t}\right]$$

$$C_{z_{\dot{\theta}}} = -\frac{l_t S_t}{\bar{c} S_m}\left(1 - \frac{d\varepsilon}{d\alpha}\right) C_{L\alpha_t} + \frac{l_m C_{L\alpha_m}}{\bar{c}} - \frac{K_t \pi}{2\bar{c}}\left(\bar{C}_m + \frac{\bar{C}_t S_t}{S_m}\right)$$

$$C_{z_{\ddot{\theta}}} = -\frac{K_t \pi S_t \bar{C}_t}{2 S_m \bar{c}}\left(\frac{l_t + \frac{\bar{C}_t}{4}}{\bar{c}}\right) + \frac{K_m \pi \bar{C}_m}{2\bar{c}}\left(\frac{l_m - \frac{\bar{C}_m}{4}}{\bar{c}}\right)$$

$$C_{z\dot{h}} = \frac{K_m \pi \bar{C}_m}{2\mu} - \frac{K_t \pi \bar{C}_t S_t}{2\mu S_m}$$

$$C_{m_\theta} = \frac{l_m}{\mu} C_{L\alpha_m} + \frac{d_m}{\mu} C_{L_m} - \frac{l_t S_t}{\mu S_m} C_{L\alpha_t}\left(1 - \frac{d\varepsilon}{d\alpha}\right)$$
$$+ \frac{d_t S_t}{\mu S_m} C_{L_t} - \frac{2 d_m}{\mu} C_{L_m} C_{L\alpha_m} \frac{dC_{D_m}}{dC_{L^2 m}} + \frac{l_m}{\mu} C_{D_m}$$
$$- \frac{d_t S_t}{\mu S_m}\left[2 C_{L_t} C_{L\alpha_t}\left(1 - \frac{d\varepsilon}{d\alpha}\right)\frac{dC_{D_t}}{dC_{L^2_t}} + \frac{d\varepsilon}{d\alpha} C_{L_t}\right.$$
$$\left. + \frac{d\varepsilon}{d\alpha}\left(\frac{C_{L\alpha_t}}{C_{L\alpha_m}}\right) C_{L_m}\left(1 - \frac{d\varepsilon}{d\alpha}\right)\right] - \frac{l_t S_t}{\mu S_m} C_{D_t}$$

$$C_{m_{\ddot{\theta}}} = -\frac{K_m \pi \bar{C}_m}{2\mu}\left(\frac{l_m - \frac{\bar{C}_m}{4}}{\mu}\right)^2 - \frac{K_t \pi \bar{C}_t S_t}{2\mu S_m}\left(\frac{l_t + \frac{\bar{C}_t}{4}}{\mu}\right)^2$$

$$C_{m_{\dot{h}}} = \frac{l_m}{\mu} C_{L\alpha_m} - \frac{l_t S_t}{\mu S_m} C_{L\alpha_t} - \frac{2 d_m C_{L_m} C_{L\alpha_m}}{\mu} \frac{dC_{D_m}}{dC_{L^2 m}}$$
$$- \frac{d_t S_t}{\mu S_m}\left[2 C_{L_t} C_{L\alpha_t}\left(1 - \frac{d\varepsilon}{d\alpha}\right)\frac{dC_{D_t}}{dC_{L^2_t}} + \frac{d\varepsilon}{d\alpha} C_{L_t}\right.$$
$$\left. + \frac{d\varepsilon}{d\alpha}\left(\frac{C_{L\alpha_t}}{C_{L\alpha_m}}\right) C_{L_m}\left(1 - \frac{d\varepsilon}{d\alpha}\right)\right]$$

$$C_{m_{\ddot{h}}} = \frac{K_m \pi \bar{C}_m}{2\mu}\left(\frac{l_m - \frac{\bar{C}_m}{4}}{\mu}\right) - \frac{K_t \pi \bar{C}_t S_t}{2\mu S_m}\left(\frac{l_t + \frac{\bar{C}_t}{4}}{\mu}\right)$$

$$C_{x_u} = -2C_D$$

$$C_{z_u} = -2C_L$$

$$C_{m_u} = -2\left[C_{D_m}\left(\frac{d_m}{\mu}\right) + C_{D_t}\left(\frac{d_t}{\mu}\right)\left(\frac{S_t}{S_m}\right)\right]$$

$$C_{X_h} = C_L - \frac{dC_D}{d\alpha}$$

$$C_{X_\Theta} = C_L - \frac{dC_D}{d\alpha}$$

Where: $$\frac{dC_D}{d\alpha} = 2\frac{dC_{Dm}}{dC_{L_h}^2} C_{L\alpha_m}^2 \alpha_m + \frac{S_t}{S_m}\left[\frac{dC_{Dt}}{dC_{L_t}^2} C_{Lt} C_{L\alpha_t}\left(1-\frac{d\varepsilon}{d\alpha}\right) + \frac{d\varepsilon}{d\alpha} C_{Lt}\right]$$

For stabilizing foil aft, the all movable stabilizing foil control effectiveness derivatives are:

$$C_{Z\delta_t} = -\frac{S_t}{S} C_{L\alpha_t}$$

$$C_{m\delta_t} = -\frac{\ell_t S_t}{\ell S_m} C_{L\alpha_t} - \frac{d_t S_t}{\ell S_m}\left\{2\frac{dC_{Dt}}{dC_{L_t}^2} C_{L\alpha_t}^2 \alpha\left(1-\frac{d\varepsilon}{d\alpha}\right) + \frac{d\varepsilon}{d\alpha}\alpha C_{L\alpha_t}\right\}$$

For stabilizing foil forward, these derivatives are:

$$C_{Z\delta_m} = -C_{L\alpha_m}$$

$$C_{m\delta_m} = \frac{\ell_m}{\ell} C_{L\alpha_m} - \frac{d_m}{\ell} 2\frac{dC_{Dm}}{dC_{L_m}^2} C_{L\alpha_m} C_{Lm}$$

Flap control effectiveness derivatives may be computed by the methods of Ref. (9).

Note that S_m has been used as the reference area for the derivatives. The usual convention in choosing a reference area is to use the largest foil. For a configuration with the stabilizing foil forward, S_f , would be used as a reference area and the equations should then be multiplied by S_m / S_f to change to this convention.

b. Transient Approximation

Complete solutions of the longitudinal equations of motion, for the type of foil configurations under consideration here, show a quick response of pitch angle and height change when a surface is deflected by a slow change in speed. This type of solution suggests that a simplifying approximation, neglecting all speed changes, can be made for the initial response to control movements. An investigation of this approximation for some typical configurations shows very small errors in roots of the characteristic equations which govern the initial transients. Table (1) shows a comparison of the exact and approximate roots.

The transient approximation permits a tremendous simplification of the longitudinal equations of motion for servomechanism purposes. It reduces the characteristic equation of the system of equations from a quartic to a quadratic and effects a similar simplification in the control effectiveness polynomials.

The approximation is made by setting $u = 0$ in Equ. (4a, 4b, 4c) of Sec. (II, F, 2, b). The first equation is then neglected because it yields an uninteresting identity. x_h and m_h are both set equal to zero for reasons given in the last section:

$$\left(D^2\left[1-\frac{z_{\dot{h}}}{2U}\right]-D\frac{z_h}{\tau}\right)\frac{h}{l}+\left(-D^2\frac{z_{\ddot{\theta}}}{2U}-D\frac{z_{\dot{\theta}}}{\tau}-\frac{u z_\theta}{\tau^2}\right)\theta = \frac{u z_{\alpha_1}\delta}{\tau^2}$$

$$\left(-D^2\frac{m_{\ddot{h}}}{2U}-D\frac{m_{\dot{h}}}{\tau}\right)\frac{h}{l}+\left(D^2\left[1-\frac{m_{\ddot{\theta}}}{2U}\right]-D\frac{m_{\dot{\theta}}}{\tau}-\frac{u m_\theta}{\tau^2}\right)\theta = \frac{u m_{\alpha_1}\delta}{\tau^2}$$

For the purposes of a servo system analysis, it is most convenient to take the Laplace Transform of these equations. The differential operator, D, becomes the Laplace variable, s. In Ref. (16) it is given the symbol p. The variables, h , θ , δ, are replaced by their Laplace Transforms, H, Θ, Δ .

$$\left(s^2\left[1-\frac{z_h''}{\mu}\right]-s\frac{z_h'}{\tau}\right)\frac{H}{\delta}+\left(-s^2\frac{z_\theta''}{\mu}-s\frac{z_\theta'}{\tau}-\frac{\mu z_\theta}{\tau^2}\right)\theta=\frac{\mu z_\delta\Delta}{\tau^2}$$

$$\left(-s^2\frac{m_h''}{\mu}-s\frac{m_h'}{\tau}\right)\frac{H}{\delta}+\left(s^2\left[1-\frac{m_\theta''}{\mu}\right]-s\frac{m_\theta'}{\tau}-\frac{\mu m_\theta}{\tau^2}\right)\theta=\frac{\mu m_\delta\Delta}{\tau^2}$$

These are now a pair of simultaneous linear equations in two unknowns. Solving for $\frac{H/\ell}{\Delta}$ and θ/Δ gives the <u>longitudinal transfer functions</u> for this system:

$$\frac{H/\ell}{\Delta}=\frac{1}{\Omega}\left\{\frac{s^2}{\tau^2}\left[m_\delta z_\theta''+\mu z_\delta\left(1-\frac{m_\theta''}{\mu}\right)\right]\right.$$

$$+\frac{s}{\tau^3}\left[-\mu z_\delta m_\theta'+\mu m_\delta z_\theta'\right]$$

$$\left.+\frac{\mu^2}{\tau^4}\left[-z_\delta m_\theta+z_\theta m_\delta\right]\right\}$$

$$\frac{\theta}{\Delta}=\frac{1}{\Omega}\left\{s\left(\frac{s}{\tau^2}\left[\left\{1-\frac{z_h''}{\mu}\right\}\mu m_\delta+z_\delta m_h''\right]\right.\right.$$

$$\left.\left.+\frac{1}{\tau^3}\left[-\mu z_h' m_\delta+\mu m_h' z_\delta\right]\right)\right\}$$

$$\Omega=s\left\{s^3\left[\left(1-\frac{z_h''}{\mu}\right)\left(1-\frac{m_\theta''}{\mu}\right)-\frac{z_\theta'' m_h''}{\mu^2}\right]\right.$$

$$+\frac{s^2}{\tau}\left[-m_\theta'\left(1-\frac{z_h''}{\mu}\right)-z_h'\left(1-\frac{m_\theta''}{\mu}\right)-\frac{z_\theta'' m_h'}{\mu}\right.$$

$$\left.-\frac{z_\theta' m_h''}{\mu}\right]$$

$$+\frac{s}{\tau^2}\left[-\mu m_\theta\left(1-\frac{z_h''}{\mu}\right)+z_h' m_\theta'-m_h'' z_\theta\right.$$

$$\left.-z_\theta' m_h'\right]$$

$$\left.+\frac{1}{\tau^3}\left[\mu m_\theta z_h'-\mu z_\theta m_h'\right]\right\}$$

NOTE: The last term in the expression for Δ is identically zero because $m_{\theta}\dot{z}_h = z_{\theta} m_{\dot{h}}$

The physical and mathematical significance of the transfer function is explained in some detail in Sec. 2.18 of Ref. (16). In brief, $\frac{\Delta H}{\delta}$ represents the response in change of height, h , of a craft due to a control deflection, δ . This response may be to a steady sinusoidal control deflection or to almost any arbitrary periodic or non-periodic variation of δ . The transfer function is of the most fundamental importance in determining the nature of the control deflections necessary to achieve the modes of stability not inherently present in a hydrofoil craft.

c. Feedback Loops

The transfer functions which were derived in a previous section give the response of a craft to longitudinal control deflections. The amount and direction of the control deflections can be determined by a manual operation or by an actuator which deflects the controls in response to some measured motion or attitude of the craft. The type of system where the control deflection is determined by some measured attitude of the craft and this attitude is then altered by the control deflection is called a feedback loop.

The longitudinal mode of stability which is most conspicuously lacking in all-underwater hydrofoil configurations is height stability. In order to impose this mode on the craft artificially it is necessary to measure the height of the craft and deflect the controls when the height is not correct. In principal, some device which measures mean altitude above the water would accomplish this purpose. However, such a device would not also provide response to waves, which is desirable in rough water. A water level measuring device provides both features. Physical means of measuring the water level are discussed elsewhere in this report.

Control of riding qualities and possibly stabilization of an otherwise unstable system could be accomplished by providing feedback loops which measure such quantities as pitch angle, pitch rate, vertical acceleration or vertical velocity. Any or all of these feedback loops can be provided and the individual strengths of the loops adjusted. The same type of analysis is used for all these types of feedback.

One convenient means of representing a feedback loop is the "block

diagram." Such a schematic diagram shows the paths along which the signals flow in a servomechanism. Each element in the system is represented by a box which stands for its transfer function. As an example of a "block diagram," consider a hydrofoil craft system which operates to move control surfaces when the water level on the struts is not at the desired point. Note that all displacements are divided by the craft reference length to conform with the dynamic analysis:

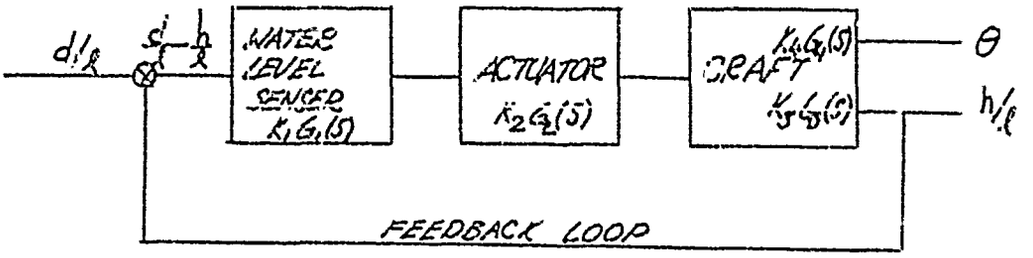

Let d be the height of the wave surface from the mean water level at the craft strut, δ the control surface deflection, and θ and h/ℓ the responses in pitch angle and height to control deflection. The transfer functions of the elements in the loop are indicated in functional notation in their respective boxes. The height stability and wave response characteristics of this system are specified by the complete transfer function.

$$\frac{h/\ell}{d/\ell} = \frac{K_1 K_2 K_3 G_1(S) G_2(S) G_3(S)}{1 + K_1 K_2 K_3 G_1(S) G_2(S) G_3(S)}$$

The stability of this system can be investigated most simply by cutting the feedback loop and tracing a signal through the system. This result is called the open-loop transfer function:

$$\frac{h/\ell}{d/\ell - h/\ell} = K_1 K_2 K_3 G_1(S) G_2(S) G_3(S)$$

The symbols, K_1 , K_2 , K_3 , represent the magnitude of the amplification of steady signals as they pass through each element. They are called gain constants. $G_1(S)$, $G_2(S)$, $G_3(S)$ are the complex phase and attenuation functions of each element.

A useful approximation for preliminary design purposes assumes that the water level senser and the actuator are perfect machines so that their transfer functions are unity times their gain constants. The resulting open loop transfer function is:

$$\left(\frac{h/\ell}{d/\ell - h/\ell}\right)_{APPROX.} = K_1 K_2 K_3 G_3(S)$$

The transfer function $K_3 G_3(S)$ was previously derived from the craft equations of motion and given the symbol $\frac{H/\ell}{\Delta}$. The product of the two gains K_1, and K_2 is the control deflection per unit height error, δ/h. In terms of these parameters, the perfect stabilizer open loop transfer function becomes:

$$\left(\frac{h/\ell}{d/\ell - h/\ell}\right)_{APPROX.} = \left(\delta/\frac{h}{\ell}\right)\left(\frac{H/\ell}{\Delta}\right)$$

After the components of the stabilization system are selected and their time constants determined, it is possible to refine the analysis by including the characteristics of the stabilization system in the open loop transfer function. In general the overall system gain will not change but the time constants of the components will affect the phase and attenuation of the system frequency response.

Feedback loops using other than height error signals can be provided for a hydrofoil craft and the analysis of their characteristics is similar to the one outlined above. The present study indicates that satisfactory longitudinal dynamic stability can be achieved by height feedback alone and it was felt that the direction of useful further investigation could be best determined by study of the actual results of operation of a hydrofoil craft based on this principal.

The general study of feedback loops is treated in detail in Ref. (16), and the very brief discussion above is intended only to show the direction in which the longitudinal stabilization investigation of this report was pursued.

4. LATERAL SYSTEM.

A hydrofoil craft with all foils submerged and the hull supported on struts appears to have unsatisfactory lateral dynamic stability characteristics if no control stabilization system is provided. With controls fixed, the craft has slight roll stability due to gravity and no tendency to follow waves in roll. The directional stability depends on the strut configuration. The dynamic stability appears usually to have the "spiral" instability which is sometimes found in aircraft and is discussed in Ref. (14). Some type of roll angle or lateral wave location stabilization appears to be necessary for this type of craft.

a. Calculation of Stability Derivatives.

The calculation of lateral stability derivatives for aircraft is usually much less accurate than the longitudinal case. For hydrofoil craft the situation is further confused by the proximity of the water surface. The usual method of calculating lateral stability derivatives for aircraft employs the "quasi-steady" method, which was used in deriving the longitudinal formulae. Ordinarily such refinements as additional apparent mass and sidewash terms are neglected for aircraft because they are usually small and because the poor probable accuracy of the other terms obscures their effects. For a hydrofoil craft, the additional apparent mass terms can be very important so they should not be neglected without investigating their magnitude.

Probably the most reliable means of obtaining lateral stability derivatives is by model tests in a towing tank or water tunnel. These can be static tests to find such values as directional stability or oscillatory tests to find damping and apparent mass values. To date no applicable data appear to be available on any such tests.

In theabsence of reliable test data it is necessary to make some rather crude assumptions in order to compute lateral stability derivatives. The contributions of the foils to stability derivatives can be approximated quite accurately by the theoretical methods which are used for aircraft. The contributions of the struts can be approximated by assuming a lift curve slope for their underwater portions. The lower end of the strut is end plated and the upper end intersects a free surface. A reasonable assumption for the characteristics of such a surface is that the lift curve slope is the same as the wetted portion of the strut would have if it were isolated in an infinite fluid. The vertical location of the force on this strut section is probably below the mid-point and most likely near a point $4/3\pi$ times the depth of submersion up from the foil.

Based on the assumptions above, it is possible to write formulae for the lateral stability derivatives in terms of wetted strut areas and foil characteristics. The accuracy of these expressions in representing the stability derivatives is so uncertain that these formulae are not presented here since they might be more misleading than useful. The lateral control effectiveness derivatives can be computed in much the same manner as the longitudinal values. In Sec. (III, c, 1) the lateral stability derivatives for a specific configuration are estimated by this method since it represents the only available means for obtaining such estimates.

b. Feedback Loops.

The type of servomechanism analysis applicable to the lateral case is similar to the longitudinal analysis outlined in Sec. (II, H, 3, c). The feedback loop of most interest in the lateral case involves two asymmetrically located water level sensing devices which cause asymmetrical control surface deflections in response to differences in their measured water levels. This type of system gives roll stability and also response to waves coming from the side. The "block diagram" for such a system is presented below:

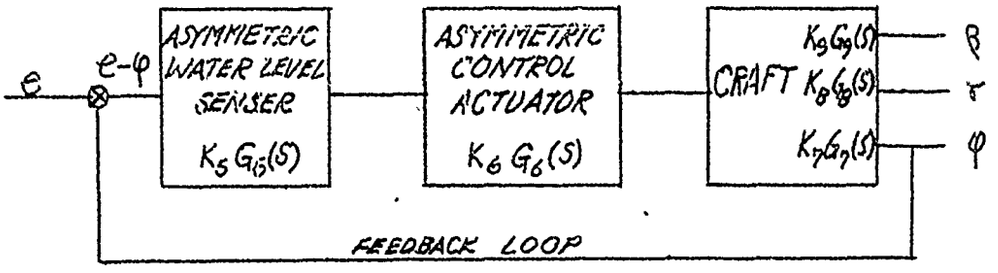

In the block diagram, φ is the apparent measured roll angle from the water level difference on the struts; σ is the control deflection; and β, γ, φ are the motions of the craft resulting from control deflection.

Other feedback loops which measure such quantities as rate of roll or sideslip angle can be incorporated into the craft in much the same way. It has been the aim of the analysis of this report to try to achieve satisfactory dynamic lateral stability and lateral wave response by water level sensing alone and further development of lateral stabilization can best be directed by the results of operating tests.

I. SUMMARY AND CONCLUSIONS

The philosophy of stabilization followed in this report is to develop a hydrofoil system which best meets a design performance specification and then stabilize the configuration in a manner which imposes the least performance penalty. For a design to achieve high speed as the major aim, the most serious problems appear to be cavitation and wave response. Both of these phenomena can best be studied by experimental means. The main effort of this report is to study the problem of stabilization of a craft designed for best lift-to-drag ratio. Configurations best suited to this purpose can be investigated theoretically for performance, strength and stability.

The hydrofoil configuration which offers the most promise for high lift-to-drag ratio is a single straight high aspect ratio foil, operating completely below the surface, supporting the main weight of the craft on struts. This foil can be stabilized by small foils which seek the water surface or by completely submerged stabilizing foils and movable controls which are operated to correct errors in the orientation of the craft with respect to the water surface.

Surface seeking foils must be arranged so that they give both height and roll stability. In order to stabilize an all underwater foil, they must be located forward of the main foil and their underwater side area kept low enough so as not to cause unsatisfactory directional stability. In general, it is not possible to predict the characteristics of surface foils theoretically. Experimental investigation of this type of stability arrangement appears to be the most satisfactory way to achieve a final design. There is some indication that surface seeking foils impose a greater performance penalty on the overall configuration than the completely submerged stabilizing foils which would provide the same permissible center of gravity travel.

The characteristics of fully submerged foils can be computed with fair accuracy. Control effectiveness and hinge moments can be estimated from wind tunnel data. With this information it is possible to calculate theoretically the static and dynamic behavior of craft stabilized by movable foils or flaps.

The control system for this type of hydrofoil craft requires a device which determines the location of the water surface. An investigation of the principals upon which such devices can be based indicates that using the difference in hydrodynamic pressure in air and water or the difference in electrical conductivity will probably result in the simplest and most reliable control system.

The power and frequency response requirements for actuators to move primary flap controls can be met most conveniently by the use of hydraulic cylinders. Other possibilities for flap actuation are pneumatic systems or special amplidynes. Electrical actuators with irreversible drives are satisfactory for slow speed trim purposes. A craft which is "flown" by a pilot by means of movable controls should be possible if some means is available for the pilot to determine the height of the craft above the water. Such an arrangement might be useful for a test vehicle but it would probably not be satisfactory for continued service.

The configuration with a completely submerged main foil and small submerged stabilizing foils forward of the main foil has two inherent difficulties. In order to achieve longitudinal static stability, the center of gravity must be moved forward to the point where the stabilizing foils are loaded so that they tend to stall. Thus there is an inadequate allowable center of gravity travel. Furthermore, the struts supporting the stabilizing foils tend to cause directional instability which, in certain cases, might have to be balanced by vertical area aft.

The configuration with small submerged stabilizing foils aft appears to offer satisfactory overall stability characteristics. A craft which uses movable stabilizing foils as primary controls to maintain height above the water surface is apparently unstable with a control system which measures only the location of the surface. The use of flap controls on the main foil offers an apparently satisfactory solution to obtaining height stability by water level sensing alone.

The same configuration appears also to be satisfactory laterally when the main foil flaps are operated differentially to give roll stability which is otherwise insufficient.

It should be emphasized that detailed results of the dynamic stability analyses are necessarily subject to some error because of the uncertain values of stability derivatives. However, it is felt that the general range of the solutions is correct for this type of craft and that satisfactory configurations can be developed along the lines recommended in this report.

Experimental investigation of the type of hydrofoil craft recommended in this report was conducted on two types of manned test vehicles. A configuration with all fixed foils, using planing foils for stability, was operated extensively. Data on its operation are presented in a division of this report devoted to the subject and some remarks on its stability properties are included in Sec. II, B, 5 of this division. A second configuration, not contemplated as a part of the original contract, using an automatic stabilization system operating flaps on the main foil and an all-movable tail foil was operated successfully shortly before the end of the contract period. This test vehicle is described in Sec. III, D of this report. While the somewhat limited experimental operation of these hydrofoil craft is not a conclusive demonstration of the validity of the principles presented in this report, it is a strong indication that it is possible to build hydrofoil craft of the type recommended with performance and riding qualities markedly superior to comparable surface craft.

III. DESIGN OF THE TEN-TON TEST VEHICLE

One of the primary purposes of the test vehicle which is described in the following portion of this report is to obtain operating experience and data on the use of movable controls as a means of stabilizing a hydrofoil craft. The portions of the configuration which are concerned with stability and the entire control system are designed specifically as components which best fit the requirements of a test vehicle. The design of a military or transportation craft might be quite different since each has special requirements which reflect its intended use. The information which can be obtained from the proposed test craft will be of the greatest assistance in determining the direction in which to proceed with the design of craft to perform specific useful functions.

A. CONFIGURATION AND OPERATING CONDITIONS.

The underwater configuration for which this stability analysis applies may differ in details from the drawings of the craft. At the time when this analysis was performed, the design was still being refined and changes made as detail design features were worked out. The configuration presented here is representative of the overall design and while dimensions may differ slightly from the proposal drawing, the changes in the basic stability properties of the craft will be small. In the preliminary design stages there is no justification for trying to follow relatively minor design changes with the cumbersome stability analysis.

Fig. (4) shows a sketch of the foil configuration, with the center of gravity travel indicated. The attitude corresponds to cruise conditions with design center of gravity location.

Table (2) shows the tabulated properties and dimensions of the foils.

The longitudinal stability properties of the craft are studied for five conditions. All conditions correspond to full load. Three speeds are considered: take-off at 15 knots and $C_L = .748$; cruise at 20 knots and $C_L = .420$; high speed at 30 knots and $C_L = .180$. For take-off and high speed the fore and aft center of gravity locations are considered. For cruise the design center of gravity is chosen.

Lateral stability is studied for the cruise condition with design center of gravity location only.

B. LONGITUDINAL ANALYSIS.

1. TRIM CURVES

Fig. (5, 6 and 7) show curves of θ and $C_{m_{TRIM}}$ as functions of C_L and δ_t for three center of gravity locations. These curves were computed from the equations of Sec. (II, E, a, 2). The geometry is determined from the values of i_t , i_m , d_t , and d/m shown in Fig. (4) for $\theta = 4.82^0$ and modified for other angles of pitch by the appropriate formulae in Sec. (II, E, a, 2). For these curves it is assumed that the thrust and drag act along the same line so there is no resulting couple. Lift coefficients and stabilizing foil settings for the three design conditions are indicated. Flaps are assumed to remain neutral

2. STATIC STABILITY CURVES

Figs. 8,9 and10) show curves of C_m and $C_{m_{STABILITY}}$ as functions of C_L and δ_t for three center of gravity locations. These curves are computed for the case where the thrust passes through the center of gravity so that the magnitudes of pitching moments are not correct. However, the slopes of the curves, which are of the greatest interest, are correct and the proper values of dC_m/dC_L can be measured at the intersection of the desired C_L value and the δ_t corresponding to trim for that C_L . The curves were drawn this way to illustrate the differences in slope between the trim and stability curves for this configuration.

3. STABILITY DERIVATIVES AND STABILITY COEFFICIENTS

Table (3) shows values of stability derivatives and control effectiveness derivatives for this configuration. They were computed from the formulae in Sec. (II, H, 3, a) using the foil properties shown in Fig. (4). Flap effectiveness is estimated from Ref. (8).

Table (4) gives values of stability coefficients computed from the derivatives in Table (3) by means of the formulae in Sec. (II, F, 2, a). The values of μ and τ for each condition are indicated. For all conditions a value of $\rho/k_y = 4.00$.

The number of significant figures shown in Tables (3 and 4) are not intended to be representative of the probable accuracy of the tabulated values.

4. SOLUTION TO EQUATIONS OF MOTION

In order to justify the use of the longitudinal transient approximation which was developed in Sec. (II, H, 3, b), it is advisable to

compute the roots of the longitudinal characteristic equations for both the exact and the approximate equations and compare them. Table (1) shows this comparison for the five conditions under investigation. The approximations to the real roots is well withir the probable error due to uncertainties in stability derivatives. The exact roots were obtained by substituting values of stability coefficients and α and γ from Table (4) into Equation (4a, 4b, 4c) of Sec. (II, F, 2, b), expanding the resulting system of equations into a quartic and then factoring the quartic to find the roots. Approximate solutions were obtained by substituting values from Table (4) into the expression for Ω in Sec. (II,H,3,b) and factoring the resulting quadratic. These roots have the dimensions of 1/sec.

5. PERFECT SERVOMECHANISM CURVES.

In the absence of detailed information about the time constants of the servo system components required to operate the fast response controls, the only phase and attenuation plots which can be presented are those corresponding to perfect servo components. These plots do not indicate whether a complete system will work, but only whether it is possible under ideal conditions for it to work. The main effort of this phase of the investigation is to determine which controls offer the best prospects for a stable system which operates by determining the location of the water surface only.

It was first thought that moving the stabilizing foils alone might provide a height correction system which was stable. In order to investigate this situation, the stability coefficients and the stabilizing foil effectiveness coefficients from Table (3) were substituted into the expression for the open loop transfer function corresponding to this feedback loop as developed in Sec. (II, H, 3,). This transfer function was then factored and plotted on an attenuation-phase diagram as shown in Ref. (16). Fig. (11) shows this plot for the cruise condition and design center of gravity location. Notice that no phase margin is possible for any value of system gain so there is no possibility of obtaining a stable system by this means alone.

The next step was to investigate the use of flaps on the main foil as a means of obtaining the desired height stability and a stable system. The values of stability coefficients and the flap effectiveness coefficients of Table (4) were substituted into the expression for the open loop transfer function and the resulting equation plotted on an attenuation-phase diagram. Figs. (12 to 16) show these plots for the five conditions under investigation. Note that all five conditions demonstrate phase margins of 56° or better. Ref. (16) recommends

a phase margin of at least 30° and preferably 45°. Thus it is apparent that this system can almost certainly be made stable provided that the servo components are carefully selected to have sufficiently small time constants.

Fig. (17) shows the longitudinal frequency response of the craft at cruise condition and design center of gravity location. The feedback gain corresponds to a flap deflection per unit height error of $\delta_f / \frac{h}{z} = 10$ which gives physically reasonable flap dimensions and deflections.

C. LATERAL ANALYSIS

1. STABILITY DERIVATIVES.

Four separate components of the underwater configuration of the proposed test craft contribute to lateral stability derivatives. They are the main foil, the stabilizing foils, the wetted portions of the main struts and the wetted portions of the stabilizing foil struts. In addition, there are three lateral control systems: the main foil flaps, the stabilizing foils and the rudders. Fig. (4) shows the portions of the geometry of the configuration required to compute approximate lateral stability derivatives. The lift curve slopes of the wetted portions of the struts are assumed to be $C_{L_\alpha} = 3.5$ for the main struts and $C_{L_\alpha} = 3.3$ for the stabilizing foil struts.

The component contributions to the lateral stability derivatives and the total values are shown in Table (5). The contribution of the foils are computed assuming elliptic loading and "strip theory." Based on such assumptions, the important main foil stability derivatives are as follows:

$$C_{l_{\dot{\varphi}_{MAIN\ FOIL}}} = -\frac{1}{16} C_{L_{\alpha_m}}$$

$$C_{l_{r_{MAIN\ FOIL}}} = C_{n_{\dot{\varphi}_{MAIN\ FOIL}}} = -\frac{1}{16} C_{L_m}$$

Strut contributions are computed by the assumption of quasi-steady conditions. As an example, the formula for C_{l_r} of the stabilizing foil strut will be derived. The side velocity of the stabilizing foil struts due to a rate of yaw, r, is $r\ell_t$. The apparent

side slip angle is $-\frac{r\ell_t}{v}$. The side force due to this angle is $3.3\,\frac{r\ell_t}{v}\,q\,S_{S_t}$. The rolling moment due to this force is $-3.3\,\frac{r\ell_t}{v}\,q\,S_{S_t}\,d_S$. The rolling moment coefficient is $-3.3\left(\frac{r\ell_t}{v}\right)\left(\frac{S_{S_t}}{S}\right)\left(\frac{d_S}{b}\right)$. Dividing by $\frac{rb}{v}$ gives:

$$(C_{l_r})_{STABILIZING\ FOIL\ STRUTS} = -3.3\,\frac{S_{S_t}}{S}\,\ell_t\,d_S$$

$$= -\frac{3.3 \times 8.24 \times 20 \times 5.73}{46.73 \times 31.4 \times 31.4} = -.0676$$

Control effectiveness derivatives were computed by means of Ref. (9).

The mass distribution of the finished test vehicle can only be estimated roughly in the preliminary design stage. For the lateral analysis it was assumed that in the cruise attitude the principal axis of inertia in roll points in the direction of motion so that $I_{XZ} = 0$. The radii of gyration k_Z and k_X then became principal radii of gyration and their values were estimated to be such that $b/k_X = 4.5$ and $b/k_{z_t} = 3.5$.

Table (6) shows values of stability coefficients based on the stability derivatives of Table (5) and the assumed mass distribution. They were computed by the formulae of Sec. (II, F, 3, a). Values of M and γ shown are for design gross weight and cruise speed.

Without the stabilization system, the derivatives l_φ and n_φ are both zero. With the stabilization system operating there are equivalent stability derivative values for l_φ and n_φ which correspond to the flap deflection per unit roll angle. The longitudinal analysis indicated that a value of $\delta_f = 10\,h/\ell$ was satisfactory for longitudinal stability. In physical units this means that $\delta_f = \frac{h}{2}$ or the flaps deflect one radian for a two foot error in water level at a strut. If this two foot error in water level occurs because of a roll angle, it corresponds to a roll angle of .255 radians because the strut is 7.85 feet from the centerline of the craft. Thus $\delta_f = 3.92\varphi$ and:

$$C_{l_\varphi} = \frac{\delta_f}{\varphi}\,C_{l_{\delta_f}} = 3.92(-.187) = -.733$$

$$C_{n_\varphi} = 3.92(.00780) = .0306$$

The effective stability coefficients are:

$$l_\varphi = -7.42$$

$$n_\varphi = .187$$

2. PERFECT SERVOMECHANISM ANALYSIS

The lateral dynamic characteristics of the test craft can be determined by substituting the lateral stability coefficients in Table (6) into the lateral equations of motion of Sec. (II, F, 3, b). Note that without the flaps operating, l_φ and n_φ are zero. It is of interest first to study the characteristic equation of this system.

$$S^4 + 29.3S^3 + 202.8S^2 + 351.7S - 81.06 = 0$$

Factoring this equation yields:

$$(S + 20.09)(S + 6.30)(S + 3.119)(S - .206) = 0$$

Notice that there is no lateral oscillation of the type usually found in aircraft but that the familiar "spiral" root is present and it is divergent in this case. Thus, the hydrofoil craft without the flaps to provide roll stability would not hold its course or remain level, but it would go into a slow spiral with increasing heel angle until the hulls finally hit the water. The size of this root indicates that this tendency could probably be overcome rather easily by the rudders operating from command signals alone.

For the purposes of studying the characteristic equation, the equivalent stability derivatives due to the flaps can be used in the lateral equations of motion. Using the values of l_φ and n_φ computed in the previous section, the characteristic equation becomes:

$$S^4 + 29.3S^3 + 239.09S^2 + 700.13S + 702.4 = 0$$

In the factored form it is:

$$(S + 18.12)(S + 6.46)(S + 2.360 + .655i)(S + 2.360 - .655i) = 0$$

These factors show that the craft is stable and is strongly damped with the flaps operating.

The roll response to waves approaching the craft from the side can be investigated by the servomechanism analysis. The divergent "spiral" root indicates that the open loop transfer function has a pole in the right half plane, which means that it is "non-minimum phase" in the nomenclature of Ref. (16). In addition, the craft has a slight sensitivity to roll angle because of the vertical established by the gravity vector. This means that the servo system will not be a "zero displacement error" system in the nomenclature of Ref. (16). By properly recognizing these two facts, it is possible to construct the attenuation-phase diagram for the open loop transfer function as well as the closed loop frequency response curve. Fig. (18) shows the attenuation-phase diagram for this case with the gain indicated. There is a satisfactory phase margin.

Fig. (19) shows the roll angle wave response which is the closed loop characteristics of the craft. Note that at zero frequency the response curve does not approach zero decibels. This is because of the slight roll angle sensitivity of the unstabilized craft.

The lateral analysis indicates that the craft should be well damped in all lateral modes. The frequency response in roll angle to wave disturbances appears to be in the proper range for satisfactory operation of this type of hydrofoil craft in a beam sea.

3. STEADY TURN

The turning properties of the proposed test vehicle can be computed for both flap and rudder turns by means of the equations derived in Sec. (II, F, 3, d).

The turning radius and heel angle due to a rudder deflection can be found by substituting the stability coefficients and rudder effectiveness coefficients in Table (6) and the values of ℓ_φ and n_φ computed in Sec. (III, C, 1) into the expressions for R_ζ and φ_ζ . Note that the formulae use σ_r in radians and hat φ_ζ comes out in radians.

Turning properties of the craft with flap deflection are computed in a somewhat different manner. Because the flaps are used for stabilization purposes, it is not possible simply to substitute a value of σ_f into the expressions for R_ζ and φ_ζ and use ℓ_φ and n_φ also. The way in which a flap turn can be made is to shift the water surface reference points asymmetrically on the two main foil struts. This can be done by electrical means in the stabili-

zation system. In this way it is possible to select a heel angle to which the flaps are to stabilize the craft. The turning radius corresponding to a selected heel angle can be found by computing the value of φ_t / σ_f from the formula in Sec. (II, F, 3, d) and the stability coefficients and flap effectiveness coefficients from Table (6). An apparent value of σ_f corresponding to the selected value of φ_t can be found by $\sigma_f = \varphi_t / \varphi_t$ This value of σ_f is then used to find R_t . The actual flap deflection can be found by substracting $3.92\,\varphi_t$ from the apparent value of σ_f . This is done in order to compensate for the flap deflection which was assumed in using the equivalent stability derivatives f_ψ and n_φ . As an example, consider the flap deflection required to obtain a 5° heel angle for the operating conditions under consideration. From the formula for φ_t a value of $\varphi_t/\sigma_f = -.2035$ is obtained. The apparent flap angle corresponding to $\varphi_t = .0873$ is $\sigma_f = .429$. The actual flap angle is $.429 - 3.92(.0873) = .0870$ radians or 4.97°. The radius of turn for this condition is computed from $\sigma_f = .429$ and comes out 663 feet.

The following values summarize the steady turning properties of the proposed test vehicle at cruise speed and design center of gravity location.

Turning Radius
- Rudders only - 279 ft.
- Flaps only - 663 ft.
- Rudders and Flaps - 193 ft.

Heel Angle (Roll into turn)
- Rudders only - 0.53°
- Flaps only - 5.00°
- Rudders and Flaps - 5.53°

In addition to the steady turning properties of the craft, it is possible to predict the response to a sudden control deflection by computing the transient response of the lateral equation of motion.

Methods for computing transient responses are given in Ref. (13).

D. DESCRIPTION OF CONTROL SYSTEM

The stability analysis thus far has been concerned principally with the behavior of the craft, provided that it has a perfect stabilization system. Such an analysis is of great assistance in the selection of system components to give a satisfactory craft. Figs. (12 to 19) show that the stabilization system must have a flat frequency response

up to at least two cycles per second for small amplitudes of flap movement. Once the components are selected and their time constants determined, it is possible to refine the attenuation-phase analysis and get more realistic frequency response curves for the craft.

Fig. (20) shows a schematic diagram of the automatic control system proposed for the 10-ton test vehicle. Fig. (21) shows an electrical circuit diagram of the servo system. The purpose of this system is to position the craft so that the water surface remains at a desired level on both front struts. An added requirement is that in steady, undisturbed operation on calm water, the flaps must have only small deflections from the neutral position.

As shown in Fig. (20), the electrical water contacts at (1) are the means of measuring the level of the water surface on the strut. These contacts are small brass buttons arranged so that the water completes an electrical circuit when it touches them. The bottom button provides a ground connection and there is an open circuit voltage between the bottom button and the others of 28 v D.C. When a circuit is completed through the water, current flows and a relay is closed in the bridge box (2) . There is a relay for each button. These relays are arranged, as shown in Fig. (21), with resistances in series with their contact points. The resistance of the parallel circuit is so arranged that as each relay is closed, a similar increment of resistance is added to the circuit. This change in resistance is used to unbalance a Wheatstone bridge when the water level is not at the desired button. The bridge unbalance causes a current to flow in the measuring leg of the bridge and this current energizes one of a pair of solenoids depending on the direction of current flow. Each solenoid is made to respond only to current in a chosen direction by germanium crystal diodes in series with the coils. The two solenoids are arranged to operate a hydraulic valve at (3) in a direction determined by the polarity of the bridge unbalance. The valve motion operates a hydraulic cylinder which positions the flap at (5) . Attached to the hydraulic cylinder is a follow-up potentiometer (4) , which forms one resistance leg of the bridge and nulls the bridge unbalance when the hydraulic cylinder has moved the required distance. The hydraulic system uses a 1500 psi variable displacement pump driven by an electric motor.

The trim system is operated by relays which move the trim actuator (6) whenever the water level is not at the proper position. There is no follow-up potentiometer on the trim actuator, which is an electric motor and worm gear arrangement. The actuator moves the stabilizing foil (7) by means of cables.

There are two independent control systems which use a common hydraulic pump and electrical power source, but are otherwise not connected. Each system is mounted in and above its own front strut and operates the flap at the base of the strut and the stabilizing foil diagonally opposite. This cross rigging gives the proper roll trim direction.

The hydraulic flap actuators are selected to provide required hinge moment, actuating power and frequency response. The hinge moment requirements are determined from the flap characteristics which were estimated from curves and formulae of Ref. (9). The flaps extend over 25% of the chord and 30% of the main foil span. The trailing edge angle is 21°. Maximum hinge moment at full deflection and high speed for this configuration, in the notation of Ref. (9), is:

$$C_{h_\alpha} = -.0012 \qquad C_{h_\delta} = -.0090$$

$$q = 2560 \text{ LB/FT}^2 \qquad \alpha = 2.2^\circ$$

$$C_h = \{(-.0012)(2.2) + (-.0090)\,20^\circ = -.184$$

Maximum Hinge Moment = $(-.184)(2560)(.407)^2(4.72) = -368$ lb.ft. per set of flaps on one side of craft

Flap actuation power is computed assuming a maximum flap speed of two cycles per second, and a maximum hinge moment of 368 lb. ft. per set of flaps. This gives a maximum required hydraulic system power of 2.96 horsepower for the craft. At a system pressure of 1500 psi the maximum required flow is 3.39 gallons per minute.

Frequency response far beyond the required two cycles per second can be obtained by a valve-on-cylinder hydraulic servo which is used in aircraft control systems. The cable system between the hydraulic servo and the flaps must be carefully designed and preloaded in order to give satisfactory frequency response characteristics.

The solenoid and hydraulic valve combination has been used successfully for guided missile applications. It has the characteristic that the flow rate to the cylinder is proportional to the coil current. The follow-up potentiometer has also been used successfully for this type of application.

The electrical trim actuator is a standard aircraft linear actuator. The most satisfactory trim speed and trim deadband can be determined only by actual operation. Provision must be made in the test vehicle to vary these properties in order to determine the desired settings. Provision must also be made for a trim cut-out which prevents the trim actuators from moving when the craft is in a turn. Since there is no follow-up on the trim system, the roll angle of the craft in a turn will cause the trim actuators to operate continuously so that the craft will be out of roll trim when it resumes a straight course unless trim cut-out is provided.

The electrical contact button array must be designed to prevent false signals from blown spray, rain or water run-off. Tests on a mock-up of a single button and relay show that the electrical portion of the system works very well but that the water run-off problem requires further a ntion.

The control system described above was designed specifically for use in a test vehicle. It was considered desirable to design a system which used as many proven and readily available components as possible and which could be adjusted and modified simply and inexpensively. The electrical sensing system permits adjustment of gain and ranges, simple electrical measurement of operating properties, and a wide variety of functional modifications.

A 14-foot manned test vehicle using flaps and a control system somewhat similar to the one described above was operated successfully. Height sensing was accomplished by means of pressure orifices along the leading edge of the struts. The flaps on the main foil were operated by small electrical servo-motors. The single tail foil was actuated by an electric motor for trim purposes only. The craft took off easily and operated foil-borne at the proper height, stabilized by the flap action alone on many flights of 500 yards or better with a crew of two. The flights usually terminated because a mechanical looseness in the flap actuation mechanism permitted the craft to develop a vertical hunting motion which often became severe enough to require landing. On several occasions the hunting oscillation damped of its own accord and the craft continued smoothly. It was the opinion of the crew that the hunting motion was caused entirely by the looseness of the actuation mechanism and that tightening the system would result in a completely smooth-operating craft. This testing was conducted at the end of the contract period as an extra effort and time did not permit the relatively minor mechanical changes which were required to correct mechanical deficiencies in the control system.

E. ALTERNATIVE CONTROL SYSTEMS

The control system described in Sec. III, D is intended to be flexible enough to that major functional modifications can be made with relatively minor equipment and circuit changes.

One of the most important changes that may be necessary is to arrange the entire control system so that it operates as separate longitudinal and lateral systems. This might be required because of coupling between motions or in order to vary the gains of the systems independently. This modification may be accomplished by using different solenoid coils and altering the circuits.

The electrical button contacts can be replaced by pressure switches along the leading edges ofthe struts. The change required is to remove the bank of relays and wire the button leads directly to the pressure switches.

Gyroscope or accelerometer feedback loops can be included in the system by modifications in the solenoid coils and some changes in wiring.

The entire electrical system can be converted to 400 cycle alternating current if some need, such as the use of precision gyroscopes, requires this modification.

Provision for "flying" the craft by command signals alone can be made. It is also possible to provide command signal control and still retain the stabilization features of the control system.

These provisions for major modifications are incorporated into the design in an effort to anticipate difficulties which might arise in the course of operating the craft and to provide as many means as possible of correcting the difficulties without making major physical changes in the stabilization system.

REFERENCES

1. German Hydrofoil Research and Development, Sachsenberg Bros., F2-S-435-47.

2. Bigelow, Henry B., and Edmondson, W.T.; Wind Waves at Sea Breakers and Surf; Hydrographic Office, U. S. Navy, HO 602, 1947.

3. Tietjens, Phil O.; Das Tragflachenboot (Boat with Supporting Foils); Werft, Reederei, Hafen; April 1, 1937.

4. Benson, James M. and Land, Norman S.; An Investigation of Hydrofoils in the NACA Tank I - Effect of Dihedral and Depth of Submersion; NACA ACR, Sept. 1942.

5. Weaver, Vance W.; Are Hydrofoils Practical?; Motorboating, Aug. 1949.

6. Guidoni, A.; Seaplanes - Fifteen Years of Naval Aviation; RAS Journal, Vol. XXXII, No. 205, Jan. 1926.

7. Keldysach, N.V. and Laurentiev, M.A.; On the Motion of an Aerofoil under the Surface of a Heavy Fluid, i.e., a Liquid; Science Translation Service, Nov. 1949.

8. Benson, James M. and Douglas A. King; Preliminary Tests to Determine the Dynamic Stability Characteristics of Various Hydrofoil Systems for Seaplanes and Surface Boats; NACA RB-62, Nov. 1943.

9. Toll, Thomas A.; Summary of Lateral Control Research; NACA TN 1245, 1947.

10. Bates, William R.; Collection and Analysis of Wind-Tunnel Data on the Characteristics of Isolated Tail Surfaces with and without End Plates; NACA TN 1291, 1947.

11. Hook, Christopher; The Hydrofoil Boat for Ocean Travel; Transactions of Liverpool Engineering Society, Vol. LXIII, Nov. 1947.

12. Schuster; Six Component Measurements of Hydrofoils Interrupted at the Keel; Sachsenberg Bros., Rep. F2 2082.

13. Churchill, Ruel V.; Modern Operational Mathematics in Engineering; McGraw-Hill, New York. 1944.

14. Durand, W.F.; Aerodynamic Theory; Vol. V., Div. N., Chap. 5, Calif. Inst. of Tech., 1943.

15. Measurements of the Dynamic Longitudinal Stability of a Free-to-Trim and Heave Hydrofoil System in Smooth Water; John H. Carl and Sons, Rep. No. 2, 1949.

16. James, Hubert M.; Nichols, Nathaniel B.; and Phillips, Ralph S.; Theory of Servomechanisms; McGraw-Hill, New York 1947.

17. Lamb, Sir Horace; Hydrodynamics; Dover, New York, 1945.

18. Durand, W. F.; Aerodynamic Theory; Vol. 1, Div. C, Chap. VIII Calif. Inst. of Tech., 1943.

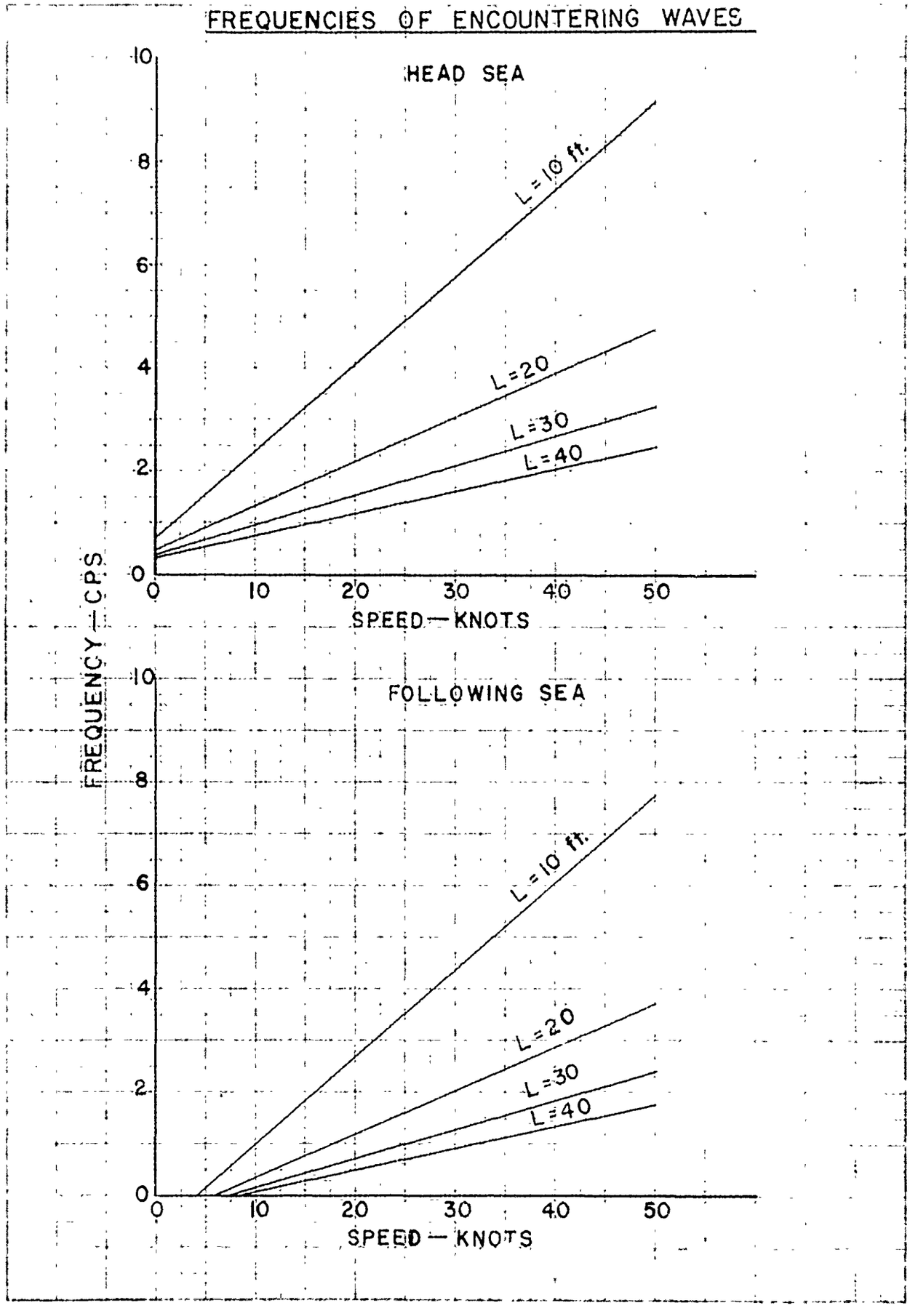
FREQUENCIES OF ENCOUNTERING WAVES
HEAD SEA
FREQUENCY — CPS
SPEED — KNOTS
L = 10 ft.
L = 20
L = 30
L = 40
FOLLOWING SEA
FREQUENCY — CPS
SPEED — KNOTS
L = 10 ft.
L = 20
L = 30
L = 40

ORBITAL VELOCITIES AND WAVE HEIGHTS
VELOCITY OF WAVE PROPAGATION — FT/SEC
VELOCITY OF WAVE HEIGHT
WAVE VELOCITY AT SURFACE
ORBITAL VELOCITY AT 1 FT. DEPTH
VELOCITY AT 2
3
4
5
WAVE LENGTH — FT.
WAVE HEIGHT — FT
VELOCITY OF ORBITAL MOTION FT/SEC.

INERTIA COEFFICIENT FOR ELLIPTIC FLAT PLATE WITH INITIAL ACCELERATION NORMAL TO PLATE FACE

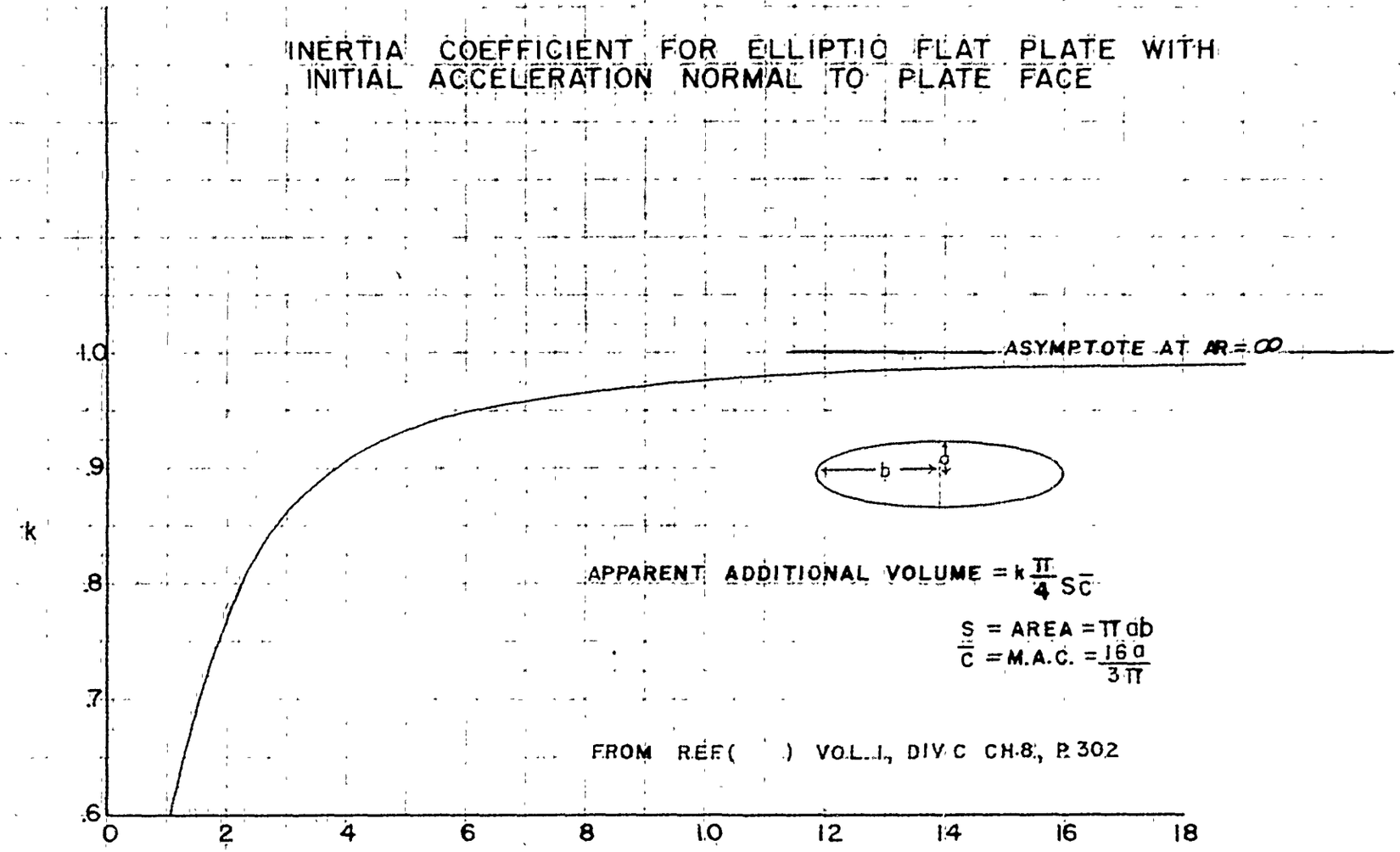

APPARENT ADDITIONAL VOLUME $= k\frac{\pi}{4} S\bar{c}$

S = AREA $= \pi ab$

$\bar{c}$ = M.A.C. $= \frac{16a}{3\pi}$

FROM REF( ) VOL. I., DIV C CH-8., P. 302

Figure 2-10

FOIL CONFIGURATION AND CENTER OF GRAVITY LOCATIONS
10 TON TEST CRAFT

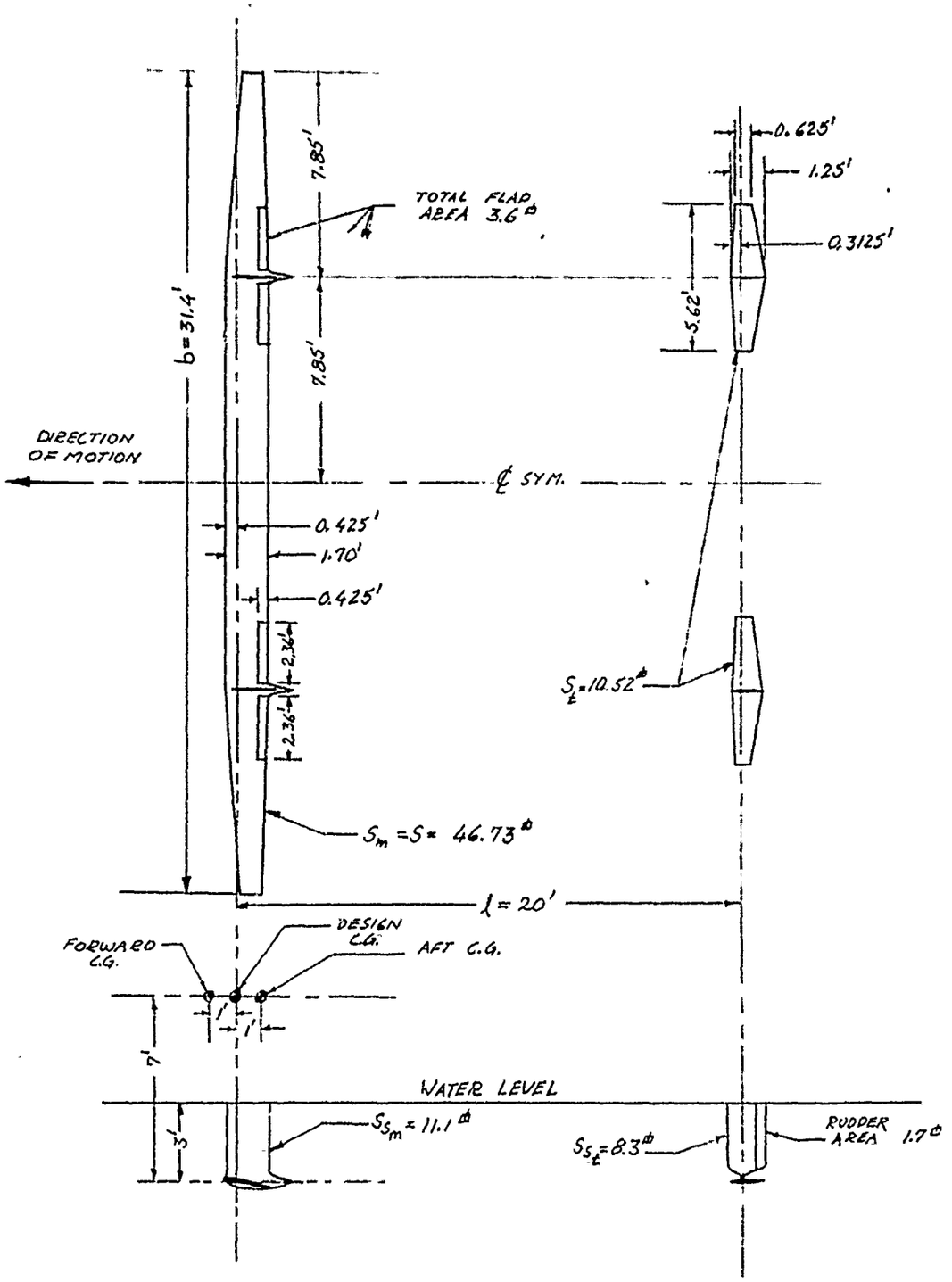

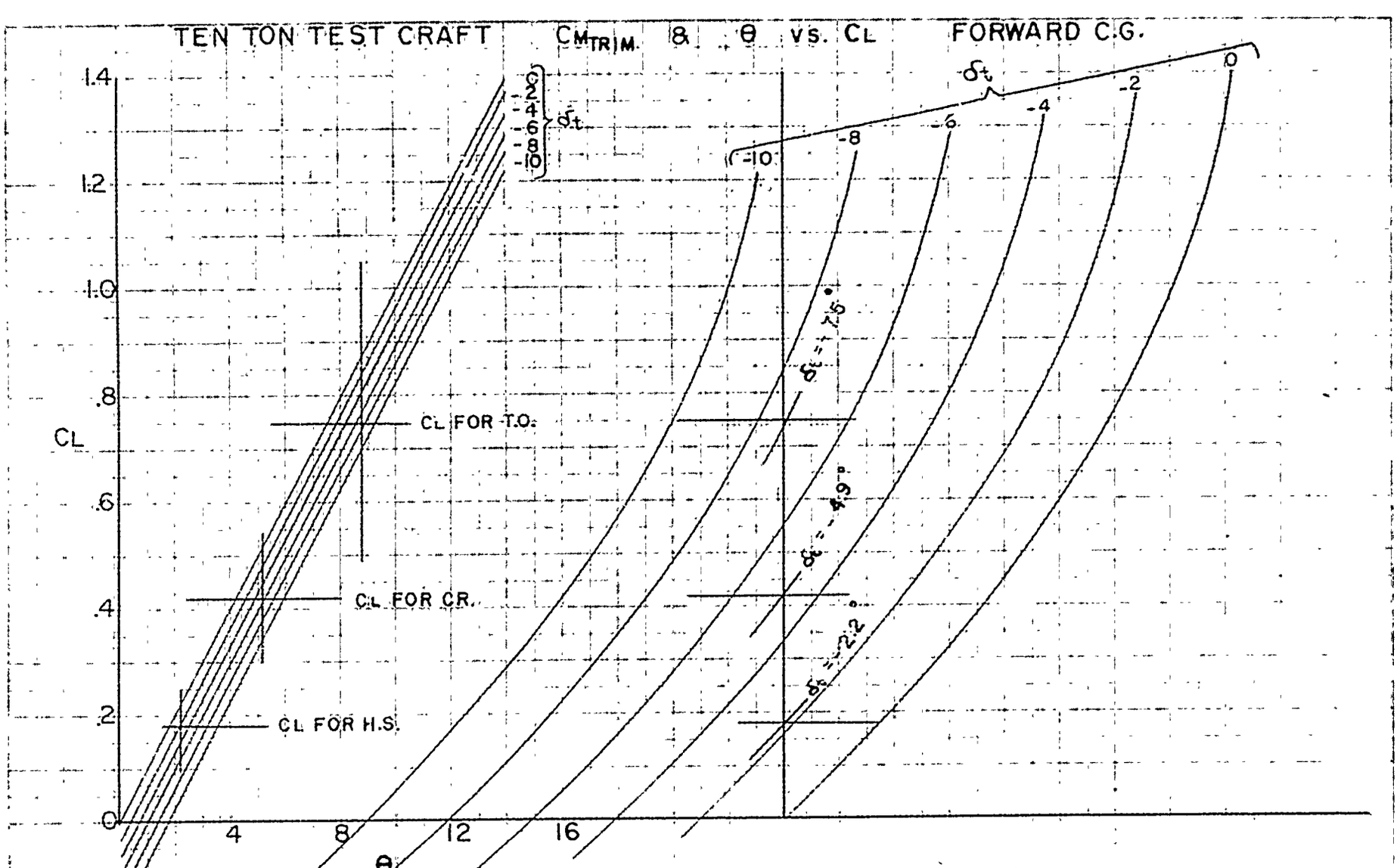
TEN TON TEST CRAFT CMTRIM. & θ vs. CL FORWARD C.G.
CL
1.4
1.2
1.0
.8
.6
.4
.2
0
CL FOR T.O.
CL FOR CR.
CL FOR H.S.
0
-2
-4
-6
-8
-10
δt
δt = -7.5°
δt = -4.9°
δt = -2.2°
4
8
12
16
θ
.20
.16
.12
.08
.04
0
-.04
-.08
-.12
-.16
-.20
CMTRIM

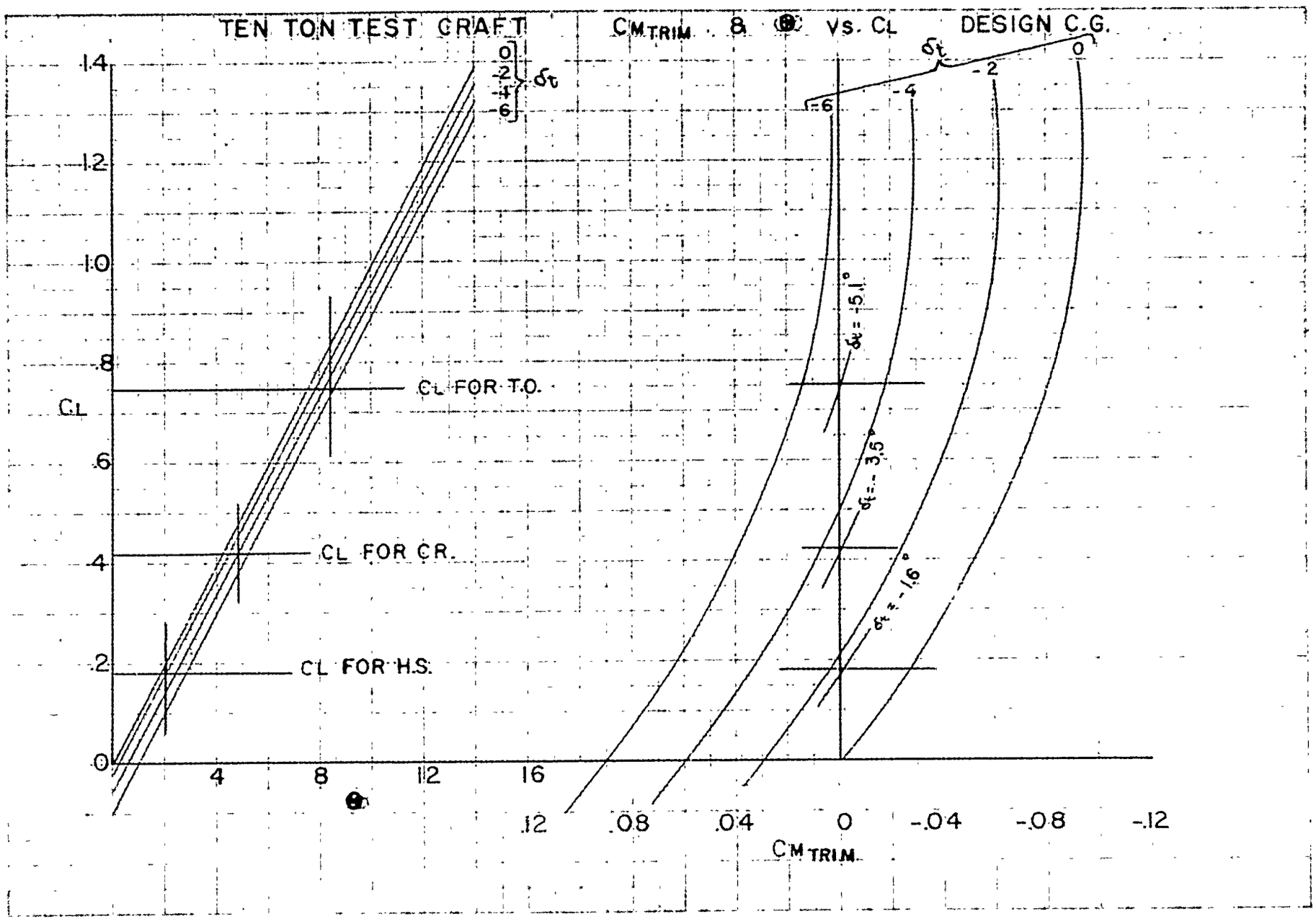
TEN TON TEST CRAFT
CM TRIM . δt Vs. CL DESIGN C.G.
δt
0
-2
-4
-6
CL
CL FOR T.O.
CL FOR CR.
CL FOR H.S.
δt = -5.1°
δt = -3.5°
δt = -1.6°
1.4
1.2
1.0
.8
.6
.4
.2
0
4
8
12
16
α
.12
.08
.04
0
-.04
-.08
-.12
CM TRIM

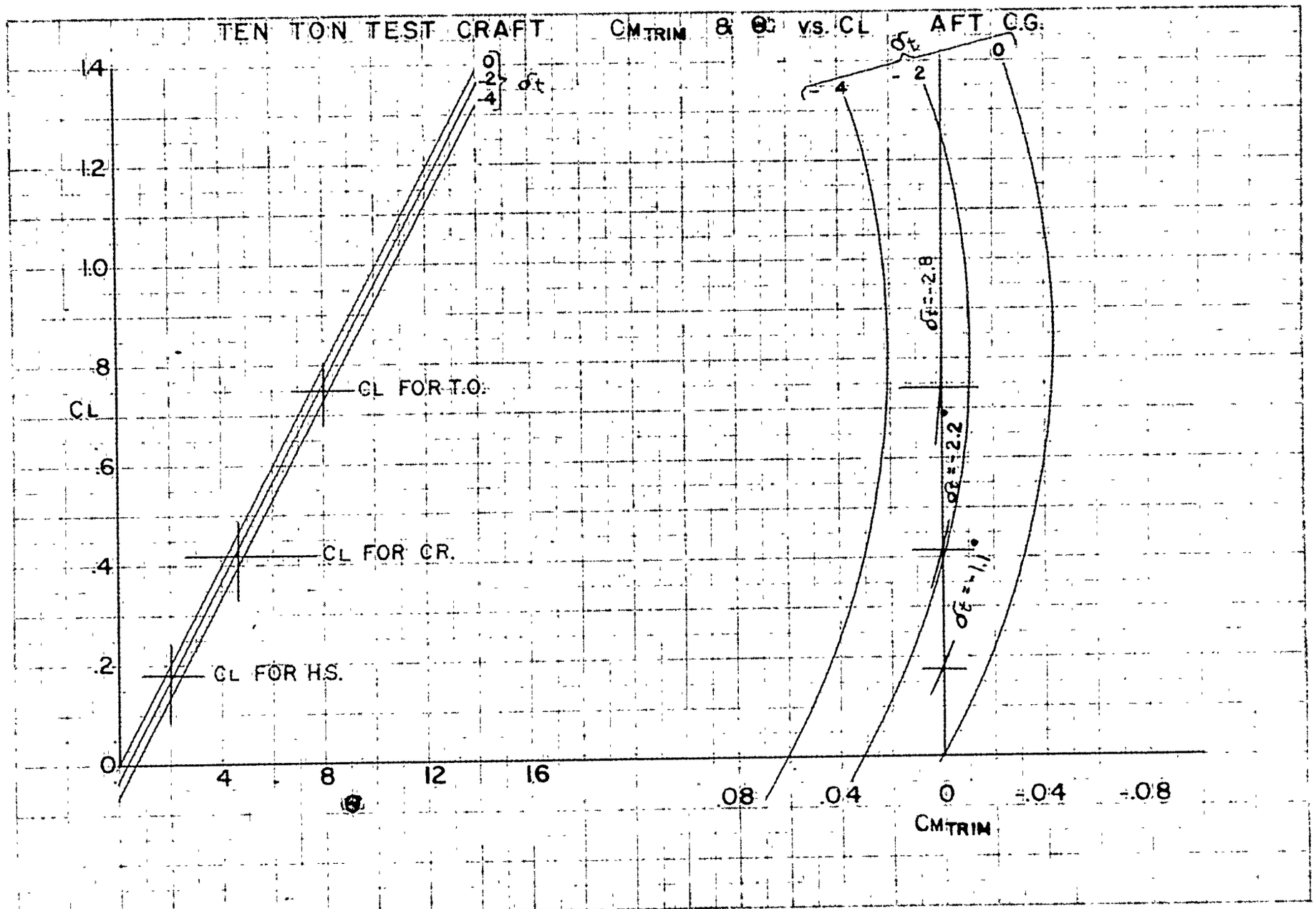
TEN TON TEST CRAFT CM TRIM & α vs. CL AFT C.G.
0
-2
-4
δt
1.4
1.2
1.0
.8
CL
.6
.4
.2
0
CL FOR T.O.
CL FOR CR.
CL FOR H.S.
4
8
12
16
α
δt
0
-2
-4
δt=-2.8
δt=-2.2
δt=-1.1
.08
.04
0
-.04
-.08
CM TRIM

Page 95.
Fig. 7

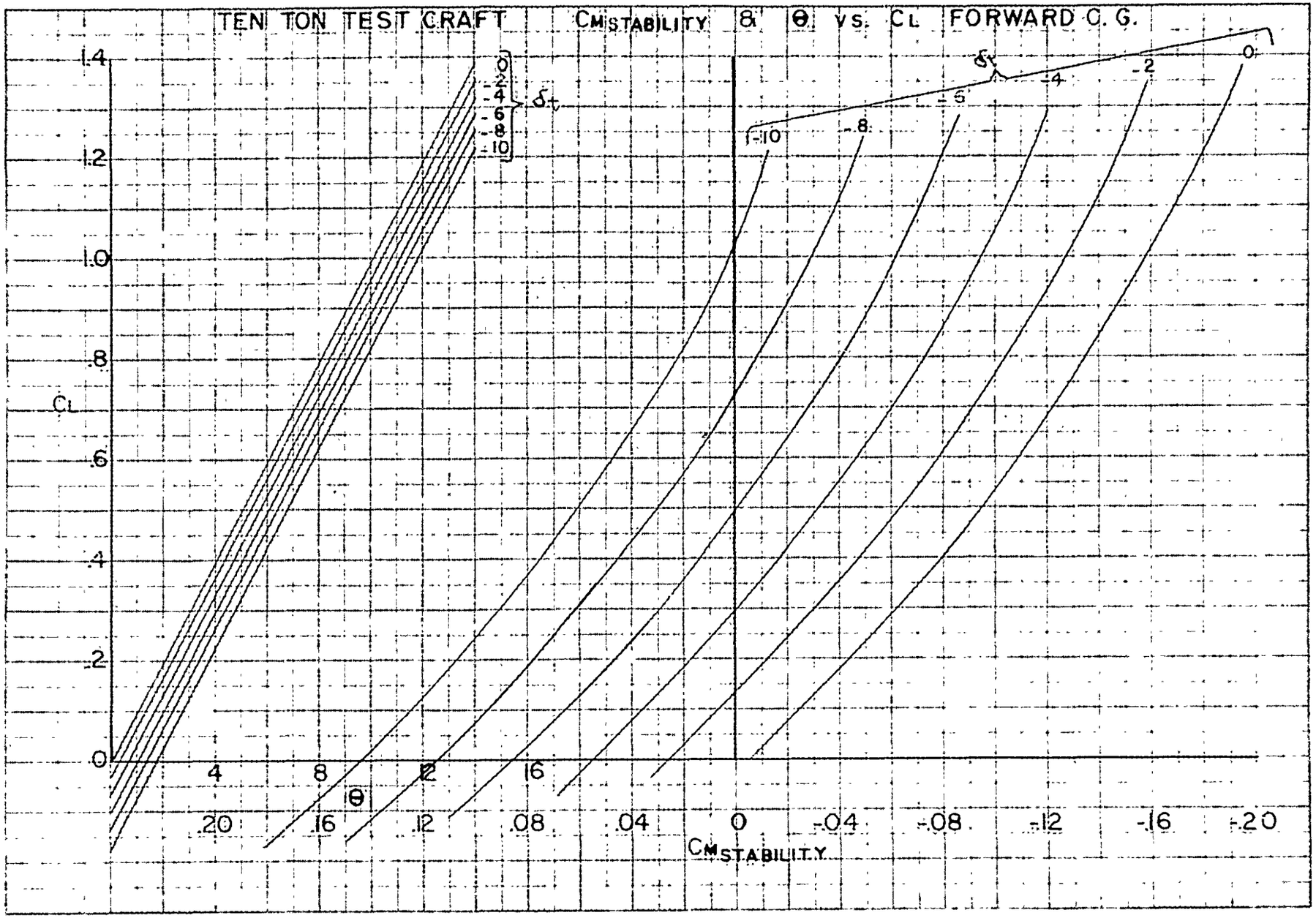
TEN TON TEST CRAFT
CM STABILITY
δt θ VS. CL FORWARD C.G.
CL
θ
CM STABILITY
δt
0
-2
-4
-6
-8
-10
1.4
1.2
1.0
.8
.6
.4
.2
0
4
8
12
16
.20
.16
.12
.08
.04
0
-.04
-.08
-.12
-.16
-.20

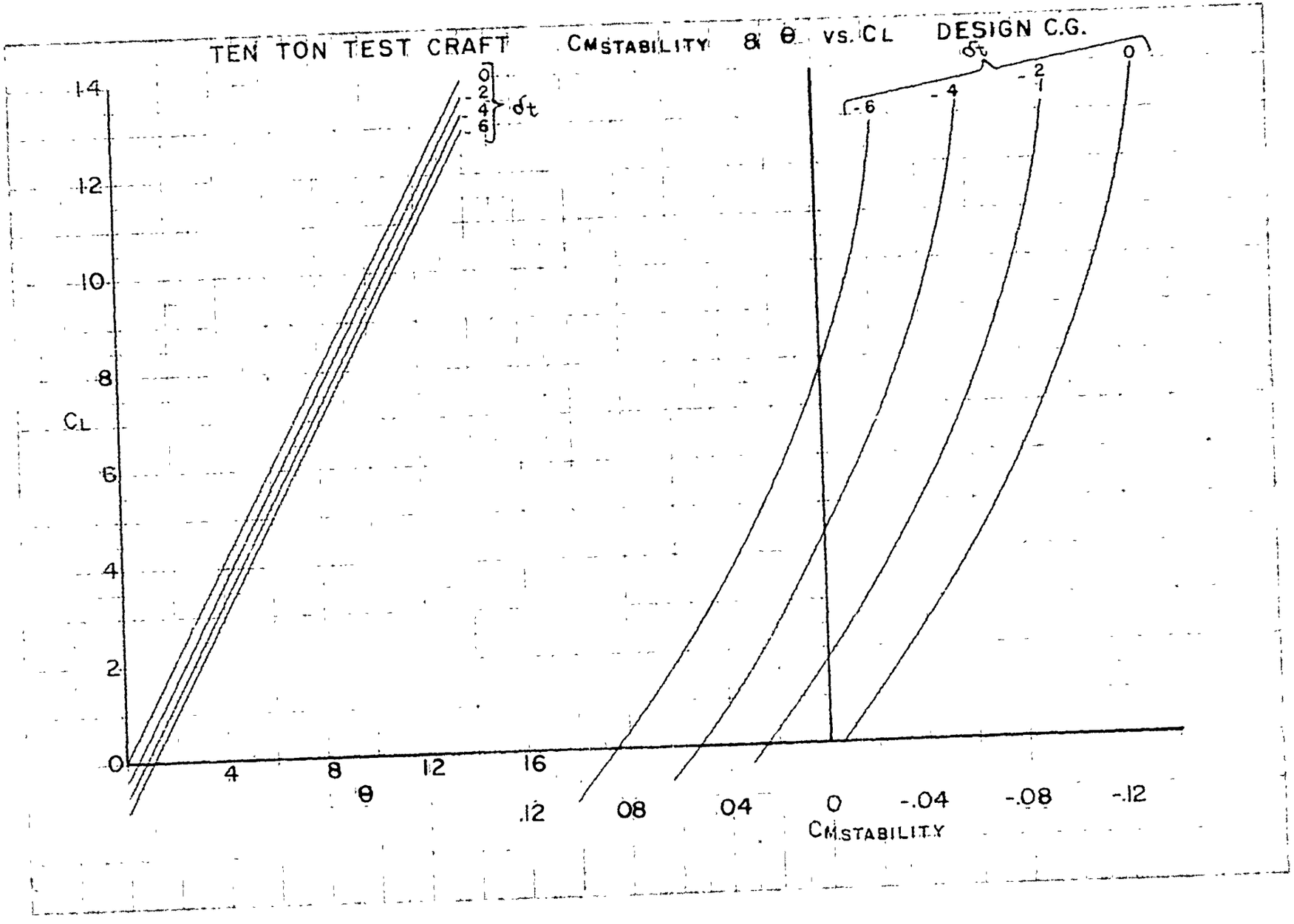
TEN TON TEST CRAFT CMSTABILITY & θ VS. CL DESIGN C.G.
δt
0
-2
-4
-6
CL
14
12
10
8
6
4
2
0
4
8
12
16
θ
.12
08
04
0
-.04
-.08
-.12
CMSTABILITY

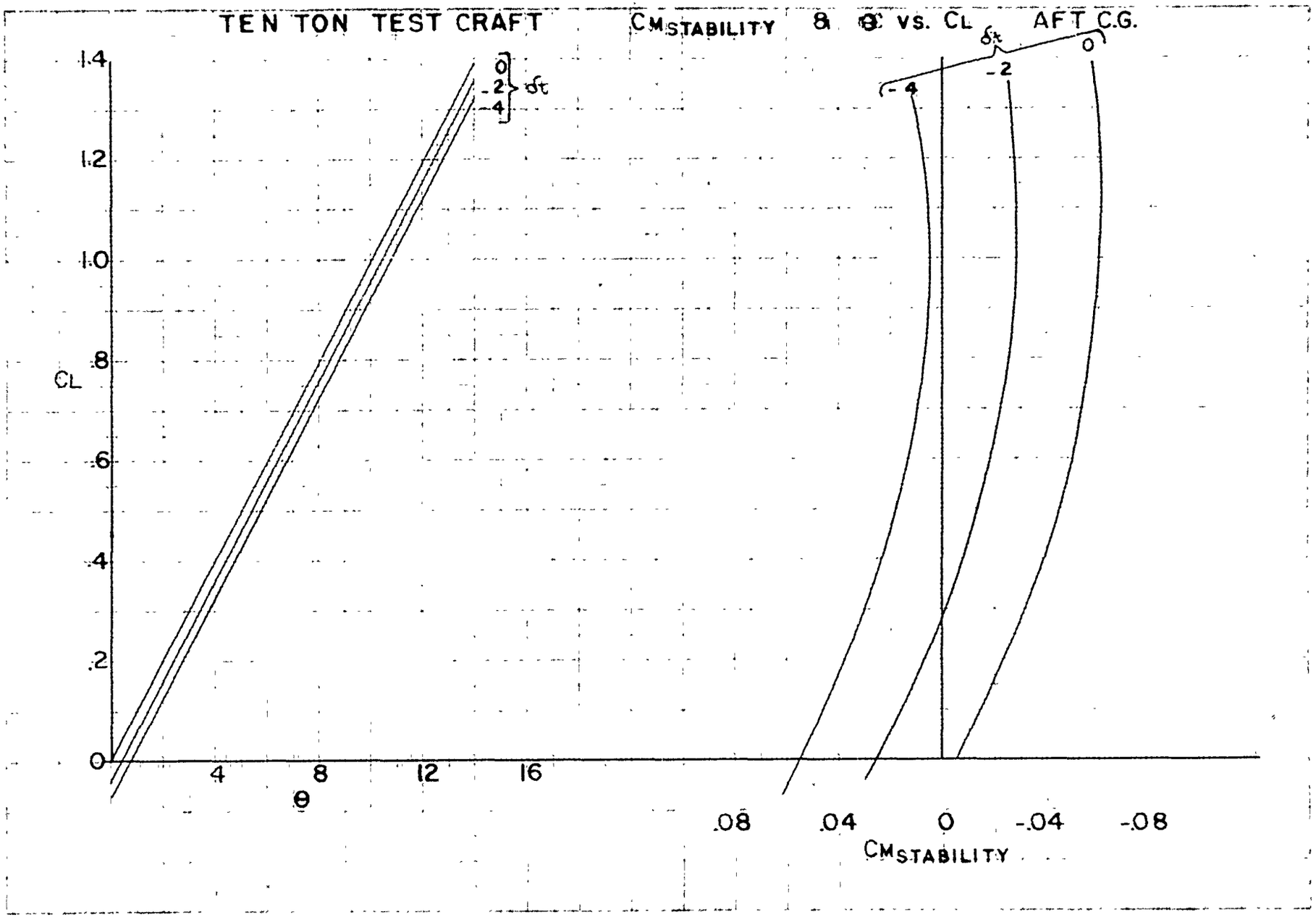
TEN TON TEST CRAFT
CM STABILITY & Θ VS. CL AFT C.G.
CL
Θ
δt
0
-2
-4
1.4
1.2
1.0
.8
.6
.4
.2
0
4
8
12
16
.08
.04
0
-.04
-.08
CM STABILITY

KEUFFEL & ESSER CO., N. Y. NO. 359-71
Semi-Logarithmic 3 cycles x 10 to the ½ inch
MADE IN U. S. A.

ATTENUATION AND PHASE VS. FREQUENCY — CRUISE — STABILIZING FOILS AS CONTROL SURFACES

ASYMPTOTIC ATTENUATION

NOTE: this is a non-minimum phase transfer function

PHASE ANGLE

ATTENUATION db

20
10
0
-10
-20
-30

PHASE ANGLE — DEG.

90
0
-90
-180

1
10
10.0
100.0

FREQUENCY — RAD./SEC.

Page 96.
Fig. 11

KEUFFEL & ESSER CO. N. Y. No. 359-71
Semi-Logarithmic, 3 Cycles X 10 to the by Inch
MADE IN U.S.A.

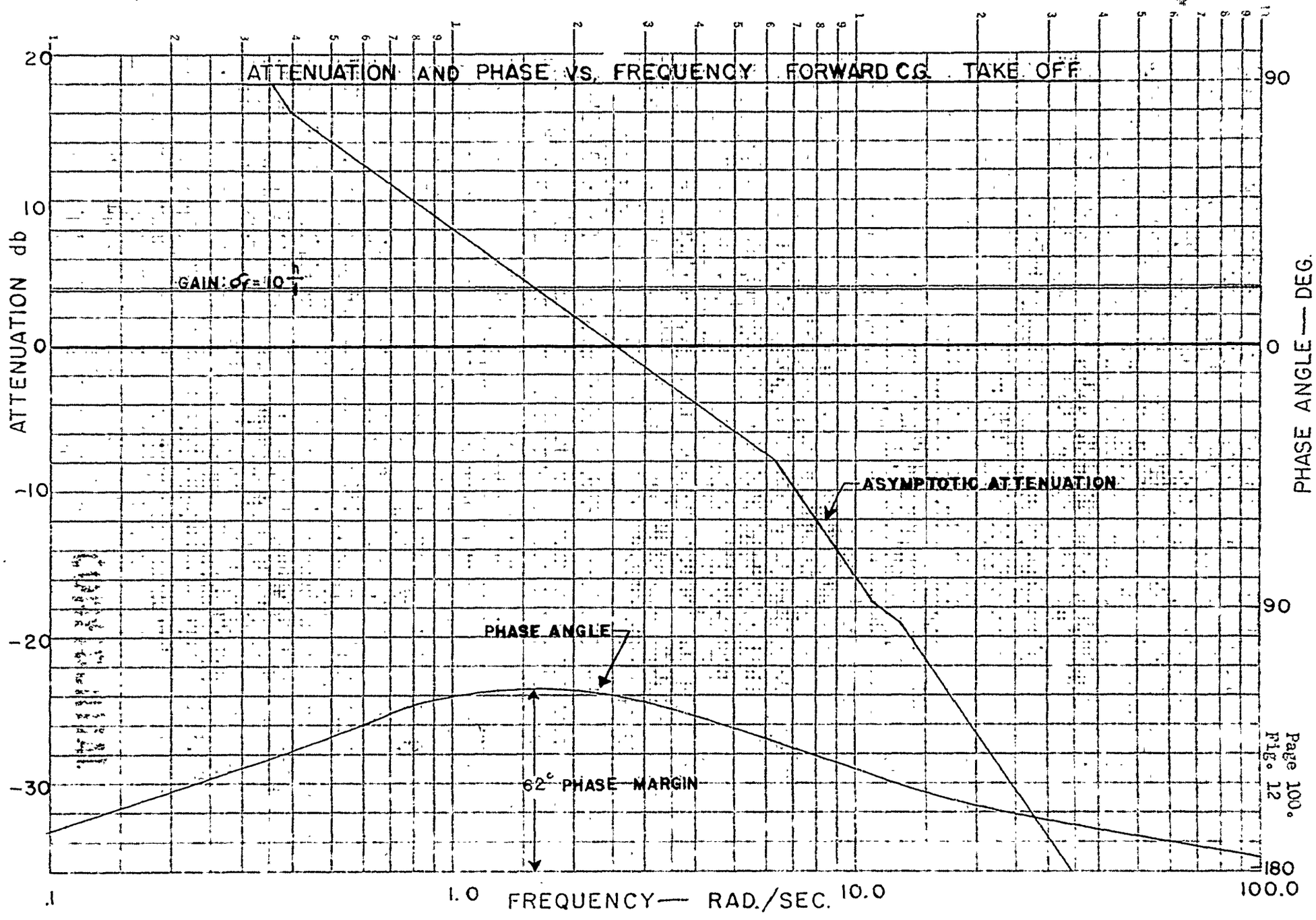

Page 100.
Fig. 12

KEUFFEL & ESSER CO., N. Y. NO. 359-73
Semi-Logarithmic, 3 cycles × 10 to the ½ inch.
MADE IN U.S.A.

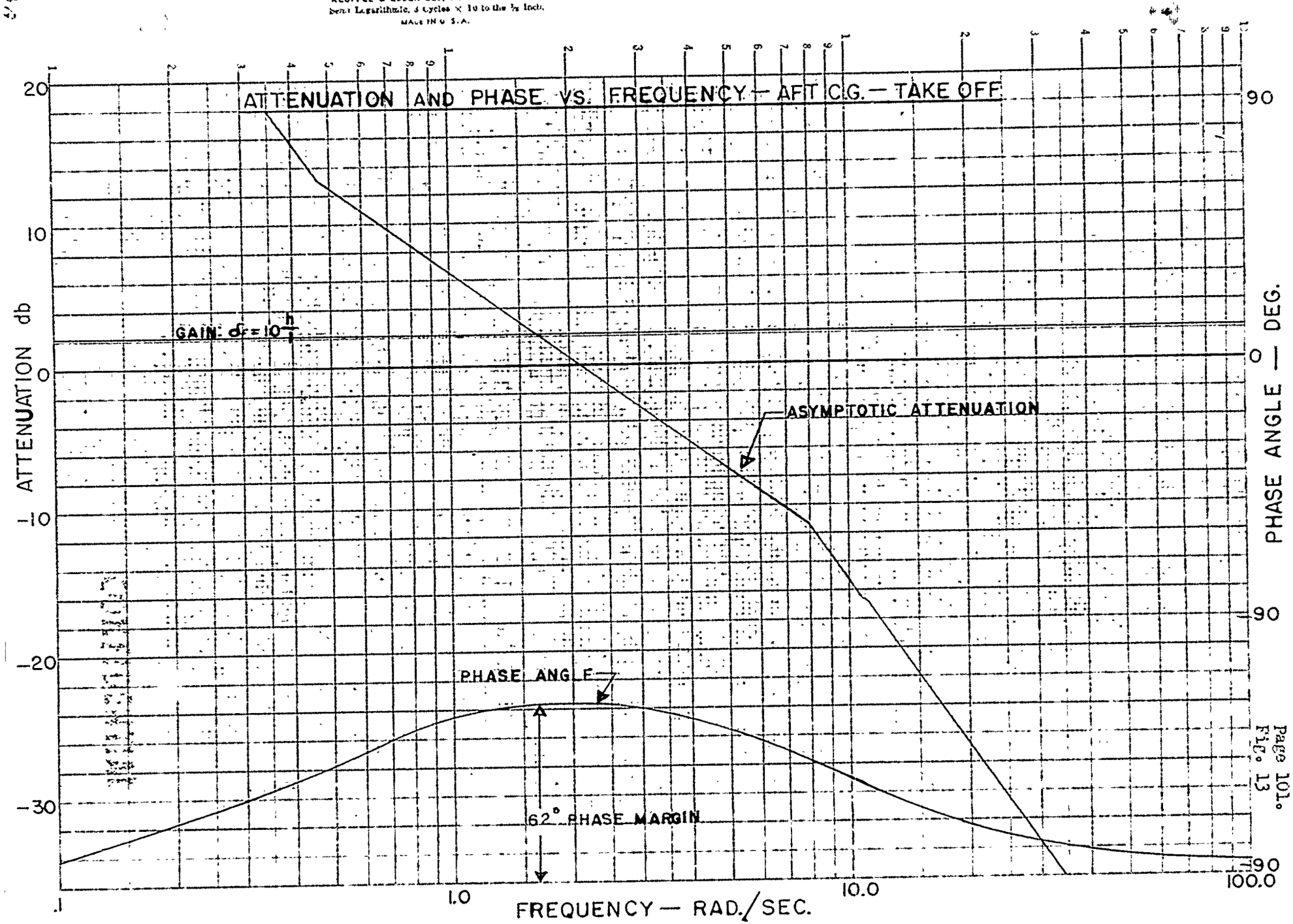

Page 101.
Fig. 13

KEUFFEL & ESSER CO N Y NO 359-72
Semi-Logarithmic: 3 Cycles X 10 to the ½ Inch
MADE IN U.S.A.

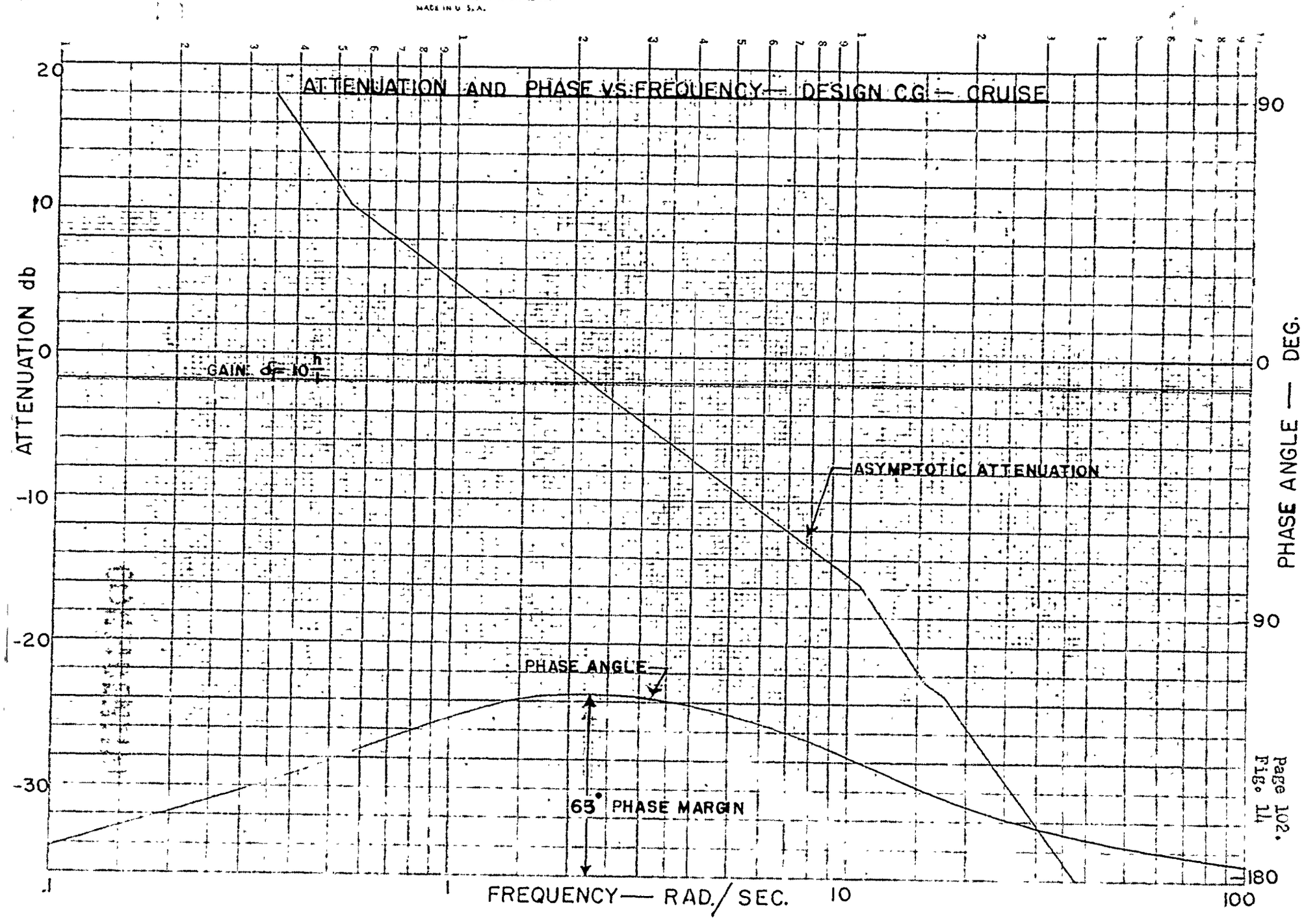

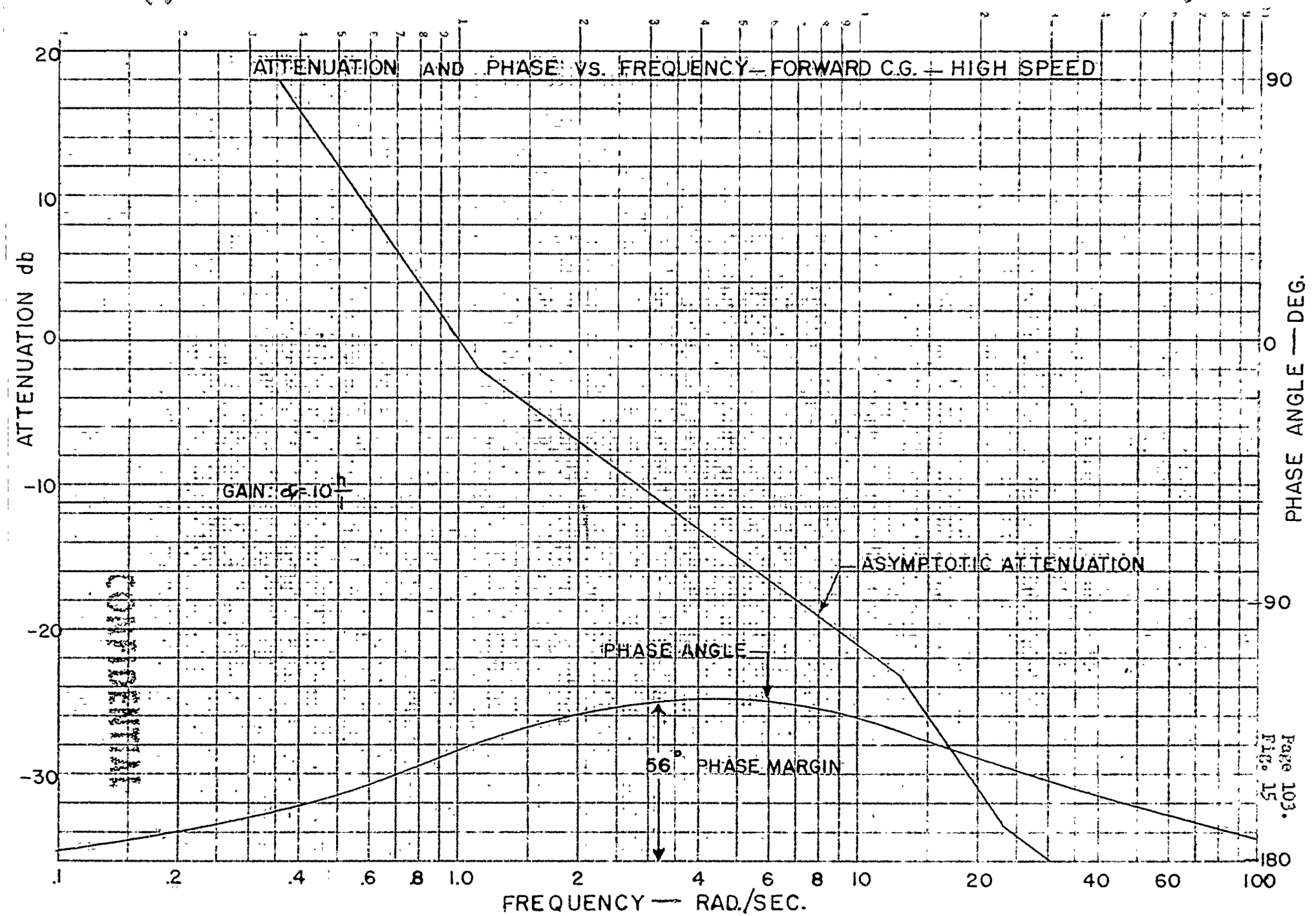

Page 103.
Fig. 15

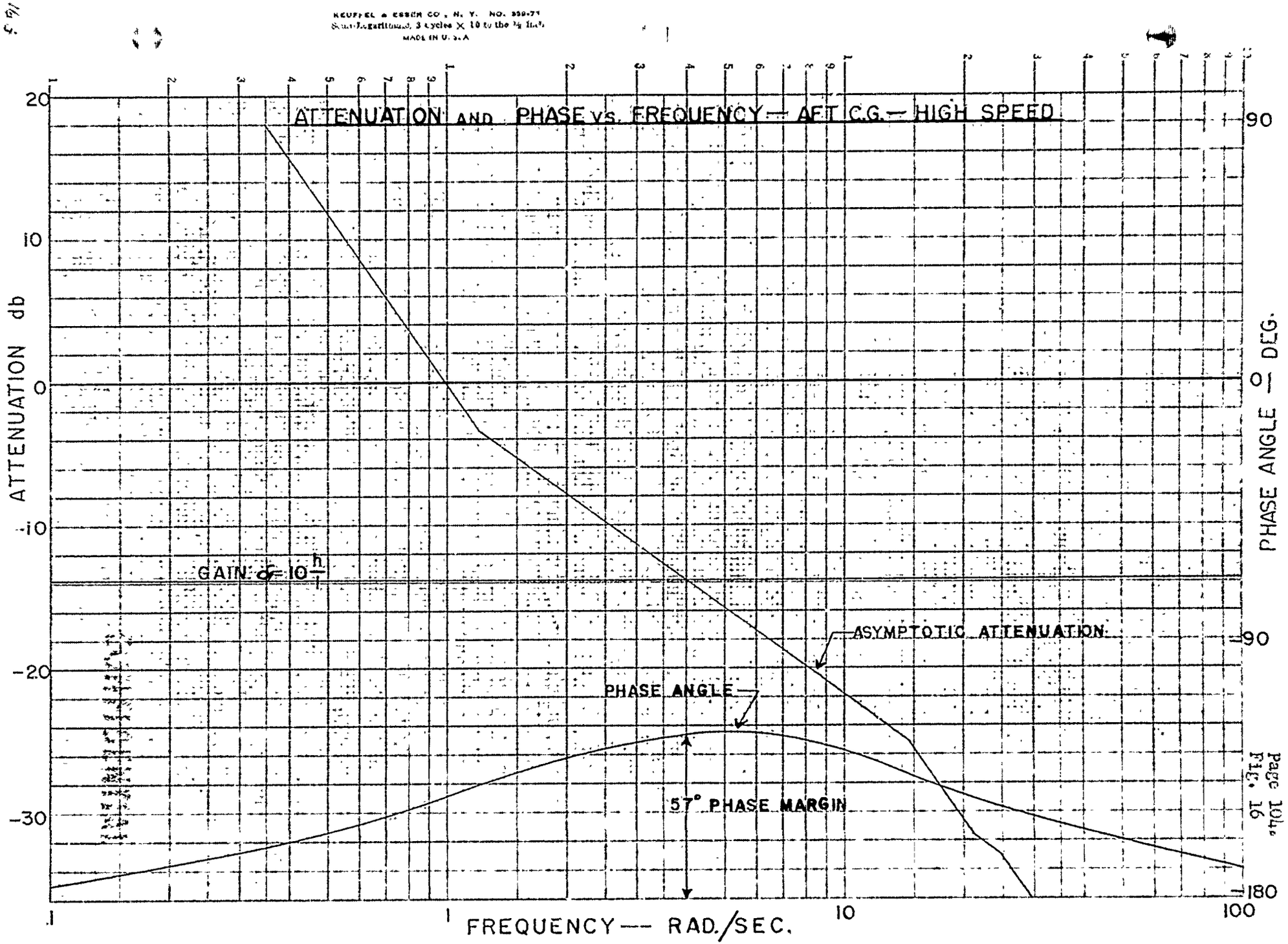
ATTENUATION AND PHASE vs. FREQUENCY — AFT C.G. — HIGH SPEED
ATTENUATION db
PHASE ANGLE — DEG.
20
10
0
-10
-20
-30
90
0
-90
-180
GAIN $\alpha = 10\frac{h}{l}$
ASYMPTOTIC ATTENUATION
PHASE ANGLE
57° PHASE MARGIN
1
10
100
FREQUENCY — RAD./SEC.

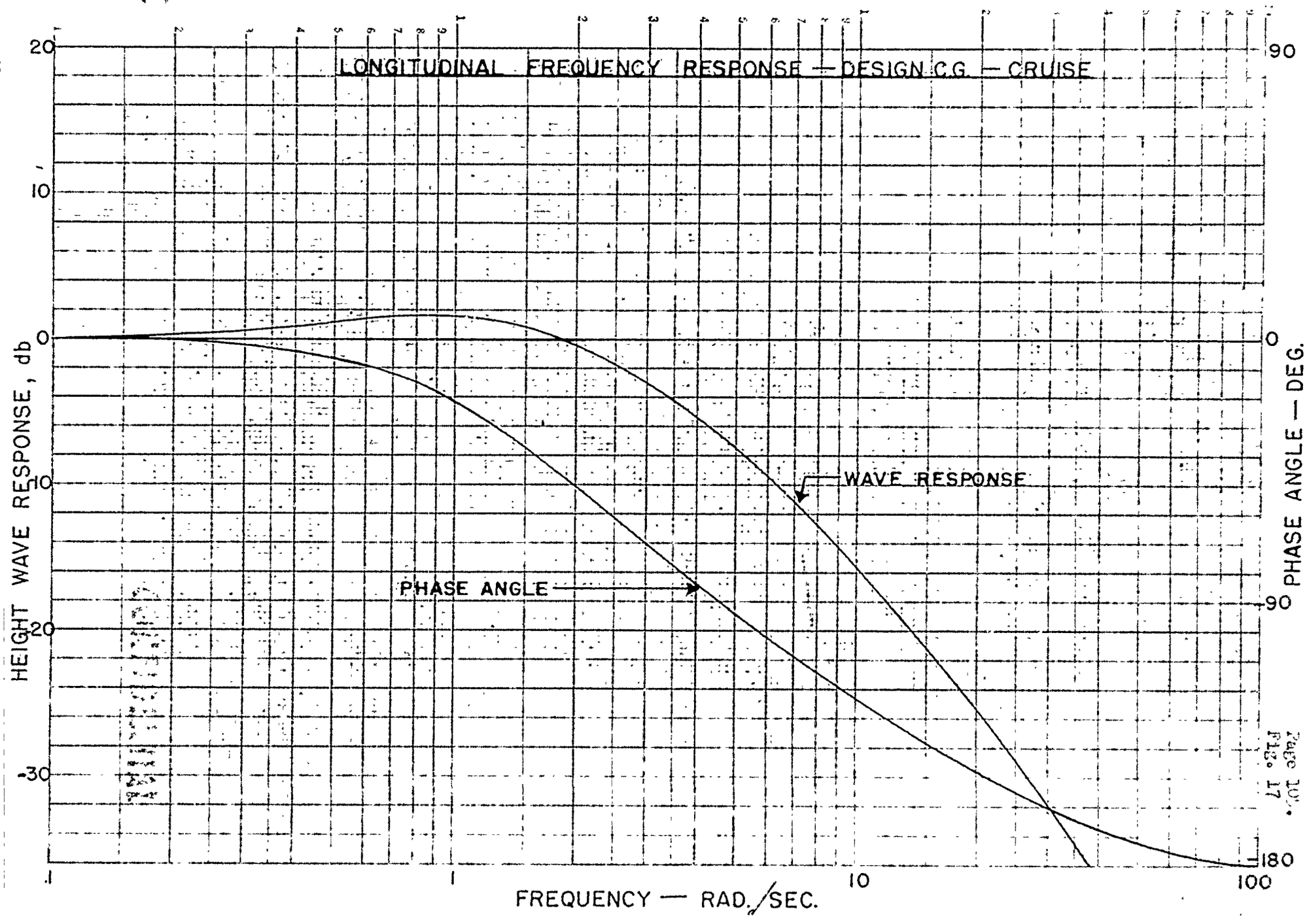
LONGITUDINAL FREQUENCY RESPONSE — DESIGN C.G. — CRUISE
HEIGHT WAVE RESPONSE, db
PHASE ANGLE — DEG.
WAVE RESPONSE
PHASE ANGLE
FREQUENCY — RAD./SEC.
20
10
0
-10
-20
-30
90
0
-90
180
.1
1
10
100

KEUFFEL & ESSER CO., N. Y. No. 359-71

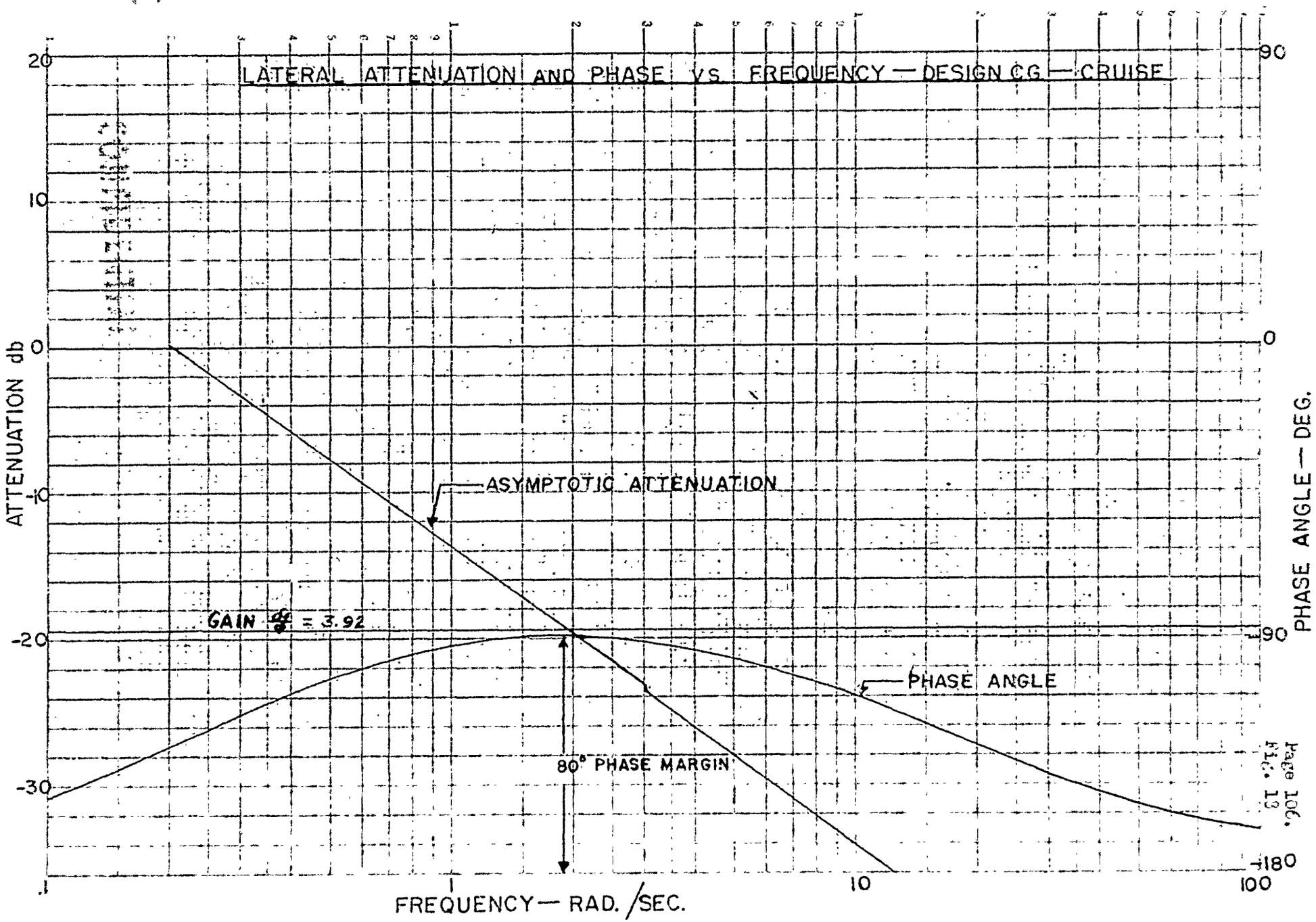

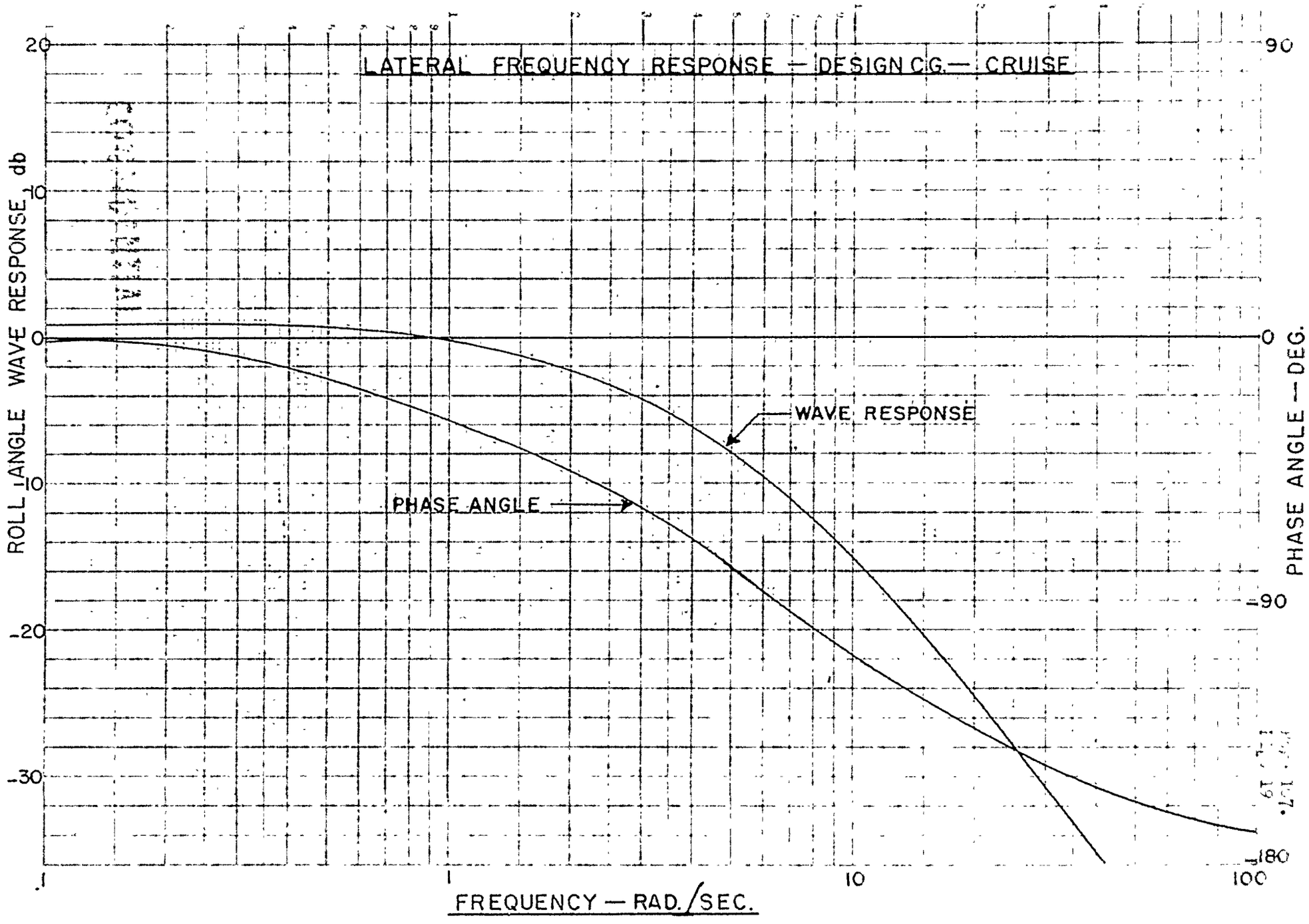
LATERAL FREQUENCY RESPONSE — DESIGN C.G. — CRUISE
ROLL ANGLE WAVE RESPONSE, db
PHASE ANGLE — DEG.
20
10
0
-10
-20
-30
90
0
-90
-180
WAVE RESPONSE
PHASE ANGLE
.1
1
10
100
FREQUENCY — RAD./SEC.

HYDROFOIL TEST VEHICLE
SCHEMATIC DIAGRAM - STABILIZATION AND TRIM SYSTEM

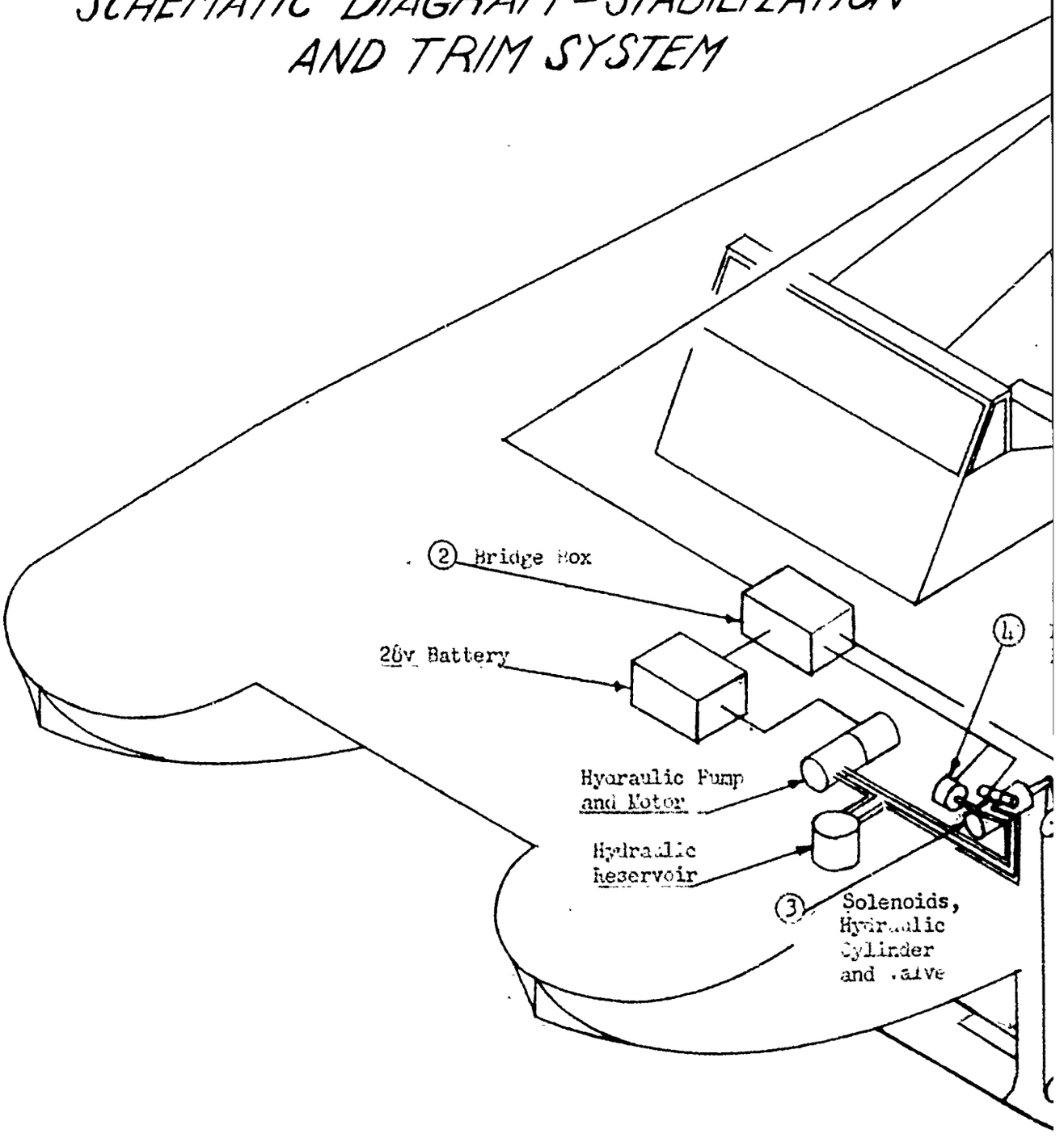

T VEHICLE
STABILIZATION
STEM

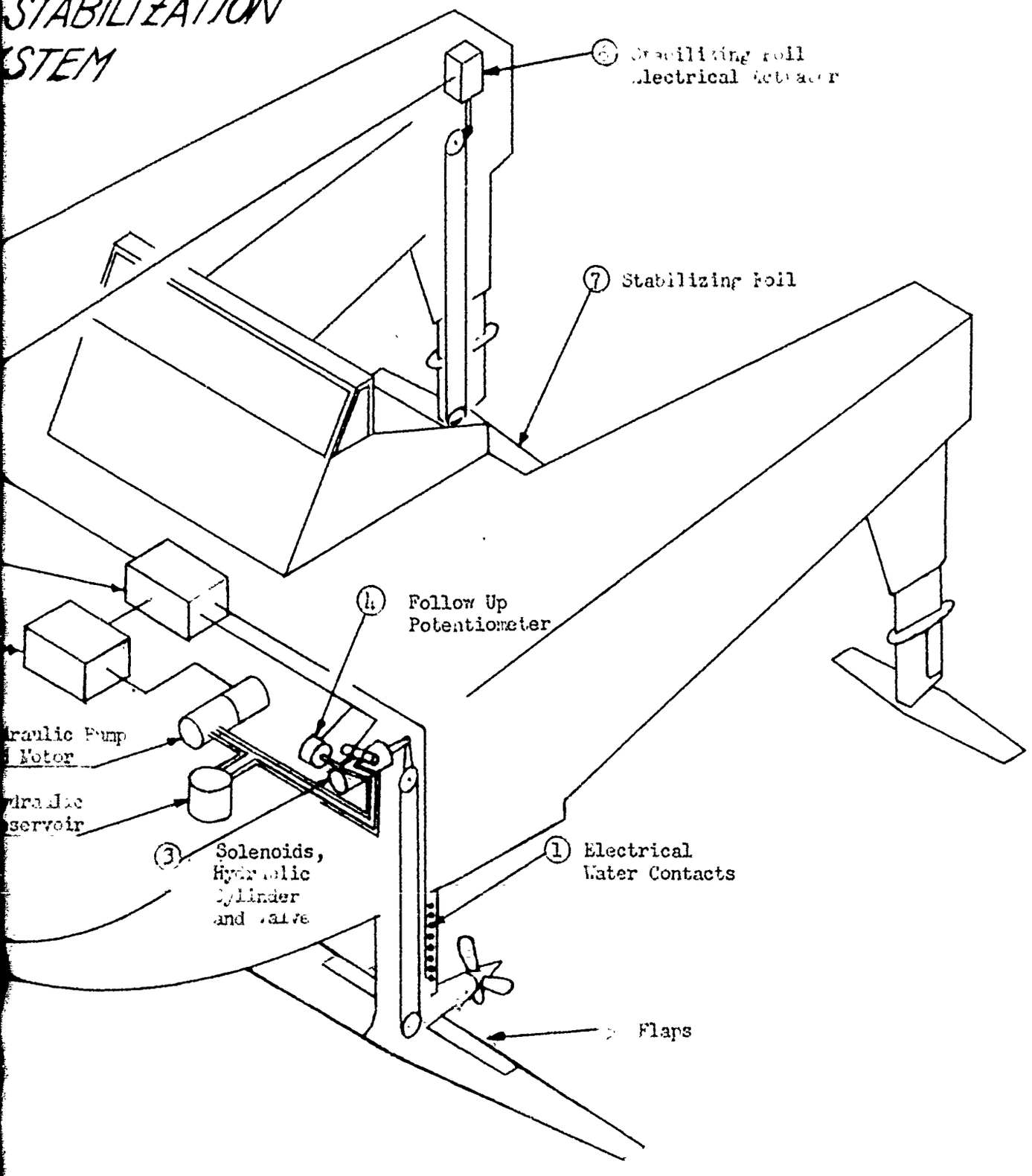

CIRCUIT DIAGRAM OF A TYPICAL 10 CONTACT ELECTRICAL FLIGHT SENSING STABILIZATION SYSTEM

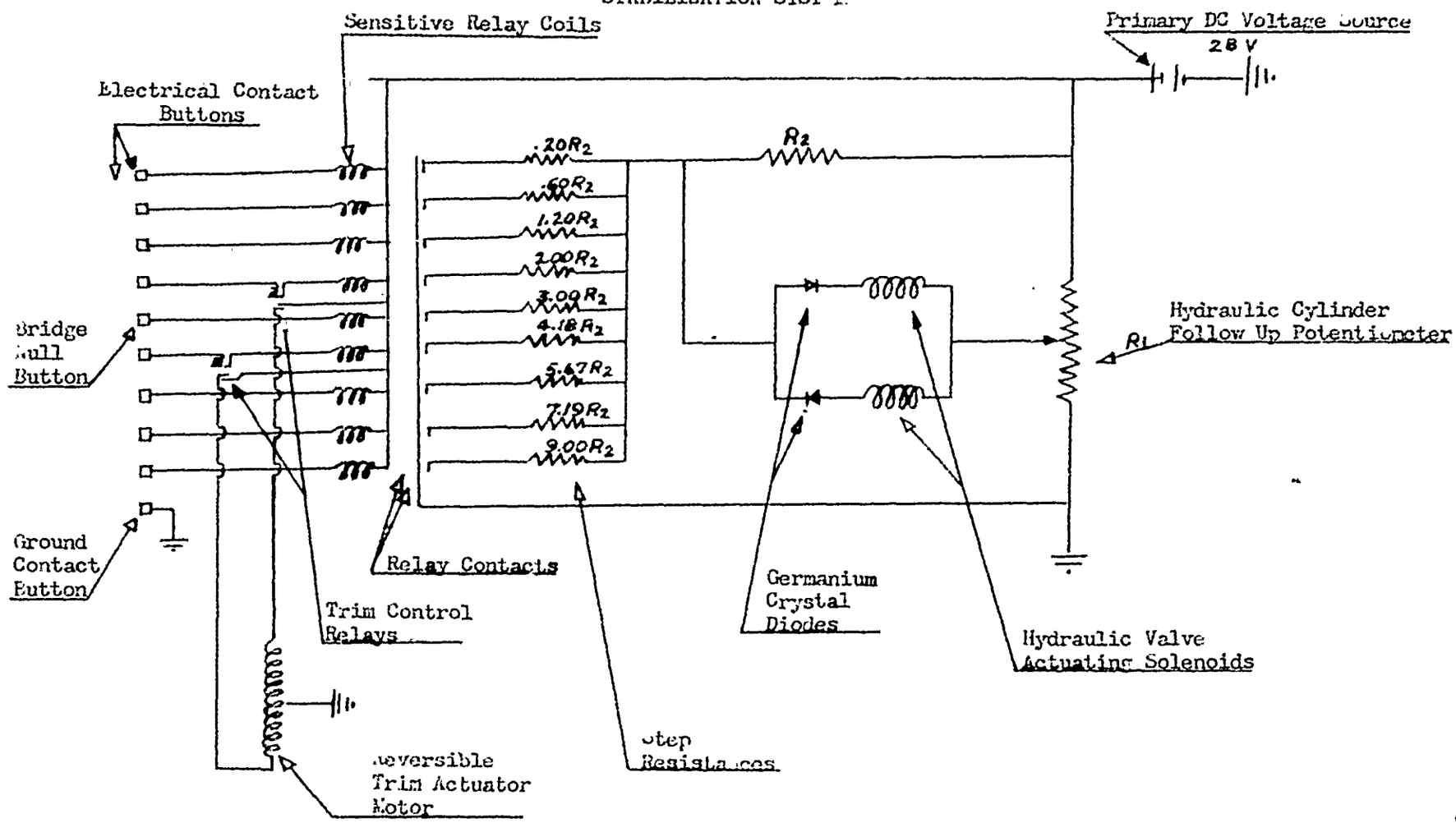

FORM 20-20

Page 105
Fig. 21

TEN-TON TEST CRAFT

Roots of Longitudinal Characteristic Equations

C.G.	Design		Aft		Aft		Forward		Forward	
Speed	CR.		T.O.		H.S.		T.O.		H.S.	
Equation	Exact	Approx.	Exact	Approx.	Exact	Approx.	Exact	Approx.	Exact	Approx.
Real Root	-16.72	-16.74	-10.54	-10.55	-23.20	-22.79	-12.45	-12.91	-28.62	-28.63
Real Root	-10.06	-10.12	- 7.98	- 8.19	-15.25	-15.71	- 7.16	-7.325	-13.51	-13.53
Complex Roots Real	-.0836		-16.56		-.0613		-.1569		.0609	
Complex Roots Imag.	±.3110i		±.115i		±.154i		±.436i		±.255i	

Page 110.
Table 1

CONFIGURATION PROPERTIES
OF
TEN-TON TEST CRAFT

$C_{L\alpha_m}$	=	4.98	S_t/S	=	0.225
C_{D0_m}	=	0.00963	ℓ	=	20'
dC_{Dm}/dC_L^2	=	0.0335	S_m	=	S = 46.73
$d\varepsilon/d\alpha$	=	0.281	$\bar{C}_m$	=	1.53'
k_m	=	0.990	b_m	=	b = 31.4'
$d\varepsilon/dC_{L_m}$	=	0.0563	AR_m	=	21.1
$C_{L\alpha_t}$	=	4.39	S_t	=	10.52
C_{D0_t}	=	0.01695	$\bar{C}_t$	=	0.972
dC_{Dt}/dC_L^2	=	0.0800	b_t	=	5.62'
ℓ_{n_t}	=	0.950	AR_t	=	6.00

TEN-TON TEST CRAFT

LONGITUDINAL STABILITY DERIVATIVES

C.G.	Design	Aft	Aft	Forward	Forward
Speed	C_{ruise}	T.O.	H.S.	T.O.	H.S.
Load	Full	Full	Full	Full	Full
C_{Z_θ}	-5.6903	-5.6903	-5.6903	-5.6903	-5.6903
$C_{Z_{\dot\theta}}$	-1.4006	-0.9374	-1.1864	-1.5888	-1.8181
$C_{Z_{\ddot\theta}}$	-0.0188	-0.0088	-0.141	-0.0229	-0.0279
$C_{Z_{\dot h}}$	-5.6903	-5.6903	-5.6903	-5.6903	-5.6903
$C_{Z_{\ddot h}}$	-0.1353	-0.1353	-0.1353	-0.1353	-0.1353
Cm_θ	-0.6223	-0.1403	-0.4799	-0.6967	-1.0541
$Cm_{\dot\theta}$	-1.3113	-1.1240	-1.1984	-1.3542	-1.4900
$Cm_{\ddot\theta}$	-0.0164	-0.0147	-0.0156	-0.0180	-0.0198
$Cm_{\dot h}$	-0.6223	-0.1403	-0.4799	-0.6967	-1.0541
$Cm_{\ddot h}$	-0.0188	-0.0088	-0.141	-0.0229	-0.0279
$C_{Z_{\sigma_t}}$	-0.9878	-0.9878	-0.9878	-0.9878	-0.9878
Cm_{σ_t}	-1.0107	-0.9575	-0.9614	-1.0647	-1.0617
$C_{Z_{\sigma_f}}$	-0.748	-0.748	-0.748	-0.748	-0.748
Cm_{σ_f}	-0.0297	0.0356	0.0159	-0.0423	-0.0599

TEN-TON TEST CRAFT

LONGITUDINAL STABILITY COEFFICIENTS

C.G	Design	Aft	Aft	Forward	Forward
Speed	Cruise	T.O.	H.S.	T.O.	H.S.
Load	Full	Full	Full	Full	Full
Z_θ	-2.8452	-2.8452	-2.8452	-2.8452	-2.8452
$Z_{\dot\theta}$	-0.7003	-0.4687	-0.5932	-0.7944	-0.9091
$Z_{\ddot\theta}$	-0.0094	-0.0044	-0.0071	-0.0115	-0.0140
Z_h	-2.8452	-2.8452	-2.8452	-2.8452	-2.8452
$Z_{\dot h}$	-0.0677	-0.0677	-0.0677	-0.0677	-0.0677
m_θ	-1.9447	-0.4384	-1.4997	-2.1772	-3.2941
$m_{\dot\theta}$	-4.0978	-3.5125	-3.7450	-4.2319	-4.6563
$m_{\ddot\theta}$	-0.0513	-0.0459	-0.0488	-0.0563	-0.0619
m_h	-1.9447	-0.4384	-1.4997	-2.1772	-3.2941
$m_{\dot h}$	-0.0588	-0.0275	-0.0441	-0.0716	-0.0872
Z_{δ_f}	-0.4939	-0.4939	-0.4939	-0.4939	-0.4939
m_{δ_f}	-3.1584	-2.9922	-3.0044	-3.3272	-3.3178
Z_{δ_s}	-0.374	-0.374	-0.374	-0.374	-0.374
m_{δ_s}	-0.0928	0.1113	0.0497	-0.1322	-0.1872
μ	0.373	0.373	0.373	0.373	0.373
τ	0.220	0.294	0.147	0.294	0.147
k_y/l	0.400	0.400	0.400	0.400	0.400
X_u	-0.0193	-0.0326	-0.0145	-0.0321	-0.0147
Z_u	-0.420	-0.748	-0.180	-0.748	-0.180
$X_{\dot h}$	0.1403	0.2444	0.0595	0.2528	0.0607
X_θ	0.1403	0.2444	0.0595	0.2528	0.0607
k	0.2100	0.3740	0.0900	0.3740	0.0900
m_u	-0.0419	-0.0731	-0.0306	-0.0719	-0.0306

LATERAL STABILITY DERIVATIVES

CRUISE SPEED DESIGN C.G.

	Main Foil	Main Strut	Stabilizing Foil	Stabilizing Foil Strut	TOTAL
$C_{l_{\dot{\varphi}}}$	-.311	-.0278	-.0676	-.0194	-.426
$C_{n_{\dot{\varphi}}}$	.0261	0	0	-.0676	-.0415
$C_{y_{\dot{\varphi}}}$	0	.152	0	.106	.258
C_{l_r}	.0261	0	0	-.0676	-.0415
C_{n_r}	0	0	0	-.236	-.236
C_{y_r}	0	0	0	.371	.371
C_{l_β}	0	.152	0	.106	.258
C_{n_β}	0	0	0	.371	.371
C_{y_β}	0	-.831	0	-.582	-1.413
$C_{l_{\delta_f}}$	-.187	——	——	——	-.187
$C_{n_{\delta_f}}$	.0078	——	——	——	.0078
$C_{l_{\delta_r}}$	——	——	——	.0432	.0432
$C_{n_{\delta_r}}$	——	——	——	.151	.151
$C_{y_{\delta_r}}$	——	——	——	-.236	-.236
$C_{l_{\delta_z}}$	——	——	-.247	——	-.247
$C_{n_{\delta_z}}$	——	——	0	——	0

LATERAL STABILITY COEFFICIENTS

CRUISE SPEED - DESIGN C.G.

$l_{\dot{\phi}}$	=	-4.30	n_{δ_f}	=	.0475
$n_{\dot{\phi}}$	=	-.253	l_{δ_r}	=	.436
$y_{\dot{\phi}}$	=	.129	n_{δ_r}	=	.922
l_v	=	-.418	y_{δ_r}	=	-.118
n_v	=	-1.440	l_{δ_s}	=	-2.49
y_r	=	.185	n_{δ_s}	=	0
l_v	=	2.61	μ_1	=	.237
n_v	=	2.27	τ	=	.220
y_v	=	-.706	k	=	.210
l_{δ_f}	=	-1.800			

C O N F I D E N T I A L

CONSIDERATION

OF

HYDROFOIL-CRAFT PROPULSION

June 1950

M. W. Beardsley

Contract No. N9onr-93201

TABLE OF CONTENTS

	Page
SUMMARY	1
INTRODUCTION	2
ANALYSIS AND DISCUSSION	3
AIR PROPELLER	5
SHROUDED AIR PROPELLER	7
MARINE PROPELLER	11
SHROUDED MARINE PROPELLER	16
CONCLUSIONS	25
REFERENCES	26
SYMBOLS	27
SUBSCRIPTS	28

C O N F I D E N T I A L

CONSIDERATION OF HYDROFOIL-CRAFT PROPULSION

SUMMARY:

Following a review of many known types of marine propulsion systems, more detailed consideration is given to systems appearing to demonstrate reasonable efficiency in the speed range of immediate interest for hydrofoil craft — 15 to 50 knots.

A shrouded air-driving propeller is shown to be capable of efficiencies comparable to those of conventional marine propellers, but it might have undesirable operating characteristics because of the fact that it is operating in a different medium than the hydrofoil craft itself.

High-speed propulsion systems, the direct hydropulse, the gasoline-air hydropulse and the hydroduct have been reviewed briefly. They offer interesting possibilities for very high speed craft but are considered uneconomical at this time for the range of speeds considered in this phase.

Investigation of the performance of conventional marine propellers indicates that cavitation will be encountered at speeds greater than about 30 knots, the deleterious effects on performance increasing with speed until they become unacceptably large at about 50 knots. An analysis is made to show that theoretically cavitation might be eliminated for high speeds if the propeller is made to operate in an encircling shroud. A theoretical study of shrouded propeller performance and design considerations indicates that efficiencies comparable to those of medium-speed conventional marine propellers may be achieved at any desired speed.

The utilization of a marine propeller requires that it be installed at some distance below the hull and requires either right angle gear drives or slanting shafts, both of which have been used with success. The use of right angle drives allows the drive shaft to be housed in the main foil supporting struts and is cleaner hydrodynamically. However, as powers increase, the design and size of gears become a serious problem and other types of power transmission should be considered. Because of time and money limitations the present report does not include consideration of this subject.

Another propulsive requirement which is of particular interest in hydrofoil craft is the necessity for providing high thrust at relatively slow forward speeds in the region of the hump in the resistance curve, coupled with reasonable propeller efficiency at considerably higher speeds. A controllable pitch propeller appears to offer the best promise to satisfy these needs.

It is believed that a shrouded marine propeller can be developed to produce acceptable propulsive efficiency at high speeds.

INTRODUCTION

The efficiency of hydrofoil craft appears to be superior to that of other types of marine craft at comparatively high speeds. If this performance advantage is to be realized, the craft propulsion system must demonstrate a reasonably high efficiency so that the overall fuel consumption per ton mile is satisfactory. Thus the major propulsion system requirement appears to be that of reasonably high efficiency at high speeds.

In an effort to leave nothing overlooked, many known types of propulsion systems have been considered and some, by their nature, are quickly dismissed as inefficient or unsuitable.

Af first glance, the direct hydropulse, the gasoline-air hydropulse, the hydroduct, the marine propeller and the air-driving propellers appear to have performance characteristics which make them worthy of more detailed consideration. These propulsion system types are analyzed and discussed in the following individual sections on each type.

ANALYSIS & DISCUSSION

The Hydropulse, Gasoline-Air Hydropulse, and Hydroduct

Reference #1 describes the hydropulse, the gasoline-air hydropulse, and the hydroduct and it presents analyses and test results concerning them.

The direct hydropulse is similar to an air pulse-jet engine except that the fluid concerned is water and the energy is supplied by the reaction of lithium or aluminum borohydride injected into the water in the "combustion chamber." This propulsion system has been developed to the point where it is stated to have a lower fuel consumption than that obtained in any modern torpedo engine regardless of type. The best fuel consumption obtained in the reported tests was 5.2 lb. fuel per thrust hp. hr. at 40 knots. (A marine-propeller propulsion system having a 50% propeller efficiency, 90% gearing efficiency, and an engine specific fuel consumption of 0.6 lb. per hp. hr. would show an overall specific fuel consumption of 1.33 lb. per thrust hp. hr.)

Thus, it may be seen that the fuel consumption of the direct hydropulse is considerably higher than might be expected for a conventional marine propeller drive for speeds up to perhaps 40 knots. In addition, it must be appreciated that the "fuel" for this hydropulse is lithium or aluminum borohydride which are expensive and difficult to handle as compared to petroleum fuels. It is felt that this hydropulse does not merit serious consideration as a propulsion system for hydrofoil craft for speeds less than 100 knots.

The main body of the gasoline-air hydropulse is very similar to that of the direct hydropulse, but it has, in addition, a gasoline-air combustion chamber connected through a flap-type valve to the main duct just aft of the duct inlet valve grid. In operation, a gasoline-air mixture is drawn into the combustion chamber and then ignited when the main duct is filled with water. The pressure of the combustion forces the water out of rear end of the duct at high velocity, thus developing thrust.

The unit tested demonstrated a specific fuel consumption of approximately 5 lb. per thrust hp. hr. at a speed of 8 knots. This unit is simple and light, but as long as the fuel-air mixture is not compressed prior to combustion, this type engine will never be able to realize high specific thrust or low specific fuel consumption. If a method of effecting this pre-compression could be obtained, this type of propulsion system should be able to show good efficiency for high speed operation. In its present form, however, the gasoline-air hydropulse engine does not appear attractive for use in high-speed hydrofoil craft.

The hydroduct is similar to a ram-jet aircraft power plant. It consumes a continuous flow of water and the thrust-developing energy is supplied by the reaction of molten lithium which is injected into the "combustion" chamber. The hydroduct is very simple and can be housed in a well streamlined body, and for those reasons is attractive for propulsion of high-speed craft. The specific fuel consumption, however, is several times as large as that of the direct hydropulse and thus this type of propulsion system appears out of the question for driving marine service craft.

Air-Driving Propeller

It has been suggested that because of the relatively low forward velocities involved, propulsion by an air-driving propeller is impractical and uneconomical for hydrofoil craft. This study analyzes the factors involved and makes specific recommendations concerning the application of the air propeller to hydrofoil-craft propulsion.

Conventional Propeller:

It is generally well known that the propulsive efficiency of a propeller decreases as the forward speed is reduced. This characteristic is clearly illustrated by the equation for propulsive efficiency:

$$\eta = \frac{F V_o}{P} \qquad (1)$$

where F = thrust.
V_o = forward velocity
P = power input

As the forward velocity, V_o drops to zero, the efficiency also decreases to zero. This expression also indicates that a high ratio of thrust to power is desirable.

As shown in any standard text on propeller theory, the ideal propulsive efficiency, based on the simple momentum theory, is expressed as:

$$\eta_i = \frac{2 V_o}{V_o + V_3} \qquad (2)$$

where V_3 is the velocity of the propeller slip stream at atmospheric pressure. This relation indicates that the propulsive efficiency increases as the slipstream velocity is reduced to a value approaching that of the forward velocity.

The propeller thrust is expressed:

$$F = m (V_3 - V_o) \qquad (3)$$

where m = the mass rate of flow through the propeller. Since equation (1) indicates that the thrust should be great, and equation (2) shows that V_3 should be as nearly as possible equal to V_0, then equation (3) discloses that the rate of mass flow through the propeller must be large. This rate of

mass flow can be expressed:

$$m = \rho A_1 V_1 \qquad (4)$$

where A_1 = the propeller disc area
V_1 = velocity at propeller disc

Since $V_1 = \frac{V_3 + V_0}{2}$, (Ref. 5), it is not an independent variable. And since ρ , the air density, cannot be controlled, the propeller disc area, A_1 , is the only factor which can be increased to give high rates of mass flow.

From these very basic considerations it may be seen that the propulsive efficiency attainable for low-speed operation will be determined chiefly by maximum allowable propeller diameter.

An expression relating thrust, propeller disc area, and ideal propulsive efficiency has been developed by Weick (Ref. 5):

$$\frac{\eta_i^2}{1-\eta_i} = \frac{4}{C_f} \qquad (6)$$

where

$$C_f = \frac{F}{\frac{1}{2}\rho V_0^2 A_1}$$

This relation between ideal efficiency, η_i , and the thrust coefficient, C_f , is illustrated in Fig. 1. This curve for the unshrouded propeller shows very clearly that for a given speed and thrust, the propulsive efficiency increases with increasing propeller disc area. In order to give an idea of the order of magnitude of the terms of this relationship, it might be pointed out that a propeller developing 1000 lb. of thrust at 30 knots will show an ideal propulsive efficiency of 60% if its diameter is 10 ft.

This is an air propeller

It should be made clear that the ideal propulsive efficiency does not include any losses caused by propeller blade drag or slipstream rotation. Thus, with a propeller blade efficiency of 85%, the overall propulsive efficiency for the above example would be 51%.

Shrouded Air Propeller:

If the propeller is encircled by a shroud, control of the mass flow of air through the propeller can be made much more effective. As pointed out in Ref. 4, the shroud functions to increase the propeller inflow and thus decrease to a non-stalling value the blade angle of attack, and also to increase the cross-sectional area of the slipstream.

From continuity of flow, (See Fig. 3)

$$\rho A_1 V_1 = \rho A_3 V_3 \qquad (7)$$

Thus, with a shrouded propeller, the thrust may be expressed, from equation (3),

as: $$F = \rho A_3 V_3 (V_3 - V_0) \qquad (8)$$

or: $$F = 2 g_0 A_1 \left(\frac{A_3}{A_1}\right)\left(\frac{V_3}{V_0}\right)\left(\frac{V_3}{V_0} - 1\right) \qquad (9)$$

The thrust coefficient is therefore:

$$C_F = \frac{F}{g_0 A_1} = 2\left(\frac{A_3}{A_1}\right)\left(\frac{V_3}{V_0}\right)\left(\frac{V_3}{V_0} - 1\right) \qquad (10)$$

The ideal propulsive efficiency is still the same as expressed in equation (2). The variation of propulsive efficiency with thrust coefficient for various area ratios is illustrated in Fig. 1.

It may be observed that for a given thrust coefficient the propulsive efficiency is increased appreciably by incorporating a shroud with a large exit area ratio. Or, if a given value of propulsive efficiency is specified, the thrust coefficient can be increased considerably. For the example of 1000 lb. thrust and 60% ideal propulsive efficiency, the propeller diameter can be reduced from 10 ft. to 6.7 ft. if a shroud with an exit area ratio of 1.6 is employed. Or, for this exit ratio, the propulsive efficiency could be increased to approximately 72% for the 10 ft. propeller developing the same thrust.

As developed in Ref. 4, the theoretical relative thrust of shrouded and unshrouded propellers for static conditions and the same power input can be expressed:

$$\frac{F_{shrouded}}{F_{unshrouded}} = 1.26\left(\frac{A_3}{A_1}\right)^{\frac{1}{3}} \qquad (11)$$

The test results reported in this reference, however, show that the thrust superiority of the shrouded propeller is actually greater than indicated in equation (11) because blade stalling of the unshrouded propeller prevents the development of thrust approaching the theoretical values. The thrust actually developed by the shrouded propellers tested was very close to the ideal calculated values.

Comparison of Propellers with and without Shroud:

It is quite apparent that the shrouded propeller gives a static and low-speed performance which is superior to that of a conventional unshrouded propeller. For the same thrust and efficiency the shrouded propeller can be of considerably smaller diameter than an unshrouded one. Since a shroud will also serve as a safety guard, which should be incorporated with a propeller driving a hydrofoil craft, its employment requires no great amount of additional work or expense.

The propeller operating within the shroud, however, may necessarily be of special design or require modification from any standard model available if the desired high performance is to be realized. This point must be investigated for each individual installation, but it is probable that the propeller must have more than two blades. An unshrouded propeller would probably also require a special design because of the unusually large diameter for a given power output.

After considering all factors it is recommended that a shrouded propeller be used if air propulsion is to be employed for hydrofoil-type craft.

Design Considerations for Shrouded Air Propeller Installation:

With air propulsion, it should be borne in mind that the hydrofoil and its driving system are operating in different and independent media. For calm conditions this factor is unimportant, but with a relatively strong breeze, the operation of the water craft may be undesirably restricted. For instance, if the hydrofoil were running at 30 knots into a 30 knot wind, the power required to drive the air propeller would be approximately 50% greater than under no-wind conditions. The required thrust horsepower is twice as great, but the ideal propulsive efficiency increases substantially so that the engine shaft power increases less rapidly than the thrust power.

Thus, if an air propeller installation incorporated a power plant producing 100% power at the design craft speed under no-wind conditions, the hydrofoil craft must be run down wind or cross wind if design high speed is to be obtained. This limitation is, of course, undesirable. But, on the other hand, the hydrofoil test craft may not be operated under windy conditions because of the rough water. The installation could, of course, be designed to incorporate sufficient power to run into a wind determined to be the maximum in which the craft could operate because of rough water considerations.

The influence of the propeller installation on stability and balance must also be considered. The propeller thrust line will be high so that there will be a substantial negative pitching moment about the center of gravity. The propeller slipstream and the area of the shroud itself will affect the yawing forces on the craft and the fore-and-aft location of the shrouded propeller should be given careful consideration.

It is probable that the simplest installation would incorporate an air-cooled aircraft engine. Since the engine must operate at full power and low forward speeds for long periods of time, careful attention must be devoted to engine cooling. The actual cooling system design would be determined by the airflow requirements and physical features of the engine employed, but it is reasonably certain that satisfactory cooling could be obtained.

As a general cooling plan, it is suggested that the engine be mounted forward of the propeller with the cooling air admitted at the nose of the engine cowl. The cylinder baffling should be arranged to conduct the air flow over the cylinders, rearward and in to the base of the propeller hub. The hub would have radial vanes so that it functioned as a centrifugal blower. The spinner would enclose the propeller hub and be arranged so that the cooling air is exhausted as a rearward-moving jet through an annular area directly behind the propeller. With this system there is a continuous pressure gradient present and it should cause the flow of sufficient cooling air.

If it should appear, upon further detailed study, that the foregoing scheme would not provide sufficient cooling, then a system employing the engine exhaust as jet ejectors could be worked out. It is established that such systems can be designed to provide satisfactory cooling for static conditions, but the design and development of such a system would probably require more labor and cost than the first proposal.

A rough sketch of a possible installation is shown in Fig.5. For this sample, a 10-ton hydrofoil test craft, the propulsion requirements and performance estimates are presented in Fig. 4. A reasonable solution for this example might be the selection of two five-foot propellers having shrouds with exit area ratios of 1.4. The ideal propulsive efficiency is 60% and for the design speed requirement two engines of approximately 110 BHp. each are required.

The thrust and efficiency of a shrouded propeller is substantially superior to that of an unshrouded propeller of equal diameter. Since the shroud serves also as a propeller guard, the additional work, etc., required for its employment is a small price to pay for the benefits obtained. Hydrofoil-type craft can be driven by shrouded propellers with propulsive efficiencies comparable to those of marine drives. However, since the propeller and the hydrofoil are operating in different media, some undesirable operating restrictions may be imposed. From a sample preliminary design study, it appears that the power and dimensions of a shrouded propeller installation are of reasonable values for the case of a 10-ton hydrofoil craft.

Marine Propellers

The general performance characteristics of marine propellers operating at low speeds and non-cavitating conditions are well understood and established. In the speed range of interest to hydrofoil craft, however, the cavitation phenomenon is encountered and exerts a major influence on the propeller performance. For this reason the attention of this study is focused chiefly upon the conditions which influence cavitation and upon means for controlling these conditions so that the deleterious effects of cavitation can be ameliorated or eliminated.

Dr. V. Bush has suggested in private discussions that propeller design concepts would probably have to be changed if reasonable efficiencies are to be realized at high speeds. These discussions with Dr. Bush gave considerable impetus to these studies on marine propellers.

Conventional Marine Propeller:

It is well known that the thrust and propulsive efficiency of marine propellers suffer marked deterioration under high-speed operating conditions because of the effects of cavitation. It is generally accepted that cavitation-free operation is limited by blade tip speed, thrust loading, and cavitation number (Ref. 2 and 3). Gawn, Ref. 3, recognizes the occurence of cavitation as "commencing at such vectorial speed of the propeller that the maximum local peak suction on the back of the blade begins to exceed the hydrostatic head available."

It appears from the literature that it is still difficult to closely predict the occurence of cavitation because this phenomenon is considered as being influenced by too many variables. These variables are such quantities as "tons of thrust per square foot of developed area," and tip speed in knots. Such terms do not directly define the critical pressure developed on the back of the blade, and it would appear that cavitation could be more accurately predicted and understood if the subject were analyzed in somewhat more fundamental terms.

Fig. 6, taken from Ref. 3, illustrates the general relationship between blade C_L and "location cavitation number" for two particular series of propellers. The data on reduced thrust conditions is interesting but perhaps a more fundamental approach would consider the blade section pressure coefficient - since this is a direct indication of cavitation condition - rather than C_L.

Although no mention of it has been found in the literature, the increase of velocity, and decrease in pressure of the flow entering the propeller appears to be worthy of consideration. By incorporating this "inflow effect", the conditions of flow in which the propeller blades operate can be directly defined without reference to less closely related factors.

As sketched in Fig. 2 and developed in Ref. 5 and 6, the flow into a propeller operating in a free stream has its velocity increased over the free-stream value as indicated in the expression:

$$V_1 = \frac{V_0 + V_3}{2} \tag{12}$$

Since no energy is added to this flow entering the propeller, Bernoulli's theorem is applicable:

$$p_0 - p_1 = \frac{\rho V_1^2}{2} - \frac{\rho V_0^2}{2} \tag{13}$$

where p_1 is the static pressure in the fluid just entering the propeller.

From (12),

$$\frac{V_1}{V_0} = \frac{1}{2}\left(\frac{V_3}{V_0} + 1\right) \tag{14}$$

Dividing (13) by q_0 gives:

$$\frac{p_0 - p_1}{q_0} = \left(\frac{V_1}{V_0}\right)^2 - 1 \tag{15}$$

Substituting equation (14) in (15):

$$\frac{p_0 - p_1}{q_0} = \frac{1}{4}\left(1 + \frac{V_3}{V_0}\right)^2 - 1 \tag{16}$$

Cavitation will occur in the stream flow entering the propeller when the left side of equation (16) is equal to the location cavitation number.

The variation of this inflow pressure drop coefficient, Equation (16), with slipstream velocity ratio, $\left(\frac{V_3}{V_0}\right)$,

is illustrated in Fig. 7. Physically, this means that when the suction required to accelerate the flow into the propeller becomes sufficiently great, it causes the flow entering the propeller to "burst" into vapor. Under this condition there will be complete back cavitation and part of the blade face may also be operating in vapor. Under such conditions the thrust and efficiency are drastically reduced.

According to Ref. 3 a thrust coefficient as low as 0.5 tons per square foot of developed blade area may be necessary for such applications as small, fast motor torpedo boats - as compared with the "time-honored pressure coefficient of 0.75 tons per square foot of developed blade area." It is interesting to make a comparison between these thrust coefficients and the values of C_f of Equation (6). For a three-bladed propeller with a mean width ratio of 0.4 - such as might be found in a high-speed craft - the ratio of developed area/disc area as calculated by Taylor's formula is: $A_d/A_1 = 0.509 \times 3 \times 0.4 = 0.61$. Thus, 1000 pounds per square foot of developed area is equal to 610 pounds per square foot of disc area. At 50 knots this is equivalent to $C_f = 610/84.5^2 = 0.0855$. This value corresponds to a slip stream velocity ratio of about 1.043 and is well below the slip stream ratio of 1.275 at which inflow cavitation would occur at 50 knots (on the surface) because of acceleration into the propeller.

In most discussions of propeller cavitation, the expression for the dynamic pressure is usually given as $\rho\frac{V_0^2}{2}$, $\rho\frac{U^2}{2}$, or $\frac{\rho(V_0^2+U^2)}{2}$, where U is the circumferential tip speed of the propeller. In an effort to better express the actual conditions in which the blades are operating, consideration should be given to the increased velocity of the entering flow and the location pressure coefficient expressed in terms of this velocity.

From a simple vector diagram it can be seen that the velocity of the flow relative to the blade tip is $\sqrt{V_1^2+U^2}$, and thus,

$$q_t = \frac{\rho}{2}(V_1^2+U^2) \qquad (17)$$

Dividing and multiplying by V_o^2, and substituting for V_1 from Equation (14) gives:

$$q_t = q_o\left[\frac{1}{4}\left(\frac{V_s}{V_o}+1\right)^2+\left(\frac{U}{V_o}\right)^2\right] \qquad (18)$$

Since $U=\pi nD$,

$$q_t = q_o\left[\frac{1}{4}\left(\frac{V_s}{V_o}+1\right)^2+\left(\frac{\pi}{J}\right)^2\right] \qquad (19)$$

where the advance coefficient,

$$J=\frac{V_o}{nD}$$

In order to be able to determine the maximum allowable operating C_L for a known blade profile, it is necessary to develop an expression for pressure coefficient in terms of the dynamic pressure of the flow relative to the blade, q_t. From Bernoulli's theorem for the flow relative to the blade:

$$p_1+q_t = p_b+q_b \qquad (20)$$

where p_b and q_b are the local pressure and dynamic pressure at any point on the propeller blade. It follows that

$$\frac{p_1-p_b}{q_t}=\frac{q_b}{q_t}-1=C_{p_b} \qquad (21)$$

Substituting for p_1 from Equation (16)

$$\frac{p_o-p_b}{q_t}=\frac{q_b}{q_t}-1+\frac{q_o}{q_t}\left[\frac{1}{4}\left(\frac{V_s}{V_o}+1\right)^2-1\right] \qquad (22)$$

Substituting from Equation (19), this can be written

$$\frac{p_o-p_b}{q_t}=C_{p_b}+\frac{\left[\frac{1}{4}\left(\frac{V_s}{V_o}+1\right)^2-1\right]}{\left[\frac{1}{4}\left(\frac{V_s}{V_o}+1\right)^2+\left(\frac{\pi}{J}\right)^2\right]} \qquad (23)$$

where C_{p_b} is the local pressure coefficient of the blade as determined by the profile shape. (In this case the sign

of the C_{p_b} term is opposite to the convention usually employed in presenting airfoil section data.) Dividing and multiplying the left side of (23) by q_o yields:

$$\left(\frac{p_o - p_b}{q_o}\right)\frac{q_o}{q_t} = C_{p_b} + \frac{\rho - 1}{\rho + \left(\frac{\pi}{J}\right)^2} \qquad (24)$$

where $\rho = \frac{1}{A}\left(\frac{V_s}{V_o} + 1\right)^2$.

Multiplying both sides by q_t/q_o from equation (19) gives:

$$\frac{p_o - p_b}{q_o} = \left[\rho + \left(\frac{\pi}{J}\right)^2\right] C_{p_b} + \rho - 1 \qquad (25)$$

For use in determining the maximum blade operating C_L that can be employed without cavitation, equation (23) can be most conveniently written as:

$$C_{p_b} = \frac{\delta - \rho + 1}{\rho + \left(\frac{\pi}{J}\right)^2} \qquad (26)$$

where δ is the location cavitation member as determined by depth of immersion and free stream velocity. In use, the value of C_{p_b} is calculated by equation (26) and, referring to the pressure distribution of the selected airfoil section data, the maximum allowable value of C_L is determined. This value, of course, applies only to the blade tip; and for actual propeller design the allowable values for other radii could be calculated by modifying the above equations.

Equation (26) is plotted in Fig. 8. The great effect of speed is readily apparent, and the variation of the advance coefficient, J, is also seen to exert a substantial influence. The effect of thrust loading is secondary since most conventional propellers appear to operate with a thrust coefficient of 0.1 to 0.4. These curves suggest that the struggle for increased speeds will lead to propellers designed with higher advance coefficients (blade pitch angles) or the incorporation of variable pitch mechanisms.

The values of C_L obtainable for various C_{P_s} values for an NACA 66-006 section airfoil are indicated in the vertical axis of Fig. 8. These C_L values are typical for a symmetrical blade section of 6% thickness, which is a reasonably low practical thickness. Although this analysis may not give values which are of exactly correct magnitudes, it does, nevertheless, indicate that it will be almost impossible to operate conventional propellers without serious cavitation at speeds greater than about 50 knots. Speeds of this order will also require high blade angles which may be impractical for operation at lower speeds unless pitch-changing mechanisms are employed.

In short, it appears that it will be impossible to secure satisfactory performance with conventional propeller drive on service vessels required to operate continuously at speeds greater than about 50 knots.

Cavitation Elimination: The Shrouded Propeller

Rather than be resigned to this speed limitation as inevitable, it is considered worthwhile to investigate methods of modifying the propeller or its operating conditions in such a manner that it can demonstrate a satisfactory performance at high speeds.

It is obvious that if the ambient pressure in the zone of propeller operation could be sufficiently increased, the propeller could operate without cavitation. In addition, any decrease in the velocity of the fluid relative to the propeller blades would also decrease cavitation. Both of these effects can be secured by enclosing the propeller in a shroud, as illustrated in Fig. 9.

By the design of the shroud the velocity of the entering flow is decreased and hence the pressure is increased. From Bernoulli's theorem again:

$$\frac{p_o - p_i}{q_o} = \frac{q_i}{q_o} - 1 \qquad (27)$$

Substituting for q_1 and q_0 gives:

$$\frac{P_2 - P_1}{q_0} = \left(\frac{V_1}{V_0}\right)^2 - 1 \qquad (28)$$

Considering Bernoulli's Theorem for the flow conditions under which the blades operate:

$$\frac{P_1 - P_b}{q_t} = \frac{q_b}{q_t} - 1 = C_{p_b} \qquad (29)$$

where the subscript, b, denotes any location on the blade. Equation (29) can be rewritten as:

$$\left(\frac{P_0 - P_b}{q_0}\right)\left(\frac{q_0}{q_t}\right) - \left(\frac{P_2 - P_1}{q_0}\right)\left(\frac{q_0}{q_t}\right) = C_{p_b} \qquad (30)$$

From a vector diagram of the flow velocity relative to the blade:

$$q_t = \frac{\rho}{2}(V_1^2 + U^2) \qquad (31)$$

$$\text{or, } q_t = \frac{\rho V_0^2}{2}\left(\frac{V_1}{V_0}\right)^2\left[1 + \left(\frac{U}{V_1}\right)^2\right] \qquad (32)$$

Substituting (32) in (30) gives:

$$C_{p_b} = \frac{\left(\frac{P_0 - P_b}{q_0}\right) - \left(\frac{P_2 - P_1}{q_0}\right)}{\left(\frac{V_1}{V_0}\right)^2\left[1 + \left(\frac{U}{V_1}\right)^2\right]} \qquad (33)$$

If the minimum absolute pressure on the blade surface is just equal to the fluid vapor pressure, or at incipient cavitation; then, $\frac{P_0 - P_b}{q_0} = \sigma$, the location cavitation number. Thus, at incipient cavitation, the maximum local pressure coefficient allowed on the blade is:

$$C_{P_b} = \frac{\delta - \left(\frac{V_1}{V_o}\right)^2 + 1}{\left(\frac{V_1}{V_o}\right)^2 \left[1 + \left(\frac{U}{V_1}\right)^2\right]} \qquad (34)$$

From Fig. 10 it may be noted that the shrouded propeller can be designed to be less critical from the standpoint of cavitation effects than a hydrofoil or other part of the vessel travelling at the speeds considered. Cavitation may occur on the outside of the shroud, however, at a speed depending on the shroud shape. In general, the shroud length must increase with the speed.

Since all of this analysis has been based upon the assumption of an incompressible fluid, the equations are valid only for such conditions. The effects of compressibility will probably start to appear at about 2000 knots since the accoustic velocity of water is approximately 2900 knots. Since such a high speed is not considered attainable in the forseeable future, Equation 34 can be considered as valid for any speed likely to be of interest, and it indicates that a relatively great value of allowable C_{P_b} can always be obtained without cavitation with the shrouded propeller. This is distinctly superior to the conventional unshrouded propeller (see Equation 26), for which the maximum allowable C_{P_b} is zero for $\delta = 0$ even for the no-thrust condition, $\frac{V_3}{V_o} = 1.0$.

It appears that for ship speeds of the order of 50 knots or higher, the performance of conventional propellers will be adversely affected by unavoidable cavitation losses. These losses will be so large that continuous operation at speeds of this magnitude will be decidedly impractical from the standpoint of economy. In attempting to secure higher speeds the design trend will probably be toward thinner blade sections and higher values of advance coefficient and possibly pitch varying mechanisms.

Based on theoretical considerations, it appears that propeller blade cavitation can be completely eliminated at very high speeds by enclosing the propeller in a shroud designed to establish a region of high pressure and relatively low velocity in which the propeller blades operate.

Shrouded Propeller Design and Performance Analysis:

It has been shown that propeller cavitation can theoretically be eliminated by the incorporation of an enclosing shroud. Since the conditions of flow through the propeller are obviously changed by the shroud, they should be analyzed to determine the following major points for use in design and performance estimates:

1. What parameters most greatly influence cavitation, and the values of these parameters which are necessary to eliminate cavitation for any specified operating conditions.

2. What parameters most greatly influence the overall performance (efficiency and thrust), and the values of these parameters which will give the optimum performance.

Considering that the chief function of the shroud is to decrease the velocity and increase the static pressure at the propeller, it is evident that two major factors will be the axial velocity at the propeller operating section and the efficiency of the pressure recovery in the flow up to this section. One convenient means of expressing pressure recovery is as "ram pressure recovery ratio." This parameter is defined as:

$$\eta_r = \frac{H_1 - P_0}{q_0} \tag{35}$$

or,

$$\eta_r = \frac{P_1 - P_0}{q_0} + \frac{q_1}{q_0} \tag{36}$$

and

$$\eta_r = \frac{P_1 - P_0}{q_0} + \left(\frac{V_1}{V_0}\right)^2 \tag{37}$$

Substituting Equation (37) in Equation (30), the expression for blade pressure coefficient becomes:

$$C_{P_b} = \frac{q_0}{q_b}\left[\frac{P_b - P_0}{q_0} + \eta_r - \left(\frac{V_1}{V_0}\right)^2\right] \tag{38}$$

If the lowest absolute pressure on the blade, p_b , is equal to the vapor pressure of the fluid, then, at incipient cavitation:

$$\frac{p_o - p_b}{g_o} = \frac{p_o - p_v}{g_o} = \delta \qquad (39)$$

Substituting (39) in Equation (38), the propeller blade pressure coefficient at incipient cavitation is expressed:

$$C_{p_b} = \frac{g_o}{g_t}\left[\delta + \eta_r - \left(\frac{V_1}{V_o}\right)^2\right] \qquad (40)$$

Since,

$$g_t = \frac{\rho}{2}\left[V_1^2 + (\pi n D)^2\right] \qquad (41)$$

$$C_{p_b} = \frac{\delta + \eta_r - \left(\frac{V_1}{V_o}\right)^2}{\left(\frac{V_1}{V_o}\right)^2\left[1 + \left(\frac{\pi n D}{V_1}\right)^2\right]} \qquad (42)$$

This is the expression for the propeller blade pressure coefficient at incipient cavitation in terms of the major parameters affecting cavitation. The variation of this maximum allowable C_{p_b} value (at incipient cavitation) with speed is illustrated in Fig. 10.

In actual shroud design calculations it is probable that the value of the blade pressure coefficient will be predetermined from blade efficiency considerations. As a result, the propeller operating velocity ratio must be solved for, and from Equation (42), the propeller operating velocity ratio is derived to be:

$$\frac{V_1}{V_o} = \sqrt{\frac{\delta + \eta_r}{1 + C_p\left[1 + \left(\frac{\pi n D}{V_1}\right)^2\right]}} \qquad (43)$$

This equation expresses the velocity ratio at the propeller operating section for the condition that incipient cavitation exists at the minimum pressure point of the propeller blades. The relationship between this velocity ratio and the blade pressure coefficient is illustrated in Fig. 11 for speeds of 30 knots and 60 knots, and in Fig. 12 for extremely high speeds, i.e. $\delta = 0$.

Since the shroud presents additional surface to cause resistance, it is to be expected that there will be internal and external losses which will tend to decrease the performance of the propeller. The internal losses are the more important and can be considered in terms of pressure loss in the flow through the shroud.

If the flow through the shroud suffered no losses, the total pressure added to the fluid stream by the propeller would, for this ideal condition, be expressed as:

$$\Delta H_i = H_3 - H_0 \qquad (44)$$

The actual total pressure added to the flow by the propeller is:

$$\Delta H_a = H_2 - H_1 \qquad (45)$$

If the volume rate of flow is equal for the ideal and actual cases, the shroud efficiency (considering internal flow only) can be expressed as:

$$\eta_s = \frac{\Delta H_i}{\Delta H_a} = \frac{H_3 - H_0}{H_2 - H_1} \qquad (46)$$

The total pressure of the flow leaving the jet discharge nozzle may be expressed:

$$H_3 = H_2 - f q_3 \qquad (47)$$

where f = fraction of dynamic head lost because of friction.

(The application of the friction factor to the jet dynamic pressure is conservative since the friction actually occurs while the flow velocity is lower and in a region of favorable pressure gradient between the propeller discharge and the jet nozzle exit.) Substituting for H_1 from Equation (35), and for H_2 from Equation (47) in Equation (46) gives:

$$\eta_s = \frac{H_3 - H_0}{H_3 + f q_{d_3} - H_1} = \frac{p_3 + q_3 - p_0 - q_0}{p_3 + q_3 + f q_3 - \eta_r q_0 - p_0} \quad (48)$$

Since $p_3 = p_0$, the pressure terms cancel, and,

$$\eta_s = \frac{q_3 - q_0}{q_3(1+f) - \eta_r q_0} \quad (49)$$

Dividing through by q_0 and cancelling ($\rho/2$) gives:

$$\eta_s = \frac{\left(\frac{V_3}{V_0}\right)^2 - 1}{\left(\frac{V_3}{V_0}\right)^2 (1+f) - \eta_r} \quad (50)$$

In this expression the friction factor, f , represents the fraction of the dynamic head (of the flow from the propeller through the jet nozzle) which is lost because of friction. This is the same factor regularly employed in expressing the pressure loss for fluid flow through pipes, etc., and thus can be estimated with reasonable accuracy for given conditions of Reynold's Number, shroud diameter, etc.

The overall propulsive efficiency of the shrouded propeller installation may be expressed:

$$e = \eta_s \cdot \eta_b \cdot \eta_i \quad (51)$$

where η_i is the ideal propulsive efficiency, Equation (2), and η_b is the propeller blade efficiency which is largely determined by the blade pitch angle and lift/drag ratio. The propeller blade efficiency is also defined:

$$\eta_b = \frac{(H_2 - H_1) Q}{P} \quad (52)$$

where Q is the volume flow through the propeller, and P is the power input into the propeller shaft.

The shroud efficiency as a function of the major parameters is illustrated in Fig. 13. It will be noted that the jet velocity ratio is the most influential parameter and that at high jet velocity ratios the other parameters--within the range of values to be reasonably expected--are relatively unimportant. At jet velocity ratios in the probable working range, eg. 1.2 to 1.5, the ram pressure recovery ratio, η_r , is of considerable importance. It is obvious that any installation should be designed with the objective of obtaining the maximum possible ram pressure recovery and minimum internal friction losses.

The shrouded propeller is especially attractive because of its freedom from cavitation at high speeds, but it also supplies several other effects which may cause a net increase in propeller efficiency at all speeds. One major result is the end-plate effect caused by the shroud around the end of the blades. This effect will reduce tip losses and should make possible the attainment of blade profile characteristics approaching those of infinite aspect ratio airfoils.

An indication of the order of magnitude of this effect may be secured by considering a propeller operating under the following conditions:

Loading.....	1500#/ft.^{2} developed area.
Vessel speed.....	30 knots.
Advance Coef.	J = 1.0.
Propeller Diam.	8 ft.
Calculated Mean C_L.....	0.10 approx.
Induced Drag	0.004 approx.

Considering that the profile drag coefficient of a propeller blade section is perhaps $C_{D_p} = 0.010$, it will be seen that elimination of the induced drag would decrease the total blade drag by approximately 30% with the consequent increase in overall efficiency.

Another result which may be even more important is the

realization of operation with a blade section C_L which gives the highest attainable values of L/D or propeller efficiency. For instance, curves in Ref. 2 show that for typical airfoil blade sections, aspect ratio = 6, the lift/drag ratio at C_L = 0.1 is of the order of 13; whereas, if an operating C_L = 0.3 could be realized without cavitation, a lift/drag ratio of approximately 25 could be achieved with a 6% thick section. It is interesting to note that with an infinite aspect ratio this same section reaches its peak L/D = 70 at a value of C_L = 0.6. Compared on the basis of simple blade-element propeller theory, for an advance angle of 20°, the blade efficiency for those L/D values is:

L/D = 13,	Blade Efficiency = 0.802
25	0.888
70	0.953

Operation at higher C_L would also mean that smaller, more easily fabricated blades could be employed.

By judicious control of the internal cross-sectional area of the shroud, the propeller blades could be made to operate in a region of favorable pressure gradient with consequent additional reduction in drag losses.

In order to get an idea of the order of magnitude of the overall efficiency of the shrouded propeller, assume a blade efficiency, η_b = 0.90. For a jet velocity ratio, V_3/V_0 = 1.3, and a ram pressure recovery, η_r = 0.90, from Fig. 13 the product $\eta_i \cdot \eta_s$ = 0.714. Thus, from Equation (51) the overall efficiency is:

$$\epsilon = 0.714 \times 0.90 = 0.642$$

This is not as good as the efficiency of conventional low-speed propellers, but it is decidedly superior to the efficiency realized on high-speed racing craft, etc. Again it might be stated that theoretically this order of efficiency is obtainable for very high speeds.

CONCLUSIONS:

It is believed to be theoretically possible to develop a propulsion system to drive hydrofoil craft at very high operating speeds with an overall efficiency comparable to that of a moderate-speed marine propeller.

High-speed propulsion systems such as the hydropulse, the gasoline-air hydropulse and the hydroduct appear to have efficiencies too low to be acceptable for propulsion of service hydrofoil craft where long-range and large pay load characteristics are desired.

Propulsion by a shrouded air-driving propeller appears capable of operating with acceptable efficiency and makes possible a light-weight and simple installation for small craft. However, certain wind conditions may develop undesirable operating restrictions, and the generation of sufficient power for larger craft may be difficult of impossible to obtain.

The conventional marine propeller gives satisfactory propulsion for speeds up to perhaps 30 knots. For greater speeds the deleterious effects of cavitation become increasingly large until, at about 50 knots, the propeller efficiency is reduced to a value which is unacceptable for service operation.

Theoretical investigations indicate the possibility that the shrouded marine propeller can develop efficiencies up to very high speeds which are comparable to the efficiencies of the conventional unshrouded marine propeller at approximately 30 knots. In view of the higher operating speeds anticipated with hydrofoil craft, it appears desirable to investigate further the possibilities of better performance at higher speeds indicated theoretically through the use of shrouded marine propellers.

REFERENCES

1. Aerojet Engineering Corp.; "Research, Development and Testing of Underwater Propulsion Devices;" Report No. 387 (Semi-annual) Contract N6ori-10, Task Order No. 1, Project No. NR 22003.

2. Burrill, L.C.; "Developments in Propeller Design and Manufacture for Merchant Ships;" Trans. Institute of Marine Engineers, Oct., 1943.

3. Gawn, R.W.L.; "Cavitation of Screw Propellers." Preprint of Paper presented to N-E Coast Inst. of Engrs. & Shipbuilders, Mar. 11, 1949.

4. Platt, Robert J.; "Static Tests of A Shrouded and An Unshrouded Propeller;" NACA RM No. L7H25, Feb. 9, 1948.

5. Weick, Fred E.; "Aircraft Propeller Design;" McGraw Hill Book Company, 1930.

6. Wislicenus, G.F.: "Fluid Mechanics of Turbomachinery;" McGraw-Hill Book Company, pg. 398.

Terminology and Symbols

A	Area , sq. ft.
$C_f = \frac{F}{q_o A}$ =	Thrust coefficient
D	Diameter , ft.
F	Thrust , lb.
H	Total Pressure, H = $p+q$, lb./sq. ft.
$J = \frac{V_a}{nD}$	Advance coefficient
L/D	Lift/drag ratio
P	Power , ft. lb./sec.
Q	Volume Flow, cu. ft./sec.
V	Velocity , ft./sec.
e	Overall Propulsive Efficiency
f	Friction Factor, f = (Press. Loss due to friction)/q
n	Revolutions per sec.
p	Static pressure
q	Dynamic pressure
σ	Location cavitation number
η	Efficiency
ρ	Density

Subscripts

o	Free stream
1	At cross-section just entering propeller
2	At cross-section just after propeller
3	At shroud discharge nozzle (or open propeller slipstream where $p_3 = p_o$)
b	Blade
f	Thrust
i	Ideal
j	Slipstream or jet
p	Pressure
t	Total relative to blade
v	Vapor of fluid.

CONFIDENTIAL

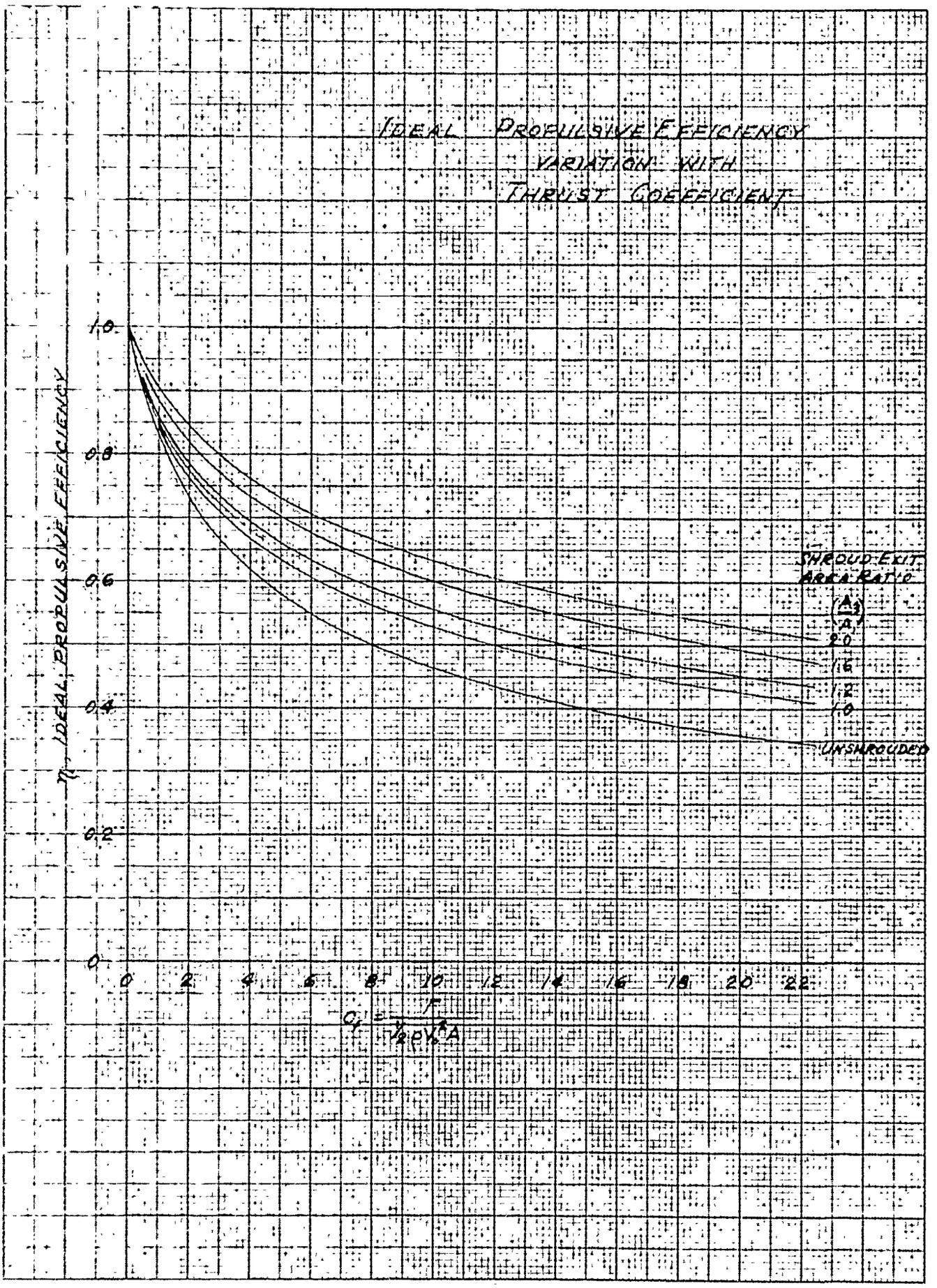

FIG. 1

FORM 20-20

CONFIDENTIAL

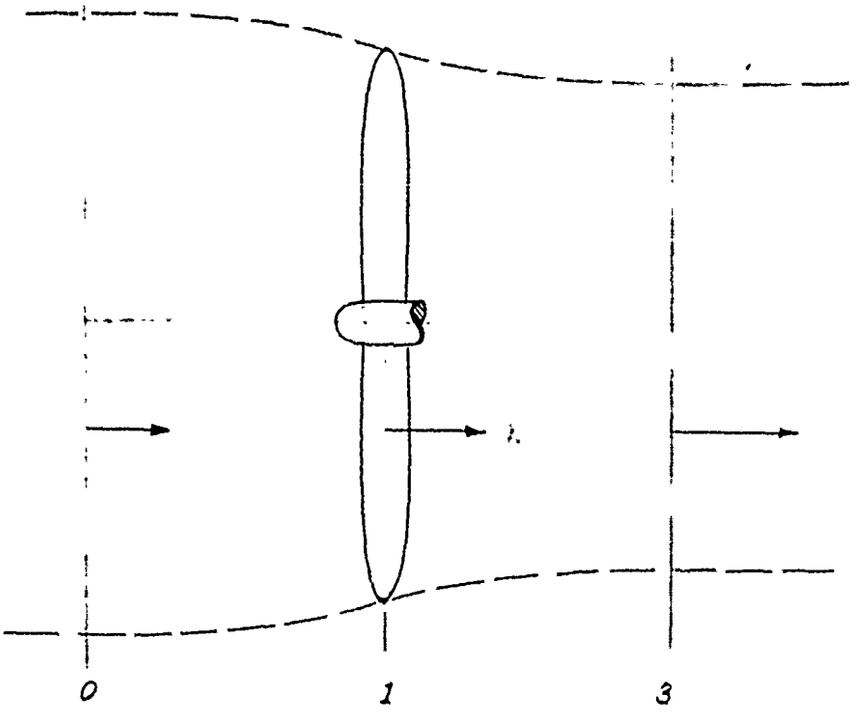

FIG. 2

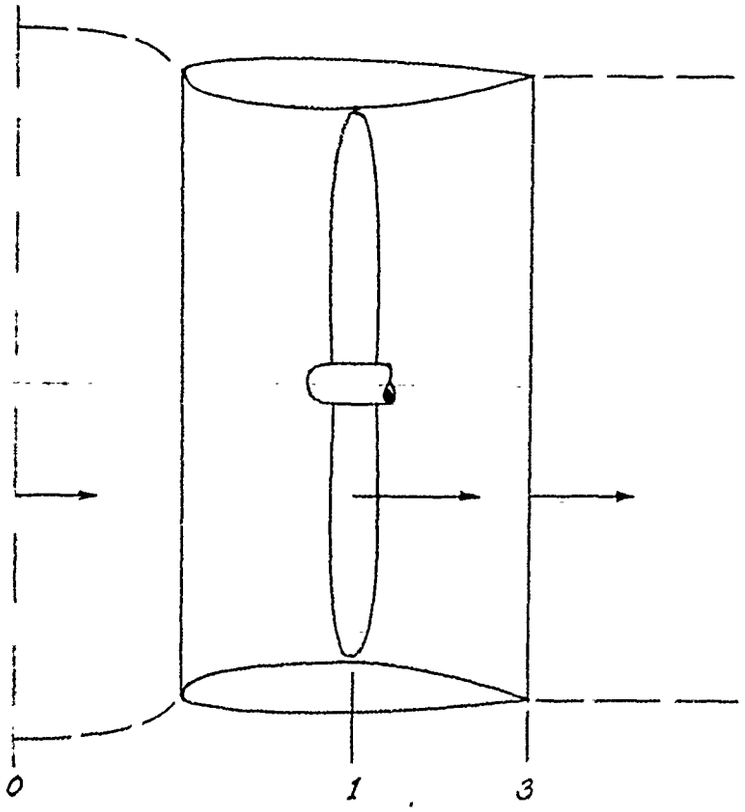

FIG. 3

CONFIDENTIAL

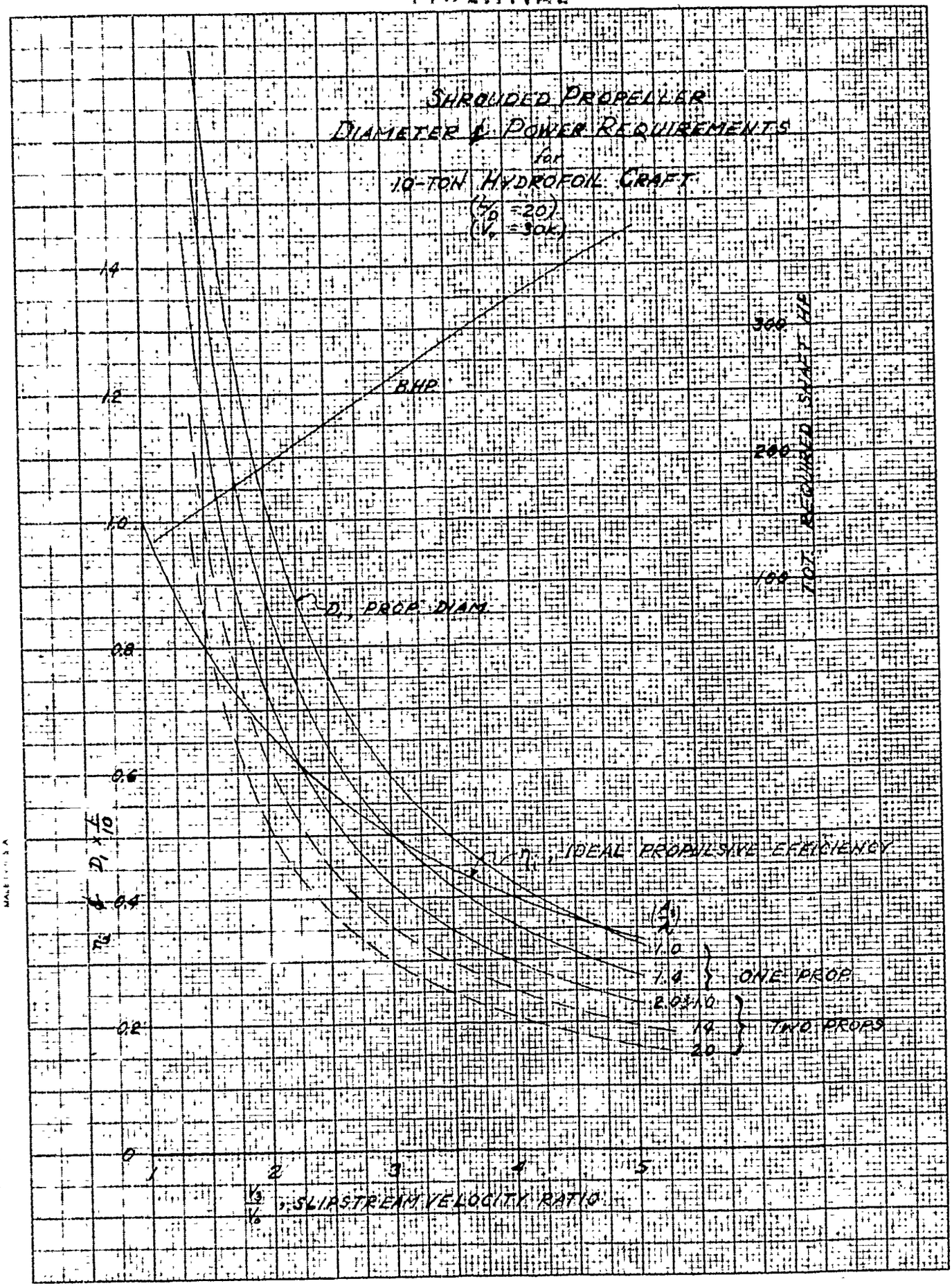

FIG. 4

3B

FORM 20-20

CONFIDENTIAL

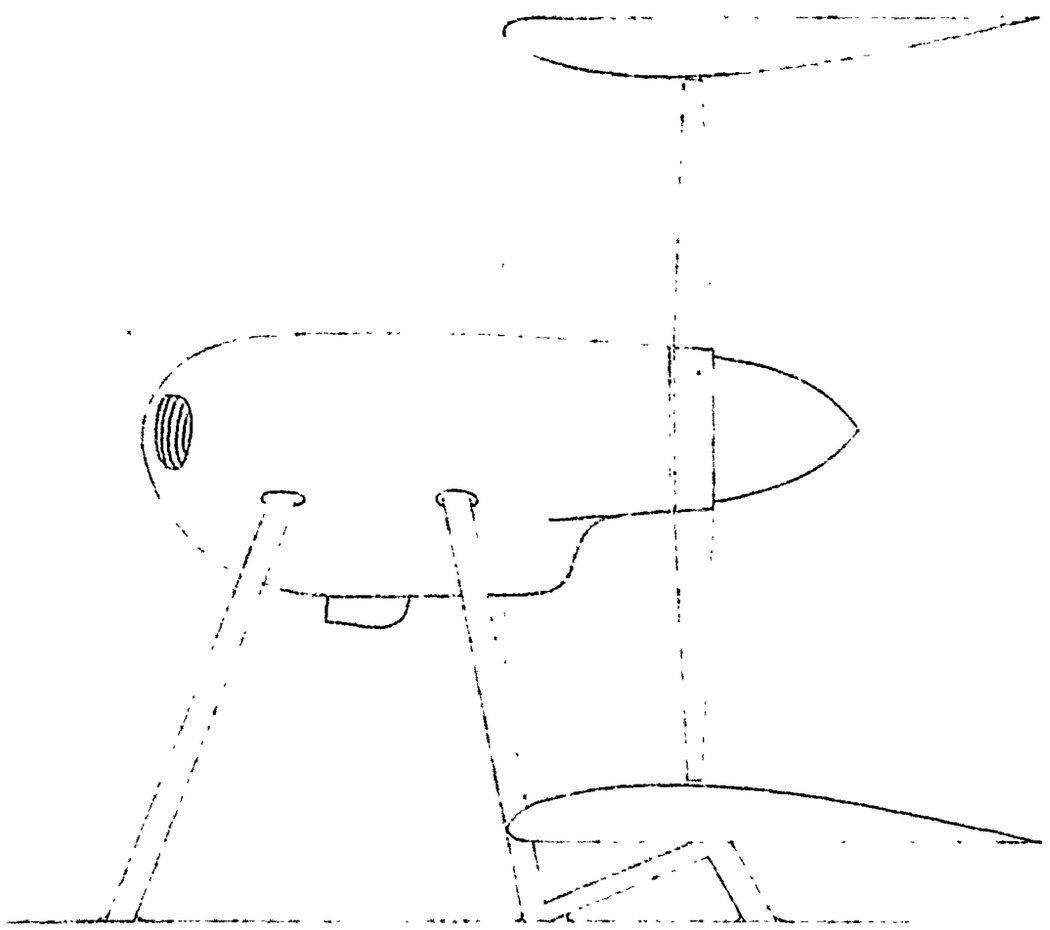

FIG. 5

CONFIDENTIAL

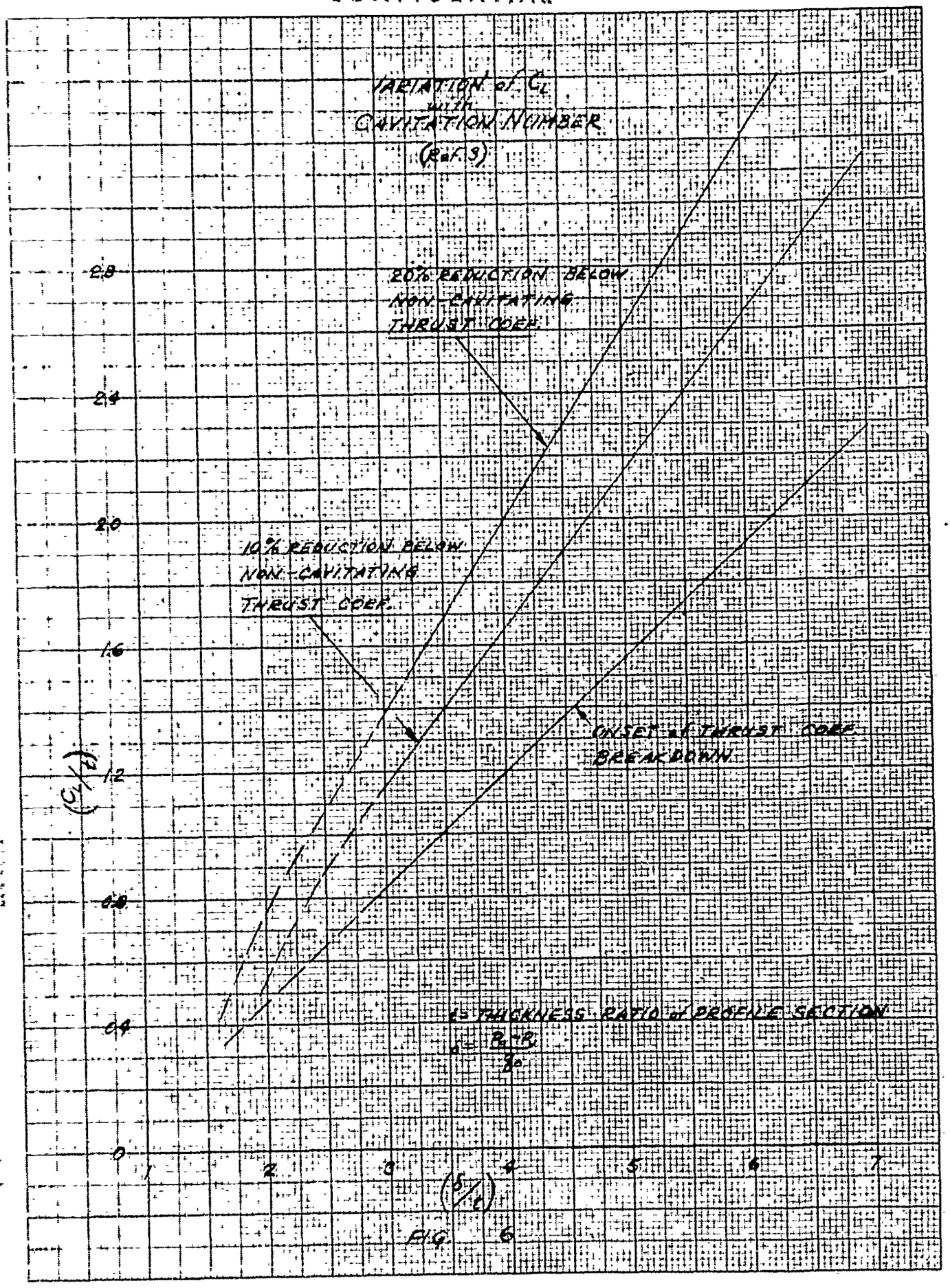

FIG. 6

CONFIDENTIAL

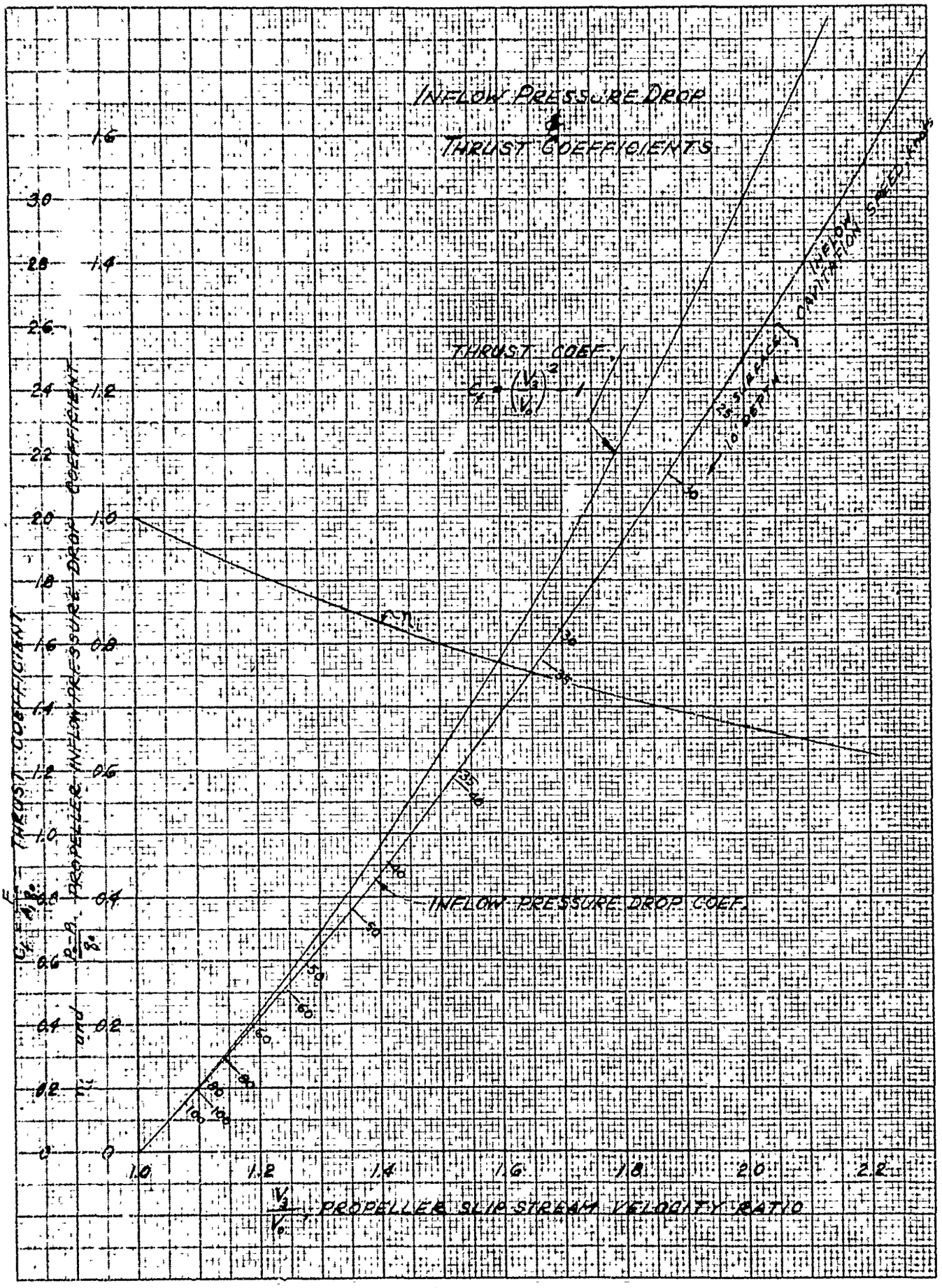

FIG. 7

CONFIDENTIAL

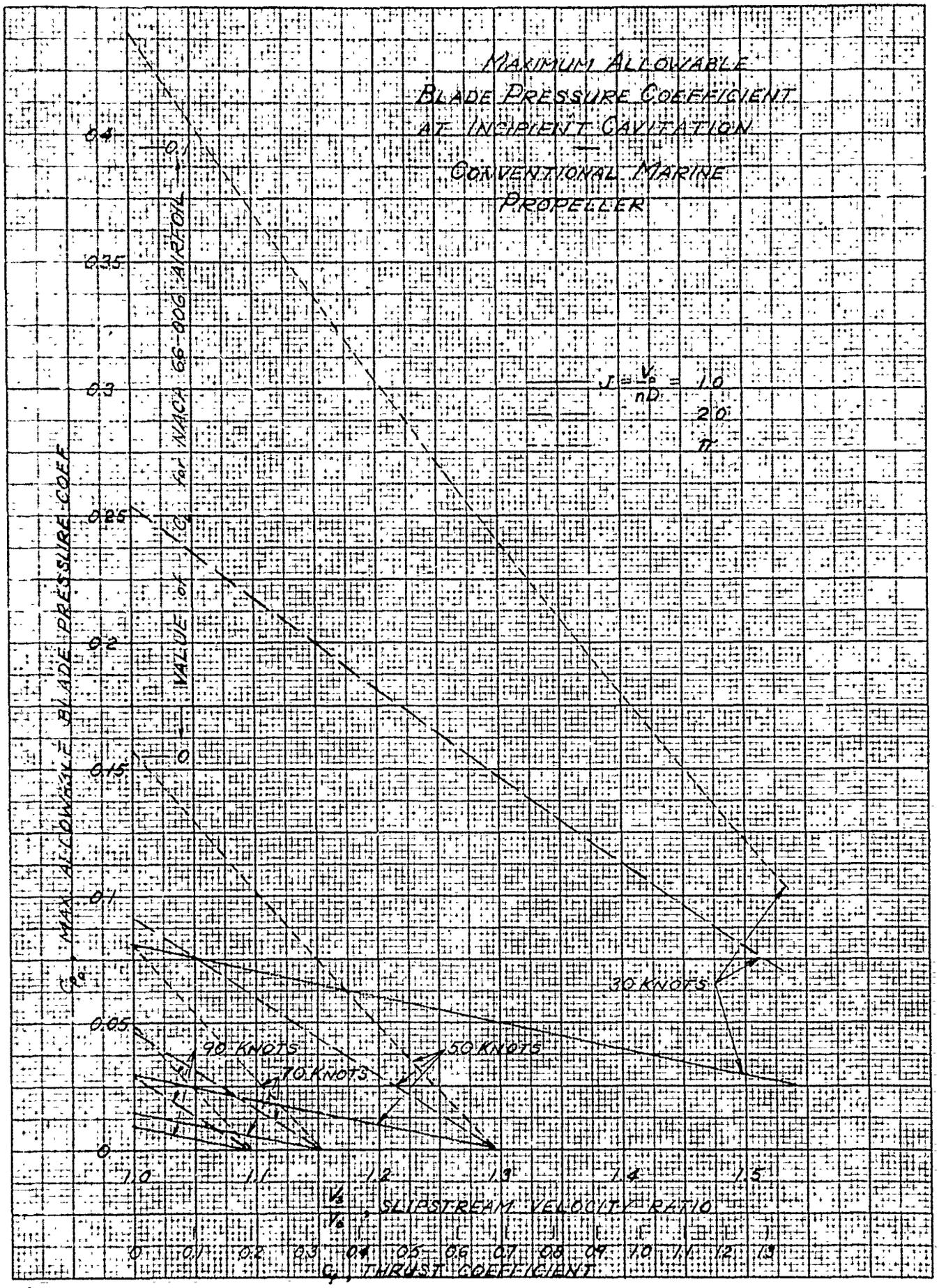

Bearing 1-18-50

FIG. 8

FORM 20-20

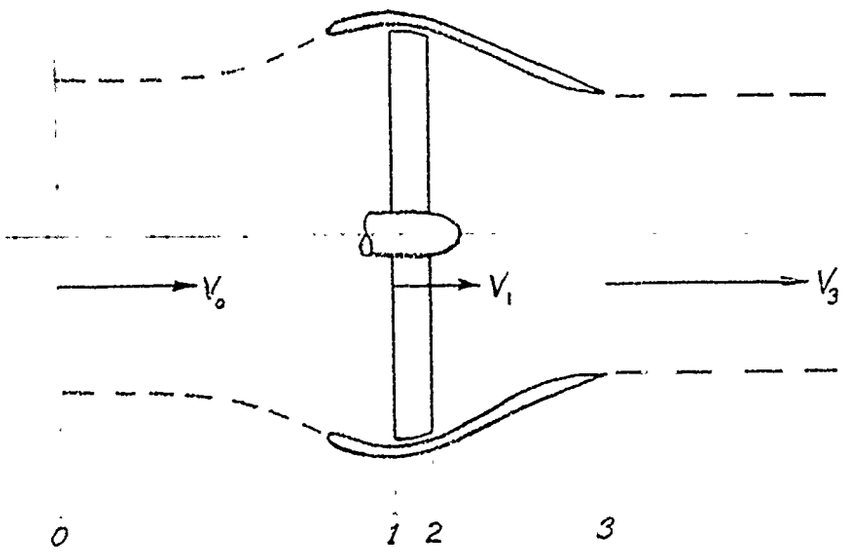

Fig. 9

Berkeley 11-16-49

8 B

CONFIDENTIAL

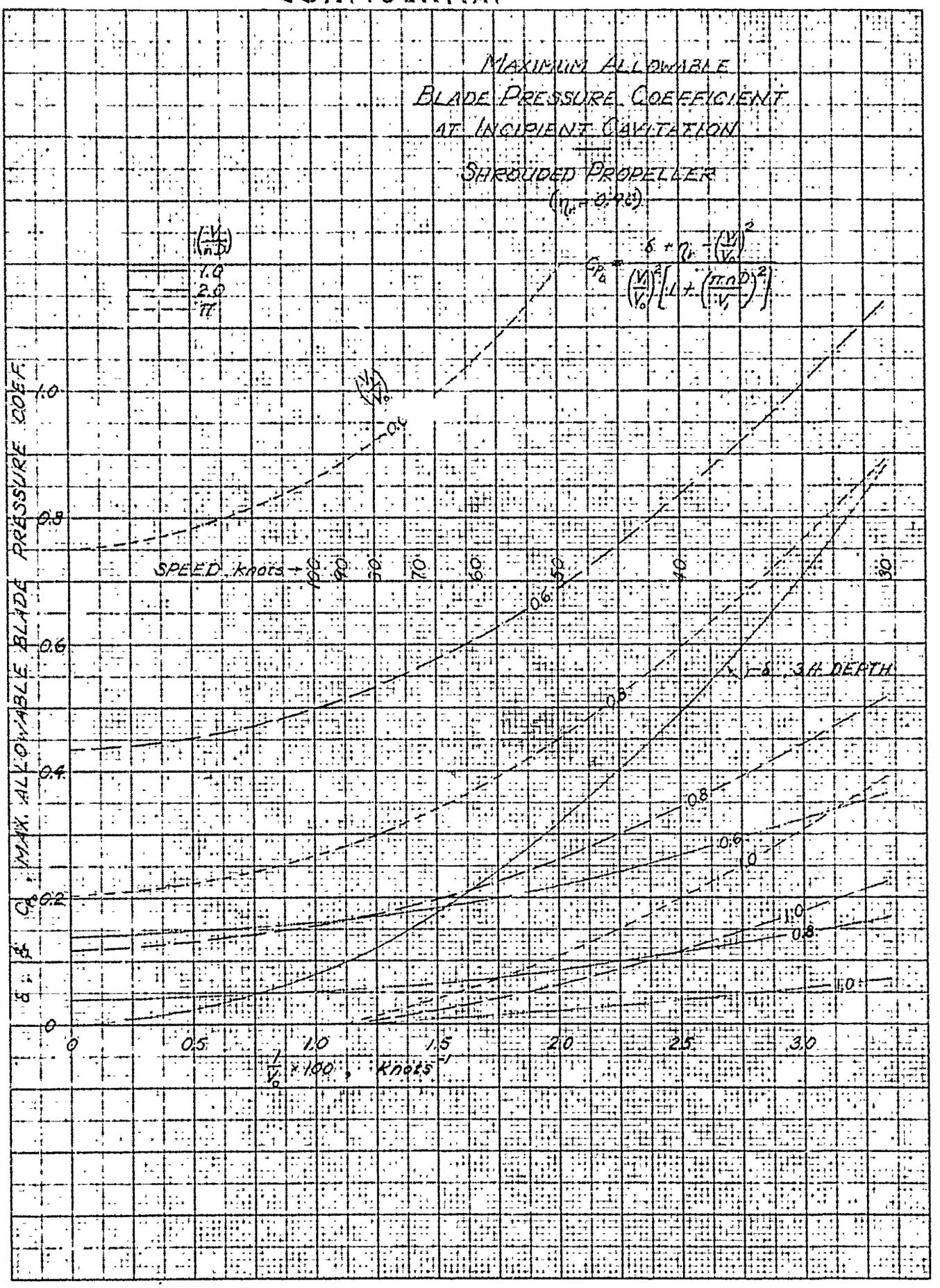

FIG. 10

9.B

CONFIDENTIAL

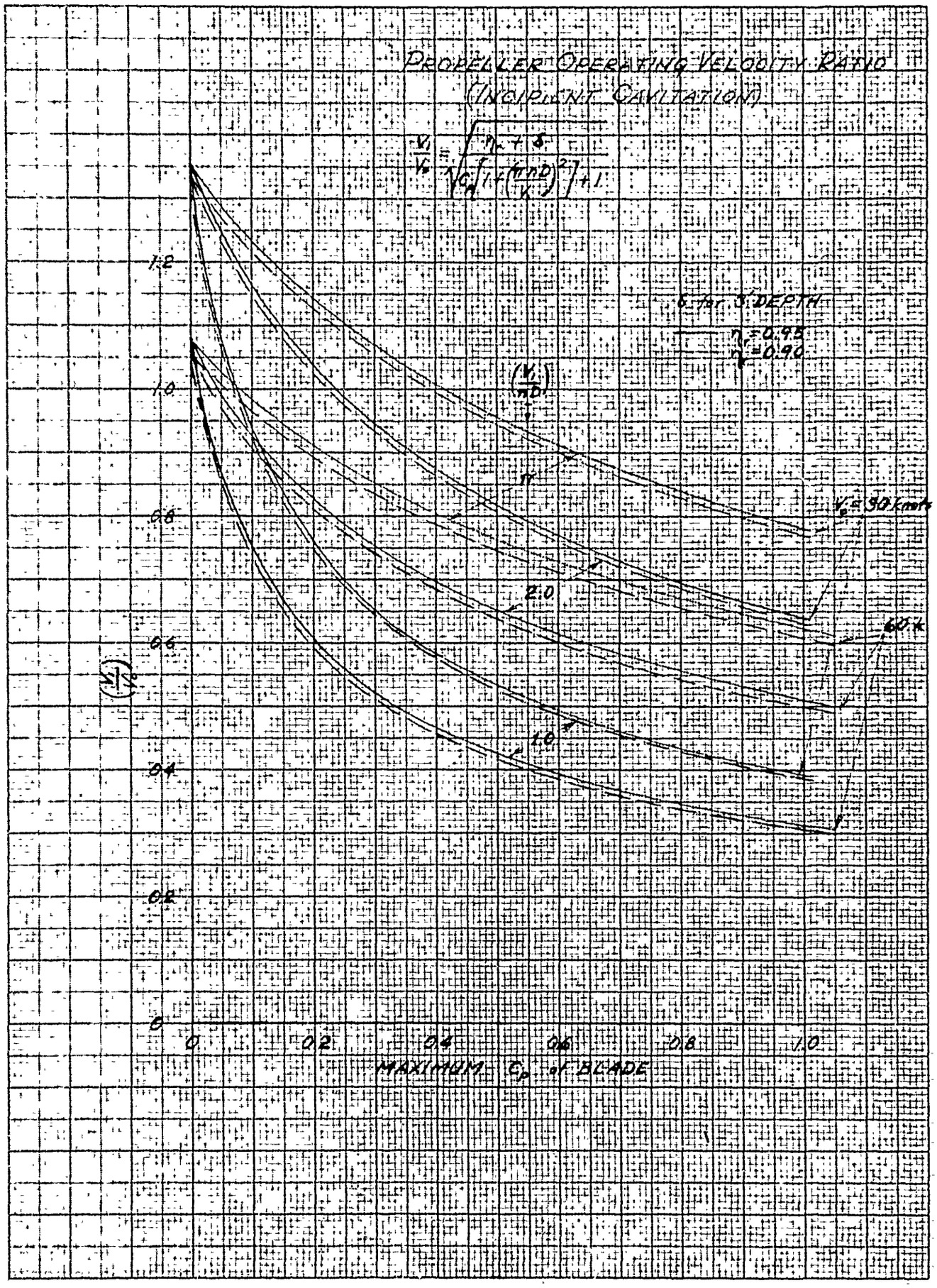

FIG. 11

CONFIDENTIAL

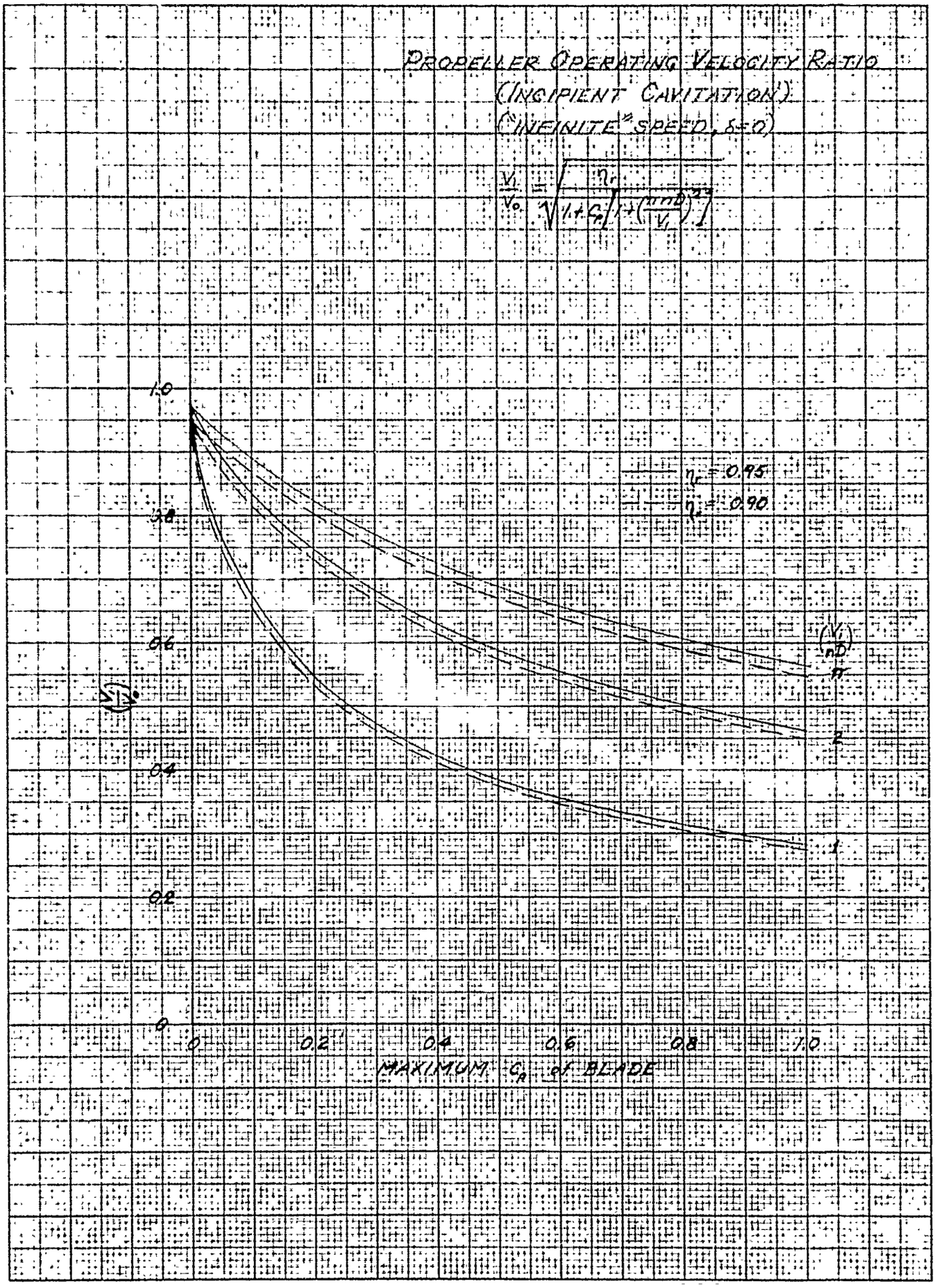

FIG. 12

CONFIDENTIAL

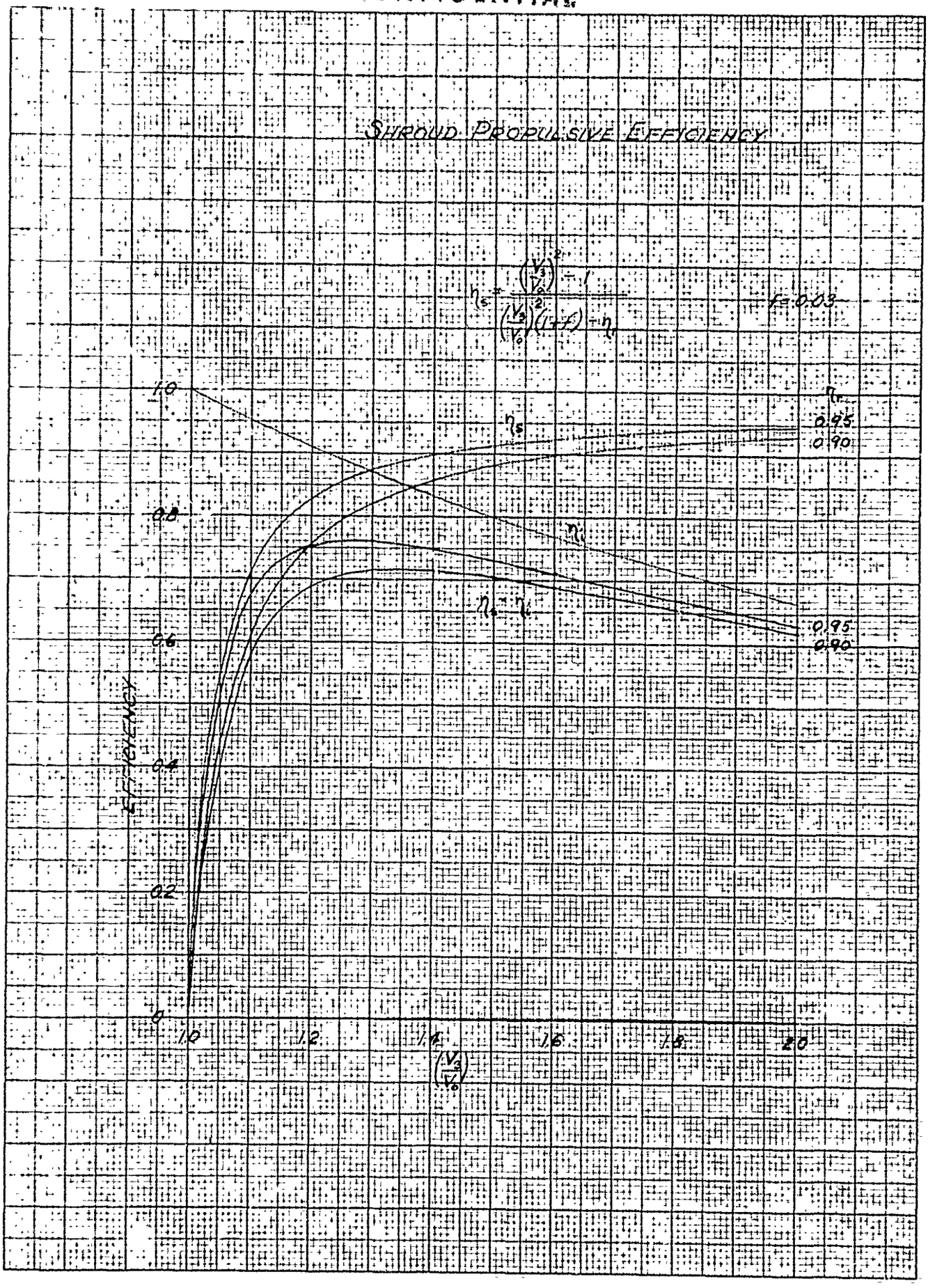

FIG. 13

KEUFFEL & ESSER CO., N. Y. NO. 359 12
10 X 10 to the ½ inch, 5th lines accented
MADE IN U.S.A.

C O N F I D E N T I A L

REPORT OF TRIALS

14-FOOT HYDROFOIL TEST CRAFT

"THE FLYING FISH"

W. C. Holmes, Jr.
W. H. Amster

Contract No. N9onr-93201

June 1950

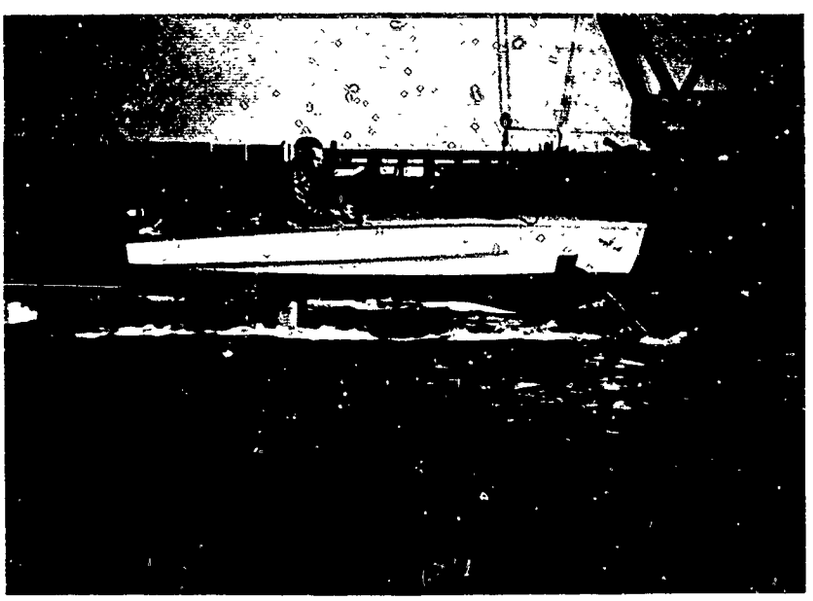

CONFIGURATION I Completely Submerged Main
Foil and Bow Planing Surfaces 28 April 1950

COLOR

3

COLOR

CONFIGURATION II Completely Submerged Main and Tail Foils With Automatic Stabilization
22 June 1950

TEST OBJECTIVES

DESCRIPTION OF CRAFT

TEST METHODS

TEST RESULTS

TOWING TESTS

SELF-PROPELLED TESTS

CONCLUSIONS

FIGURES

1. TOTAL DRAG AND EQUIVALENT HORSEPOWER
2. COMPONENT DRAGS AND EQUIVALENT HORSEPOWERS
3. OPERATING (L/D) AND GLIDING COEFFICIENT
4. EFFECT OF BOW SURFACE LOADING UPON PERFORMANCE
5. OPERATING REYNOLDS NUMBERS

PERFORMANCE ANALYSIS

GEOMETRY

BRIEF HISTORY OF CONSTRUCTION AND TESTS OF CRAFT

INTRODUCTION

Based upon theoretical investigations and reviews of available literature on the subject, certain predictions have been made with regard to performance and stability characteristics to be expected of hydrofoil craft designed to obtain high values of (L/D). It was considered highly desirable to obtain full-scale test data against which to check the theoretical analyses upon which the predictions are based. A small hydrofoil craft, designed to carry four people, was constructed for the purpose of obtaining qualitative and quantitative performance and stability test data under actual operating conditions. Primary structural components were fabricated of laminated fibreglass, in order to obtain information regarding the use of this material for hydrofoil craft construction.

TEST OBJECTIVES

The primary objective of tests of the full-scale hydrofoil craft was to verify, under actual operating conditions, the validity of methods of performance prediction developed in theoretical studies of the subject. It was also desired to obtain, as a secondary objective and as time permitted, information regarding automatic control and stabilization of a hydrofoil craft which utilized completely submerged main and auxiliary foils as its primary lifting elements. The objectives of the tests were realized by the use of two essentially separate configurations, although the same basic power plant, hull, and main strut-foil combination were used in both.

DESCRIPTION OF CRAFT * Performance Tests, Configuration I

It was desired to obtain performance test data at a minimum expenditure of time and funds. Accordingly, an existing fibreglass fourteen-foot runabout hull was modified for installation of a two-strut high aspect ratio main hydrofoil, two auxiliary bow planing stabilizing surfaces, and a standard ten horsepower outboard motor with extended shaft.

The laminated fibreglass main foil and struts were contoured by hand grinding, filing, and sanding. They are considered to represent a practical minimum of manufacturing control, since no special effort was made to hold the usual tolerances of particular profile sections. Contouring was continued, rather, until the foil was considered to represent the general characteristics of typical high-speed profiles similar to the NACA 65-015, while the strut was of rectangular section with ogival leading and trailing edges to the one-quarter and three-quarter chords, respectively.

The bow planing surfaces consist of flat steel plates, of length two feet and width one foot, supported by tubular steel struts attached to the hull. They were adjusted to planing angles of 12.5 degrees with the craft in its design cruise attitude (hull bottom 12 inches above water).

TEST METHODS * Performance Tests, Configuration I

Net drag of hydrofoil craft was determined by towing and measurement of required thrust by a simple spring scale. Runs were made at various combinations of speed, gross weight, and center of gravity location. Drag of the basic hull was determined by towing it with the main struts and foil and bow struts and foils removed. All towing runs were made with the engine removed.

Qualitative tests were made by running the craft, under its own power, in both calm and choppy water, at various combinations of speed, gross weight, and center of gravity location. Observations were made of the handling characteristics, turn performance, landing and take-off characteristics, and general operating requirements. Time and funds did not permit installation of accelerometers or other desired instrumentation.

TEST RESULTS * Performance Tests, Configuration I

Towing Tests

Results of the towing tests are indicated by Figure (1). In order to check the theoretical analyses developed for prediction of hydrofoil craft performance, performance of the test craft was predicted without reference to the test data, in accordance with the methods outlined in the Hydrodynamics section of the general Hydrofoil Studies report. As indicated by the figure, agreement between the predicted and test data is highly encouraging. Details of the method of prediction are shown in a separate section of this report.

Figure (2) indicates the order of magnitude of each of the component drags and equivalent horsepowers. As indicated, the drags and powers of the main foil and struts appear entirely acceptable, in view of the relative lack of rigid manufacturing control exercised in their fabrication. It would appear that practical, rather than laboratory, manufacturing techniques will suffice for fabrication of high performance hydrofoil craft.

Figure (2) also indicates the order of magnitude of the penalties involved in the use of stabilizing members which rely upon contact with the water surface for their action, verifying the theoretical conclusions drawn in the general Hydrofoil Studies report. It is considered probable that, although some improvement in bow surface characteristics

could be realized with more careful design, the penalties indicated appear to be of the order inherent in the type of design which relies upon planing surfaces for stabilization.

Figure (3) indicates the operating values of (L/D) and Gliding Coefficient realized with the test craft and its various components. Here, again, the main foil and struts appear entirely satisfactory, whereas the bow planing surfaces act to modify the values for the entire craft to less spectacular values. It is interesting to note, however, that the bow surfaces, although showing rather poor performance, compare favorably with conventional hull shapes at similar Froude Numbers. For example, at sixteen miles per hour, with bow surface wetted length of nine inches, load of seventy-three pounds, and drag of thirty-three pounds, the Froude Number is 4.78 and Gliding Coefficient 0.453. This compares favorably with the values given both by Tietjens and Curry, and appears to indicate that the drag breakdown derived is quite reasonable.

Figure (4) indicates the effect of bow surface loading upon total craft drag. As indicated, movement of the craft center of gravity toward the bow surfaces produces a deleterious effect upon total drag by increasing the bow surface drag at a greater rate than the main foil drag is decreased by its reduction of loading. This is, again, in accordance with the theoretical conclusion that maximum craft efficiency is obtained by carrying the greatest possible portion of the total load on the main, more efficient lifting surface.

It is encouraging to note that the theoretical predictions of performance of the test craft show excellent agreement with test results, even though the operating conditions did not in all respects represent the conditions assumed in development of the theory. As indicated in the Hydrodynamics section of the general Hydrofoil Studies report, it is expected that full-scale hydrofoil craft operations will be at Reynolds Numbers of at least 500,000 to 50,000,000, with the greater majority of cases of interest having minimum values of over one million. The operating Reynolds Numbers of the various test craft components are shown by Figure (5) and are seen to be at the lower range of values assumed in the theoretical studies. The agreement between theory and test, even at these low Reynolds Numbers, is considered to strengthen the practical usefulness of the theory.

Self-Propelled Tests

Observations of general handling and operational characteristics were made at various combinations of speed, gross weight, and center of gravity location, in both calm and rough water. Comparative trials were made in rough water, using a hull identical to the test craft hull, as the basis of comparison.

Operation in relatively rough water in the outer Los Angeles harbor on a windy day indicated that the hydrofoil craft's handling qualities in waves up to about two feet in height are remarkably smooth. Comparisons with an identical hull under the same conditions showed the hydrofoil craft, even with its susceptible bow foils planing on the water surface, much less subject to pounding, spray, or directional instability. The conventional hull, equipped with a sixteen horsepower outboard motor, could keep up with the hydrofoil craft only when the test craft's ten horsepower motor was operated at about half-throttle.

Operation in water rougher than that in the outer harbor was not attempted, although runs were made at various speeds up to about twenty knots across the wakes of large vessels, such wakes running as high as four feet, without affecting the hydrofoil craft's performance beyond the initial disturbance as the bow surfaces attempted to follow the wake contours. Complete damping after such disturbance was affected in one to two cycles.

Extensive runs made in calm and choppy water indicated that the craft is stable about all three major axes, with longitudinal (pitch) stability most positive. Directional (yaw) stability is positive, although more subject to disturbance than is the longitudinal case. This could of course be expected of a configuration which is, essentially, a canard with thrust application far aft of the main foil.

Lateral (roll) stability is positive, although somewhat more critical than are the other two cases. The craft showed a slight tendency to roll away from the direction of a turn, a characteristic which became more noticeable as the turn radius was shortened, bow surface load reduced, or speed increased. This tendency was not, however, considered at all dangerous and is, in fact, not surprising when it is realized that control of the craft was affected entirely by rudder action of the outboard motor. Present efforts are being made to modify the craft to include control surfaces on the main foil. It is anticipated that roll characteristics will be improved by this modification. The tendency to roll could also, of course, be reduced by increasing the lateral separation of the bow planing surfaces.

Attempts to determine the greatest angle to which the craft could be rolled indicated that there is little danger of upsetting a craft of this type. High speed turns were the only means by which rolls could be induced, since only rudder control was provided. The procedure then involved entering a turn at high speed, then tightening the turn until the maximum roll angle was attained, it being of course in the opposite direction from that of the turn. It was found that roll angle was limited by the angle at which the rising foil tip broke water. Lift would immediately drop on that side of the foil, and a strong restoring moment would result. The craft usually merely returned to an equilibrium attitude. At worst, the foil would stall and the craft would land.

Take-off and landing characteristics were much smoother than at first anticipated. No sudden transition, or jerk, was apparent. Both take-offs and landings, on the contrary, were characterized by gradual changes in craft height and attitude as the load was transferred from the hull to the foil. Application of full power from a standstill produced an appreciable acceleration without marked changes in equilibrium. Landings, even when power was suddenly shut off at high speed, involved merely a smooth glide to the normal displacement condition. It is anticipated that take-off and landing procedures for large hydrofoil craft will be much less complicated than for aircraft, and will be much more amenable to completely automatic control.

Although no attempt was made to design the craft for high speed, it is interesting to note that a speed of 23.9 miles per hour was maintained over a measured course, at a gross weight of 621 pounds. Take-off was at seven to eight miles per hour. Time and funds did not permit measurement of net thrust, but it is estimated that the ten horsepower outboard installation gave a net propulsive efficiency of the order of fifty percent.

Load carrying capabilities of the test craft appeared highly encouraging. Empty weight, without crew, was 451 pounds. Successful take-offs and operation up to about twenty miles per hour were made with up to four passengers at a gross weight of 1161 pounds.

A point of interest, although not part of the formal testing program, was noted when attempts were made to tow the craft with only the main foil in the water. This required movement of the center of gravity to a point over, or slight aft of, the foil center of lift, such that the bow surfaces carried no load and could be held clear of the water. In this attitude, the craft appeared to be completely oblivious of choppy surface conditions, indicating that completely smooth operation might be expected of configurations in which all lifting foils are below the water surface.

DESCRIPTION OF CRAFT * Stability Tests, Configuration II

In accordance with the secondary objective of tests of the full-scale hydrofoil craft, and after completion of the performance tests in which methods of performance prediction received verification, the craft was modified as necessary to obtain qualitative information regarding control and stabilization of a craft with completely submerged main and stabilizing hydrofoils.

The planing bow surfaces incorporated in the first configuration were removed, and a submerged tail foil was installed. In order to eliminate the necessity of relocating the main foil and struts, and to provide the proper separation between main and tail foils, the tail strut-foil combination was mounted below a tubular steel boom extending aft of the hull transom. The tail foil and strut were fabricated of laminated fibreglass by hand grinding, filing, and sanding.

Provisions for height sensing at the main struts were made by installing a series of eight pitot tubes along the leading edge of each main strut. Hydrodynamic pressure transmitted through the tubes operated bellows, which in turn controlled small electric motor flap servo-actuators. Quarter-chord, fifteen percent span trailing edge flaps were installed on the main foil adjacent to each main strut, with twenty degree positive or negative travel.

Electric power for the flap and tail position actuators was provided by four six-volt motorcycle storage batteries in series. A control panel, including flap and tail position indicators and manual overide controls, was mounted on the main dash panel of the craft. Since, as far as possible, components of the autopilot and actuator assemblies were assembled from available war-surplus items, the system can be considered to represent a minimum of design refinement.

TEST METHODS * Stability Tests, Configuration II

Tests of the stabilization system were entirely self-propelled, with qualitative observations of characteristics made both from the craft itself and from shore stations. Time did not permit installation of accelerometers, nor the collection of quantitative test data. Observations were made of handling characteristics during take-off, cruise, and landing operations, in relatively smooth water. It should be noted that termination of the basic contract prevented either refinement of the initial stabilization system, or continuation of the tests.

TEST RESULTS * Stability Tests, Configuration II

Trials of the modified test craft indicated the entire feasibility of stabilization of craft which utilize entirely submerged main and auxiliary foils. Time did not permit refinement of the tested system to the degree of perfection which would be considered desirable. The results obtained, however, were considered highly encouraging in spite of the tested system's shortcomings.

All trials of the modified configuration were conducted with either two or three passengers, at gross weights from 960 to 1160 pounds. Weight of the craft without crew was 600 pounds.

Initial runs with the craft were made with a crew of two, during which familiarization with its handling characteristics was of prime importance. After several short preliminary runs during which manual operation of the controls was affected to familiarize the crew with the craft's response characteristics, take-off was successfully attempted. Starting from rest, a run of approximately five boat lengths was required before the craft was completely foilborne. The craft climbed steadily until the depth sensing pitot tubes affixed to the main struts properly actuated the flap and tail trim servo motors. The craft responded to the flap and tail foil motions, and assumed a level flight attitude at approximately the design height above the water surface. Similar runs were repeated, with "flight" distances of 500 to 600 yards successfully attained.

During these trials the effects of design compromises in the flap actuation system became apparent. Assembly of the configuration had been made with expediency, rather than perfection, as the prime consideration. A great deal of mechanical looseness was therefore present in the actuating system. It was expected that operation of the mechanisms would be somewhat compromised by such looseness, but it was considered highly probable that proof of the basic stabilization concepts could be attained in spite of the mechanical defficiencies. Such was found to be the case.

Two types of "hunting" motion were noted, both attributed primarily to mechanical looseness of the actuation system. A rising and falling oscillatory motion sometimes developed and either damped out or became of sufficient magnitude to permit the hull to hit the water surface. A long period rolling oscillation also sometimes developed and either damped out or became excessive. Observations of the flaps during both types of oscillation indicated that elimination of the mechanical looseness present would in all

probability prevent such behavior. It is considered entirely probable that the types of oscillation observed were actually imposed upon the craft by the mechanical looseness, rather than inherent characteristics, and that a minimum of further development time is required to provide an entirely satisfactory automatic stabilization system for the test craft.

To the best knowledge of personnel of this project, operation of the modified test craft represented the first occasion in which a hydrofoil craft was successfully operated and stabilized by completely submerged main and auxiliary hydrofoil surfaces which did not rely upon contact with the water surface for their proper stabilizing action.

CONCLUSIONS

As a result of tests of the fourteen-foot hydrofoil craft, certain conclusions can be drawn with respect to the general subject of design and operation of hydrofoil craft.

1. Although a certain degree of care must be maintained in fabrication of hydrofoil components, practical, rather than laboratory, tolerances should be entirely acceptable for the design of high (L/D) craft. As in the cases of both aircraft and conventional surface craft, greater refinement of manufacturing techniques will be required as emphasis is shifted from high load-carrying to high speed requirements.

2. Power requirements of hydrofoil craft can be made much lower than those of conventional displacement or planing craft at the same gross weights and operational speeds. Top speeds, with the same power, can be increased.

3. Satisfactory stability and control characteristics can be demonstrated with hydrofoil craft, without exorbitant sacrifices of performance.

4. The configuration which utilizes a completely submerged high aspect ratio main lifting foil, plus completely submerged auxiliary control foils, appears to offer considerable promise for high-performance design.

5. Acceptable rough water performance can be demonstrated with hydrofoil craft, although more information is needed with respect to the upper limit to which this characteristic applies.

6. The most critical aspect of hydrofoil craft design appears to be concerned with power requirements during the take-off, or "hump", period immediately before the craft is fully foilborne. Every effort should be expended to arrive at a design which minimizes drag in this region.

7. Maneuverability of hydrofoil craft will probably be somewhat inferior to that of their conventional counterparts, although tactical requirements should dictate the degree to which this characteristic negates the advantages of greater speeds and lower power requirements.

CONFIDENTIAL

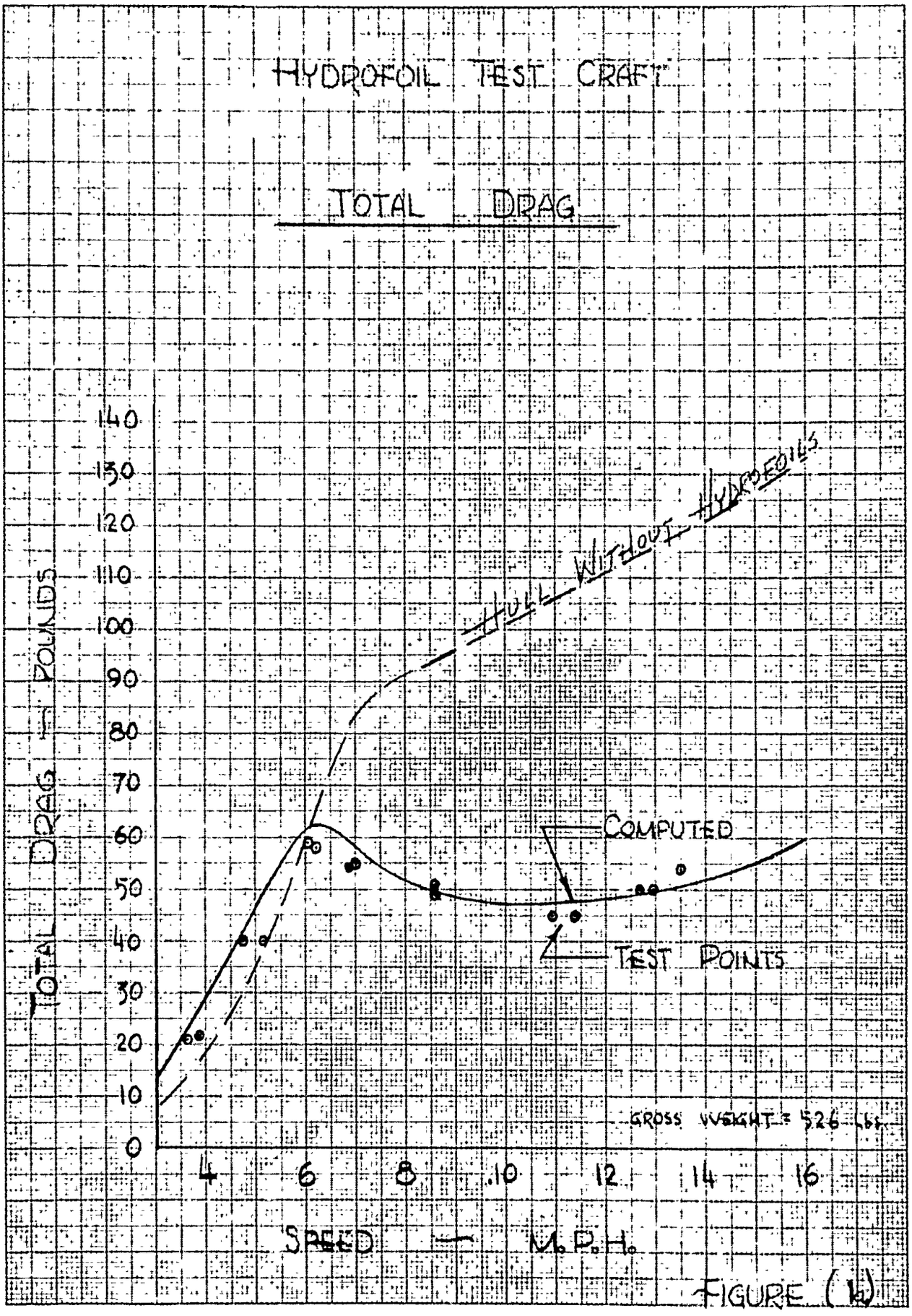

FIGURE (14)

CONFIDENTIAL

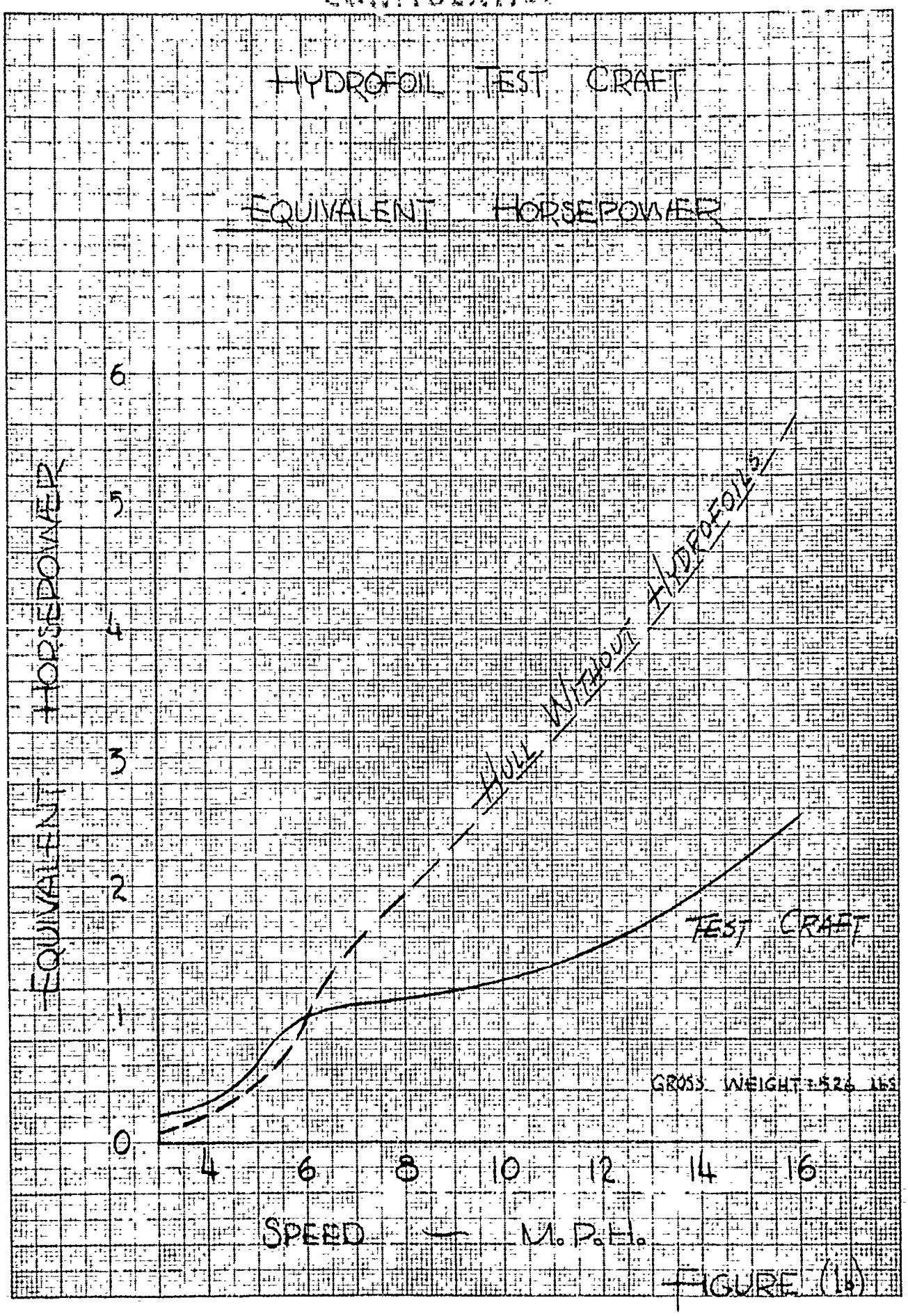

FIGURE (15)

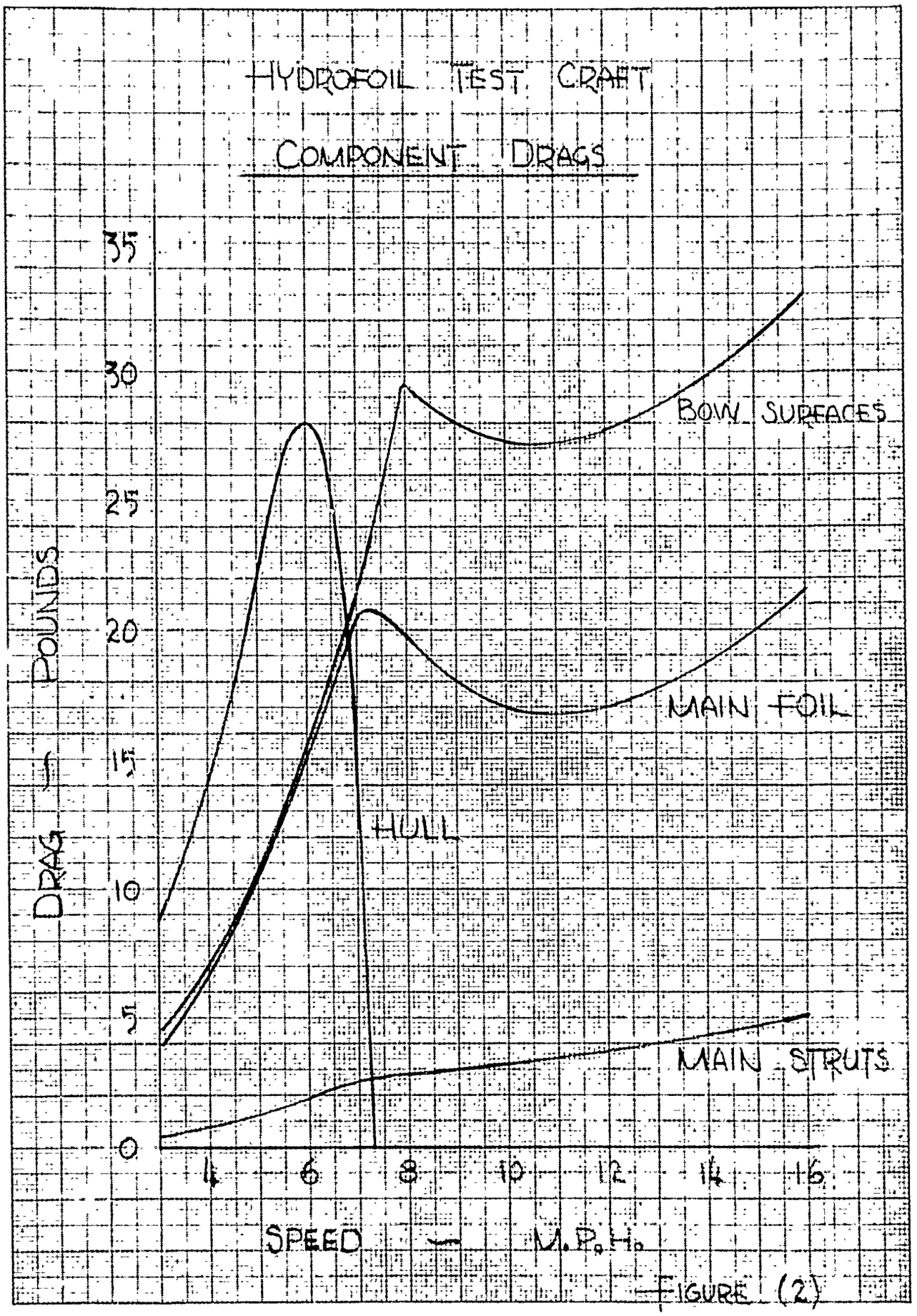
HYDROFOIL TEST CRAFT
COMPONENT DRAGS
DRAG IN POUNDS
35
30
25
20
15
10
5
0
4
6
8
10
12
14
16
SPEED — M.P.H.
BOW SURFACES
MAIN FOIL
HULL
MAIN STRUTS

FIGURE (2)

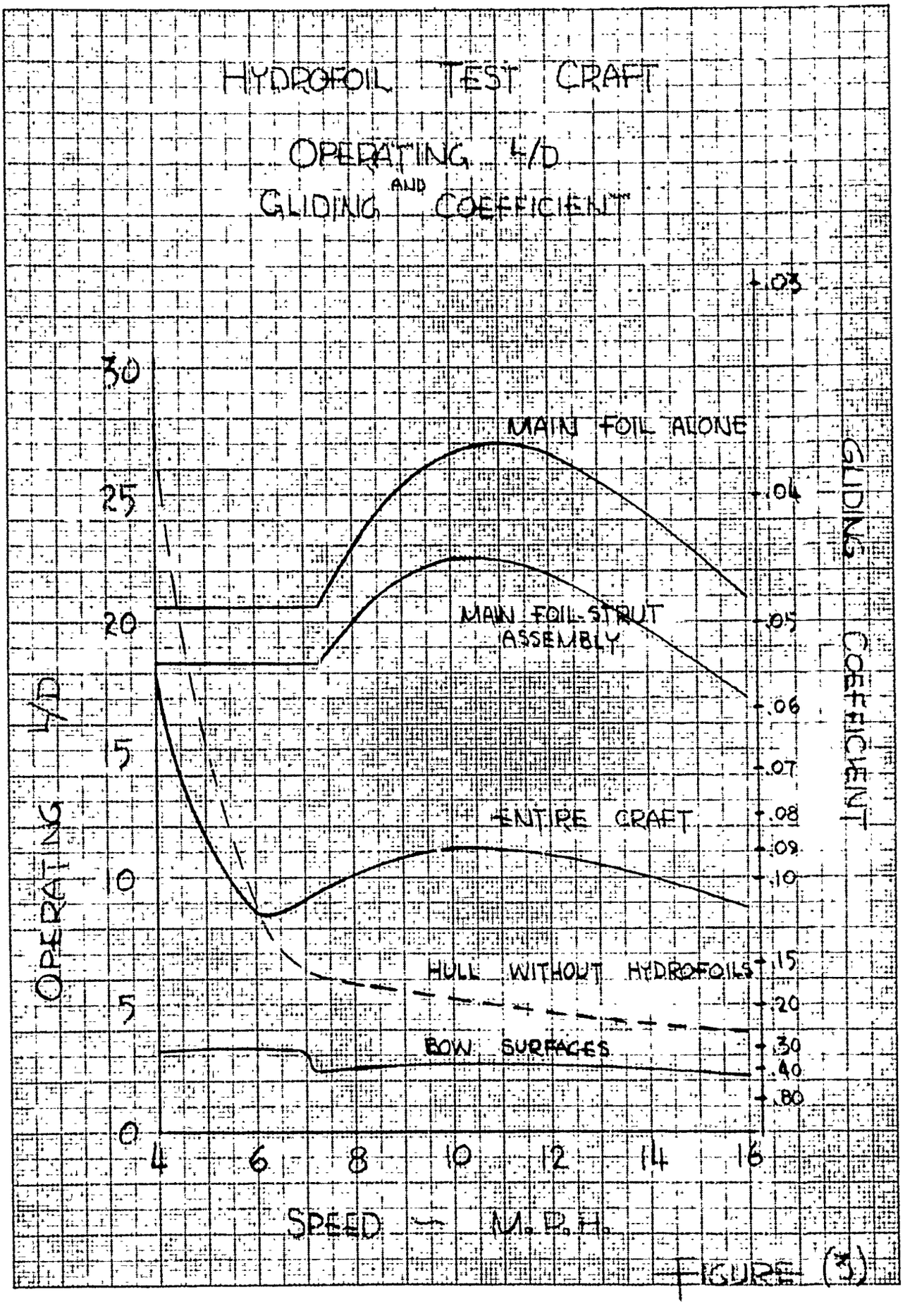
HYDROFOIL TEST CRAFT
OPERATING L/D AND GLIDING COEFFICIENT
OPERATING L/D
GLIDING COEFFICIENT
30
25
20
15
10
5
0
.03
.04
.05
.06
.07
.08
.09
.10
.15
.20
.30
.40
.80
MAIN FOIL ALONE
MAIN FOIL-STRUT ASSEMBLY
ENTIRE CRAFT
HULL WITHOUT HYDROFOILS
BOW SURFACES
4
6
8
10
12
14
16
SPEED — M.P.H.

FIGURE (3)

HYDROFOIL TEST CRAFT

EFFECT OF BOW SURFACE LOADING UPON CRAFT PERFORMANCE

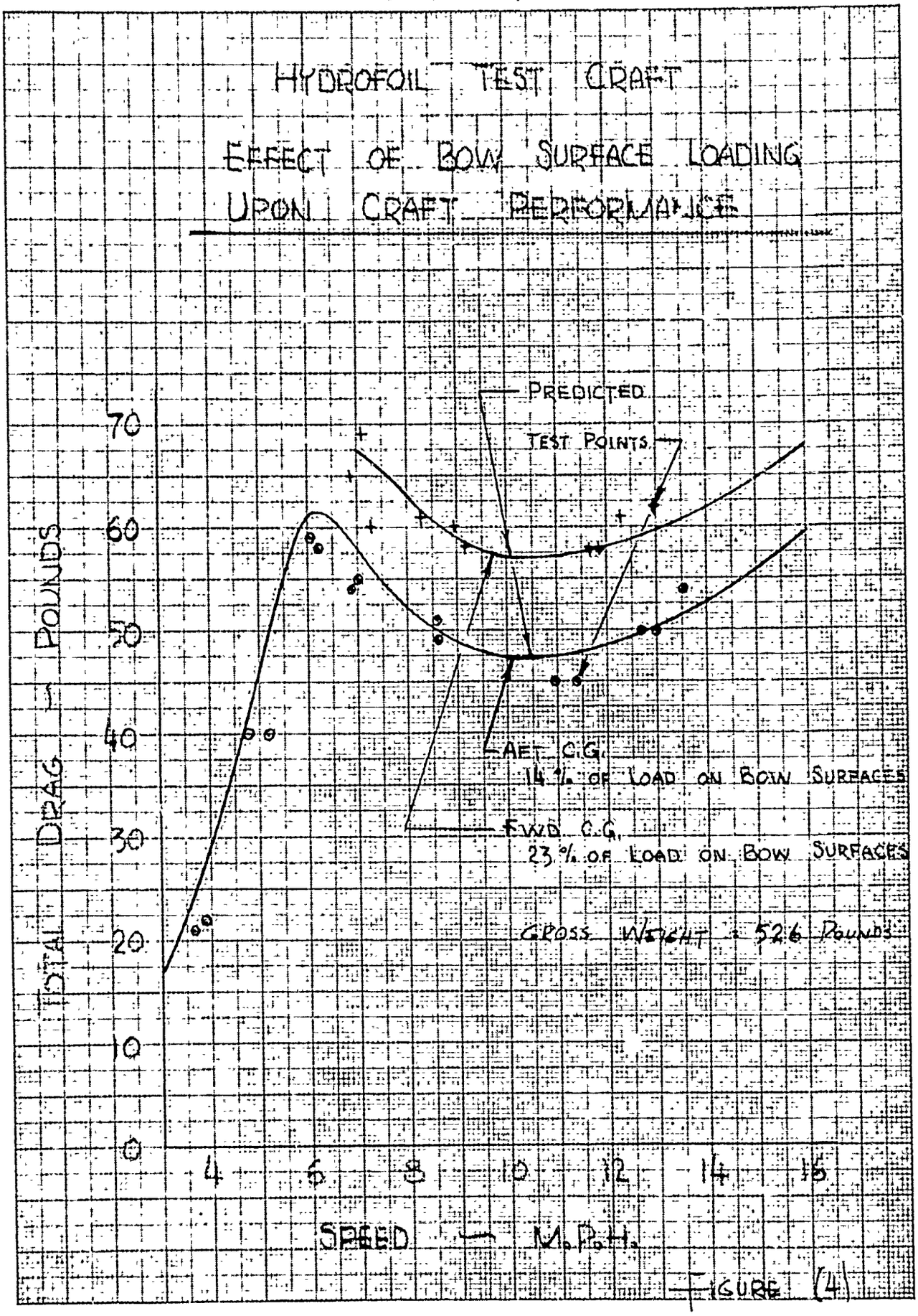

FIGURE (4)

CONFIDENTIAL

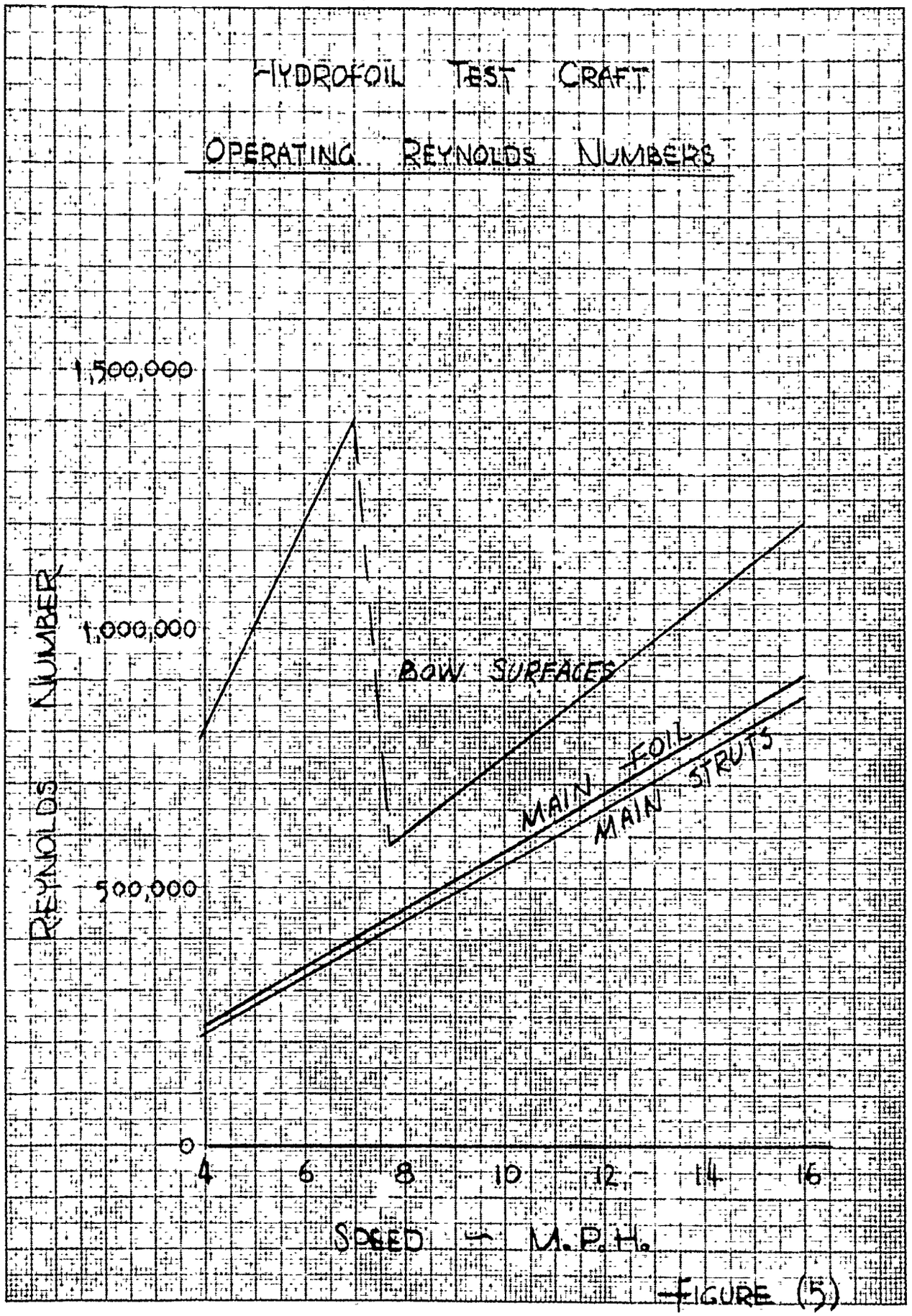

FIGURE (5)

6C

PERFORMANCE ANALYSIS

HYDROFOIL TEST CRAFT JH - 1

Prediction of performance of the hydrofoil test craft are made in accordance with the methods outlined in the Hydrodynamics section of the general Hydrofoil Studies report.

MAIN FOIL

Main foil drag is composed of profile drag (D_o), plus induced drag, (D_i).

(1) $$D_F = D_o + D_i$$

(2) $$D_o = C_{D_o} S q$$

$$C_{D_o} = 0.0048 + 0.10(t/c)_f^2 + 0.0050\, C_L^2$$

$$= 0.00705 + 0.0050\, C_L^2$$

S = foil area, 4.44 square feet

q = dynamic pressure, $2.15 V^2$

V = speed in miles per hour

$(t/c)_f$ = foil thickness in percent of chord, (0.15)

C_L = foil lift coefficient

(3) $$D_i = C_{D_i} S q$$

$$C_{D_i} = (1 + 0.025N) \frac{C_L^2}{\pi AR} (1 + \delta)(1 + \phi)$$

$$= 1.05\, C_L^2 \frac{K_i}{AR}$$

N = number of struts, (2)

AR = Aspect Ratio, (14.4)

δ = planform induction parameter

ϕ = surface reflection parameter

K_i = induced drag parameter

It is necessary to estimate the depth of submersion of the main foil at each operating speed in order to evaluate the induced drag. This can be accomplished by a process of iteration in which a lift curve slope is assumed, the corresponding foil angle of attack computed, then submersion established from the relationship

(4) $$h = 97 \tan(\alpha_F - 3^\circ) + 12.0$$

in which (h) is the submersion in inches and (α_F) the main foil angle of attack in degrees.

The process can be repeated by correcting the assumed lift curve slope as appropriate for the submersion established, then determining a new angle of attack and depth of submersion. It is considered highly probable, however, that such repetition is not warranted by the existing uncertainties with respect to exact foil characteristics and that entirely sufficient accuracy is obtained by assuming a lift curve slope corresponding to the design cruise condition and applying this value throughout the flight range.

The lift curve slope is defined by

(5) $$m = \frac{m_0}{1 + \frac{m_0}{\pi AR}(1+\tau)(1+\phi)}$$

in which (m_0) is the infinite aspect ratio section slope, (τ) is the slope induction parameter, and the other symbols are as defined previously.

For this foil,

$$m_o = 2\pi - 4(t/c)_F = 5.68$$

$$\gamma = 0.292$$

For the design cruise condition,

$$h_l = 12.0 \text{ inches}$$

$$\phi = 0.650$$

The lift curve slope is then

(6) $$m = 4.48$$

And the angle of attack at any lift coefficient can be approximated by

(7) $$\alpha_F = \frac{C_L}{m}(57.3) = 12.8\, C_L$$

in which the lift coefficient is defined by

(8) $$C_L = \frac{W_F}{Sq}$$

where (W_F) is the portion of the load carried by the main foil (453 pounds for the case under study).

At any speed after take-off, then, the depth of submersion can be determined, after which the induced drag parameter (K_i) can be established. It is tacitly assumed that prior to take-off the lift coefficient is limited to a value of 0.90.

The main foil profile and induced drags then becomes

(9) $D_o = (0.00705 + 0.0050\, C_L^2)(4.44)\, q$

$= (0.0313 + 0.0222\, C_L^2)\, q$

(10) $D_i = (1.05) C_L^2 \frac{K_i'}{R} (4.44)\, q$

$= 0.3232\, C_L^2 K_i'\, q$

MAIN STRUTS

Drag of the main struts is defined by

(11) $D_s = C_{D_s} S\, q$

$C_{D_s} = 1.5 N \frac{S_s}{S} \left[0.0048 + 0.10 \left(t/c\right)_s^2\right]$

in which (N) is the number of struts (2), (S_s) is the strut submerged area, (S) the foil area (4.44 sq.ft.), and ($t/c)_s$ the strut thickness ratio in percent of chord.

It can be assumed that the effective thickness ratio of the submerged struts is ten percent.

The submerged strut area is defined by

(12) $S_s = 6.5\, h + \frac{h^2}{32}$

whence the strut drag is

(13) $D_s = (1.5)(2)\left(6.5h + \frac{h^2}{32}\right)\left(\frac{1}{144}\right)(0.0058)\, q$

$= \left[7.86 \times 10^{-4} h + 3.78 \times 10^{-6} h^2\right] q$

HULL DRAG

Hull drag is estimated by correcting known hull characteristics for changes in displacement as lift is transferred from the hull to the hydrofoils. Towing tests of the hull, with struts and foils removed, were made to establish its resistance at the same gross weight as that of the hydrofoil craft.

Net hull displacement prior to take-off is estimated by

$$W_H = W\left[1 - \left(\frac{V}{V_{TO}}\right)^2\right] \tag{14}$$

in which (W_H) is net hull displacement

(W) is total craft gross weight (526 pounds)

(V) is speed in miles per hour

(V_{TO}) is take-off speed in miles per hour (7.26 mph at main foil lift coefficient of 0.90).

It is then assumed that hull resistance varies from the experimental values with the two-thirds power of the displacement ratio.

$$D_H = R_H \left(\frac{W_H}{W}\right)^{2/3} \tag{15}$$

in which (D_H) is the net hull resistance prior to take-off,

(R_H) is the experimental hull resistance at full gross weight.

BOW PLANING SURFACE DRAG

Drag of the bow planing surfaces is estimated by assuming that it consists of a combination of wave drag, induced drag, and friction drag.

Induced and wave drags of a body of the type used for the bow surfaces can be approximated, as pointed out by Sottorf, by

$$D_{iB} = W_B \tan \alpha_B \tag{16}$$

in which (D_{iB}) is the sum of induced and wave drags,

(W_B) is the portion of total load carried by the bow surfaces,

(α_B) is the bow surface planing angle.

The load carried by the bow surfaces can be determined as the difference between the total craft gross weight and the sum of the loads carried by the main foil and hull. For the particular case under study, it is equal to 73 pounds after take-off (453 pounds carried by main foil, none by hull).

Prior to take-off, it is assumed that the bow wave and induced drags will be equal to one-half the value indicated by equation (16), since the foils will be completely submerged, or nearly so.

Friction drag of the bow foils is estimated by

$$D_{FB} = 2 C_f S_B q \tag{17}$$

in which (C_f) is friction drag coefficient = $0.02058 R_N^{-1/6}$

(R_N) is the Reynolds Number = $\frac{V_{MPH} \ell_{FT}}{9.97} 10^6$

(S_B) is the bow surface wetted area.

In the design cruise condition, submerged length of each bow surface is nine inches, and wetted area approximately four square feet. It is assumed that these values remain essentially constant throughout the flight range after take-off. It is also assumed that the values remain constant at two feet and ten square feet, respectively, prior to take-off.

It is also assumed that the friction drag coefficient defined by a length of nine inches at eight miles per hour is sufficiently accurate for use over the entire speed range (C_f = 0.00390).

Detailed computations of the component and total hydrofoil test craft drags are outlined in Table I.

TABLE I

W - 256 lbs. S - 4.44 sq. ft. W_F - 453 lbs. T.O.@ 7.76 mph (C_L .90)

V MPH	4	5	6	7	8	10	12	14	16
q PSF	34.4	53.8	77.4	105.4	137.5	215.0	309.6	421.3	550.2
C_L	.90	.90	.90	.90	.7420	.4745	.3296	.2420	.1853
α_R Deg.	11.5	11.5	11.5	11.5	9.5	6.1	4.2	3.1	2.4
γ_T Deg.(Sr-3)	14.5	14.5	14.5	14.5	11.1	5.2	2.1	0.2	-1.1
h IN	26.5	26.5	26.5	26.5	23.1	17.2	14.1	12.2	10.9
K_4	.552	.552	.552	.552	.564	.589	.604	.615	.623
α_R Deg.	21.0	21.0	21.0	21.0	19.0	15.6	13.7	12.6	12.0
(HULL DRAG)									
$(V/V_{TO})^2$	.304	.475	.683	.930					
ω_H/ω	.696	.525	.317	.070					
W_H	366	271	167	37					
R_H	19	35	60	83	91	101	111	121	133
EHP_{RH}	.20	.47	.96	1.55	1.94	2.69	3.55	4.52	5.68
D_H	14	22	28	14					
EHP_H	.15	.29	.45	.26					
(MAIN FOIL DRAG)									
$0.022 C_L^2$	.0180	.0180	.0180	.0180	.0122	.0050	.0024	.0013	.0008
$\omega/2$	.0493	.0493	.0493	.0493	.0435	.0363	.0337	.0326	.0321
D_c	1.7	2.7	3.8	5.2	6.0	7.8	10.4	13.8	17.8
$D_i/2$	.1445	.1445	.1445	.1445	.1004	.0429	.0212	.0117	.0069
D_i	5.0	7.8	11.2	15.2	13.8	9.2	6.6	4.9	3.8
D_F	6.7	10.5	15.0	20.4	19.8	17.0	17.0	18.7	21.6
EHP_F	.07	.14	.24	.38	.42	.45	.54	.70	.92
$(L/D)_F$	20.6	20.6	20.6	20.6	22.9	26.6	26.6	24.2	21.0
(MAIN STRUT DRAG)									
$7.84 \times K^4 h$	.0208	.0208	.0208	.0208	.0182	.0135	.0111	.0096	.0086
$3.78 \times 10^{-4} h^2$	.0027	.0027	.0027	.0027	.0020	.0011	.0008	.0006	.0004
D_s/q	.0235	.0235	.0235	.0235	.0202	.0146	.0119	.0102	.0090
D_s	0.8	1.3	1.8	2.5	2.8	3.1	3.7	4.3	5.0
EHP_s	.01	.02	.03	.05	.06	.08	.12	.16	.21
$D_s + D_F$	7.5	11.8	16.8	22.9	22.6	20.1	20.7	23.0	26.6
$EHP_{(s+F)}$	.08	.16	.27	.43	.48	.54	.66	.86	1.14
$L/D_{(s+F)}$	18.4	18.4	18.4	18.4	20.0	22.5	21.9	19.7	17.0
(BOW SURFACE DRAG)									
W_B	22	40	50	68	73	73	73	73	73
D_{iB}	4.2	7.7	9.6	13.1	25.1	20.4	17.8	16.3	15.5
D_{wB}	2.7	4.2	6.0	8.2	4.4	6.9	9.9	13.5	17.6
D_B	6.9	11.9	15.6	21.3	29.5	27.3	27.7	29.8	33.1
EHP_B	.07	.16	.25	.40	.63	.73	.89	1.11	1.41
$(L/D)_B$	3.19	3.39	3.21	3.19	2.47	2.67	2.63	2.45	2.21
(TOTAL DRAG)									
D	29	46	61	58	52.1	47.4	48.4	52.8	59.7
L/D	18.1	11.4	8.6	9.1	10.1	11.1	10.9	10.0	8.8
EHP	.31	.61	.98	1.08	1.11	1.26	1.55	1.97	2.55
EHP/EHP_{RH}	1.53	1.84	1.02	.70	.57	.47	.44	.44	.45

HYDROFOIL TEST CRAFT

GEOMETRY

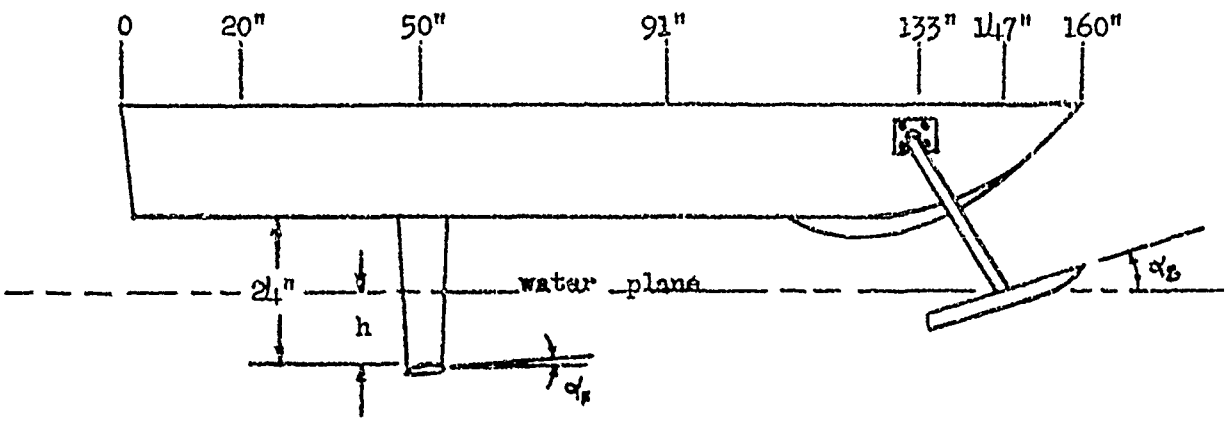

Station	Item
0	transom and outboard motor.
20"	crew seat No. 1.
50"	main foil, main struts, crew seat No. 2.
91"	Crew seat No. 3.
133"	bow strut attachment.
147"	bow planing surface.
160"	bow

MAJOR DIMENSIONS

Main Foil: span - 96.0 inches
chord - (between struts) 6.8 inches
(outboard of struts) tapered to 5.1 inches at tip.
strut separation - 48.0 inches
total area - 4.44 square feet
aspect ratio - 14.4
thickness - 15%
approximately 65-015 section

Main Struts: length below hull - 24.0 inches
chord at hull - 8.0 inches
chord at foil - 6.5 inches
thickness at hull - 1.0 inch
thickness at foil - 0.5 inch
slab sides, ogive l.e. & t.e. to .25 chord

Bow Surfaces: sheet steel 2 ft. x 1 ft. with 4 inch flanges down.

NOTE: Foil angle of attack 3.0 degrees and bow planing angle 12.5 degrees for design cruise condition of one foot submergence.

BRIEF HISTORY OF CONSTRUCTION AND TESTS OF HYDROFOIL TEST CRAFT

Theoretical studies of the general subject of hydrofoils had progressed, by February of 1950, to the point where methods of prediction of performance and stability characteristics of hydrofoil craft were proposed with some degree of confidence. It was considered highly desirable, however, to substantiate the various theories developed, by operation of a full-scale test craft under actual operating conditions. Several methods of obtaining such substantiation were considered.

The studies had shown that the most favorable configuration, from an (L/D) standpoint, would utilize completely submerged main and auxiliary hydrofoils, as contrasted with the usual practice of employing either foils or oblique struts which pierce the water surface. Simultaneous testing of a high (L/D) craft which utilized such completely submerged foils, however, was considered to involve design problems which could probably not be resolved in as short a time as desired. It was therefore decided to attack the test program from two separate philosophies. First, the performance of a high aspect ratio main foil would be determined, with stabilization of the test craft affected in the simplest manner, using forward planing surfaces which would achieve the desired stabilization without affecting performance of the main foil. Second, the effectiveness of a completely submerged foil system would be tested, after completion of the initial performance tests, with stability rather than performance as the prime consideration. It was thus considered possible to obtain information regarding performance and stability of hydrofoil craft without involving the complication and expense of an ideal test craft which combined all of the desired features at once.

A test configuration consisting of a submerged high aspect ratio foil aft, carrying most of the craft weight, and small planing surfaces forward for longitudinal and lateral stabilization, offered a simple means of obtaining performance test data without introducing distracting mechanical problems which would be associated with automatic stabilizing mechanisms. The use of laminated fibreglass as a material of construction was considered seriously because of its qualities of resistance to corrosion and fouling, and its relative ease of fabrication. Mr. L.H.Corzine, who had accumulated a great deal of experience in the construction of small fibreglass pleasure boats was employed to advise on this type of construction. After some study, the material appeared to be most desirable for construction of a fourteen-foot test craft, and Mr. Corzine and Mr. Warren Hoyt were employed to construct the craft at their facilities in Long Beach, California.

The basic design of the performance test craft was developed after brief model towing tests to insure that bow planing surfaces would provide adequate stabilization. An existing fourteen foot Triangle Boat Company laminated fibreglass runabout hull was modified for installation of a high aspect ratio, two strut, main foil and two bow planing stabilizing surfaces. Power was provided by a standard Mercury "10" outboard motor with extended shaft. The main foil and struts were fabricated of laminated fibreglass.

Provisions were made in the initial design for installation of strain gages with which to record lift and drag of the main strut-foil assembly, and net engine thrust. The laminated fibreglass main struts were designed for maximum practical rigidity, and steel strain gage mounting pads were provided between the struts and hull attachment fittings. Provisions were also included for adjustment of both depth and angle of incidence of the main struts.

Forward laminated fibreglass planing surfaces were supported by tubular steel struts, with provisions for adjustment of both height and planing angle.

Subsequent trials of the initial configuration indicated that sufficiently reliable lift and drag measurements could probably be obtained without the expense and complications of strain gage installation. Provisions were therefore made for towing the craft at various combinations of speed, main foil depth and incidence, bow surface attitude, gross weight, and center of gravity location, using a simple spring scale to measure net drag. Resistance of the basic hull, with the hydrofoil system removed, was determined by towing it at the same gross weight as that of the complete craft.

Observations made during repeated runs with the initial configuration indicated that the forward struts and planing surfaces were considerably overweight for the loads actually encountered. Modified tubular steel struts and flat plate steel planing surfaces were installed, at the height and angle of incidence considered most favorable as the result of qualitative observations of the original surfaces.

During early runs with the initial configuration, the laminated fibreglass main foil failed by fracture of the starboard tip section at the foil-strut juncture. Inspection indicated improper, or too hasty, curing as the cause of failure. A second foil was fabricated and sun cured, using more reliable methods of fabrication.

Repeated tests with the replacement foil were conducted to establish the most favorable depth of submersion and incidence angle. Modified main struts were then fabricated and installed in place of the original adjustable struts. Elimination of provisions for strain gage installation and adjustment of height and incidence angle permitted considerable reduction of the strut sizes, which in turn reduced their drag.

Final performance trials, both towed and self-propelled, were then conducted with the modified main foil and struts and bow surfaces installed. In all, some 113 trial runs were made. Empty weight of the craft was 451 pounds with the engine installed, 371 pounds with the engine removed. Towing tests were conducted with the engine removed, in order to eliminate its drag from the recorded data, at a total gross weight of 526 pounds. Self-propelled tests were conducted at gross weights varying from 606 to 1161 pounds. Center of gravity location was varied to load the bow surfaces from 2.9 to 20.0 percent of the total load.

After completion of the performance trials, the test craft was modified to incorporate completely submerged stabilizing surfaces. The bow planing surfaces were removed and a single tail strut-foil assembly was mounted below a tubular steel boom extending aft of the hull transom. Quarter-chord, fifteen percent span trailing edge flaps were added to the main foil, adjacent to each main strut.

Brief development programs indicated that a satisfactory height sensing system could be designed, using hydrodynamic pressure operated bellows as pressure switches which would control electric motor servo-actuators. The overall system designed was similar to that described in Sec.III, D of the Stability Section of the general report. Electric control circuits were incorporated into two autopilots mounted in the hull near the flap actuating motors. Power was provided by four six-volt motorcycle batteries in series. A master control panel, with manual overide controls, was mounted on the main dash panel.

During assembly of the automatic flap mechanisms it became apparent that the design was such that considerable looseness of the various connections would be inherent in the particular design used. Since there did not appear to be sufficient time available for assembly of a redesigned system, it was decided to reduce the electrical sensitivity of the autopilots to partially compensate for the mechanical defficiencies of the actuating system. It was considered probable that the essential purpose of the tests, proof of the basic stabilization concepts, could be satisfied without extended refinement of the complete system. The system was therefore assembled, with the expectation that its performance would be somewhat compromised by its lack of design perfection.

Subsequent trials, at gross weights between 960 and 1160 pounds, indicated that a craft utilizing completely submerged main and auxiliary foils could be adequately stabilized. The troubles expected as a result of looseness of the mechanisms were encountered, but in no case did they appear to negate the marked advantages of the automatic stabilization system.

It is considered entirely probable that a completely adequate system of stabilization of the fourteen foot test craft can be developed with a minimum further expenditure of time and funds. Such was not done during the tests reported, however, due to termination of the basic study contract under which these, and the other, tests were conducted.

DEPARTMENT OF THE NAVY
OFFICE OF NAVAL RESEARCH
875 NORTH RANDOLPH STREET
SUITE 1425
ARLINGTON, VA 22203-1995

IN REPLY REFER TO:
5513
Ser 43/056

AUG 3 0 2010

From: Chief of Naval Research
To: Commander, Naval Surface Warfare Center, Carderock Division, DET Norfolk

Subj: MANDATORY DECLASSIFICATION REVIEW

Ref: (a) SECNAVINST M-5510.36
(b) NSWCCD ltr of 13 Oct 09

Encl: (1) Final Report - Hydrofoil Studies and Preliminary Studies Data (U)

1. In accordance with reference (a), a declassification review has been conducted as requested by reference (b) of enclosure (1). This document is hereby downgraded from CONFIDENTIAL to UNCLASSIFIED and is approved for public release with unlimited distribution. However, all classified references associated and listed in this document must be removed prior to release, since those classified references may not have been reviewed and approved for declassification.

2. You may contact Mr. Derrick Shack (ONR 43) at 703-696-1499 or by email at derrick.shack@navy.mil for any questions regarding this matter.

8/30

NEVIN P. CARR, JR.
Rear Admiral, U.S. Navy

COPY